CAPITAL UNIVERSITY OF SCIENCE AND TECHNOLOGY, ISLAMABAD

Gene Expression Mining for Relapse Biomarkers in Multiple Myeloma: Implications for Drug Repurposing

by

Sana Elahi

A dissertation submitted in partial fulfillment for the degree of Doctor of Philosophy

in the

Faculty of Health and Life Sciences
Department of Bioinformatics and Biosciences

2024

Gene Expression Mining for Relapse Biomarkers in Multiple Myeloma: Implications for Drug Repurposing

By

Sana Elahi

(DBI163003)

Dr. Muhammad Usman Hadi, Assistant Professor

Ulster University, Belfast, UK

(Foreign Evaluator 1)

Dr. Sheheryar Khan, Lecturer

The Hongkong Polytechnic University, Hongkong

(Foreign Evaluator 2)

Dr. Sahar Fazal

(Research Supervisor)

Dr. Syeda Marriam Bakhtiar

(Head, Department of Bioinformatics and Biosciences)

Dr. Sahar Fazal

(Dean, Faculty of Health and Life Sciences)

DEPARTMENT OF BIOINFORMATICS AND BIOSCIENCES

CAPITAL UNIVERSITY OF SCIENCE AND TECHNOLOGY

ISLAMABAD

2024

I dedicate this dissertation to my family, whose unconditional love, unwavering support, and endless encouragement have been my pillars of strength throughout this challenging journey.

CAPITAL UNIVERSITY OF SCIENCE & TECHNOLOGY
ISLAMABAD
Expressway, Kahuta Road, Zone-V, Islamabad
Phone:+92-51-111-555-666 Fax: +92-51-4486705
Email: info@cust.edu.pk Website: https://www.cust.edu.pk

CERTIFICATE OF APPROVAL

This is to certify that the research work presented in the dissertation, entitled "**Gene Expression Mining for Relapse Biomarkers in Multiple Myeloma: Implications for Drug Repurposing**" was conducted under the supervision of **Dr. Sahar Fazal**. No part of this dissertation has been submitted anywhere else for any other degree. This dissertation is submitted to the **Department of Bioinformatics & Biosciences, Capital University of Science and Technology** in partial fulfillment of the requirements for the degree of Doctor in Philosophy in the field of **Biosciences**. The open defence of the dissertation was conducted on **August 01, 2024.**

Student Name : Sana Ilahi (DBI163003)

The Examination Committee unanimously agrees to award PhD degree in the mentioned field.

Examination Committee :

(a) External Examiner 1: Dr. Sobia Tabassum
Professor
IIU, Islamabad

(b) External Examiner 2: Dr. Malik Badshah
Associate Professor
QAU, Islamabad

(c) Internal Examiner : Dr. Sohail Ahmed Jan
Associate Professor
CUST, Islamabad

Supervisor Name : Dr. Sahar Fazal
Professor
CUST, Islamabad

Name of HoD : Syeda Marriam Bakhtiar
Associate Professor
CUST, Islamabad

Name of Dean : Dr. Sahar Fazal
Professor
CUST, Islamabad

AUTHOR'S DECLARATION

I, **Sana Ilahi** (Registration No. **DBI163003)**, hereby state that my dissertation titled, '**Gene Expression Mining for Relapse Biomarkers in Multiple Myeloma: Implications for Drug Repurposing**' is my own work and has not been submitted previously by me for taking any degree from Capital University of Science and Technology, Islamabad or anywhere else in the country/ world.

At any time, if my statement is found to be incorrect even after my graduation, the University has the right to withdraw my PhD Degree.

(**Sana Ilahi**)

Dated: 01, August, 2024

Registration No : DBI163003

PLAGIARISM UNDERTAKING

I solemnly declare that research work presented in the dissertation titled "**Gene Expression Mining for Relapse Biomarkers in Multiple Myeloma: Implications for Drug Repurposing**" is solely my research work with no significant contribution from any other person. Small contribution/ help wherever taken has been duly acknowledged and that complete dissertation has been written by me.

I understand the zero-tolerance policy of the HEC and Capital University of Science and Technology towards plagiarism. Therefore, I as an author of the above titled dissertation declare that no portion of my dissertation has been plagiarized and any material used as reference is properly referred/ cited.

I undertake that if I am found guilty of any formal plagiarism in the above titled dissertation even after award of PhD Degree, the University reserves the right to withdraw/ revoke my PhD degree and that HEC and the University have the right to publish my name on the HEC/ University Website on which names of students are placed who submitted plagiarized dissertation.

(Sana Ilahi)

Dated: 01, August, 2024

Registration No : DBI163003

List of Publications

It is certified that following publication(s) have been made out of the research work that has been carried out for this dissertation:-

1. S. Elahi, and S. Fazal, "Gene Expression Profiling to Predict Prognostic Biomarkers for Relapse in Multiple Myeloma". Advancements in Life Sciences, vol. 11, no. 2, pp. 329-337, May 2024.

(Sana Elahi)
Registration No: DBI163003

Acknowledgement

With love, First and foremost I would like to dedicate this work to the Almighty ALLAH, Who bestowed me with the courage and faith to complete this work. I have to thank my family for their prayers, love and support throughout this difficult voyage, my mentors for their continuous guidance.

(Sana Elahi)

Abstract

Multiple Myeloma (MM), an untreatable form of Plasma Cells (PCs) cancer, ranks as the second most prevalent hematological malignancy. Its primary drivers are structural alterations, including chromosomal aberrations and somatic mutations. Majority of the patients acquired resistance against standard therapeutic approaches for MM and experience relapse despite the continuous advances in MM therapies. Differential Gene Expression (DGE), literature mining and SNV analysis of Gene Expression profiles of Newly Diagnosed MM (NDMM) and Relapsed/Refractory MM (RRMM) were performed. The selected Differentially Expressed Genes (DEGs) were subjected to functional enrichment and pathway analysis. Immune cells infiltration analysis was also performed to estimate immune cells variations in the Tumor Microenvironment (TME) of RRMM. The 3D structures of selected biomarkers were predicted, refined and assessed using computational tools. The Solvent Accessible Surface Area (SASA) was also assessed computationally to evaluate the solubility of biomarkers. Additionally the Molecular Dynamic (MD) simulations of biomarkers with SNVs were also performed to assess the stability of wild and mutated structures. Lastly drug repurposing against selected biomarkers were performed to find out most suitable existing compounds that can be added to RRMM treatment regimens to enhance their effectiveness. MD simulations of protein-drug complex were conducted to investigate whether the drugs could potentially exert an inhibitory effect on the proteins by perturbing their 3D conformation, thereby aiding in the inhibition of the protein's pathogenic function. CSF1R, VCAN, NRP1, COL22A1, BPI, BIRC5, MNX1, FAT1, ERG, TCL1A, AFF3, NRAS, IL1B, CD4, ITGAM, PTPRC, TYROBP, and KRAS were selected after DGE, literature mining, hub genes and SNV analysis as candidate relapse biomarkers. The functional enrichment of these candidate relapse biomarkers showed significant enrichment for positive regulation of cell population proliferation, serene/threonine kinase activity, endothelial cell proliferation, cytokine binding, G protein activity and GDP binding, whereas KEGG pathway analysis revealed vital role of PI3K-Akt signaling pathway along with various cancer

pathways. The immune cells infiltration analysis revealed the higher count of neutrophils and lesser level of T cells (CD8+) in TME of RRMM. Mutations ERG-E353Q and AFF3-P1129L induced structural changes in the Ets domain (ERG) and AF4/FMR2, C-terminal homology domain (AFF3), respectively. Whereas, the mutations of FAT1 effected the Cadherin-like domains of protein. The small GTP-binding domain of KRAS and NRAS proteins was observed with drastic structural changes due to mutations. The mutations KRAS-G12V and KRAS-A59E caused significant disruption, altering the function of the small GTP-binding protein domain essential for signaling functions of RAS proteins. The mutants TCL1A-T38I, KRAS-K117N and KRAS-Q61E were significantly stable indicating their crucial role in RRMM as compared to wild-type models. Meanwhile ERG-E353Q, AFF3-P1129L, KRAS-Q61R, KRAS-G12R, KRAS-A59E, NRAS-Q61H, NRAS-Q61K, NRAS-Q61R, NRAS-G13R, NRAS-E153Q and MNX1-P392L have been identified as more unstable conformtionally, with respect to their wild structures indicating that these structural alterations may have disrupt the native of these proteins in RRMM. The molecular docking results with 141 drug compounds showed that adapalene, ponatinib, glycyrrhizic acid, and pralsetinib showed the best binding affinities with all the proteins except for two complexes. Adapalene showed the best binding affinities with 17 protein models out of 44 protein models, followed by Ponatinib (15), Glycyrrhizic acid (9), and Pralsetinib(3). The MD simulation of protein–drug compound revealed that all drug compounds have great potential to inhibit the activity of biomarkers by destabilizing their structure. However, all the drugs were the best inhibitors for both wild and mutant models of the MNX1 and AFF3 proteins as these proteins were extremely unstable when docked with the drug compounds. In summary, our study identified potential relapse biomarkers in RRMM, characterized their structural alterations, and highlighted promising drug candidates for enhanced treatment effectiveness. These findings offer a foundation for targeted therapies and warrant further preclinical and clinical investigations. Future research endeavors should focus on validating the clinical relevance of the identified biomarkers, conducting in vitro and in vivo experiments to confirm the inhibitory effects of the selected drug candidates, and exploring combination therapies to address the complexity of RRMM.

Contents

List of Figures

List of Tables

Abbreviations

3D	Three Dimensional
AA	African Americans
ADT	AutoDockTool
AML	Acute Myeloid Leukemia
API	Application Programming Interface
ASCT	Autologous Stem Cell Transplantation
AURKA	Aurora Kinase A Activity
B Cells	B Lymphocytes
BM	Bone Marrow
BP	Biological Process
CA	Caucasians American
CAFs	Cancer Associated Fibroblasts
CAR-T	Chimeric Antigen Receptor T-cell
CC	Cellular Component
CNVs	Copy Number Variations
CoMMpass	Clinical Outcomes in Multiple Myeloma to Personal Assessment of Genetic Profile study
CRC	Colorectal Cancer
CTCs	Circulating Tumor Cells
DEGs	Differentially Expressed Genes
DGE	Differential Gene Expression
DOPE	Optimized Protein Energy score
DSS	Durie-Salmon Staging
EGFR	Epidermal Growth Factor Receptor

EMD	Extramedullary Disease
FACS	Fluorescence Activated Cell Sorting
FISH	Fluorescence in-situ Hybridization
FLC	Free Light Chain
FPKM	Fragments per Kilobase Million
GO	Gene Ontology
GVHD	Graft-Versus-Host Disease
HCC	Hepatocellular Carcinoma
HLA	Human Leukocyte Antigen
HRD	Hyperdiploid
HTS	High-Throughput Sequencing
IHC	Immunohistochemistry
IMWG	International Myeloma Working Group
ISS	International Staging System
LDH	Lactase Dehydrogenase
M proteins	Monoclonal Paraprotein
MD	Molecular Dynamic
MDC	Myeloid Dendritic Cells
MDE	Myeloma Defining Event
MDSCs	Myeloid-Derived Suppressor Cells
MeSH	Medical Subject Headings
MF	Molecular Function
MGUS	Monoclonal Gammopathy of Undetermined Significance
MM	Multiple Myeloma
MMRF	Multiple Myeloma Research Foundation
MRD	Minimal Residual Disease
NCBI	National Centre for Biotechnology Information
NCI	National Cancer Institute
NDMM	Newly Diagnosed MM
NGS	Next Generation Sequencing
NK	Natural Killer Cells
NLM	National Library of Medicine

NMR	Nuclear Magnetic Resonance
non-HRD	non-Hyperdiploid
OS	Overall Survival
PCL	Plasma Cell Leukemia
PCs	Plasma Cells
PDB	Protein Data Bank
PDL1	Programmed Cell Death Ligand 1
PEA	Pathway Enrichment Analysis
PFS	Progression Free Survival
PPIs	Protein-Protein Interactions
ProSA	Protein Structure Analysis
RBCs	Red Blood Cells
RISS	Revised International Staging System
RMSD	Root Mean Square Deviation score
RMSF	Root Mean Square Fluctuation
RRMM	Relapsed/Refractory MM
SASA	Solvent Accessible Surface Area
SIFE	Serum Immunofixation Essay
SMM	Smoldering Multiple Myeloma
SNPs	Single Nucleotide Polymorphisms
SNV	Single Nucleotide Variant
SPEP	Serum Protein Electrophoresis
TME	Tumor Microenvironment
Treg	regulatory T cells
TRM	Treatment Related Mortality
TTP	Time to Progression
UniProtKB	UniProt Knowledgebase
WBC	White Blood Cell

Symbols

α	Alpha
β	Beta
κ	Kappa

Chapter 1

Introduction

1.1 Background

Multiple Myeloma (MM) is a Plasma Cells (PCs) neoplasm. PCs develops from B lymphocytes (B cells), a type of White Blood Cell (WBC) produce in the Bone Marrow (BM). During an immune response to bacteria or viruses, some of the B cells will transform into PCs to make antibodies to fight off the infection. In PCs neoplasm, abnormal PCs (myeloma cells) grow aberrantly and form tumors in the bones or soft tissues of body and produce monoclonal paraprotein (M proteins) or immunoglobulin Free Light Chain (FLC). These abnormal antibodies do not help body in fighting off infection rather deposited at different sites in body. In MM, myeloma cells forms tumors in many bones of body that not only restrains BM from producing enough Red Blood Cells (RBCs), WBCs and platelets but also cause lytic bone lesion that also damage and weaken the bone. With the increase of myeloma cells in BM there is a gradual decrease in healthy blood cells and immunity of the body [1–3].

1.2 Multiple Myeloma (MM)

MM is approximately 1% of all neoplastic illnesses and the second most common hematologic malignancy. The highest incident rate has been observed in Australia, New Zealand, North America, and Europe. In Asia, the incidence rate is low as compared to Western countries, but recently few reports showed the increasing prevalence of MM in some Asian countries [4]. According to the global cancer statistics 2020, the number of cases and fatalities were recorded as 176,404 and 117,077 for MM respectively [5]. The yearly age-adjusted incidence in Western nations is 5 patients per 100,000 people. MM is slightly more prevalent in men as compared to women. The risk of developing MM is twice in African-Americans then Caucasians [6]. The mean age of the onset of myeloma is about 68 and 70 years for men and women respectively. Less than 2% of patients have been observed under age 40 and 50% were above age 70 years [7–12]. The means age of disease onset observed in Pakistani population was 58 years (ranging from 23 to 86 years). However, the response to therapy is adequate and survival is comparable to western patients [13].

Etiology of MM is not clear yet, many factors collectively contribute to disease causation e.g. age, gender, race, chemical and radiation exposure, obesity, family history, and other plasma cell disorders [14–18]. Familial transmission of the disease has not been observed except few incidences in African-America patients [18]. Certain chemical (benzene, asbestos, petroleum products, arsenic, lead, carbon monoxide, pesticides) and radiations are also thought to be causative agents but clear evidence is missing [19]. The role of Epstein bar virus in the progression of MM has been explored by two groups recently [20, 21].

The pathophysiology of MM affects bone, blood, kidney, and neurological processes. MM follows a multi-step process of pathogenesis initiating from precursor disorders i.e. Monoclonal Gammopathy of Undetermined Significance (MGUS) and smoldering myeloma that progresses to MM [22]. These are non-cancerous stages, can be diagnosed through routine blood and urine test. In most cases, these stages are devoid of any indications, symptoms, or health issues (www.cancer.gov/

types/ myeloma/patient/ myeloma-treatment-pdq). Malignant PCs invade different organs and cause a variety of symptoms. Bone health complications are observed in almost 60% of MM patients and develop fractures at some point during disease. Myeloma cells disrupt bone remodeling process, as fewer healthy osteocytes are present in bone leading to skeletal problems i.e. fractures and pain and high calcium levels in blood. Overgrowth of myeloma cells in BM crowd out normal blood cells leads to low blood count causing anemia, neutropenia and thrombocytopenia in patients. Almost 50% of patient experiences kidney problems because of M protein or FLC buildup in body. Nervous system complications are rear (1%) in MM but do exist. MM patients have higher probability of developing infections as abnormal antibodies cannot provide immunity against pathogens [1][22].

Genomic instability in MM encompasses a range of abnormalities, both large and small in scale. Significant alterations includes insertions, deletions, translocations, and inversions on a large scale, whereas minor alteration includes small insertions and deletions (indels), Loss of Heterozygosity (LOH), Copy Number Varations (CNVs), and base-level mutations. Individuals diagnosed with MM are categorized into two molecular subgroups: Hyperdiploid (HRD) and non-Hyperdiploid (non-HRD). HRD is identified by the presence of extra copies of odd-numbered chromosomes, while non-HRD is linked to chromosomal translocations. Structural abnormalities in chromosomes are prevalent in nearly 60% of MM cases, with IgH translocations being a common occurrence. These translocations often involve various genes, such as those in the cyclin D family, MMSET/FGFR3, and MAF group. Additionally, mutations in genes like NRAS, ATM, DIS3, BRAF, KRAS, CCND1, FAM46C, and TP53 are associated with MM. Epigenetic modifications, particularly PC demethylation, also play a role in the development of MM. High-risk MM groups are identified based on these genetic abnormalities. Notably, recent research has identified driver genes in MM, including KRAS, TP53, NRAS, DIS3, BRAF, FAM46C, TRAF3, EGR1, ROBO1, FAT3, and SP140. These genes are involved in various pathways such as MAPK, DNA repair, NF-kB, RNA processing, and cell migration [23–26].

Moreover immune system of many MM patients has been observed dysfunctional

i.e. low expression of tumor antigens and Human Leukocyte Antigen (HLA), presence of Regulatory T Cells (Tregs) and Myeloid-Derived Suppressor Cells (MDSCs), and enhanced expression of Programmed Cell Death Ligand 1 (PCD-L1) [27]. Considering the crucial role of the immune system in MM, quantitative elucidation of the infiltrating immune cells in the TME can contribute significantly in the cancer treatment as it provides the information regarding the extent of immune evasion as well as cancer growth and progression [28].

1.2.1 Diagnosis and Treatment of MM

The diagnosis of MM can be classified into three groups of procedures: i) Blood or urine tests to rule out abnormal antibodies, beta-2 microglobulin, albumin, Lactase Dehydrogenase (LDH) and calcium level, ii) Tracking of cancerous PCs by BM biopsy (Fluorescence in-situ hybridization, sequencing techniques) and iii) Bone lesions assessment by medical imaging (x-rays, CT scan and MRI) [29]. The ISS staging system is the most commonly used staging system for MM.

It is a simple and reproducible system that is used to predict prognosis and treatment response. The diagnostic criteria for ISS stage I includes presences of Monoclonal (M) protein (Serum beta2-microglobulin <3.5 mg/L, albumin ≥ 3.5 g/dL, and LDH normal) in serum or urine. Whereas he ISS Stage II criteria includes $>10\%$ clonal PCs in BM and elevated LDH along with M protein in serum or urine upto the level specified in stage I. Similarly, presences of M protein, end-organ damage, HyperCalcemia (Ca >11 mg/dl), Renal insufficiency, Anemia (Hb <10 g/dl), bone lesions, and high risk cytogenetics are the features of ISS Stage III MM [30][31].

Symptomatic myeloma typically needs prompt medical attention. The main focus of MM treatment is to target malignant PC to address sign and symptoms of the disease. The treatment is usually delayed or limited to clinical trials for asymptomatic myeloma [32]. Autologous Stem Cell Transplantation (ASCT) is the standard of treatment for patients less than 65 years old or those aged 65–70 with minor comorbidities. Prior getting transplant, patients generally receive 3–6

rounds of induction therapy with the goal of achieving a full or near complete response [33]. Bisphosphonates, RBC transfusion, and erythropoietin are prescribed to manage skeletal issues and anemia along with the main drug to control plasma cell propagation. A combination of steroids (dexamethasone and prednisone), antibiotics (doxorubicin), alkylating agents (cyclophosphamide, melphalan), immunomodulatory drugs (thalidomide, lenalidomide, and pomalidomide), proteasome inhibitor (bortezomib, carfilzomib, and ixazomib), monoclonal antibodies targeting CD38 (Daratumumab and isatuximab) and SLAMF7 antigens (elotuzumab, panobinostat, and selinexor) appears to produce the best possible outcomes [34, 35].

1.2.2 Relapse in MM

The cause for the relapse in MM is still unknown, however drug resistance is one of most agreed upon factor. Multiple causes including genetic and epigenetic variations, abnormal drug transport and metabolism, persistence of cancer stem cells, dysfunctional TME, immunotherapy, antigens and dysregulation of apoptosis dictate drug resistance in MM [36].

Relapse has been categorized into relapsed but not refractory, relapsed and refractory, and primary refractory forms. These are the aggressive forms of MM that become non-responsive or recur/relapse after the initial or several treatments [27]. Recently, most promising therapies against RRMM are Chimeric Antigen Receptor T-cell (CAR-T) Therapy, Cereblon E3 Ligase Modulators (CELMoDs), and Bispecific T-cell Engagers (BITEs).

However, there are still challenges in terms of limited access to these therapies as well as the continual increased cases of relapses [37]. The underlying mechanisms of cancer progression, development and drug resistance are still not understood completely, however with the advancement in genomic technologies and integrated approaches, several new treatment approaches are being investigated that can be promising against cancer [38–40].

1.2.3 High Throughput Sequencing & Computational Approaches to Identify Biomarkers

High-Throughput Sequencing (HTS) techniques have revolutionized the field of biology, enabling researchers to sequence entire genomes, transcriptomes, and epigenomes. RNA-Seq is a Next-Generation Sequencing (NGS) approach that involves converting RNA into cDNA and offers comprehensive and quantitative insights into gene expression levels. Its applications are far-reaching, especially in the realm of cancer research, where it has been extensively employed to unveil the genomic and mutational landscape of cancer. Moreover, it aids in the identification of specific biomarkers crucial for early diagnosis, relapse prediction, and the understanding of drug resistance mechanisms [41–43].

In tandem with HTS, computational biology plays a pivotal role in analyzing biological data, system modeling, and gaining insights into intricate biological processes. These approaches are essential for integrating and analyzing vast biological datasets and instrumental in both the discovery and validation of biomarkers carrying diagnostic, prognostic, or predictive significance. This advancement contributes to personalized medicine and enhances patient outcomes [44, 45].

Differential Gene Expression (DGE) analysis, which examines the patterns of gene expression at the transcriptional level under specific conditions, is a powerful tool for unraveling the molecular mechanisms behind biological processes and diseases. It facilitates the identification of Differentially Expressed Genes (DEGs) among various conditions or cell types and sheds light on dysregulated pathways in disease states. The applications of DEG span a wide spectrum, encompassing drug discovery, biomarker identification, disease diagnosis, prognosis, and the realization of personalized medicine. Literature mining, a process that extracts information from scientific literature, contributes significantly to the identification of biomarkers associated with clinical outcomes, such as tumor stage, grade, and survival [46]. It enables the synthesis of knowledge from existing research to inform biomarker discovery. Moreover, function enrichment analysis, and Pathway

Enrichment Analysis (PEA) are computational method, expedite the identification of enriched biological processes, molecular functions, cellular components, and overrepresented biological functions within sets of genes or proteins. These analyses shed light on the functional roles, mechanistic intricacies, and dysregulated pathways in disease processes [47].

By integrating function enrichment and pathway analysis with gene expression data, researchers can prioritize and validate biologically relevant biomarkers, thereby enhancing our understanding of the molecular basis of diseases. These insights hold immense value for diagnostic, prognostic, and therapeutic purposes [47]. DGE along with other computation methods has great potential to identify relapse biomarkers in various diseases. The role of dysregulated proteins in relapse and drug resistance of Acute Myeloid Leukemia (AML), breast cancer, Colorectal (CRC) and prostate cancer has been identified by employing DGE on RNA-seq data [48–52]. These are just a few examples of the many studies that have been conducted to identify relapse biomarkers in cancer using DGE.

Similarly, DGE has also been utilized to identify various prognostic signatures for MM. The HZDCD, a ten gene prognostic signature for progression-free survival (PFS) has been proposed by Dickens et al. [53]. Likewise, a 92-gene signature (EMC-92) was derived from the Gene Expression Profiling (GEP) of 400 MM patients, demonstrating its reliability as a predictor of Overall Survival (OS) in individuals with MM [54]. Another famous genetic signature (70-gene) for prognosis of OS and PFS was also proposed by assessing the gene expression profiles of MM tumor of 532 patients [55]. Most recently, 5-gene RNA sequencing-based signature was proposed by analyzing RNA-seq data of 1200 MM patients [56]. The signature has been proven to be a reliable predictor of survival in patients with MM [56].

1.3 Research Problem

Managing relapses in cancer poses various difficulties. One significant challenge lies in dealing with resistance to treatments that were previously effective, complicating the search for alternative therapies to combat relapse. Successful relapse

management necessitates a personalized, comprehensive strategy that takes into account the individual's particular medical condition and their distinctive situation. Furthermore, continuous exploration and advancement of treatment choices play a pivotal role in enhancing the results of relapse management.

1.4 Research Objective

- To identify differentially express genes as candidate biomarkers causing relapse of MM using gene expression profiles.
- To perform functional and pathway annotation of candidate relapse biomarkers.
- To predict 3D structure of candidate relapse biomarkers.
- To carry out drug repurposing against candidate relapse biomarkers.

1.5 Research Philosophy

Presence of abnormal proteins or altered protein expression is a key aspect of cancer. Cancer can be understood as a result of alterations in the normal functioning of proteins involved in cell growth, division, and regulation. Proteins play critical roles in maintaining the balance between cell proliferation and cell death, as well as in controlling various signaling pathways within cells. When these proteins become dysfunctional or their regulation is disrupted, it can lead to uncontrolled cell growth and the development of cancer. Certain proteins known as oncogenes, when mutated or over expressed, can promote cell proliferation and inhibit cell death, leading to the formation of tumors. On the other hand, there are proteins called tumor suppressor proteins that normally regulate cell growth and prevent the development of cancer. These proteins help in maintaining genomic stability, repairing damaged DNA, and inducing cell death if necessary. However, mutations or inactivation of tumor suppressor genes can lead to a loss of their normal functions, allowing cells to divide uncontrollably and form tumors. In addition to

oncogenes and tumor suppressor genes, other proteins and signaling pathways contribute to the development and progression of cancer. These can include proteins involved in angiogenesis (formation of new blood vessels), invasion of surrounding tissues, and metastasis (spread of cancer to distant sites in the body).

Cancer cells employ various mechanisms to become resistant to drugs including, altered drug targets, activation of alternative pathways, enhanced DNA damage repair caused by chemotherapy drugs to reduce the effectiveness of treatment, increased drug efflux, epigenetic changes and cancer stem cells. Relapse occurs due to the survival of a small number of drug-resistant cancer cells that were not eliminated during the initial treatment.

These cells can give rise to new tumors or metastasize to other parts of the body, leading to more aggressive and difficult-to-treat disease. Addressing drug resistance and relapse is a major focus of cancer research. Strategies to overcome resistance include the development of combination therapies, where multiple drugs with different mechanisms of action are used simultaneously, as well as the identification of novel targets and the development of targeted therapies. Additionally, understanding the molecular mechanisms underlying drug resistance and finding ways to reverse or prevent them is crucial in improving treatment outcomes and preventing relapse.

1.6 Research Hypothesis

Genetic heterogeneity and the emergence of drug resistance constitute significant etiological factors contributing to relapse in MM. An approach to elucidate the underlying mechanisms responsible for relapse involves the analysis of differential gene expression profiles of patients at initial disease presentation and subsequently at relapse episodes. Such an understanding of these mechanisms carries the potential to unveil novel therapeutic targets and facilitate the development of pharmacological agents tailored to these targets, ultimately enhancing the efficacy of treatments for MM relapse.

1.7 Research Methodology

The approach used to conduct this research is segmented into various stages, from identification of biomarkers with therapeutic potential to control relapse, 3D structure modeling and MD simulation of these biomarkers, and identification of suitable drug compounds for these biomarkers.

1.7.1 Retrieval of Genetic and Gene Expression Profiles (GEP) of MM Patients

This study utilized the RNA-Seq data (GEP) of newly diagnosed MM (NDMM) and relapse or refractory MM (RRMM) patients. The RNA-Seq and variant data was retrieved from National Cancer Institute Genomic Data Commons (NCI-GDC) data Portal utilizing the MMRF CoMMpass study data (portal.gdc.cancer.gov).

1.7.2 Differential Gene Expression (DGE) of RRMM and NDMM

Differential gene expression (DGE) of GEP was performed by using DESeq2 (1.38.3), an R (4.2.2) package. Differentially expressed genes (DEGs) were selected on the basis of following threshold $2.0 < \text{Log2FC} < -2.0$ and $p < 0.05$.

1.7.3 Protein-Protein Interactions & Identification of Hub Genes

Protein-Protein Interactions (PPIs) of DEGs was constructed using STRING. Whereas the complex PPI network was visualized through Cytoscape and CytoHubba module was utilized to identify hub genes from the network.

1.7.4 Literature Mining for Identification of Relapse Biomarkers

Literature mining was conducted to identify biomarkers involved in recurrence of multiple types of cancers including MM using Google Scholar (scholar.google.com) and PubMed (pubmed.ncbi.nlm.nih.gov).

1.7.5 Short Listing of Candidate Relapse Biomarkers

The genes were selected as candidate genes if meeting the following criteria 1) a gene retrieved as relapse biomarker in literature mining and also upregulated in DGE, 2) a gene carrying SNV and also upregulated in DGE, 3) top five hub genes and 4) frequently mutated genes with higher no of SNVs.

1.7.6 Functional and Pathway Annotation of Candidate Relapse Biomarkers

Functional and pathway enrichment analysis of both DEGs and shortlisted candidate relapse biomarkers were performed by GeneCodis 4 (genecodis.genyo.es) separately, to identify GO (Gene Ontology) terms (biological process (BP), cellular component (CC), molecular function (MF)) and KEGG pathway.

1.7.7 Impact of Immune Cells on Tumor Micro Environment

The immune cells infiltration of GEP of the RRMM vs NDMM patients was carried out by two deconvolution methods quanTIseq and MCPcounter, computational techniques that utilizes bulk RNA-Seq data to measure the content of immune cells in the samples.

1.7.8 Retrieval of Protein Sequence of Candidate Relapse Biomarkers

The protein sequences of the selected candidate relapse biomarkers were obtained from UniProt (https://www.uniprot.org/). UniProt Knowledgebase (UniProtKB) is an integral component of The Universal Protein Resource (UniProt), which serves as a comprehensive repository for protein sequences and annotation information.

1.7.9 Identification of Protein Domains and Families for Candidate Relpase Biomarkers

The information pertaining to protein domains and families was obtained from the InterPro database, a comprehensive resource that integrates protein families, domains, and functional sites from multiple sources.

1.7.10 3D Structure Modeling of Candidate Relapse Biomarkers

Various tools were employed to model 3D structure of proteins. MODELLER 10.3 was used for homology modeling of proteins with already available 3D templates. Whereas, AlphaFold, OmegaFold and Genome3D were used for other proteins. The optimization and refinement of all predicted structures were performed by using UCSF chimera.

1.7.11 Structural Assessment of Predicted 3D Models

The quality assessment of all predicted 3D models were performed using various structural evaluation tools ERRAT, ProSa and QMEAN.

1.7.12 Assessment of Solvent-Accessible Surface Area (SA-SA) of 3D Structures

The solvent accessibility of protein is dictated by composition of surface residues. Quantitative assessment of polar, apolar, buried and exposed residues on surface of protein was performed using tool GETAREA.

1.7.13 Visualization and Structure Comparison of Wild and Mutant Candidate Relapse Biomarkers with SNVs

The predicted wild and mutated structures of candidate relapse biomarkers with SNVs were superimposed on each other to visualize the impact of mutations on the 3D structures of proteins. PyMol was employed to visualized these superimposed structures and all other predicted 3D structures of proteins.

1.7.14 Molecular Dynamics (MD) Simulation of Wild and Mutant Candidate Relapse Biomarkers with SNVs

MD simulation was performed to assess the conformational stability of both and wild and mutated predicted 3D structures of candidate relapse biomarkers with SNVs by employing Desmond Maestro 12.0. The MD simulations were performed at 300K temperature for 50 nanoseconds.

1.7.15 Retrieval of Drug Compounds for Drug Repurposing

The drug compounds for repurposing were retrieved from DRUGBANK, selected on the basis of following criteria i) retrieved in target sequence search of selected proteins, ii) reported for relapse treatment of other cancers, iii) FDA approved, or iv) EMA approved.

1.7.16 Molecular Docking of Drug Compounds with Candidate Relapse Biomarkers

Docking of selected drug compounds with shortlisted candidate relapse biomarkers was performed using AutoDock Vina (20) to identify lead compounds. AutoDock Vina (20) is widely used software for predicting the binding modes and affinities of small molecules to target protein. The best binding pose between the ligand and the target protein was chosen based on the binding energy score.

1.7.17 MD Simulation of Candidate Relapse Biomarker-Ligand Complexes

The MD Simulation of candidate relapse biomarkers complex with shortlisted drug compounds was performed to evaluate the conformational stability of complex by employing Desmond Maestro 12.0. The MD simulations were performed at 300K temperature for 50 nanoseconds.

Chapter 2

Literature Review

2.1 Disease Overview

MM is an untreatable malignancy originating from terminally differentiated B lymphocytes called PCs, which reside within the Bone Marrow (BM) and produce immunoglobulins [57]. MM accounts for one percent of all cancer cases and constitutes ten percent of all hematologic malignancies [58, 59]. Each year, over 32,000 new cases are identified in the United States, with nearly 13,000 individuals losing their lives to the disease. MM exhibits a slightly higher incidence in men compared to women and is twice as common among African-Americans (AA) when compared to Caucasians-Americans (CA) [60]. MM predominantly impacts older individuals, with a median patient age of 65 at diagnosis. The clinical signs and symptoms of MM include hypercalcemia, renal impairment, anemia, and bone-related issues, often referred to as CRAB manifestations [61]. MM induces bone lesions that obstructs the the formation of new bone [62]. Bone disease stands as the primary contributor to morbidity, and its most effective detection relies on advanced medical imaging techniques [63]. Approximately 1% to 2% of patients are diagnosed with Extramedullary Disease (EMD) at the outset, with an additional 8% developing EMD as the disease continues to progress [64]. MM is characterized by a challenging prognosis, as the overall 5-year survival rate stands at 48.5% [57].

2.1.1 Pre-clinical Phase of Multiple Myeloma

An essential feature of MM is the distinct clinical phase linked to each stage of its advancement. Both Monoclonal Gammopathy of Undetermined Significance (MGUS) and Smouldering Multiple Myeloma (SMM) represent first stages of pre-malignancy. MGUS is a medical condition that is typically asymptomatic. It is characterized by less than 10% PC count in the BM whereas progression rate of approximately 1% per year to MM development has been observed. MGUS, sometime become more serious and develop conditions i.e. amyloidosis, or kidneys, heart, or nerves problems (https://www.cancer.gov/types/myeloma/patient). Additionally, SMM is also asymptomatic and occurs subsequent to MGUS. It is characterized more than 10% clonal PCs and progression rate of approximately 10% or more per year to MM development. Consequently, the transition between MGUS, SMM, and MM's progression is governed by a genomic hierarchy, involving inherited factors that raise susceptibility to MM, initial triggering events, and subsequent acquisition of genetic abnormalities that eventually trigger disease advancement and resistance to treatment[65] [Figure 2.1].

2.1.2 Genetic Predisposition and Familial Transmission of Multiple Myeloma

The recognized genetic predisposition to MM is firmly established, with an estimated hereditary influence of approximately 15% for MGUS and 17% for MM [66]. In 2010, a Swedish investigation demonstrated that individuals who are first-degree relatives of MM patients face an elevated relative risk of developing MM, MGUS and other heamotological melagnancies [67]. In the same vein, a greater likelihood of developing MGUS and MM was identified among the immediate family members participating in the studies conducted at Minnesota and the Mayo Clinic [68].

Recent advancements in genetic research, specifically Genome-Wide Association Studies (GWAS), have pinpointed specific Single-Nucleotide Polymorphisms (SNPs)

linked to the risk of developing MM, Offering perspectives into risk factors associated with genetics [69]. Recent advancements in genetic research, specifically Genome-Wide Association Studies (GWAS), have pinpointed specific SNPs linked to the risk of developing MM, Offering perspectives into risk factors associated with genetics [70, 71]. Almost 13% familial risks are associated with the distinct loci including 2p23.3 on chromosome 2, 3p22.1 and 3q26 on chromosome 3, 6p21.33 on chromosome 6 , 7p15.3 on chromosome 7, 17p11.2 on chromosome 17, and 22q13 on chromosome 22 [72].

Moreover, American African (AA) experiences an increased frequency of MM than Caucasioan American (CA) of European lineage. According to Costa et al., AA men have a 2.24-times higher rate of MM than CA. Individuals of African descent were among the highest 10% of polygenic risk scores showed a 1.82-time higher suspectability of MM in contrast those with an average risk [73–77]. Similarly, a GWAS investigation identified a greater relationship in AA between the genetic site 7p15.3 and MM, the risk allele associated with increased CDCA7L, indicating MM germline risk to IRF4-MYC [78–80]. Furthermore, an NGS investigation revealed ethnic disparities in MM patients with higher frequency of mutations in BI3BP, ANKRD26, AUTS2, BCL7A, BRWD3, DDX17, GRM7, IRF4, MYH13, PARP4, PLD1, PTCHD3, RPL10, RYR1, SPEF2, STXBP4, and TP53, genes and essential involvement of MM-associated translocations [81, 82].

2.1.3 Cytogenetics in Multiple Myeloma

The cytogenetic perspective reveals that the onset and advancement of MM entail both primary and secondary events. PCs immortalization predominantly arises from primary events, which are divided into two groups: hyperdiploid (HRD) and non-hyperdiploid (non-HRD). The HRD group is characterized by the trisomies (presence of extra copies) of specific chromosomes 3, 5, 7, 9, 11, 15, 19, and 21 (odd-numbered), while the non-HRD group is distinguished by translocations of chromosomes. Whereas, the precise mechanism responsible for HRD remains unclear. One hypothesis speculates that a single catastrophic event during mitosis

leads to the acquisition of extra chromosomes, rather than a gradual accumulation over time [83]. The molecular classification of MM patients on the basis of cytogenetic abnormalities and their impact on the prognosis and Overall Ssurvival (OS) is compiled in Table 2.1 and Figure 2.1.

2.1.3.1 Primary Translocations in Multiple Myeloma

In more than 90% of non-HRD cases, primary chromosomal translocations, have a notable impact on the transcriptionally active IgH locus located on chromosome 14q32. As a consequence, these translocations lead to the upregulation cancer associated genes such as MAF, MAFB, CCND1, CCND3 and MMSET/FGFR3 [84, 85]. About 50% of individuals diagnosed with MGUS encounter these initial translocations. These events occur within the germinal center within the lymphatic system as part of the natural processes of class-switch recombination and somatic hypermutation [86]. HRD and non-HRD events, either directly or indirectly, can lead to the disruption of transition point of cell cycle (G1/S) by causing a hyperexpression of cyclinD genes. This represents a critical early molecular abnormality in MM [65]. The translocations in MM exhibit varying prevalence and clinical implications. The t(11;14) (q13;32) translocation, affecting 15%-20% of MM cases, leads to the over-expression of the Cyclin D1 Gene (CCND1), playing a crucial role in development of MM. Research is actively investigating CCND1 inhibitors for potential MM treatment [87, 88]. In contrast, the t(4;14) (p16.3;q32.3) translocation, found in approximately 15% of MM cases, is characterized with a unfavorable outcomes. It leads to the hyperexpression of FGFR3 and MMSET genes, contributing to disease progression. The use of the Proteasome Inhibitors (PI) holds potential for enhancing the survival prospects of individuals bearing this translocation [89–95]. Moreover, the t(14;16) (q32.3;q23) translocation, occurring in 5%-10% of MM cases, initially considered a poor prognostic factor, leads to over-expression of c-MAF, up-regulating CCND2 and APOBEC3A/B, resulting in a high mutation rate with an APOBEC signature [96–98]. Additionaly, a rare (2%) translocation event t(6;14) (p21;q32) in MM, carries a neutral

prognosis. It involves the repositioning of CCND3, directly leading to the up-regulation of CCND3 expression [99]. Lastly, the t(14;20) (q32;q12) translocation, the rarest among major translocations (1% of MM cases), is generally associated with a adverse outcomes. It leads to MAFB gene upregulation and, in some cases, mutant MAFB, contributing to CCND2 deregulation and the development of the APOBEC mutational signature. Its clinical implications remain enigmatic [98, 100–102] (Table 2.1).

2.1.3.2 Secondary Cytogenetic Abnormalities

Secondary cytogenetic abnormalities, referred to as secondary events, become apparent during the progression of MM. These events include the gain of 1q, deletion of 1p, deletion of 17p, deletion of 13q, secondary translocations involving MYC, and various other genetic alterations such as LOH, CNV, acquired mutations, and epigenetic modifications [57, 86]. One of the secondary translocations in MM often associated with proto-oncogene, c-MYC. These translocations, including t(8;14) the most common at 14q32.3, lead to c-MYC over-expression and are associated with a poor outcomes [98, 103]. Similarly, gain of the 1q arm, occurring in 30% - 40% of MM cases, is linked to poor prognosis and involves amplification of specific regions on 1q, including candidate oncogenes such as CKS1B, ANP32E, and BCL9 [57, 86, 104, 105]. Moreover, loss of 1p, observed in 30% of MM cases, involves deletion of specific regions on 1p and affects genes like FAM46C and CDKN2C [106–108]. Likewise, loss of 13q, present in 45%-50% of MM cases, causes absence of crucial tumor suppressor (RB1), DNA replication regulatory enzyme (RNASEH2B), and various miRNAs, often co-occurs with t(4;14) and is linked with poor prognosis [86, 109, 110]. However, deletion of 17p, affecting the entire p arm of chromosome 17 and leading to TP53 dysfunction, is linked to aggressive MM and extramedullary involvement [86, 111–113].

Additionally, miscellaneous chromosomal gains and losses impact various genes involved in MM progression. Gain of 8q24.2 and 11q13.2 upregulates MYC and CCND1, respectively, in a subset of MM patients [57]. Deletion events affecting genes like BIRC2, BIRC3, TRAF3, CYLD, and WWOX have been observed in

different MM cases, contributing to adverse prognosis [109]. Deletion of 8p leads to downregulation of apoptosis associated gene TRAIL, promoting immune evasion of tumor cells, enabling them to evade cytotoxic T lymphocytes and natural killer cells [114]. These secondary cytogenetic alterations add complexity to MM pathogenesis and may guide future therapeutic strategies [Table 2.1].

TABLE 2.1: Cytogenetic Abnormalities, Prognosis and Median Overall Survival (OS) in MM [81]

Subtypes	**Gene(s)/chromosomes affected**	**Approximate % of myeloma patients**	**Prognosis & Survival**
Primary Cytogenetic Abnormalities			
Hyperdiploid (HRD)	Recurrent trisomies involving odd-numbered chromosomes with the exception of chromosomes 1, 13, and 21	45	Good prognosis, standard-risk MM, median OS 7-10 years. Most have myeloma bone disease at diagnosis. Excellent response to lenalidomide-based therapy
non-HRD (NHRD) MM		40	
t(11;14) (q13;q32)	*CCND1* (cyclin D1)	20	Good prognosis, standard-risk MM, median OS 7-10 years
t(6;14) (p21;q32)	*CCND3* (cyclin D3)	5	Good prognosis, standard-risk MM, median OS 7-10 years
t(4;14) (p16;q32)	*NSD2*	10	Intermediate-risk MM, median OS 5 years Needs bortezomib-based initial therapy, early ASCT (if eligible), followed by bortezomib-based consolidation/maintenance
t(14;16) (q32;q23)	*C-MAF*	4	High-risk MM, median OS 3 years. Associated with high levels of FLC and 25% present with acute renal failure as initial MDE
t(14;20) (q32;q11)	*MAFB*	<1	High-risk MM, median OS 3 years
Secondary Cytogenetic Abnormalities			

Subtypes	**Gene(s)/chromosomes affected**	**Approximate % of myeloma patients**	**Prognosis & Survival**
Secondary Translocation Affecting MYC	*c-MYC*	15	High risk, poor prognosis, OS almost 2 years
Gain of the 1q	*CKS1B, ANP32E, BCL9, PDZK1, ADAR1, PSMD4, ILF2, IL6R,* and *MCL1*	45	Intermediate-risk MM, median OS 5 years
Loss of 1p	*FAM46C, FAF, CDKN2C DC14A, MTF2*	30	High-risk, Poor prognosis OS 4 years
Loss of 13q	*RB1, RCBTB2, RNASEH2B, EBPL*	45	low-risk, Good prognosis
Loss of 17p	*TP53*	10	High-risk MM, median OS 3 years

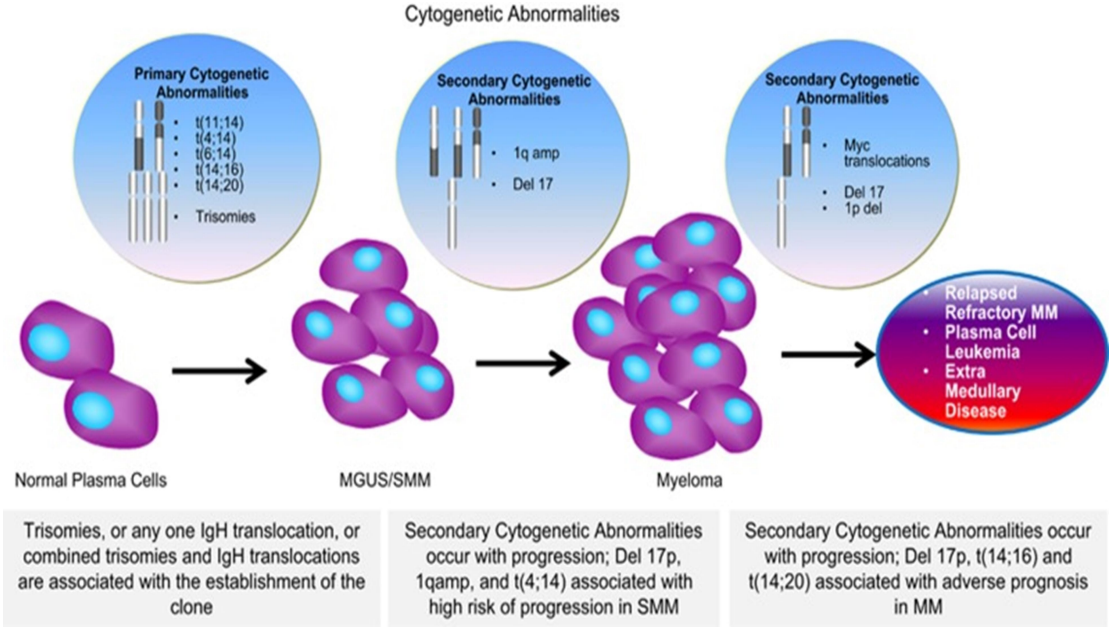

FIGURE 2.1: Cytogenetic abnormalities in the inception and maturation of MM [81].

2.1.4 Genetic Heterogeneity in Multiple Myeloma

Genetic irregularities are central in initiating and progressing MM [81]. These encompass several manifestations that impact the entirety of the genome, resulting in two distinct categories of anomalies: those of significant magnitude, referred to as large-scale aberrations, and those of a more subtle kind, known as small-scale aberrations [81].

Large-scale genetic aberrations, encompassing inversions, translocations insertions, and deletions are observable in cancer cells throughout different phases of their cell cycle. Techniques like Giemsa banding and karyotyping are used to visualize these aberrations during the metaphase of mitosis whereas, molecular cytogenetic methods like FISH, can identify such aberrations even in interphase cells [115–117].

Similarly, small-scale genetic aberrations comprise indels, CNVs, LOH, and substitution mutations. CNVs encompass alterations in DNA, leading to either the gain or loss of genetic material. These variations encompass focal deletions and amplifications, changes in chromosomal arms, and HRD. CNVs are pivotal in promoting genomic instability, either by triggering the excessive expression of cancer promoting genes or the depletion of cnacer suppressor genes. As a result, CNVs play a substantial role in driving the onset and advancement of MM [57, 81, 109]. Detecting these small-scale aberrations is possible through NGS techniques, including Whole-Genome Sequencing (WGS).

2.1.5 Epigenetic Modification

The epigenetic changes implicated in MM can be categorized into three main groups: i) modification of gene expression through transcription factors, ii) dysregulation of miRNAs, and iii) DNA methylation. SIRT6, RECQ1, and HOXA9 regulate transcription factors in MM cells. SIRT6 is associated with an unfavorable prognosis and interacts with ELK1 and ERK signaling genes. RECQ1 preserves chromosome integrity, and MM cells show elevated RECQ1 expression. HOXA9,

a transcription factor, regulates cell differentiation and gene expression. Disrupting HOXA9 gene expression in MM cells reduces competitive advantage compared to normal expression [81, 107]. Similarly, miRNAs can negatively regulate genes and pathways associated with MM development, with dysregulation of miRNA molecules revealing potential therapeutic targets [118, 119]. Lastly, DNA methylation is crucial in gene expression regulation and contributes to the progression of MM from pre-cancerous stages [120].

2.1.6 Clonal Heterogeneity

The presence of intra-clonal heterogeneity is a prevalent characteristic in MM, which aligns with the principles of clonal evolution as described by Darwinian Theory. The process commences at a premalignant phase and proceeds through either linear or branched evolutionary trajectories. The aspects of clonal stability and the presence of similar clonal and sub-clonal heterogeneity both before and after therapy are other noteworthy considerations. The examination of intra-clonal heterogeneity is of paramount importance in comprehending the etiology of diseases, as it has the potential to uncover the mechanisms that contribute to relapse and the emergence of drug resistance in the context of cancer treatments [57, 86].

2.1.7 Bone Marrow Microenvironment

The BM microenvironment is pivotal in mediating the interaction between cancerous PCs and non-malignant stromal cells. This interaction encompasses adhesion molecules and the exchange of signaling molecules through autocrine and paracrine pathways. Stromal cells release a variety of cytokines, such as FGFs, IL-6, MIP-1a, VEGF, RANKL, IL-1b, IL-10, IGFs, TGF-b, MMP-1, and TNF-a [121]. These cytokines influence B cell differentiation, proliferation, and apoptosis inhibition in MM. Factors secreted by BM can influence chemo and radiation therapy efficacy and disease progression [122].

2.1.8 Cellular Pathways

Numerous signaling pathways in MM exhibit dysregulation, impacting processes such as proliferation, apoptosis, survival, migration, and drug resistance, thereby contributing to the disease's pathogenesis. NF-κB signaling pathway was found active in 50% of MM cases. NF-κB, a transcription factor, promotes cellular proliferation, maturation, survival, inflammation, and immunity activates cancer promoting genes and inactivates cancer suppressor gene in pathway [123–125]. The pathway's involvement indicates the significance of PI in the treatment of MM [125].

Cellular growth pathways in MM encompass the MAPK, JAK-STAT, and the PI3K pathway. Inflammatory cytokines activates MAPK pathway and regulates gene expression [126]. Two dominant oncogenes, NRAS and KRAS, have mutations that contribute to advancement of disease [98].

Mutations in RAS are associated with adverse outcomes, while BRAF-MAPK mutations suggest potential therapeutic inhibitors for MM patients [86, 127]. The JAK-STAT path- way is activated in 50% of myeloma cases, triggered by cytokine IL-6 [86, 128]. Over-activation of STAT3 leads to chemoresistance by overexpressing of Bcl-x (an anti-apoptotic protein) [129]. In vitro inhibition with atiprimod, curcumin, and AG490 has shown fair results in inhibiting MM survival and sensitizing U266 cells to apoptosis [130, 131].

Signal transduction through PI3K-Akt pathway facilitates cellular development and viability in reaction to external stimuli [132]. The activation of PI3K occurs through the interaction of IL-6 and IGF-1, resulting in the phosphorylation of AKT. This phosphorylation event is significant in regulation of cell proliferation and the development of resistance to apoptosis. Notably, this molecular pathway has been found to be implicated in around 50% of MM cases [133]. The investigation of therapeutic strategies aimed at targeting PI3K has emerged as a prominent focus in MM research [86].

2.1.9 Cell Cycle Deregulation

Cyclin D gene overexpression and negative G1/S cell cycle regulatory genes are key factors in early molecular abnormalities in MM [86]. CDKN2C downregulation deregulates the G1/S transition [108]. p15, p16, and p18 inhibitors are crucial for cell cycle regulation. p21 inhibits CDK2, CDK1, and CDK4/6 complexes, protecting cells from apoptosis [134]. RB1 inactivation also affects the G1/S transition [109].

2.1.10 Defective DNA Repair

The DNA repair score in MM is a predictor of Progression Free Survival [PFS] [135]. Comprehending DNA repair mechanisms is essential for devising effective therapeutic strategies. One such strategy is synthetic lethality, where the simultaneous dysfunction of two genes leads to cell death. This approach has been applied to treat MM patients with impaired functioning of BRCA1 and BRCA2. Moreover, PARP inhibitors have shown promise in carcinomas with flawed homologous recombination mediated repairing of DNA [135]. Additionally, a noncoding RNA known as MALAT1 plays a crucial role in the binding of LIG3 and PARP1, suggesting its potential as an innovative therapeutic target [136–138].

2.1.11 Post-Transcriptional RNA Processing

The significance of post-transcriptional RNA processing in maintaining the genomic integrity in MM cannot be overstated, as alterations in genes responsible for mRNA processing and translation of proteins can play a role in the development of cancer [139]. Patients with a genetic predisposition to aggressive myeloma frequently have an elevated expression of RBP-ILF2, a crucial regulator involved in the repair of DNA double-strand breaks by homologous recombination. The inhibition of the ILF2 signalling system has the potential to enhance the efficacy of DNA-damaging drugs in the treatment of MM [140, 141].

2.2 Diagnosis of Multiple Myeloma

The latest diagnostic guidelines defined by the International Myeloma Working Group (IMWG) for MM are outlined as follows: It is necessary to have least one Myeloma Defining Event (MDE) to diagnose MM in conjugation with presences 10% or more clonal PCs or plasmacytoma confirmed through BM examination or biopsy respectively [58]. MDE encompasses the well-recognized features including elevated calcium levels, kidney dysfunction, reduced RBC count, or bone damage (lytic lesions), along with three specific biomarkers: PCs≥60% in BM , FLC ratio ≥100 mg/L in serum , and multiple focal lesions on MRI [58].

M proteins can be identified using different diagnostic methods such as serum protein electrophoresis, serum immunofixation, and serum FLC assay. The prevalence of true non-secretory illness in individuals with MM is estimated to be 2%, and the utilization of the serum FLC assay proves to be beneficial in such cases [61, 142, 143]. The quantification of M protein concentration is achievable when it reaches a level of 1 gram per deciliter (g/dL) in serum or 200 milligrams per day (mg/day) in urine. The assessment of therapy response is conducted on a monthly basis, whilst the monitoring of probable renal complications is performed using urine protein electrophoresis [144].

Similarly as part of the initial diagnostic evaluation, BM examinations should encompass karyotyping and FISH to identify specific chromosomal translocations, trisomies, hypodiploidy, deletions and gains [145]. GEP can offer supplementary prognostic insights by providing Carboxy-Terminal Collagen Crosslinks (CTX) through Serum Cross Laps that may serve as a valuable tool in evaluating bone turnover and ascertaining the effectiveness of bisphosphonate treatment [146, 147].

The most effective method to evaluate the extent of bone involvement is low-dose whole-body CT or PET/CT scans [63, 148]. MRI scans serve a crucial role in ruling out focal BM lesions which may manifest before true osteolytic disease develops if performed at SMM stage. It is also valuable for assessment of EMD, impingement of spinal cord, or in depth imaging of a particular indicative region is necessary [63, 148].

2.3 Prognosis and Risk Stratification

The survival predictions for patients with MM exhibit variability depending on the source of data. Within the framework of controlled randomized trials, it has been noted that the median survival duration spans roughly 6 years [149]. However, when considering patients eligible for ASCT, it has been found that their 4-year survival rates surpass 80% [150]. Furthermore, the median OS for this specific cohort exceeds 8 years. Furthermore, the median OS for this specific cohort exceeds 8 years [151, 152].

The median OS of elderly patients is shown to be 5 years [99]. The current survival probabilities may be underestimated as a result of the presence of pre-existing monoclonal antibodies and the introduction of new therapeutic medicines. Nevertheless, these benchmarks hold significant value and can be used to NDMM patients who possess a strong performance status, thereby making them generalizable.

Prognosis in MM is determined by host characteristics, tumor burden, genetic irregularities, and treatment outcomes [88, 96]. The assessment of tumor load is conducted through the utilization of the Durie-Salmon Staging (DSS) and the International Staging System (ISS) [153–155].

The disease biological characteristics are most accurately represented by factors such as molecular subtype, cytogenetic anomalies, and indicators of disease aggressiveness, including LDH increased levels in serum and circulating PCs. The Revised International Staging System (RISS) is a comprehensive prognostic indicator that incorporates tumor density, high-hazard genetic anomalies and higher levels of LDH (Table 2.2).

It facilitates the process of clinical decision-making and enables the comparison of data. Nevertheless, current therapy encounters certain restrictions, particularly in cases where patients with high-risk classes may come into contact with others who have standard risk disease. The Mayo Clinic mSMART risk assessment provides more information regarding therapy approaches (Table 2.3)[151].

TABLE 2.2: Revised International Staging System for Myeloma[151]

Stage	
Stage 1	
All of the following:	
	Serum albumin ≥3.5 gm/dL
	Serum beta-2-microglobulin <3.5 mg/L
	No high risk cytogenetics
	Normal serum lactate dehydrogenase level
Stage II	
	Not fitting Stage I or III
Stage III	
Both of the following:	
	Serum beta-2-microglobulin >5.5 mg/L
	High risk cytogenetics [t(4;14), t(14;16), or del(17p)] or
	Elevated serum lactate dehydrogenase level

TABLE 2.3: Mayo Clinic Risk Stratification for Multiple Myeloma (mSMART) [151]

Risk Group	**Percentage of newly diagnosed patients with the abnormality**
Standard Risk	60%
Trisomies	
t(11;14)	
t(6;14)	
High Risk	40%
t(4;14)	
t(14:16)	
t(14;20)	
del(17p)	
gain(1q)	
Double-Hit myeloma:	
Any 2 high risk factors	
Triple-Hit myeloma:	
Any 3 or more high risk factors	

2.4 Treatment for Multiple Myeloma

Symptomatic MM typically requires immediate medical attention. The survival rates of MM patients have demonstrated a substantial improvement during the last 15 years. The most favorable treatment outcomes appear to result from the use of a combination of various drugs, including steroids (such as dexamethasone and prednisone), antibiotics (like doxorubicin), alkylating agents (such as cyclophosphamide and melphalan), Immunomodulatory Drugs (IMiDs) such as thalidomide, lenalidomide, and pomalidomide, PI including bortezomib, carfilzomib, and ixazomib, as well as monoclonal antibodies targeting CD38 (such as Daratumumab and Isatuximab) and Signaling Lymphocytic Activation Molecule F7 (SLAMF7) antigens (including Elotuzumab), along with panobinostat, Selinexor, Belantamab Mafodotin, and Chimeric Antigen Receptor T (CAR-T) cell therapies. [156–160].

The medications employed for MM treatment operate through various mechanisms, some of which are not entirely elucidated. Thalidomide, lenalidomide (R), and Pomalidomide (Pd) are classified as IMiDs agents, and they interact with cereblon, leading to the activation of cereblon E3 ligase activity. Consequently, this triggers the swift ubiquitination and subsequent degradation of two specific B cell transcription factors, IKZF1 and IKZF3. IMiDs can potentially induce cytotoxic effects through the generation of DNA damage mediated by free radicals. Additionally, they possess anti-angiogenic, immunomodulatory, and properties that inhibit tumor necrosis factor alpha. Bortezomib, carfilzomib, and ixazomib fall into the category of PI. Elotuzumab is focused on SLAMF7, while CD38 is precisely target of daratumumab and isatuximab. Humanized antibody (Belantamab mafodotin) was developed to bind B cell maturation antigen. Recently authorized CAR-T therapies directed against BCMA including Idecabtagene vicleuceland and ciltacabtagene autoleucel exhibited efficacy in cases of RRMM [156–160].

2.4.1 Hematopoietic Stem Cell Transplantation

The transplantation of autologues stem cells has been found to considerably increase the median OS in patients with MM by a duration of 12 months. However,

there is ongoing dispute regarding the ideal timing for ASCT, as early transplantation has demonstrated comparable outcomes to delayed transplantation, which is often reserved for cases of recurrence [161–163]. Tandem ASCT might be considered for selected high-risk patients not achieving complete response after the initial transplant but is not recommended as standard practice outside of clinical trial settings [164–168].

Post-transplant consolidation therapy, involving additional VRd chemotherapy cycles after ASCT followed by lenalidomide maintenance, did not result in significant improvements in PFS or OS instead patients were recommended to proceed with regular maintenance regimen [168].

2.4.2 Treatment of Newly Diagnosed Multiple Myeloma Eligible for Autologus Stem Cell Transplant

The treatment of NDMM is dependent on eligibility for ASCT and risk classification. ASCT is the established treatment approach for patients under 65 years of age or those aged 65–70 with minor comorbidities. Before undergoing the transplant procedure, patients usually undergo 3–6 cycles of induction therapy, aiming to achieve a complete or nearly complete response. Bortezomib, lenalidomide, and dexamethasone (VRd) is the preferred first-line therapy, with daratumumab, lenalidomide, and dexamethasone (DRd) as an option [149, 169]. For individuals ineligible for transplantation, DRd presents a viable alternative to VRd [133]. In situations where lenalidomide is inaccessible or in cases of acute kidney failure, bortezomib-based regimens with relpacemt of lenadomide with thalidomide (VTd) or like cyclophosphamide (VCd)can serve as suitable substitutes for VRd [170]. Peripheral neuropathy associated with bortezomib therapy mitigate by weekly subcutaneous administration once [171, 172]. However, the combination of carfilzomib, lenalidomide, and dexamethasone is currently being investigated with a focus on potential concerns related to toxicity [173, 174]. Quadruplet regimens usually recommended for high risk MM incuding daratumumab with (VTd) or VRd show promise, but further data are required to establish their superiority

over VRd in terms of OS [175, 176]. Multi-drug combinations are valuable for aggressive cases such as PCL or multiple extramedullary plasmacytomas Currently, quadruplets are recommended for high-risk double or triple-hit myeloma patients [94, 177, 178].

2.4.3 Treatment of Newly Diagnosed Multiple Myeloma Ineligible for Autologus Stem Cell Transplant

VRd and DRd is also a viable option for patients ineligible for ASCT because of age or concurrent medical conditions. While treatments including melphalan are not advisable due to concerns regarding harm to stem cell and the possible emergence of secondary cancers. Therapies incorporating bortezomib have demonstrated improved survival outcomes and are a best available option for initial therapy in patients ineligible for ASCT [134, 149]. DRd has shown superior PFS of 30 months in comparison to Rd, with higher minimal residual disease (MRD) negative rates (24.2% vs. 7.3%, P<0.001) [169]. Alkylator-based regimens, particularly those using melphalan, are only considered when there are difficulties accessing lenalidomide. In that case, melphalan can be substituted by cyclophosphamide to avoid associated the risks with melphalan [121, 179].

2.4.4 Treatment of Refractory or Relapse Multiple Myeloma

The majority of MM patients will experience relapse at some point, and with each subsequent treatment regimen, the duration of remission tends to decrease [180]. Selecting an appropriate regimen upon relapse is an intricate decision effected by several features, such as the timing of relapse, the patient's response to prior therapy, the severity of the relapse, and their current performance status. Patients eligible for ASCT should be evaluated for the procedure if they have not previously undergone it or experienced a prolonged remission of minimum 3 years or more along with maintenance therapy. Triplet drug regimen that includes minimum two

new drugs to which the patient is not resistant is advisable when it comes to drug therapy [181].

Resistance of lenalidomide and bortezomib in RRMM patients is associated with poor outcomes (median PFS = 5 months and OS = 9 months) [182]. For patients categorized as lenalidomide-refractory, a possible course of action is to contemplate treatment regimens centered around pomalidomide. Bortezomib-based treatment protocols are deemed appropriate for patients who have discontinued therapy subsequent to obtaining a bortezomib-based triplet regime. The bortezomib-based regimens are deemed appropriate and are associated with reduced expenses and risks [183, 184].

Daratumumab has demonstrated efficacy in the treatment of RRMM. It is specifically authorized for individuals who have undergone a minimum of three prior treatment regimens, including both PI and IMiDs drugs. Considering the available evidence, treatment regimen including daratumumab seems to offer the most substantial reduction in disease progression, making them a preferable choice for initial relapse treatment, considering factors like availability and cost [185–187].

Carfilzomib (K), a newly developed keto-epoxide tetrapeptide proteasome inhibitor, received its initial approval in 2013 for the therapeutic management of RRMM. Previous treatment with lenalidomide and bortezomib is considered essential prior giving approval for utilizing carfilzomib [188]. The efficacy of the calfilzomib in combination of Rd has been demonstrated in a randomized study, establishing it as a prominent therapeutic choice for the management of recurrent illness. Carfilzomib-based treatment regimens provide significant alternatives for patients refractory to bortezomib [189, 190]. Carfilzomib exhibits a reduced propensity for neurotoxicity in comparison to bortezomib, however, it is important to note that a minority of individuals (5%) may encounter significant cardiac adverse effects.

Pomalidomide is a pharmaceutical compound that shares structural similarities with lenalidomide and thalidomide. It was first granted approval in 2013 for the therapeutic management of RRMM and notably effective for lenalidomide refractory patients [191, 192]. Pomalidomide including triplet regimens either with

daratumumab and dexamethasone or carfilzomib and dexamethasone, is crucial for patients experiencing recurrence. Similarly, the doublet regimen of pomalidomide with dexamethasone is a consideredable option for patients who are weak or experiencing indolent recurrence [191, 192].

The combination of Elotuzumab, that specifically targets the SLAMF7, has demonstrated synergistic effects when used in conjunction with Rd. The drug has demonstrated a high level of tolerability and got first approval in 2015 for its application in treating RRMM patients with one to three previous therapeutic interventions [193]. Nevertheless, it has been observed that the efficacy of elotuzumab is potentially higher when used in conjunction with pomalidomide as opposed to lenalidomide [193].

Ixazomib is an orally administered PI that has demonstrated efficacy in the treatment of both NDMM and RRMM [194]. The medication possesses the benefit of being administered on a weekly basis and was recommended by FDA for those diagnosed with MM and undergone at least one prior treatment. In comparison to bortezomib, it exhibits a higher incidence of gastrointestinal adverse effects, while demonstrating a reduced likelihood of neurotoxicity [194, 195].

Selinexor functions by inhibiting the activity of Exportin 1 (XPO1), resulting in the buildup and activation of many tumor suppressor proteins, while also impeding the nuclear factor kappaB. The FDA has approved selinexor for individuals diagnosed with RRMM and undergone a minimum of four previous therapies [196]. Most common adverse effects encompass thrombocytopenia, tiredness, nausea, and anorexia [197].

Istutuximab, targets CD38, has demonstrated potential in the treatment of RRMM. Isatuximab, pomalidomide, and dexamethasone (Isa-Pd) in a randomised trial resulted in better PFS when compared to the use of pomalidomide and dexamethasone alone in RRMM patients. The FDA has granted approval to isatuximab for the management of RRMM in individuals who had undergone a minimum of two prior treatment regimens, which encompassed the use of lenalidomide and PI. In the context of myeloma treatment, it may be argued that isatuximab presents

a viable option to daratumumab. The selection between these two monoclonal antibodies may depend on factors such as the cost incurred by the patient, the accessibility of treatment, and scheduling considerations [198].

Both Doxorubicin and Liposomal Doxorubicin exhibit limited efficacy as standalone treatments for MM. Findings from a phase III randomized trial showed a notable increase in the median Time To Progression (TTP) when bortezomib was paired with pegylated liposomal doxorubicin compared to the use of bortezomib alone. Doxorubicin-based therapy protocols, have demonstrated potential efficacy in managing aggressive MM cases that have shown resistance to conventional myeloma therapies. Venetoclax, although not currently licensed for the treatment of MM, is readily accessible on the market. It has demonstrated efficacy as a standalone treatment primarily in patients with the t(11;14). The findings of a randomized trial revealed a notable increase in mortality rates linked with the administration of venetoclax in RRMM patient, Hence, it is most appropriate to regard venetoclax as an exploratory treatment, and its administration should be limited to individuals with t(11;14) who have experienced disease relapse and possess few therapeutic alternatives [199, 200].

CAR-T cell treatment is highly promising and innovative immunotherapeutic approach for RRMM patients. Both idecabtagene vicleucel and ciltacabtagene autoleucel have demonstrated substantial clinical efficacy in phase 2 trials. FDA recommended CAR-T cell therapies for the management of patients showing refractriness from at least four or more previous treatment protocols [201]. Belantamab mafodotin is proposed as a potential therapeutic agent. Among RRMM patients who had seen unsuccessful outcomes with three or more lines of therapy, it was shown that approximately 33% of these individuals exhibited a positive response to subsequent therapeutic interventions. Keratopathy was shown to be the prevailing grade 3-4 toxicity, affecting roughly 25% of the patient population [202].

2.5 Relapse in Multiple Myeloma

The recurrence of MM is impacted by genetic alterations, the microenvironment of the BM, and the immune system of the individual. The development of genetic mutations inside genes, the deliberate targeting of gene mutations and the upregulation of drug transporters have been identified as factors contributing to cellular resistance against therapeutic interventions. Epigenetic modifications have the potential to induce resistance to pharmaceutical interventions. The BM microenvironment plays a crucial role in providing essential nutrients, growth.

Reduce efficacy of a therapeutic agent e.g. antimicrobial or antineoplastic to combat a disease is considered as drug resistance [203]. The term is widely used to refer to the resistance that a pathogen or various malignancies developed during treatment. Presently antimicrobial and antineoplastic drug resistance is a big challenge facing by clinical caregivers and researchers. The major reason for the inexorable failure of chemotherapy or targeted therapy to treat cancer is the drug resistance that restricts the effectiveness of therapy and reduces the survival rate [204].

Corticosteroids triggers following resistance mechanism in MM cells causing relapse, dysfunctional glucocorticoid receptor, heightened secretion of pro-survival cytokines within the BM microenvironment, elevated expression of the oncogenes FGFR3 and MYC, and epigenetic silencing of RASD1. Whereas overexpression of P-gp (reduced drug influx), ABCG2 (drug absorption), RECQ1 (DNA repair) and Bcl-xL (anti- apoptotic) have been observed following use of alkylating drugs. Likewise resistance due to PI has been observed in variety of ways e.g. Up-regulation of the proteasomal system, modification and loss of 8p21, XBP1 suppression and increased expression of the MARCKS (cell cycle regulation), ABCB1 (drug influx), CXCR4 (receptor synthesis); TXN, TXNDC5 (protection from oxidative stress) and MAF (proto-oncogene). Irregularities in cell growth, proliferation, and faulty B-cell differentiation has been observed due to reduced expression of CRBN and IRF4 following use of immunomodulatory drugs. Moreover Monoclonal antibodies showed their resistance mechanism in MM cell

by enhancing complement system (CD55), inhibiting apoptosis (CD59) and malignant B-cell growth and survival. Combination therapy targets specific genes or pathways, while targeted therapy boosts the immune system. Combination therapy, targeted therapy, and immunotherapy are effective methods to prevent drug resistance hence relapse in MM [204].

2.6 Significance of Biomarkers in Cancers

Cancer, which is often referred to as a "tumor," fundamentally arises from genetic changes at the cellular level, and these alterations within tumors can be quantified [205]. Biomarkers, serving as indicators of these genetic modifications, can be broadly grouped into three categories: DNA biomarkers, DNA tumor biomarkers, and general biomarkers [206]. DNA plays a pivotal role in encoding the instructions for creating essential proteins required for cellular structure and function, necessitating the preservation of genetic information within it [207]. DNA biomarkers encompass variations at the DNA sequence level, including insertions, deletions, SNPs, and short tandem repeats [208–210]. Among these, SNPs are the most commonly utilized type of DNA alterations, typically exhibiting three possible genotypes in various applications [211].

In contrast, DNA tumor biomarkers are unique to a specific cancerous tumor and hold substantial potential for enhancing cancer treatment outcomes and reducing cancer-related fatalities when properly employed for early cancer detection, selection of treatment strategies, or identification of patient subgroups responsive to a particular therapy [212, 213]. Additionally, DNA tumor biomarkers can be employed for prognostic purposes, predicting a patient's overall outcome [70]. Conversely, general biomarkers tend to be less specific to a particular cancer type and consequently find limited utility in prognosis or prediction of treatment outcomes [206]. Prognostic biomarkers aim to forecast the progression of a disease, while predictive biomarkers are intended to gauge a patient's response to treatment [214, 215]. Differentiating between predictive and prognostic biomarkers

with confidence necessitates data from randomized, controlled studies, as single-arm studies can yield misleading results [216, 217].

The process of developing new biomarkers involves a multifaceted journey that begins with their discovery and preliminary investigation in basic research studies. Subsequently, validation through clinical studies is undertaken to ascertain their potential to diagnose the disease, either retrospectively or prospectively. Finally, clinical implementation follows [218]. The ultimate objective of this entire process is to establish clinically reliable biomarkers that support decision-making and enhance patient outcomes [219]. Relying on biomarkers based on invalid or poorly-defined surrogate endpoints can result in a lack of predictive power. Despite being trained on archived specimens, only a limited number of prognostic gene-expression signatures have been validated in previous studies [220].

2.7 Gene Expression Profiles for Identification of Biomarkers in Cancers

GEP is a vital tool for understanding disease mechanisms and identifying novel biomarkers. It analyzes transcriptomic changes in diseases, revealing altered pathways and potential therapeutic targets. GEP can identify cancer and resistance biomarkers, aiding in the identification of diagnostic, prognostic, and predictive biomarkers for various diseases. It also assist in understanding disease mechanisms, aiding to devising new drugs and treatments.

Genomic profiles exclusively ascertain mutational occurrences relevant to treatment, although they do not comprehensively encompass the intricacies of the disease. The integration of transcriptional profiling is a promising approach to overcome the restriction in Non-Small Cell Lung Cancer (NSCLC) management. This technique holds potential for patient stratification and therapy recommendations, particularly in instances of acquired resistance to targeted therapies or the absence of targetable genetic changes.

Prognostic biomarkers play a crucial role in monitoring anti-cancer therapy, assessing cancer grade, and detecting resistance and relapse in individual patients [221, 222]. Prognostic biomarkers, their clinical utility, and significance for breast, colorectal, prostate and NSCL cancers identified through utilization of HTS data has been assembled in Table 2.4.

Genetic mutations in certain genes, such as BRCA1, BRCA2, TP53, and ATM, increase the risk of breast cancer, some of which can be inherited [106]. For instance, mutations in the BRCA2 gene can impair its protein synthesis and disrupt the DNA repair system, hence regular screening and examinations is necessary for assessment of risk for incidence of breast cancer to individuals [223]. Likewise, alterations in the genetic makeup of glutathione S-transferase genes (GSTP1 and GSTM1) and the presence of G158A polymorphism in the prostate-specific antigen gene may increase the susceptibility to prostate cancer [224]. Similarly, adenomatous polyposis due to constitutive genetic mutations in the Adenomatous Polyposis Coli (APC) gene are linked to, a hereditary condition that raises the risk of developing intestinal polyps and Colorectal Cancer (CRC) [225].

GWAS and pharmacogenetic biomarkers enable the efficient identification of genetic mutations in intricate genetic conditions [208]. Expression analysis, as demonstrated by MammaPrint Symphony, employs a 70-gene panel to dynamically evaluate the progression of neoplastic processes and classify breast cancer patients as either high or low risk for relapse. This assists oncologists in making informed decisions regarding suitable chemotherapy and hormonal therapy [198, 226, 227].Similarly, as illustrated by Nguyen et al that variations in the gene expression levels of specific genes among breast cancer patients prior to treatment can serve as predictive indicators for treatment outcomes [123]. Furthermore, Circulating Tumor Cells (CTCs) present in the bloodstream have been identified as a prognostic indicator, exhibiting a significant correlation with the occurrence of metastasis and the development of secondary tumors. This association implies an unfavorable prognosis, even in cases when only a small number of CTCs are detected, such as one cell per 10 milliliters of blood [129, 130, 228].

TABLE 2.4: The clinical utility and importance of prognostic biomarkers in specific types of cancer [221]

Cancer	**Biomarker**	**Clinical Utility & Significance**	**Refs.**
Breast cancer	*PR*	PR-positive patients having higher survival rate than PR-negative patients	[171]
	ER	ER-positive patients having better survival than ER-negative patients	[172] [173]
	BRCA1	High BRCA1 expression indicating worse prognosis for untreated patients	[174]
	HER2	Patients with HER2-positive tumors having worse prognosis and more aggressive cancer than HER2-negative patients	[175]
	MammaPrint	A 70-gene assay used to stratify patients into groups with high or low risk for relapse	[74]
	Oncotype DX	A 21-gene multiplex assay used for determining recurrence score	[176]
Colorectal cancer	*CEA*	Elevated serum levels of CEA associated with poor prognosis in patients	[177] [178] [179]
	LOH at 18q	Associated with metastasis and poor prognosis in patients.	[180]
Prostate cancer	*BRCA2*	Patients carrying BRCA2 mutations having an increased cancer risk and poor prognosis	[181]
	CTCs	Increased CTCs in peripheral blood associated with poor prognosis	[182]
	PSCA	High PSCA expression correlated with higher stage, metastasis, and poor prognosis	[183]

Cancer	Biomarker	Clinical Utility & Significance	Refs.
	uPA	Elevated serum level and increased expression of uPA associated with occurrence of bone metastasis of prostate cancer	[184]
Non-small cell lung cancer	BRCA1	High BRCA1expression conferring worse prognosis in untreated patients	[185]
	TP53	High TP53 expression indicating poor prognosis in untreated cases	[186]
	KRAS	KRAS mutation associated with poor prognosis, worse OS, and shorter disease-free survival	[186] [187]
	RRM1	High RRM1 expression conferring better prognosis in untreated patients	[188]

Predictive biomarkers provides information about the response expected to a specific therapy and can aid in guiding treatment decisions [131, 132]. Few example of predictive biomarkers identifies through analysis of HTS data has been assembled in Table 2.5. One prominent example is the KRAS gene mutation, which can occur early in colorectal carcinogenesis. Mutations in 12 and 13 codons of the KRAS gene serve as predictive markers for the efficacy of targeted therapy, specifically in progressive colorectal cancer treated with monoclonal antibodies like cetuximab or panitumumab that target EGFR signaling pathways [175]. These therapies suppress cancer cell progression and increase apoptosis. Patients without KRAS mutations are considered positive predictive biomarkers for this therapy. However, it's important to note that patients with increased EGFR expression even in the absences of these mutations may not respond well, specifically in the presences of SNVs 61 or 146 codon of KRAS or SNVs in BRAF gene [175].

In addition to KRAS, ERCC1 is another predictive biomarker, particularly in hepatic and lung cancer. High ERCC1 expression is associated with cisplatin

resistance in HCC and NSCLC patients, suggesting its value in predicting therapy response [134]. Upregulation of mTOR and cerb-B2 genes may also associated with adverse hepatic carcinogenesis [134].

Furthermore, the detection of CTCs at different stages of treatment can serve as a valuable predictive tool. Molecular characterization of CTCs can help predict treatment response, as demonstrated by the decline in mammaglobin1 mRNA expression in CTCs from advanced breast cancer patients, providing insights into their response to anti-cancer treatment [135].

TABLE 2.5: The clinical utility and importance of predictive biomarkers in specific types of cancer [221]

Cancer	**Biomarker**	**Clinical Utility & Significance**	**Refs.**
Breast cancer	*PR*	High *PR* expression predicting beneficial response to tamoxifen therapy	[189]
	ER	High cellular *ER* expression predicting benefit from tamoxifen-based chemotherapy in node-negative patients	[114] [190]
	BRCA1	High *BRCA1* expression predicting response to chemotherapy	[191]
	HER2	Overexpression of *HER2* predicting response to treatment with trastuzumab as an adjuvant therapy or in the metastatic cases	[175] [192]
	Akt kinase isoform	Akt kinase isoforms and activity predicting response to trastuzumab-based therapy in HER2-positive metastatic cancer patients	[193]
Colorectal cancer	*LOH* at 18q	Predicting benefit from 5-FU based adjuvant chemotherapy	[180]
	EGFR1	*EGFR1* amplification predicting response to anti-EGFR1 antibody therapy	[194]
	KRAS	*KRAS* mutation negatively predicting benefit from EGFR-targeted therapy	[152] [195] [196]

Cancer	Biomarker	Clinical Utility & Significance	Refs.
Non-small cell lung cancer	*BRCA1*	High *BRCA1* expression predicting resistance to chemotherapy	[197]
	TP53	High TP53 expression predicting sensitivity to cisplatin; *TP53* mutations predicting resistance to cisplatin	[186] [198]
	KRAS	*KRAS* mutation predicting lack of response to adjuvant chemotherapy in early disease and resistance to treatment with EGFR-targeted or TKI in advanced disease	[199]

2.8 Drug Repurposing

The process of drug discovery often spans a duration of 10 to 15 years. The majority of the compounds that have been subjected to testing are unable to proceed to the advanced phases, as stated by DiMasi, *et al.* [229]. Since 1995, a mere 10 percent of compounds subjected to phase 1 investigation have successfully advanced to the clinical phase. Hence, computational techniques such as molecular docking are being increasingly employed across the entire drug development process to facilitate the identification and elimination of potential targets. However, despite the assistance of computer technology, the process of drug discovery remains time consuming.

Drug repurposing is considered as one of the ways that might be employed to expedite this process. Drug repurposing, sometimes referred to as drug repositioning or reprofiling, is a method employed to identify novel applications for pre-existing medications that extend beyond their initial medical indications [230]. Bypassing a significant portion of the pipeline, this methodology guarantees a rapid time to market, an established supply chain, reduced expenses, and, in certain instances, substantial quantities of clinical data. The inclusion of clinical data holds significant value due to its potential to streamline the progression of pre-clinical and clinical testing phases. Moreover, it has been shown that a significant proportion of drug lead failures, namely 45%, can be attributed to toxicity and safety concerns

[230]. Consequently, adopting this technique will likely enhance the likelihood of achieving favorable outcomes.
Drug repurposing has been effectively employed in numerous locations, resulting in favorable outcomes. For instance, the pharmaceutical company Pfizer repurposed and marketed the drug Viagra, which was initially created as an anti hypertensive medication, for the treatment of erectile dysfunction [231]. Another illustration involves the repurposing of the cancer treatment Zidovudine for use as an anti-HIV medication. Thalidomide, was initially formulated and utilized as a sedative during the 1950s, represents another prominent illustration. However, subsequent research led to its repurposing as a treatment for leprosy and MM [232].

Nevertheless, medication repurposing also presents its own set of obstacles. Pharmaceutical agents are often authorized for use in specific medical conditions and prescribed at specific dosages. When a medicine undergoes repurposing, it necessitates the repetition of clinical trials and the determination of suitable dosage regimens. Another concern that arises pertains to the delivery methods. The utilization of a modified molecule with a specific tissue targeting capability may necessitate the implementation of an alternative targeting mechanism, hence including certain stages within the overall process. Furthermore, it is imperative to investigate the potential interactions between a repurposed drug and other medications employed for the new indication [233]. Despite the various hurdles involved, the effective repurposing of a medicine would expedite its development and ultimately lead to the preservation of human lives.

Utilizing computational methodologies represents the most effective approach for augmenting potential avenues for drug repurposing. All three computational methods are suitable for implementing this strategy. Virtual screening is a computational approach employed to find pharmacological compounds that have been approved and has the ability to interact with a certain protein responsible for causing a particular disease. Alternatively, a targeted examination can be conducted wherein a particular medicinal molecule is assessed for potential interactions with the crystal structures contained inside various databases. The exploration of molecule libraries enables the identification of therapeutic targets that

possess enhanced drugability, improved efficacy, or increased affordability. By leveraging network analysis, it becomes possible to identify commonalities across diseases and biological processes. Consequently, medications that have demonstrated efficacy in one example can be explored for potential application in other related cases. Molecular docking is employed in a wide range of settings.

2.9 Research Gap

The continuously advancing landscape of MM treatment has provided significant benefits to patients dealing with recurrent disease. However, the abundance of available treatment options calls for a thorough examination of various factors that could impact patient results. Utilizing multiple drug combinations has generally led to enhancements in response rates and overall survival. However, this approach can sometimes result in elevated toxicity levels, highlighting the importance of diligent clinical oversight and a tailored approach based on the patient's individual characteristics. The swift progress of high-throughput techniques has facilitated the emergence of integrated omics technologies, encompassing comprehensive platforms such as genomics, transcriptomics, proteomics, epigenomics, and metabolomics analyses. These techniques facilitate the detection of mutations, gene profiles, microRNA, protein expression patterns, and epigenetic changes. These findings can yield prognostic and diagnostic biomarkers, opening up new possibilities for therapeutic targets. Ultimately, the integration of these novel treatments alongside established approaches in the initial treatment phase will bring us closer to achieving a cure.

2.10 Research Question

1. Which gene/ biomarkers are differentially expressed in gene expression profiles of refractory or relapse MM patients?
2. What are the functional implications of differentially expressed genes / biomarkers in refractory or relapse MM?

3. What are the existing drugs that can be repurposed for the treatment of refractory or relapse MM?

Chapter 3

Materials and Methods

Significant roles are played by the interconnected concepts of cancer relapse, drug resistance, and repurposing in the realm of cancer treatment and research. A common contributor to cancer recurrence is the development of drug resistance. A subset of cancer cells may sustain initial treatment with chemotherapy, targeted therapy, or other therapies, can repopulate and contribute to the recurrence of the disease. Drug resistance may arise as a result of genetic mutation, altered drug target expression, activation of alternative pathways, or other processes. The utilization of drug repurposing as a strategic approach holds significant value in the context of combating medication resistance and perhaps mitigating the occurrence or postponing the onset of cancer relapse. DGE help guided drug repurposing by identifying biomarkers and dysregulated pathways in disease conditions, constructing interaction networks, identifying potential drug targets. These insights can help identify drugs with similar impact on disease pathways, predict drug efficacy, and target specific subgroups for repurposed drugs.

DGE compares gene expression levels across conditions (e.g., disease versus relapse) to identify genes that are substantially upregulated or downregulated. Popular tools for this purpose include DESeq2, edgeR, and limma, which detect differential expression using statistical methods that account for biological variability

FIGURE 3.1: Flow chart of research methodology

and data distribution. Functional annotation tools like DAVID, GO (Gene Ontology) enrichment, and pathway analysis tools (KEGG, Reactome) help annotate DEGs with functional information and biological pathways.

Identifying appropriate target proteins is a fundamental step in drug discovery. The structure of a protein is intricately linked to its function. The precise arrangement of amino acids within a protein dictates its conformation, active sites, and binding sites. These structural characteristics determine the manner in which the protein interacts with other molecules, substrates, ligands, and inhibitors. Often, the effectiveness of a drug depends on its ability to bind to a specific target protein. The structure of the protein influences how well a drug molecule can fit into the active site of the protein, thereby inhibiting or modulating its activity. In addition, they predict drug interactions, thereby decreasing off-target effects and adverse reactions. Modern techniques such as X-ray crystallography, Nuclear Magnetic Resonance (NMR) spectroscopy, and computational modelling have significantly improved our ability to determine and analyze protein structures, resulting in more efficient and targeted drug discovery and design processes.

The computational tools available for 3D protein modelling can be categorized based on the method used to anticipate the structure. MODELLER is used for homology or comparative modelling, Rosetta is used for ab-initio modelling, PHYRE2 is used for threading, I-TASSER is used for integrated threading and ab-initio modelling, and AlphaFold and OmegaFold are used for machine learning and AI-based structure prediction. Structure-based virtual screening entails docking candidate ligands into the protein's binding site and evaluating their binding modes and energies. The goal is to anticipate which ligands will interact well with the protein, hence identifying prospective therapeutic candidates. AutoDock Vina is a popular and frequently used molecular docking software for virtual screening and ligand-receptor docking investigations. It is especially useful for predicting ligand interaction with the binding site of a target protein and rating these interactions based on their binding affinities.

The research approach employed in this study is structured into three distinct parts. Proteins with therapeutic promise for the management of relapse in MM

have been identified in the first stages using the gene expression profiles of patients. The second phase of the study aimed to utilize a range of computational approaches and tools in order to predict the 3D structures of candidate proteins and their variants. Drug repurposing against these candidate proteins was the focus of the third phase.

The computational analysis has been performed on experimental data collected from clinical studies on the relapse of MM in patients by the Multiple Myeloma Research Foundation. This analysis demonstrates the validity of the data. Recommendations for future research has been proposed to focus on the clinical translation of recommended biomarkers for the treatment and personalized medicine of RRMM.

3.1 Tools

3.1.1 Genomic Data Commons (GDC) and CoMMpass Data Set

GDC is a centralized portal established by the National Cancer Institute (NCI) to facilitate the sharing, access, and analysis of cancer genomic data (gdc.cancer.gov). It provides a user-friendly interface for researchers searching and extracting data from various cancer types, including studies on humans and mice. This information is a valuable resource to identify new cancer-causing genes, develop novel treatments, and devising cancer prevention strategies. Additionally, the GDC promotes collaboration between researchers, thereby accelerating the pace of research and identifying novel cancer treatment methods. Among many available cancer projects on GDC, CoMMpass is a Multiple Myeloma Research Foundation (MMRF)-led research initiative (portal.gdc.cancer.gov/projects). The objective of the project is to collect comprehensive genomic and clinical data from patients with MM in order to better understand the disease and enhance patient outcomes. Clinical information, treatment histories, and genetic profiles of MM patients were

collected as part of this study. Genetic profiling entails analyzing the DNA of tumor cells in order to identify specific genetic mutations that may be fueling the disease [234].

3.1.2 Google Scholar

It is a web-based search engine designed to find scholastic literature, such as articles, conference papers, theses, patents, and academic books. It provides extensive coverage across multiple disciplines, citation monitoring, author profiles, alerts, full-text article links, advanced search filters, and Google Scholar metrics (scholar.google.com).

3.1.3 PubMed

PubMed is a free database maintained by the National Centre for Biotechnology Information (NCBI) and the National Library of Medicine (NLM) of the United States of America (pubmed.ncbi.nlm.nih.gov). It employs Medical Subject Headings (MeSH) to classify articles according to subject. Users can set up email notifications to be notified of newly published articles. It provides access to a vast assortment of articles, research papers, and publications in numerous disciplines, including medicine, healthcare, and life sciences. Accessible to anyone with an internet connection, PubMed provides a comprehensive overview of the most recent research in these disciplines. It provides comprehensive search capabilities, direct links to the full text, and citation data for each article.

3.1.4 UniProt Knowledgebase (UniProtKB)

It is a comprehensive resource for protein-related data, provides protein characteristics, extensive annotations, taxonomic information, and cross-references to external databases (www.uniprot.org). It also contains bibliographic references, information on protein variants, isoforms, 3D protein structures, and computational methods for predicting protein function. Users are able to conduct text

and sequence searches, extract data, and utilize tools and services for sequence similarity searching, multiple sequence alignment, and batch retrieval.

3.1.5 Protein Data Bank (PDB)

The RCSB PDB is a globally recognized resource for storing and disseminating 3D structural data of biological macromolecules (www.rcsb.org) [235]. It primarily focuses on proteins and nucleic acids, containing crystallographic, NMR, and EM structures.

The PDB provides free and open access to its data through a user-friendly website and various data download options. The data is stored in a standardized file format known as pdb format, and the database undergoes rigorous validation procedures to ensure its quality and accuracy. The PDB is regularly updated and integrated with software tools, making it a vital resource for the global scientific community.

3.1.6 DrugBank

DrugBank is a comprehensive and user-friendly repository provides valuable information regarding drugs, their corresponding targets, and associated pharmaceutical details (go.drugbank.com/) [236].

The database assembled the diverse information encompassing a wide range of data, including chemical structures, molecular formulas, drug classifications, trade name, properties, mechanisms of action, pharmacology, pharmacokinetics, indications, and side effects for both approved and investigational drugs.

Furthermore, DrugBank extends its utility by offering an Application Programming Interface (API) designed to facilitate the seamless integration of drug-related information into diverse applications and research endeavors. To ensure its continued relevance, this repository undergoes regular updates, staying current with new drug approvals and the latest research findings.

3.1.7 Packages of R 4.2.2

R is a widely used open-source language for statistical analysis, data visualization, and data manipulation in academia and industry [237]. It provides an extensive range of applications and functions for conducting a variety of statistical analyses, including descriptive statistics and advanced modelling techniques. R extensive repository of packages and libraries extends its functionality to numerous domains, such as genomics, bioinformatics, machine learning, and natural language processing. It is a scripting language that enables repetitive duties and supports a variety of data import and export formats. R has a large user community with extensive documentation, resources, and IDEs such as RStudio. It encourages reproducible research via tools such as R Markdown. R operates on Windows, macOS, and Linux platforms.

3.1.7.1 Immunedeconv

The immunedeconv package in R 4.2.2 is a computational method for estimating the proportions or abundance of various immune cell types within a heterogeneous cell population, especially in gene expression data [238]. This is essential for gaining an understanding of the immune microenvironment in disease, particularly in cancer research. This method is being utilized to make up for the limited usability and economic hurdles that are encountered with techniques such as Fluorescence Activated Cell Sorting (FACS) or Immunohistochemistry (IHC)-staining [238]. It employs a Bayesian methodology that can account for data uncertainty. It can, however, be computationally intensive. The package contains a number of deconvolution algorithms, such as CIBERSORT, xCell, MCP-counter, quanTIseq and TIMER, which are commonly used for immune cell deconvolution. The input data is typically RNA-seq or microarray data, and the package provides estimates for T cells, B cells, and macrophages, among other immune cell types. The package may also include tools for investigating the results visually. quanTIseq is an established method that has been used for many years to deconvolute immune cell populations from aggregate RNA-seq data [239]. It is an NMF technique that is

comparatively quick and simple to implement. Whereas, MCPcounter is a more recent method based on the MCP strategy. It has been demonstrated to be effective at deconvolving immune cell populations from aggregate RNA-seq data, and is relatively quick and simple to use [240].

3.1.7.2 DESeq2 (1.38.3)

DESeq2 (1.38.3), an R (4.2.2) package, is used for differential expression analysis on RNA-sequencing data [241]. It is part of the Bioconductor project (bioconductor .org), a collection of open-source software tools for biological data analysis. It identifies genes with differential expression between experimental conditions in RNA-Seq experiments, commonly used in genomics and transcriptomics research. The package normalizes data using raw read count to account for library size and sequencing depth variations.

The negative binomial distribution model evaluates differential gene expression, generating a list of genes with significant differential expression. This model yields a list of genes that exhibit significant differential expression, accompanied by statistical data such as log2 fold changes, p-values, and adjusted p-values.

The adjusted p-values are typically computed to account for multiple testing, employing methods such as the Benjamini-Hochberg procedure. It also offers graphical capabilities for data visualization and can be integrated with other Bioconductor programs and R libraries.

3.1.7.3 EnhancedVolcano

EnhancedVolcano is an R tool that generates publication-ready volcano graphics for differential expression analysis [242]. It includes features like as colorization based on the significance of the results, labelling, annotations, and customization of the plot's design.

It is user-friendly and well-maintained making it an effective visualizations tool. It also includes annotations and is updated on a regular basis with new features and problem fixes [242].

3.1.8 GeneCodis4

GeneCodis4 is a bioinformatics tool that analyses gene lists or gene sets to determine overrepresented biological annotations or pathways (genecodis.genyo.es) [243]. Comparing a user-supplied list of genes with predefined gene sets or annotations, it conducts Gene Set Enrichment Analysis (GSEA).

Tests based on statistics evaluate the enrichment of specific annotations. GeneCodis4 supports multiple databases and annotation sources, offers visualizations options, and lets users upload their own annotation files. It also exports results in a number of formats for easy integration into research reports and corrects for multiple testing.

3.1.9 STRING

STRING is an online database and web application that investigates PPIs and functional protein associations in various organisms [244]. It offers interactive network visualization tools, enrichment analysis, and database integration and widely used in biological and biomedical research. Researchers can upload their own protein or gene catalogues and analyze their interactions.

3.1.10 Cytoscape

Cytoscape is a platform for visualizing, analyzing, and modeling complex biological networks like genes, proteins, and metabolites [245]. It supports multiple network types, data integration, and network analysis tools. It is also compatible with pathway databases, supports data import, integration, scripting, and automation, and has an active user community and comprehensive documentation base.

3.1.11 CytoHubba

CytoHubba is a Cytoscape plugin that ranks network nodes based on topological properties, including Degree, Betweenness, and Closeness Centrality [246]. It can identify hub genes or proteins, generate ranked lists, and integrate with Cytoscape for network analysis.

3.1.12 InterPro

InterPro is a well-recognized and well reputed bioinformatics resource and database that assumes a crucial role in the annotation and categorization of proteins [246]. This resource offers extensive and in-depth information pertaining to protein domains, families, and functional locations, hence facilitating researchers in their comprehension of protein activities and attributes across diverse animals.

The comprehensive data and methods provided by InterPro make a substantial contribution to bioinformatics analysis and efforts in protein annotation.

3.1.13 MODELLER (10.3)

MODELLER (10.3) is a widely used software package for protein structure modeling [247–250]. It performs homology modeling by aligning the target protein's sequence with the template protein's sequence. It uses force-field optimization techniques to refine the initial model.

The software uses scoring functions to evaluate the quality and reliability of the generated models. Users can choose template structures based on sequence similarity and structural relevance. MODELLER can handle modeling missing regions or loops in the target protein structure. It can be integrated with other software for tasks like sequence alignment and energy minimization. Its GUI is user-friendly and available for academic and commercial use.

3.1.14 Alpha Fold

AlphaFold, a deep learning-based approach to predict protein structures with remarkable accuracy (alphafold.com) [251]. Protein structures are predicted utilizing deep neural networks, specifically Transformer. AlphaFold's accuracy is a result of its training on an enormous set of PDB-provided known protein structures. It has revolutionized the discipline by resolving decades-old protein folding issues.

The understanding of protein function, interactions, and disease mechanisms is profoundly affected by the accuracy of protein structure predictions. AlphaFold has garnered global prominence in the Critical Assessment of Structure Prediction (CASP) competition and is an open-source programme. It could be used in drug discovery, vaccine development, and structural biology.

3.1.15 OmegaFold

OmegaFold is a structure prediction method that uses protein language model to predict protein structure [252]. It is the first computational method to predict high-resolution protein structure from a single primary sequence. Using a deep learning model trained on a massive protein dataset, it learns to predict protein structure by considering protein sequence and amino acid properties. It has shown high accuracy, comparable to experimental methods like X-ray crystallography.

3.1.16 Genome 3D

Genome3D is a user-friendly web-based interface allows researchers to explore annotations complete genome sequences, providing structural insights into protein-coding genes and gene products [253].

It integrates data from multiple databases and prediction methods, identifying protein domains and domain boundaries. Genome3D uses homology modeling to predict protein 3D structures, providing insights into protein molecule arrangement. It also aids in functional annotation by associating protein domains with

known functions. Genome3D is suitable for genome-wide structural analysis and can analyze genomic variations affecting protein structures.

3.1.17 UCSF Chimaera

The flexible molecular visualizations and analysis software UCSF Chimaera, widely used in computational chemistry and structural biology to examine the 3D molecular structures of proteins, nucleic acids, and complexes [254]. The software offers sophisticated visualization features, like as ball-and-stick and space-filling representations, and supports a number of molecular file types.

Additionally, it offers analysis tools for measuring atomic surfaces, angles, distance, docking, and electron density maps. Chimaera has a vibrant user base, is extendable via Python programming, and supports 3D printing. Since the software is open-source and free, users are allowed to alter and expand it as necessary. To enhance performance and meet user needs, updates are made on a regular basis.

3.1.18 ERRAT

ERRAT is a user friendly web based tool used to evaluate protein structure quality (saves.mbi.ucla.edu) [255]. It is available on the UCLA Molecular Biology Institute's website for researchers and structural biologists to access and validate protein structures.

3.1.19 Protein Structure Analysis (ProSA)

Protein Structure Analysis (ProSA) is a tool used to evaluate protein structures, assessing their quality, stability, and potential errors [256, 257] (prosa.ac.at/prosa). The ProSA web server provides a user-friendly interface for researchers and structural biologists to upload protein structure files for analysis. It uses statistical potentials and energy calculations to evaluate the energy profile and overall quality of a structure. ProSA calculates the Z-score, a statistical measure that quantifies

the energy of an input structure compared to high-resolution protein structures in the PDB. The Z-score plot helps identify potential errors or inaccuracies in the structure.

3.1.20 Qualitative Model Energy Analysis

QMEAN is a computational method used to assess and score protein structure models (swissmodel.expasy) [258]. The SwissModel web server offers a user-friendly interface for QMEAN analyses, allowing researchers to upload their models or access precomputed models. It provides quantitative measures of the quality and reliability of these models by evaluating structural features and properties.

It helps researchers identify the most accurate and biologically relevant protein structure models among a set of candidate models. It calculates a composite scoring function that combines energy-based and statistical terms, considering structural features like geometry, solvent accessibility, and torsion angles. It also employs statistical potentials and energy calculations to evaluate the energetics and stability of the protein model.

3.1.21 GETAREA

GETAREA, a tool used in computational chemistry and structural biology to calculate molecular surface areas (SASA) and related properties of molecules (curie.utmb.edu/getarea) [259]. It is crucial for understanding molecular interactions, ligand binding, and biophysical and biochemical processes. GETAREA uses mathematical algorithms and numerical methods to compute SASA values for individual atoms and residues within a molecule, considering the shape, size, and radius of solvent molecules.

It provides quantitative values in square angstroms (A^2) for different atoms, residues, or specific regions of a molecule. GETAREA can be integrated with other software for comprehensive molecular structure analyses. It is used in research and drug discovery to assess protein-ligand interaction, aiding in the design of potential drug candidates.

3.1.22 PyMOL

PyMOL is a popular molecular visualizations software in computational chemistry and structural biology (pymol.org) [260]. It enables the creation of intricate 3D visualizations of a variety of molecular structures, including complexes, proteins, nucleic acids, tiny molecules, and other compounds. PyMOL offers an interactive interface for real-time manipulation and supports a number of file formats. It may be scripted and mechanized using Python, enabling users to carry out complicated operations and produce figures appropriate for publishing. Additionally, it offers support for plugins and advanced rendering capabilities, analysis tools, selections and labels, superposition, and alignment.

3.1.23 AutoDock Vina (Version 20)

Molecular docking software, used to forecast the affinities and patterns of binding of small compounds to biological macromolecules, usually proteins. It is an updated version of AutoDock software created by the Scripps Research Institute's Olson group. The main use for AutoDock Vina is molecular docking simulations, which are essential for drug discovery and the study of molecular interactions [261, 262]. It rates potential binding poses according to anticipated energies to assess the binding affinity between a ligand and a protein receptor. Because of its effectiveness, adaptability, and simultaneous support for multiple ligand binding, it is easily usable by researchers with little or no computing background. It is an open-source software and users are free to change and expand its features as desired.

3.2 Methodology

3.2.1 Retrieval of Genetic and Gene Expression Profiles (GEP) of MM Patients

Genomic and clinical data of various cancer projects is available on GDC data Portal (portal.gdc.cancer.gov) including Clinical Outcomes in Multiple Myeloma

to Personal Assessment of Genetic Profile (CoMMpass). The Gene Expression Profiles (GEPs) and variant data of MM patients enrolled in the CoMMpass study was accessed from GDC data portal using accession ID: MMRF-CoMMpass. The GEPs of newly diagnosed MM (NDMM) and Relapse and Refractory MM (RRMM) patients has been retrieved in TSV format. Each TSV files contains the gene ID and raw read counts of gene expression of 59000 genes. Similarly the SNV data for primary blood drive cancer –Bone Marrow (BM), and recurrent blood (RC) derived cancer from BM was retrieved in csv format from GDC data portal. The variant file contains multiple information regarding each SNVs. Only the SNVs with missense mutation were selected to evaluate their role in relapse of MM.

3.2.2 Differential Gene Expression (DGE) of RRMM and NDMM

DGE analysis of RNA-seq data was performed by using DESeq2 (1.38.3), an R (4.2.2) package [241]. GEPs were provided as input and Differentially Expressed Genes (DEGs) were selected on the basis of two measures p-Value and Log2FC. The threshold of 2.0 < Log2FC < -2.0 and < 0.05, was employed for Log2FC and p-value respectively to filter out up and downregulated genes in CSV format. Furthermore, the EnhancedVolcano 1.16.0 package was used to visualize volcano plot of DEGs [242].

3.2.3 Protein-Protein Interactions (PPIs) and Identification of Hub Genes

PPI analysis reveals critical insights into how proteins interact and collaborate in complex cellular processes, offering a holistic view of molecular mechanisms underlying biology, disease, and drug action. STRING, was employed to construct PPI network of DEGs. The list of HGNC (HUGO Gene Nomenclature Committee) gene symbols of DEGs was provided as input and with default parameters

to predict the interactions and results were downloaded in TSV format. The computational tool Cytoscape [245] was used to visualize the complex network of PPIs obtained from STRING. hub genes in a network provides valuable insights into the central regulators of biological processes, disease mechanisms, and potential targets for interventions hence facilitating a deeper understanding of complex systems. After that, the STRING data were used as input for Cyto-Hubba, a Cytoscape module, which identified hub genes from the PPI network. The degree of each gene, or the number of connections (edges) it has with other genes in the network, was used to identify hub genes. Higher degree genes are thought to be more central to the network, indicating that they may play a significant role in controlling biological processes associated with the illness or condition under study.

3.2.4 Literature Mining for Identification of Relapse Biomarkers

Literature mining is a robust technique for extracting, organizing, and utilizing knowledge from textual data across multiple disciplines. It facilitates knowledge discovery, hypotheses generation, and the decision support in research and industry. The literature mining was conducted to identify biomarkers involved in the recurrence of multiple types of cancers using the search terminologies on Google Scholar (scholar.google.com) and PubMed pubmed.ncbi.nlm.nih.gov as "recurrence in cancer", "cancer relapse, "recurrent genes involved in lung cancer", "recurrent genes involved in pancreatic cancer", "recurrent genes involved in bladder cancer", "recurrent genes involved in breast cancer", "recurrent genes involved in colorectal cancer" and "recurrent genes involved in prostate cancer". The genes retrieved through literature mining were compared with the list of DEGs (obtained at step 3.2) to verify if these were already reported as relapse biomarker for MM or other cancers. Furthermore, genes associated with the recurrence of MM were also identified through a literature mining using the terminologies "Relapse" "RRMM", "cancer relapse" and "multiple myeloma".

3.2.5 Short Listing of Candidate Relapse Biomarkers

The genes were selected as candidate biomarkers if meeting any one of the following four criteria 1) a gene retrieved as relapse biomarker in literature mining and also upregulated in DGE, 2) a gene carrying SNV and also upregulated in DGE, 3) top five hub genes 4) Frequently mutated genes with higher no of SNVs. The selected genes were designated as "candidate relapse biomarkers" hereafter in text.

3.2.6 Functional and Pathway Annotation of DEGs and Candidate Relapse Biomarkers

Functional and pathways Annotation is a valuable method to get significant insights from extensive datasets. This analytical approach involves the identification of biological functions, processes, and pathways that exhibit a strong association with a specific set of genes or proteins. It was performed twice, once for both upregulated and downregulated DEGs identified through DGE analysis and secondly for shortlisted candidate relapse biomarkers. The analysis was conducted by providing the list of HGNC symbols of DEGs as input to the web tool GeneCodis4, genecodis.genyo.es [243]. The tool retrieved the GO (Gene Ontology) terms (biological process (BP), cellular component (CC), molecular function (MF)) and KEGG pathway both in tabulated and graphical format.

3.2.7 Impact of Immune Cells on Tumor Micro Environment

The fundamental process of immune cell infiltration has far-reaching implications for both health and disease condition. The immune cells infiltration of GEP of the RRMM vs NDMM patients was carried out by using the immunedeconv 2.1.0 package of R 4.2.2 [238]. The gene expression matrix was normalized to Fragments per Kilobase Million (FPKM) using the count2FPKM function of RNAAgeCalc 1.10.0 package [263]. The FPKM normalized matrix was further subjected to

deconvolution methods to perform immune cell infiltration. Two deconvolution methods of immunedeconv 2.1.0 package, quanTIseq and MCPcounter were used for immune cell infiltration analysis of GEP. Whereas the ggplot2 version 3.4.1 was used to visualize the results in the form of a bar chart and dot plot [239, 240]. Both tools utilize bulk RNA-Seq data (GEPs) as input to measure the content of immune cells in Tumor Micro Enviorment (TME) of samples. The quanTIseq perform deconvolution of the tumor to provide an estimated fraction of 10 immune cell types as well as the uncharacterized cells. Whereas the MCPcounter gives the absolute count of immune and stromal cells across all samples with respect to each cell type individually. Both tools provide the results in tabulated as well graphical format for each individual.

3.2.8 Retrieval of Protein Sequence of Candidate Relapse Biomarkers

The protein sequences of shortlisted candidate relapse biomarkers were retrieved from UniProtKB www.uniprot.org. The HGNC name was provided to the database and it returned the list of orthologues of the protein in different species. The Human orthologue of the proteins were selected to retrieve the FASTA format of protein sequence. In addition, in-silico mutagenesis was conducted using a text editor to generate mutant sequences for 7 candidate relapse biomarkers (selected based on criteria 2 and 4 as mentioned in 3.5) by replacing the wild-type residues with mutant residue.

3.2.9 Identification of Protein Domains and Families for Candidate Relpase Biomarkers

Protein domain information is critical for elucidating protein functions, evolutionary relationships, and structural features. The information pertaining to protein domains and families was obtained from the InterPro database (www.ebi.ac.uk/

interpro) [246]. The gene IDs were provided to the tool and it returned the comprehensive details regarding domains, families and functions of protein collected from various sources in tabulated format.

3.2.10 3D Structure Modeling of Candidate Relapse Biomarkers

3D protein structure modeling offers crucial insights into molecular architecture of proteins that facilitate the understanding of disease mechanisms and drug designing. Various methods were used to model the 3D structures of all the selected biomarkers. Homology modelling was employed to model proteins with already-known suitable templates. Protein Data Bank (PDB) was used for seeking and retrieving templates, protein accession IDs were provided to the database, which returned a list of relevant templates (www.rcsb.org) [235]. The optimal models encompassing the greatest number of amino acids present in the query were chosen. The retrieved templates were provided as input to the MODELLER 10.3 for 3D structure modelling which predicts 10 different conformations [247–250]. The resultant predicted models were selected on the basis of the minimum Discrete Optimized Protein Energy (DOPE) score.

Proteins for which no suitable templates were available, modelled using ab-initio techniques. AlphaFold and OmegaFold follows machine learning and artificial intelligence to predict the 3D structure of proteins from ab-initio (alphafold.com) [251, 252]. Upon providing protein name, AlphaFold retrieved a catalogue of available 3D structures of various orthologues of the query protein. The 3D structures of human protein orthologues were chosen for this study. In contrast, OmegaFold utilizes FASTA-formatted amino acid sequences of protein for 3D structure modelling. Genome3D was used to retrieve the 3D structure of wild and mutant domains of one protein (www.genome3d.net) [253]. The FASTA sequences of domains were provided as input, and the tool returned the list of all protein domain orthologues along with their 3D structures. All modelled 3D structures were downloaded in pdb format for further examination. The optimization and refinement of

all predicted structures were performed using UCSF chimera [254]. The software employs the steepest descent algorithm to gradually refine the positions of atoms, systematically lowering the total energy of the protein by moving in the direction that offers the most significant energy reduction.

In contrast, the conjugate gradient algorithm optimizes atomic positions efficiently through iterative updates along mutually orthogonal directions, seeking the configuration that minimizes energy most effectively.

3.2.11 Structural Assessment of Predicted 3D Models

For evaluating the quality of predicted 3D structures of candidate relapse biomarkers, the models were subjected to bioinformatics structural evaluation tools such as ERRAT, ProSa and QMEAN. All tools required the input of protein 3D structures in the pdb format. The ERRAT algorithm provided a range of values between 0 and 100, with higher scores indicating a stronger level of agreement between the model and the experimental data.

The ProSa web utilized to compute the z-score for the purpose of assessing the quality of a given structure. It is important to note that a lower z-score indicates a greater level of structural quality. In contrast, the QMEAN algorithm produces scores ranging from 0 to 1, with higher scores indicating a higher quality of structure.

3.2.12 Assessment of Solvent-Accessible Surface Area (SASA) of 3D Structures

The assessment of SASA of all predicted protein structures was performed utilizing the GETAREA. The tool takes the protein structure in pdb format, and returned a quantitative assessment of the polar and apolar area across the protein surface. Additionally, it also provides information on the number of residues that were buried and exposed over protein surface.

3.2.13 Visualization & Structure Comparison of Wild & Mutant Candidate Relapse Biomarkers with SNVs

The molecular visualization software PyMol was used to visualize and compare the wild and mutant proteins. The pdb files of both wild and mutant proteins structures were provided to the tool along with the command for superimposition. The tool returned the superimposed structures with the Root Mean Square Deviation (RMSD) score. Additionally mutant amino acids were highlighted and differences in intra-hydrogen bond interactions were also measured and figure was saved in PNG format.

3.2.14 Molecular Dynamics Simulation of Wild & Mutant Candidate Relapse Biomarkers with SNVs

MD simulation was performed to assess the conformational stability of both wild and mutant predicted protein structures of candidate relapse biomarker with SNVs by Desmond Maestro 12.0. The tool follows a multistep process to evaluate the conformational stability of protein structure upon receiving protein structure in pdb format. In first step, the "protein preparation wizard", water molecules were removed under preprocessing step. During second step, "System Builder", H-bonds were optimized, TIP3P water force field was selected as the solvent model and salts were added for removal of any charge from protein surface. Lastly, MD simulations were carried out for 50 nanoseconds (ns) at 300K temperature with default parameters. The RMSD and Root Mean Square Fluctuation (RMSF) graphs were retrieved in PNG format for further analysis using the simulation interaction diagram module.

3.2.15 Retrieval of Drug Compounds for Drug Repurposing

Virtual screening of ligands efficiently identifies potential drug candidates by evaluating their interactions with target proteins, enabling rapid and cost-effective discovery of novel therapeutic agents, reducing experimental costs and advancing

medicine and biotechnology. The drug compounds for virtual screening were retrieved from DrugBank. The FASTA sequences of proteins were provided to the sequence search feature of Drugbank database to retrieve drug compounds. The criteria for selecting a compound included: i) Inhibitors designed against input proteins or other members of the same protein family ii) reported for the treatment of relapse of other malignancies iii) FDA or EMA-approved. The approved and experimental drug compounds were utilized for virtual screening because of their well-known ADMET properties and efficacy in treating other cancer.

3.2.16 Molecular Docking of Drug Compounds with Candidate Relapse Biomarkers

Molecular docking is of immense significance as it enables the prediction of how molecules interact at the atomic level, facilitating drug discovery, protein-ligand binding studies, and the design of novel therapeutics with applications in pharmaceuticals, biotechnology, and materials sciences. Docking of selected drug compounds with shortlisted candidate relapse biomarkers was performed using AutoDock Vina (20) to identify lead compounds [261, 262]. AutoDock Vina (20) is widely used software for predicting the binding modes and affinities of small molecules to target protein. Firstly PDBQT (.pdbqt) and config (.config) files of both proteins and ligands were prepared and placed in different directories. The ADT (AutoDockTool), part of AutoDock Vina (20) suite, gets the structure in pdb format and assign charges and types to atoms in protein and ligands to convert them into pdbqt format. The config file containing the information regarding coordinates of search space, scoring function, number of runs and exhaustiveness, was prepared using text editor. The best binding pose between the ligand and the target protein was chosen based on the least binding energy score. The best-docked complexes for both wild-type and mutant models were selected and visualized on PyMOL. To make them stand out from one another, the ligands (drug molecules) and proteins were given distinct colours. The bond lengths of the polar contacts were also used to emphasise them. The compounds with the

highest binding affinity among all the selected proteins and their mutants were selected.

3.2.17 MD Simulation of Candidate Relapse Biomarker-Ligand Complexes

The MD Simulation of candidate relapse biomarkers complex with shortlisted drug compounds were performed to evaluate the conformational stability of protein ligand complex by employing Desmond Maestro 12.0. As mentioned previously (3.14) same steps regarding preprocessing, building and MD simulation of docked protein-ligand complex were performed to assess the stability of complex. The MD simulations were performed at 300K temperature for 50 nanoseconds. The Root Mean Square Deviation (RMSD) and Root Mean Square Fluctuation (RMSF) plots were retrieved in PNG format for further analysis using the simulation interaction diagram module.

Chapter 4

Results and Analysis

This chapter provides a step-by-step explanation of the results achieved using the approaches presented in chapter 3. The report covers study methodology and concludes with a summary of findings. The results have been divided into three phases according to the objective of studies.

1. Identification of biomarkers responsible for relapse of multiple myeloma through gene expression profiles
2. 3D structure modeling of these biomarkers (wild and mutated)
3. Drug repurposing against these biomarkers

4.1 Retrieval of Genetic & Gene Expression Profiles (GEP) of MM Patients

This GEP of Newly Diagnosed Multiple Myeloma (NDMM) and Recurrent and Refractory Multiple Myeloma (RRMM) patients and Small Nucleotide Variant data (SNV) were obtained from GDC data portal utilizing the MMRF-CoMMpass study data. The query "Data type = RNA-seq and Sources = Bone Marrow (BM) tumor" yielded gene expression data of 842 patients. Out of the total sample,

742 individuals were identified as NDMM, while 80 individuals were classified as having recurrent or RCMM. The dataset included the expression levels of 59,900 genes for each patient. Among these genes, a total of 7,409 were excluded from the analysis as they exhibited no expression in any of the samples. A total of 37,409 genes were chosen for subsequent analysis.

The nature and location of the mutation within the protein leads to the specific consequences in cellular processes. Mutations can lead to both beneficial and detrimental effects on protein structure and function, and they are central to the concept of genetic diversity and evolution. SNVs serve an essential role in genomics, biomarker discovery, disease research, and personalized medicine.

Their identification and analysis allow for a deeper understanding of disease mechanisms, development of targeted therapies, and the optimization of treatment strategies based on an individual's genetic composition, ultimately resulting in more effective and individualized healthcare. The variant data retrieved form GDC revealed that 2007 SNVs were affecting 454 genes in NDMM patients whereas 226 SNVs were associated with 152 genes in RRMM (Annexure Table 1).

4.2 Differential Gene Expression (DGE) of RRMM & NDMM

The DGE of the BM samples of NDMM and RRMM patients revealed a total of 1562 dysregulated genes. Among them 908 genes were significantly upregulated in RRMM (Log2FC $>$ 2, p-value $<$ 0.05) whereas 654 genes were downregulated (Log2FC $<$ -2, p-value $<$ 0.05) as shown in Figure 4.1. Furthermore, top 10 upregulated and downregulated Differentially Express Genes (DEGs) were filtered out on the basis of highest and lowest Log2FC values were assembled in Table 4.1. The top 10 significantly upregulated DEGs include ACTL8, NPTX1, MAGEA4, KLRF2, EGFLAM, UNC13C, GABRA5, NPFFR2, LINC01414, OR7E22P, whereas the top 10 significantly downregulated DEGs were FGFR3, SSTR1, RBM24, LINC030 20, HAPLN1, PEG3, IRS4, SLITRK2, RNF128 and AGR2.

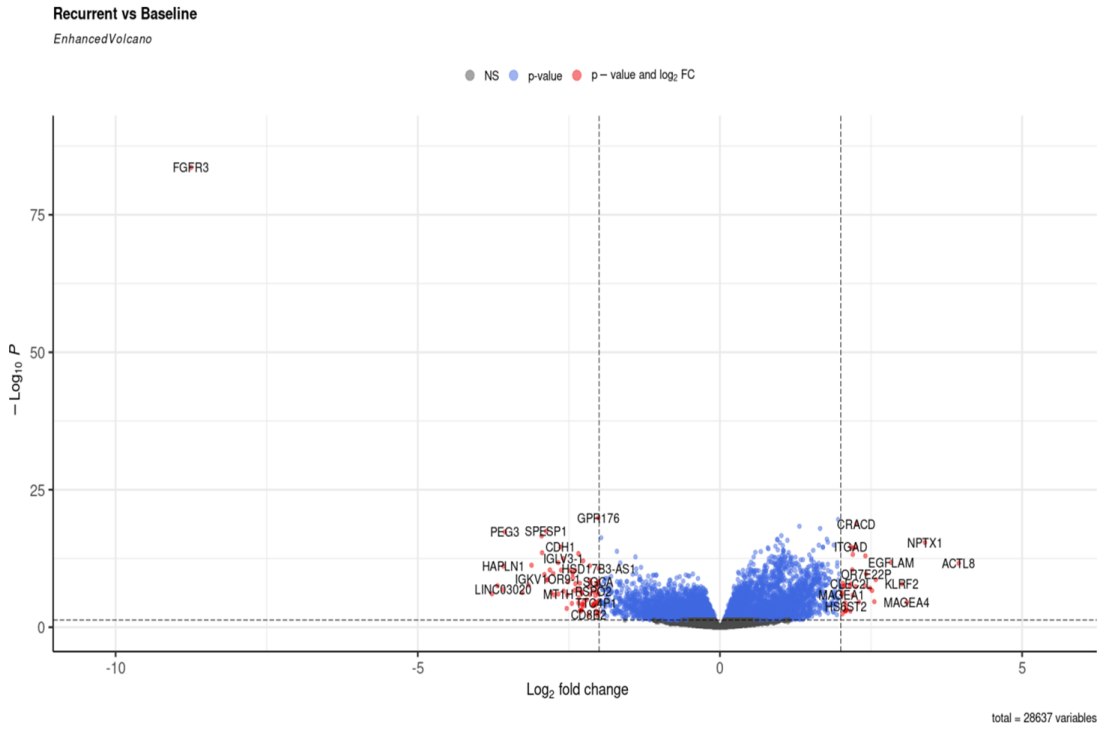

FIGURE 4.1: Enhanced Volcano plot representing differentially expressed genes in RRMM (shown in red dots) where biologically significant genes are plotted on x-axis w.r.t the Log2FC set at a cutoff of ± 2 whereas y-axis depicts statistically significant genes w.r.t the P-value at a cutoff < 0.05.

TABLE 4.1: List of top 10 upregulated and downregulated DEGs in RRMM patients retrieved through DGE Analysis

S No.	Genes	P-value	Log2FC	Expression
1	*ACTL8*	8.56E-10	3.951062	Overexpression
2	*NPTX1*	7.67E-13	3.393056	Overexpression
3	*MAGEA4*	0.000595	3.094468	Overexpression
4	*KLRF2*	1.05E-06	3.010071	Overexpression
5	*EGFLAM*	6.98E-10	2.82841	Overexpression
6	*UNC13C*	2.50E-07	2.57908	Overexpression
7	*GABRA5*	0.000478	2.553968	Overexpression
8	*NPFFR2*	1.07E-05	2.516253	Overexpression
9	*LINC01414*	4.89E-06	2.482189	Overexpression
10	*OR7E22P*	3.47E-08	2.418929	Overexpression
11	*FGFR3*	2.49E-84	-8.74914	Underexpression
12	*SSTR1*	8.23E-07	-3.77321	Underexpression

S No.	Genes	P-value	Log2FC	Expression
13	*RBM24*	2.92E-08	-3.68247	Underexpression
14	*LINC03020*	1.42E-07	-3.58844	Underexpression
15	*HAPLN1*	8.11E-12	-3.58337	Underexpression
16	*PEG3*	4.68E-18	-3.55825	Underexpression
17	*IRS4*	4.83E-07	-3.27126	Underexpression
18	*SLITRK2*	2.35E-08	-3.16896	Underexpression
19	*RNF128*	5.26E-12	-3.11795	Underexpression
20	*AGR2*	2.63E-17	-2.95198	Underexpression

4.3 Protein-Protein Interactions (PPIs) & Identification of Hub Genes

PPIs of the dysregulated genes were predicted using STRING database. Regarding the possible connections and functional links between DEGs, these PPIs offer important information. The intricate links between the dysregulated genes within MM were highlighted by the PPI network visualisations made possible by Cytoscape, as shown in Figure 4.2.

The hub genes playing crucial role in that intricate network with regulatory implications were identified through CytoHubba. The hub genes were selected on the basis of higher number of "Degree", as it represents the number of connection a gene have with other genes. The hub genes were selected on the basis of higher number of "Degree", as it represents the number of connection a gene have with other genes.

The interaction network of top 10 hub genes with each other and their ranking according to decreasing degree are assembled in Figure 4.3 and Table 4.2. The top 5 highly interconnected genes were IL1B (Interleukin 1 Beta), CD4 (cluster of differentiation 4), ITGAM (Integrin Subunit Alpha M), PTPRC (protein tyrosine phosphatase receptor type C) and TYROBP (TYRO Protein Tyrosine Kinase Binding Protein).

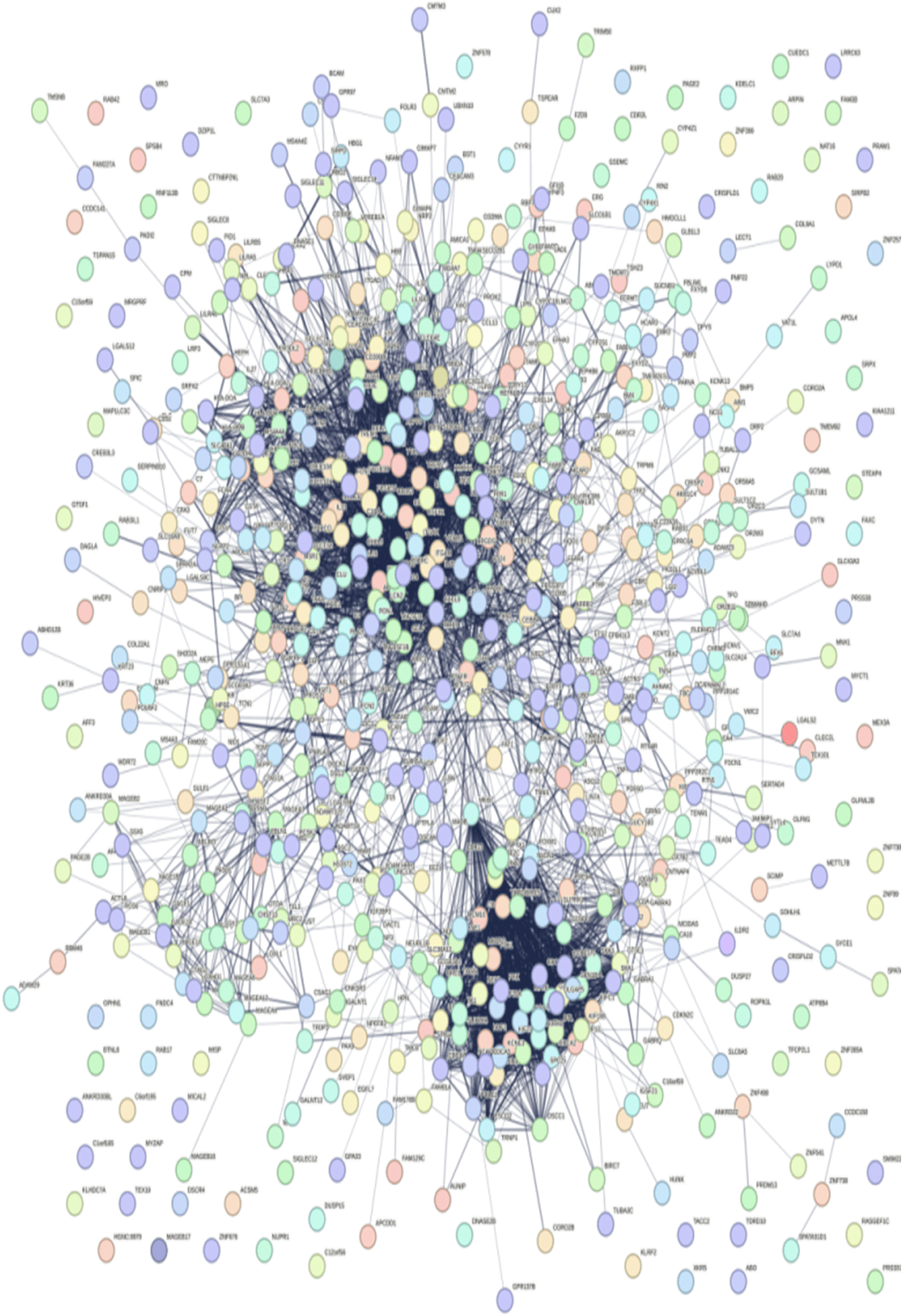

FIGURE 4.2: Protein-Protein Interaction network of DEGs constructed through STRING and Visualized through Cystoscope

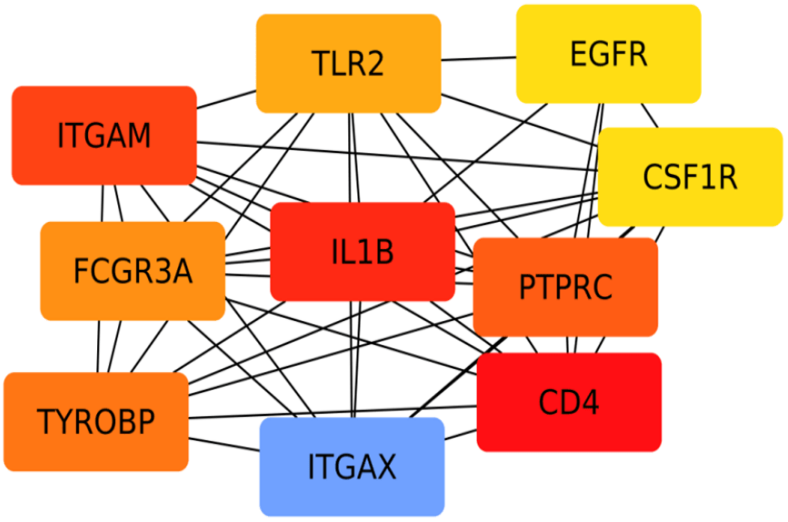

FIGURE 4.3: Interaction network of hub genes identified through CytoHubba

TABLE 4.2: Rank table of hub genes identified through PPIs with highest number of degree

Rank	Name	Degree
1	*CD4*	224
2	*IL1B*	204
3	*ITGAM*	202
4	*PTPRC*	194
5	*TYROBP*	192
6	*FCGR3A*	182
7	*TLR2*	166
8	*ITGAX*	150
9	*EGFR*	148
10	*CSF1R*	148

4.4 Literature Mining for Identification of Relapse Biomarkers

Literature mining for the exploration of relapse biomarkers of MM and other cancers already reported in literature retrieved 136 genes with significant role

in relapse of various cancers (Table 4.3). Among them 40 genes were found to be involved in relapse of MM (Table 4.3).

Analysis of results revealed that KRAS, NRAS, TP53, NF1, STK11 and DNMT3A that were found as relapse biomarker in MM also reported for relapse in others cancers. Although these biomarkers were not found upregulated in our DGE analysis but mutations in these gene is reported by various researches in RRMM.

TABLE 4.3: List of Genes involved in relapse of multiple cancers retrieved through Literature Mining

Sr No.	**Cancer**	**Gene**
1	Bladder Cancer	*FGFR3, NEB, FGFR1, SDHC, OGG1, TP53, MDM2, p53, PSCA, p16, Ki67, IFT140,UBE2I, FAHD1, NME3, EOMES, HOXA9, POU4F2, TWIST1,VIM, ZNF154*
2	Breast Cancer	*STAT3, ES41, FANCD2, FOX1, ARID1A, NF1, ARID1B, BRCA1, PIK3R1, AKT1, TP53, ESR1-CCDC170, SEC16A-NOTCH1, SEC22B-NOTCH2, ESR1-YAP1, FGFR1, ESR1, PTEN, ABCB1, BARD1, BRCA2, HER3*
3	Colorectal Cancer	*LEMD1, SERPINE1, SIAE, SERP2, EFEMP2, FBN1, SPARC, LINC0219, CC2D1B, PCDHB15, CSF1R, ATM, C11ORF65, APC, TP53, KRAS, PIK3CA, FBXW7, SMAD4, TCF7L2, NRAS, ADAM8, LYN, S100A9, VCAN*
4	Leukemia	GAS6, *PSD3, PLCB4, DEXI, JMY, NRP1, C10orf55, NCOR2, USH2A, NT5C2, DNMT3A, RUNX1, ASXL1, TP53, GTF2I–PDGFRB, IKZF1–TYW1, ARID1A, CSF1R, IKZF1, KANSL1, NIPBL, ARID1B, BCORL1, CREBBP, NRAS, PTPN11, FLT3, HOXA7, S100A11, S100A10, IFI44L, WT1*
5	Lung Cancer	*ATR,ERBB3, KDR, MUC6, GOPC-ROS1, NTRK1-SH2D2A, TTN, MUC16, CSMD3, RYR2, LRP1B, ZFHX4, USH2A, KRAS, FLG, TP53, SLC8A1, AHNAK, KCNU1, COLA5A2, COL22A1, PKHD1L1, SMARCA4*
6	Pancreatic Cancer	*KRAS, CDKN2A, TP53, SMAD4, ARID1B, NF1, PPP6C, AKT1, PIK3CA, CHD8, STK11, MGA, NOTCH1, MYC, NUTD15, BPI, C6orf58, CD177, MCM7, NUDT15*
7	Prostate Cancer	*BCL-2, C-MYC, CAVEOLIN, SLC14A1, NDUFA13, UQCR11, USP34, TP53, BIRC5, BCR-ABL1, BRCA1, BRCA2, PTEN, RB1, MYC*

Sr No.	Cancer	Gene
8	Multiple Myeloma	*BFL-1, BCL-XL, BCL-2, KRAS, NRAS, TP53, FAM46C, TRAF2, LTB, FAM154B, NF1, XBP1, IDH2, GNAQ, PMS1, CREB1, NSUNS2, PIK3CG, ROS1, PMS2, FIT4, KDM5A, STK11, ZFHX3, CD40, TNFRSF17, IL6ST, PRKCD, IRF4, TRAF3, NFKB2, FGFR3, DNMT3A, SETD2, DIS3, IGLL5, KMT2B, SP140, MALRD1, L1TD1*

4.5 Shortlisting of Candidate Relapse Biomarkers

Genes were shortlisted as relapse biomarkers on the basis of following four criteria

1. A gene retrieved as relapse biomarker in literature mining and also upregulated in DGE,
2. A gene carrying SNV and also upregulated in DGE,
3. Top five hub genes
4. Frequently mutated genes retrieved through SNV analysis

A total of 18 genes were shortlisted following all criteria. Among them 6 DEGs were selected according to first criteria including CSF1R (Colony-Stimulating Factor-1 Receptor), VCAN, NRP1 (Neuropilin1), COL22A1 (Collagen Type XXII Alpha 1 Chain), BPI (Bactericidal Permeability Increasing Protein) and BIRC5 (Baculoviral inhibitor of apoptosis repeat-containing 5). These DEGs were upregulated in our analysis but reported as relapse biomarkers for other cancers in literature (Table 4.3). Similarly, 5 DEGs were selected in accordance to second criteria included MNX1(Motor Neuron and Pancreas Homeobox 1), FAT1 (FAT Atypical Cadherin 1), ERG (ETS Transcription Factor ERG), TCL1A (TCL1 Family AKT Coactivator A) and AFF3 (ALF Transcription Elongation Factor 3). These DEGs showed upregulation along with SNV in RRMM patients. Moreover,

the genes selected following third criteria, top five hub genes, were IL1B, CD4, ITGAM, PTPRC and TYROBP. The detailed analysis of genetic profiles revealed that KRAS and NRAS were highly mutated genes whereas the most frequent mutations in both NDMM and RRMM were assembled in Table 4.4. All the DEGs shortlisted as candidate relapse biomarkers were assembled in Table 4.5. These DEGs are reported as diagnostics, prognostics, therapeutic and relapse biomarkers for various other cancers but their role in relapse of MM needs to be explored.

TABLE 4.4: Top 5 mutations in RRMM and NDMM with %age of affected cases

Sr. No	**Mutations**	**No. of Affected Cases in Cohort**	**% of Affected Cases in Cohort**	**No. of Affected Cases in Cohort**	**% of Affected Cases in Cohort**
1	Missense NRAS Q61R	63 / 833	7.56%	7 / 94	7.45%
2	Missense KRAS Q61H	56 / 833	6.72%	6 / 94	6.38%
3	Missense NRAS Q61K	45 / 833	5.40%	5 / 94	5.32%
4	Missense BRAF V640E	29 / 833	3.48%	4 / 94	4.26%
5	Missense KRAS G12D	28 / 833	3.36%	4 / 94	4.26%

TABLE 4.5: Shortlisted Candidate Relapse Biomarkers

Criteria No.	**Gene Name**	**Reason**
1 (upregulated DEGs in RRMM retrieved as relapse biomarkers in other cancers)	*CSF1R*	Colorectal + leukemia
	VCAN	Colorectal Cancer
	NRP1	Leukemia
	COL22A1	Lung Cancer
	BPI	Pancreatic Cancer
	BIRC5	Prostate Cancer
2 (upregulated DEGs in RRMM having SNV)	MNX1	P392L
	FAT1	N3716K
	ERG	E353Q
	TCL1A	T38I

Criteria No.	**Gene Name**	**Reason**
3 (Hub genes retrieved through PPI Analysis)	*AFF3*	P1129L
	IL1B	Hub gene
	CD4	Hub gene
	ITGAM	Hub gene
	PTPRC	Hub gene
	TYROBP	Hub gene
4 (Top mutated genes retrieved through SNV analysis)	*KRAS*	Q61H, Q61R, G13D, G12V, G12R, Q61E, K117N, A59E, G12D
	NRAS	Q61R, Q61K, Y64D, Q61H, G13R, G13D, E153Q, G12D

Literature review of six gene (CSF1R, VCAN, NRP1, COL22A1, BPI and BIRC5) identified by combine analysis of literature mining and DGE revealed their potential in modulating TME and disease progression. CSF1R, a receptor tyrosine kinase, inhibition is reported as potential antitumor strategy. Activated CSF1R are recruited by tumor-associate macrophages and release cytokine that modulated TME to pro-tumoral phenotype. CSF1R activation also initiates many downstream pro survival signaling cascades including PI3K/AKT, ERK1/2, and JNK [264]. Similarly BIRC5 is also an immune-related gene that inhibits apoptosis and promotes cellular proliferation. High expression of BIRC5 regulates DNA methylation hence is reported as potential target for developing immunotherapies [265]. Moreover, NRP1 is an independent predictor of relapse and poor survival in NSCLC. It is also reported as novel potential therapeutic target in NSCLC because of its critical role in tumorigenesis, cancer invasion, and angiogenesis through VEGF, PI3K, and Akt pathways [266]. Whereas, VCAN and COL22A1 are reported as prognostic biomarkers in various cancers. VCAN mRNA are specifically expressed in cancer-associated fibroblasts and associated with poor relapse free survival of stage II-III patients in CRC. It is a promising biomarker to identify stage II-III patients with high risk of relapse in CRC [267]. While COL22A1 is an integral part of novel prognostic immune related gene signature in CRC [268]. Additionally, COL22A1 is also reported as poor prognosis and relapse biomarker in Head and Neck Squamous Cell Carcinoma (HNSCC) [269]. Furthermore, BPI

is associated with human neutrophils as they secrete BPI in response to inflammation, along with many other cytotoxic proteins. Neutrophils can promote tumor metastasis by forming so-called Neutrophil Extracellular Traps (NETs).

High levels of circulating and intra-tumoral neutrophils have been shown to correlate with poor survival in pancreatic cancer and pancreatic ductal adenocarcinoma [269]. These results were also consistent with our immune cell infiltration analysis which revealed the presences of higher neutrophils count in RRMM.

The DGE and SNV analysis of dataset retrieved five genes (MNX1, FAT1, ERG, TCL1A, AFF3) harboring mutation and upregulation in RRMM. These mutations include MNX1 (P392L), FAT1 (N3716K), ERG (E353Q), TCL1A (T38I), and AFF3 (P1129L). KRAS and NRAS, although not found in DGE but are the most mutated genes in both NDMM and RRMM patients according to SNV data. Both KRAS and NRAS are proto-onco genes, belong to the Ras family of proteins, small GTPase, involve in regulation of biological processes particularly cell growth, proliferation and apoptosis [270]. It has been reported that newly acquired mutations and pre-treatment sub-clonal mutations of KRAS and NRAS in MM possibly induce chemo resistance and relapse [271]. Mutation in KRAS and NRAS have been reported to be more common in relapsed patients (>70% patients) [272, 273]. The codons G12, Q61 and G13 are mutation hotspots for both KRAS and NRAS but various substitutions in each codon elicit different signaling pathway, hence express distinct pathophysiology [274]. In our study all the three hotspots were found substituted with various codon (NRAS: Q61H, Q61R, Q61E, G12V, G12D, G12R, G13D KRAS: Q61K, Q61H, G12D, G13R, G13D) along with few new codons (NRAS: K117N, A59E KRAS: Y64D, E153Q) in RRMM. The impairment of PI3K pathway due to KRAS (G12R) mutation is reported in literature and is also consistent with our results of pathway analysis [275] (Figure 4.5).

Additionally MNX1 encodes a transcription factor (HB9) that contains a homeodomain. The overexpression of MNX1 has been reported in many cancers (prostate, colon, liver, breast and bladder cancer, glioma and pancreatic progenitor tumors and acute myeloid leukemia) and has been suggested as potential diagnostic and

prognostic biomarker [276, 277]. Upregulation of MNX1 stimulates the Wnt/β-catenin signaling and via expression of downstream genes c-Myc and CCND1, hence plays a vital role in CRC progression [278]. FAT1 is among the most frequently mutated genes in many types of cancer. The role of FAT1 in cancer progression is highly dependent upon cancer type. In some cancers epithelial-mesenchymal transition (EMT) and the formation of cancer initiation/stem-like cells is promoted by loss of FAT1 function promotes whereas overexpression of FAT1 leads to EMT in others. The paired analysis of diagnosis and relapse sample in B-cell acute lymphoblastic leukemia overexpression of FAT1 was found correlated with shorter relapse-free and overall survival [279]. Several studies have reported a correlation of FAT1 mutation or expression with prognosis in various cancers, such as breast cancer, NSCLC, gastric cancer and T-cell lymphoma [280]. Positive correlation of FAT1 overexpression with proliferation and WNT/β-catenin signaling pathway in T-cell acute leukemia (T-ALL) is recently reported in a study [281]. ERG encodes a transcription factor involved in development and differentiation affecting vasculogenesis, haematopoiesis, angiogenesis and embryogenesis, and is associated with regulation of cellular processes [282]. ERG over expression is associated with poor prognosis and oncogenesis promotion, in prostate cancer, ewing's sarcoma, acute myeloid leukemia, acute T-lymphoblastic leukemia [283]. ERG high expression stimulate gene fusion event (ERG-TMPRSS2) that leads to early relapse in AML [283]. Upregulation of ERG is also associated with upregulation of PI3K/AKT pathway [284]. TCL1A is a proto-oncogene expressed in embryonic stem cells, activated T and B lymphocytes and coactivator of kinases and interacting partners crucial in signaling pathways (PI3K and NF-κB) and cellular activities [285]. Dysregulated TCL1A has a well-documented role in hematopoietic malignancies i.e, development of T-cell leukemia, correlation of overexpression with aggressiveness, deregulation of the cell cycle and genomic instability in chronic lymphocytic leukemia [46]. It is also suggested as prognostic biomarker for stage II/III CRC [286], therefor, proposed as potential biomarker for colorectal and hematological malignancies [45, 47]. AFF3 is primarily expressed in B cells and encodes a protein involved in transcription regulation [287]. AFF3 upregulation has been found in many cancers (gastric, breast, Adrenocortical and

AML), also involve in modulating TME thus suggested as target for immune therapy [287–289]. In gastric cancer, dysregulated AFF3 is a potential marker for diagnosis and prognosis as well as correlated with immune checkpoints response whereas in breast cancer overexpression is associated with drug (tamoxifen) resistance therefore suggested as predictive marker for ER+ breast cancer [287, 289]. Moreover, AFF3 meditate oncogenic effects of β-catenin as constitutive activation of Wnt/β-catenin signaling pathway in mice leads to formation of malignant adrenocortical tumors [290].

4.6 Functional and Pathway Annotation of Candidate Relapse Biomarkers

Functional and pathway annotation was performed for the following data sets

1. Upregulated and downregulated DEGs identified through differential expression analysis
2. Shortlisted candidate relpase biomarkers (4.5)

The GO term analysis of DEGs revealed that upregulated DEGs were found to be significantly enriched in the following Biological functions (BP), immune response, immune system process, inflammatory response, cell adhesion, positive regulation of T cell activation, antigen processing and presentation of peptides, peptide antigen assembly with MHC class II, immunoglobulin production, antigen processing and presentation of exogenous peptides and neutrophil chemotaxis (Annexure Figure 1a) . However, the downregulated DEGs were notably associated with adaptive immune response, positive regulation of B cell activation, phagocytosis recognition and engulfment, complement activation and development of central nervous system among many others (Annexure Figure 1b). Similarly, the significant cellular component (CC) terms for upregulated DEGs were plasma membrane, extracellular region and extracellular space whereas, collagen-containing extracellular matrix, external side of plasma membrane, tertiary granule membrane, cell surface,

ficolin-1-rich granule lumen and MHC class II protein complex were also notable terminologies (Annexure Figure 2a). However, the downregulated DEGs were also enriched in plasma membrane, extracellular region and extracellular space, collagen-containing extracellular matrix, external side of plasma membrane along with immunoglobulin complex, synapses, and glutamatergic synapse (Annexure Figure 2b). Additionally, the significant Molecular Function (MF) retrieved for the upregulated DEGs through GO analysis were carbohydrate binding, signaling receptor activity, transmembrane signaling receptor activity and cytokine activity (Annexure Figure 3a). While the antigen binding, sequence-specific DNA binding was the most significant MF related to downregulated DEGs among many others (Annexure Figure 3b).

The pathway analysis of upregulated and downregulated DEGs revealed their enrichment in various essential pathways (Figure 4.4). The upregulated DEGs were found significantly enriched in numerous disease pathways including Staphylococcus aureus infection, rheumatoid arthritis, malaria, tuberculosis, asthma, leishmaniasis, graft versus host disease along with phagosome and hematopoietic cell lineage (Figure 4.4a). The downregulated DEGs, on the other hand, were found to be enriched in diverse signaling pathways including cAMP signaling, calcium signaling, hippo signaling, signaling pathways regulating pluripotency of stem cells along with Neuroactive ligand-receptor interaction and various synapses as depicted in Figure 4.4b.

Furthermore, the functional enrichment of these shortlisted candidate relapse biomarkers showed significant enrichment of the following BP ontologies, positive regulation of cell population proliferation, multicellular organism development, positive regulation of serene/threonine kinase activity and positive regulation of endothelial cell proliferation more significantly among many others (Annexure Figure 4). The shortlisted DEGs showed CC enrichment more significantly in focal adhesion. In contrast, G protein activity, GDP-binding, and cytokine binding were enriched MF ontologies (Annexure Figure 5 and 6). Moreover, KEGG pathways analysis revealed significant enrichment in prostate cancer, colorectal cancer

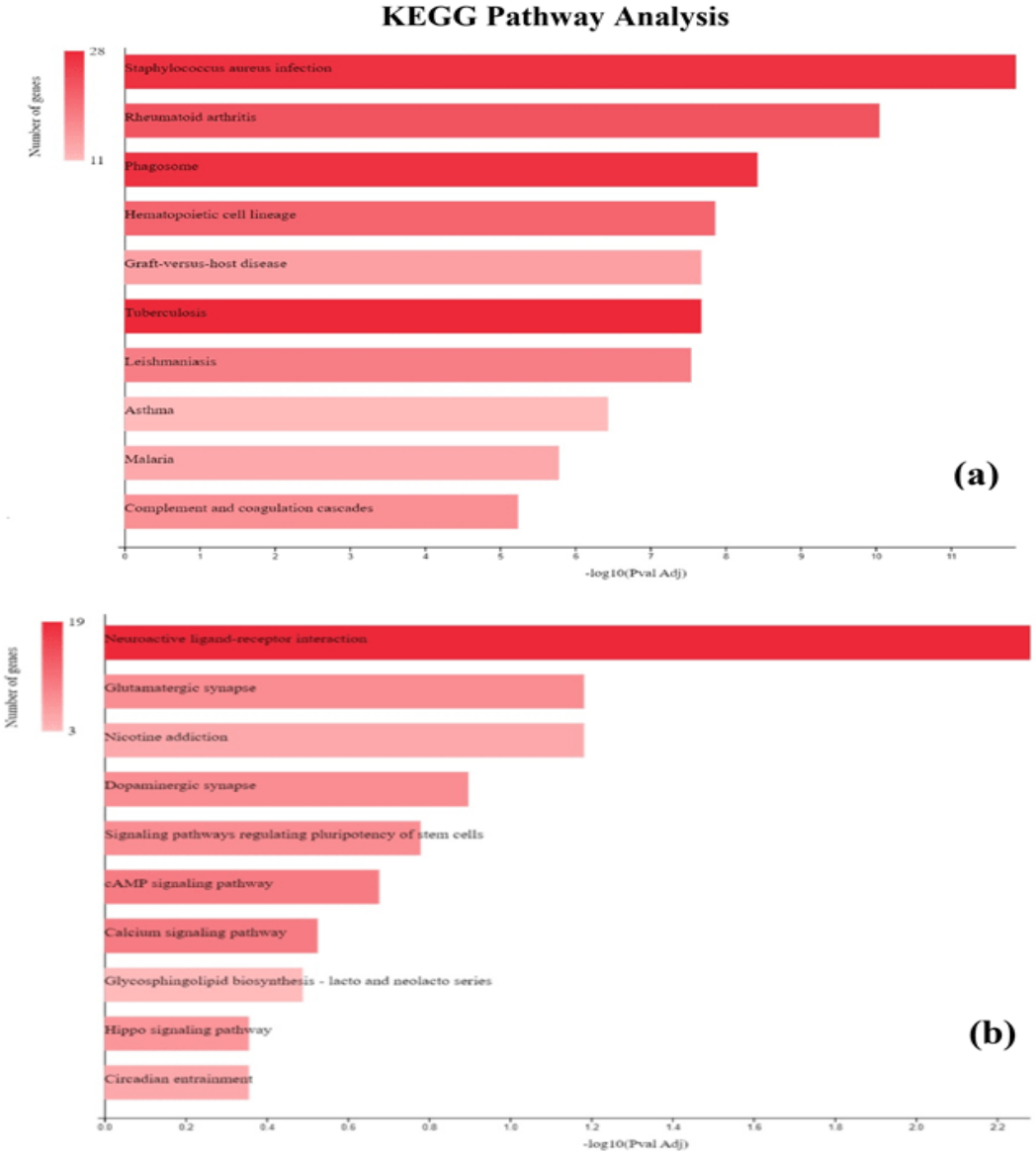

FIGURE 4.4: Pathways (KEGG) enrichment analysis of (a) upregulated and (b) downregulated DEGs in RRMM

(CRC), acute myeloid leukemia, chemical carcinogenesis receptor activation and PI3K/AKT signaling pathway (Figure 4.5).

It can be inferred that KRAS and NRAS mutants may affect the activation and hydrolysis due to dysregulation of G protein activity, GDP and GTP binding, and GTPase activity. The aberrant GTPase activity due to KRAS mutations has been reported to affect the GTP-hydrolysis [291]. Furthermore, enrichment of PI3K-Akt signaling pathway that was also consistent with our other results as upregulation

FIGURE 4.5: The KEGG pathways analysis of shortlisted candidate relapse biomarkers

of CSF1R, NRP1, TCL1A and ERG activate PI3K-Akt signaling [284, 292]. This pathway is crucial to many cellular processes, and plays a significant role in cancer proliferation and multidrug resistance. Decrease in cellular apoptosis is mediated by continuous phosphorylation of various transcription factors by AKT, thus the promotion of the proliferation, angiogenesis, and survival of cell [293]. However, the PI3K-Akt signaling pathway is crucial for pathophysiology of MM and is associated with therapy resistance [294, 295].

Moreover, Wnt/β-catenin signaling plays a dual and disease stage-specific role in the pathogenesis of MM. Wnt/β-catenin pathway activation during MM disease progression is mediated through epigenetic silencing by antagonists which facilitates pathway activation and proliferation of MM cells [296]. The pathway although not found enriched in pathway analysis but the 3 DEGs (MNX1, AFF3, and FAT1) among the 5 selected candidate genes are found to have direct relationship in upregulation of wnt/β-catenin pathway [278, 290].

4.7 Impact of Immune Cells on Tumor Micro Environment

The results of immune cell infiltration analysis were assembled in Figure 4.6 and 4.7. The meticulous analysis of results revealed that, T cell (CD4), natural killer cells (NK), monocytes, macrophages and myeloid dendritic cells (MDC) counts was marginally raised for RRMM in comparison to NDMM. Cytotoxicity score of endothelial cells and Cancer Associated Fibroblasts (CAFs) calculated through MCPcounter showed the similar trend of slightly higher count in RRMM as compared to NDMM. Similarly, regulatory T cell (Tregs) estimated by quanTIseq was somewhat more in RRMM then NDMM. The only discrepancy was observed in the count of B cells as it was more at RRMM then NDMM according to MCPcounter whereas it was higher in NDMM then RRMM according to quanTIseq. Moreover T cell (CD8+) count declined and Neutrophils count amplified in RRMM in comparison to NDMM according to both methods (Figure 4.6, Figure 4.7).

The immune cells infiltration analysis in our study corroborated the previously reported role of immune dysfunction in MM invasion and progression [264]. Development of effective therapeutic strategies against neutrophils for treating cancer and various other diseases has already been in consideration. According to recent studies the neutrophils have multiple phenotypes that perform diverse functions, particularly modulation of inflammation and immune response [297]. Similarly

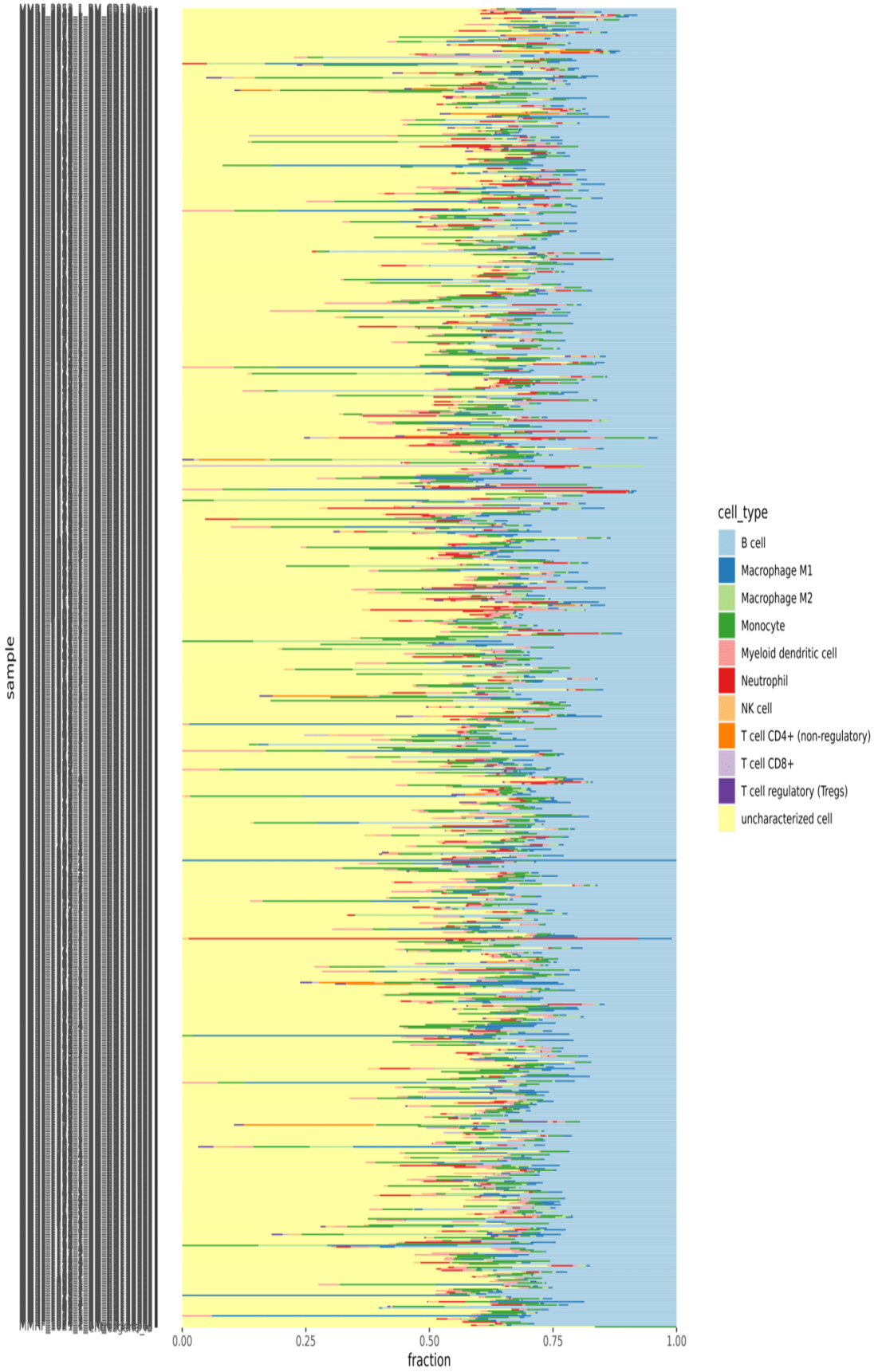

FIGURE 4.6: The immune cells infiltration analysis through quanTIseq plot represents count of immune cells in NDMM and RRMM samples where samples are plotted on y-axis whereas x-axis shows the fraction of cells.

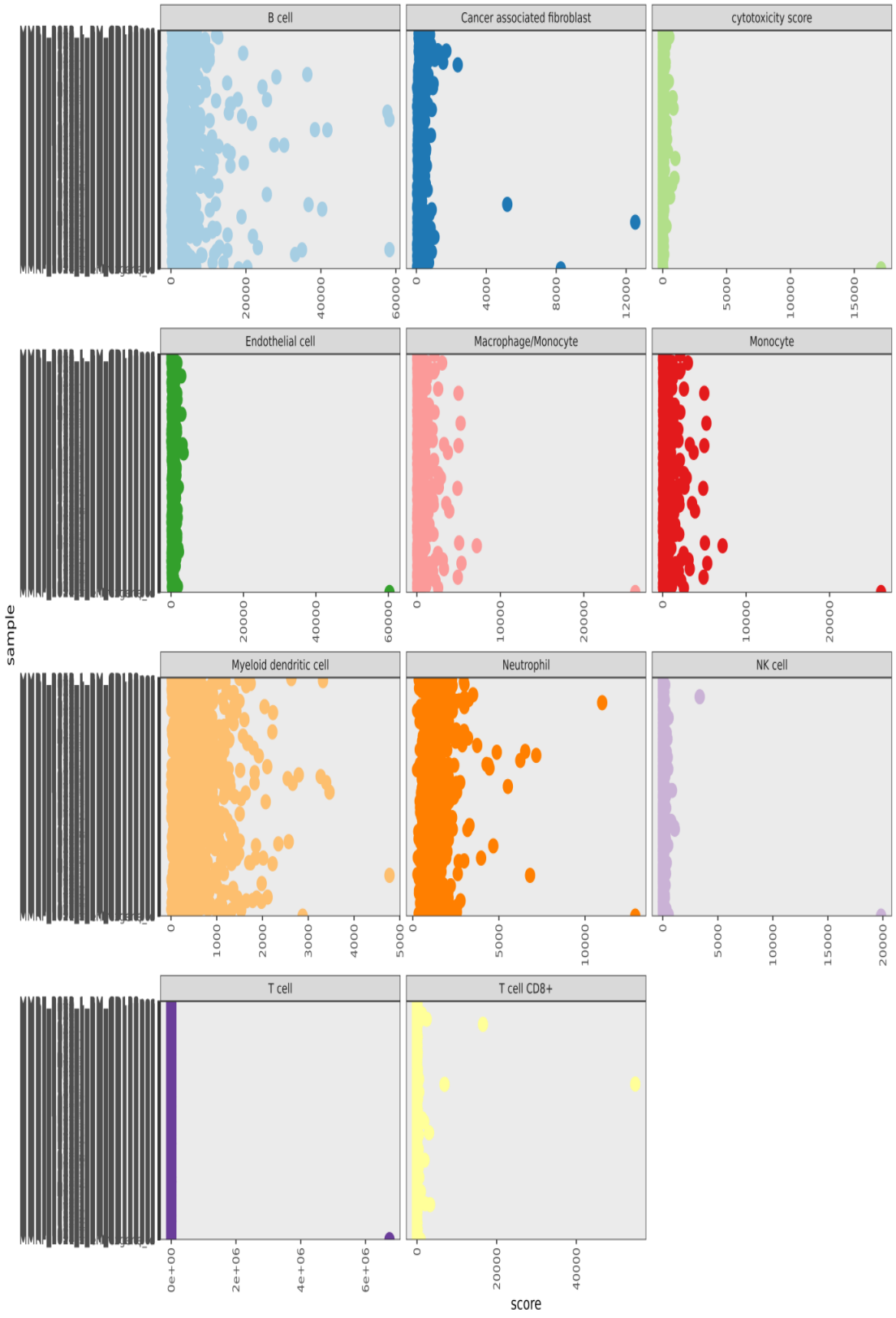

FIGURE 4.7: The immune cells infiltration analysis through MCPcounter plot represents immune cells content in baseline and recurrent cancer samples where x-axis represents scores for cell-type fractions whereas y-axis shows samples.

another study mentioned the impairment of immune response in MM due to reduced phagocytic activity of neutrophils in comparison to healthy control [298]. Moreover, the role of neutrophils in facilitating tumor progression through immune deregulation and increased vulnerability to infection in MUGS and MM has already established [299]. The count of CD8+ T cells, which are crucial for defending against intracellular pathogens (viruses, bacteria) and for tumor surveillance, was found to be decreased in NDMM. The trafficking or transporting of CD8+ T cells into the TME is crucial to exert its anti-tumor function. The elevated levels of CD8+ T cells in the TME are linked with positive anti-tumor effects and good prognosis in breast, colorectal, glioblastoma, and cervical cancers [300]. Hence the lower count of CD8+ T in TME is not only linked with cancer progression/relapse or poor prognosis but also with the increased risk of secondary viral or bacterial infection. The lower count of CD8+ T cells retrieved through immune infiltration investigation also supports our findings of pathway analysis which showed enrichment of various other cancer and bacterial infections pathways in RRMM (Figure 4.5).

4.8 Retrieval of Protein Sequence of Candidate Relapse Biomarkers

The protein sequences of all shortlisted candidate relapse biomarkers were retrieved through UniProt database (https://www.uniprot.org/) (The UniProt Consortium, 2023). The database returned the FASTA format of protein sequences along with the protein IDs which are as follows: MNX1 (ID: P50219), ERG (ID: P11308), TCL1A (ID: P56279), AFF3 (ID: P51826), FAT1 (ID: Q14517) KRAS (ID: P01116), NRAS (ID: P01111), BIRC5 (ID: O15392), CD4 (ID: P01730), IL1B (ID: P01584), ITGAM (ID: P11215), TYROBP (ID: O43914), PTPRC (ID: P08575), CSF1R (ID: P07333), VCAN (ID: P13611), NRP1 (ID: O14786), COL22A1 (ID: Q8NFW1) and BPI (ID: P17213). The protein sequences were assembled in Annexure Table 2. The IDs and FASTA sequence were further used to identify domains and template for predicting 3D structure of proteins.

4.9 Identification of Protein Domains & Families for Candidate Relapse Biomarkers

Domains play a crucial role as structural components, and any alterations in the amino acid sequence have the potential to influence the structure and function of both the domain and the protein as a whole. Hence, the inclusion of domain information was deemed necessary in order to evaluate the impact of SNVs on the protein's structural integrity. The domain information for the proteins obtained from the InterPro database included comprehensive details about the numbers and size of domains present.

This information is provided for all candidate relapse biomarkers in Annexure Table 3. However, Table 4.6 presents the findings derived from the domain analysis of biomarkers associated with SNVs. The analysis of MNX1's domain indicates that the protein possesses a single domain, the Homeobox domain. However, the SNV was not found within this domain region. In the ERG protein, two distinct domains, namely Pointed Domain and ETS Domain, were identified. Additionally, SNV (E353Q) was observed specifically inside the ETS domain (Figure 4.8a). In addition, the SNV (P1129L) was observed inside the domain (AF4/FMR2) of the AFF3 protein (Figures 4.8b).

Furthermore, the FAT1 protein was observed to possess a total of 43 domains, along with three specific SNVs (D2382A, P4309S, and M739I). All the SNVs were located within the Cadherin-like domain (Figure 4.8c, d and e). Nevertheless, TCL1A did not exhibit any identifiable domain. Furthermore, it was observed that both KRAS and NRAS contain a common domain known as the Small GTP-binding protein domain.

The various SNVs of KRAS (Q61H, Q61R, G13D, G12V, G12R, Q61E, K117N, A59E, G12D) and NRAS (Q61R, Q61K, Y64D, Q61H, G13R, G13D, E153Q, G12D) were observed to be situated inside the domain, suggesting significant disruption to both the structural and functional aspects, as seen in Figures 4.9a and Figures 4.9b, respectively.

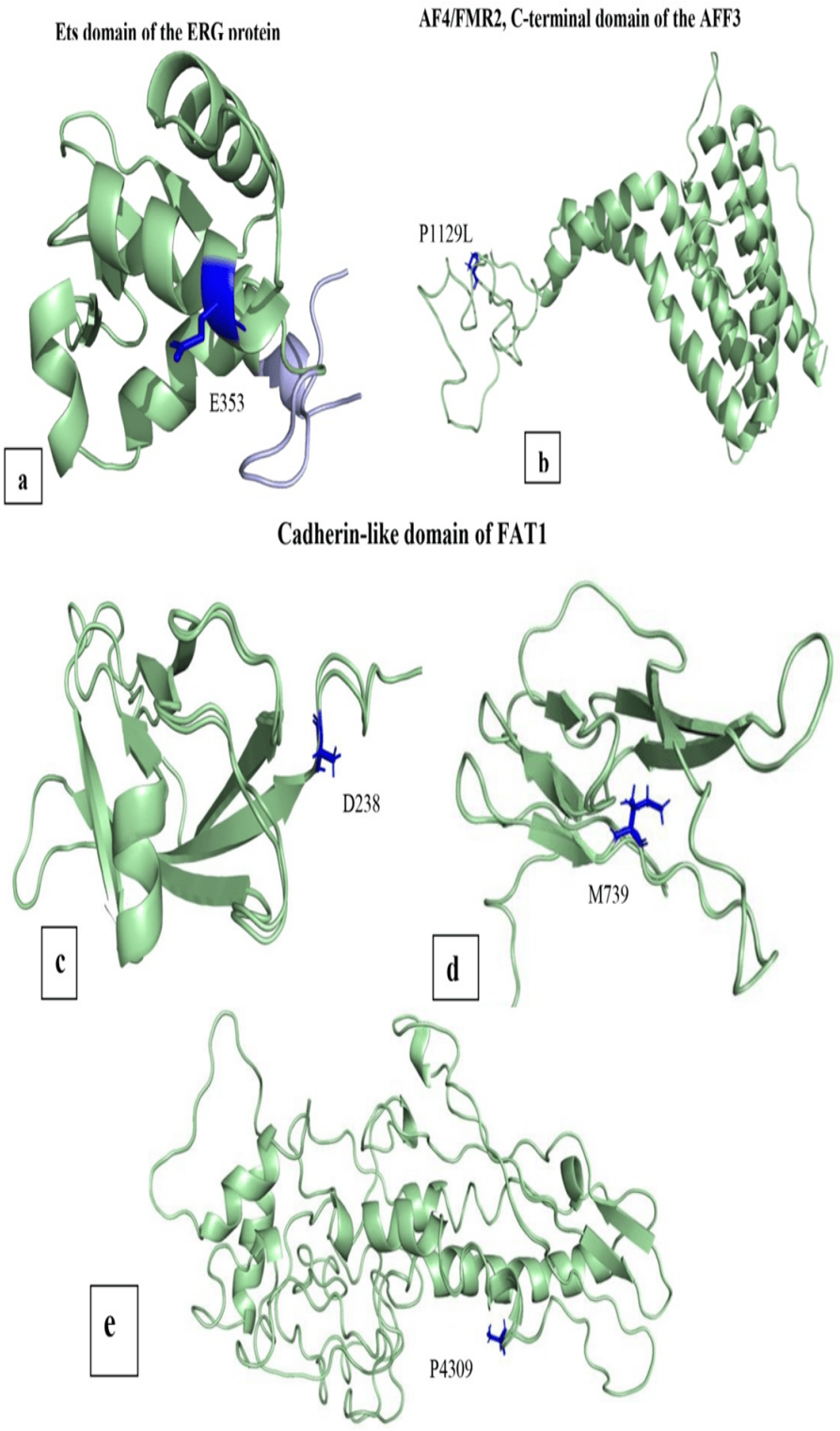

FIGURE 4.8: Domain analysis of candidate relapse biomarkers with SNVs. The (a) E353Q mutation affects the Ets domain of the ERG protein (b) the P1129L mutation that affects the AF4/FMR2, C-terminal domain of the AFF3 protein (c) D2382A mutation (d) M739I mutation and (e) P4309S mutation affects the Cadherin-like domain of FAT1 protein.

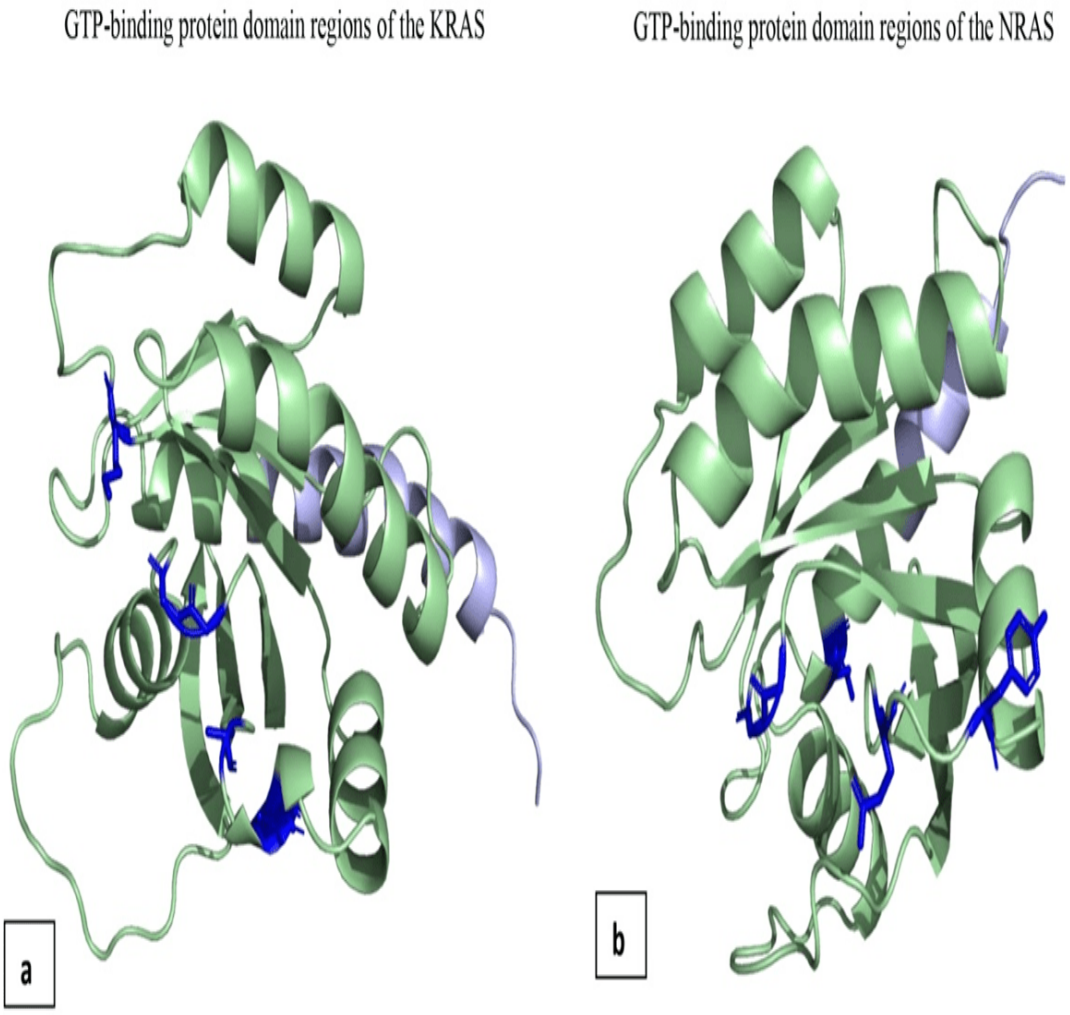

FIGURE 4.9: The depiction of mutations (Q61H, Q61R, G13D, G12V, G12R, Q61E, K117N, A59E, and G12D) that affect the Small GTP-binding domain regions of the KRAS protein. The green color represents the domain while blue color shows the mutated residues.

TABLE 4.6: Domain Analysis of Candidate Relapse Biomarkers with SNVs

Genes	Number of domains	Domain	Mutation in Domain	DNA Change	Amino acid Change
MNX1	1	Homeobox domain	No	chr7:g.157005551G>A	P392L
ERG	2	Pointed domain,		chr21:g.38383807C>G	E353Q
TCL1A		ETS domain	Yes	chr14:g.95713954G>A	T38I
AFF3	1	-	-	chr2:g.99554707G>A	P1129L

Genes	Number of domains	Domain	Mutation in Domain	DNA Change	Amino acid Change
FAT1	43	AF4/FMR2, C-terminal homology domain	Yes	chr4:g.186619441T>G	D2382A
				chr4:g.186596615G>A	M739I
				chr4:g.186707611C>T	P4309S
KRAS	1	Cadherin-like domain	Yes	chr12:g.25227341T>G	Q61H,
				chr12:g.25227342T>C	Q61R,
				chr12:g.25245347C>T	G13D,
				chr12:g.25245350C>A	G12V,
				chr12:g.25245351C>G	G12R,
				chr12:g.25227343G>C	*Q61E*,
				chr12:g.25225713T>A	K117N,
				chr12:g.25227348G>T	A59E,
				chr12:g.25245350C>T	G12D
NRAS	1	Small GTP-binding protein domain	Yes	chr1:g.114713908T>C	Q61R,
				chr1:g.114713909G>T	Q61K,
				chr1:g.114713900A>C	Y64D,
				chr1:g.114713907T>G	Q61H,
				chr1:g.114713907T>A	G13R,
				chr1:g.114716124C>G	G13D,
				chr1:g.114716123C>T	E153Q,
				chr1:g.114708648C>G	G12D
				chr1:g.114716126C>T	

The mutations ERG-E353Q and AFF3-P1129L were observed to induce structural changes in the Ets domain (ERG) and AF4/FMR2, C-terminal homology domain (AFF3), respectively. The slight change was expected in the conformation of the Ets domain of ERG by E353Q as arginine-threonine and glutamic-acid glutamine are of the same amino acids category (polar and hydrophilic). Similarly, the structure of AF4/FMR2, C-terminal homology domain (AFF3) was inferred to be affected little as proline, a nonpolar and hydrophobic amino acid, was substituted by a similar type of amino acid leucine. The AF4/FMR2, C-terminal homology domain, common among AFF protein family members (AFF1, AFF2, AFF3, and AFF4), is involved in AFF1-AFF4 heterodimer formation and is crucial in regulation of breast cancer gene ESR1 through interactions of AFF4-super elongation

complex with ESR1 transcription start site associated H3K27 [301]. Mechanistic investigations revealed that higher expression of AFF3 led to the activation of the ER signaling pathway and the transcriptional enhancement of a specific group of genes regulated by ER. Clinical examination further indicated that elevated AFF3 levels in ER+ breast tumors were linked to resistance to tamoxifen treatment and correlated with poorer overall survival outcomes [302]. Ets domains are DNA-binding transcription factors regulating gene expression. It has been studied that Ets domains are very specific and any change in their amino acid sequence can alter their functionality affecting their binding specificity with DNA [303].

Moreover, within the Cadherin-like domain of FAT1, three mutations (D2382A, M739I, and P4309S) were identified. The replacement of Methionine with Isoleucine involved amino acids from the same group (nonpolar and hydrophobic). In contrast, the substitutions of Aspartic acid (a polar amino acid) to Alanine (a nonpolar amino acid) in D2382A and Proline (a nonpolar amino acid) to Serine (a polar amino acid) in P4309S did not involve amino acids from the same chemical group. Concrete evidence underscores the significant role played by FAT1 in organ maintenance and developmental processes. Its expression appears to be specific to particular tissues. FAT1's activity involves triggering various signaling pathways through interactions with other proteins. These pathways include Wnt/β-catenin, Hippo, and MAPK/ERK, which exert influence over critical cellular functions like proliferation, migration, and invasion. Mutation in FAT1 leads to dysregulation of expression could contribute to tumorigenesis and potentially influence prognosis. FAT1 might hold promise as a therapeutic target in the context of cancer treatment [304].

Moreover, Small GTP-binding protein domain of KRAS and NRAS proteins was observed with the observable structural changes as all the mutations of KRAS (Q61R, Q61H, Q61E, K117N, G13D, G12V, G12R, G12D, A59E) and NRAS (E153Q, G12D, G13D, G13R, Q61H, Q61K, Q61R, Y64D) studied in this study were found to be affecting this domain at different regions. Among all aforementioned mutations of KRAS and NRAS, significant disruption occurred by the KRAS-G12V and KRAS-A59E mutations. In KRAS-G12V, glycine (polar,

hydrophilic) was substituted with nonpolar and hydrophobic amino acid valine inducing a large structural change. Similarly, the substitution of nonpolar and hydrophobic alanine by polar and hydrophilic glutamic acid in the KRAS-A59E model has been observed to affect the small GTP-binding protein domain drastically. These conformational changes may alter the function of the small GTP-binding protein domain which plays a crucial role in signaling functions of RAS proteins controlling cellular growth, division and survival [305].

4.10 Structure Modeling of Candidate Relapse Biomarkers

The fundamental criterion for selecting a methodology for protein structure prediction is the availability of suitable templates for 3D modelling. Due to the unavailability of appropriate templates for all biomarkers, diverse methodologies were utilized in order predict their structure. The AlphaFold Protein Structure Database was utilized to obtain the structural information of eight biomarkers, including CD4, COL22A1, IL1B, NRP1, PTPRC, TYROBP, VCAN, and CSF1R. The human orthologues corresponding to the biomarkers identified by the IDs P01730, Q8NFW1, P01584, O14786, P08575, O43914, P13611, and P07333 were chosen and downloaded in pdb format for further analysis (Figure 4.10a-h). Conversely, the OmegaFold, an ab-initio method, was employed for the 3D structure prediction of the MNX1 protein due to the absence of an appropriate template for homology modelling and the low quality structure provided by AlphaFold. The protein sequence of MNXI was provided in FASTA format as input and the predicted structure was obtained as pdb file for further processing. The procedure was replicated for the structural prediction of the mutant MNX1 (MNX1-P392L) as depicted in Figure 4.11 a-b. However, the FAT1 is a large molecule consisting of 4,588 amino acids. Due to its considerable length, the computational tools available for predicting the 3D structure of proteins were unable to effectively model it. Consequently, only the specific domains of FAT1 that carries SNVs were subjected to structural modelling by utilizing the Genome3D platform. The

protein sequence of FAT1 (Q14517) in FASTA format was provided to the tool and the anticipated structures of CATH domains were obtained using a homologous recognition methodology. For further analysis, the Cadherin-like domains that feature the SNVs D2382A, M739I, and P4309S were specifically chosen and obtained in pdb format. The aforementioned procedure was replicated for determining the structure of FAT1 mutants after incorporating SNVs in the sequence Figure 4.12. All the predicted models were minimized at 1000 steepest descent and conjugate gradient steps using the structure minimization module to ensure removal of possible steric clashes and stable structural conformation.

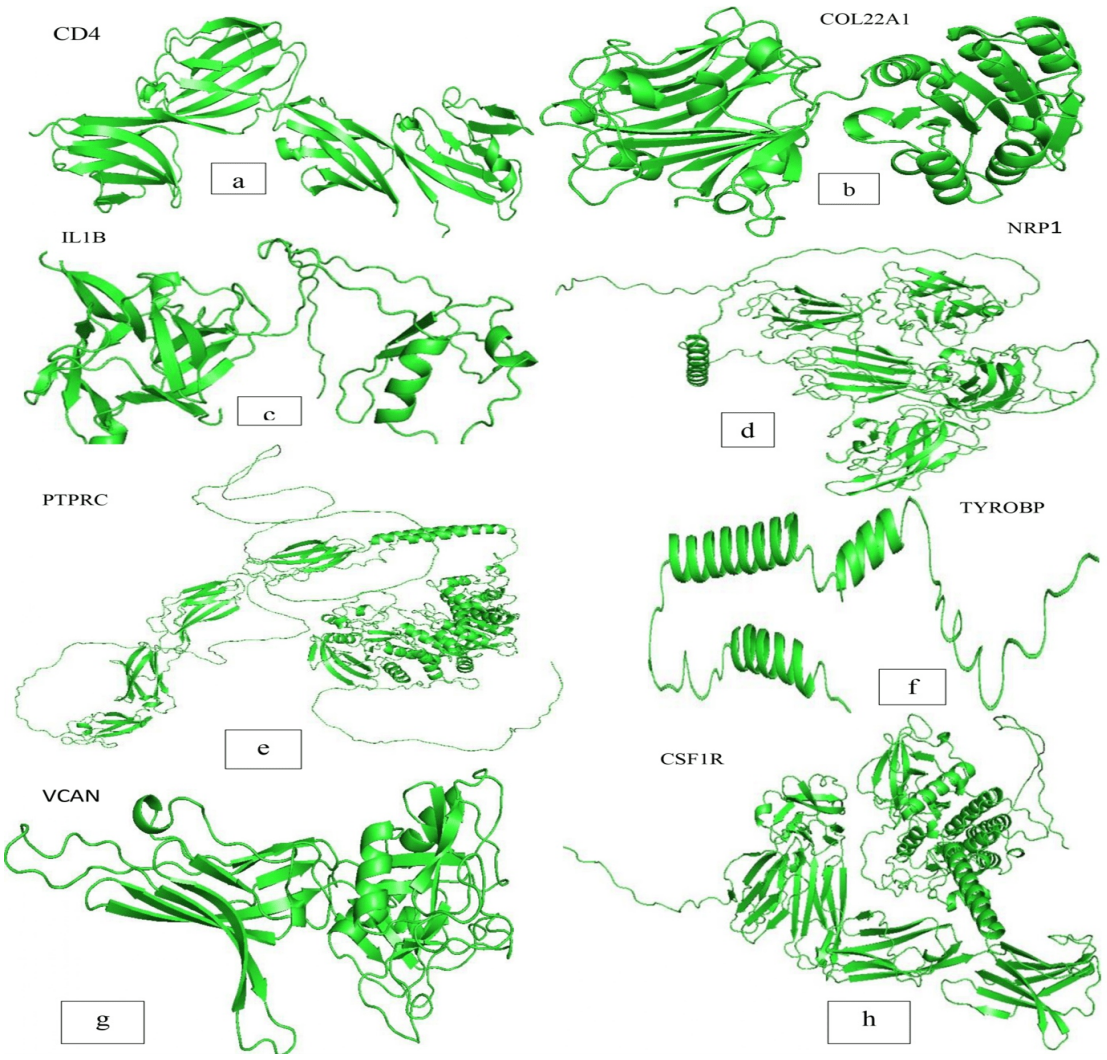

FIGURE 4.10: 3D models of (a) CD4 (P01730) (b) COL22A1 (Q8NFW1) (c) IL1B (P01584) (d) NRP1 (O14786) (e) PTPRC (P08575) (f) TYROBP (O43914) (g) VCAN (P13611) and (h) CSF1R (P07333) retrieved from Alphafold.

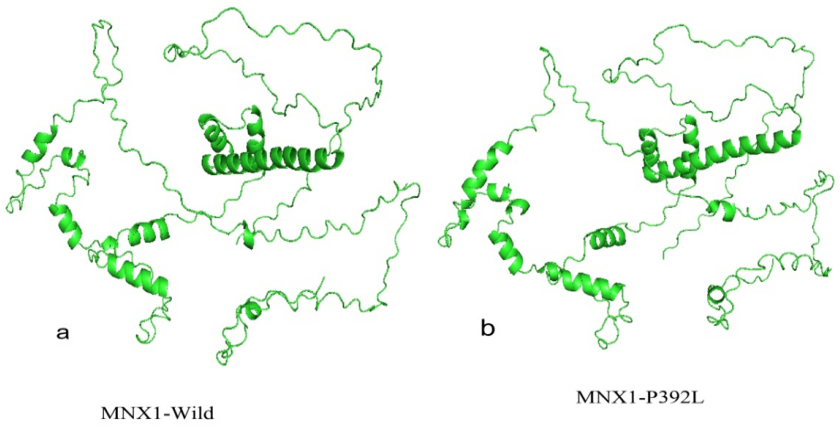

FIGURE 4.11: Wild and mutated 3D models of MNX1 retrieved from Omegafold.104

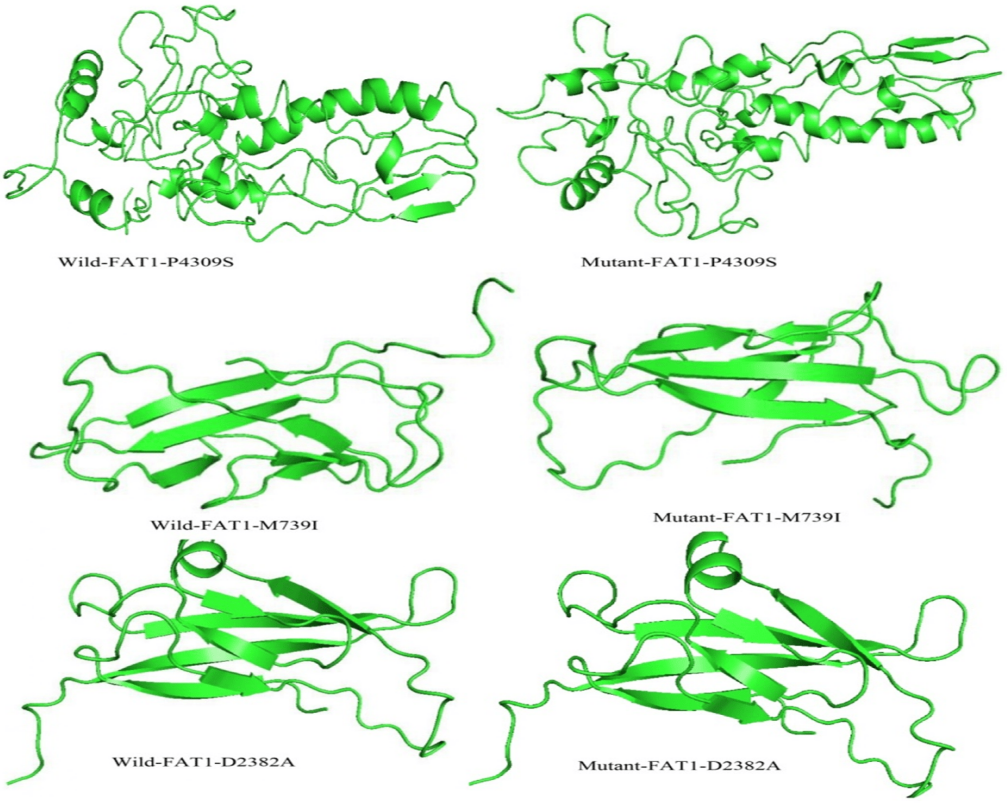

FIGURE 4.12: Wild and mutated 3D models of Cadherin like domains of FAT1 constructed from Genome3D

However, the suitable templates for eight biomarkers namely TCL1A, ERG, AFF3, KRAS, NRAS, BIRC5, BPI, and ITGAM, were found on PDB thus homology

modeling was performed for these biomarkers. These templates structures for these biomarkers were downloaded in pdb format from PDB. The chosen templates exhibited the maximum query coverage and high resolution. The information pertaining to biomarkers and structure IDs corresponding to the selected template used for the homology modelling has been consolidated in Table 4.7.

TABLE 4.7: Templates IDs and resolutions selected for homology modeling of DEGs

Sr.#	**Biomarkers**	**Template ID**	**Resolution**
1	*TCL1A*	1JSG	2.50 Å
2	*ERG*	4IRH	2.10 Å
3	*AFF3*	6KN5	2.20 Å
4	*KRAS*	5TAR	1.90 Å
5	*NRAS*	6ZIO	1.55 Å
6	*BIRC5*	1E31	2.71 Å
7	*BPI*	1BP1	2.40 Å
8	*ITGAM*	7USL	2.7 Å

Homology modelling of both wild and mutated biomarkers using template structures was performed by MODELLER 10.3. (Table 4.7). The predicted models were chosen based on the minimum DOPE score. The wild and mutated models of TCL1A, ERG, AFF3, KRAS, and NRAS were chosen for further analysis based on their respective DOPE scores (-12042.28 and -11815.05 for TCL1A, -11079.66 and -10813.77 for ERG, -11079.66 and -10813.77 for AFF3, -20292.62, -20219.83, -20196.07, -20009.27, -20028.12, -20107.05, -20218.21, -20191.55, -20084.79, -20075.51 for KRAS, and -19549.66, -19406.07, -19526.53, -19402.41, -19399.37, -19298.97, -19270.29, -19367.64, -19235.67 for NRAS) (Table 4.8 and Figures 4.13, 4.14, and 4.15).

Wild-type 3D models were exclusively generated for BIRC5, BPI, and ITGAM, as no SNVs were identified for these biomarkers (Figure 4.16). The 3D models of BIRC5, BPI, and ITGAM were selected for further investigation based on their respective DOPE scores of -13211.27, -53158.93, and -98373.27 (Table 4.8).

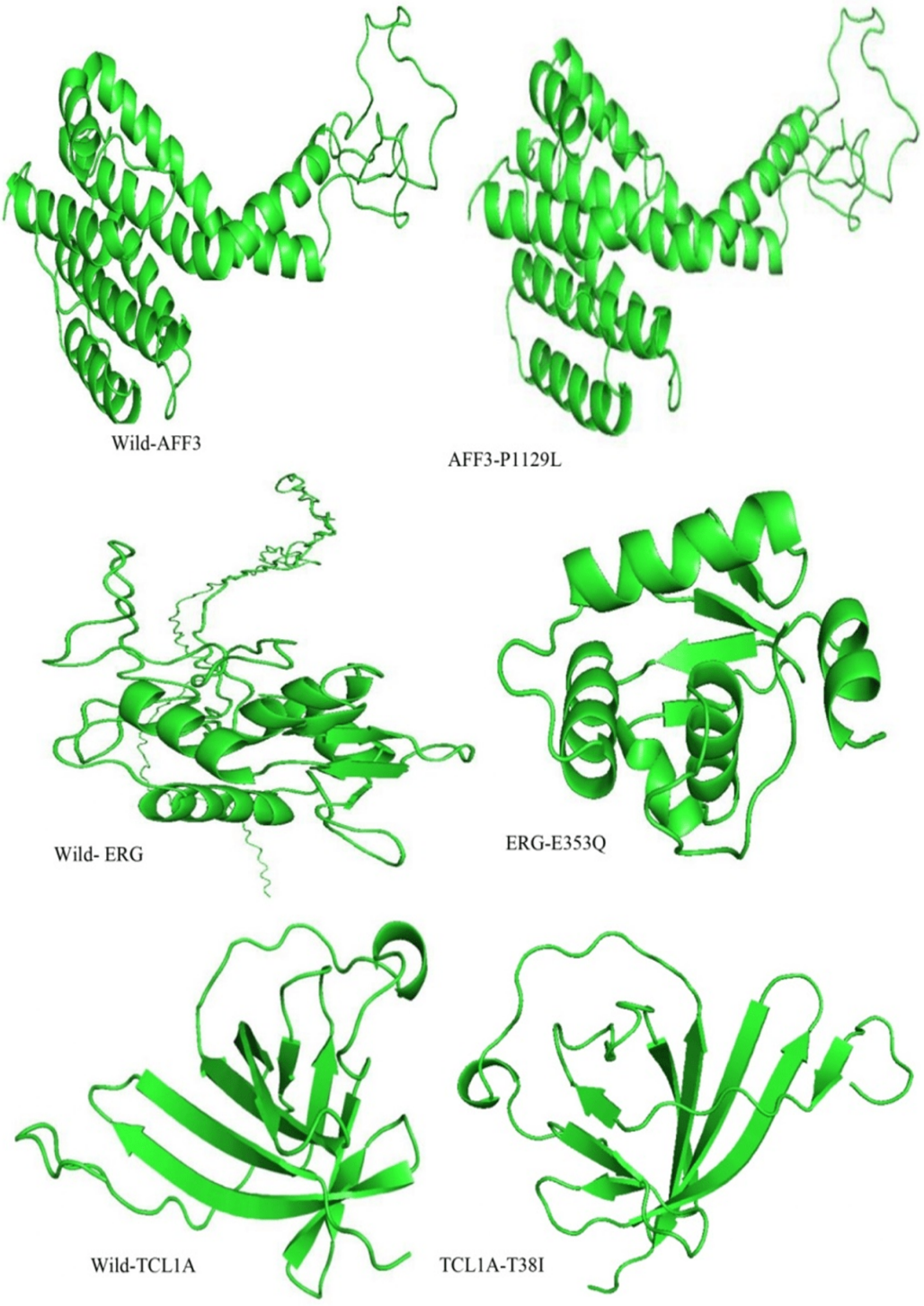

FIGURE 4.13: Wild and mutated 3D models of AFF3, ERG and TCL1A modeled using MODELLER 10.3.

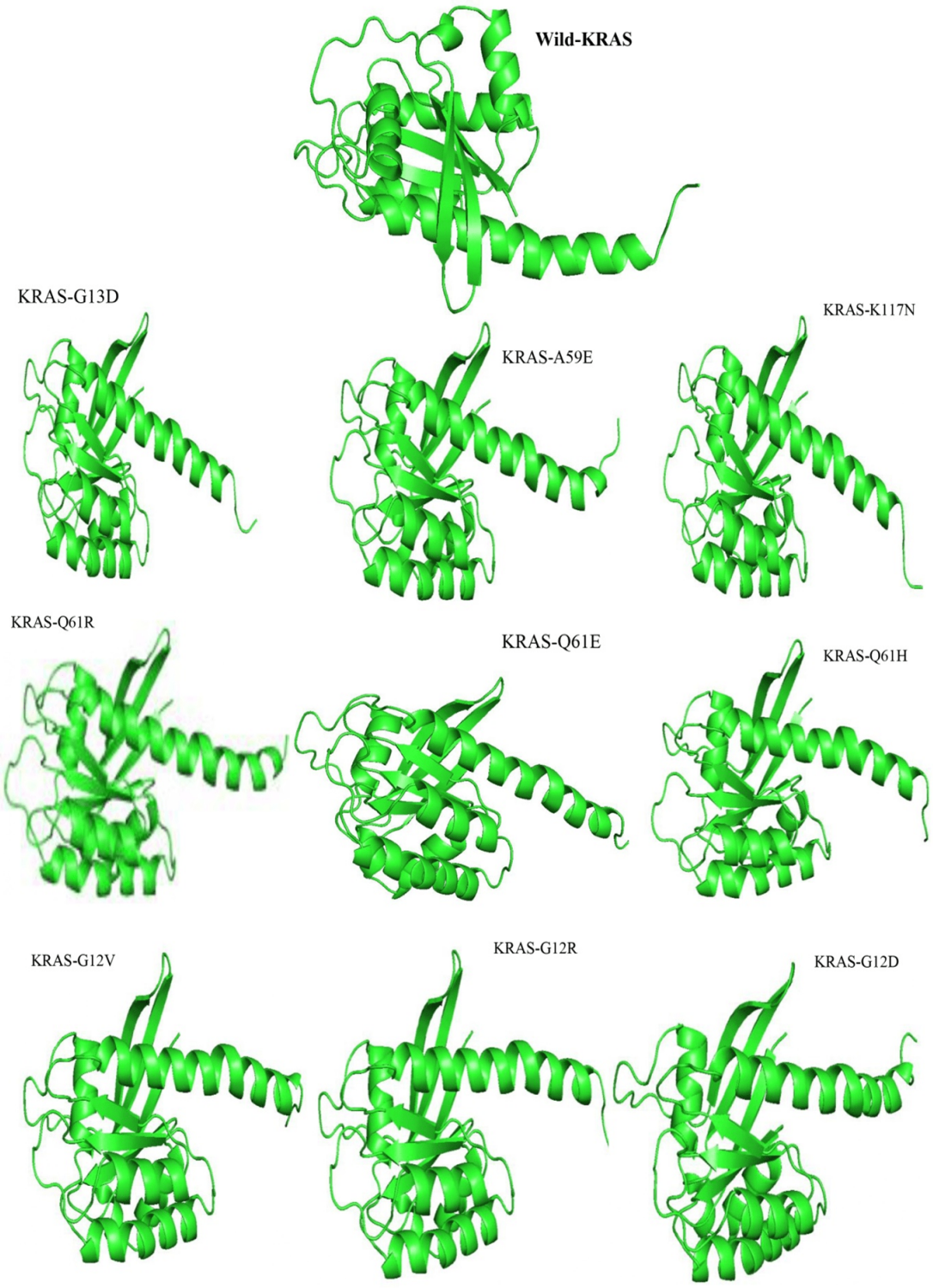

FIGURE 4.14: Wild and mutated 3D models of KRAS modeled using MODELLER 10.3.

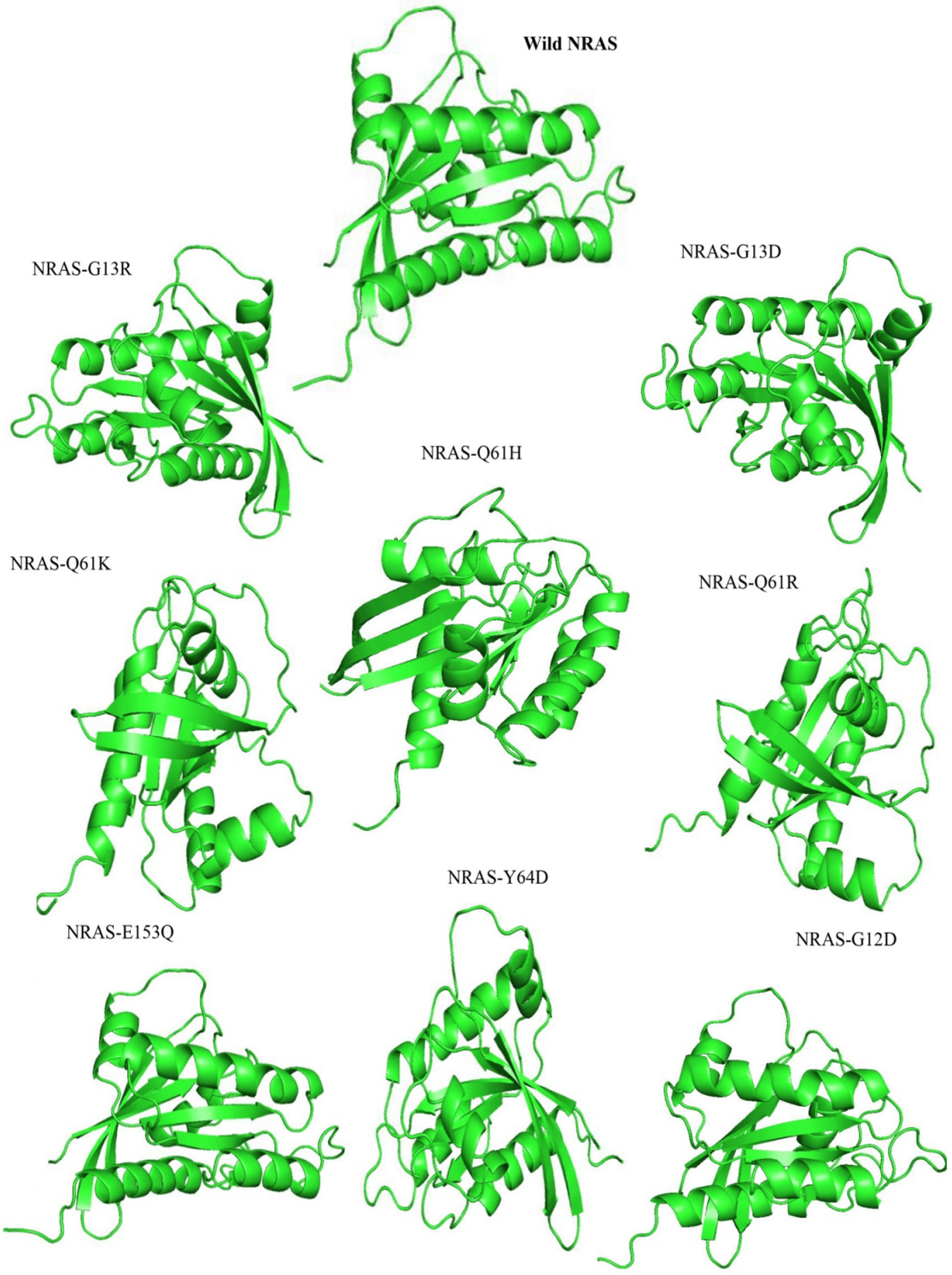

FIGURE 4.15: Wild and mutated 3D models of NRAS modeled using MODELLER 10.3.

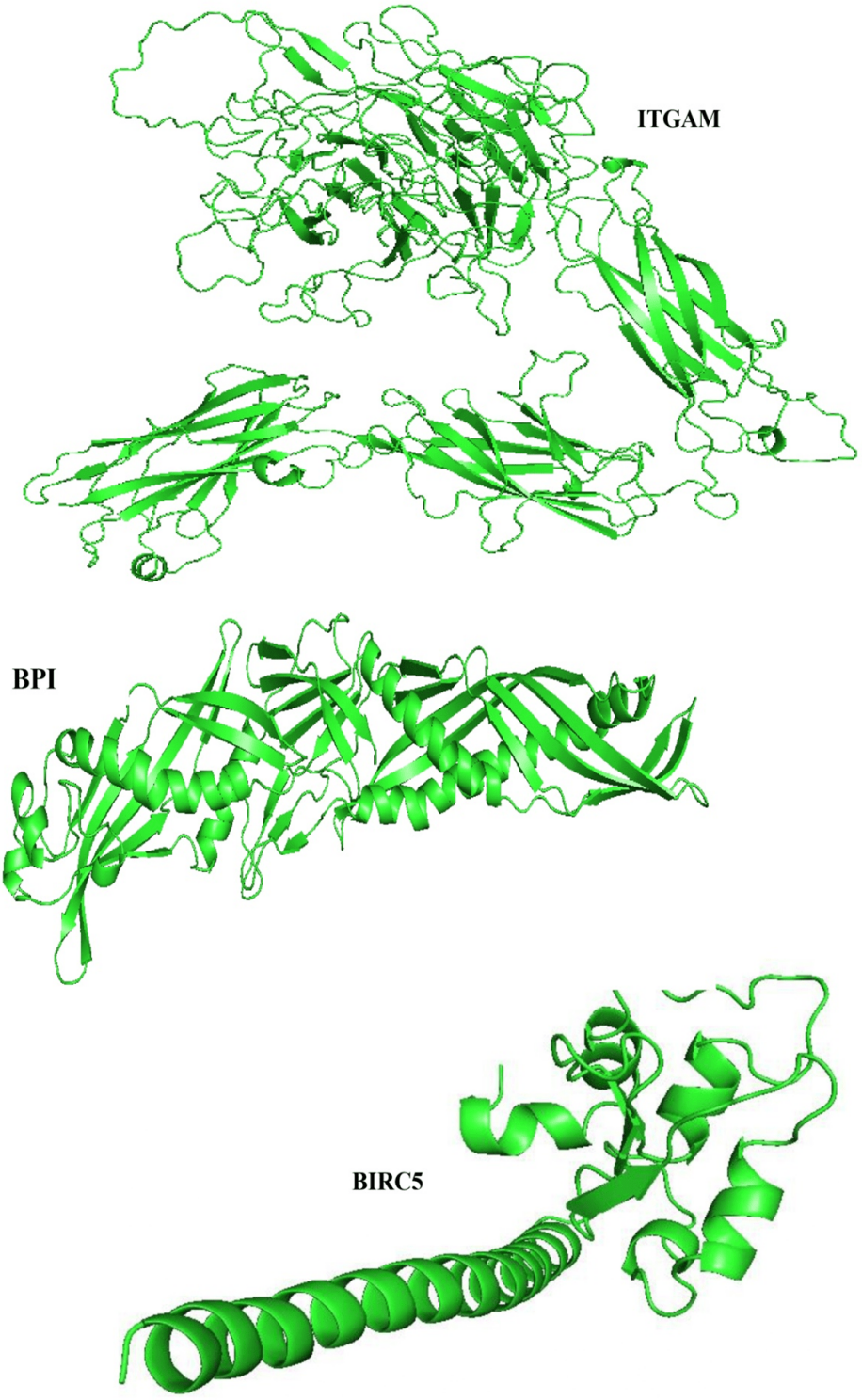

FIGURE 4.16: 3D structure of ITGAM, BP1, and BIRC5 modeled using MODELLER 10.3

TABLE 4.8: DOPE scores of homology modeling based wild-type and mutant predicted structures

Sr.#	**Protein Model**	**DOPE Score**
1	TCL1A-wild	-12042.28
2	TCL1A-T38I	-11815.05
3	ERG-wild	-11079.66
4	ERG-E353Q	-10813.77
5	AFF3-wild	-27135.50
6	AFF3-P1129L	-27109.84
7	BIRC5	-13211.27
8	BPI	-53158.93
9	ITGAM	-98373.27
10	KRAS-wild	-20292.62
11	KRAS-Q61R	-20219.83
12	KRAS-Q61H	-20196.07
13	KRAS-Q61E	-20009.27
14	KRAS-K117N	-20028.12
15	KRAS-G13D	-20107.05
16	KRAS-G12V	-20218.21
17	KRAS-G12R	-20191.55
18	KRAS-G12D	-20084.79
19	KRAS-A59E	-20075.51
20	NRAS-wild	-19549.66
21	NRAS-E153Q	-19406.07
22	NRAS-G12D	-19526.53
23	NRAS-G13D	-19402.41
24	NRAS-G13R	-19399.37
25	NRAS-Q61H	-19298.97
26	NRAS-Q61K	-19270.29
27	NRAS-Q61R	-19367.64
28	NRAS-Y64D	-19235.67

4.11 Structural Assessment of Predicted 3D Models

In order to evaluate the quality and precision of the models, several metrics were computed, such as ERRAT, ProSA, and QMEAN. The ERRAT score serves as a metric for assessing the integrity and reliability of a given protein structure. The calculation involves a comparison of non-bonded interactions among various atom types inside the protein structure with a statistical distribution of non-bonded interactions derived from meticulously polished protein structures. The ERRAT score is a numerical metric that ranges from 0 to 100, where higher values signify a stronger level of concordance between the model and the empirical observations. The ERRAT score was acquired by submitting protein structure pdb files to the web server of the UCLA-DOE LAB (saves.mbi.ucla.edu/) and using the ERRAT option. The same methodology was employed for each individual structure in an orderly manner. The ProSA score, which is commonly employed for the purpose of assessing potential errors in protein structure models, calculates a Z-score to analyse the varience of the input protein structure from the energy profile of a random coil. The Z-score value can be classified into three distinct categories: -6 or lower, -6 to 0, and greater than 0. These categories correspond to the assessment of good quality, acceptable quality, and low quality, respectively, in relation to the 3D structure of a protein. The protein data bank (PDB) structure was utilized as input for the ProSA-web server (prosa.services.came.sbg.ac.at), which subsequently generated the Z-score and a graphical representation of the overall quality of the protein structure. The QMEAN scoring function is a composite method that may calculate absolute quality estimates for both the entire structure (global) and individual residues (local) using a single model. The scores range from 0 to 1, with a score of 1 indicating a high level of excellence. The QMEAN scorer was accessed by submitting the pdb file to the QMEAN webserver (swissmodel.expasy.org/qmean/), followed by selecting the QMEAN option and initiating the submission process.

The assessment scores for all predicted structures were assembled in Table 4.9. It was noted that both the wild and mutant versions of TCL1A exhibited good

quality based on the ERRAT (80.58, 84.76) and QMEAN (0.93, 0.89) scores. Additionally, the ProSA scores (-3.69, -3.66) fell within an acceptable range. In a comparable manner, it was shown that both the wild and mutant modelled structures of MNX1 exhibited satisfactory quality based on the ERRAT scores (71.65, 77.08) and ProSA analysis, however they demonstrated low quality as indicated by the QMEAN scores (0.34, 0.36). Furthermore, the ERRAT score for both the wild-type and mutant forms of the three domains of FAT1 was above 70, with the exception of Wild-FAT1-M739I, which had a value of 68.54. The ProSA score demonstrated that the wild and mutant structures of two domains (FAT1-M739I, FAT1-D2382A) exhibited a high level of quality, However, the score indicated a poor level of quality for both the wild and mutated structures of the third domain (FAT1-P4309S). Additionally, the QMEAN analysis revealed that all predicted structures of the FAT1 domains were of low quality. In contrast, the anticipated conformations of the wild and mutated ERG, wild and mutated AFF3, wild KRAS, all variants of KRAS, Wild NRAS, and all variants of NRAS exhibited a high level of quality as determined by the three scoring metrics (Table 4.9). However, the ERRAT score revealed the good quality (> 80) of all other biomarkers (without SNVs) except ITGAM (66.54) (Table 4.8). Similarly, all the predicted structures were either of "good quality" or "acceptable quality" according to ProSA score. Moreover, according to QMEAN score all structure were of acceptable category except TYROBP (Table 4.8).

TABLE 4.9: ERRAT, ProSa and QMEAN evaluation of predicted protein structures

Sr.#	**Model**	**ERRAT**	**ProSA**	**QMEAN**
1	Wild -TCL1A	80.58	-3.69	0.93
	TCL1A-T38I	84.76	-3.66	0.89
2	Wild- ERG	94.68	-7.52	0.77
	ERG-E353Q	85.11	-7.39	0.74
3	Wild-AFF3	83.40	-7.12	0.69
	AFF3-P1129L	86.06	-7.22	0.70
4	Wild -MNX1	71.65	-4.77	0.34

Sr.#	Model	ERRAT	ProSA	QMEAN
	MNX1-P392L	77.08	-4.66	0.36
5	Wild-FAT1-D2382A	73.20	-5.28	0.62
	Mutant-FAT1-D2382A	85.57	-5.27	0.59
	Wild-FAT1-M739I	68.54	-4.01	0.49
	Mutant-FAT1-M739I	72.41	-4.27	0.47
	Wild-FAT1-P4309S	72.92	-1.45	0.32
	Mutant-FAT1-P4309S	75.35	-1.61	0.32
6	Wild-KRAS	89.14	-7.6	0.78
	KRAS-Q61R	93.14	-7.75	0.78
	KRAS-Q61H	86.29	-7.63	0.78
	KRAS-Q61E	85.71	-7.6	0.78
	KRAS-K117N	85.14	-7.53	0.78
	KRAS-G13D	88	-7.65	0.77
	KRAS-G12V	77.14	-7.5	0.78
	KRAS-G12R	81.71	-7.41	0.78
	KRAS-G12D	89.14	-7.77	0.77
	KRAS-A59E	90.29	-7.44	0.80
7	Wild-NRAS	87.20	-6.32	0.83
	NRAS-E153Q	81.71	-6.44	0.82
	NRAS-G12D	75	-6.47	0.83
	NRAS-G13D	81.71	-6.15	0.83
	NRAS-G13R	79.88	-6.4	0.82
	NRAS-Q61H	77.44	-6.32	0.83
	NRAS-Q61K	75.61	-6.32	0.82
	NRAS-Q61R	71.95	-6.26	0.82
	NRAS-Y64D	78.05	-6.4	0.82
8	BIRC5	95.3846	-5.31	0.86
9	BPI	83.0357	-8.92	0.84
10	CD4	80.2469	-7.42	0.79
11	COL22A1	90.4393	-9.74	0.65
12	CSF1R	80.1735	-10.46	0.68

Sr.#	Model	ERRAT	ProSA	QMEAN
13	IL1B	85.7988	-4.02	0.61
14	ITGAM	66.54	-7.97	0.52
15	NRP1	86.4384	-8.77	0.68
16	PTPRC	90.102	-12.13	0.68
17	TYROBP	83.10	-0.49	0.46
18	VCAN	87.931	-8.34	0.60

4.12 Assessment of Solvent-Accessible Surface Area (SASA) of 3D Structures

The SASA is a key structural parameter that can influence protein structure, stability, and function. It provides information about a protein's surface exposure, flexibility, hydrophobicity, and potential interaction sites. Understanding SASA is crucial for elucidating the mechanisms of protein folding, binding, enzymatic activity, and other biological processes. The SASA analysis for the wild and mutant models revealed the accessibility of the residues to the solvent. The pdb structures of both wild and mutant proteins provide to GETAREA generated a quantitative assessment of the polar and apolar areas across the protein surface were compiled in Table 4.9.

Variety of trends was observed by all biomarkers that would affect the protein structure stability and interaction with polar solvent and other proteins. The results revealed that the there was a significant decrease in polar area (2714.03 → 1975.66) and buried residues (387 → 368) and an increase in apolar (4736.64 → 4813.82) and exposed residues (562 → 582) on surface of TCL1A due to SNV T38I. The SNV P392L modulated the MNX1 structure by decreasing the surface polar area (11992.58 → 11224.04), apolar area (29532.61 → 28968.57), exposed residues (2396 → 2385) and increasing buried residues (461 → 473). However opposite trend was followed by AFF3 due to P1129L, increase in polar area (3625.58 →

3966.75), buried residues (835 → 926) and decrease in apolar area (10415.28 → 9979.09) and exposed residues (1219 → 1129).

The number of surface interacting residues and buried residues were obtained as 562 and 387 for TCL1A, 485 and 351 for ERG, 1174 and 880.5 for AFF3, 2390.5 and 467 for MNX1, 525 and 278 for FAT1-D2382A-wild, 524 and 228 for FAT1-M739I-wild, 1694 and 696 for FAT1-P4309S-wild, 833.1 and 639.3 (KRAS), 770.22 and 602.33 (NRAS).

Additionally, it was observed that ERG did not experience major changes in polar and apolar areas with respect to the ERG-wild. Among KRAS and NRAS models, the least difference of polar areas was obtained for KRAS-G13D, KRAS-G12D, and NRAS-Y64D, while minimum apolar changes were observed for KRAS-Q61R, KRAS-Q61E, KRAS-117N, KRAS-G13D, KRAS-A59E, NRAS-G12D, NRAS - G13R, NRAS-Q61H, NRAS-Q61K, and NRAS-Y64D.

The major changes in values of surface and buried residues were obtained for AFF3-P1129L, while the least differences were observed for ERG-E353Q, KRAS-Q61R, KRAS-Q61H, KRAS-G12V, KRAS-G12D, NRAS-E153Q, NRAS-G12D, NRAS-Q61R, and NRAS-Y64D. Moreover, a drastic decrease in the polar area was observed for TCL1A-T38I and MNX1-P392L, while a significant decrease in apolar values was observed for AFF3-P1129 and MNX1-P392L.

TABLE 4.10: Assessment of Solvent-Accessible Surface Area (SASA) of 3D Structures

Structure Name	**Polar Area / Energy**	**Apolar Area**	**Surface residues**	**Buried Residues**
TCL1A-wild	2714.03	4736.64	562	387
TCL1A-T38I	1975.66	4813.82	582	368
ERG-wild	2549.63	3608.81	488	348
ERG-E353Q	2516.90	3515.55	482	354
AFF3-wild	3625.58	10415.28	1219	835
AFF3-P1129L	3966.75	9979.09	1129	926
MNX1-wild	11992.58	29532.61	2396	461
MNX1-P392L	11224.04	28968.57	2385	473
FAT1-D2382A-wild	2429.61	4190.30	525	278

Structure Name	**Polar Area / Energy**	**Apolar Area**	**Surface residues**	**Buried Residues**
FAT1-D2382A-mutant	2330.67	4238.38	526	274
FAT1-M739I-wild	1991.81	4480.98	524	228
FAT1-M739I-mutant	2007.38	4497.42	537	215
FAT1-P4309S-wild	6100.98	11670.53	1694	696
FAT1-P4309S-mutant	6123.97	11639.47	1712	677
KRAS-wild	4070.23	6042.71	831	639
KRAS-Q61R	3967.16	6048.95	833	639
KRAS-Q61H	3983.64	6118.92	832	639
KRAS-Q61E	3984.05	6068.53	849	621
KRAS-K117N	3996.11	6026.78	843	626
KRAS-G13D	4029.49	6047.97	854	620
KRAS-G12V	3840.33	6163.72	827	646
KRAS-G12R	3941.12	6175.92	822	655
KRAS-G12D	4032.99	5930.52	831	643
KRAS-A59E	3866.16	6058.73	809	665
Mean	3971.13	6068.28	833.1	639.3
NRAS-wild	3892.46	5208.81	778	593
NRAS-E153Q	3716.75	5270.77	785	586
NRAS-G12D	3728.07	5187.68	783	592
NRAS-G13D	3743.66	5271.77	761	614
NRAS-G13R	3805.41	5194.31	764	614
NRAS-Q61H	3646.61	5254.90	754	618
NRAS-Q61K	3720.43	5212.96	752	619
NRAS-Q61R	3773.72	5278.54	781	592
NRAS-Y64D	3843.49	5180.96	774	593
Mean	3763.4	5228.97	770.22	602.33

4.13 Visualization and Structure Comparison of Wild and Mutant Candidate Relapse Biomarkers with SNVs

The RMSD analysis aimed to assess the impact of mutation on the 3D structure of the proteins was conducted for the candidate relapse biomarkers with SNVs. The mutant models were superimposed over their corresponding wild-type protein structures in order to determine the RMSD values, which quantify

the structural variations between the mutant and wild-type structures. The results were presented in Table 4.10 indicated that RMSD values for the TCL1A-T38I, ERG-E353Q, AFF3-P1129L, MNX1-P392L, FAT1-D2382A, FAT1-M739I, and FAT1-P4309S variants, when compared to their respective wild-type counterparts (TCL1A, ERG, AFF3, MNX1, FAT1-D2382A, FAT1-M739I, and FAT1-P4309S), were found to be 1.04, 0.13, 0.52, 0.53, 0.13, 0.14, and 0.06, respectively. The mutant models NRAS-E153Q, NRAS-Q61H, NRAS-Q61R, and NRAS-Y64D exhibited the RMSD value of 0.09 when compared to NRAS-wild. In contrast, elevated values were noted for NRAS-G13R (0.14), NRAS-G12D (0.13), NRAS-G13D (0.10), and NRAS-Q61K (0.10). Furthermore, the examination of RMSD disparities among different KRAS mutants demonstrated that the most substantial RMSD deviation was detected in the case of KRAS-A59E (0.23), followed by KRAS-Q61H (0.17), KRAS-Q61E (0.15), KRAS-K117N (0.14), KRAS-G13D (0.14), and KRAS-G12V (0.14). The model KRAS-Q61R, KRAS-G12R, and KRAS-G12D had the lowest RMSD value of 0.13. To summarize the aforementioned results, it can be concluded that RMSD values for TCL1A-T38I (1.04), AFF3-P1129L (0.52), MNX1-P392L (0.53), FAT1-M739I (0.14), ERG - E353Q (0.13), and FAT1-D2382A (0.13) demonstrate substantial structural alterations in the mutant forms when compared to the corresponding wild-type structures, as illustrated in Figures 4.17 and 4.18. The significant structural alterations of all KRAS variations are evident from the RMSD values, as depicted in Figure 4.19. In contrast, the evaluation of NRAS mutants indicated the absence of significant structural alterations, as evidenced by the minor RMSD differences seen for all the models depicted in Figure 4.20.

TABLE 4.11: RMSD values of the wild and mutant candidate relapse biomarkers with SNV

Sr.#	**Structure Name**	**RMSD (Angstroms)**
1	Wild TCL1A- TCL1A-T38I	1.04
2	Wild ERG -ERG-E353Q	0.13
3	Wild AFF3 - AFF3-P1129L	0.52
4	Wild MNX1-MNX1-P392L	0.53

Sr.#	Structure Name	RMSD (Angstroms)
5	Wild FAT1-D2382A-FAT1-D2382A-mutant	0.13
6	Wild FAT1-M739I-FAT1-M739I-mutant	0.14
7	Wild FAT1-P4309S-FAT1-P4309S-mutant	0.06
8	Wild-KRAS - KRAS-Q61R	0.13
9	Wild-KRAS - KRAS-Q61H	0.17
10	Wild-KRAS - KRAS-Q61E	0.15
11	Wild-KRAS - KRAS-K117N	0.14
12	Wild-KRAS - KRAS-G13D	0.14
13	Wild-KRAS - KRAS-G12V	0.14
14	Wild-KRAS - KRAS-G12R	0.13
15	Wild-KRAS - KRAS-G12D	0.13
16	Wild-KRAS - KRAS-A59E	0.23
17	Wild NRAS - NRAS-E153Q	0.09
18	Wild NRAS - NRAS-G12D	0.13
19	Wild NRAS - NRAS-G13D	0.10
20	Wild NRAS - NRAS-G13R	0.14
21	Wild NRAS - NRAS-Q61H	0.09
22	Wild NRAS - NRAS-Q61K	0.10
23	Wild NRAS - NRAS-Q61R	0.09
24	Wild NRAS - NRAS-Y64D	0.09

4.14 Molecular Dynamics (MD) Simulation of Wild and Mutant Candidate Relapse Biomarkers with SNVs

MD simulations of wild and mutated models of candidate relapse biomarkers were performed to assess the effects of mutation over structure stability of protein.

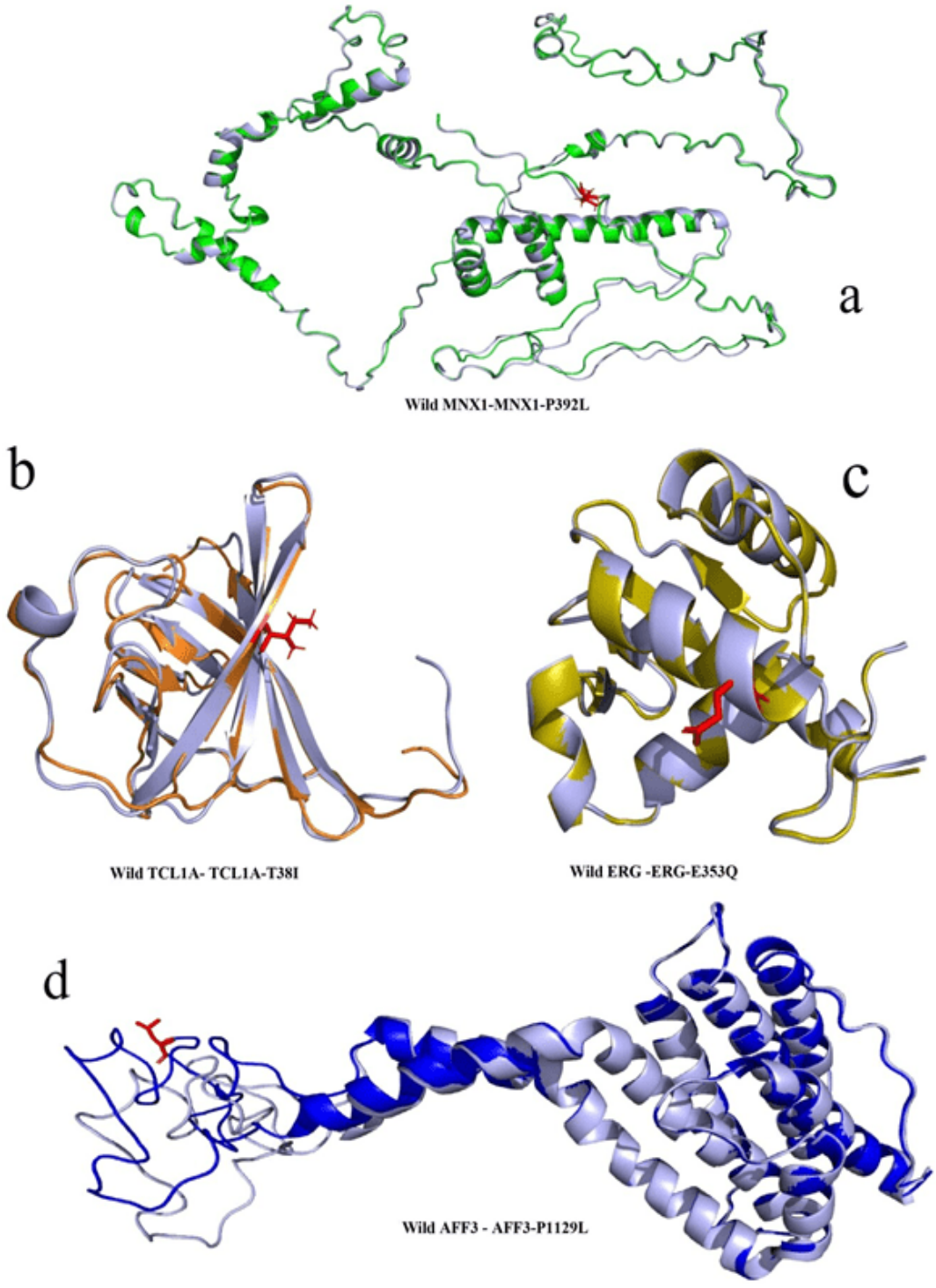

FIGURE 4.17: Superimposition of (a) the MNX1-wild (light blue) and mutant MNX1-P392L (green) (b) TCL1A-wild (light blue) and mutant TCL1A-T38I (orange) (c) ERG-wild (light blue) and mutant ERG-E353Q (olive) (d) AFF3-wild (light blue) mutant AFF3-P1129L (dark blue) illustrating structural deviations with respect to mutant residue represented as a red stick.

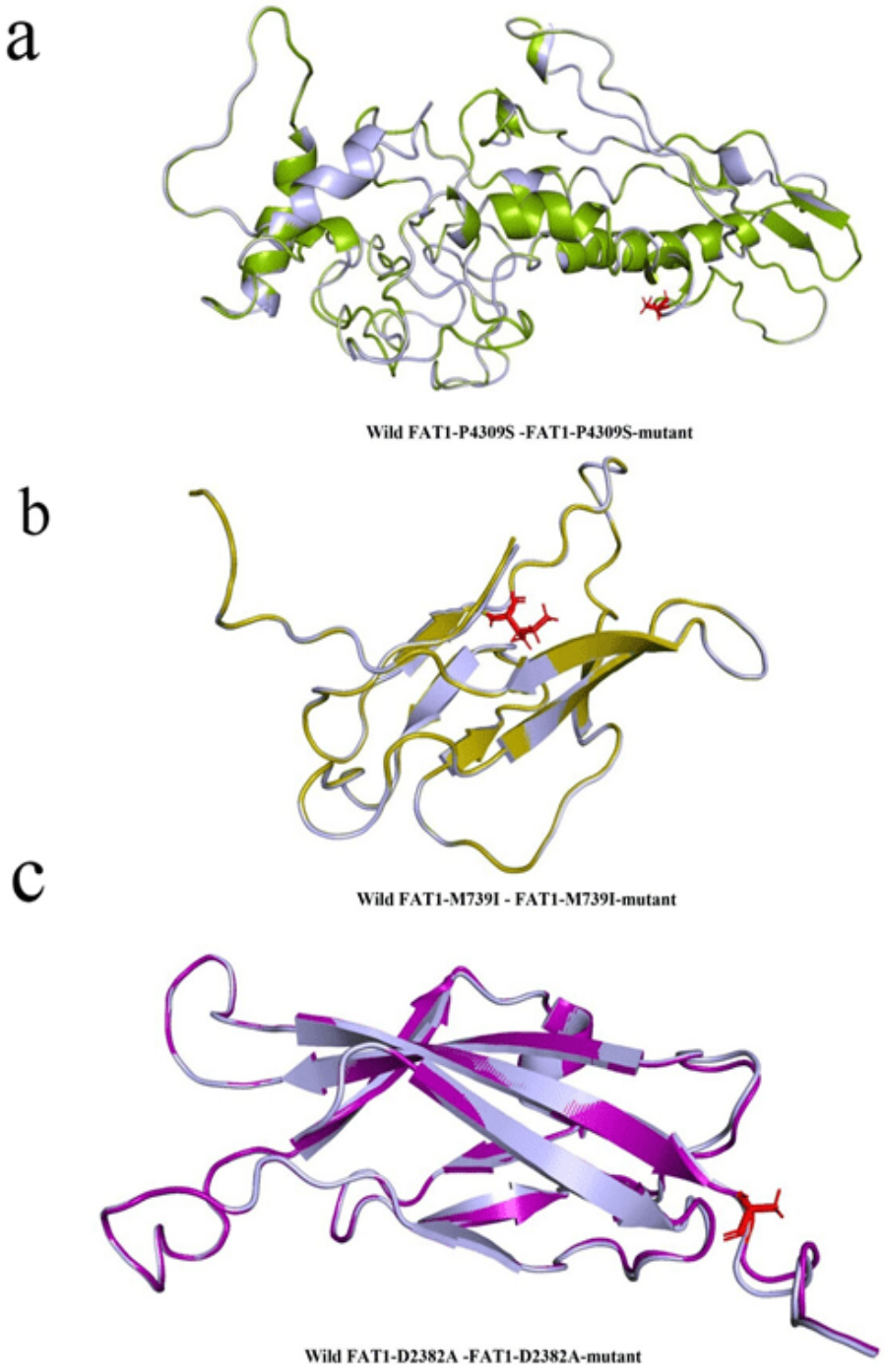

FIGURE 4.18: Superimposition of the (a) FAT1-P4309S-wild (light blue) and mutant FAT1-P4309S (green) (b) FAT1-M739I-wild (light blue) and mutant FAT1-D2382A (olive) and (c) FAT1-D2382A-wild (light blue) and mutant FAT1-D2382A (purple) illustrating structural deviations with respect to mutant residue represented as a red stick.

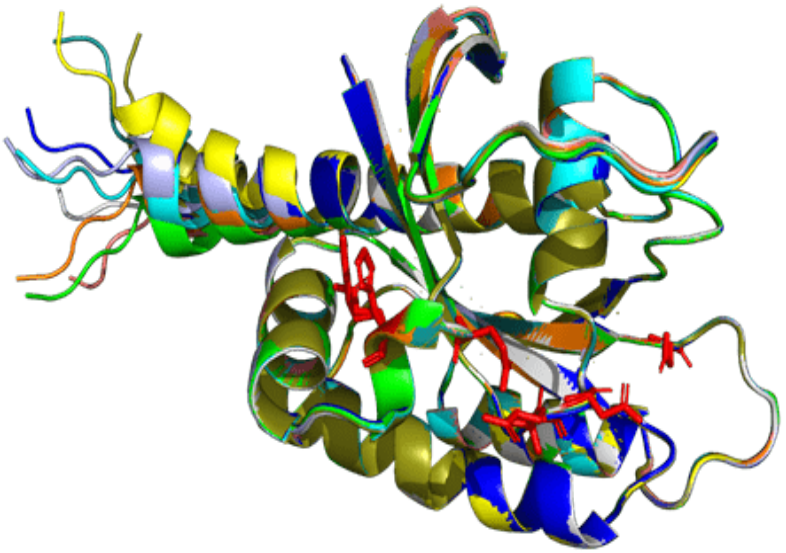

FIGURE 4.19: Superimposition of the KRAS-wild (light blue) and mutant models KRAS-K117N (salmon), KRAS-G12D (teal), KRAS-G13D (gray), KRAS-G12V (cyan), KRAS-Q61H (green), KRAS-G12R (orange), KRAS-Q61R (yellow), KRAS-Q61E (dark blue), KRAS-A59E (olive) illustrating structural deviations with respect to mutant residues represented as red sticks.

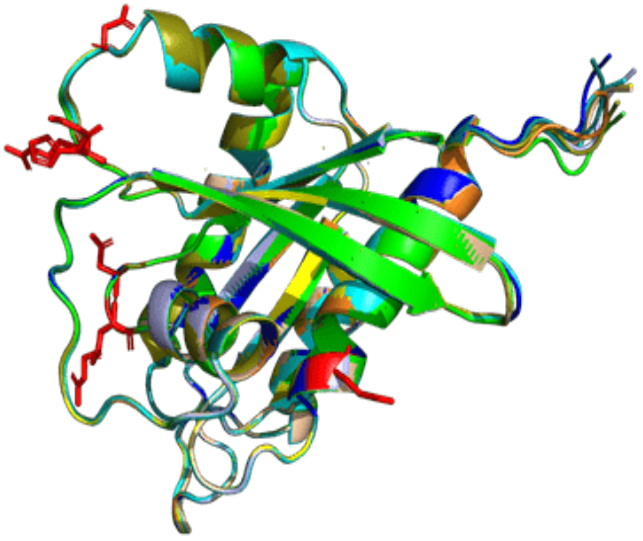

FIGURE 4.20: Superimposition of the NRAS-wild (light blue) and mutant models NRAS-E153Q (dark blue), NRAS- G12D (cyan), NRAS-G13D (yellow), NRAS-G13R (green), NRAS- Q61H (teal), NRAS-Q61K (orange), NRAS-Q61R (wheat) and NRAS- Y64D (olive) illustrating structural deviations with respect to mutant residues represented as red sticks.

4.14.1 MD Simulations of TCL1A Wild & Mutant (TCL1A-T38I) Model

As shown in Figure 4.21(b), the RMSD analysis for TCL1A-wild revealed the stability of this model throughout the simulation period, however, minor fluctuations were observed from the start till 27.0 ns. It was observed that the protein obtained optimal stability around the RMSD value of 3 A after 27.0 ns till the end, showing the least fluctuations. At the end of the simulation run (50.0ns), TCL1A-wild exhibited fluctuation of 3.35 Å. On the other hand, the RMSD analysis of TCL1A-mutant indicated that the model was found stable overall with only minor conformational changes indicated at the start of the simulation, however, stability was attained after 26.0 ns whereas the optimal stability was observed from 39.0 ns to 50.0 ns. At the end of the simulation, this mutant model of TCL1A attained the RMSD of 3.26 A. Furthermore, the RMSF analysis for TCL1A-wild indicated in Figure 4.21(a) revealed stability of overall amino acids residue as major fluctuating parks were only obtained for the terminal amino acids. The amino acids residues of TCL1A-wild that showed considerably large RMSF values included MET-1 (9.41 Å), ALA-2 (8.55 Å), GLU-3 (7.02 Å), CYS-4 (5.76 Å) and PRO-5 (4.78 Å). Meanwhile, it was observed that the TCL1A-mutant residues did not experience any significant fluctuations except for the residues lying at terminal positions. The large RMSF values were obtained for MET-1 (7.16 Å), ALA-2 (4.45 Å), and PRO-5 (4.21 Å).

4.14.2 MD Simulation of ERG Wild & Mutant (ERG-E353Q) Model

As depicted in Figure 4.22(a), the RMSD results obtained for ERG-wild depict the stability of this model throughout the simulation in the ranges of 1-2Å RMSD values. It was observed that this model experienced no major fluctuations indicating no significant conformational instability. At the end of the simulation run of 50.0 ns, ERG-wild attained an RMSD value of 1.67 A. Meanwhile, the RMSD

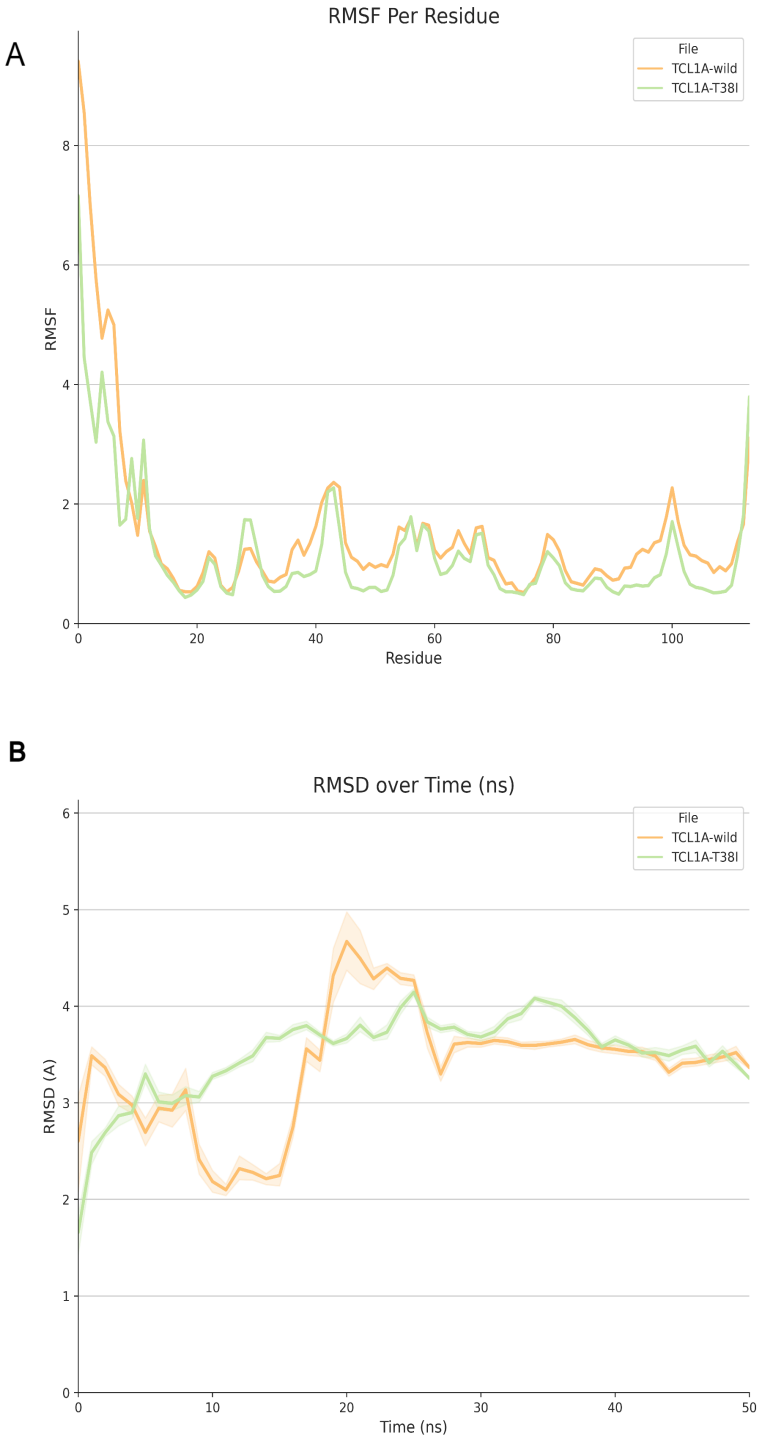

FIGURE 4.21: a) RMSF graph representing the structural fluctuations observed for amino acid residues between TCL1A-wild and TCL1A-T38I during a simulation period of 50 ns. b) RMSD graph representing the conformational differences between TCL1A-wild and TCL1A-T38I observed during a simulation period of 50 ns.

analysis of the mutant model of ERG showed that it experienced no major fluctuation throughout the simulation period with RMSD values in the range of 1-2 A, whereas the optimal stability was not observed at any time duration. At the end of the simulation (50.0 ns), 2.60 Å RMSD was observed for the ERG-mutant model. Moreover, the RMSF analysis indicated no significantly large fluctuating peaks indicating conformational stability of overall amino acids residues shown in Figure 4.22(b). The maximum RMSF value of 3.90Å was observed for the residue PRO at the position 102. On the other hand, it was observed that no significantly large fluctuating peaks were observed for the amino acids of the mutant model of ERG. The maximum RMSF value of 3.39Å was obtained for the residue SER at 26 positions.

4.14.3 MD Simulations of AFF3 Wild & Mutant (AFF3-P1129L)

It was observed that the AFF3-wild was found to be stable with no major fluctuations indicating conformational instability as depicted in Figure 4.23(a). However, the optimal stability was only observed during the simulation period of 9.0 ns-25.0 ns around the RMSD value of 5 Å. The number of fluctuations was found to be decreasing towards the end of the simulation ending at 6.59Å RMSD (50.0 ns). Meanwhile, the RMSD analysis of the AFF3-mutant showed significant fluctuations throughout the simulation period indicating conformational instability. The optimal stability has been depicted from start till 25.0 ns and from 37.0 ns-47.0 ns. At the end of the simulation run, 13.33Å RMSD was obtained at 50.0 ns. Furthemore, the RMSF analysis for AFF3-wild revealed the large fluctuating peaks for amino acid residues suggesting that these residues were not stable during the simulation as highlighted in Figure 4.23(b).

The large RMSF values indicating instability were obtained for the significant number of residues including LYS-1 (4.70 Å), GLU-61 (4.35 Å), SER-62 (4.26 Å), LYS-132 (4.03 Å), ASN-133 (4.11 Å), SER-135 (4.07 Å), LYS-136 (4.56 Å), ALA-137 (4.34 Å), ALA-140 (4.89 Å), PRO-141 (5.04 Å), SER-142 (6.18 Å), PRO-143

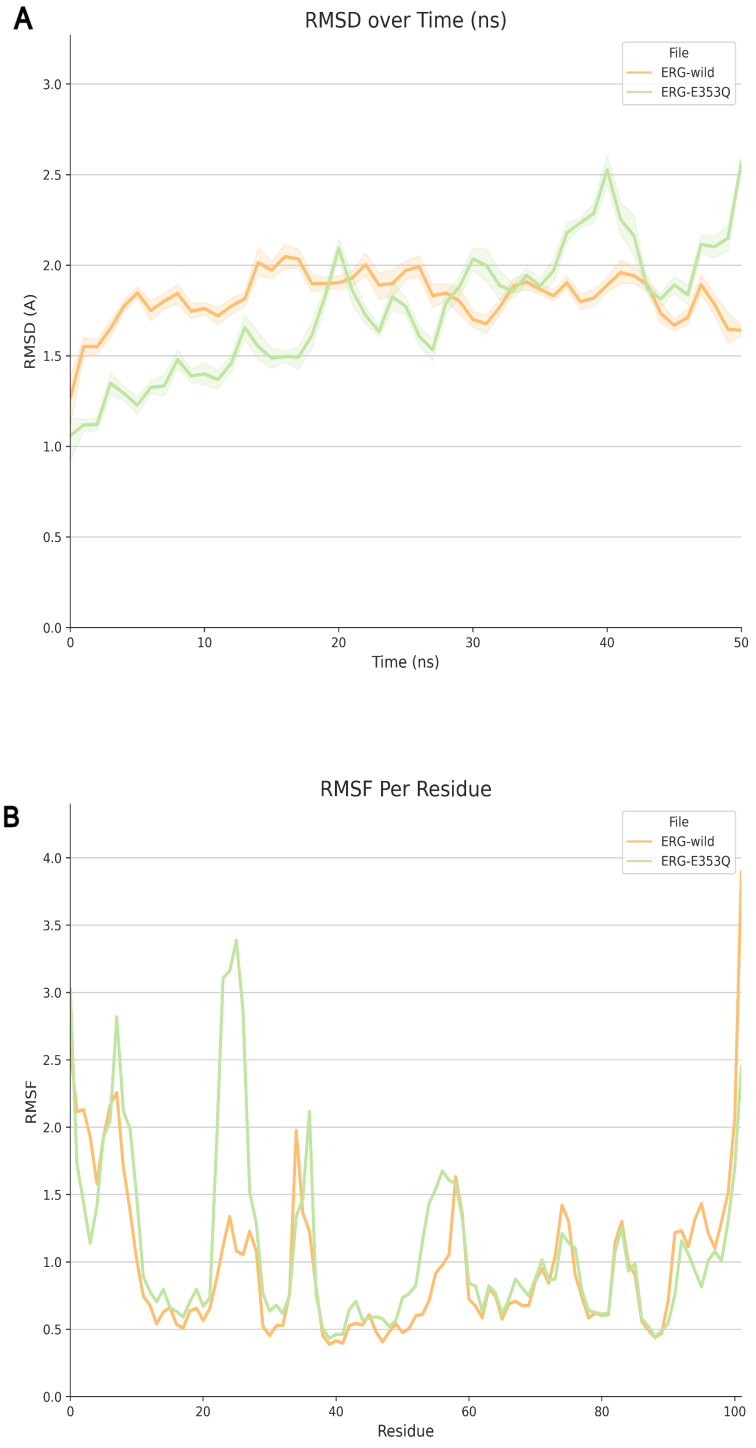

FIGURE 4.22: (a) RMSD graph representing the conformational differences between ERG-wild and ERG-E353Q observed during a simulation period of 50 ns. (b) RMSF graph representing the structural fluctuations observed for amino acid residues between ERG-wild and ERG-E353Q during a simulation period of 50 ns.

(7.27 Å), TRP-144 (8.67), GLY-145 (10.97 Å), ALA-146 (11.06 Å), SER-147 (10.92 Å), GLY-148 (9.71 Å), LYS-149 (9.32 Å), SER-150 (9.13 Å), THR-151 (8.13 Å), GLY-152 (7.61 Å), THR-153 (7.75 Å), PRO-154 (7.93 Å), SER-155 (6.90 Å), PRO-156 (5.58 Å), MET-157 (5.49 Å), SER-158 (7.48 Å), PRO-159 (9.73 Å), ASN-160 (10.28 Å), PRO-161 (9.54 Å), SER-162 (9.58 Å), PRO-163 (8.31 Å), ALA-164 (8.80 Å), SER-165 (8.75 Å), PRO-166 (9.79 Å), VAL-167 (10.05 Å), GLY-168 (10.68 Å), SER-169 (10.46 Å), GLN-170 (9.64 Å), GLY-161 (7.97 Å), SER-172 (6.50 Å), LEU-173 (5.67 Å), SER-174 (5.54 Å), ASN-175 (5.89 Å), ALA-176 (4.70 Å), SER-177 (5.74 Å), ALA-178 (4.43 Å), PRO-181 (4.31 Å), VAL-185 (4.14 Å), SER-186 (4.43 Å) and HIS-261 (4.92 Å).

Whereas the RMSF analysis of the mutant model of AFF3 indicated significant fluctuations experienced by the most of the amino acid residues in the form of fluctuating peaks. It was observed that the residues HIS-26 (6.98 Å), LYS-27 (7.02 Å), ALA-28 (6.93 Å), ASP-29 (8.24 Å), ALA-30 (8.61 Å), MET-31 (8.00 Å), VAL-32 (8.67 Å), GLU-33 (7.90 Å), LYS-34 (7.15 Å), PHE-35 (6.09 Å), GLY-36 (6.29 Å), LYS-37 (6.38 Å), GLU-61 (6.05 Å), SER-62 (6.00 Å), ARG-81 (6.22 Å), LEU-82 (6.33 Å), GLY-87 (6.87 Å), PRO-88 (6.89 Å), ASN-89 (6.53 Å), SER-135 (6.33 Å), LYS-136 (6.21 Å), ALA-137 (6.39 Å), ALA-138 (6.69 Å), GLN-139 (7.45 Å), ALA-140 (8.67 Å), PRO-141 (8.32 Å), SER-142 (9.93 Å), PRO-143 (11.76 Å), TRP-144 (11.99 Å), GLY-145 (14.86 Å), ALA-146 (16.11 Å), SER-147 (15.28 Å), GLY-148 (14.03 Å), LYS-149 (13.51 Å), SER-150 (14.36 Å), THR-151 (15.57 Å), GLY-152 (16.37 Å), THR-153 (14.59 Å), PRO-154 (14.54 Å), SER-155 (12.87 Å), PRO-156 (11.70 Å), MET-157 (11.18 Å), SER-158 (9.44 Å), PRO-159 (8.85 Å), ASN-160 (8.23 Å), PRO-161 (9.37 Å), SER-162 (9.47 Å), PRO-163 (9.85 Å), ALA-164 (9.86 Å), SER-165 (8.88 Å), LEU-166 (9.04 Å), VAL-167 (7.65 Å), GLY-168 (6.64 Å), SER-169 (6.78 Å), GLN-170 (7.61 Å), GLY-171 (7.28 Å), SER-172 (6.70 Å), LEU-173 (7.56 Å), SER-174 (6.47 Å), ALA-176 (7.12 Å), SER-177 (7.85 Å), ALA-178 (9.99 Å), LEU-179 (10.39 Å), SER-180 (9.63 Å), PRO-181 (10.04 Å), SER-182 (9.15 Å), THR-183 (8.81 Å), ILE-184 (7.14 Å), VAL-185 (6.85 Å), SER-186 (6.43 Å), ASN-203 (6.92 Å), SER-204 (6.05 Å), ILE-205 (6.04 Å), LEU-206 (6.67 Å), ALA-260 (6.57 Å) and HIS-261 (8.04 Å) obtained significantly large RMSF values.

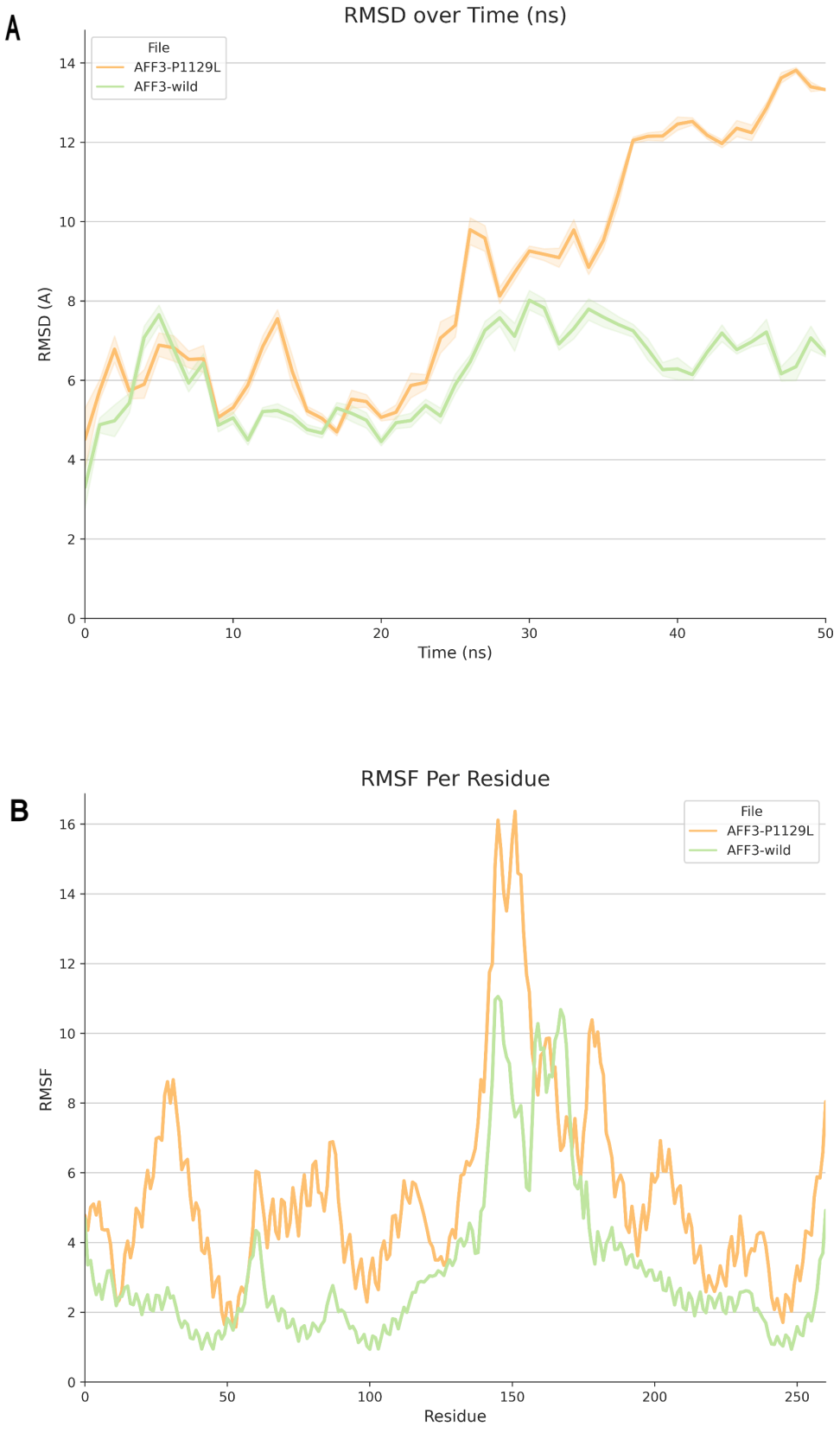

FIGURE 4.23: (a) RMSD graph representing the conformational differences between AFF3-wild and AFF3-P1129L observed during a simulation period of 50 ns. (b) RMSF graph representing the structural fluctuations observed for amino acid residues between AFF3-wild and AFF3-P1129L during a simulation period of 50 ns.

4.14.4 MD Simulation of MNX1 Wild & Mutant (MNX1-P392L) Model

As shown in Figure 4.24(a), the RMSD analysis revealed that the protein showed good stability throughout the simulation period. It was observed that minimum fluctuations were observed overall with the exception for only a small time duration at the start of the simulation before 4.0 ns. It was observed that the RMSD differences in the range of 1-3 Å were obtained for the protein from 4.00-50.0 ns time duration, indicating optimal conformation. At the end of the simulation run (50 ns), a 22.59 Å RMSD value was obtained for MNX1-wild. Meanwhile, the RMSD results for MNX1-P392L revealed that overall this model did not experience any major conformational changes as the fluctuations were obtained before 22 ns. The optimal stability was observed after 22 ns till the end of a simulation period of 50 ns in the range of RMSD differences of 1-3 Å. This model was found to attain the RMSD value of 30.53 Å at the end of the simulation.

Moreover, in Figure 4.24(b) the RMSF analysis showed that a significant number of residues experienced fluctuations as large RMSF values were obtained. The residues that obtained significantly large RMSF values included MET-1 (7.92 Å), SER-4 (7.28 Å), PRO-18 (7.04 Å), ARG-19 (7.53 Å), ALA-20 (7.89 Å), ALA-21 (8.21 Å), SER-22 (8.89 Å), ALA-23 (8.36 Å), GLN-24 (7.61 Å), SER-25 (7.70 Å), ALA-26 (7.04 Å), GLY-48 (7.80 Å), GLY-49 (8.67 Å), ALA-50 (8.06 Å), SER-51 (7.98 Å), GLY-52 (8.22 Å), GLY-53 (7.56 Å), THR-54 (7.06 Å), SER-55 (7.10 Å), GLY-56 (7.67 Å), SER-57 (9.0 Å), CYS-58 (9.72), SER-59 (9.88 Å), PRO-60 (10.52 Å), ALA-61 (10.94 Å), SER-62 (10.05 Å), SER-63 (10.12 Å), GLU-64 (9.21 Å), PRO-65 (8.63 Å), ALA-85 (7.82 Å), ALA-86 (7.99 Å), HIS-87 (7.97 Å), CYS-88 (7.75), ALA-89 (7.53 Å), ALA-99 (7.72 Å), GLY-100 (7.20 Å), GLY-144 (7.69 Å), GLY-145 (7.26 Å), ALA-146 (7.33 Å), GLN-147 (8.25 Å), GLY-148 (8.87 Å), GLY-149 (7.94 Å), ALA-150 (8.49 Å), GLY-151 (8.71 Å), LEU-152 (7.92 Å), PRO-153 (8.19 Å), ALA-154 (7.90 Å), GLN-155 (7.18 Å), GLN-190 (7.02 Å), PRO-194 (7.20 Å), ALA-195 (8.03 Å), HIS-196 (8.12 Å), PRO-197 (7.54 Å), ALA-198 (7.39 Å), GLY-329 (7.62 Å), ALA-330 (7.58 Å), GLU-331 (7.33 Å), GLU-332 (7.50 Å), LEU-333 (7.70 Å), LEU-334 (7.95 Å), GLY-335 (7.26 Å), ARG-349 (7.23 Å),

ASN-372 (7.93 Å), GLY-373 (8.24 Å), ALA-374 (7.26 Å), ALA-378 (7.83 Å), ALA-379 (8.31 Å), SER-380 (8.81 Å), SER-381 (9.28 Å), ASP-382 (10.01 Å), CYS-383 (10.35 Å), SER-384 (11.09 Å), SER-385 (11.94 Å), GLU-386 (10.55 Å), ASP-387 (11.04 Å), ASP-388 (11.35 Å), SER-389 (11.55 Å), PRO-390 (10.68 Å), PRO-391 (10.04 Å), PRO-392 (10.94), ARG-393 (10.48 Å), PRO-394 (11.61 Å), SER-395 (11.85 Å), HIS-396 (13.16 Å), GLN-397 (14.24 Å), PRO-398 (15.56 Å), ALA-399 (16.90 Å), PRO-400 (18.95 Å) and GLN-401 (20.86 Å). On the other hand, the RMSF analysis for the mutant model of MNX1 revealed that amino acid residues of the MNX1 mutant experienced significant conformational instability as a huge gap in RMSF values was obtained as compared to the wild protein residues. It was observed that major fluctuating peaks were obtained for the N-terminal residues, indicating the instability induced in these residues due to mutation. The maximum RMSF values were obtained for ASN-6 (20.03 Å), PHE-7 (22.15 Å), ARG-8 (22.05 Å), ILE-9 (21.88 Å), ASP-10 (21.25 Å) and GLN-24 (20.14 Å). Moreover, the RMSF values of the first 75 residues were found to be greater than 10 Å while the residues at positions 119-170 and 368-375 were also observed with RMSF value >= 10 Å.

4.14.5 MD Simulations of FAT1 Wild and Mutants (FAT1-D2382A, FAT1-M739I, FAT1-P4309S) Models

The RMSD analysis of the FAT1-D2382A wild and mutant model, as depicted in Figure 4.25(a), demonstrated that the stability of the wild-type protein between 21.40 ns -26.90 ns period, however, it varied from the simulation's beginning to the 17.60 ns period. On the other hand, The mutant model ranged between 13.35 and 21.90 ns in time, and it demonstrated stability from 26.70 ns until the end of the experiment. At the conclusion of the simulation period, the RMSD values for the wild and mutant models were 5.39 Åand 3.27 Å, respectively. Figure 4.25(b) displays the RMSF plot of the wild and mutant models of protein. It shows that the wild-type protein residues fluctuated at positions 1 and 102-105, with PRO (6.13 Å) fluctuating at position 105 the highest, followed by ALA (5.64 Å) at position 1, ASP (5.52 Å) at position 102, and ASN (5.13 Å) at position 103. On

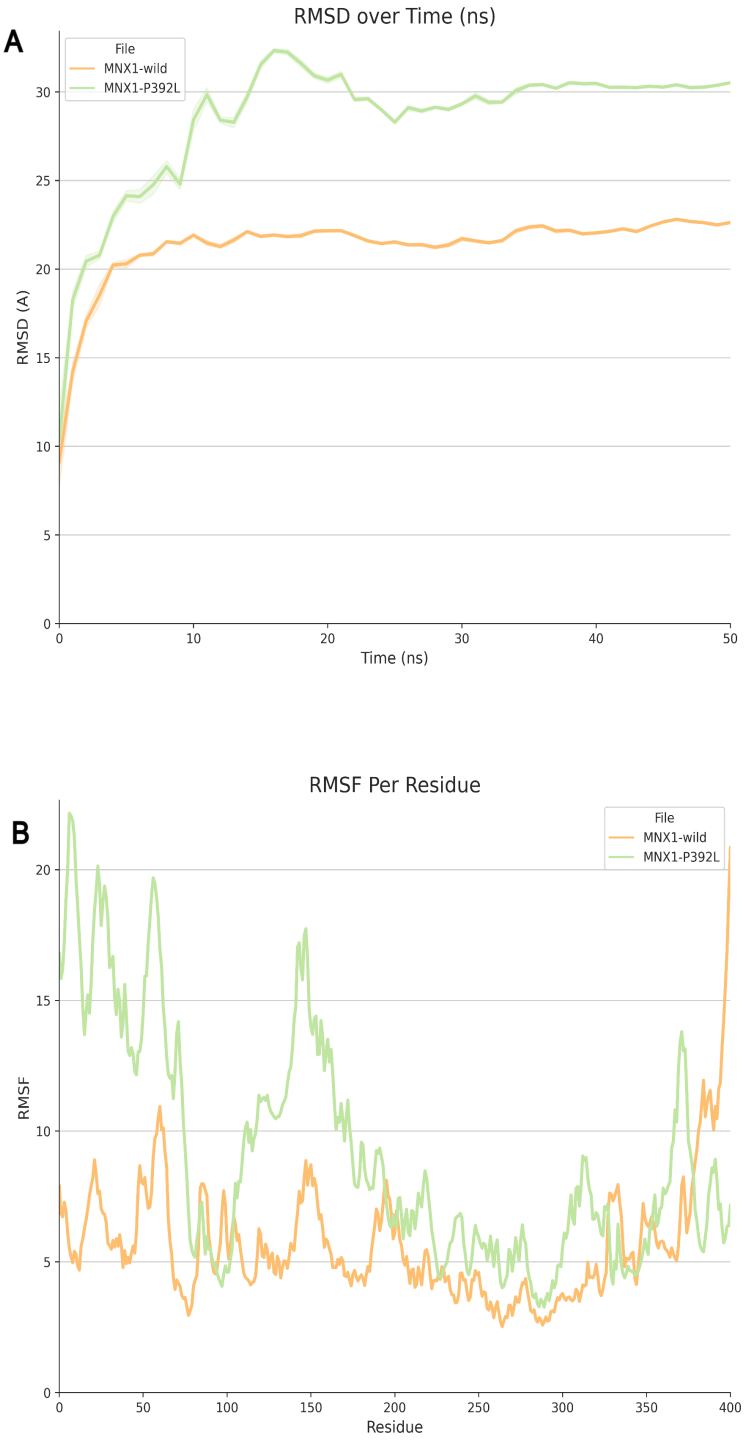

FIGURE 4.24: (a) RMSD graph representing the conformational differences between MNX1-wild and MNX1-P392L observed during a simulation period of 50 ns. (b) RMSF graph representing the structural fluctuations observed for amino acid residues between MNX1-wild and MNX1-P392L during a simulation period of 50 ns

the other hand, the mutant model's residues fluctuated at positions 84,85 and 103-105. PRO (10.37 Å) at position 105 had the greatest fluctuating residue, followed by PRO (7.60 Å) at position 104, ASN (5.46 Å) at position 103, PRO (4.90 Å) at position 85, and MET (4.72 Å) at position 84.

Similar to this, Figure 4.25(a)'s RMSD analysis of the FAT1-M739I wild and mutant model revealed that, while exhibiting oscillations from 15.10 ns to 30.70 ns, the wild-type protein was found to be generally stable between 8.60 ns and 14.25 ns. Alternatively, the protein mutant model exhibited stability from 36.60 ns to the simulation's conclusion. It was found to be generally fine, but it fluctuated most (6.28 Å) at 25.20 ns. At the conclusion of the simulation period, the RMSD values for the protein's wild-type and mutant models were 3.77 Åand 4.12 Å, respectively. On the other hand, the RMSF plot of the wild-type and mutant model of the protein, as shown in Figure 4.25(b), showed that only two wild-type protein residues, PRO (5.99 Å) and PRO (4.80 Å), fluctuated at positions 97 and 98, respectively, however, the mutant model protein residues fluctuated at positions 95-98.

Furthermore, the FAT1-P4309S wild-type and mutant models' RMSD analyses, which are displayed in Figure 4.25(a), revealed that the wild-type protein fluctuated between 22.35 and 34.55 ns in time but demonstrated stability between 5.55 and 19.05 ns. On the other hand, the protein mutant model was seen to exhibit variations from 33.45 ns until the simulation's conclusion, and to be stable between 22.65 ns and 32.30 ns in time. At the conclusion of the simulation, the value of RMSD for the wild-type and mutant protein models were 6.82 Åand 7.84 Å, respectively. Additionally, the RMSF plot of the protein's wild-type and mutant models, as shown in Figure 4.25(b), revealed that the protein's wild-type model exhibited notable oscillations at positions 1-5, 58-66, 204–214, and 283-294. ARG (7.37 Å) at position 206, PHE (9.32 Å) at position 207, LEU (8.90 Å) at position 209, ARG (7.37 Å) at position 206, VAL (6.86 Å) at position 60, and VAL (6.64 Å) at position 59 were the positions with the most fluctuating residues. Conversely, the protein mutant model had variable residues at positions 1-3, 152-158, and 264-295. The residue with the highest fluctuation was ILE (9.12 Å) at

position; it was followed by PRO (7.39 Å) at position 2, TYR (6.97 Å) at position 287, GLY (6.94 Å) at position 293, THR (6.77 Å) at position 266, SER (6.75 Å) at position 265, ASP (6.52 Å) at position 286, SER (6.47 Å) and ASP (6.47 Å) at positions 156 and 157, respectively, GLU (6.02 Å) at position 288, and GLU (5.85 Å) at position 3.

4.14.6 MD Simulations of KRAS Wild and Mutant Models

The results of MD simulations of wild KRAS with its nine variants are describe in details as follows (Figure 4.26, Figure 4.27). The RMSD analysis of KRAS-wild revealed that the model was found stable with RMSD fluctuations lying in the range of 1-5 Å as shown in Figure 4.26. It was observed that the major fluctuations were recorded at the start of the simulation till 23.0ns while the optimal stability was attained after 38.0ns till the end. This model attained the RMSD value of 4.75 Å at the end of the 50.0ns simulation trajectory. Additionally, as indicated in Figure 4.27, the RMSF analysis of the wild model of KRAS protein suggested that no significant instability was experienced by its amino acids residues except for the few terminal amino acids. The amino acids observed with the considerably large RMSF values included GLU-62 (4.13 Å), GLU-174 (5.09 Å), LYS-175 (5.82 Å), THR-176 (7.34 Å), PRO-177 (8.66 Å), GLY-178 (8.72 Å), CYS-179 (8.31 Å), VAL-180 (10.10 Å), LYS-181 (9.71 Å), ILE-182 (11.11 Å) and LYS-183 (11.88 Å).

The RMSD results for the mutant KRAS-Q61R shown in Figure 4.26 suggested structural instability throughout the simulation period. However, it was observed that major fluctuations were observed before 18.0ns while optimal stability was shown during the simulation periods of 19.0-29.0ns and 40.0-50.0ns. At the end of a simulation run, a 7.09 Å RMSD value was recorded for KRAS-Q61R. Moreover, the RMSF analysis showed that the overall majority of the amino acid residues were found to be stable, however some fluctuating peaks were observed for the residues suggestive of the structural changes as depicted in Figure 4.27. It was observed that the residues ASP-29 (4.15 Å), GLU-30 (4.48 Å), TYR-31 (4.33 Å), ASP-32 (4.90 Å), PRO-33 (5.42 Å), THR-34 (4.84 Å), GLU-173 (5.01 Å), GLU-174 (5.10 Å), LYS-175 (5.96 Å), THR-176 (7.75 Å), PRO-177 (9.85 Å), GLY-178

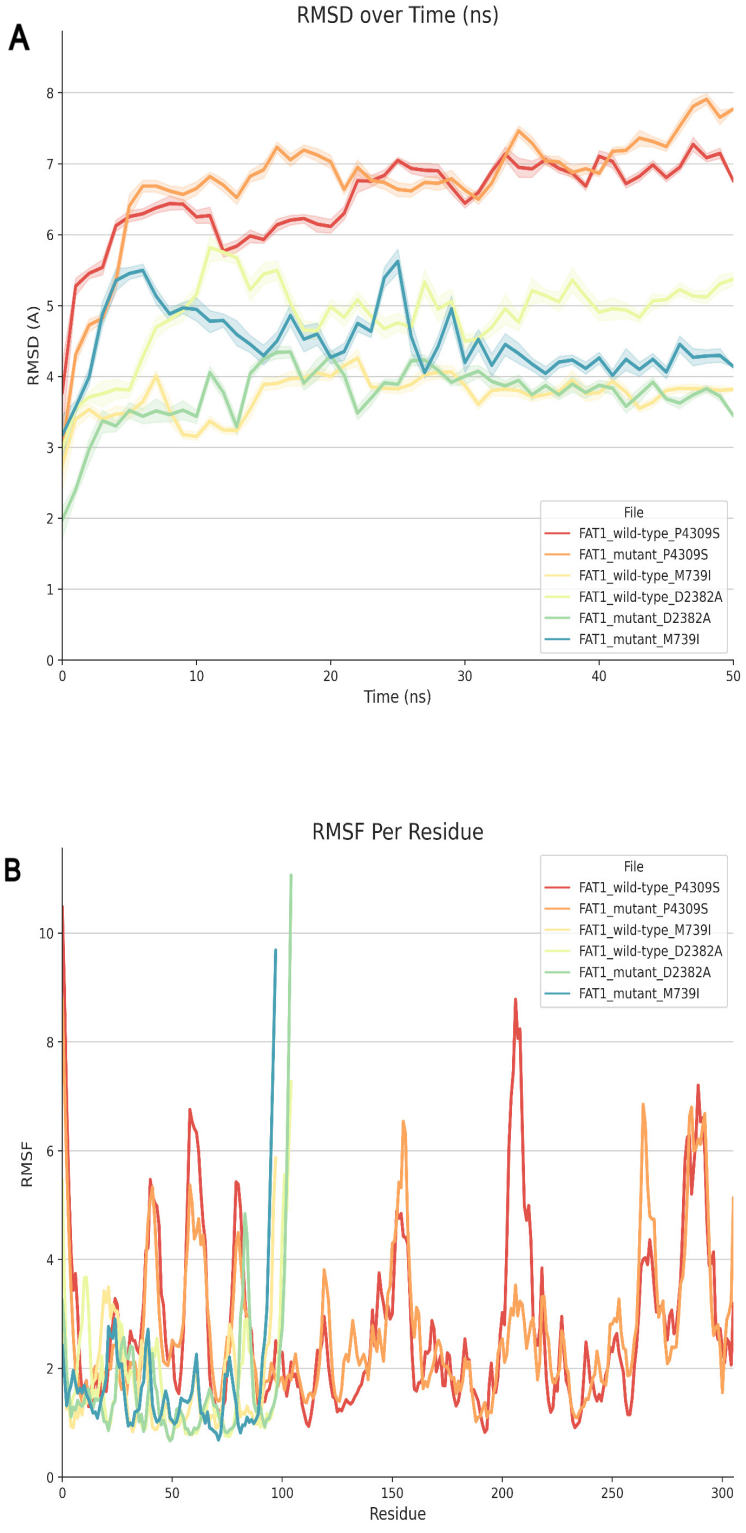

FIGURE 4.25: (a) RMSD graph representing the conformational differences between FAT1 wild domains and FAT1-mutants domains observed during a simulation period of 50 ns. (b) RMSF graph representing the structural fluctuations observed for amino acid residues between FAT1-wild and FAT1 mutant (D2382A, P4309S and M739I) domains during a simulation period of 50 ns.

(11.63 Å), CYS-179 (13.71 Å), VAL-180 (14.10 Å), LYS-181 (15.11 Å), ILE-182 (16.12 Å) and LYS-183 (17.14 Å).

Similarly, the RMSD analysis of the KRAS mutant G12D revealed the conformational stability throughout the simulation trajectory Figure 4.26. Overall, minimum RMSD fluctuations were observed with the major fluctuations recorded before 17.0ns. The optimal stability was exhibited during a simulation period of 18-30ns and 43-50 ns. At the end of the simulation, this mutant attained the RMSD of 4.83 Å. Furthermore, the RMSF analysis revealed that the amino acid residues were found stable as fluctuating peaks were observed only for a few terminal residues as indicated in Figure 4.27. The residues that observed large RMSF values included THR-176 (4.04 Å), PRO-177 (5.18 Å), GLY-178 (6.36 Å), CYS-179 (7.13 Å), VAL-180 (8.08 Å), LYS-181 (9.60 Å), ILE-182 (10.55 Å) and LYS-183 (12.74 Å).

Additionally, It was revealed through RMSD analysis that this mutant, although experienced fluctuations, attained stability towards the end of the simulation trajectory as shown in Figure 4.26. The major fluctuations were obtained before a simulation time of 20.0ns after which the stability was inferred till the end in the range of 1-2 Å RMSD differences. At the end of the simulation run, 6.02 Å RMSD was recorded by the mutant KRAS-G12R. Additionally, the results of RMSF indicated conformational instability for some residues as fluctuating peaks were observed. As depicted in Figure 4.27, the significantly large RMSF values were obtained for the residues ALA-65 (4.01 Å), GLU-174 (4.80 Å), LYS-175 (5.64 Å), THR-176 (5.56 Å), PRO-177 (5.87 Å), GLY-178 (7.64 Å), CYS-179 (7.61 Å), VAL-180 (8.30 Å), LYS-181 (8.33 Å), ILE-182 (8.95 Å) and LYS-183 (9.98 Å).

For the KRAS-A59E model minimum fluctuations were found, indicating conformational stability overall (Figure 4.26). It was observed that the protein experienced few fluctuations at the start of the simulation, however stability was attained moving towards the end of the simulation trajectory after 14.0ns run time. The optimal conformational stability was obtained during the simulation period of 33-50 ns and the protein showed the RMSD value of 7.00 Å at 50.0ns. Furthermore, indicated in Figure 4.27, the RMSF analysis of this mutant model

of KRAS revealed conformational stable amino acid residues except for some terminal residues for which large fluctuating peaks were obtained. The KRAS-A59E residues SER-171 (4.13 Å), GLU-174 (4.84 Å), LYS-175 (4.86 Å), THR-176 (5.76 Å), PRO-177 (6.44 Å), GLY-178 (6.95 Å), CYS-179 (6.88 Å), VAL-180 (7.75 Å), LYS-181 (7.92 Å), ILE-182 (8.12 Å) and LYS-183 (7.40 Å) showed large RMSF values.

Moreover The RMSD analysis of KRAS-G12V depicted in Figure 4.26 revealed that this model was found stable throughout the simulation trajectory. The optimal stability was obtained by this protein after the simulation time period of 22.0ns. At the end of the simulation run of 50.0ns, this mutant model of KRAS was observed with an RMSD value of 4.49 Å. Moreover, the RMSF results obtained for KRAS-G12V revealed the conformational instability for some amino acid residues as large fluctuations peaks were recorded. It was observed that the residues ASP-32 (4.53 Å), PRO-33 (4.63 Å), GLU-62 (5.12 Å), TYR-63 (4.54 Å), SER-64 (4.29 Å), LYS-172 (4.27 Å), GLU-173 (5.14 Å), GLU-174 (4.84 Å), LYS-175 (5.43 Å), THR-176 (7.02 Å), PRO-177 (6.51 Å), GLY-178 (6.13 Å), CYS-179 (5.14 Å), LYS-181 (4.42 Å), ILE-182 (5.45 Å) and LYS-183 (7.04 Å) experienced large fluctuations as illustrated in Figure 4.27.

The RMSD results of the mutant model KRAS-G13D were observed with fluctuations throughout the simulation period of 50.0ns inferring conformational instability as indicated in Figure 4.26. The minimum fluctuations were observed by this mutant model during the period of 27-34ns and 43-50 ns. At the end of the simulation period, a 4.62 Å RMSD value was obtained by KRAS-G13D. Additionally, as shown in Figure 4.27, the RMSF analysis revealed that the instability was observed by some of the amino acid residues of KRAS-G13D, however conformational stability was observed for the maximum residues. It was observed that the residues GLU-30 (4.14 Å), LYS-172 (4.55 Å), GLU-173 (4.67 Å), GLU-174 (5.00 Å), LYS-175 (6.73 Å), THR-176 (6.72 Å), PRO-177 (6.70 Å), GLY-178 (6.09 Å), CYS-179 (5.84 Å), VAL-180 (7.81 Å), LYS-181 (8.88 Å), ILE-182 (9.81 Å) and LYS-183 (11.41 Å) obtained maximum RMSF values.

The RMSD results revealed large fluctuations for KRAS-K117N indicating that this complex was found unstable throughout the simulation period as indicated in Figure 4.27. The maximum fluctuations were observed for this mutant protein before the simulation time of 30.0ns. At the end of the simulation run (50.0ns), the protein attained the RMSD value of 3.11 Å. Furthermore, the RMSF analysis revealed stability for a maximum number of amino acid residues of KRAS-K117N except for the some residues for which considerably large RMSF values were obtained. The KRAS-K117N residues that were found with maximum RMSF values included SER-64 (4.16 Å), ALA-65 (4.01 Å), GLU-174 (4.81 Å), LYS-175 (5.62 Å), THR-176 (6.05 Å), PRO-177 (7.87 Å), GLY-178 (8.55 Å), CYS-179 (10.42 Å), VAL-180 (10.38 Å), LYS-181 (9.48 Å), ILE-182 (10.40 Å) and LYS-183 (11.56 Å) as shown in Figure 4.27.

The mutant model KRAS-Q61E was found unstable as a significantly large number of fluctuations were observed throughout the simulation trajectory of 50.0ns as depicted in Figure 4.26. However, a decrease in the number of fluctuations was observed after the simulation time of 36.0ns till the end. This mutant model was found with the RMSD value of 3.64 Å at 50.0ns simulation time. Moreover, the RMSF results as depicted in Figure 4.27 indicated that the overall maximum number of amino acid residues did not fluctuate and were found stable. However, few residues were found with large fluctuating peaks and were inferred as conformationally unstable. The aforementioned unstable residues included THR-1 (4.81 Å), GLU-36 (4.10 Å), GLU-174 (4.18 Å), LYS-175 (6.22 Å), THR-176 (7.51 Å), PRO-177 (8.45 Å), GLY-178 (9.38 Å), CYS-179 (11.13 Å), VAL-180 (11.97 Å), LYS-181 (12.10 Å), ILE-182 (13.71 Å) and LYS-183 (14.42 Å).

The RMSD analysis for the mutant model KRAS-Q61H revealed the conformational stability as a minimum number of fluctuations were observed as shown in Figure 4.26. It was observed that fluctuations were obtained at the start of the simulation trajectory, however stability was obtained after the time period of 22.0ns. At the end of the simulation run of 50.0ns, the protein attained the RMSD value of 4.85 Å. Furthermore, the RMSF results depicted in Figure 4.27 for KRAS-Q61H indicated the stability for most of the amino acid residues except

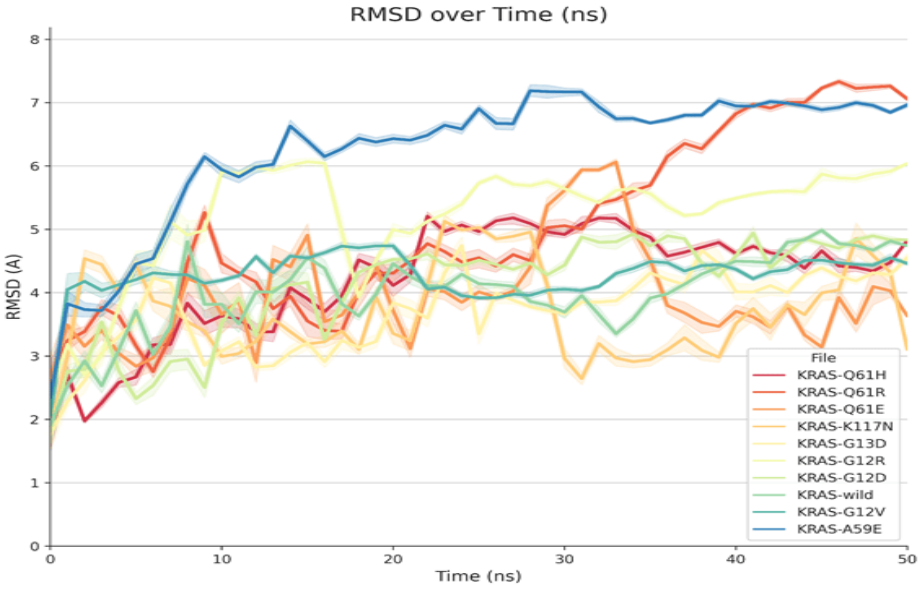

FIGURE 4.26: RMSD graph representing the conformational differences between KRAS-wild and KRAS-mutants (9 mutants) observed during a simulation period of 50 ns.

for some of the residues that were found with large RMSF values. The residues of KRAS-Q61H that were found with large RMSF values included GLU-30 (5.14 Å), TYR-31 (5.55 Å), ASP-32 (5.18 Å), PRO-33 (4.84 Å), THR-176 (4.35 Å), PRO-177 (6.21 Å), GLY-178 (6.14 Å), CYS-179 (6.84 Å), VAL-180 (8.77 Å), LYS-181 (10.31 Å), ILE-182 (12.15 Å) and LYS-183 (14.04 Å).

4.14.7 MD Simulations of NRAS Wild with Mutant Models

The MD Simulations of NRAS Wild with its eight variants were discussed in details as follows (Figure 4.28, Figure 4.29). The RMSD results obtained for the NRAS-wild model revealed the conformation stability throughout the simulation period as only minor fluctuations were observed in the range of 1-3 Å RMSD as depicted in Figure 4.28. The optimal stability was observed during the simulation period of 20.0-30.0ns, while protein attained the RMSD value of 2.47 Å at the end of the simulation run (50.0ns). Moreover, the RMSF analysis of the wild model of NRAS revealed that the protein amino acids residues have not experienced conformation

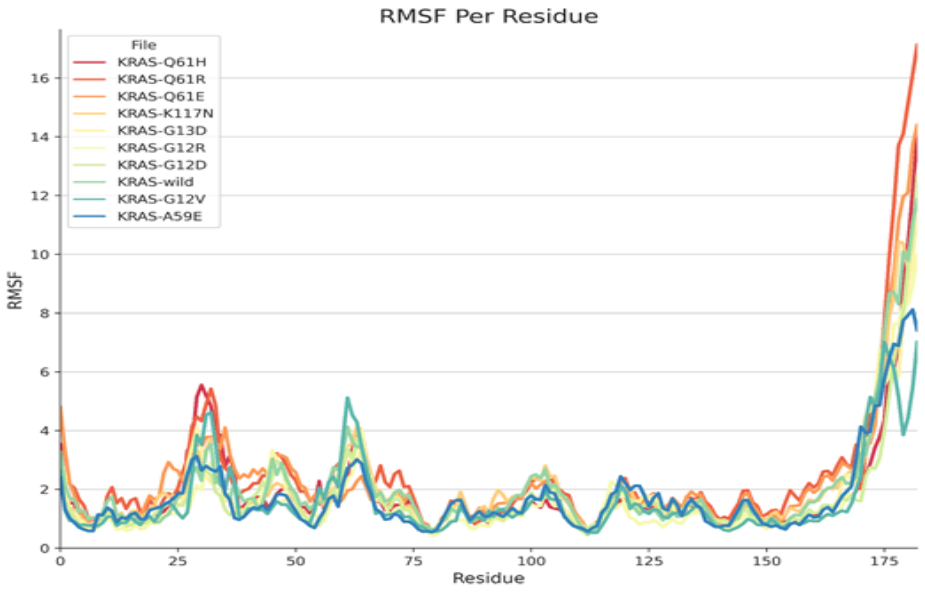

FIGURE 4.27: RMSF graph representing the structural fluctuations observed for amino acid residues between KRAS-wild and KRAS-mutants during a simulation period of 50 ns.

instability as negligible RMSF values were observed with the exception of some terminal residues as shown in Figure 4.29. The maximum RMSF values were obtained for the amino acid residues LYS-170 (4.75 Å), LEU-171 (6.46 Å) and ASN-172 (8.16 Å).

As shown in Figure 4.28, the RMSD analysis of the NRAS-Y64D revealed that this model was found conformationally stable throughout the simulation trajectory. It was observed that only minor fluctuations were recorded at the start of the trajectory while the optimal stability was shown during the simulation periods of 9-30ns and 40-50 ns. At the end of the simulation run of 50 ns, this mutant model attained the RMSD value of 2.79 Å. Furthermore, the RMSF results depicted in Figure 4.29 revealed that the overall amino acid residues of this model were found stable. The maximum RMSF value was obtained for only one residue ASN-172 (6.11 Å) whereas the other considerable RMSF values were obtained for the residues ASP-64 (2.58 Å), LYS-170 (2.97 Å) and LEU-171 (3.93 Å).

The RMSD results, as shown in Figure 4.28, analyzed for the mutant model NRAS-Q61H revealed that the minimum fluctuations were observed in the range of RMSD

differences of 1-3 Å indicating conformational stability throughout the simulation period. The optimal stability was observed after the simulation period of 33ns till the end. This model was found with an RMSD value of 3.14 Å at the end of the simulation run. Moreover, the RMSF analysis depicted in Figure 4.29 revealed that the amino acid residues did not experience the significant fluctuations as large RMSF values were found for only a few residues. The maximum RMSF value was recorded for ASN-172 (6.95 Å) whereas the LYS-169 (2.96 Å), LYS-170 (4.21 Å) and LEU-171 (5.63 Å) were also observed with the significant RMSF values.

Similarly, The RMSD analysis for the mutant NRAS-Q61K indicated the conformational stability from the start of the simulation period till the time period of 43.0ns as indicated in Figure 4.28. It was observed that the RMSD value showed a slight increase moving towards the end, however it started decreasing after the simulation time of 45.3ns. At the end of the simulation, the RMSD value was observed as 2.96 Å. Whereas, the RMSF results depicted in Figure 4.29 obtained for this mutant model of NRAS indicated that the majority of the amino acid residues were conformationally stable throughout the simulation, however some of the residues were observed with large RMSD values indicating their instability. These residues included ASP-33 (3.08 Å), PRO-34 (4.15 Å), THR-35 (4.68 Å), ILE-36 (3.94 Å), GLU-37 (3.19 Å), GLU-63 (3.04 Å), TYR-64 (3.53 Å), SER-65 (3.10 Å), ALA-66 (3.39 Å), LEU-171 (4.46 Å) and ASN-172 (6.53 Å).

The RMSD graph for NRAS-Q61R indicated that this model was not conformationally stable as fluctuations were observed at various time frames shown in Figure 4.28. The major fluctuations were observed before 18.0ns and after the simulation time of 35.0 ns. On the other hand, optimal stability was only observed for a duration of 18-35ns while the protein attained the RMSD value of 3.59 Å at 50.0 ns. Moreover, the RMSF analysis indicated that the conformational instability was experienced by some of the amino acid residues as large fluctuating peaks were recorded whereas the majority of the residues were found stable throughout the simulation. The residues that were found with large RMSF values included ASP-30 (3.39 Å), GLU-31 (4.30 Å), TYR-32 (3.91 Å), ASP-33 (4.54 Å), PRO-34 (5.03 Å), THR-35 (5.46 Å), ILE-36 (3.63 Å), GLU-37 (3.08 Å), SER-65 (4.00 Å),

ALA-66 (4.32 Å), LYS-170 (4.10 Å), LEU-171 (5.88 Å) and ASN-172 (7.31 Å) as indicated in Figure 4.29.

As shown in Figure 4.28, the RMSD analysis of NRAS-G13R revealed that this model experienced fluctuations at the start and towards the end of the simulation indicating its unstable behavior. Moreover, the number of fluctuations decreased after 16.0ns while the optimal stability was exhibited only during the simulation period of 18-42 ns. It was observed that this mutant model obtained an RMSD value of 3.92 Å at the end of the simulation period. While the RMSF results obtained for the mutant model NRAS-G13R shown in Figure 4.29 revealed that the majority of the amino acid residues were found with minimum RMSF values indicating their stability. However, significantly large RMSF values were observed for some of the residues that included ASP-33 (3.85 Å), PRO-34 (5.77 Å), THR-35 (6.72 Å), ILE-36 (4.95 Å), GLU-37 (5.15 Å), LYS-169 (3.35 Å), LYS-170 (4.57 Å), LEU-171 (6.28 Å) and ASN-172 (7.91 Å).

The RMSD analysis of the NRAS-E153Q revealed the fluctuations at different time frames in the range of RMSD differences of 1-4 Å throughout the simulation trajectory as shown in Figure 4.28. However, the number of RMSD fluctuations was minimal after the simulation time of 33ns indicating that it attained the stability towards the end. At the simulation time of 50.0ns, the RMSD value of 3.08 Å was recorded for NRAS-E153Q. Moreover, the RMSF results obtained for this mutant model indicated that the amino acid residues were majorly found conformationally stable with the exception of only few residues for which fluctuating peaks were observed. As depicted in Figure 4.29 It was observed that the residues PRO-34 (3.30 Å), THR-35 (3.57 Å), SER-89 (3.35 Å), LYS-170 (3.90 Å), LEU-171 (5.26 Å) and ASN-172 (7.34 Å) were observed with considerably large RMSF values, thus have been predicted as unstable residues.

In Figure 4.28, the RMSD results obtained for the mutant model KRAS-G12D revealed that the structure experienced several minor fluctuations throughout the simulation indicating structural changes. Overall, the fluctuations were recorded in the range of RMSD differences of 1-3 Å with optimal stability observed only for a duration of 30-39.55ns. At the end of the simulation period of 50.0ns, a 2.65

Å RMSD value was obtained for KRAS-G12D. Moreover, the RMSF analysis depicted in Figure 4.29 revealed that the amino acid residues were found to be conformationally stable as fluctuating peaks were observed for only a few terminal residues. The residues that were observed with significantly large RMSF values included ASP-30 (2.42 Å), LYS-170 (3.38 Å), LEU-171 (5.55 Å) and ASN-172 (7.92 Å), suggesting that these residues have experienced instability.

As shown in Figure 4.28 the RMSD results of NRAS-G13D revealed that throughout the trajectory, the RMSD differences of 1-4 Å were observed with fluctuations exhibited at different time frames. The minimum fluctuations and maximum stability were exhibited during the simulation periods of 8-23ns and 24.5-32.5ns while the RMSD value of 2.70 Å was obtained at the end of the simulation period (50.0ns). Moreover, the RMSF analysis shown in Figure 4.29 indicated stability for the majority of the amino acid residues as a negligible number of fluctuation peaks were observed throughout. It was observed that the residues GLN-61 (2.72 Å), LYS-170 (3.72 Å), LEU-171 (5.02 Å) and ASN-172 (6.81 Å) experienced significant structural changes as large RMSF values were obtained for them. The RMSF results indicate that overall amino acid residues for this mutant model were conformationally stable.

During the simulation, it was observed that TCL1A-T38I had a lower RMSD value of 3.26 Å compared to the wild-type TCL1A with an RMSD of 3.35 Å. Similarly, the ERG-Wild protein exhibited a lower RMSD of 1.67 Å compared to ERG-E353Q, which had an RMSD of 2.60 Å. Conversely, the AFF3-P1129L mutation showed a significantly higher RMSD value of 13.33 Å compared to its wild-type AFF3 protein, which had an RMSD of 6.59 Å. Moreover, the RMSF analysis of TCL1A, ERG and AFF3 revealed that the amino acid residues of TCL1A-T381 and AFF3-wild were found to be more stable with minimum fluctuations as compared to their counterparts while no considerable fluctuations were observed for ERG models. These results indicated that the mutant of TCL1A was found more stable conformationally, thus this stable mutant protein may have adopted an important role in RRMM while on the other hand ERG and AFF3 (ERG-E353Q, AFF3-P1129L) mutants were found to be unstable as compared to their

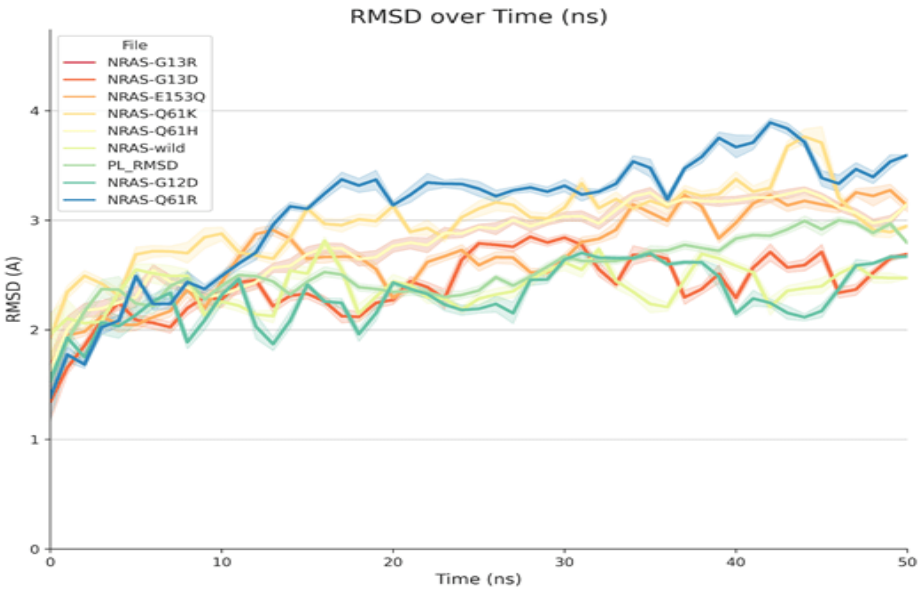

FIGURE 4.28: RMSD graph representing the conformational differences between NRAS-wild and NRAS-mutants observed during a simulation period of 50 ns. Each Variant is represented with different color.

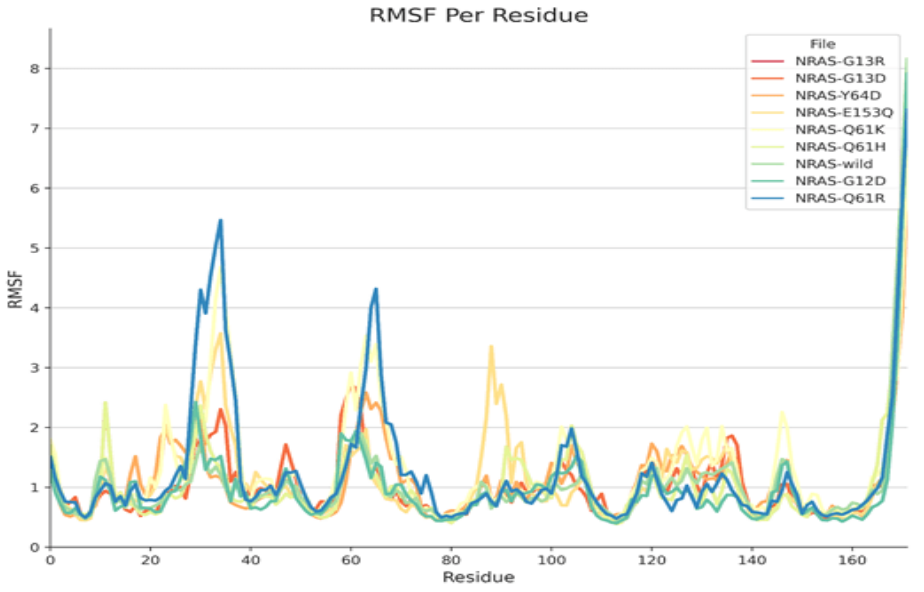

FIGURE 4.29: RMSF graph representing the structural fluctuations observed for amino acid residues between NRAS-wild and NRAS-mutants during a simulation period of 50 ns.Each Variant is represented with different color.

wild proteins.

Furthermore, the RMSD and RMSF analysis indicated that MNX1-P392L was significantly unstable as compared to the wild protein as distinct differences were observed between both indicating that the mutation may have induced large structural and functional changes,. At the end of the simulation, a huge gap in RMSD values was observed between MNX1-wild (22.59 Å) and MNX1-P392L (30.53 Å) while the greater number of RMSF fluctuating peaks was observed for amino acid residues of the MNX1-P392L indicating their instability compared to the MNX1-wild residues.

It was inferred from the RMSD analysis of KRAS that 5 out of 9 mutants KRAS-Q61R (7.09 Å), KRAS-G12D (4.83 Å), KRAS-G12R (6.02 Å), KRAS-A59E (7.00 Å), KRAS-Q61H (4.85 Å) were more conformationally unstable than the KRAS-Wild (4.75 Å) as they were obtained with greater RMSD values at 50.0ns indicating more fluctuations while on the other hand stability was observed for the KRAS-G12V (4.49 Å), KRAS-G13D (4.62 Å), KRAS-K117N (3.11 Å), KRAS-Q61E (3.64 Å) mutants as compared to the wild protein. Furthermore, KRAS RMSF analysis showed that no significant differences were observed in fluctuating peaks for the mutants as compared to the KRAS-wild, however a slight increase in the number of fluctuating residues was observed for KRAS-Q61R and KRAS-G12V. The aforementioned analysis indicate that large increase in RMSD values obtained for KRAS-Q61R, KRAS-G12R and KRAS-A59E suggest the increased structural disruption induced by these mutations while KRAS-K117N and KRAS-Q61E have been found to be more stable than wild protein, thus are recommended as more functionally important in RRMM.

The RSMD analysis unveiled that the NRAS mutants were found conformationally unstable as NRAS-Y64D (2.79 Å), NRAS-Q61H (3.14 Å), NRAS-Q61K (2.96 Å), NRAS-Q61R (3.59 Å), NRAS-G13R (3.92 Å), NRAS-E153Q (3.08 Å), NRAS-G12D (2.65 Å) and NRAS-G13D (2.70 Å) showed higher RMSD values as compared to NRAS-wild (2.47 Å) at the end of 50.0ns simulation run. Moreover, the RMSF analysis declared amino acid residue of NRAS-Q61K, NRAS-Q61R, NRAS-G13R, and NRAS-E153Q as more unstable with respect to NRAS-wild as

an increase in RMSF values were obtained for these mutants. Consequently, a significant increase observed in RMSD and RMSF values of NRAS-Q61H, NRAS-Q61K, NRAS-Q61R, NRAS-G13R, NRAS-E153Q recommend these mutations as capable of disrupting the structure of NRAS protein drastically altering the functional properties.

Hence, this study proposes TCL1A-T38I, KRAS-K117N and KRAS-Q61E as significantly stable indicating their crucial functional role in RRMM as compared to wild-type models. Meanwhile ERG-E353Q, AFF3-P1129L, KRAS-Q61R, KRAS-G12R, KRAS-A59E, NRAS-Q61H, NRAS-Q61K, NRAS-Q61R, NRAS-G13R, NRAS-E153Q and MNX1-P392L have been identified as more unstable conformtionally, with respect to their wild structures indicating that these structural alterations may have disrupt the native function of these proteins in RRMM.

4.15 Retrieval of Drug Compounds for Drug Repurposing

The drug compounds were retrieved from the DrugBank by using a target sequence search of the proteins (MNX1, ERG, TCL1A, AFF3, FAT1, KRAS, NRAS, CD4, ITGAM, PTPRC, TYROBP, IL1B, CSF1R, VCAN, NRP1, COL22A1, BPI, and BIRC5) and different search terms were also used such as “relapsed cancers”, “FDA approved drugs for cancers” and “EMA approved drugs for cancers”. The drug compounds that were retrieved from the DrugBank were FDA and EMA-approved, furthermore, they were also previously used in the experimental validation of the drugs against relapses of multiple cancers. The approved and experimental drug compounds were used because of their already-known ADME properties and the efficiency of the compounds in treating other cancers. A comprehensive set of 141 drug compounds, including experimental, approved, and those under clinical evaluation, known as inhibitors for diverse protein types associated with different diseases, including various cancers, was retrieved and assembled in Table 4.12.

Among them 94 were approved drugs, 21 were investigational drugs (clinical trials), whereas 26 were experimental drugs (pre-clinical trials).

TABLE 4.12: Drug compounds retrieved from DrugBank for Drug Repurposing

Sr.#	IDs	Compounds	Groups
1	DB00210	Adapalene	Approved
2	DB00280	Disopyramide	Approved
3	DB00308	Ibutilide	Approved
4	DB00321	Amitriptyline	Approved
5	DB00457	Prazosin	Approved
6	DB00458	Imipramine	Approved
7	DB00480	Lenalidomide	Approved
8	DB00489	Sotalol	Approved
9	DB00557	Hydroxyzine	Approved
10	DB00570	Vinblastine	Approved
11	DB00590	Doxazosin	Approved
12	DB00619	Imatinib	Approved
13	DB00661	Verapamil	Approved
14	DB00675	Tamoxifen	Approved
15	DB00795	Sulfasalazine	Approved
16	DB00836	Loperamide	Approved
17	DB00843	Donepezil	Approved
18	DB00852	Pseudoephedrine	Approved
19	DB01035	Procainamide	Approved
20	DB01100	Pimozide	Approved
21	DB01162	Terazosin	Approved
22	DB01182	Propafenone	Approved
23	DB01211	Clarithromycin	Approved
24	DB01218	Halofantrine	Approved
25	DB03796	Palmitic Acid	Approved
26	DB04855	Dronedarone	Approved
27	DB05294	Vandetanib	Approved
28	DB06207	Silodosin	Approved
29	DB08896	Regorafenib	Approved
30	DB09063	Ceritinib	Approved
31	DB09079	Nintedanib	Approved
32	DB01411	Pranlukast	Investigational
33	DB01645	Genistein	Investigational

Sr.#	IDs	Compounds	Groups
34	DB03701	Vanoxerine	Investigational
35	DB04891	Becocalcidiol	Investigational
36	DB04957	Azimilide	Investigational
37	DB05212	HE3286	Investigational
38	DB05767	Andrographolide	Investigational
39	DB05785	LGD-1550	Investigational
40	DB05786	Irofulven	Investigational
41	DB05943	Resatorvid	Investigational
42	DB06080	Linifanib	Investigational
43	DB06457	Tecastemizole	Investigational
44	DB06486	Enzastaurin	Investigational
45	DB06641	Perifosine	Investigational
46	DB11752	Bryostatin 1	Investigational
47	DB12742	Amuvatinib	Investigational
48	DB12816	Terpinen-4-ol	Investigational
49	DB08846	Ellagic acid	Investigational
50	DB12116	Epigallocatechin Gallate	Investigational
51	DB12039	Epicatechin	Investigational
52	DB00199	Erythromycin	Approved, Investigational
53	DB00136	Calcitriol	Approved, Nutraceutical
54	DB00252	Phenytoin	Approved, Vet approved
55	DB03017	Lauric acid	Approved, Experimental
56	DB13751	Glycyrrhizic acid	Approved, Experimental
57	DB00176	Fluvoxamine	Approved, Investigational
58	DB00204	Dofetilide	Approved, Investigational
59	DB00276	Amsacrine	Approved, Investigational
60	DB00908	Quinidine	Approved, Investigational
61	DB01026	Ketoconazole	Approved, Investigational
62	DB01097	Leflunomide	Approved, Investigational
63	DB01118	Amiodarone	Approved, Investigational
64	DB01136	Carvedilol	Approved, Investigational
65	DB01142	Doxepin	Approved, Investigational
66	DB01296	Glucosamine	Approved, Investigational
67	DB03756	Doconexent	Approved, Investigational
68	DB06217	Vernakalant	Approved, Investigational
69	DB06595	Midostaurin	Approved, Investigational
70	DB00398	Sorafenib	Approved, Investigational

Sr.#	IDs	Compounds	Groups
71	DB00455	Loratadine	Approved, Investigational
72	DB00482	Celecoxib	Approved, Investigational
73	DB00537	Ciprofloxacin	Approved, Investigational
74	DB01029	Irbesartan	Approved, Investigational
75	DB01074	Perhexiline	Approved, Investigational
76	DB01268	Sunitinib	Approved, Investigational
77	DB08814	Triflusal	Approved, Investigational
78	DB08865	Crizotinib	Approved, Investigational
79	DB08875	Cabozantinib	Approved, Investigational
80	DB08901	Ponatinib	Approved, Investigational
81	DB08908	Dimethyl fumarate	Approved, Investigational
82	DB09078	Lenvatinib	Approved, Investigational
83	DB11363	Alectinib	Approved, Investigational
84	DB11633	Isavuconazole	Approved, Investigational
85	DB11642	Pitolisant	Approved, Investigational
86	DB11697	Pacritinib	Approved, Investigational
87	DB11718	Encorafenib	Approved, Investigational
88	DB11800	Tivozanib	Approved, Investigational
89	DB12010	Fostamatinib	Approved, Investigational
90	DB12130	Lorlatinib	Approved, Investigational
91	DB12141	Gilteritinib	Approved, Investigational
92	DB12267	Brigatinib	Approved, Investigational
93	DB12364	Betrixaban	Approved, Investigational
94	DB12500	Fedratinib	Approved, Investigational
95	DB12978	Pexidartinib	Approved, Investigational
96	DB15035	Zanubrutinib	Approved, Investigational
97	DB15685	Selpercatinib	Approved, Investigational
98	DB15822	Pralsetinib	Approved, Investigational
99	DB00228	Enflurane	Approved, Investigational, Vet approved
100	DB01110	Miconazole	Approved, Investigational, Vet approved
101	DB00477	Chlorpromazine	Approved, Investigational, Vet approved
102	DB11386	Chlorobutanol	Approved, Investigational, Vet approved
103	DB00604	Cisapride	Approved, Investigational, Withdrawn

Sr.#	IDs	Compounds	Groups
104	DB01025	Amlexanox	Approved, Investigational, Withdrawn
105	DB06144	Sertindole	Approved, Investigational, Withdrawn
106	DB11186	Pentoxyverine	Approved, Investigational, Withdrawn
107	DB00472	Fluoxetine	Approved, Vet approved
108	DB00945	Acetylsalicylic acid	Approved, Vet approved
109	DB00679	Thioridazine	Approved, Withdrawn
110	DB01149	Nefazodone	Approved, Withdrawn
111	DB01195	Flecainide	Approved, Withdrawn
112	DB01244	Bepridil	Approved, Withdrawn
113	DB00342	Terfenadine	Approved, Withdrawn
114	DB00637	Astemizole	Approved, Withdrawn
115	DB01750	1-naphthaleneacetic acid	Experimantal
116	DB01809	1-Ter-Butyl-3-P-Tolyl-1h-Pyrazolo[3,4-D]Pyrimidin-4-Ylamine	Experimantal
117	DB01863	Inositol 1,3,4,5-Tetrakisphosphate	Experimantal
118	DB03309	N-cyclohexyltaurine	Experimental
119	DB03459	Sparfosic acid	Experimental
120	DB03721	N-acetyl-alpha-neuraminic acid	Experimental
121	DB04147	Dodecyldimethylamine N-oxide	Experimental
122	DB06732	beta-Naphthoflavone	Experimental
123	DB06884	4-HYDROXY-N'-(4 - ISOPROPYL-BENZYL) BENZOHYDRAZIDE	Experimental
124	DB06980	(2S)-2-(1H-indol-3-yl)hexanoic acid	Experimental
125	DB06981	(2S)-2-(1H-indol-3-yl)pentanoic acid	Experimental
126	DB06982	(2S)-8-[(tert-butoxycarbonyl)amino]-2-(1H-indol-3-yl)octanoic acid	Experimental
127	DB07167	5 - CYANO - FURAN - 2 - CARBOXYLIC ACID [5 - HYDROXYMETHYL- 2- (4 - METHYL - PIPERIDIN - 1 - YL) - PHENYL] - AMIDE	Experimental
128	DB07202	6-CHLORO-3-(3-METHYLISOXAZOL-5-YL)-4-PHENYLQUINOLIN-2(1H)-ONE	Experimental

Sr.#	IDs	Compounds	Groups
129	DB07584	N-[2-(5-methyl-4H-1,2,4-triazol-3-yl)phenyl]-7H-pyrrolo[2,3-d]pyrimidin-4-amine	Experimental
130	DB07585	5-(5-chloro-7H-pyrrolo[2,3-d]pyrimidin-4-yl)-4,5,6,7-tetrahydro-1H-imidazo[4,5-c]pyridine	Experimental
131	DB07812	N-[(1S)-2-amino-1-phenylethyl]-5-(1H-pyrrolo[2,3-b]pyridin-4-yl)thiophene-2-carboxamide	Experimental
132	DB07859	4-(4-CHLOROPHENYL)-4-[4-(1H-PYRAZOL-4-YL)PHENYL]PIPERIDINE	Experimental
133	DB07947	ISOQUINOLINE-5-SULFONIC ACID (2- (2- (4 - CHLOROBENZYLOXY) ETHYLAMINO) ETHYL) AMIDE	Experimental
134	DB07950	Indoleacetic acid	Experimental
135	DB08073	(2S)-1-(1H-INDOL-3-YL)-3-{[5-(3-METHYL-1H-INDAZOL-5-YL)PYRIDIN-3-YL]OXY}PROPAN-2-AMINE	Experimental
136	DB08231	Myristic acid	Experimental
137	DB08341	4-{[4-{[(1R,2R)-2-(dimethylamino)cyclopentyl]amino}-5-(trifluoromethyl)pyrimidin-2-yl]amino}-N-methylbenzenesulfonamide	Experimental
138	DB09221	Polaprezinc	Experimental
139	DB04419	D-norleucine	Experimental
140	DB14059	SC-236	Experimental, Investigational
141	DB02709	Resveratrol	Investigational
142	DB04216	Quercetin	Experimental, Investigational

4.16 Molecular Docking of Drug Compounds with Candidate Relapse Biomarkers

The molecular docking of the wild-type and mutant models of MNX1, FAT1, ERG, TCL1A, AFF3, KRAS, and NRAS with the FDA and EMA-approved drug compounds was performed using AutoDock Vina, showing variable binding affinities. Furthermore, the wild-type CD4, ITGAM, PTPRC, TYROBP, and IL1B proteins were also docked with the retrieved drug compounds; however, the proteins CSF1R, VCAN, NRP1, COL22A1, BPI, and BIRC5 were docked only with those compounds (Adapalene, Poatinib, Glycyrrhizic acid, and Pralsetinib) that showed significant binding affinities among all of the other proteins. The binding affinities of all the complexes ranged from as high as-3.1 kcal/mol of the wild-type TYROBP protein with D-norleucine (DB04419) and dimethyl fumarate (DB08908) to as low as -10.9 kcal/mol of the wild-type ITGAM protein with glycyrrhizic acid (DB13751).The complete results of binding affinities of all proteins with all selected compounds are given in Annexure Table 4. However, the detailed analysis of results revealed that out of 141 compounds four compounds namely adapalene (DB00210), ponatinib (DB08901), glycyrrhizic acid (DB13751), and pralsetinib (DB15822) showed significant binding affinities with all wild as well as mutant proteins. Adapalene, a synthetic compound derived from retinoic acid, is a topical retinoid commonly employed in clinical settings to manage various skin conditions [306]. Extensive research has explored the pharmacological properties of ADA, encompassing its ability to reduce comedones, mitigate inflammation, and demonstrate anticancer potential [307]. Within the realm of anticancer investigations, one study revealed that ADA exerts formidable anticancer effects by inhibiting CDK2 in colorectal cell lines [308]. In contrast, retinoic acid, employed as an anticancer agent, promotes cellular differentiation, potentially linked to its inherent cytotoxic and pro-apoptotic properties [309]. Recent findings have indicated that ADA impedes the growth of ovarian cancer ES-2 cells by targeting glutamicoxaloacetic transaminase 1 (GOT1) and induces apoptosis by regulating the Bax/Bcl-2 ratio in hepatocyte cells [310, 311]. ADA also triggers cell cycle arrest in the G1 phase of colorectal cancer cells and hinders the proliferation of melanoma

cells by inducing cell cycle arrest in the S phase, along with inhibiting apoptosis through DNA damage induction [312, 313]. A recent study investigating adapalene's potential in treating prostate cancer found that it effectively suppressed the growth of prostate cancer cells, induced programmed cell death (apoptosis), and halted the cell cycle during the S-phase. Furthermore, in vitro experiments showed that adapalene slowed down both tumor growth and the degradation of bone tissue (osteolytic bone lesion) [314]. Ponatinib is a novel Bcr-Abl tyrosine kinase inhibitor that is especially effective against the T315I mutation for the treatment of chronic myeloid leukemia (CML). Ponatinib is approved for treating adults with various phases of CML and Philadelphia chromosome positive acute lymphoblastic leukemia (Ph+ALL) who have not responded to previous tyrosine kinase inhibitor therapy or cannot tolerate it [315]. It functions as a multi-target kinase inhibitor with its main target being the Bcr-Abl tyrosine kinase protein, which plays a key role in driving CML. This protein results from the fusion of the Bcr and Abl genes found in the Philadelphia chromosome. Ponatinib is particularly effective against resistant CML because it can inhibit the tyrosine kinase activity of Abl and T315I mutant kinases. The T315I mutation makes cells resistant to other Bcr-Abl inhibitors by preventing their binding to the Abl kinase. Additionally, ponatinib targets various other kinases like VEGFR, PDGFR, FGFR, EPH receptors, SRC families, as well as KIT, RET, TIE2, and FLT3. Experiments in rats have shown a reduction in tumor size in cases expressing both native and T315I mutant BCR-ABL [316]. Glycyrrhizic acid, derived from the root of the licorice plant (Glycyrrhiza glabra), is a triterpene glycoside containing glycyrrhetinic acid, known for its diverse pharmacological and biological properties. In its extracted form, it can be found as ammonium glycyrrhizin and mono-ammonium glycyrrhizin. Japan and China have developed it as a hepatoprotective medication for chronic hepatitis cases [317]. This compound has found applications in various formulations due to its reported anti-inflammatory, anti-ulcer, anti-allergic, antioxidant, anti-tumor, anti-diabetic, and hepatoprotective attributes. Its uses encompass treating conditions such as premenstrual syndrome, viral infections, lipid and blood sugar regulation, as well as remedies for peptic ulcers and other gastrointestinal issues [318]. Additionally, It is also known to be

used as a remedy for peptic ulcer and other stomach diseases [319]. Glycyrrhizic acid has demonstrated anti allergic, antiviral, and anti-inflammatory properties, along with potential benefits in improving glucose tolerance. a recent study revealed the potential of glycyrrhizic acid in inhibiting the proliferation, invasion, and migration of colorectal cancer cells, and induced their apoptosis by SIRT3 inhibition [320]. Pralsetinib is a targeted medication designed to inhibit the RET receptor tyrosine kinase, primarily used for treating metastatic non-small cell lung cancer (NSCLC) in adult patients with confirmed RET gene fusions [321, 322]. It is also employed in adult and pediatric patients aged 12 and above who have advanced or metastatic RET fusion-positive thyroid cancer, particularly when radioactive iodine therapy is not suitable [317, 323]. The approval for thyroid cancer is based on accelerated approval criteria, contingent upon further confirmation of clinical benefits in subsequent trials. Pralsetinib achieves its anti-tumor effects by specifically targeting RET tyrosine kinase, including various oncogenic RET fusions, mutated RET kinase domains with gatekeeper mutations, and RET kinases harboring various activating single point mutations. Notably, pralsetinib exhibits a high level of selectivity for RET over other kinases both in laboratory settings and in living organisms, making it a safer option compared to previously utilized multi-kinase inhibitors [324]. These binding affinity score of these compounds with all protein along with the binding residues information obtained from Protein-Ligand Interaction Profiler (PLIP) were compiled in Table 4.13. Lastly, the visualization of docked complexes on PyMOL also disclosed the proteins binding residues and their positions that were showing interactions with the drug compounds and are shown in Figure 4.30 - 4.34.

TABLE 4.13: Protein-Ligand Interaction Profiler (PLIP) of all the docked complexes of the TCL1A, AFF3, MNX1, ERG FAT1 and their variants proteins with selected drug compunds, representing the binding residues, their positions and distances between hydrogen-acceptor and donor-acceptor molecules

Proteins		**Binding Affinity**	**Residue**	**AA**	**Distance H-A**	**Distance D-A**
TCL1A-wild	TCL1A-Adapalene	-8.7	62A	MET	2.06	2.85

Proteins		**Binding Affinity**	**Residue**	**AA**	**Distance H-A**	**Distance D-A**
	TCL1A-ponatinib	-8.3	-	-	-	-
	TCL1A-glycyrrhizic acid	-7.2	66A	GLN	2.54	3.31
	TCL1A-pralsetinib	-8.5	28A, 55A, 56A, 56A	ASP, ASP, VAL, VAL	3.00, 2.13, 3.36, 2.51	3.83, 3.06, 4.02, 3.33
TCL1A-T38I	TCL1A-Adapalene	-8.3	20A, 74A	ALA, ILE	2.56, 2.24	3.11, 2.70
	TCL1A-ponatinib	-7.7	23A	LYS	3.27	3.63
	TCL1A-glycyrrhizic acid	-7.5	11A, 94A, 97A, 97A	VAL, LEU, HIS, HIS	2.66, 2.02, 2.16, 2.24	3.13, 2.90, 2.87, 3.22
	TCL1A-pralsetinib	-7.8	-	-	-	-
AFF3-wild	AFF3-Adapalene	-8.2	29A, 29A, 74A	ASP, ASP, GLU	3.70, 2.05, 3.62	4.07, 2.99, 3.92
	AFF3-ponatinib	-8	95A, 222A, 224A	LYS, ASN, GLU	3.10, 2.47, 2.25	4.06, 3.43, 3.18
	AFF3-glycyrrhizic acid	-8	213A, 219A, 223A, 227A, 227A	GLU, ALA, ARG, ASN, ASN	2.41, 3.01, 3.21, 2.35, 3.32	2.93, 3.92, 3.78, 3.01, 4.08
	AFF3-pralsetinib	-7.9	103A, 117A, 238A	ARG, ARG, LEU	3.39, 3.02, 2.21	3.89, 3.89, 3.08
AFF3-P1129L	AFF3-Adapalene	-8.4	40A	ASN	2.27	3.17
	AFF3-ponatinib	-8.6	83A	LYS	2.18	3.14

Proteins		**Binding Affinity**	**Residue**	**AA**	**Distance H-A**	**Distance D-A**
	AFF3-glycyrrhizic acid	-8	22A, 25A, 41A, 71A, 71A, 75A	LYS, LYS, TYR, GLU, GLU, LEU	3.11, 1.96, 2.17, 1.95, 2.03, 3.39	3.99, 2.92, 3.09, 2.84, 2.84, 3.71
	AFF3-pralsetinib	-8.1	102A, 102A	TYR, TYR	2.37, 2.40	3.30, 3.30
ERG-wild	ERG-Adapalene	-9	-	-	-	-
	ERG-ponatinib	-8.1	23A, 27A, 55A	SER, ASN, ARG	3.13, 2.23, 3.36	3.96, 3.19, 3.88
	ERG-glycyrrhizic acid	-8.3	16A, 26A, 27A, 50A, 51A, 55A, 55A	GLN, SER, ASN, ARG, ARG, ARG, ARG	2.79, 2.70, 2.06, 2.97, 2.61, 2.60, 1.92	3.32, 3.10, 2.71, 3.69, 3.14, 3.33, 2.82
	ERG-pralsetinib	-8.1	23A, 51A, 54A, 55A, 55A	SER, ARG, GLU, ARG, ARG	2.17, 3.31, 3.18, 2.27, 3.06	3.11, 4.01, 4.03, 3.09, 4.01
ERG-E353Q	ERG-Adapalene	-9	33A	TRP	2.89	3.64
	ERG-ponatinib	-8.2	75A, 83A	ASP, HIS	3.31, 2.24	4.04, 3.10
	ERG-glycyrrhizic acid	-8.3	67A, 67A, 71A, 71A, 83A	SER, SER, ARG, ARG, HIS	3.12, 2.35, 1.82, 2.81, 2.55	3.69, 2.90, 2.81, 3.53, 3.36

Proteins		**Binding Affinity**	**Residue**	**AA**	**Distance H-A**	**Distance D-A**
	ERG-pralsetinib	-8.3	23A, 23A, 27A	SER, SER, ASN	2.60, 2.31, 2.35	3.20, 3.11, 3.26
MNX1-wild	MNX1-Adapalene	-8.2	-	-	-	-
	MNX1-ponatinib	-8.3	290A, 290A	ASN, ASN	2.59, 2.68	3.20, 3.21
	MNX1-glycyrrhizic acid	-7.9	185A, 185A, 187A, 187A, 189A, 191A	TYR, TYR, GLN, GLN, GLN, ALA	3.57, 2.56, 3.22, 1.97, 1.87, 2.14	4.09, 2.91, 3.68, 2.96, 2.87, 3.04
	MNX1-pralsetinib	-8.2	290A, 290A	ASN, ASN	2.59, 2.68	3.20, 3.21
MNX1-P392L	MNX1-Adapalene	-8.3	-	-	-	-
	MNX1-ponatinib	-8.7	185A	TYR	2.94	3.43
	MNX1-glycyrrhizic acid	-7.2	216A, 217A, 219A	SER, THR, GLY	1.82, 2.43, 2.99	2.74, 2.81, 3.35
	MNX1-pralsetinib	-8.2	239A	LYS	3.23	3.76
FAT1-D2382A	FAT1-D2382A-Adapalene	-6.9	99A, 99A	ASP, ASP	2.08, 3.01	2.95, 3.69
	FAT1-D2382A-ponatinib	-7.4	26A, 56A	ASP, THR	2.49, 2.19	3.34, 3.09
	FAT1-D2382A-glycyrrhizic acid	-7.8	1A, 89A, 90A	ALA, SER, ASP	2.52, 2.58, 2.69	2.91, 3.50, 3.65
	FAT1-D2382A-pralsetinib	-7.5	43A, 74A	HIS, THR	2.61, 2.25	3.19, 3.13
FAT1-D2382A	FAT1-D2382A-Adapalene	-7.1	-	-	-	-
	FAT1-D2382A-ponatinib	-7.2	1A, 89A	ALA, SER	2.21, 3.19	3.22, 4.08

Proteins		**Binding Affinity**	**Residue**	**AA**	**Distance H-A**	**Distance D-A**
	FAT1-D2382A-glycyrrhizic acid	-7.3	71A, 71A, 99A, 102A, 102A, 102A	ARG, ARG, ALA, ASP, ASP, ASP	3.20, 2.45, 2.07, 2.87, 2.38, 2.34	3.94, 3.33, 3.00, 3.25, 3.23, 3.17
	FAT1-D2382A-pralsetinib	-7.2	25A, 25A, 26A, 29A, 32A, 33A	THR, THR, ASP, SER, ASN, ARG	2.92, 3.46, 2.79, 2.70, 2.60, 3.20	3.72, 3.97, 3.73, 3.17, 3.42, 4.04
FAT1-M739I-wild	FAT1-M739I-Adapalene	-7.4	-	-	-	-
	FAT1-M739I-ponatinib	-8.5	74A, 84A	ASP, ARG	2.21, 2.62	2.86, 3.23
	FAT1-M739I-glycyrrhizic acid	-8.1	13A, 18A, 18A, 21A, 21A, 22A, 23A, 24A, 25A, 26A, 28A	SER, ASN, ASN, ASP, ASP, LEU, ASP, THR, GLY, PHE, GLY	2.92, 2.90, 2.43, 3.14, 2.42, 2.49, 2.78, 2.36, 2.62, 2.32, 3.52	3.66, 3.82, 3.26, 3.76, 3.20, 3.17, 3.37, 3.20, 3.61, 3.04, 3.98
	FAT1-M739I-pralsetinib	-7.4	18A, 19A, 21A, 22A	ASN, SER, ASP, LEU	3.28, 2.20, 2.70, 2.96	3.97, 2.88, 3.64, 3.97
FAT1-M739I	FAT1-M739I-Adapalene	-7.6	79A	GLN	2.11	3.04

Proteins		**Binding Affinity**	**Residue**	**AA**	**Distance H-A**	**Distance D-A**
	FAT1-M739I-ponatinib	-8.5	74A, 84A	ASP, ARG	2.20, 2.62	2.85, 3.24
	FAT1-M739I-glycyrrhizic acid	-8.1	13A, 18A, 21A, 22A, 23A, 24A, 25A, 26A, 28A	SER, ASN, ASP, LEU, ASP, THR, GLY, PHE, GLY	2.87, 2.40, 3.21, 2.60, 2.73, 2.33, 2.45, 2.33, 3.50	3.61, 3.23, 3.84, 3.24, 3.31, 3.18, 3.44, 3.06, 3.96
	FAT1-M739I-pralsetinib	-7.4	18A, 19A, 21A, 22A	ASN, SER, ASP, LEU	2.81, 1.99, 2.75, 2.86	3.30, 2.81, 3.70, 3.85
FAT1-P4309S	FAT1-P4309S-Adapalene	-8.6	296A	GLU	2.01	2.93
	FAT1-P4309S-ponatinib	-9.6	181A, 189A, 189A, 225A, 280A	GLN, ARG, ARG, GLN, SER	2.41, 2.78, 1.95, 2.02, 3.34	3.10, 3.52, 2.91, 3.02, 4.07
	FAT1-P4309S-glycyrrhizic acid	-8.9	190A, 196A, 196A	ASP, SER, SER	3.15, 3.75, 3.51	3.51, 4.07, 4.07
	FAT1-P4309S-pralsetinib	-8.9	102A, 104A, 104A, 305A	ASN, TYR, TYR, SER	2.66, 2.08, 1.92, 3.10	3.40, 2.81, 2.81, 3.72
FAT1-P4309S	FAT1-P4309S-Adapalene	-9.4	285A	SER	2.32	3.3
	FAT1-P4309S-ponatinib	-8.8	102A, 305A	ASN, SER	2.56, 2.63	2.97, 3.54

Proteins		**Binding Affinity**	**Residue**	**AA**	**Distance H-A**	**Distance D-A**
	FAT1-P4309S-glycyrrhizic acid	-8.1	179A, 180A, 181A, 181, 200A, 225A	SER, ASN, GLN, GLN, SER, GLN	2.18, 2.63, 2.19, 2.05, 2.30, 2.91	3.03, 3.10, 3.19, 2.89, 3.25, 3.49
	FAT1-P4309S-pralsetinib	-9.1	259A, 279A	PRO, GLU	1.93, 2.53	2.89, 3.37

4.16.1 Molecular Docking of Wild-type and Mutant Model (T38I) of the TCL1A Protein with Selected Drug Compounds

The binding affinities of the wild-type and mutant model (T38I) of the TCL1A protein were found to be -9.1 (kcal/mol) and -9.2 (kcal/mol) with midostaurin (DB06595) and carvedilol (DB01136), respectively. Nevertheless, the outcomes pertaining to the binding affinities observed with the chosen compounds were also of notable importance. Both the wild and mutant forms exhibited the highest binding affinity for adapalene, with binding scores of -8.7 and -8.3, respectively. This was followed by pralsetinib with scores of -8.5 and -7.8, Ponatinib with scores of -8.3 and -7.7, and glycyrrhizic acid with scores of -7.2 and -7.5 (Figure 4.30. and Table 4.13). The wild-type TCL1A protein complexes with the Adapalene, Ponatinib, Glycyrrhizic acid, and Pralsetinib showed the interacting residue, MET, at 62 position with adapalene, showed no interactions with ponatinib, GLN at position 66 with glycyrrhizic acid, ASP and VAL at positions 28, 55 and 56 (ASP interacted at positions 28 and 55, while VAL at position 56 showed two interactions) with pralsetinib (Figure 4.30a). However, the mutant (T38I) TCL1A complexes showed the interacting residues, ALA and ILE, at positions 20 and 74 with adapalene, LYS at position 23 with ponatinib, VAL, LEU, HIS at 11,94 and

97 positions (HIS at position 97 showed two interactions) with glycyrrhizic acid but showed no interactions with the pralsetinib (Figure 4.30b).

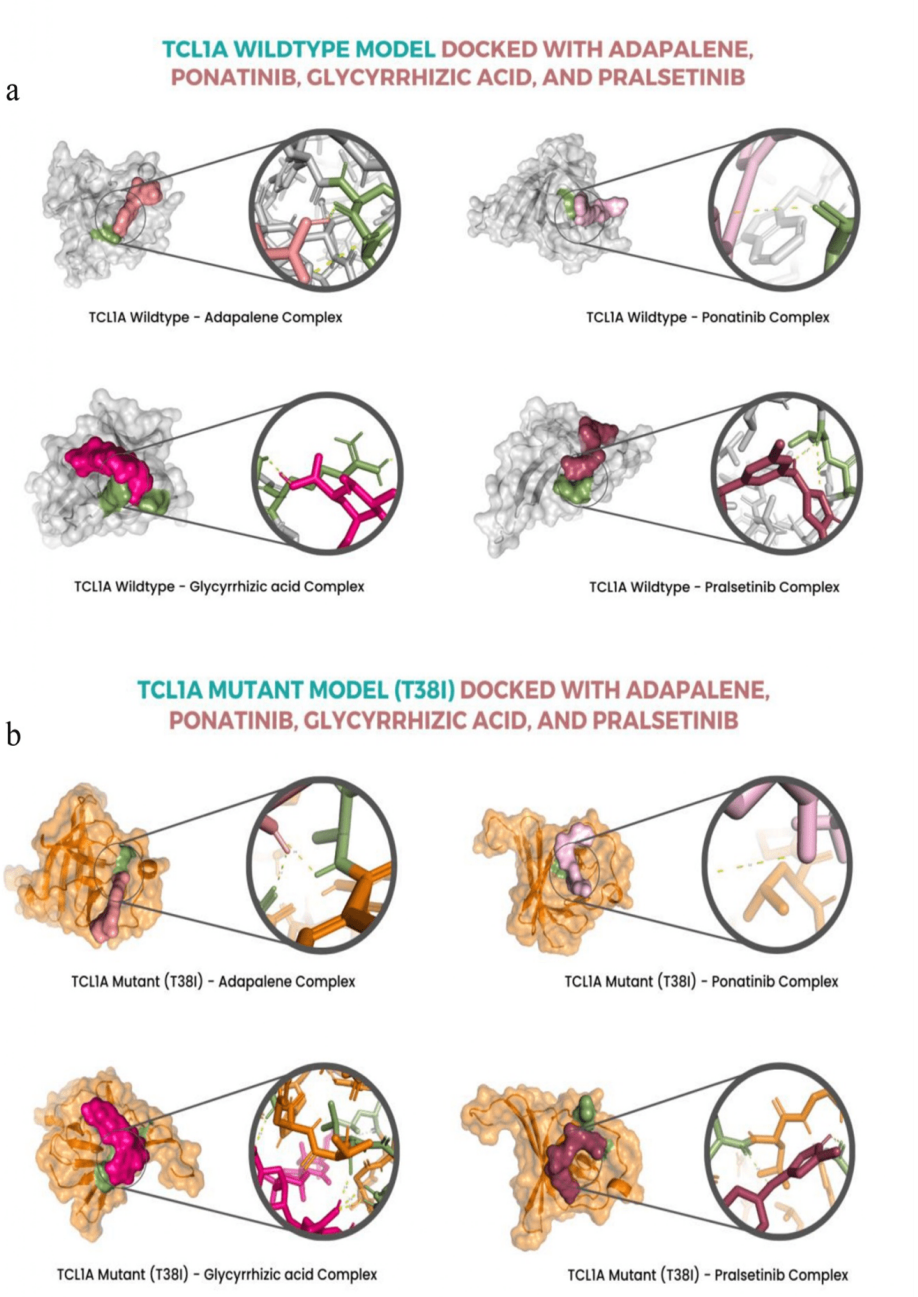

FIGURE 4.30: (a) Visualization of wild-type TCL1A protein docked with Adapalene, Ponatinib, Glycyrrhizic acid and Pralsetinib on PyMOL, showing interactions of the ligand molecules with the protein residues. (b) Visualization of mutant model (T38I) of TCL1A protein docked with Adapalene, Ponatinib, Glycyrrhizic acid and Pralsetinib on PyMOL, showing interactions of the ligand molecules with the protein residues.

4.17 Molecular Docking of Drug Compounds with Candidate Relapse Biomarkers

The molecular docking of the wild-type and mutant models of MNX1, FAT1, ERG, TCL1A, AFF3, KRAS, and NRAS with the FDA and EMA-approved drug compounds was performed using AutoDock Vina, showing variable binding affinities. Furthermore, the wild-type CD4, ITGAM, PTPRC, TYROBP, and IL1B proteins were also docked with the retrieved drug compounds; however, the proteins CSF1R, VCAN, NRP1, COL22A1, BPI, and BIRC5 were docked only with those compounds (Adapalene, Poatinib, Glycyrrhizic acid, and Pralsetinib) that showed significant binding affinities among all of the other proteins. The binding affinities of all the complexes ranged from as high as -3.1 kcal/mol of the wild-type TYROBP protein with D-norleucine (DB04419) and dimethyl fumarate (DB08908) to as low as -10.9 kcal/mol of the wild-type ITGAM protein with glycyrrhizic acid (DB13751).The complete results of binding affinities of all proteins with all selected compounds are given. However, the detailed analysis of results revealed that out of 141 compounds four compounds namely adapalene (DB00210), ponatinib (DB08901), glycyrrhizic acid (DB13751), and pralsetinib (DB15822) showed significant binding affinities with all wild as well as mutant proteins. These binding affinity score of these compounds with all protein along with the binding residues information obtained from Protein-Ligand Interaction Profiler (PLIP) were compiled in Table 4.13. Lastly, the visualization of the docked complexes on PyMOL also disclosed the proteins binding residues and their positions that were showing interactions with the drug compounds and are shown in Figure 4.30 – 4.34.

4.17.1 Molecular Docking of Wild-type and Mutant Model (T38I) of the TCL1A Protein with Selected Drug Compounds

The binding affinities of the wild-type and mutant model (T38I) of the TCL1A protein were found to be -9.1 (kcal/mol) and -9.2 (kcal/mol) with midostaurin

(DB06595) and carvedilol (DB01136), respectively. Nevertheless, the outcomes pertaining to the binding affinities observed with the chosen compounds were also of notable importance. Both the wild and mutant forms exhibited the highest binding affinity for adapalene, with binding scores of -8.7 and -8.3, respectively. This was followed by pralsetinib with scores of -8.5 and -7.8, Ponatinib with scores of -8.3 and -7.7 and glycyrrhizic acid with scores of -7.2 and -7.5 (Figure 4.30 and Table 4.13). The wild-type TCL1A protein complexes with the Adapalene, Ponatinib, Glycyrrhizic acid, and Pralsetinib showed the interacting residue, MET, at 62 position with adapalene, showed no interactions with ponatinib, GLN at position 66 with glycyrrhizic acid, ASP and VAL at positions 28, 55 and 56 (ASP interacted at positions 28 and 55, while VAL at position 56 showed two interactions) with pralsetinib (Figure 4.30a). However, the mutant (T38I) TCL1A complexes showed the interacting residues, ALA and ILE, at positions 20 and 74 with adapalene, LYS at position 23 with ponatinib, VAL, LEU, HIS at 11,94 and 97 positions (HIS at position 97 showed two interactions) with glycyrrhizic acid but showed no interactions with the pralsetinib (Figure 4.30b).

4.17.2 Molecular Docking of Wild-type and Mutant AFF3-P1129L of the AFF3 Protein with Selected Drug Compounds

In addition, the AFF3 wild type had the most significant binding interaction of -8.5 (kcal/mol) with pranlukast (DB01411), whereas the AFF3-P1129L variant demonstrated the highest binding interaction of -8.6 (kcal/mol) with ponatinib (DB08901). In a similar manner, the significant interaction between the wild and mutant (P1129L) AFF3 model and other selected drugs, Adapalene (-8.2, -8.4), Glycyrrhizic acid (-8, -8), and Pralsetinib (-7.9, -8.1), was seen. Furthermore, the wild-type AFF3 protein complexes exhibited specific residue interactions. Specifically, ASP displayed two interactions at position 29 and GLU at position 74 with adapalene. Additionally, LYS, ASN, and GLU at positions 95, 222, and 224 interacted with ponatinib. Moreover, GLU, ALA, and ARG at positions 213, 219,

and 223 interacted with glycyrrhizic acid. Furthermore, ASN displayed two interactions at position 227 with glycyrrhizic acid, LEU at position 238, and ARG at positions 103 and 117 interacted with pralsetinib (Figure 4.31a). In contrast, the mutant (P1129L) AFF3 complexes exhibited specific residue interactions. Specifically, the residue ASN at position 40 interacted with adapalene, LYS at position 83 interacted with ponatinib, and LYS at positions 22 and 25 interacted with TYR and LEU at positions 41 and 75, respectively. Additionally, GLU displayed two interactions at position 71 with glycyrrhizic acid, while TYR exhibited two interactions at position 102 with pralsetinib (Figure 4.31b and Table 4.13).

4.17.3 Molecular Docking of Wild-type and Mutant ERG-E153Q of the ERG protein with Selected Drug Compounds

Furthermore, it was observed that both the wild-type and mutant (E153Q) models of the ERG protein exhibited binding affinities of -9 (kcal/mol) and -8.3 with adapalene and glycyrrhizic acid, respectively. In contrast, the combination of -8.1 and -8.2 with ponatinib, as well as the combination of -8.1 and -8.3 with pralsetinib, exhibit certain effects. In addition, it was observed that the wild-type ERG protein complexes did not exhibit any interactions with adapalene. However, they did display interactions with ponatinib, specifically with the residues SER, ASN, and ARG at positions 23, 27, and 55, as well as ARG at positions 50, 51, and 55 (with two interactions occurring at position 55). Furthermore, interactions were observed with glycyrrhizic acid, involving the residues GLN, SER, and ASN at positions 16, 26, and 27, respectively. Additionally, interactions were observed with pralsetinib, involving the residues SER and GLU at positions 23 and 54, as well as ARG at positions 51 and 55 (with two interactions occurring at position 55) (Figure 4.32a). Similarly, the ERG complexes harboring the mutant (353Q) exhibited specific residue interactions. Specifically, TRP at position 33 interacted with adapalene, while ASP and HIS at positions 75 and 83 respectively interacted with ponatinib. Additionally, SER and ARG displayed two interactions at

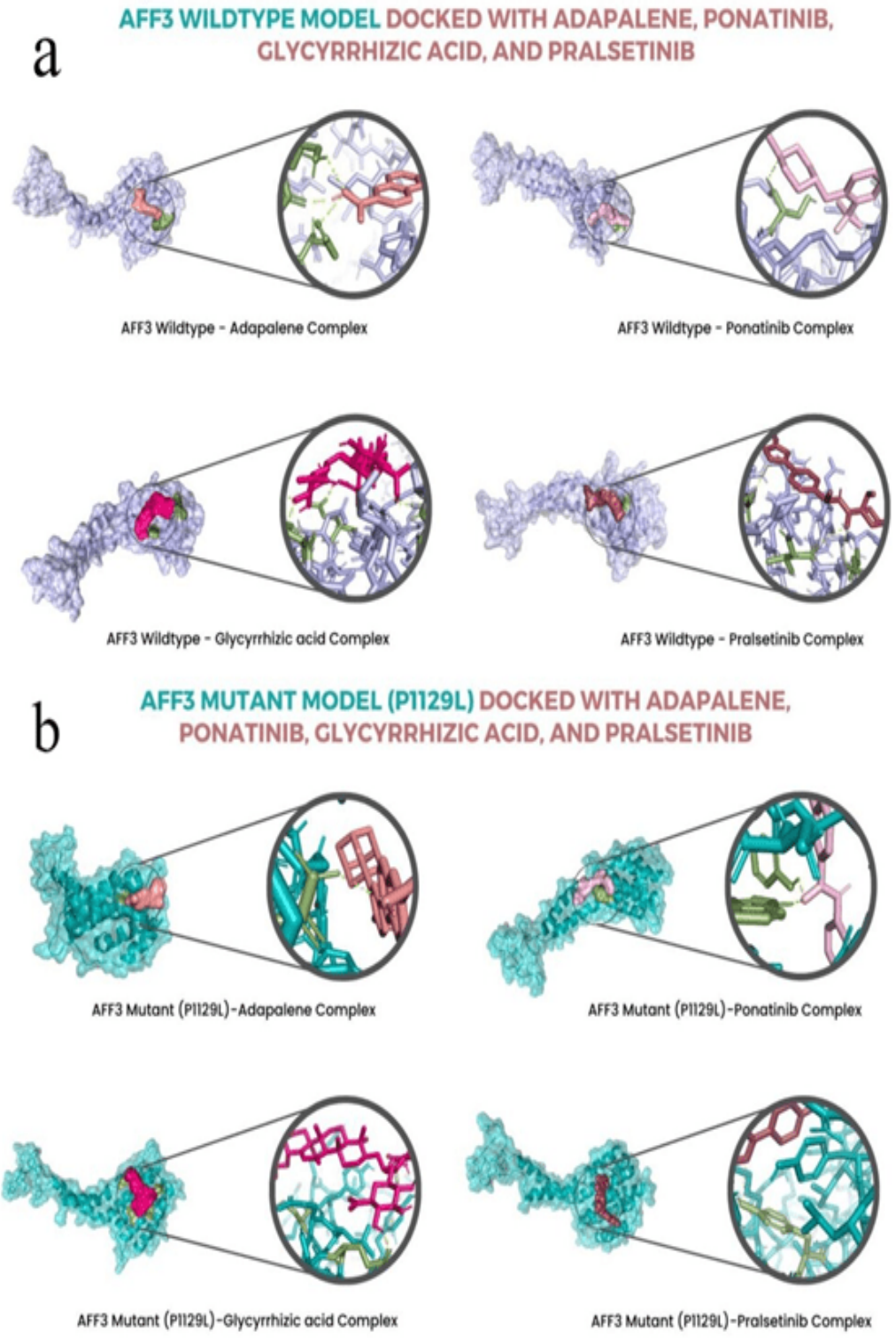

FIGURE 4.31: Visualization of (a) AFF3-wild and (b) mutant AFF3- P1129L protein docked with Adapalene, Ponatinib, Glycyrrhizic acid and Pralsetinib on PyMOL, showing interactions of the ligand molecules with the protein residues

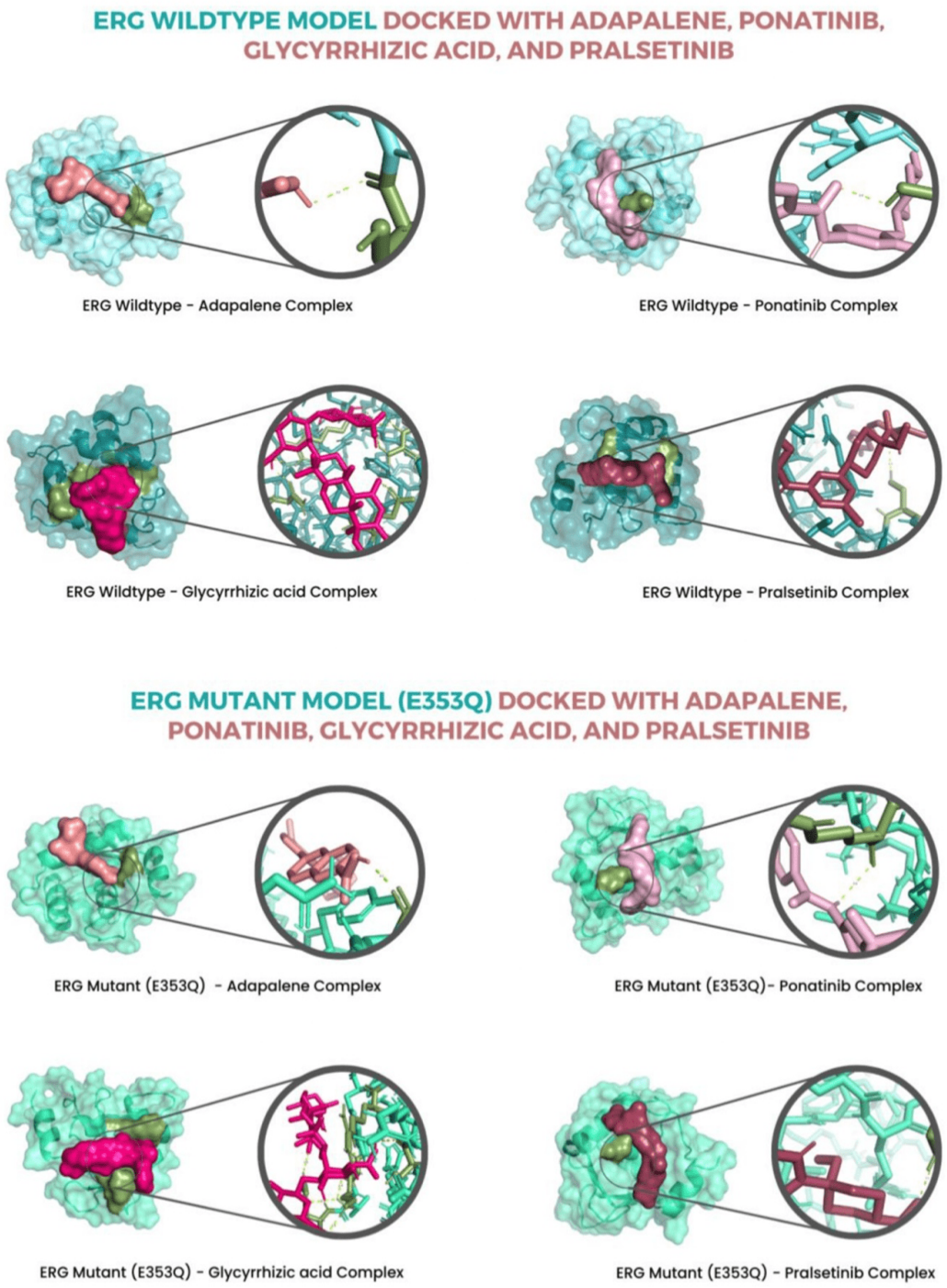

FIGURE 4.32: Visualization of (a) ERG-wild (b) mutant ERG-E353Q protein docked with Adapalene, Ponatinib, Glycyrrhizic acid and Pralsetinib on PyMOL, showing interactions of the ligand molecules with the protein residues.

positions 67 and 71, while HIS at position 83 interacted with glycyrrhizic acid. Furthermore, SER interacted twice at position 23 and ASN at positions 27 with pralsetinib (Figure 4.32b and Table 4.13).

4.17.4 Molecular Docking of Wild-type and Mutant MNX1 - P392L of the MNX1 Protein with Selected Drug Compounds

Furthermore, the docking simulations revealed that the wild-type and mutant (P392L) models of the MNX1 protein exhibited binding affinities of -8.3 (kcal/-mol) and -8.7 (kcal/mol) respectively, towards ponatinib. Similarly, the affinities towards adapalene were -8.2 and -8.3, towards pralsetinib were -8.2 and -8.2, and towards glycyrrhizic acid were -7.9 and -7.2. In addition, it was observed that the wild-type MNX1 protein complexes did not exhibit any interactions with adapalene. However, it was found that the amino acid ASN at position 290 displayed two interactions with ponatinib. Furthermore, TYR and GLN at positions 185 and 187 respectively demonstrated two interactions, while ALA at position 191 and GLN at position 189 interacted with glycyrrhizic acid. Lastly, ASN at position 290 exhibited an interaction with pralsetinib (Figure 4.33a). In addition, it was shown that the mutant MNX1 complexes with the P392L mutation also did not exhibit any interactions with adapalene. However, these complexes did exhibit interactions with other compounds. Specifically, the residue TYR at position 185 was found to connect with ponatinib, while the residues SER, THR, and GLY at positions 216, 217, and 219 respectively, were found to interact with glycyrrhizic acid. Additionally, the residue LYS at position 239 was found to interact with pralsetinib (Figure 4.33b, Table 4.13).

4.17.5 Molecular Docking of Wild-type and Mutant models of the FAT1 Protein with Selected Drug Compounds

The binding affinities of the domains of wild-type FAT1 (D2382A, M739I, and P4309S) with ponatinib were -7.4 kcal/mol, -8.5 kcal/mol, and -9.6 kcal/mol, respectively. Similarly, the binding affinities with glycyrrhizic acid were -7.8 kcal/-mol, -8.1 kcal/mol, and -8.9 kcal/mol, and with pralsetinib were -7.5 kcal/mol,

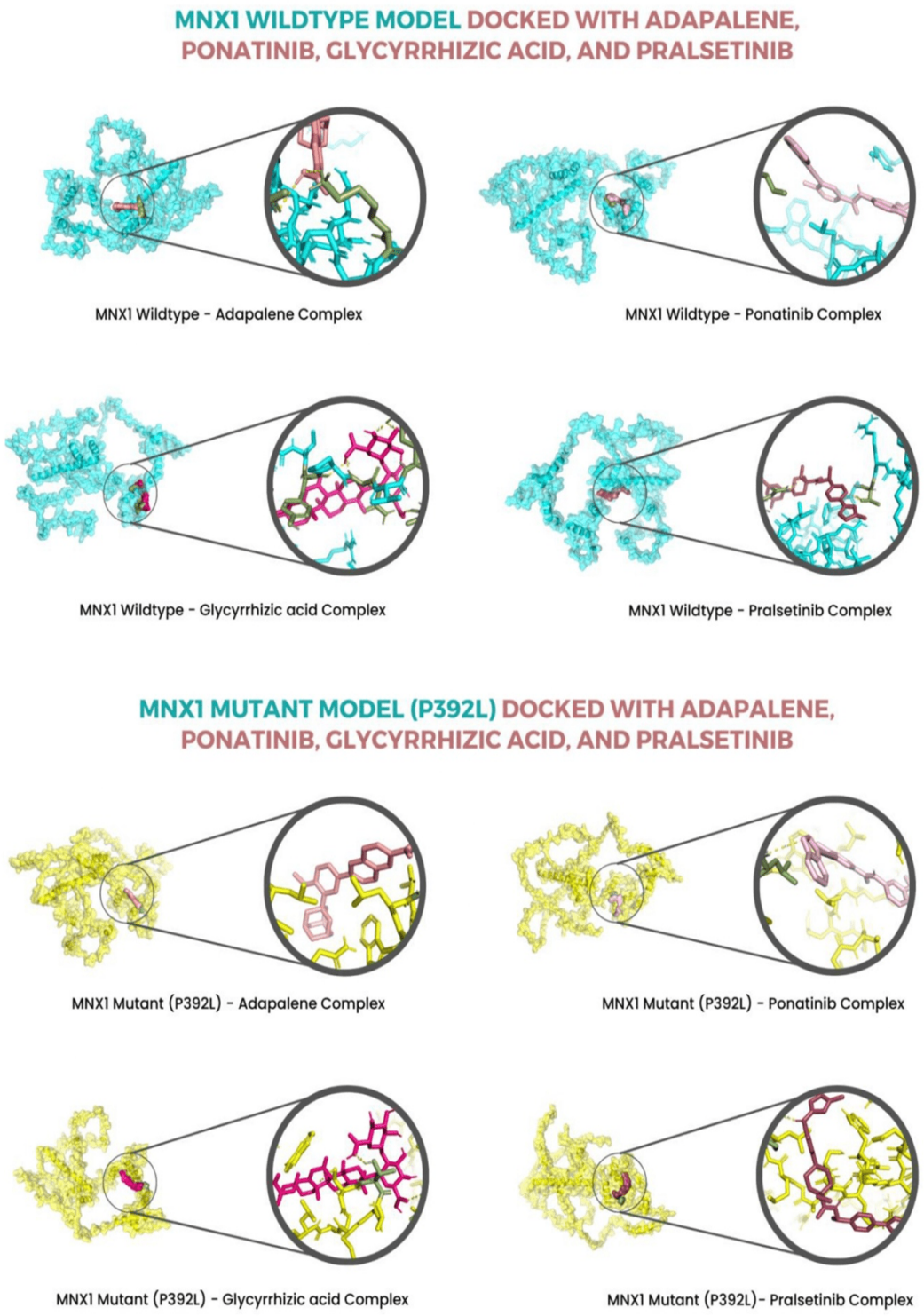

FIGURE 4.33: Visualization of (a) MNX1-wild and (b) mutant MNX1- P392L protein docked with Adapalene, Ponatinib, Glycyrrhizic acid and Pralsetinib on PyMOL, showing interactions of the ligand molecules with the protein residues.

-7.4 kcal/mol, and -8.9 kcal/mol. In contrast, the FAT1 mutant model (D2382A, M739I, and P4309S) exhibited the most favourable binding affinities of -7.3 kcal/-mol, -8.5 kcal/mol, and -9.4 kcal/mol towards glycyrrhizic acid, ponatinib, and adapalene, respectively.

Furthermore, the wild-type (D2382A) FAT1 protein complexes exhibited specific interactions between certain residues. Specifically, ASP residues at position 99 interacted with adapalene, while ASP and THR residues at positions 26 and 56 interacted with ponatinib. Additionally, ALA, SER, and ASP residues at positions 1, 89, and 90 interacted with glycyrrhizic acid, and HIS and THR residues at positions 43 and 74 interacted with pralsetinib (Figure 4.34). In contrast, the mutant model (D2382A) FAT1 complexes exhibited a lack of interaction with adapalene, ALA, and SER at position 1 and 89, as well as with ponatinib and ALA at position 99. However, ARG demonstrated two interactions at position 71, while ASP displayed three interactions at position 102 with glycyrrhizic acid. Additionally, ASP, SER, ASN, and ARG at positions 26, 29, 32, and 33 respectively, exhibited interactions with pralsetinib (Figure 4.34). The wild-type FAT1 (M739I) protein complexes, did not exhibit any interaction with adapalene, ASP, ARG at positions 74, 84, or with ponatinib, SER, LEU, ASP, THR, GLY, PHE at positions 13, 22, 23, 24, and 26. However, GLY demonstrated two interactions at positions 25 and 28, while ASP also displayed two interactions at position 21, with glycyrrhizic acid, ASN, SER, ASP, LEU at positions 18, 19, 21, and 22, in the presence of pralsetinib (Figure 4.34). The mutant model (M739I) of the FAT1 protein exhibited specific residue interactions with various compounds. Specifically, GLN at position 79 interacted with adapalene, while ASP and ARG at positions 74 and 84, respectively, interacted with ponatinib. Additionally, SER, ASN, LEU, THR, and PHE at positions 13, 18, 22, 24, and 26, respectively, interacted with ponatinib. ASP displayed two interactions at positions 21 and 23, while GLY also exhibited two interactions at positions 25 and 28 with glycyrrhizic acid. Furthermore, ASN, SER, ASP, and LEU at positions 18, 19, 21, and 22, respectively, interacted with pralsetinib (Figure 4.34).

The wild-type (P4309S) FAT1 protein complexes exhibited specific residue interactions. Notably, GLU at position 296 interacted with adapalene, SER at position 280, ARG at position 189 displayed two interactions, and GLN at positions 181 and 225 exhibited two interactions with ponatinib. Additionally, ASP at position 190, SER at position 196 had two interactions with glycyrrhizic acid and ASN, and SER at positions 102 and 305 interacted with pralsetinib (Figure 4.34). The mutant model (P4309S) of the FAT1 protein exhibited specific residue interactions with various compounds. Specifically, SER at position 285 interacted with adapalene, while ASN and SER at positions 102 and 305 interacted with ponatinib. ASN at position 180 also showed an interaction, while SER exhibited two interactions at positions 179 and 200. Additionally, GLN displayed three interactions with glycyrrhizic acid and PRO, with two interactions occurring at position 181 and one at position 225. Finally, GLU at positions 259 and 279 interacted with pralsetinib (Figure 4.34, Table 4.13).

4.17.6 Molecular Docking of Wild-type and Mutant Models of the KRAS Protein with Selected Drug Compounds

In addition, the wild-type KRAS protein exhibited the highest binding affinity of -8.7 (kcal/mol) towards silandrin. In contrast, the mutant models of the KRAS protein exhibited the most favorable binding affinities with hydnocarpinD, midostaurin (DB06595), enzastaurin (DB06486), enzastaurin (DB06486), nintedanib (DB09079), glycyrrhizic acid (DB13751), midostaurin (DB06595), brigatinib (DB 12267), and ponatinib (DB08901), with respective values of -9 kcal/mol (mutant_Q61H), -9.1 kcal/mol (mutant_Q61R), -8.9 kcal/mol (mutant_G13D), -8.8 kcal/mol (mutant_G12V), -8.6 kcal/mol (mutant_G12R), -8.5 kcal/mol (mutant _Q61E), -8.7 kcal/mol (mutant_K117N), -8.7 kcal/mol (mutant_A59E), and -9.6 kcal/mol (mutant _G12D). Nevertheless, the measured binding affinities between wild-type KRAS and its variations, as well as all selected compounds, were found to be significant according to the data presented in Table 4.13.

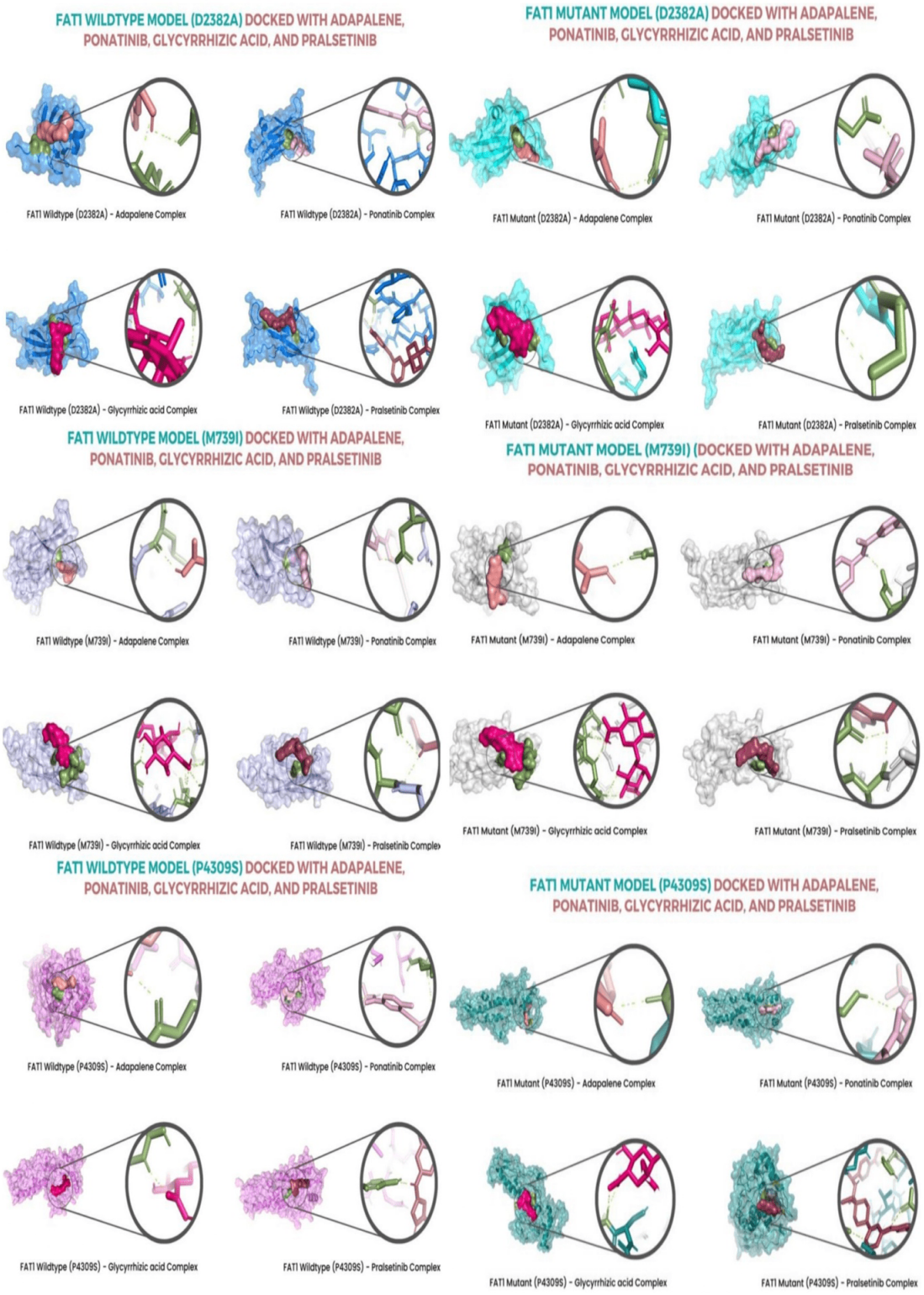

FIGURE 4.34: Visualization of wild-type FAT1 (D2382A M739I and P4309S) domains and mutant FAT1 (D2382A M739I and P4309S) domains docked with Adapalene, Ponatinib, Glycyrrhizic acid and Pralsetinib on PyMOL, showing interactions of the ligand molecules with the protein residues.

In addition, the wild-type KRAS complexes exhibited binding residues that included ASP and ASN at positions 32 and 115 in interaction with adapalene, THR and GLU at positions 34 and 36 in association with ponatinib, and GLY, SER, ASP, and ALA at positions 12, 16, 32, and 58 in conjunction with glycyrrhizic acid. Furthermore, GLY and LYS at positions 12 and 116 were found to interact with pralsetinib (Figure 4.35).

The mutant model (A59E) exhibited interactions between specific residues and various compounds. Adapalene interacted with ALA and LYS at positions 145 and 146, ponatinib interacted with GLN and TYR at positions 24 and 39, glycyrrhizic acid interacted with SER and GLY at positions 16 and 59, and glycyrrhizic acid also interacted with ASP at positions 32 and 56, as well as GLU at positions 30 and 36. Additionally, pralsetinib interacted with ARG at position 163 (Figure 4.35).

The G12D mutant variant of KRAS did not exhibit any interaction with adapalene. However, ponatinib demonstrated interactions with residues THR and GLN at positions 34 and 60, respectively. Glycyrrhizic acid interacted with ASP, GLY, LYS, SER, and ASP residues at positions 11, 12, 14, 15, 16, and 32, with GLY specifically interacting at positions 12 and 14. Pralsetinib, on the other hand, showed interactions with GLN, THR, and TYR residues at positions 24, 34, and 39, respectively(Figure 4.35).

The G12R mutant model of KRAS exhibited interactions between specific residues. Specifically, SER at position 16 interacted with adapalene, THR at position 34 interacted with ponatinib, and GLY, LYS, SER, ALA, ASP, THR, and GLU were found at positions 12, 14, 15, 16, 17, 29, 34, and 36, respectively (with GLY interacting at positions 12 and 14) with glycyrrhizic acid. Additionally, GLU, GLN, and ARG were observed at positions 61, 98, and 101, respectively, and were found to interact with pralsetinib (Figure 4.35).

The G12V mutant variant of KRAS exhibited interactions with adapalene at positions 29 and 30, specifically with the residues ASP and GLU. However, no interactions were observed between the mutant KRAS and ponatinib, as well as the

residues THR, ARG, GLU, and VAL at positions 1, 72, 75, 166, and 180 (although ARG did interact at positions 72 and 166) with glycyrrhizic acid. Additionally, pralsetinib showed interactions with the residues GLU and LYS at positions 97 and 100 with the mutant KRAS (Figure 4.35).

The mutant model (G13D) exhibited residue interactions between SER and LYS at positions 16, 144, and 146 (specifically, SER interacted at positions 16 and 144) with adapalene. ARG interacted at positions 148, 160, and 160 with ponatinib. LYS, ASP, HIS, and GLN at positions 87, 91, 94, and 98 interacted with glycyrrhizic acid. GLN, PHE, ARG, VAL, GLU, and ASP residues interacted at positions 130, 140, 148, 150, 151, 152, and 153 (notably, ARG interacted at positions 148 and 150) with pralsetinib (Figure 4.35).

The mutant model of KRAS, specifically the K117N variant, exhibits interactions with various residues when exposed to different compounds. Adapalene interacts with LYS and GLU residues at positions 103 and 173, respectively. Ponatinib, on the other hand, interacts with ARG residues at positions 148, 150, and 160. Glycyrrhizic acid interacts with GLY, LYS, ASP, THR, and GLU residues at positions 12, 14, 15, 29, 32, 34, and 36. Notably, GLY interacts at positions 12 and 14, while ASP interacts at positions 29 and 32. Lastly, pralsetinib interacts with ASN, ASP, and LYS residues at positions 116, 118, and 146 (Figure 4.35).

The Q61E mutant variant of the KRAS protein exhibited interactions with several residues. Specifically, it displayed interaction with ILE at position 138 when exposed to adapalene. Moreover, when exposed to ponatinib, the mutant variant showed interactions with LYS and SER at positions 4 and 38, respectively. Additionally, glycyrrhizic acid elicited interactions with GLU, LYS, SER, ARG, ASP, and THR at positions 2, 4, 38, 40, 53, 60, and 73. Lastly, pralsetinib induced interactions with HIS, GLU, and ASP at positions 94, 97, and 104, respectively (Figure 4.35).

The Q61H mutant model of KRAS demonstrated interactions between specific residues, namely GLN and GLU at positions 24 and 36, with adapalene. However, no interactions were observed between ponatinib and the residues GLY, LYS,

SER, ALA, ASP, TYR, ASP, THR at positions 14, 15, 16, 17, 29, 31, 32, and 34 (except for ASP, which interacted at positions 29 and 32) with glycyrrhizic acid. Additionally, pralsetinib exhibited interactions with LYS, ARG, and GLN at positions 15, 67, and 98, respectively (Figure 4.35).

The Q61R mutant variant of KRAS exhibited interactions between specific amino acid residues, namely GLU and ASP at positions 36 and 56, with adapalene. Additionally, VAL and ARG at positions 44 and 160 were found to interact with ponatinib. Furthermore, glycyrrhizic acid was observed to interact with GLY, SER, ASP, and ASN at positions 12, 16, 32, and 84, respectively. Lastly, pralsetinib was found to interact with HIS, GLU, ARG, and TYR at positions 93, 97, 101, and 136, respectively (Figure 4.35), Table 4.14).

TABLE 4.14: Protein-Ligand Interaction Profiler (PLIP) of the docked complexes of the KRAS wild-type and KRAS variants with selected drug compounds, representing the binding residues, their positions and distances between hydrogen-acceptor and donor-acceptor molecules

Proteins		**Binding Affinity**	**Residue**	**AA**	**Distance H-A**	**Distance D-A**
KRAS -wild	KRAS-Adapalene	-7.8	32A, 115A	ASP, ASN	1.80, 3.58	2.80, 3.99
	KRAS-ponatinib	-8.1	34A, 36A, 36A	THR, GLU, GLU	2.88, 2.65, 3.30	3.63, 3.61, 3.88
	KRAS-glycyrrhizic acid	-8.1	12A, 16A, 32A, 32A, 58A	GLY, SER, ASP, ASP, ALA	2.11, 2.03, 2.23, 2.24, 2.58	3.11, 2.96, 3.14, 3.15, 3.29
	KRAS-pralsetinib	-7.6	12A, 116A	GLY, LYS	1.98, 2.77	2.90, 3.68
KRAS-A59E	KRAS-A59E-Adapalene	-8.3	145A, 146A	ALA, LYS	3.34, 2.82	4.01, 3.78
	KRAS-A59E-ponatinib	-8.5	24A, 39A	GLN, TYR	1.98, 3.51	2.96, 4.03
	KRAS-A59E-glycyrrhizic acid	-8.6	16A, 30A, 32A, 32A, 36A, 36A, 56A, 59A	SER, GLU, ASP, ASP, GLU, GLU, ASP, GLY	1.96, 2.17, 1.86, 3.38, 3.51, 2.63, 1.90, 2.31	2.83, 3.13, 2.86, 4.06, 3.92, 3.20, 2.75, 3.24
	KRAS-A59E-pralsetinib	-7.8	163A, 163A, 163A	ARG, ARG, ARG	3.04, 2.38, 2.25	3.69, 3.16, 3.17

Proteins		**Binding Affinity**	**Residue**	**AA**	**Distance H-A**	**Distance D-A**
KRAS-G12D	KRAS-G12D-Adapalene	-7.8	-	-	-	-
	KRAS-G12D-ponatinib	-9.6	34A, 60A, 60A	THR, GLN, GLN	2.18, 2.95, 3.00	3.02, 3.40, 3.76
	KRAS-G12D-glycyrrhizic acid	-8.3	11A, 12A, 12A, 14A, 15A, 16A, 16A, 32A	ASP, GLY, GLY, GLY, LYS, SER, SER, ASP	2.32, 2.55, 2.53, 2.61, 2.75, 2.89, 2.23, 3.25	2.97, 3.41, 3.09, 3.28, 3.12, 3.32, 3.21, 3.93
	KRAS-G12D-pralsetinib	-8.6	24A, 34A, 39A	GLN, THR, TYR	2.86, 2.62, 2.82	3.50, 3.10, 3.17
KRAS-G12R	KRAS-G12R-Adapalene	-8.2	16A	SER	2.53	3.35
	KRAS-G12R-ponatinib	-8.3	34A	THR	2.57	3.15
	KRAS-G12R-glycyrrhizic acid	-7.9	12A, 14A, 15A, 16A, 16A, 17A, 29A, 34A, 36A	GLY, GLY, LYS, SER, SER, ALA, ASP, THR, GLU	2.14, 2.47, 3.35, 2.81, 2.02, 2.91, 2.77, 2.23, 2.48	3, 3.40, 4.09, 3.67, 2.91, 3.80, 3.68, 3.17, 3.29
	KRAS-G12R-pralsetinib	-7.5	61A, 98A, 101A	GLU, GLN, ARG	2.18, 2.75, 3.03	2.99, 3.68, 3.63
KRAS-G12V	KRAS-G12V-Adapalene	-8.2	29A, 30A	ASP, GLU	2.37, 2.20	3.04, 3.22
	KRAS-G12V-ponatinib	-7.4	-	-	-	-
	KRAS-G12V-glycyrrhizic acid	-7.9	1A, 72A, 75A, 166A, 166A, 180A	THR, ARG, GLU, ARG, ARG, VAL	3.38, 3.07, 2.71, 2.10, 3.26, 2.88	4.02, 3.92, 3.38, 3.04, 3.91, 3.22
	KRAS-G12V-pralsetinib	-8.1	97A, 100A	GLU, LYS	2.26, 3.06	2.94, 3.98
KRAS-G13D	KRAS-G13D-Adapalene	-8.2	16A, 144A, 146A	SER, SER, LYS	2.94, 3.37, 3.22	3.75, 3.96, 4.07
	KRAS-G13D-ponatinib	-7.9	148A, 160A, 160A	ARG, ARG, ARG	2.07, 2.68, 2.62	2.95, 3.28, 3.23

Proteins		**Binding Affinity**	**Residue**	**AA**	**Distance H-A**	**Distance D-A**
	KRAS-G13D-glycyrrhizic acid	-8.1	87A, 91A, 94A, 98A, 98A	LYS, ASP, HIS, GLN, GLN	2.39, 3.27, 2.21, 2.98, 2.11	2.80, 4.02, 3.03, 3.96, 2.96
	KRAS-G13D-pralsetinib	-7.4	130A, 140A, 148A, 150A, 151A, 152A, 153A	GLN, PHE, ARG, ARG, VAL, GLU, ASP	3.06, 2.94, 3.01, 2.85, 3.14, 2.53, 3.06	3.53, 3.85, 3.84, 3.50, 3.87, 3.40, 3.99
KRAS-K117N	KRAS-K117N-Adapalene	-8.5	103A, 173A	LYS, GLU	3.15, 2.47	4.08, 3.05
	KRAS-K117N-ponatinib	-8	148A, 150A, 160A, 160A	ARG, ARG, ARG, ARG	2.65, 3.37, 2.49, 2.14	3.10, 4.07, 3.23, 2.97
	KRAS-K117N-glycyrrhizic acid	-7.3	12A, 14A, 15A, 29A, 32A, 32A, 34A, 36A	GLY, GLY, LYS, ASP, ASP, ASP, THR, GLU	3.07, 2.23, 3.00, 1.97, 2.20, 1.97, 2.17, 2.48	4.03, 3.15, 3.70, 2.72, 3.10, 2.82, 3.02, 3.23
	KRAS-K117N-pralsetinib	-8.3	116A, 118A, 146A	ASN, ASP, LYS	2.80, 3.37, 2.98	3.79, 4.09, 3.65
KRAS-Q61E	KRAS-Q61E-Adapalene	-7.5	138A	ILE	3.66	3.99
	KRAS-Q61E-ponatinib	-7.8	4A, 38A	LYS, SER	2.79, 2.53	3.43, 3.37
	KRAS-Q61E-glycyrrhizic acid	-8.5	2A, 4A, 38A, 40A, 53A, 60A, 73A	GLU, LYS, SER, ARG, ASP, GLU, THR	2.13, 3.55, 2.25, 3.51, 3.04, 3.15, 2.52	2.98, 4.05, 3.17, 4.04, 3.63, 3.70, 3.09
	KRAS-Q61E-pralsetinib	-7.7	94A, 97A, 104A	HIS, GLU, ASP	3.07, 2.52, 3.32	4.04, 3.19, 4.05
KRAS-Q61H	KRAS-Q61H-Adapalene	-7.9	24A, 36A	GLN, GLU	3.20, 3.38	4.05, 3.89
	KRAS-Q61H-ponatinib	-7.8	-	-	-	-

Proteins		**Binding Affinity**	**Residue**	**AA**	**Distance H-A**	**Distance D-A**
	KRAS-Q61H-glycyrrhizic acid	-8.1	14A, 15A, 16A, 16A, 17A, 29A, 31A, 32A, 34A, 34A	GLY, LYS, SER, SER, ALA, ASP, TYR, ASP, THR, THR	2.64, 2.84, 3.10, 2.34, 3.64, 2.07, 3.00, 2.25, 1.96, 2.09	3.31, 3.24, 3.98, 3.31, 4.10, 3.02, 3.58, 3.09, 2.85, 3.01
	KRAS-Q61H-pralsetinib	-7.5	15A, 67A, 67A, 98A, 98A	LYS, ARG, ARG, GLN, GLN	2.47, 3.28, 3.07, 3.42, 3.19	3.41, 3.99, 3.88, 3.83, 3.96
KRAS-Q61R	KRAS-Q61R-Adapalene	-8.8	36A, 36A, 56A	GLU, GLU, ASP	3.45, 2.28, 2.94	4.01, 3.08, 3.75
	KRAS-Q61R-ponatinib	-7.5	44A, 44A, 160A	VAL, VAL, ARG	2.40, 3.24, 3.31	3.42, 3.90, 3.97
	KRAS-Q61R-glycyrrhizic acid	-8.5	12A, 16A, 32A, 84A	GLY, SER, ASP, ASN	2.13, 2.06, 2.94, 2.96	3.03, 3.00, 3.91, 3.58
	KRAS-Q61R-pralsetinib	-7.4	93A, 97A, 101A, 136A, 136A	HIS, GLU, ARG, TYR, TYR	2.80, 2.26, 3.73, 2.49, 2.36	3.23, 3.02, 4.10, 3.20, 3.20

4.17.7 Molecular Docking of Wild-type and Mutant Models of the NRAS Protein with Selected Drug Compounds

In a similar vein, the wild-type NRAS protein exhibited the most favorable binding affinity of -8.6 (kcal/mol) with theaflavine. Conversely, the mutant variants of the NRAS protein displayed the following optimal binding affinities: -7.8 kcal/mol (mutant_Q61R), -8.8 kcal/mol (mutant_Q61K), -8.3 kcal/mol (mutant_Y64D), -8.2 kcal/mol (mutant_Q61H), -8.9 kcal/mol (mutant_G13R), -7.8 kcal/mol (mutant_G13D), -8.6 kcal/mol (mutant_E153Q), and -8.8 kcal/mol (mutant_G12D) with enzastaurin (DB06486), epicatechin, isavuconazole (DB11633),

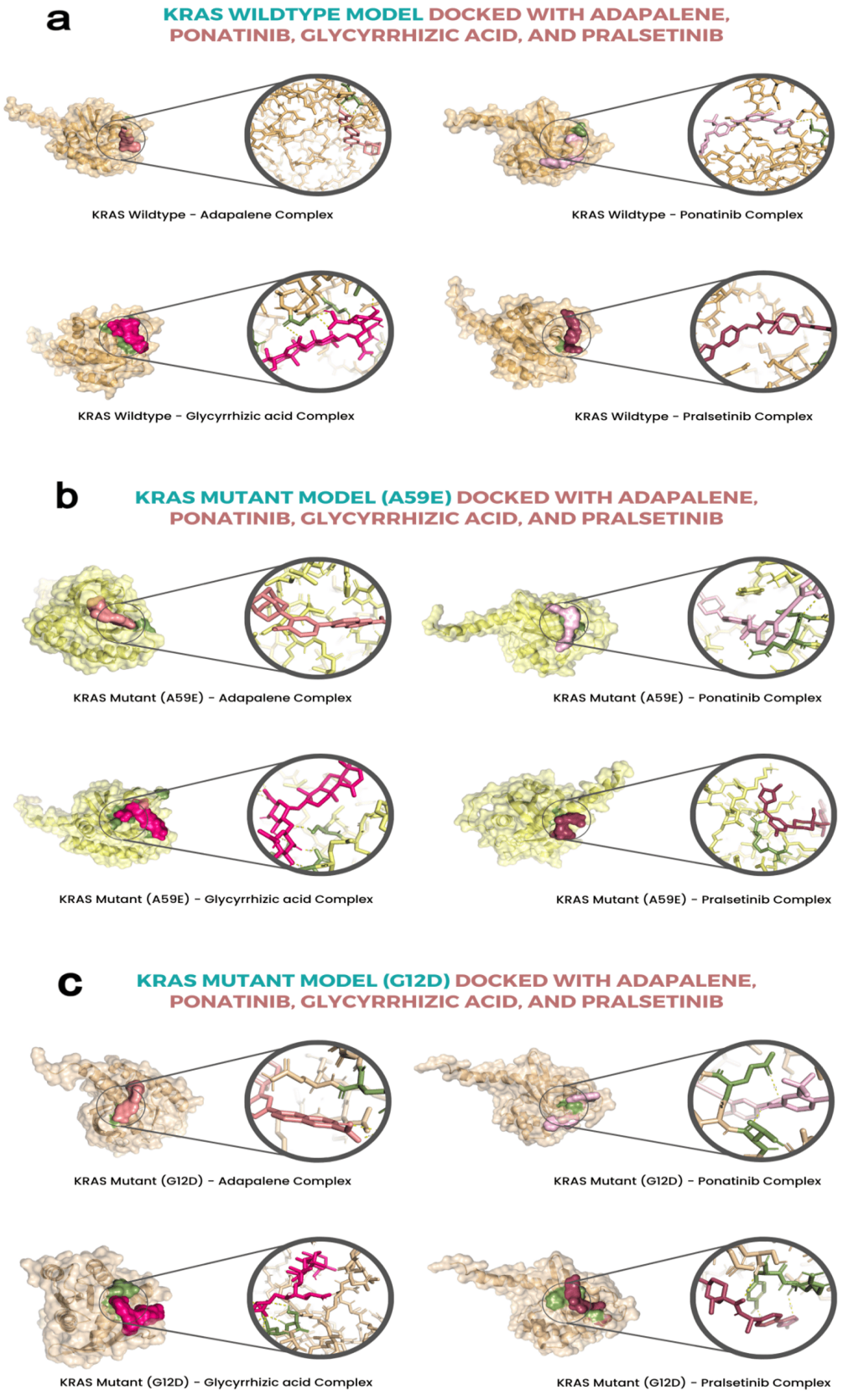
a
KRAS WILDTYPE MODEL DOCKED WITH ADAPALENE, PONATINIB, GLYCYRRHIZIC ACID, AND PRALSETINIB
KRAS Wildtype - Adapalene Complex
KRAS Wildtype - Ponatinib Complex
KRAS Wildtype - Glycyrrhizic acid Complex
KRAS Wildtype - Pralsetinib Complex
b
KRAS MUTANT MODEL (A59E) DOCKED WITH ADAPALENE, PONATINIB, GLYCYRRHIZIC ACID, AND PRALSETINIB
KRAS Mutant (A59E) - Adapalene Complex
KRAS Mutant (A59E) - Ponatinib Complex
KRAS Mutant (A59E) - Glycyrrhizic acid Complex
KRAS Mutant (A59E) - Pralsetinib Complex
c
KRAS MUTANT MODEL (G12D) DOCKED WITH ADAPALENE, PONATINIB, GLYCYRRHIZIC ACID, AND PRALSETINIB
KRAS Mutant (G12D) - Adapalene Complex
KRAS Mutant (G12D) - Ponatinib Complex
KRAS Mutant (G12D) - Glycyrrhizic acid Complex
KRAS Mutant (G12D) - Pralsetinib Complex

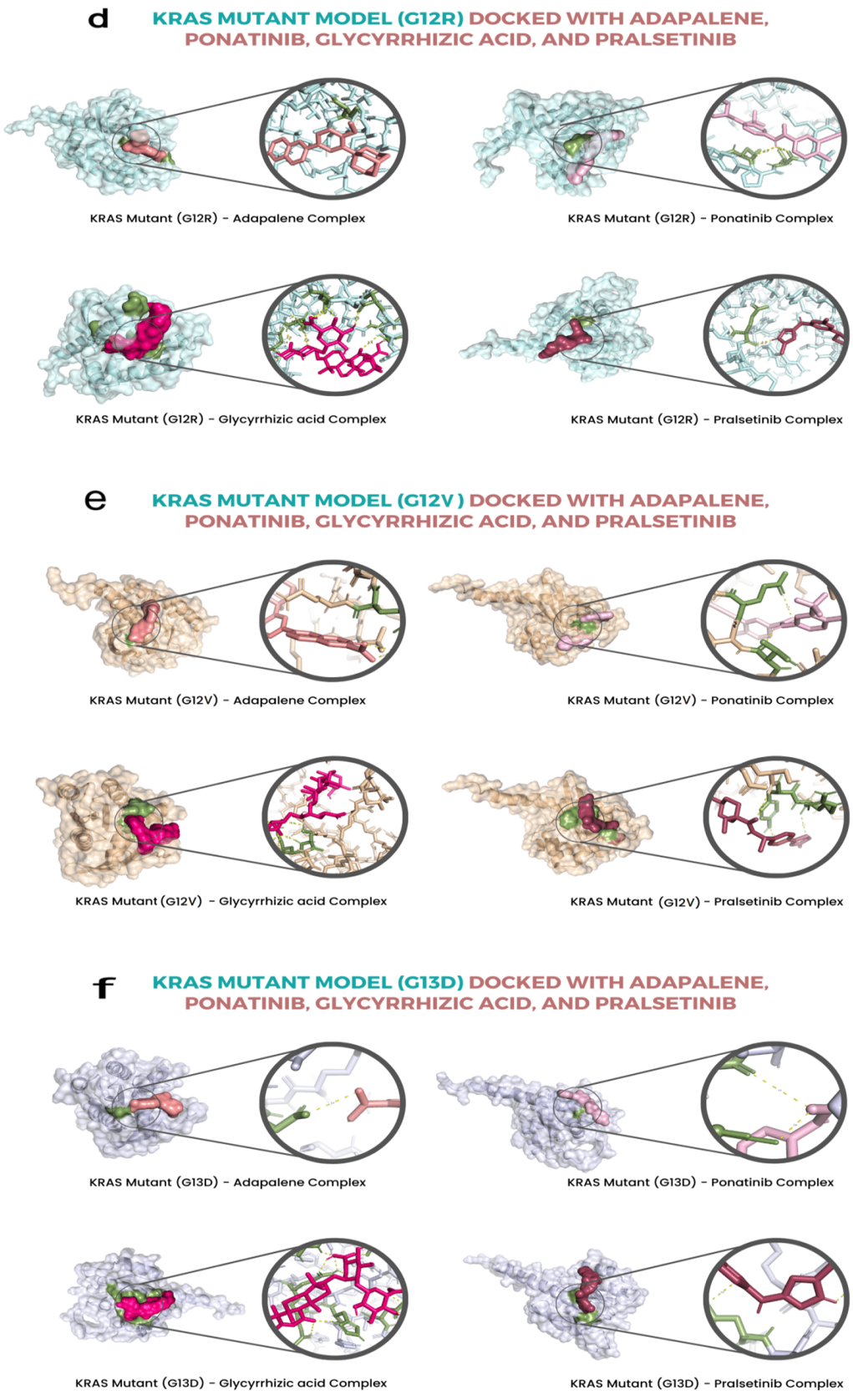
d
KRAS MUTANT MODEL (G12R) DOCKED WITH ADAPALENE, PONATINIB, GLYCYRRHIZIC ACID, AND PRALSETINIB
KRAS Mutant (G12R) - Adapalene Complex
KRAS Mutant (G12R) - Ponatinib Complex
KRAS Mutant (G12R) - Glycyrrhizic acid Complex
KRAS Mutant (G12R) - Pralsetinib Complex
e
KRAS MUTANT MODEL (G12V) DOCKED WITH ADAPALENE, PONATINIB, GLYCYRRHIZIC ACID, AND PRALSETINIB
KRAS Mutant (G12V) - Adapalene Complex
KRAS Mutant (G12V) - Ponatinib Complex
KRAS Mutant (G12V) - Glycyrrhizic acid Complex
KRAS Mutant (G12V) - Pralsetinib Complex
f
KRAS MUTANT MODEL (G13D) DOCKED WITH ADAPALENE, PONATINIB, GLYCYRRHIZIC ACID, AND PRALSETINIB
KRAS Mutant (G13D) - Adapalene Complex
KRAS Mutant (G13D) - Ponatinib Complex
KRAS Mutant (G13D) - Glycyrrhizic acid Complex
KRAS Mutant (G13D) - Pralsetinib Complex

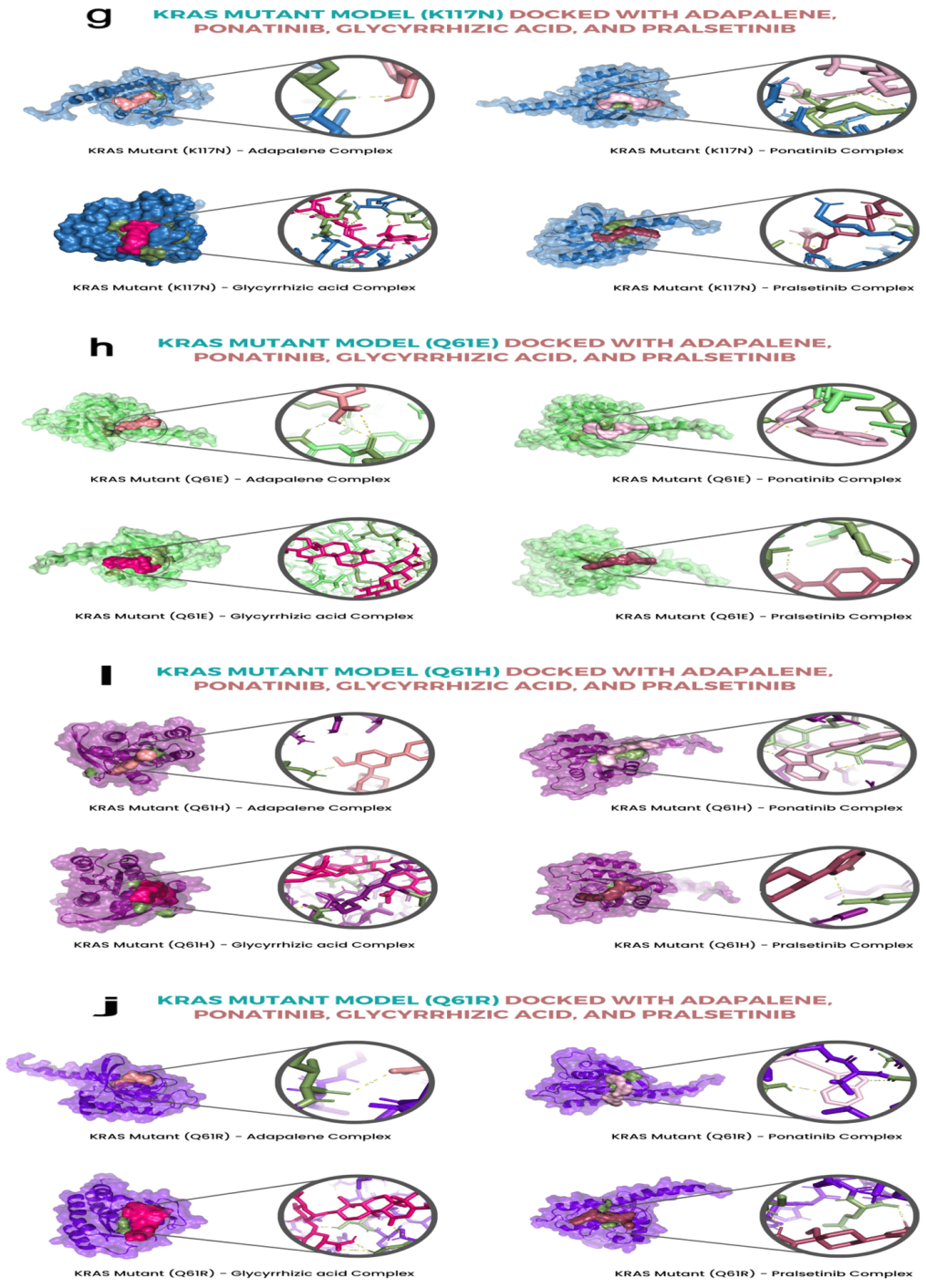

FIGURE 4.35: Visualization of wild-type KRAS (a) and KRAS variants ((A59E), (G12D), (G12R), (G13D), (K117N), (Q61E), (Q61H) and (Q61R)) (b-j) docking with Adapalene, Ponatinib, Glycyrrhizic acid and Pralsetinib on PyMOL, showing interactions of the ligand molecules with the protein residues.

hydnocarpinD, glycyrrhizic acid (DB13751), pacritinib (DB11697), alectinib (DB 11363), and theaflavine, respectively. The binding affinities of both NRAS-wild and its variations with the chosen compounds exhibited significant strength, as

indicated in Table 4.15. The wild-type NRAS protein complexes exhibited residue interactions involving LYS at position 147 with adapalene, GLY, LYS, ASN at positions 13, 16, and 116 with ponatinib, GLY, TYR, ARG at positions 12, 96, and 102 with glycyrrhizic acid, and GLY, ASN, LYS at positions 13, 85, and 147 with pralsetinib (Figure 4.36).

The mutant model (E153Q) of NRAS exhibited interactions with adapalene at positions 170 and 171 involving the residues LYS and LEU, and with ponatinib at positions 104 and 166 involving the residues LYS and TYR. Additionally, interactions were observed with glycyrrhizic acid at positions 151, 152, and 153 involving the residues GLY, VAL, and GLN, and with pralsetinib at positions 26, 150, 32, 85, and 147 involving the residues ASN, GLN, TYR, ASN, and LYS, respectively (Figure 4.36). The NRAS mutant model (G12D) exhibited interactions with adapalene at residues VAL and ARG located at positions 103A and 167, respectively. Additionally, it displayed interactions with ponatinib at residues GLY and LYS located at positions 13 and 16, and with residues HIS, LYS, GLY, and ARG located at positions 131, 135, 138, and 161. On the other hand, the ASP mutant model demonstrated two interactions with glycyrrhizic acid at positions 47 and 154, and interactions with pralsetinib at residues TYR and GLY located at positions 137 and 138 (Figure 4.36). The NRAS mutant model (G13D) exhibited specific interacting residues with various compounds. Adapalene interacted with ALA and ASP residues at positions 18 and 30, respectively. Ponatinib showed interactions with SER and ARG residues at positions 106 and 167. LEU and ILE residues at positions 23 and 24, respectively, were involved in interactions with TYR at position 157. GLN exhibited four interactions with glycyrrhizic acid, three at position 43 and one at position 25. SER and LYS residues at positions 17 and 147, respectively, interacted with pralsetinib, while ASP showed interactions at positions 13, 30, and 119 (Figure 4.36). The G13R mutant model of NRAS exhibited specific residue interactions. Specifically, ALA at position 59 interacted with adapalene, while ASP and LYS at positions 33 and 147 also showed interactions. Additionally, TYR displayed interactions at position 32 with ponatinib, as well as with GLY, ASN, ASP, TYR, and GLN at positions 12, 86, 92, 96, and 99, respectively. Furthermore, SER demonstrated two interactions at position 89

with glycyrrhizic acid, and with TYR, ASN, and LYS at positions 32, 85, and 147, respectively, in relation to pralsetinib (Figure 4.36). The NRAS mutant model (Q61H) exhibited no discernible interaction with adapalene, GLY, and GLU at positions 151 and 153, respectively, when exposed to ponatinib. Similarly, no interactions were observed with GLY, LYS, ALA, VAL, GLU, TYR, ASN, and THR at positions 15, 16, 18, 29, 31, 32, 85, and 122. However, the mutant model did exhibit four interactions with SER at position 17 when exposed to glycyrrhizic acid, ASN, and GLN at positions 94 and 129, respectively, in the presence of pralsetinib (Figure 4.36). The NRAS mutant model (Q61K) exhibited specific residue interactions with various compounds. Adapalene displayed an interaction with VAL at position 103, TYR at position 157, and two interactions with VAL at position 45. Ponatinib demonstrated two interactions with ARG at position 161, as well as interactions with GLY, ALA, ASP, GLU, and ASN at positions 13, 18, 30, 31, and 86, respectively. Glycyrrhizic acid exhibited interactions with ARG at position 68 (two interactions) and position 73. Lastly, pralsetinib displayed three interactions with ARG, two at position 68 and one at position 73 (Figure 4.36). The NRAS mutant model (Q61R) exhibited specific interactions with various compounds. Adapalene interacted with the residue ASP at position 107, ponatinib interacted with the residues GLU and GLY at positions 143 and 151, glycyrrhizic acid interacted with the residues GLY, SER, ASP at positions 12, 16, 32, and 84, and pralsetinib interacted with the residue TYR at position 136. Additionally, the residues HIS, GLU, and ARG at positions 93, 97, and 101 were involved in interactions (Figure 4.36). The NRAS mutant model (Y64D) exhibited specific interacting residues with various compounds. Adapalene interacted with TYR and LEU at positions 32 and 120, respectively. Ponatinib interacted with LEU at position 95. SER, ASN, and ASP at positions 17, 116, and 119, respectively, were involved in interactions. GLY displayed two interactions at positions 12 and 15. LYS demonstrated three interactions at positions 16, 117, and 147. ALA exhibited two interactions at positions 18 and 146 with glycyrrhizic acid. Lastly, ASN and LYS at positions 85 and 147 interacted with pralsetinib ((Figure 4.36, Table 4.15)).

TABLE 4.15: Protein-Ligand Interaction Profiler (PLIP) of the docked complexes of the NRAS wild-type and NRAS variants with selected drug compounds, representing the binding residues, their positions and distances between hydrogen-acceptor and donor-acceptor molecules.

Proteins		**Binding Affinity**	**Residue**	**AA**	**Distance H-A**	**Distance D-A**
NRAS-Wild	NRAS-Adapalene	-7.3	147A	LYS	2.15	3.14
	NRAS-ponatinib	-7.4	13A, 16A, 116A	GLY, LYS, ASN	2.55, 2.73, 3.21	3.21, 3.47, 3.78
	NRAS- glycyrrhizic acid	-8	12A, 96A, 102A	GLY, TYR, ARG	3.76, 2.14, 3.33	4.08, 2.89, 4.07
	NRAS-pralsetinib	-7.6	13A, 85A, 147A	GLY, ASN, LYS	3.43, 3.14, 3.44	3.95, 4.07, 3.94
NRAS-E153Q	NRAS-E153Q-Adapalene	-7.7	170A, 171A	LYS, LEU	2.13, 2.16	2.80, 3.17
	NRAS-E153Q-ponatinib	-7.5	104A, 166A	LYS, TYR	2.28, 2.36	3.18, 3.12
	NRAS-E153Q- glycyrrhizic acid	-7.5	26A, 26A, 150A, 150A, 151A, 152A, 153A	ASN, ASN, GLN, GLN, GLY, VAL, GLN	2.10, 2.34, 2.89, 2.63, 2.51, 2.62, 2.19	2.96, 3.17, 3.25, 3.30, 3.14, 3.12, 3.17
	NRAS-E153Q-pralsetinib	-7.5	32A, 85A, 147A	TYR, ASN, LYS	2.31, 2.34, 2.23	3.31, 3.28, 3.13
NRAS-G12D	NRAS-G12D-Adapalene	-7.6	103A, 167A	VAL, ARG	2.29, 3.09	3.03, 4.05
	NRAS-G12D-ponatinib	-7.4	13A, 16A	GLY, LYS	2.51, 2.97	3.03, 3.89
	NRAS-G12D-ponatinib	-7.2	47A, 131A, 135A, 138A, 154A, 161A	ASP, HIS, LYS, GLY, ASP, ARG	2.54, 2.51, 2.96, 3.39, 2.55, 3.18	2.89, 3.27, 3.92, 3.85, 3.33, 4.09
	NRAS-G12D- glycyrrhizic acid	-7.1	137A, 138A	TYR, GLY	2.53, 2.63	2.92, 3.12
NRAS-G13D	NRAS-G13D-Adapalene	-7.4	18A, 30A	ALA, ASP	2.97, 2.32	3.38, 3.11
	NRAS-G13D-ponatinib	-7.5	106A, 167A	SER, ARG	3.19, 3.18	3.87, 4.05

Proteins		**Binding Affinity**	**Residue**	**AA**	**Distance H-A**	**Distance D-A**
	NRAS-G13D-glycyrrhizic acid	-7.6	23A, 24A, 25A, 43A, 43A, 43A, 157A, 157A	LEU, ILE, GLN, GLN, GLN, TYR, TYR	2.32, 2.25, 2.76, 2.19, 2.28, 2.87, 2.90, 2.70	2.71, 2.91, 3.11, 2.88, 3.29, 3.76, 3.59, 3.59
	NRAS-G13D-pralsetinib	-7.7	13A, 17A, 30A, 119A, 147A	ASP, SER, ASP, ASP, LYS	2.61, 2.42, 2.06, 2.16, 2.64	3.14, 2.92, 2.99, 2.99, 3.41
NRAS-G13R	NRAS-G13R-Adapalene	-8	59A	ALA	2.39	3.16
	NRAS-G13R-ponatinib	-7.5	32A, 32A, 33A, 147A	TYR, TYR, ASP, LYS	2.68, 3.32, 2.53, 2.44	3.59, 3.83, 3.07, 3.01
	NRAS-G13R-glycyrrhizic acid	-8.9	12A, 86A, 89A, 89A, 92A, 96A, 99A	GLY, ASN, SER, SER, ASP, TYR, GLN	2.35, 2.58, 2.42, 2.63, 1.85, 3.48, 2.47	3.18, 3.22, 3.15, 3.08, 2.70, 3.79, 3.17
	NRAS-G13R-pralsetinib	-7.8	32A, 85A, 147A	TYR, ASN, LYS	2.81, 2.12, 2.00	3.81, 3.11, 2.85
NRAS-Q61H	NRAS-Q61H-Adapalene	-7.1	-	-	-	-
	NRAS-Q61H-ponatinib	-7.4	151A, 153A	GLY, GLU	2.72, 2.03	3.09, 2.90
	NRAS-Q61H-glycyrrhizic acid	-7.5	15A, 16A, 17A, 17A, 17A, 17A, 18A, 29A, 31A, 32A, 85A, 122A	GLY, LYS, SER, SER, SER, ALA, VAL, GLU, TYR, ASN, THR	3.63, 2.99, 2.68, 2.89, 2.22, 2.25, 2.46, 3.00, 3.17, 2.82, 3.54, 2.75	3.97, 3.83, 3.34,
	NRAS-Q61H-pralsetinib	-7.7	94A, 129A	ASN, GLN	2.97, 3.69	3.61, 4.04

Proteins		**Binding Affinity**	**Residue**	**AA**	**Distance H-A**	**Distance D-A**
NRAS-Q61K	NRAS-Q61K-Adapalene	-7.3	103A	VAL	2.61	3.21
	NRAS-Q61K-ponatinib	-7.9	45A, 45A, 157A, 161A, 161A	VAL, VAL, TYR, ARG, ARG	2.50, 3.02, 2.69, 3.33, 2.40	3.51, 3.86, 3.30, 4.05, 3.33
	NRAS-Q61K-glycyrrhizic acid	-7.6	13A, 18A, 30A, 31A, 86A	GLY, ALA, ASP, GLU, ASN	2.62, 2.65, 2.24, 2.10, 3.14	3.34, 3.32, 2.7I, 2.89, 3.98
	NRAS-Q61K-pralsetinib	-7	68A, 73A, 73A	ARG, ARG, ARG	3.04, 2.61, 1.79	4.06, 3.38, 2.79
NRAS-Q61R	NRAS-Q61R-Adapalene	-7.3	107A	ASP	2.41	3.01
	NRAS-Q61R-ponatinib	-7.1	143A, 151A	GLU, GLY	1.99, 1.94	2.99, 2.92
	NRAS-Q61R-glycyrrhizic acid	-7.3	12A, 16A, 32A, 84A	GLY, SER, ASP, ASN	2.13, 2.06, 2.94, 2.96	3.03, 3.00, 3.91, 3.58
	NRAS-Q61R-pralsetinib	-7.3	93A, 97A, 101A, 136A, 136A	HIS, GLU, ARG, TYR, TYR	2.80, 2.26, 3.73, 2.49, 2.36	3.23, 3.02, 4.10, 3.20, 3.20
NRAS-Y64D	NRAS-Y64D-Adapalene	-7.9	32A, 120A	TYR, LEU	2.50, 2.94	3.30, 3.35
	NRAS-Y64D-ponatinib	-8.1	95A	LEU	3.1	3.56
	NRAS-Y64D-glycyrrhizic acid	-7.7	12A, 15A, 16A, 17A, 18A, 116A, 117A, 119A, 146A, 147A	GLY, GLY, LYS, SER, ALA, ASN, LYS, ASP, ALA, LYS	2.48, 2.30, 3.36, 3.20, 2.63, 2.63, 3.47, 3.56, 3.09, 2.28	3.18, 3.07, 4.00, 4.05, 3.14, 3.14, 4.03, 4.05, 3.99, 3.28
	NRAS-Y64D-pralsetinib	-8.2	85A, 147A	ASN, LYS	2.88, 2.84	3.90, 3.67

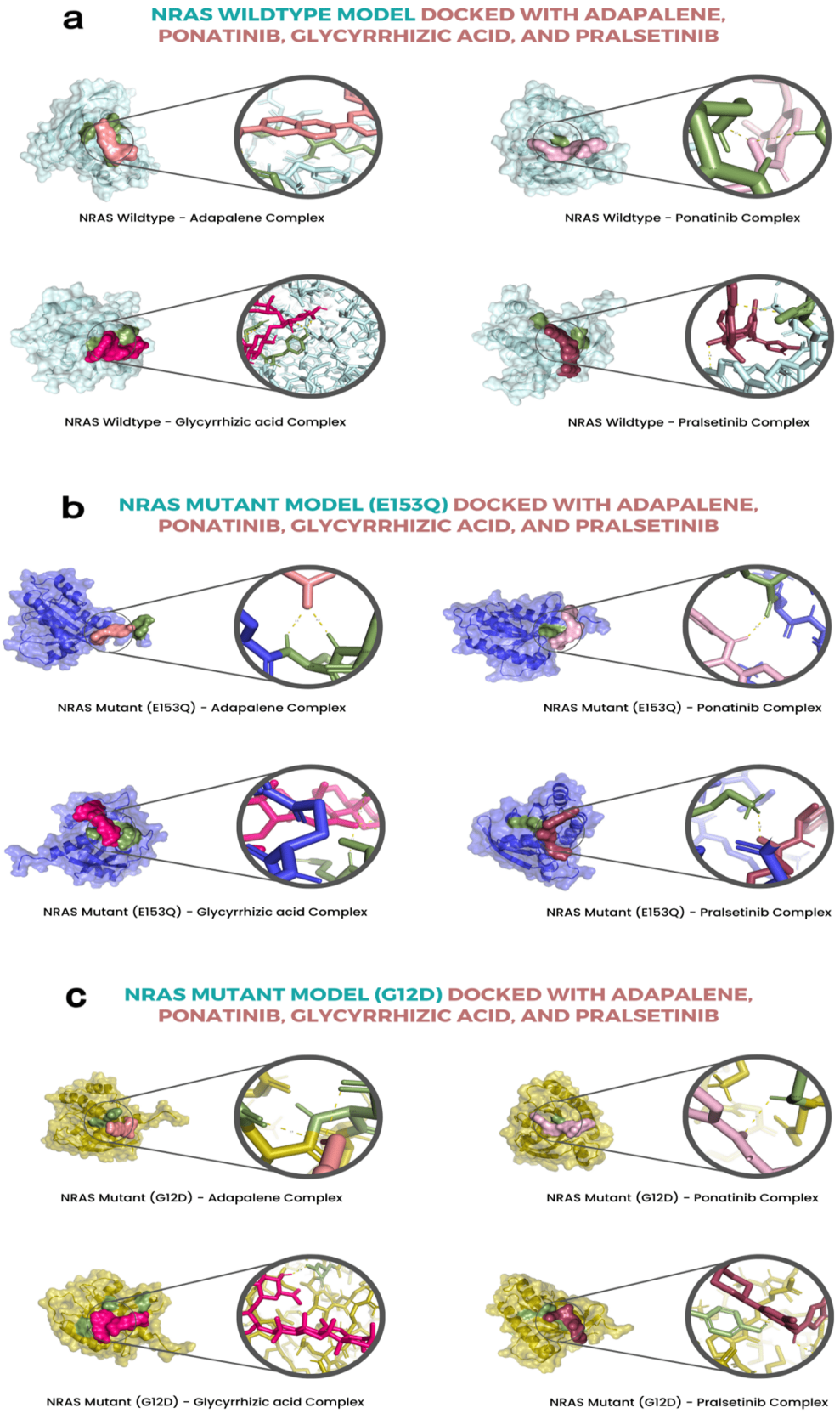
a
NRAS WILDTYPE MODEL DOCKED WITH ADAPALENE, PONATINIB, GLYCYRRHIZIC ACID, AND PRALSETINIB
NRAS Wildtype - Adapalene Complex
NRAS Wildtype - Ponatinib Complex
NRAS Wildtype - Glycyrrhizic acid Complex
NRAS Wildtype - Pralsetinib Complex
b
NRAS MUTANT MODEL (E153Q) DOCKED WITH ADAPALENE, PONATINIB, GLYCYRRHIZIC ACID, AND PRALSETINIB
NRAS Mutant (E153Q) - Adapalene Complex
NRAS Mutant (E153Q) - Ponatinib Complex
NRAS Mutant (E153Q) - Glycyrrhizic acid Complex
NRAS Mutant (E153Q) - Pralsetinib Complex
c
NRAS MUTANT MODEL (G12D) DOCKED WITH ADAPALENE, PONATINIB, GLYCYRRHIZIC ACID, AND PRALSETINIB
NRAS Mutant (G12D) - Adapalene Complex
NRAS Mutant (G12D) - Ponatinib Complex
NRAS Mutant (G12D) - Glycyrrhizic acid Complex
NRAS Mutant (G12D) - Pralsetinib Complex

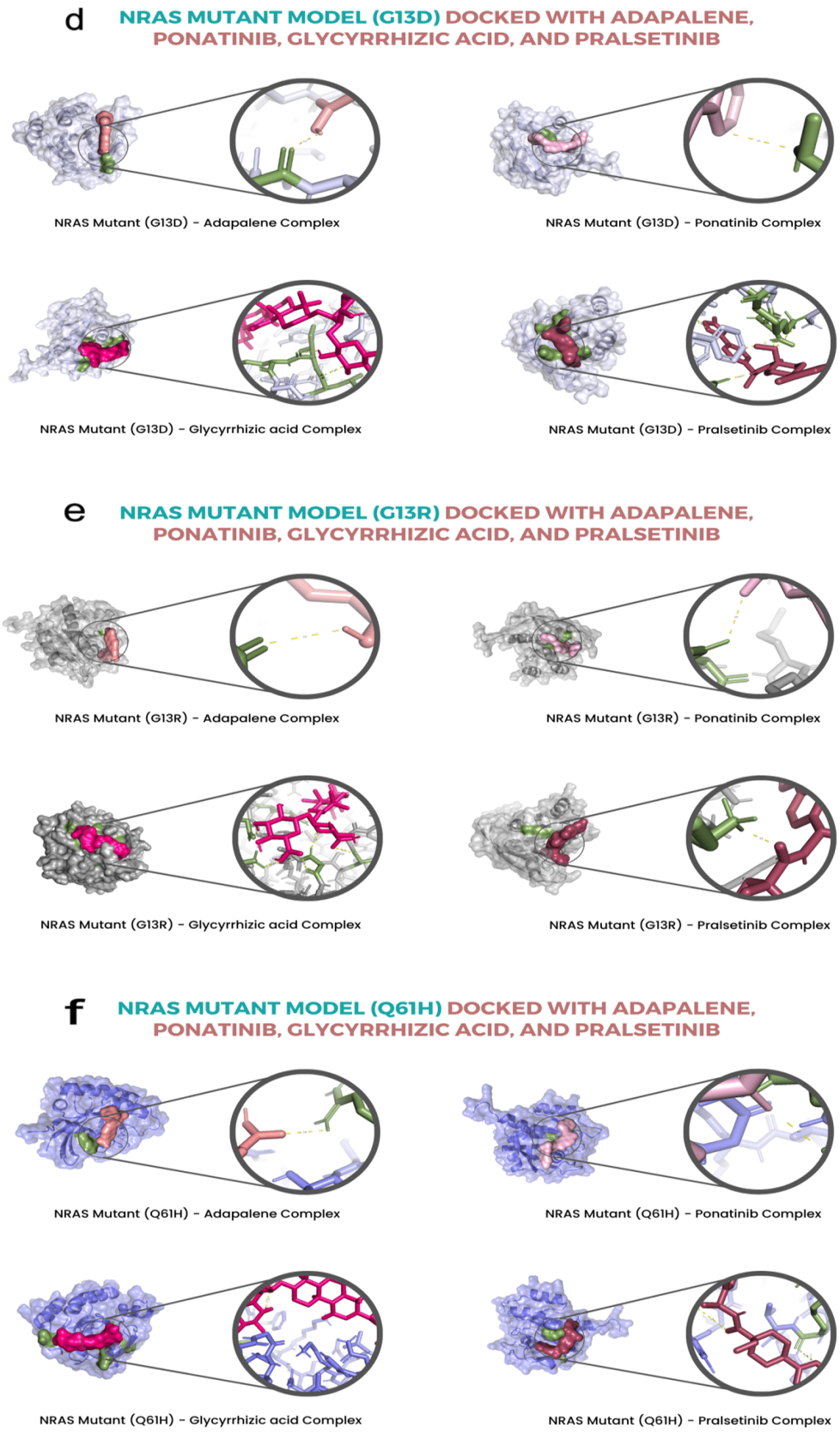
d
NRAS MUTANT MODEL (G13D) DOCKED WITH ADAPALENE, PONATINIB, GLYCYRRHIZIC ACID, AND PRALSETINIB
NRAS Mutant (G13D) - Adapalene Complex
NRAS Mutant (G13D) - Ponatinib Complex
NRAS Mutant (G13D) - Glycyrrhizic acid Complex
NRAS Mutant (G13D) - Pralsetinib Complex
e
NRAS MUTANT MODEL (G13R) DOCKED WITH ADAPALENE, PONATINIB, GLYCYRRHIZIC ACID, AND PRALSETINIB
NRAS Mutant (G13R) - Adapalene Complex
NRAS Mutant (G13R) - Ponatinib Complex
NRAS Mutant (G13R) - Glycyrrhizic acid Complex
NRAS Mutant (G13R) - Pralsetinib Complex
f
NRAS MUTANT MODEL (Q61H) DOCKED WITH ADAPALENE, PONATINIB, GLYCYRRHIZIC ACID, AND PRALSETINIB
NRAS Mutant (Q61H) - Adapalene Complex
NRAS Mutant (Q61H) - Ponatinib Complex
NRAS Mutant (Q61H) - Glycyrrhizic acid Complex
NRAS Mutant (Q61H) - Pralsetinib Complex

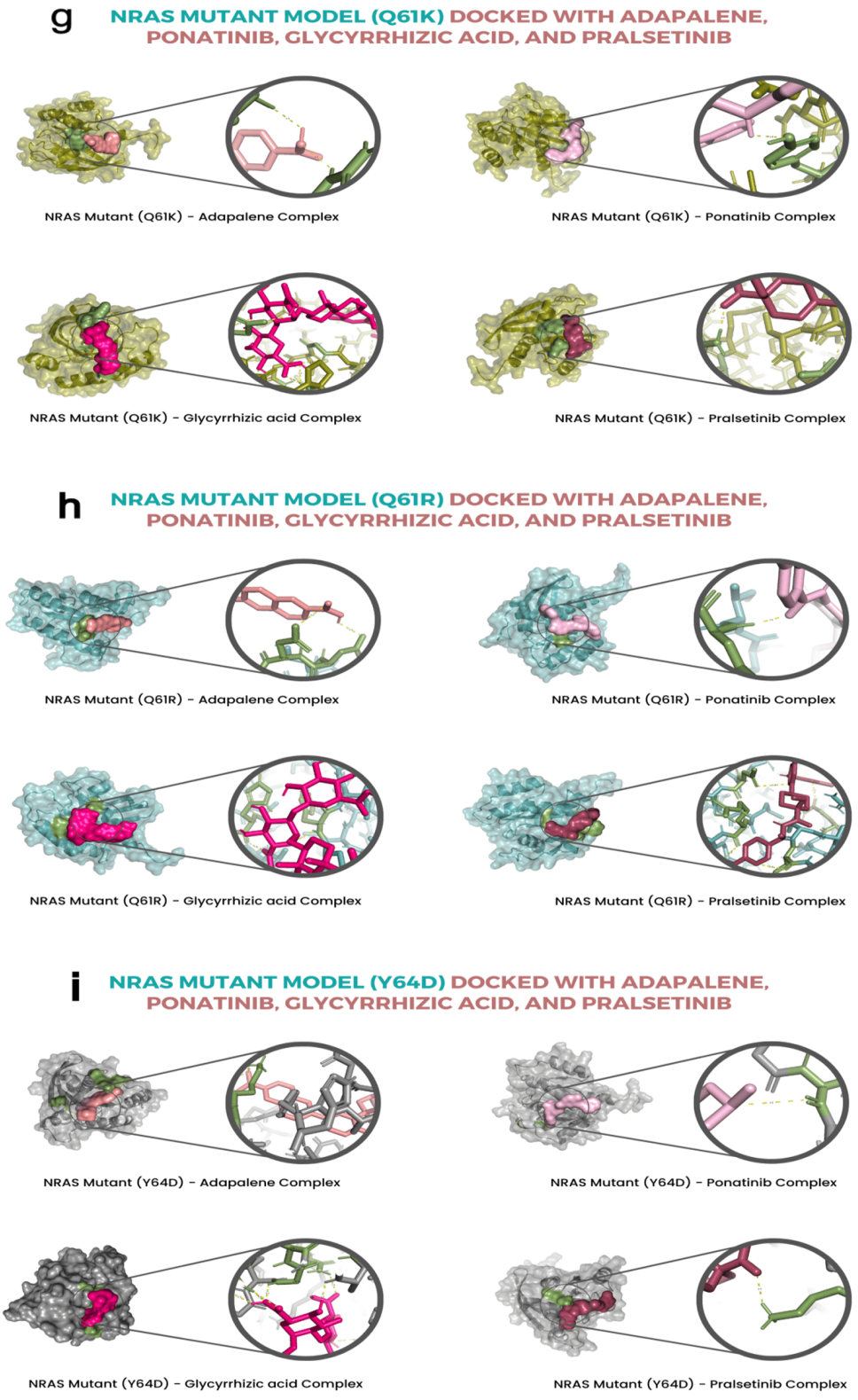

FIGURE 4.36: Visualization of wild-type NRAS and variant of NRAS protein (G13D, E153Q, G12D, G13R, Q61H, Q61K, Q61R and Y64D) docking with Adapalene, Ponatinib, Glycyrrhizic acid and Pralsetinib on PyMOL, showing interactions of the ligand molecules with the protein residues.

4.17.8 Molecular Docking of CD4 Protein with Selected Drug Compounds

The ligand that exhibited the highest docking affinity with the CD4 protein was shown to have a binding affinity of -9.4 kcal/mol with midostaurin (DB06595). Furthermore, it is worth noting that the aforementioned chemicals, namely adapalene (-7.8), ponatinib (-6.4), glycyrrhizic acid (-7.7), and pralsetinib (-7.4), demonstrate a favorable binding affinity with the target molecule. In addition, the CD4 protein complexes exhibited interactions between specific residues and other compounds. Specifically, SER at position 132 interacted with adapalene, SER at position 120 interacted with ponatinib, LEU at position 5 and THR at position 15 showed two interactions with glycyrrhizic acid, and SER at position 31 interacted with pralsetinib. (Table 4.15, Figure 4.37).

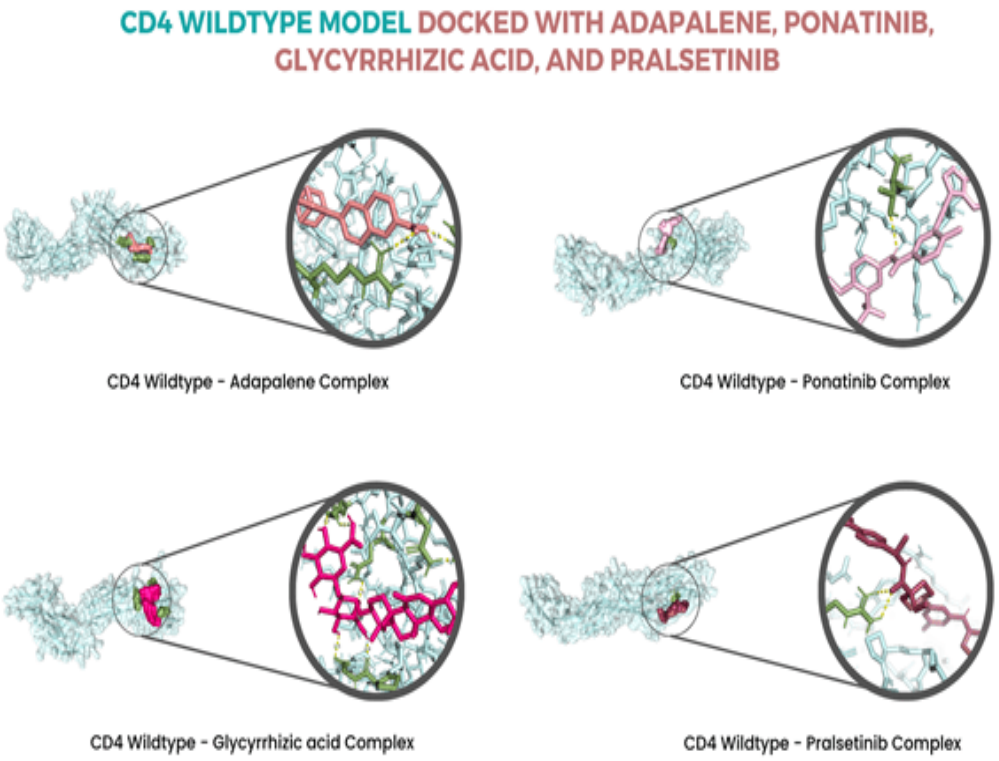

FIGURE 4.37: Visualization of wild-type CD4 protein docked with Adapalene, Ponatinib, Glycyrrhizic acid and Pralsetinib on PyMOL, showing interactions of the ligand molecules with the protein residues.

TABLE 4.16: Protein-Ligand Interaction Profiler (PLIP) of the docked complexes of the IL1B, BRIC5, BP1, CD4, CSF1R, ITGAM, NRP1, PTPRC, COL22A1, TYROBP, and VCAN with selected drug compounds, representing the binding residues, their positions and distances between hydrogen-acceptor and donor-acceptor molecules.

Proteins		**Binding Affinity**	**Residue**	**AA**	**Distance H-A**	**Distance D-A**
IL1B	IL1B-Adapalene	-9	99A	GLU	2.56	3.03
	IL1B-ponatinib	-9.4	165A, 166A, 167A	GLY, GLU, GLU	2.11, 3.32, 2.50	3.07, 4.10, 3.50
	IL1B-glycyrrhizic acid	-9.1	108A, 111A, 111A, 164A, 206A, 208 A	TRP, GLU, GLU, GLN, TYR, LYS	2.57, 2.50, 2.58, 2.30, 3.15, 3.03	3.07, 3.19, 3.19, 3.14, 3.80, 3.73
	IL1B-pralsetinib	-8.3	164A, 209A	GLN, LYS	2.29, 3.38	3.27, 4.02
BIRC5	BIRC5-Adapalene	-8.6	11A, 12A	LYS, ASP	2.19, 2.98	3.02, 3.97
	BIRC5-ponatinib	-9.2	9A, 11A, 89A	PHE, LYS, PHE	3.45, 2.41, 2.15	3.89, 3.33, 3.15
	BIRC5-glycyrrhizic acid	-8.7	58A, 61A, 61A, 76A	LYS, GLU, GLU, HIS	2.16, 1.93, 2.31, 2.46	3.05, 2.92, 3.08, 3.12
	BIRC5-pralsetinib	-9	89A, 90A, 90A	PHE, GLU, GLU	3.10, 3.52, 3.28	4, 3.86, 3.70
BP1	BPI-Adapalene	-10.6	267A	GLY	2.73	3.08
	BPI-ponatinib	-10.2	-	-	-	-
	BPI-glycyrrhizic acid	-7.8	127A, 192A, 195A, 196A, 198A, 433A, 434A	LYS, THR, VAL, MET, LYS, VAL, GLN	2.56, 3.30, 2.24, 2.05, 2.12, 2.47, 2.62	3.18, 3.73, 3.20, 2.76, 3.06, 3.13, 3.15
	BPI-pralsetinib	-10.5	263A, 416A, 420A	PHE, ARG, LYS	2.62, 2.75, 2.53	3.19, 3.18, 3.24
CD4	CD4-Adapalene	-7.8	132A	SER	3.05	3.65
	CD4-ponatinib	-6.4	120A	SER	2.93	3.91
	CD4-glycyrrhizic acid	-7.7	5A, 15A, 15A	LEU, THR, THR	2.58, 2.32, 3.28	3.19, 3.19, 3.88
	CD4-pralsetinib	-7.4	31A	SER	2.47	3.25
CSF1R	CSF1R-Adapalene	-8.9	913A	GLN	2.76	3.75
	CSF1R-ponatinib	-9.5	587A, 725A, 727A	THR, GLU, ARG	2.19, 2.73, 3.63	2.95, 3.73, 3.95

Proteins		**Binding Affinity**	**Residue**	**AA**	**Distance H-A**	**Distance D-A**
	CSF1R-glycyrrhizic acid	-8.9	803A, 806A, 811A, 861A, 866A	ILE, ASP, VAL, VAL, TYR	3.18, 2.94, 2.35, 2.66, 2.56	4.07, 3.83, 3.34, 3.10, 3.15
	CSF1R-pralsetinib	-8.6	561A, 563A, 568A	TYR, PHE, GLN	2.17, 2.71, 2.67	3.09, 3.69, 3.63
ITGAM	ITGAM-Adapalene	-10.8	77A, 143A	LEU, GLY	2.08, 3.10	2.96, 4.08
	ITGAM-ponatinib	-9.3	466A, 484A, 486A	TYR, ARG, ARG	2.45, 3.16, 3.19	2.97, 3.54, 4.08
	ITGAM-glycyrrhizic acid	-10.9	81A, 81A, 81A, 82A, 346A, 346A	THR, THR, THR, SER, ASN, ASN, ASP	3.01, 1.90, 2.97, 2.53, 2.95, 2.37, 3.23	3.80, 2.80, 3.94, 3.35, 3.88, 3.03, 3.85
	ITGAM-pralsetinib	-9.8	141A, 143A	GLY,GLY	3.63, 2.43	3.95, 3.17
NRP1	NRP1-Adapalene	-10	150A	ASN	2.64	3.21
	NRP1-ponatinib	-10.5	643A	PHE	2.4	3.23
	NRP1-glycyrrhizic acid	-9.5	227A, 232A, 237A, 289A	TYR, THR, ARG, ASP	2.03, 2.53, 2.31, 2.28	2.95, 3.13, 3.19, 3.05
	NRP1-pralsetinib	-9.9	227A, 235A, 285A, 287A, 290A, 330A,	TYR, ARG, GLU, HIS, GLN, LEU	2.25, 2.78, 1.89, 2.97, 2.61, 2.96	2.87, 3.54, 2.80, 3.80, 3.53, 3.72
PTPRC	PTPRC-Adapalene	-9.3	1190A	GLU	2.42	3.08
	PTPRC-ponatinib	-8.4	1151A, 1151A	LYS, LYS	2.19, 2.82	3.16, 3.78
	PTPRC-glycyrrhizic acid	-8.4	949A, 953A, 955A, 955A	GLN, SER, ARG, ARG	2.59, 1.97, 2.19, 3.64	3.19, 2.97, 2.78, 4.10
	PTPRC-pralsetinib	-8.1	1159A, 1160A	HIS, HIS	2.14, 3.15	3.09, 3.72
TYROBP	TYROBP-Adapalene	-8	54A	THR	1.85	2.81
	TYROBP-ponatinib	-8.1	65A	GLY	3.63	4
	TYROBP-glycyrrhizic acid	-6.7	21A, 25A, 25A	GLY, VAL, VAL	2.33, 2.91, 2.26	2.71, 3.26, 2.96

Proteins		**Binding Affinity**	**Residue**	**AA**	**Distance H-A**	**Distance D-A**
	TYROBP-pralsetinib	-7.4	70A	ARG	3.56	3.95
COL22A1	COL22A1-Adapalene	-8.7	311A, 311A, 325A	TYR, TYR, SER	3.14, 3.78, 1.96	4.08, 4.08, 2.72
	COL22A1-ponatinib	-8.1	397A	ASP	3.06	145.39
	COL22A1-glycyrrhizic acid	-8.9	171A, 171A, 220A, 221A, 223A, 225A, 225A, 244A	ARG, ARG, ASN, VAL, CYS, SER, SER, THR	3.14, 3.28, 3.14, 2.53, 3.27, 2.39, 2.17, 3.47	3.99, 3.93, 3.48, 3.24, 3.92, 3.12, 2.99, 4.06
	COL22A1-pralsetinib	-8.9	144A, 144A, 166A	GLN, GLN, HIS	1.94, 2.84, 2.52	2.94, 3.81, 3.53
VCAN	VCAN-Adapalene	-10.3	191A	ASP	2.63	3.48
	VCAN-ponatinib	-10	284A, 322A	GLN, VAL	2.61, 2.63	3.60, 3.22
	VCAN-glycyrrhizic acid	-8.6	195A, 284A, 305A, 305A, 324A, 326A, 326A, 331A	GLN, GLN, ARG, ARG, THR, TYR, TYR, GLN	3.27, 3.33, 3.31, 3.01, 3.34, 2.50, 3.30, 2.24	3.77, 4.02, 3.69, 3.69, 3.93, 3.31, 3.88, 2.88
	VCAN-pralsetinib	-8.8	260A, 295A, 296A, 296A, 296A, 316A, 317A, 324A	LYS, ASP, TYR, TYR, TYR, GLY, GLY, THR	2.81, 2.55, 3.16, 2.75, 3.17, 2.66, 2.84, 2.17	3.51, 3.28, 3.99, 3.68, 3.63, 3.13, 3.55, 3.13

4.17.9 Molecular Docking of ITGAM Protein with Selected Drug Compounds

Following that, the most highly associated complexes of ITGAM had a binding affinity of -10.9 kcal/mol with glycyrrhizic acid (DB13751). The following drugs

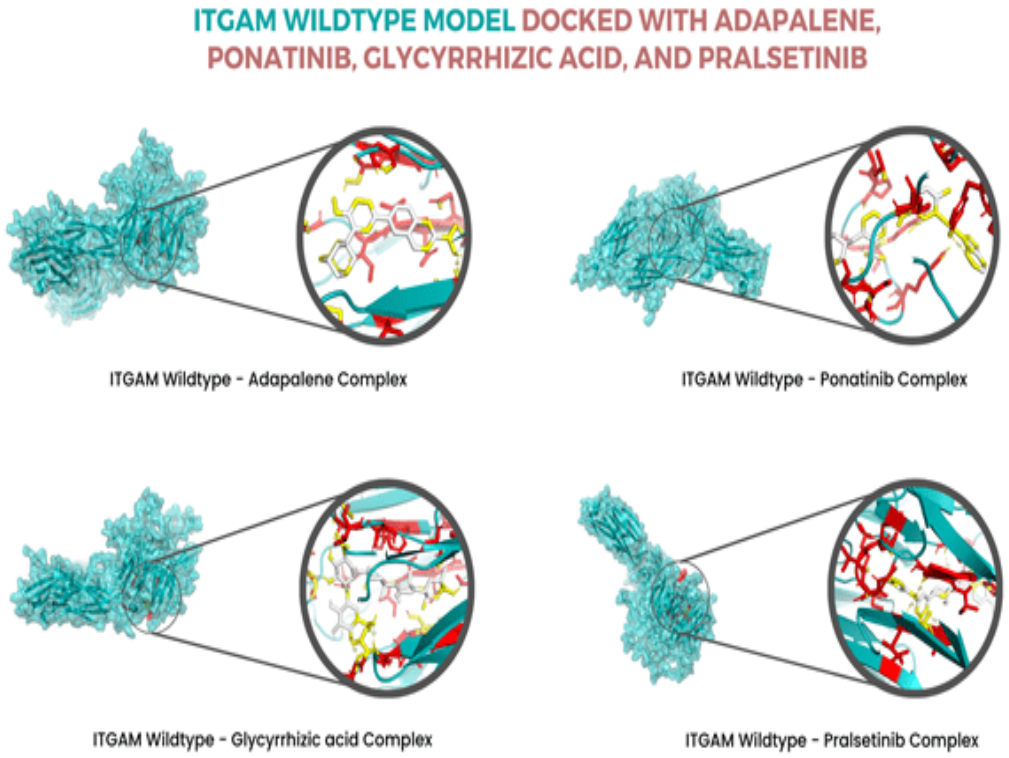

FIGURE 4.38: Visualization of wild-type ITGAM protein docked with Adapalene, Ponatinib, Glycyrrhizic acid and Pralsetinib on PyMOL, showing interactions of the ligand molecules with the protein residues.

compounds are listed in ascending order of stabality: adapalene (-10.8), pralsetinib (-9.8), and pralsetinib (-9.3). In a similar manner, the ITGAM demonstrated distinct residue interactions with diverse substances. The interaction between Adapalene and LEU and GLY residues at positions 77 and 143, respectively, was observed. Additionally, the TYR residue at position 466 was found to interact with ponatinib. The ARG residue exhibited two interactions with ponatinib at sites 484 and 486. Glycyrrhizic acid was found to interact with serine (SER) and aspartic acid (ASP) residues at positions 82 and 457, respectively. Additionally, the threonine (THR) residue demonstrated three interactions at position 81. In addition, glycyrrhizic acid exhibited an interaction with the asparagine (ASN) residue located at position 346, leading to the formation of two distinct interactions. In conclusion, pralsetinib exhibited interactions with glycine (GLY) residues located at positions 141 and 143, as documented in Table 4.15 and Figure 4.38.

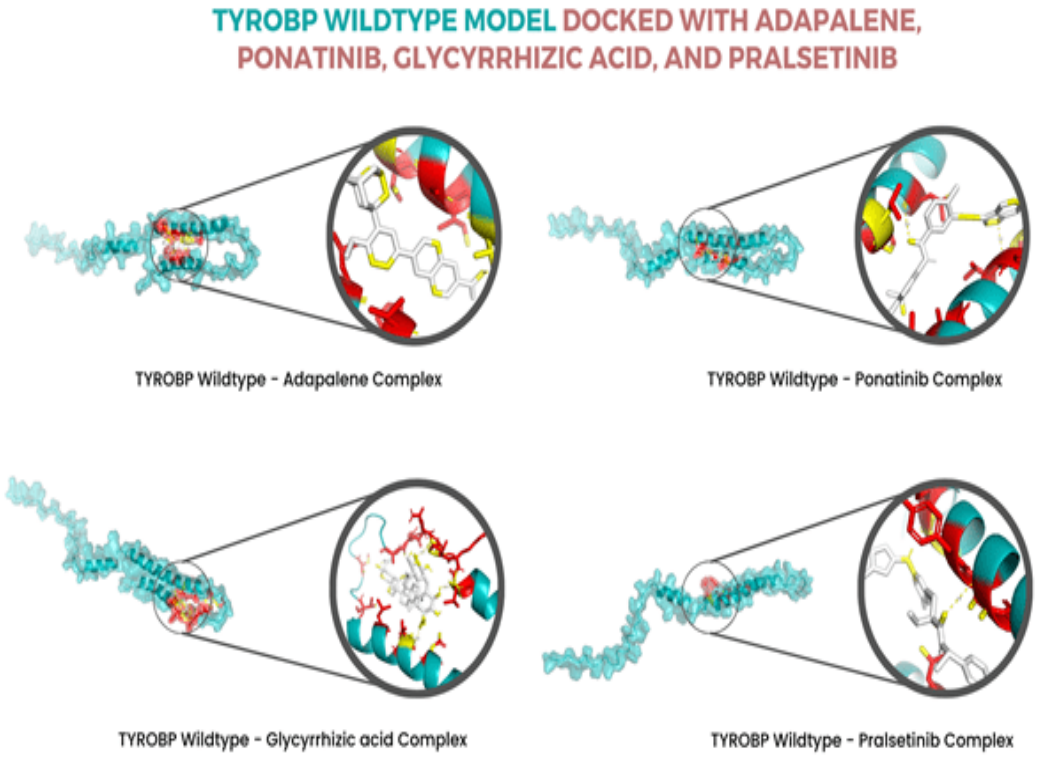

FIGURE 4.39: Visualization of wild-type TYROBP protein docked with Adapalene, Ponatinib, Glycyrrhizic acid and Pralsetinib on PyMOL, showing interactions of the ligand molecules with the protein residues.

4.17.10 Molecular Docking of TYROBP Protein with Selected Drug Compounds

In addition, the TYROBP complex exhibited the highest binding affinity for ponatinib at -8.1 kcal/mol, followed by adapalene at -8 kcal/mol, pralsetinib at -7.4 kcal/mol, and glycyrrhizic acid at -6.7 kcal/mol. Furthermore, the TYROBP protein complexes exhibited specific residue interactions. Specifically, THR was found at position 54 in compound with adapalene, GLY was present at position 65 in interaction with ponatinib, GLY was observed at position 21, and VAL displayed two interactions at position 25 with glycyrrhizic acid. Additionally, ARG was identified at position 70 in association with pralsetinib (Table 4.15 and Figure 4.39).

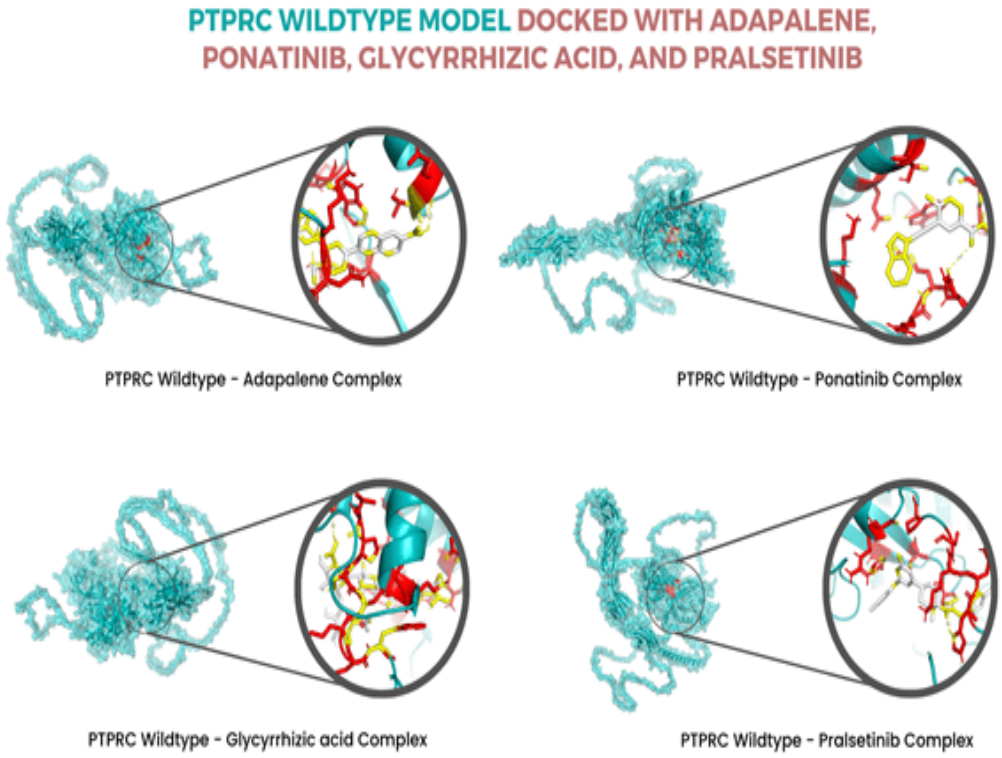

FIGURE 4.40: Visualization of wild-type PTPRC protein docked with Adapalene, Ponatinib, Glycyrrhizic acid and Pralsetinib on PyMOL, showing interactions of the ligand molecules with the protein residues.

4.17.11 Molecular Docking of PTPRC Protein with Selected Drug Compounds

The PTPRC complex exhibited the highest binding affinity for adapalene (-9.3 kcal/mol), followed by ponatinib (-8.4 kcal/mol), glycyrrhizic acid (-8.4 kcal/mol), and pralsetinib (-8.1 kcal/mol). In the wild-type PTPRC protein complexes, it was observed that the residue GLU at position 1190 interacted with adapalene. Additionally, the residue LYS at position 1151 exhibited two interactions with ponatinib, while GLN and SER residues at positions 949 and 953, respectively, also displayed interactions. Moreover, ARG residue at position 955 demonstrated two interactions with glycyrrhizic acid, and HIS residue at positions 1159 and 1160 exhibited two interactions with pralsetinib Table 4.15 and Figure 4.40.

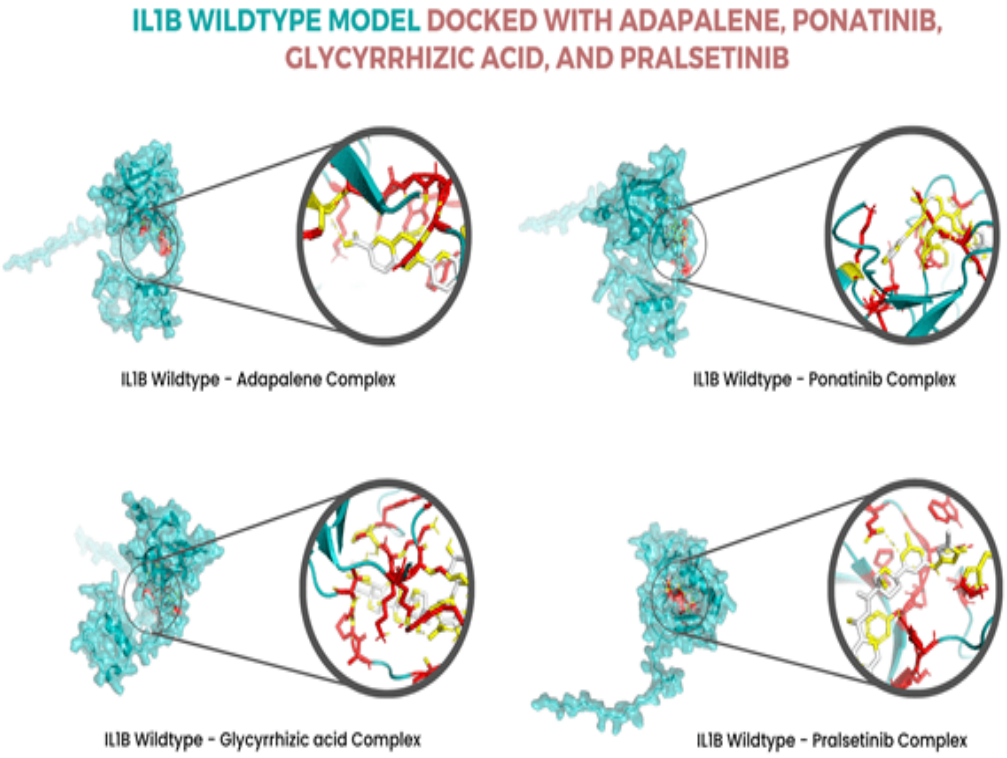

FIGURE 4.41: Visualization of wild-type IL1B protein docked with Adapalene, Ponatinib, Glycyrrhizic acid and Pralsetinib on PyMOL, showing interactions of the ligand molecules with the protein residues.

4.17.12 Molecular Docking of IL1B Protein with Selected Drug Compounds

In addition, the most favourable docked complexes of the wild-type IL1B protein demonstrated a binding affinity of -9.4 kcal/mol with ponatinib. The substances that had the highest inhibitory activity were glycyrrhizic acid (-9.1), adapalene (-9.0), and pralsetinib (-8.3). The wild-type IL1B protein complexes exhibited specific residue interactions. Adapalene interacted with GLU at position 99, while ponatinib interacted with GLY at position 165 and GLU at positions 166 and 167. Additionally, TRP, GLN, TYR, and LYS residues at positions 108, 164, 206, and 208 respectively were involved in interactions. Furthermore, glycyrrhizic acid interacted with GLU at position 111, and pralsetinib interacted with GLN at position 164 and LYS at position 209 Table 4.15 and Figure 4.41.

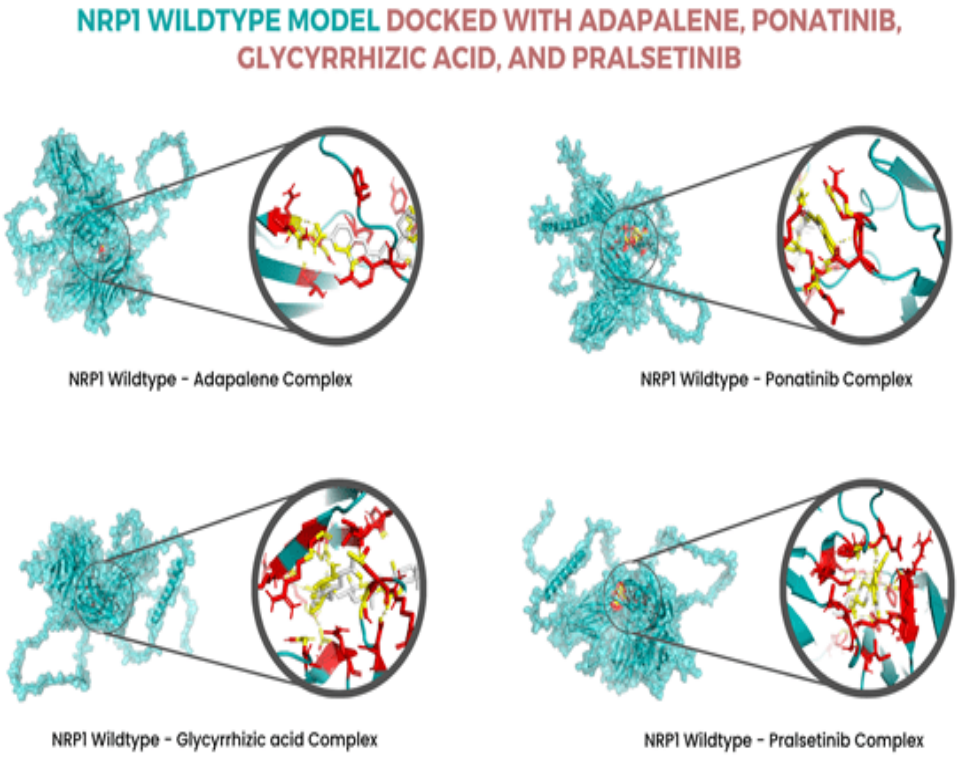

FIGURE 4.42: Visualization of wild-type NRP1 protein docked with Adapalene, Ponatinib, Glycyrrhizic acid and Pralsetinib on PyMOL, showing interactions of the ligand molecules with the protein residues.

4.17.13 Molecular Docking of NRP1 Protein with Selected Drug Compounds

In a similar manner, it was shown that NRP1 had strong binding affinities with all of the chemicals that were selected. The affinities of the compounds are as follows: ponatinib exhibits a value of -10.5, adapalene has a value of -10, pralserinib demonstrates a value of -9.9, and glycyrrhizic acid possesses a value of -9.5. The ligand binding interactions of NRP1 involve specific residues at various places. For instance, the residue ASN at position 150 interacts with adapalene, while PHE at position 643 interacts with ponatinib. Additionally, glycyrrhizic acid interacts with residues TYR, THR, ARG, and ASP at positions 227, 232, 237, and 289, respectively. Similarly, pralsetinib interacts with residues TYR, ARG, GLU, HIS, GLN, and LEU at positions 227, 235, 285, 287, 290, and 330 (Table 4.15 and Figure 4.42).

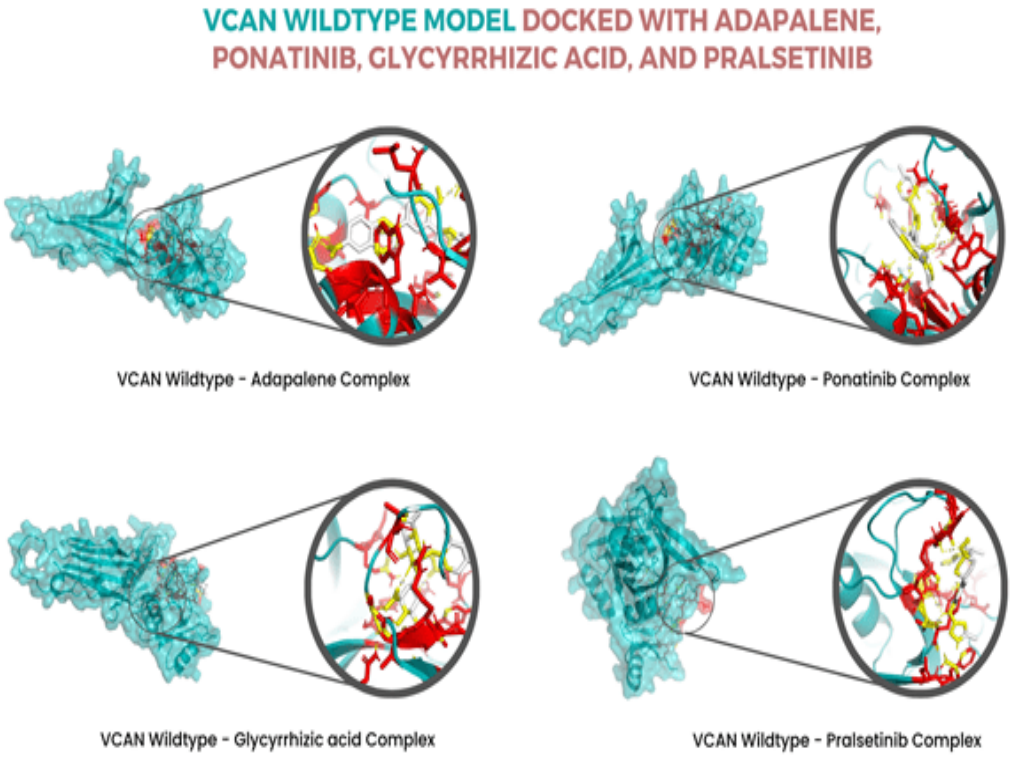

FIGURE 4.43: Visualization of wild-type VCAN protein docked with Adapalene, Ponatinib, Glycyrrhizic acid and Pralsetinib on PyMOL, showing interactions of the ligand molecules with the protein residues.

4.17.14 Molecular Docking of VCAN Protein with Selected Drug Compounds

Moreover, the most optimal complexe formed by VCAN exhibited binding affinities of -10.3 kcal/mol, towards the chemical adapalene. Moreover, the wild-type VCAN protein complexes exhibited specific residue interactions. Specifically, the residue ASP at position 191 interacted with adapalene, while GLN and VAL at positions 284 and 322 interacted with ponatinib. Additionally, THR at position 324, ARG at position 305, and TYR at position 326 displayed interactions. Furthermore, GLN at positions 195, 284, and 331 interacted with glycyrrhizic acid, LYS, ASP, and THR at positions 260, 295, and 324, respectively. TYR at position 296 exhibited three interactions, and GLY at positions 316 and 317 interacted with pralsetinib Table 4.15 and Figure 4.43.

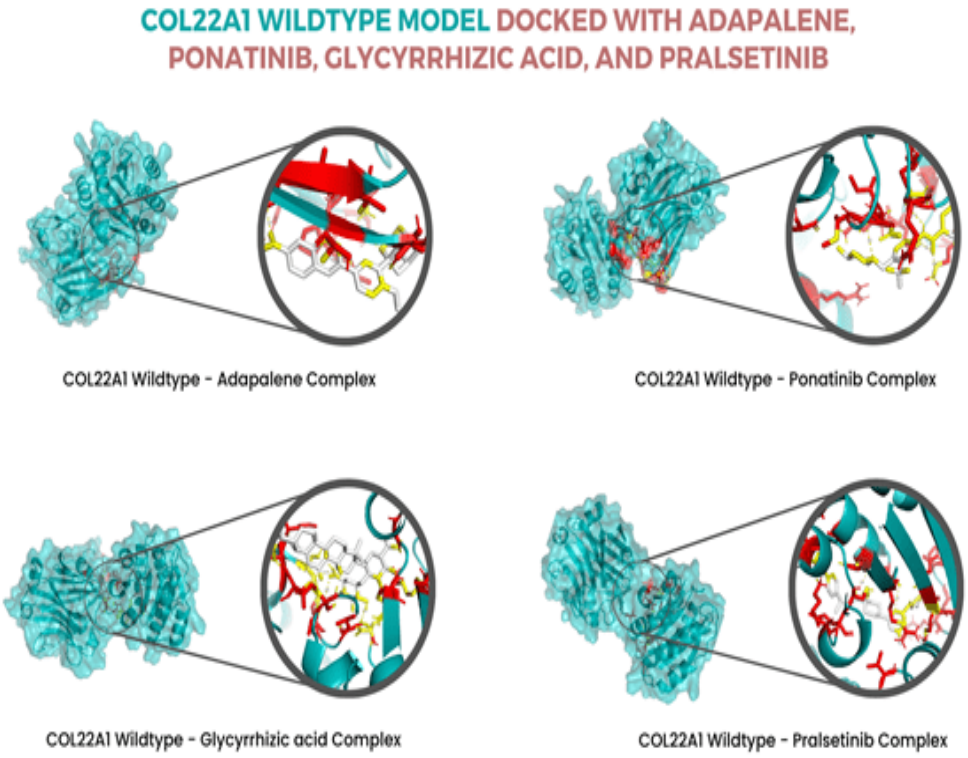

FIGURE 4.44: Visualization of wild-type COL22A1 protein docked with Adapalene, Ponatinib, Glycyrrhizic acid and Pralsetinib on PyMOL, showing interactions of the ligand molecules with the protein residues.

4.17.15 Molecular Docking of COL22A1 Protein with Selected Drug Compounds

Additionally, it is worth noting that COL22A1 exhibited the highest binding affinity, measuring -8.9 kcal/mol, towards glycyrrhizic acid (DB13751) and pralsetinib (DB15822). The protein complexes of the wild-type COL22A1 exhibited specific residue interactions. Specifically, at position 325, the interacting residue was SER. At position 311, TYR displayed two interactions with adapalene. At position 397, ASP showed an interaction with ponatinib. Positions 220, 221, 223, and 244 were associated with interactions involving ASN, VAL, CYS, and THR, respectively. Additionally, ARG and SER displayed two interactions at positions 171 and 225, respectively, with glycyrrhizic acid. Furthermore, HIS exhibited interactions at positions 144, while GLN displayed two interactions at position 144 with pralsetinib (Table 4.15 and Figure 4.44).

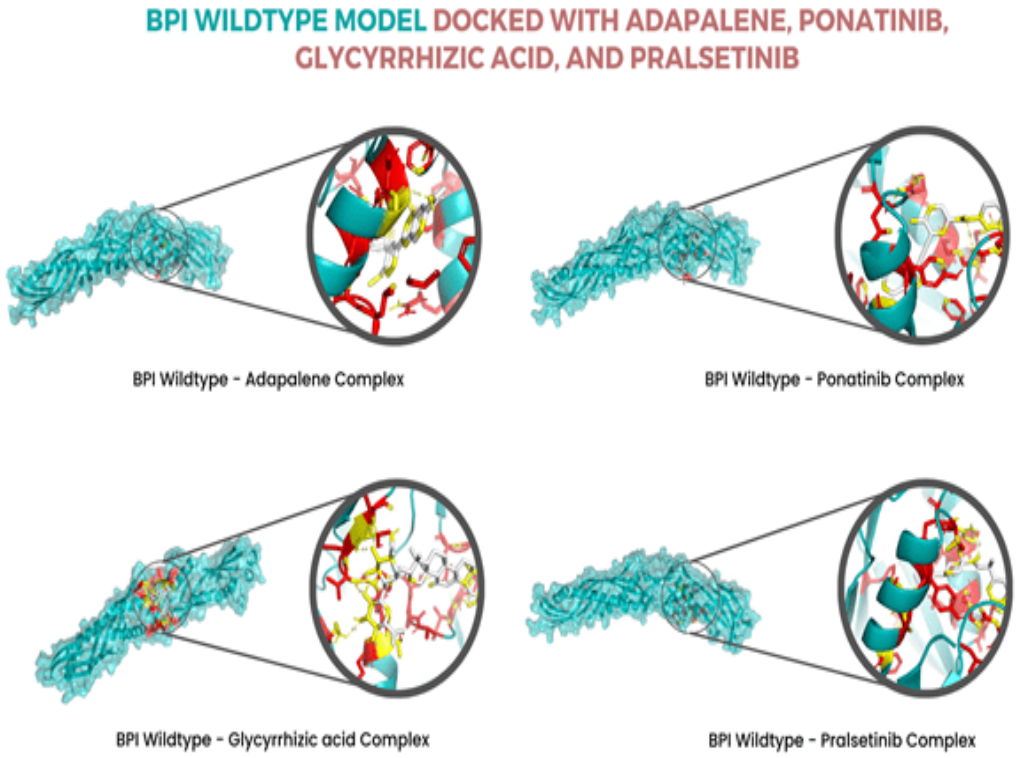

FIGURE 4.45: Visualization of wild-type BPI protein docked with Adapalene, Ponatinib, Glycyrrhizic acid and Pralsetinib on PyMOL, showing interactions of the ligand molecules with the protein residues.

4.17.16 Molecular Docking of BP1 Protein with Selected Drug Compounds

In a similar manner, BP1 demonstrates consistent interaction with the chosen chemicals, specifically -10.6, -10, -7.8, and -10.5 with adapalene, ponatinib, glycyrrhizic acid, and pralsetinib respectively, as illustrated in Table 4.15. The BPI protein complexes exhibited an interaction between the residue GLY at position 267 and adapalene, while no interactions were observed with ponatinib, THR, MET, and GLN at positions 192, 196, and 434, respectively. However, interactions were observed between LYS and positions 127 and 198, VAL and positions 195 and 433 with glycyrrhizic acid, and PHE, ARG, and LYS at positions 263, 416, and 420 with pralsetinib (Table 4.15 and Figure 4.45).

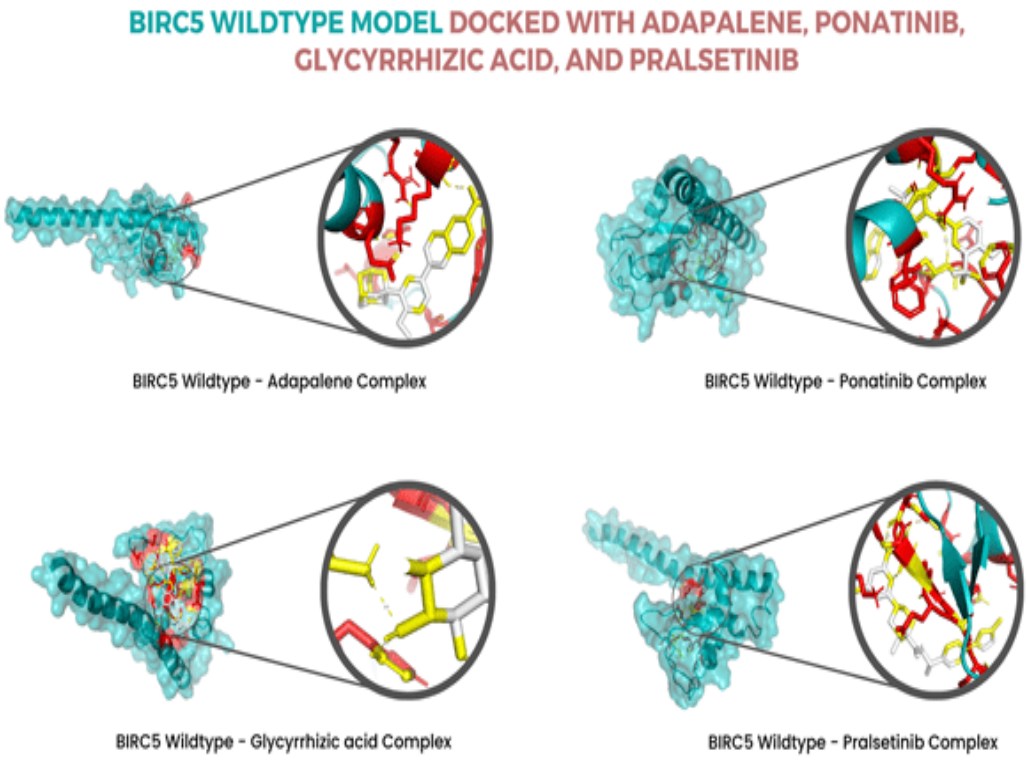

FIGURE 4.46: Visualization of wild-type BIRC5 protein docked with Adapalene, Ponatinib, Glycyrrhizic acid and Pralsetinib on PyMOL, showing interactions of the ligand molecules with the protein residues.

4.17.17 Molecular Docking of BIRC1 Protein with Selected Drug Compounds

Moreover, the BIRC5 complexes exhibited specific interacting residues, namely LYS and ASP at positions 11 and 12, respectively, with adapalene, resulting in a binding energy of -8.6. Additionally, LYS at position 11 and PHE at positions 9 and 89 were found to interact with ponatinib, yielding a binding strength of -9.2. Furthermore, LYS and HIS at positions 58 and 76, respectively, were involved in interactions, while GLU displayed two interactions at position 61 with glycyrrhizic acid, resulting in a binding energy of -8.7. Lastly, PHE at position 89 and GLU exhibited two interactions at position 90 with pralsetinib, leading to a binding strength of -9 (Table 4.15 and Figure 4.46).

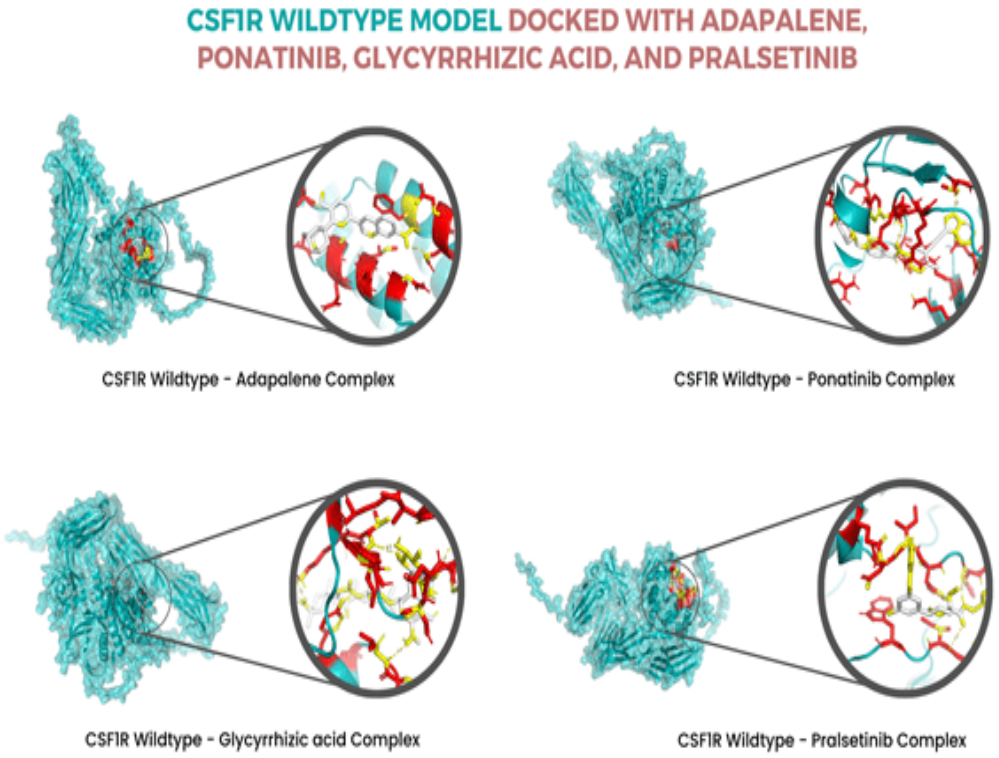

FIGURE 4.47: Visualization of wild-type CSF1R protein docked with Adapalene, Ponatinib, Glycyrrhizic acid and Pralsetinib on PyMOL, showing interactions of the ligand molecules with the protein residues.

4.17.18 Molecular Docking of CSF1R Protein with Selected Drug Compounds

The CSF1R protein demonstrated a binding affinity of -8.9 through its interaction with the residue GLN at position 913 when exposed to adapalene. Similarly, when exposed to ponatinib, the protein exhibited a binding energy of -9.5 through its interactions with the residues THR, GLU, and ARG at positions 587, 725, and 727, respectively. Furthermore, the protein displayed a binding affinity of -8.9 through its interactions with the residues ILE, ASP, and TYR at positions 803, 806, and 866, respectively. Additionally, the residue VAL demonstrated two interactions at positions 811 and 861 with glycyrrhizic acid, resulting in an affinity of -8.6. Lastly, the protein showed an affinity of -8.6 through its interactions with the residues TYR, PHE, and GLN at positions 561, 563, and 568, respectively, when exposed to pralsetinib (Table 4.15 and Figure 4.47).

Summarizing the molecular docking results of all the specified proteins (MNX1, ERG, TCL1A, AFF3, FAT1, KRAS, NRAS, CD4, ITGAM, PTPRC, TYROBP, IL1B, CSF1R, VCAN, NRP1, COL22A1, BPI, and BIRC5) with 141 drug compounds indicated that the binding affinities (docking scores) ranged from as low as -3.1 kcal/mol [TYROBP protein with D-norleucine (DB04419) and Dimethyl fumarate (DB08908)] to as high as -10.9 kcal/mol [ITGAM with glycyrrizic acid (DB13751)]. Moreover, the best docking scores of all the proteins (wild-type and mutant models) had different binding affinities with different drug compounds but the best binding affinities ranged from as low as -7.3 kcal/mol [mutant (D2382A) FAT1-glycyrrhizic acid (DB13751)] to as high as -10.9 kcal/mol for ITGAM-glycyrrhizic acid (DB13751) complex. However, the compounds adapalene, ponatinib, glycyrrhizic acid, and pralsetinib showed the best binding affinities with all the proteins except for two complexes TYROBP-Glycyrrhizic acid complex, and wild-FAT1-Adapalene (D2382A) complex, otherwise all the complexes were observed to have the binding affinities of more than -7.0 kcal/mol.

Furthermore, the TCL1A_wild, TCL1A_T38I, ERG_ E353Q, CD4, VCAN, BPI, PTPRC, AFF3_wild, FAT1_P4309S, KRAS_Q61R, KRAS_G13D, KRAS_G12V, KRAS_G12R, KRAS_K117N, NRAS_Q61R, NRAS_E153Q, and NRAS_G12D of NRAS showed the best binding affinities with the same compound, Adapalene. However, the protein models, KRAS_wild, AFF3_P1129L, IL1B, CSF1R, NRP1, BIRC5, MNX1_wild, MNX1_P392L, wild-type_FAT1_M739I, Wilds_FAT1_P4309S, KRAS_G12R, KRAS_G12D), and NRAS_Q61K showed the best binding affinities with the same compound, Ponatinib. Moreover, the Glycyrrhizic acid showed the best binding affinities with ITGAM, COL22A1, NRAS_wild, FAT1_ D2382A_wild, FAT1_ D2382A, KRAS_Q61H, KRAS_Q61E, KRAS_A59E and KRAS_G13R. Finally, the Pralsetinib showed the best binding affinities with only NRAS_Y64D, NRAS_Q61H, and NRAS_G13D). The aforementioned docking results revealed that the compound Adapalene showed the best binding affinities with 17 protein models (including the wild-type and mutant models) out of a total of 44 protein models, while the Ponatinib, Glycyrrhizic acid, and Pralsetinib showed the best binding affinities with 15, 9, and 3 protein models, respectively. This indicates that Adapalene showed the best binding affinities with most protein models, followed

by Ponatinib. Although Adapalene and Ponatinib were not showing the best binding affinities with those protein models that were with the other two compounds (Glycyrrhizic acid and Pralsetinib) but still showed considerable binding affinities with those protein models as well, ranging from -6.9 kcal/mol to -10.8 kcal/mol for Adapalene and -7.2 kcal/mol to -9.3 kcal/mol for Ponatinib. Hence, based on binding affinities, adapalene, and ponatinib are the best compounds that can be utilized against the crucial proteins except for two protein models with binding affinities less than -7.0 kcal/mol.

4.17.18.1 MD Simulations of TCL1A with Selected Drug Compounds

The protein was stable from 15.20 ns to 32.60 ns, according to the MD simulation results for the wild-type TCL1A-Adapalene docked complex, however it fluctuated from the simulation's beginning to 13.85 ns. The protein was observed to be overall stable (Figure4.48a Conversely, it was noted that the ligand varied between 30.30 ns till the simulation's conclusion and remained steady between 5.55 ns and 29.85 ns in time. At 1.70 ns in time, the protein and ligand's RMSD value differences were at their lowest. Finally, at the conclusion of the simulation period, the RMSD for the ligand and protein were 8.78 Å and 2.41 Å , respectively (Figure 4.48b). Additionally, only a small number of protein residues altered at positions 1, 2, and 114 according to the protein RMSF plot. At position 1, MET had the largest fluctuation of any protein residue (3.69 Å) (Figure4.48c).

The TCL1A protein's mutant model (T38I), when docked with adapalene, produced simulation findings that indicated the protein was only moderately stable overall, lasting from 19.45 ns to 22.35 ns. From the start of the simulation to the 10.15 ns interval, it displayed the largest fluctuations (Figure 4.48a). The ligand, on the other hand, fluctuated the most from 23.70 ns to 25.85 ns period and was likewise unstable. The RMSD values of the protein and the ligand at the conclusion of the simulation period were 2.77 Å and 3.86 Å , respectively, and the minimum difference was seen at 2.05 ns time (Figure 4.48b). Additionally, the residues at positions 1-4 that fluctuated were visible on the RMSF figure. At

position 1 (8.86 Å), MET had the largest fluctuating residue, followed by ALA at position 2 (7.68 Å) and GLu at position 3 (6.87 Å) (Figure 4.48c).

The protein exhibited stability from 34.30 ns to 40.60 ns time and was generally pretty stable, but it had the biggest variation from the beginning to 16.85 ns period, according to the simulation results of the wild-type TCL1A-Ponatinib complex (Figure 4.48a). However, the ligand fluctuated between the times of 22.20 and 20.40 ns and 45.10 ns and the simulation's completion; overall, the ligand was not very stable. Furthermore, at a time period of 0.40 ns, the disparity between the ligand and protein RMSD values was at its lowest. At the conclusion of the simulation period, the protein's and the ligand's RMSD values were 2.57 Å and 6.95 Å , respectively (Figure 4.48b). Additionally, the changing residues at positions 1–5 were visible in the protein RMSF figure. In Figure 4.48c, the residue with the largest fluctuation was MET at position 1 (10.39 Å), followed by ALA at position 2 (9.19 Å) and GLU at position 3 (7.43 Å).

According to the mutant TCL1A-Ponatinib complex simulation results, the protein remained stable between 27.30 and 33.25 ns. Overall, it was not very steady, exhibiting variable swings from the start of the simulation to 21.05 ns and from 35.95 ns to 43.15 ns time (Figure 4.48a). Additionally, the ligand was not particularly stable and fluctuated from the start of the simulation until 18.55 ns. The RMSD values of the protein and the ligand at the conclusion of the simulation period were 3.50 ns and 6.26 ns, respectively, with the minimum difference between them occurring at 2.90 ns (Figure 4.48b). The protein residues at positions 2, 5, 6, 44, and 114 that fluctuate were also visible on the protein RMSF figure. Position 114 (3.19 Å) had the largest residue fluctuation, followed by position 2 (3.00 Å) for ALA and position 5 (2.82 Å) for PRO (Figure 4.48c).

Proceeding to the simulation findings for the wild-type TCL1A-Glycyrrhizic acid complex, the RMSD plot indicated that the protein was generally unstable, fluctuating between 38.85 ns and the conclusion of the simulation period. Only the protein exhibited stability between the 17.50 and 20.10 ns interval (Figure 4.48a). However, the ligand was not consistently steady and exhibited the greatest volatility from the start of the simulation time to the 24.70 ns interval. The protein and

ligand RMSD values at 0.45 ns and 0.55 ns time showed the least difference, however at the conclusion of the simulation period, the ligand and protein RMSD values were 17.99 Åand 4.45 Å , respectively (Figure 4.48b). The protein residues varying at positions 1–5 were shown by the protein RMSF plot, which was observed. At position 3 (5.74 Å), GLU was the most highly fluctuating residue, while at position 1 (5.73 Å), MET was the second highest. The remaining residues, PRO, CYS, and ALA, at positions 5, 4, and 2, displayed fluctuations of 5.39 Å , 5.36 Å , and 5.30 Å , in that order (Figure 4.48c).

Based on simulation results of the mutant TCL1A-Glycyrrhizic acid complex, it was found that the protein remained stable between 11.90 and 21.70 ns. It was not particularly steady overall, exhibiting variations from 32.00 ns to the simulation's termination because it varied after 22.05 ns (Figure 4.48a). Conversely, the ligand exhibited the greatest variation at 33.65 ns (4.80 Å); it was also shown to be unstable, fluctuating from the beginning to 25.15 ns. The protein and ligand RMSD values differed from one another by a minimum of 33.05 ns. Similarly, at the conclusion of the simulation period, the RMSD values for the protein and ligand were 3.47 Å and 3.58. The protein RMSF showed that the residues at positions 3, 4, and 114 were varying. Position 114 (4.52 Å) had the largest fluctuating residue, ASP, followed by position 3 (3.20 Å) with GLU (Figure 4.48c).

Ultimately, the final complex of the wild-type TCL1A protein with pralsetinib was shown, showing that the protein fluctuated from the start of the simulation to the 28.20 ns period, but remained stable from 40.00 ns to the completion of the simulation duration (Figure 4.48). Overall, the protein was found to be good, however the ligand was unstable and fluctuated a lot, peaking between 32.10 and 36.40 ns in time. The RMSD values of the protein and the ligand at the conclusion of the simulation were 2.35 Å and 4.98 Å , respectively, with the minimum difference between them being detected at 0.85 ns time (Figure 4.48 b). Additionally, the protein RMSF plot's positions 1-3 showed the fluctuating protein residues. At position 1, MET had the most fluctuating residue (7.74 Å), while ALA at position 2, with an RMSF value of 6.09 Å , was the second most variable residue (Figure 4.48 c).

The protein varied from the start of the simulation to 10.05 ns time, according to the results of the mutant TCL1A-Pralsetinib complex simulation. Overall, it was deemed to be fine and stable between the 25.30 and 36.85 ns periods (Figure 4.48a). However, the ligand fluctuated from 41.05 ns to the simulation's conclusion, with the most significant fluctuation occurring between 9.25 ns and 10.45 ns, which led to the ligand's overall instability. 10.65 ns was discovered to be the smallest difference between the protein and ligand RMSD values. At the conclusion of the simulation period, the protein's and the ligand's RMSD values were 2.95 Å and 3.07 Å , respectively (Figure 4.48b). Additionally, as shown in Figure 4.48c, the protein RMSF plot showed the varying residues at positions 1-3. MET had the largest variation at position 1 (6.04 Å), followed by ALA at position 2 (4.32 Å).

4.17.19 MD simulations of MNX-1 with Selected Drug Compounds

The wild-type MNX1-Adapalene complex's simulation results showed that the protein was generally unstable and fluctuated from the start of the simulation to 29.55 ns time (Figure 4.49a). The protein was stable only from 12.60 ns to 14.25 ns time. Conversely, it was discovered that the ligand exhibited general instability, fluctuating between the start of the simulation and 30.05 ns, with the maximum fluctuation occurring at 16.75 ns and measuring 18.85 Å. At 0.05 ns, the disparity between the ligand and protein RMSD values was at its lowest. At the conclusion of the simulation period, the protein's and the ligand's RMSD values were, respectively, 29.96 Åand 14.24 Å(Figure 4.49b). Additionally, the changing residues at positions 0-81 were visible in the protein RMSF figure. ARG at position 71 (26.40 Å) had the largest varying residue, followed by LEU at position 72 (26.38 Å), GLU at location 75 (24.62 Å), and ASP at position 70 (24.35 Å) (Figure4.49c). The mutant model (P392L) MNX1-Adapalene complex's simulation findings demonstrated that the protein was stable between 25.40 and 36.17 ns in time. It was discovered to be generally unstable after fluctuating from the start of the simulation to the 14.70 ns period (Figure 4.49a). Conversely, the ligand exhibited the greatest changes from the start to 36.05 ns period, while being generally unstable

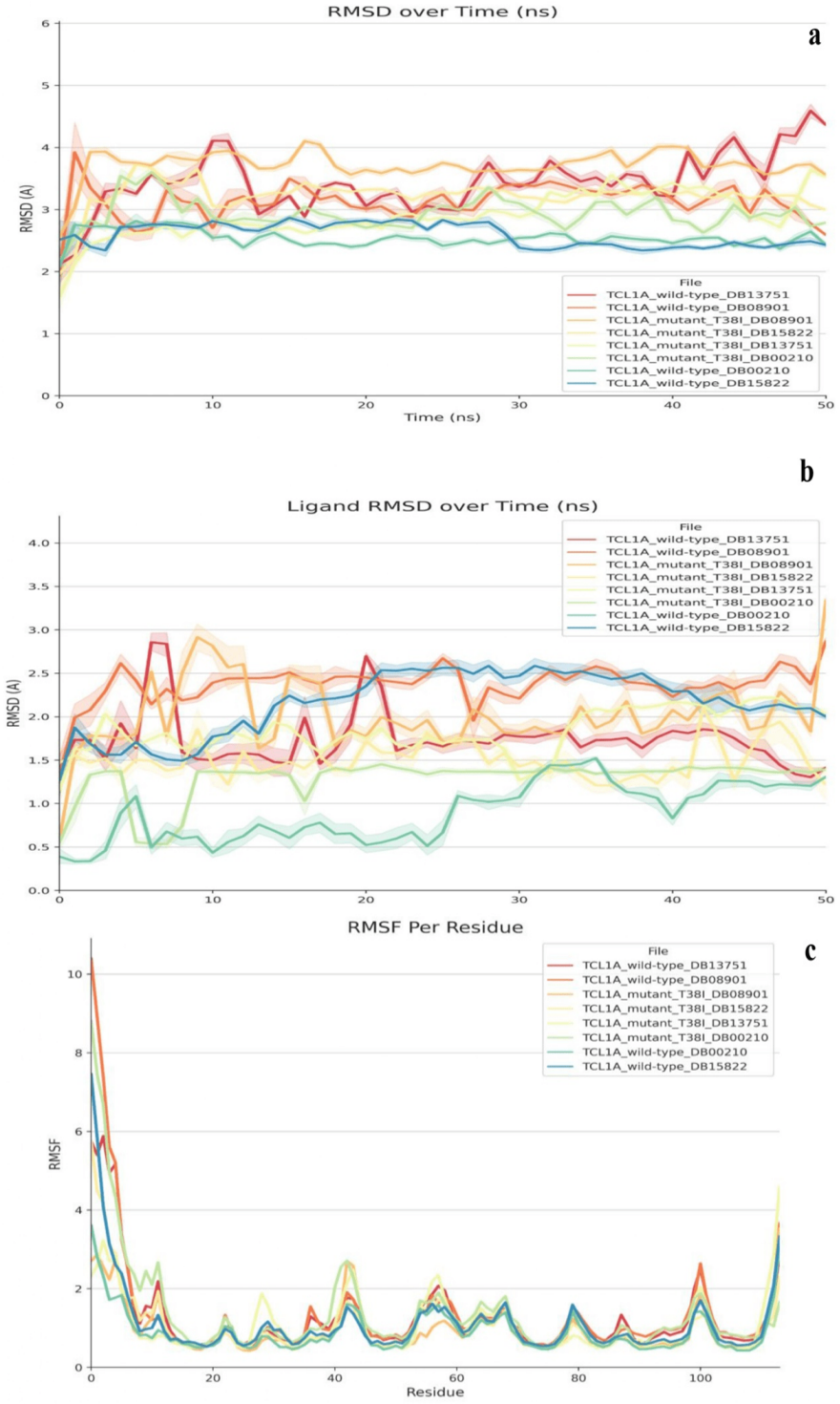

FIGURE 4.48: (a) RMSD graph of wild and mutant TCL1A representing the conformational differences while docking with selected drug compounds. (b) RMSD graph of ligands (drugs) while docking with wild and mutant TCL1A. The simulations were performed for a period of 50 ns. (c) RMSF graph representing the structural fluctuations observed for amino acid residues between the wild-types and mutant models of TCL1A protein docked with the selected compounds during a simulation period of 50 ns.

as well. At 0.05 ns, the RMSD difference between the protein and ligand was at its lowest. At the conclusion of the simulation, the RMSD values of the protein and ligand were 23.86 Åand 13.36 Å, respectively (Figure 4.49 b). Additionally, the protein RMSF revealed that the residues at positions 0-85 and 365-400 varied significantly. The residues with the highest changes were MET and ARG, which displayed 18.21 Åat positions 0 and 392, respectively. CYS (17.96 Å) at position 382, GLU (17.50 Å) at position 1, and SER (17.48 Å) at position 3 were the next highest oscillating residues (Figure 4.49c).

According to the simulation results, the protein was only stable between 42.90 and 46.90 ns for the wild-type MNX1-Ponatinib combination. It was generally unstable and varied from the start to the 28.00 ns duration (Figure 4.49). Rather, from the start to 22.35 ns, the ligand also varied. Although it was generally unstable, it was seen to be steady between 23.65 and 34.65 ns in time. The RMSD values of the protein and the ligand were 24.97 Åand 7.89 Å, respectively, at the conclusion of the simulation period (Figure 4.49b). The minimum difference between the RMSD values of the protein and the ligand was at 0.05 ns time. However the protein RMSF was found, and it showed that the residues at positions 0-4,399, and 400 were variable. At location 400 (19.60 Å), GLN had the largest fluctuating residue, followed by MET at position 0 (17.88 Å) and PRO at position 399 (17.39 Å) (Figure 4.49 c).

The protein showed stability from 35.30 ns to 40.95 ns in the simulation results of the mutant model (P392L) MNX1-Ponatinib complex, but fluctuated from the start of the simulation to 23.30 ns, with 32.33 Åshowing the biggest variation at positions 12.05 ns and 23.20 ns period. Overall instability of the protein was noted (Figure 4.49a). The ligand did, however, exhibit oscillations from the start of the simulation to 14.20 ns, when it was 29.4 Å, with the most fluctuation occurring at 47.40 ns. Additionally, an overall unstable state was noted, with the protein and ligand RMSD values differing by as little as 0.05 ns; additionally, the final simulation time RMSD values were 29.88 Åand 26.83 Å(Figure4.49b). However, the protein RMSF plot revealed that the residues at positions 0–251 and 339–400 were significantly changing. The protein residues at positions 0-251 and 339-394 all fluctuated significantly (more than 5 Å), but the residues that fluctuated the

most were GLN (33.86 Å) at position 400, PRO (32.12 Å) at position 399, ALA (31.45 Å) at position 398, PRO (30.39 Å) at position 397, GLN (28.73 Å) at position 396, and HIS (28.66 Å) at position 395.

The protein exhibited fluctuations from the beginning to 13.15 ns and from 23.90 ns to 38.85 ns period, and the simulation results of the wild-type MNX1-Glycyrrhizic acid complex were obtained. These results showed that the protein was unstable overall (Figure 4.49a). However, it was discovered that the ligand was not generally stable and that it fluctuated greatly from the start of the simulation to 13.30 ns time. The RMSD values of the protein and the ligand at the end of the simulation time were 28.26 Åand 23.41 Å, respectively. The minimum difference between the RMSD values of the protein and the ligand was at 11.25 ns time (Figure 4.49b). Furthermore, the shifting residues at positions 13, 14, 3, 99, and 400 were shown by the protein RMSF. At location 400 (14.84 Å), GLN was the residue with the largest fluctuation, while at positions 13 and 14, respectively, ALA and VAL displayed the similar oscillations (13.57 Å) (Figure 4.49c).

The protein was stable from 19.80 ns to 31.70 ns time in the simulation results of the mutant model (P392L) MNX1-Glycyrrhizic acid complex, but it fluctuated from the start of the simulation to before 19.80 ns time, with the highest fluctuation recorded at 13.05 ns time, 25.31 Å(Figure 4.49a). The ligand fluctuated from the start of the simulation to 19.80 ns and from 39.35 ns to the end of the simulation duration, and it was found to be generally unstable. The maximum variation, detected at 17.20 ns time, was 30.71 Å, indicating an overall state of instability. The RMSD values of the protein and the ligand at the conclusion of the simulation time were 22.62 Åand 25.89 Å, respectively, and the minimum difference between the two was observed at 21.35 ns and 22.55 ns periods (Figure 4.49b). Additionally, the protein-RMSF plot revealed that at positions 0-181, 185-239, 244-255, 265–291, 293-294, 304-319, 329-377, 383–400, the protein residues exhibited significant variations. ALA (12.89 Å) at position 85 had the highest fluctuation, followed by ALA (12.71 Å) at position 84, GLN (12.41 Å) at position 400, LEU (12.20 Å) at position 83, HIS (12.05 Å) at position 86, and ASP (11.59 Å) at position 358. Other protein residues fluctuated significantly (more than 5.00 Å) at positions 0-82, 87-181, 185- 239, 244-255, 265-291, 293-294, 304-319,

329-357, 359-377, and 383-399 (Figure 4.49c).

The protein was determined to be generally unstable based on simulation results for the wild-type MNX1-Pralsetinib complex. The protein was stable from 39.75 ns to 46.75 ns time but fluctuated from the start of the simulation to 27.95 ns period (Figure 4.49a). Rather, the ligand was not extremely unstable generally; it fluctuated from the start of the simulation until 22.10 ns duration. The RMSD values of the protein and the ligand at the conclusion of the simulation time were 24.97 Åand 7.89 Å, respectively (Figure 4.49a). The minimum difference between the RMSD values of the protein and the ligand was at 0.05 ns time. Additionally, the protein RMSF showed that the residues at positions 0-66 and 394-400 were variable. GLN (19.60 Å) at position 400 was the protein residue that changed the most, followed by MET (17.88 Å) at position 0, PRO (17.39 Å) at position 399, GLU (16.92 Å) at position 1, and LYS (16.13 Å) at position 2 (Figure 4.49c).The findings of the simulation for the MNX1-Pralsetinib complex in the mutant model (P392L) showed that the protein varied from the start of the simulation until the 14.10 ns period. Although it was discovered to be generally unstable, it was determined to be stable between 27.15 and 36.05 ns in time (Figure 4.49a).

Conversely, the ligand experienced fluctuations from the start of the simulation to 13.05 ns, with the maximum fluctuation occurring at 5.55 ns. Additionally, it was discovered to be somewhat stable yet unstable in relation to the protein. At 0.05 ns, the RMSD difference between the protein and ligand was at its minimum, and at the conclusion of the simulation, the RMSD values of the two substances were 28.17 Åand 9.65 Å, respectively (Figure 4.49b). Moreover, the protein-RMSF plot revealed that the protein residues varied at positions 0-76, 166-203, 95-164, and 331-400. GLN (25.08 Å) at position 400, PRO (23.15 Å) at position 399, ALA (21.16 Å) at position 398, PRO (19.36 Å) at position 397, GLN (17.88 Å) at position 396, and HIS (16.60 Å) at position 395 were the residues with the highest fluctuation (Figure 4.49c). The remaining protein residues at positions 0-76, 95-164, 166-203, and 331-394 also exhibited significant fluctuations (more than 5 Å).

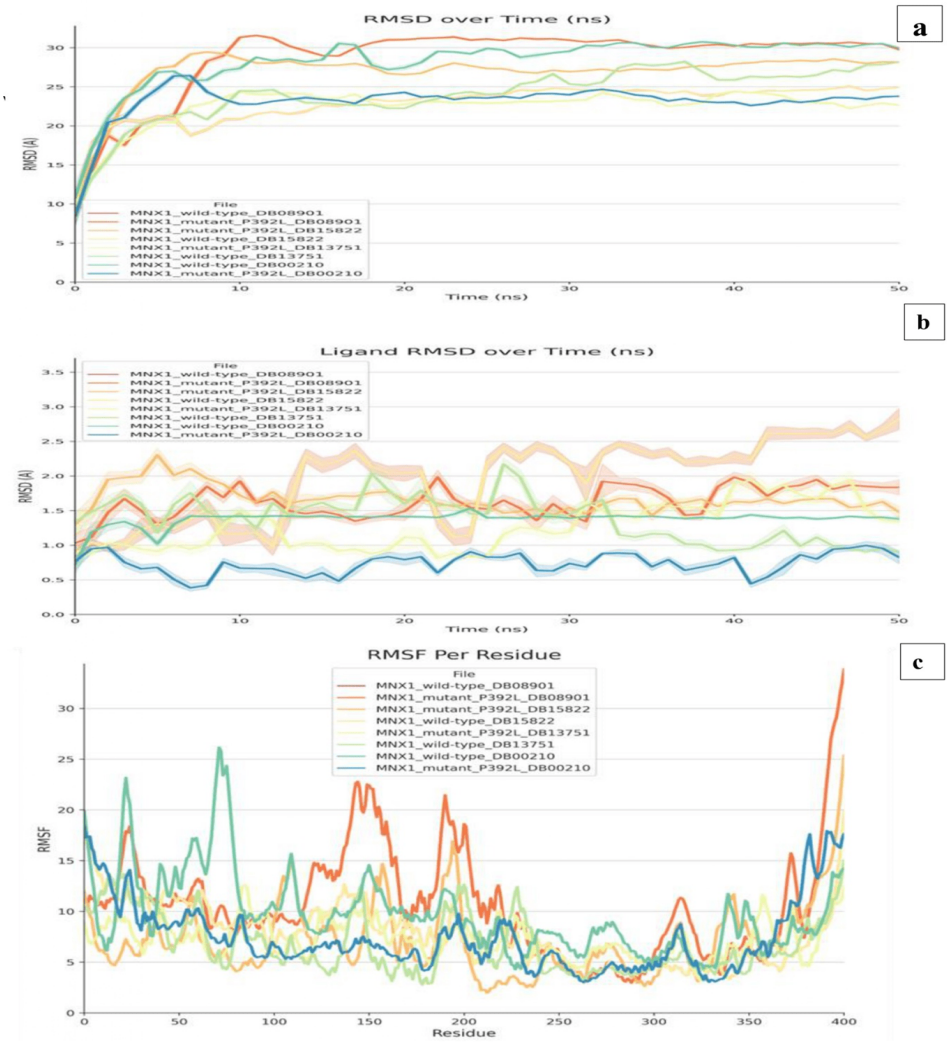

FIGURE 4.49: (a) RMSD graph of wild and mutant MNX1 representing the conformational differences while docking with selected drug compounds. (b) RMSD graph of ligands (drugs) while docking with wild and mutant MNX1. The simulations were performed for a period of 50 ns. (c) RMSF graph representing the structural fluctuations observed for amino acid residues between the wild-types and mutant models of MNX1 protein docked with the selected compounds during a simulation period of 50 ns.

4.17.19.1 MD Simulations of ERG with Selected Drug Compounds

The simulation findings of the wild-type ERG-Adapalene complex showed that the protein remained steady between 18.60 ns and 44.55 ns, but experienced fluctuations between 8.55 ns and 16.90 ns. The largest fluctuation, measuring 2.50 Å, occurred at 15.95 ns. Overall, the protein was determined to be stable (Figure 4.50a). Conversely, the ligand exhibited fluctuations throughout the simulation,

starting from the beginning and continuing until the 37.50 ns mark. The maximum variation seen was 4.81 Å, measured at two time intervals: 7.85 ns and 8.15 ns. Additionally, it was determined that the system as a whole was unstable. The RMSD values of the protein and the ligand differed by a minimum of 3.20 ns. At the end of the simulation, the RMSD values for the protein and the ligand were 2.25 Åand 1.93 A, respectively (Figure 4.50b). Furthermore, the protein-RMSF plot revealed the absence of any notable variations in protein residues. The residue with the largest fluctuation was GLN (2.46 Å) at position 98, followed by ASN (2.37 Å) at position 37, and ALA (2.27 Å) at position 99 (Figure 4.50c).

The simulation results of the mutant model (E353Q) ERG-Adapalene complex indicate that the protein remained stable for the duration of the simulation, except for a fluctuation between 23.15 ns and 42.85 ns. The highest recorded fluctuation of 3.61 Åoccurred at 24.70 ns (Figure 4.50a). The system demonstrated general stability, with little fluctuations. However, the ligand exhibited significant fluctuations, ranging from 20.95 ns till the end of the simulation period. The maximum variation, measuring 13.28 Å, occurred at a time of 21.90 ns. The data exhibited stability during the period of 13.35 ns to 20.75 ns, however it was determined to be generally unstable. The smallest difference between the RMSD values of the protein and the ligand was observed at a time of 0.95 nanoseconds. At the end of the simulation, the RMSD values for the protein and the ligand were 2.00 Åand 9.69 Å, respectively (Figure 4.50b). Furthermore, the protein-RMSF plot revealed that there were very minimal fluctuations in a small number of protein residues at positions 1-3 and 102. The residue with the greatest fluctuation was SER (6.83 Å) at position 1, followed by SER (4.93 Å) at position 2, PRO (4.87 Å) at position 102, and ARG (3.66 Å) at position 3 (Figure 4.50c).

The simulation of the wild-type ERG-Ponatinib combination showed that the protein remained stable from 37.25 ns till the end of the simulation period. The time changed between 15.05 ns and 17.65 ns, and between 26.35 ns and 33.30 ns, while being steady overall (Figure 4.50a). Conversely, the ligand exhibited fluctuations ranging from 13.95 ns until the conclusion of the simulation. The largest measured

fluctuation, measuring 15.11 Å, occurred at 21.05 ns. The system exhibited stability throughout the simulation until just before to the 13.95 ns mark, at which point it was determined to be generally unstable. The smallest discrepancy between the RMSD) values of the protein and the ligand occurred at a time of 0.20 nanoseconds. At the end of the simulation, the RMSD values for the protein and the ligand were 2.18 Åand 7.47 Å, respectively (Figure 4.50b). Moreover, the protein-RMSF plot revealed that the protein residues exhibited fluctuations at positions 1-3 and 102. The residue with the largest fluctuation was SER (7.40 Å) at position 1, followed by SER (5.99 Å) at position 2, ARG (5.16 Å) at position 3, and PRO (5.02 Å) at position 102 (Figure 4.50c).

The simulation results of the mutant (E353Q) ERG-Ponatinib complex indicate that the protein exhibited stability during the time intervals of 0 to 6.75 ns and 25.00 to 35.90 ns. Overall, the protein remained stable throughout the simulation, except for fluctuations observed between 16.30 to 24.55 ns and 37.05 ns until the end of the simulation. The highest recorded fluctuation was 3.08 Åat 4.65 ns (Figure 4.50a). Nevertheless, the ligand exhibited stability solely within the time range of 5.00 ns to 10.20 ns. The simulation exhibited significant variation, ranging from 26.20 ns until the end of the simulation period. It was observed to be generally unstable, with the largest fluctuation recorded at 36.30 ns, measuring 8.21 Å. The smallest disparity between the protein and ligand RMSD values was observed at a time of 9.15 nanoseconds. At the conclusion of the simulation, the protein and ligand had RMSD values of 2.51 Åand 7.22 A, respectively (Figure 4.50b). The protein-RMSF plot indicated that the protein residues exhibited minimal fluctuations, indicating stability. The residues with the highest fluctuations were SER (4.35 Å) at position 1, followed by PRO (3.46 Å) at position 102, and SER (2.62 Å) at position 2 (Figure 4.50c).

The simulation results of the wild-type ERG-Glycyrrhizic acid complex indicate that the protein remained stable during the time intervals of 11.00 ns and 20.25 ns. The data exhibited significant variations ranging from 25.75 ns to 29.05 ns and 42.55 ns to 45.30 ns, although it was determined to be generally stable (Figure

4.50). The ligand exhibited substantial temporal variations at time intervals ranging from 1.15 ns to 1.75 ns, 7.85 ns to 12.55 ns, and 16.45 ns to 28.30 ns. An overall instability was observed with a maximum fluctuation of 59.82 Å, which occurred at 17.40 ns. The smallest disparity between the protein and ligand RMSD measurements occurred at a time of 0.85 ns. At the conclusion of the simulation, the protein and ligand had RMSD values of 2.78 Åand 19.27 Å, respectively (Figure 4.50b). In addition, the protein-RMSF plot revealed that there were fluctuations in protein residues at positions 1, 2, and 102. The greatest variation was observed in the SER amino acid (4.89 Å) at position 1, followed by PRO (4.78 Å) at position 102, and SER (3.98 Å) at position 2 (Figure 4.50c). The simulation findings of the mutant model (E353Q) ERG-Glycyrrhizic acid complex demonstrated that the protein remained stable between 6.25 ns and 15.65 ns, but experienced fluctuations between 30.05 ns and 39.95 ns. Overall, the protein was shown to be stable (Figure 4.50a). Conversely, the ligand exhibited a range of fluctuations from 6.70 ns to 23.35 ns throughout time, with the maximum measured fluctuation of 12.46 Åoccurring at the 22.65 ns mark. The overall stability of the system was determined to be low, with the smallest difference between the RMSD values of the protein and the ligand occurring at the 0.30 ns mark. At the conclusion of the simulation, the protein had an RMSD value of 1.87 Å, while the ligand had an RMSD value of 9.90 Å(Figure 4.50a). Nevertheless, the protein-RMSF plot indicated that the protein remained stable, as there were no significant fluctuations in residues seen for this combination. The residue with the greatest magnitude of fluctuation was serine (SER) with a value of 3.55 angstroms at position 1 (Figure 4.50c).

The simulation results of the wild-type ERG-Pralsetinib complex demonstrated the protein's stability throughout the whole simulation period, which lasted 21.40 nanoseconds. The duration fluctuated between 1.65 nanoseconds and 4.80 nanoseconds, 7.75 nanoseconds and 8.45 nanoseconds, and 16.10 nanoseconds and 21.40 nanoseconds. Overall, the time was judged to be satisfactory (Figure 4.50a). Conversely, the ligand exhibited a fluctuation in time ranging from 8.95 ns to 22.45 ns. An overall instability was observed, with the largest recorded fluctuation being 15.84 Åat a time of 21.70 ns. The smallest discrepancy between the RMSD values

of the protein and the ligand occurred at a period of 1.80 ns. At the end of the simulation, the RMSD values for the protein and the ligand were 1.70 Åand 14.04 Å, respectively (Figure 4.50 b). In addition, the protein-RMSF plot revealed that there were no significant changes observed in the protein residues. The greatest variation occurred in the PRO residue, with a fluctuation of 3.56 Åat position 102, followed by the SER residue with a fluctuation of 3.23 Åat position 1 (Figure 4.50c). The simulation results of the mutant model (E353Q) ERG-Pralsetinib complex indicate that the protein remained stable from the start of the simulation until 5.95 ns. However, it exhibited fluctuations between 6.25 ns and 17.00 ns, as well as between 46.85 ns and the end of the simulation. Overall, the protein was found to be stable throughout the simulation (Figure 4.50a). However, the ligand exhibited stability only during the initial phase of the simulation, lasting until 8.65 ns. Subsequently, it displayed fluctuations from 9.15 ns until the completion of the simulation, indicating overall instability. The protein and ligand RMSD values had a minimum difference at 0.10 ns time. At the end of the simulation, the protein and ligand had RMSD values of 2.85 Åand 6.96 Å, respectively (Figure 4.50b). In addition, the protein-RMSF plot revealed that the protein residues exhibited little fluctuations, maintaining stability. The residue with the highest degree of fluctuation was SER (2.94 Å) at position 26 (Figure 4.50c).

4.17.20 MD Simulations of AFF3 with Selected Drug Compounds

The simulation findings of the wild-type AFF3-Adapalene complex indicated that the protein remained stable from 33.40 ns to the completion of the simulation. However, it exhibited fluctuations from the beginning of the simulation until 22.80 ns, suggesting overall instability (Figure 4.51a). Conversely, the ligand exhibited fluctuations from 16.40 nanoseconds until the conclusion of the simulation period. An overall instability was observed, with the largest fluctuation of 10.29 Åoccurring at 27.50 ns. The RMSD values of the protein and the ligand differed by a minimum of 15.85 ns and 19.65 ns, respectively. At the completion of the simulation, the RMSD values for the protein and the ligand were 7.63 Åand 7.24

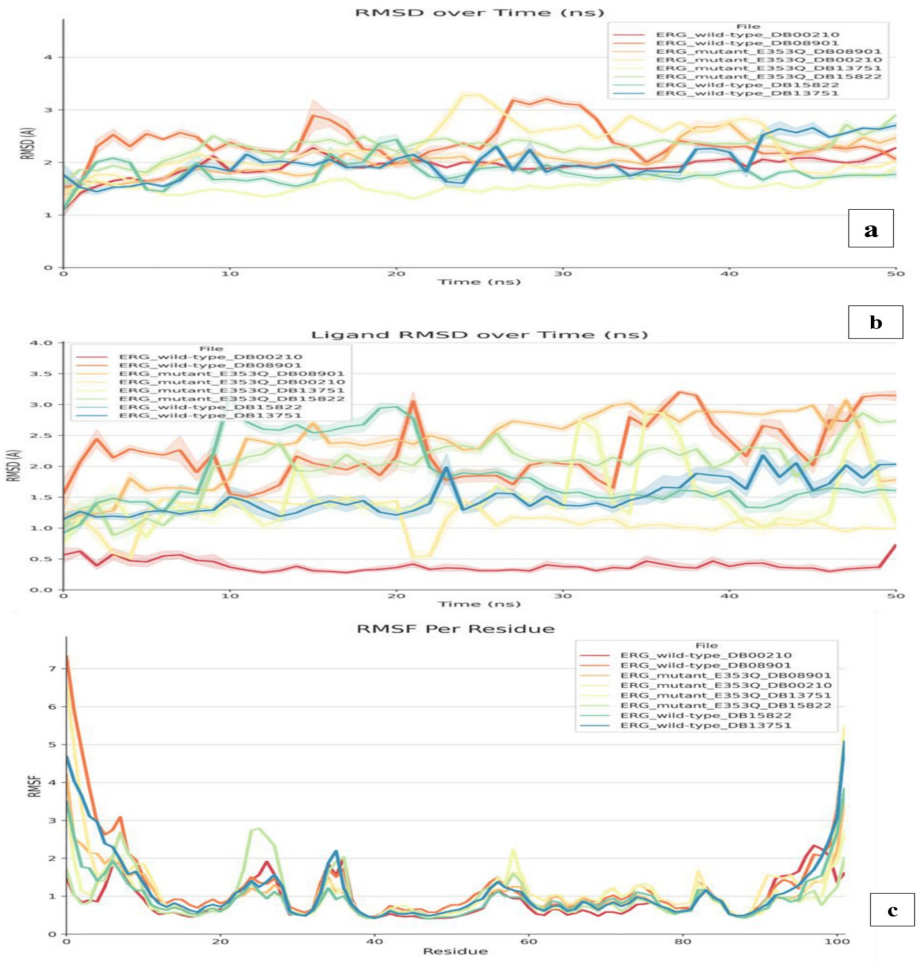

FIGURE 4.50: (a) RMSD graph of wild and mutant ERG representing the conformational differences while docking with selected drug compounds. (b) RMSD graph of ligands (drugs) while docking with wild and mutant ERG. The simulations were performed for a period of 50 ns. (c) RMSF graph representing the structural fluctuations observed for amino acid residues between the wild-types and mutant models of ERG protein docked with the selected compounds during a simulation period of 50 ns.

Å, respectively (Figure 4.51c). In addition, the RMSF plot revealed significant fluctuations in the protein residues at positions 134-159, 161-175, 178-186, and 259-261. The residue with the greatest variations was VAL (16.67 Å) at position 167. This was followed by PRO (15.84 Å) at position 166, GLY (15.77 Å) at position 168, and SER (14.52 Å) at position 169. Additionally, several other protein residues at positions 134-159, 161-165, 170-175, 178-186, and 259-261 also exhibited significant fluctuations, measuring more than 5.00 Å(Figure 4.51e).

The simulation results of the mutant model (P1129L) AFF3-Adapalene complex indicated that the protein exhibited fluctuations throughout the simulation, with the largest fluctuation of 10.06 Åoccurring at 16.40 ns. The simulation exhibited

stability from 31.45 ns until the end of the simulation time, however it was often characterised by instability (Figure 4.51b). Conversely, the ligand exhibited fluctuations ranging from 17.40 ns to the conclusion of the simulation, with a peak fluctuation of 27.00 Åoccurring at 31.70 ns. Throughout the simulation, it was noted that the system remained stable until the 17.35 ns mark. However, it was ultimately determined that the system was unstable overall. The RMSD values of the protein and the ligand at the end of the simulation were 7.69 Åand 26.54 Å, respectively. The minimum difference between the RMSD values occurred at 15.25 ns time (Figure 4.51d). Moreover, the protein-RMSF plot revealed that there were fluctuations in protein residues specifically at positions 132-174. The greatest fluctuation was recorded for the amino acid MET (10.93 Å) at position 157, followed by SER (9.97 Å) at position 147, ALA (9.78 Å) at position 146, and PRO (9.63 Å) at position 156. SER (9.62 Å) at position 158 and PRO (9.57 Å) at position 159 also showed significant fluctuations. Additionally, other protein residues at positions 132-145, 148-156, 158, and 160-174 exhibited fluctuations of more than 5 Å, respectively (Figure 4.51f).

The simulation findings of the wild-type AFF3-Ponatinib complex showed that the protein remained stable from 6.00 ns until just before 26.15 ns. The value varied between 26.15 ns and the conclusion of the simulation duration, and it was determined to be generally unstable (Figure 4.51a). Conversely, the ligand exhibited significant instability throughout the simulation, with fluctuations ranging from 16.55 ns until the conclusion of the simulation duration. The largest variation observed was 89.23 Å. The smallest discrepancy between RMSD values of the protein and the ligand occurred at 10.15 nanoseconds. At the end of the simulation, the RMSD values for the protein and the ligand were 11.27 Åand 35.94 Å, respectively (Figure 4.51c). Additionally, the RMSF plot revealed that the protein residues exhibited fluctuations at positions 134, 135, and 138-181. The largest variation was seen for PRO (15.12 Å) at position 156, followed by THR (14.88 Å) at position 153, GLY (14.64 Å) at location 152, and SER (14.58 Å) at position 147. Nevertheless, the protein residues located at positions 134, 135, 138-146, 148-151, 154, 155, and 158-181 exhibited substantial fluctuations, over 5.00 Å, as depicted in Figure 4.51e.

The simulation findings of the mutant model (P1129L) AFF3-Ponatinib complex demonstrated the protein's stability throughout the whole simulation, up to a time of 10.20 ns. The time measurements exhibited significant variations, ranging from 10.85 ns to 18.10 ns initially and from 47.60 ns until the completion of the simulation. The largest recorded fluctuation was 10.46 Åat 48.30 ns. Additionally, the protein was shown to be generally unstable (Figure 4.51b). Conversely, the ligand exhibited fluctuation from 15.90 nanoseconds to the conclusion of the simulation period. An oscillation of 15.49 Åwas seen at a time of 48.30 ns, indicating significant instability of the ligand. The protein and ligand RMSD values differed by a minimum of 27.45 ns. At the end of the simulation, the protein and ligand had RMSD values of 8.39 Åand 10.88 Å, respectively (Figure 4.51d). In addition, the protein-RMSF plot revealed significant fluctuations in protein residues at positions 140-159, 163-173, and 178-185. The residue with the highest fluctuation was GLN (11.01 Å) at position 170, followed by GLY (10.39 Å) at position 171, SER (9.84 Å) at position 150, GLY (9.69 Å) at position 148, GLY (9.62 Å) at position 152, and SER (9.06 Å) at position 169. The other protein residues at positions 140-147, 149, 151, 153-159, 163-168, 172, 173, and 178-185 showed considerable fluctuation, with RMSF values exceeding 5 Årespectively (Figure 4.51f).

The simulation findings of the wild-type AFF3-Glycyrrhizic acid complex demonstrated that the protein maintained stability from 22.90 ns to the conclusion of the experiment. The system was determined to be generally unstable and exhibited variations throughout the simulation until the 22.90 ns mark (Figure 4.51a). Conversely, the ligand exhibited fluctuations from the start of the simulation until 14.05 ns, but subsequently remained steady until the end of the experiment. The maximum variation observed was 10.82 Åat a time of 9.50 ns, although the general stability was confirmed. The protein and ligand RMSD values differed by a minimum of 3.95 ns. At the end of the simulation, the protein and ligand had RMSD values of 10.04 Åand 3.31 Å, respectively (Figure 4.51c). Furthermore, the protein-RMSF plot revealed significant fluctuations in protein residues at positions 139-173. The greatest variation was observed in the GLY residue (20.70 Å) at position 152, followed by SER (20.45 Å) at position 150, THR (19.75 Å) at position 151, and LYS (19.53 Å) at position 149 (Figure 4.51e).

The simulation findings of the mutant model (P1129L) AFF3-Glycyrrhizic acid complex showed that both the protein and the ligand were highly unstable overall, as depicted in Figure 4.51b. The RMSD values of the protein and the ligand at the conclusion of the simulation period were 7.84 Åand 6.25 Å, respectively (Figure 4.51d). The protein-RMSF plot revealed that the protein residues exhibited the highest degree of fluctuation at positions 131-174. The residue with the highest fluctuation was SER (11.97 Å) at position 147, followed by MET (11.93 Å) at position 157, PRO (11.63 Å) at position 156, SER (11.62 Å) at position 158, PRO (11.57 Å) at position 159, GLY (11.18 Å) at position 145, and GLN (11.04 Å) at position 170. In addition, there were additional protein residues that exhibited substantial variations, ranging from over 4 Åto 10.80 Å(Figure 4.51f).

The simulation findings of the wild-type AFF3-Pralsetinib complex indicated that the protein remained stable for a duration of 8.65 ns to 38.40 ns. The value varied during the simulation, starting from the beginning until 8.65 ns, and then from 38.40 ns to the end of the simulation. It was seen to be generally unstable (Figure 4.51a). Conversely, the ligand exhibited fluctuations throughout the simulation, starting from the beginning until 16.20 ns and then again from 35.90 ns to the end. It was determined to be consistently unstable. The protein and ligand exhibited a minimal difference at a time of 2.55 nanoseconds. At the end of the simulation, the protein had an RMSD value of 13.53 angstroms, while the ligand had an RMSD value of 23.48 angstroms (Figure 4.51c). Furthermore, the protein-RMSF plot revealed that the protein residues exhibited fluctuations at positions 131-137 and 140-186. The residue with the largest fluctuation was LYS (16.17 Å) at position 149, followed by GLY (16.07 Å) at position 148, THR (15.91 Å) at position 151, SER (15.46 Å) at position 150, and GLY (15.03 Å) at position 152 (Figure 4.51e).

The simulation results of the mutant model (P1129L) AFF3-Pralsetinib complex indicate that the protein remained stable during the whole simulation period, starting from 47.8 nanoseconds. The timing exhibited variations ranging from 15.95 ns to 45.25 ns and was determined to be generally unstable (Figure 4.51b). However, the ligand exhibited fluctuations ranging from 32.20 ns to the conclusion of the simulation duration. The biggest measured variation, measuring 12.16 Å,

occurred at 36.30 ns. The stability of the system was observed only between the time intervals of 15.40 ns and 18.55 ns, but it was generally unstable. The protein and ligand had a minimum difference in RMSD values at 6.35 ns. At the end of the simulation, the protein had an RMSD value of 7.67 Åand the ligand had an RMSD value of 10.00 Å(Figure 4.51d). In addition, the protein-RMSF plot revealed significant fluctuations in the protein residues at positions 62, 121-125, 128, 131-135, 137-175, 177-179, 181, 187-199, and 260-261. The residue with the highest fluctuation was PRO (14.65 Å) at position 156, followed by MET (14.16 Å) at position 157, SER (12.58 Å) at position 155, GLY (12.03 Å) at position 145, ALA (11.91 Å) at position 146, SER (11.66 Å) at position 147, PRO (11.32 Å) at position 154, and SER (11.28 Å) at position 158. The remaining protein residues at positions 62, 121-125, 128, 131-135, 137-144, 148-153, 159-175, 177-179, 181, 187-199, and 260-261 also exhibited significant fluctuations with RMSF values exceeding 5 Å, as shown in (Figure 4.51f).

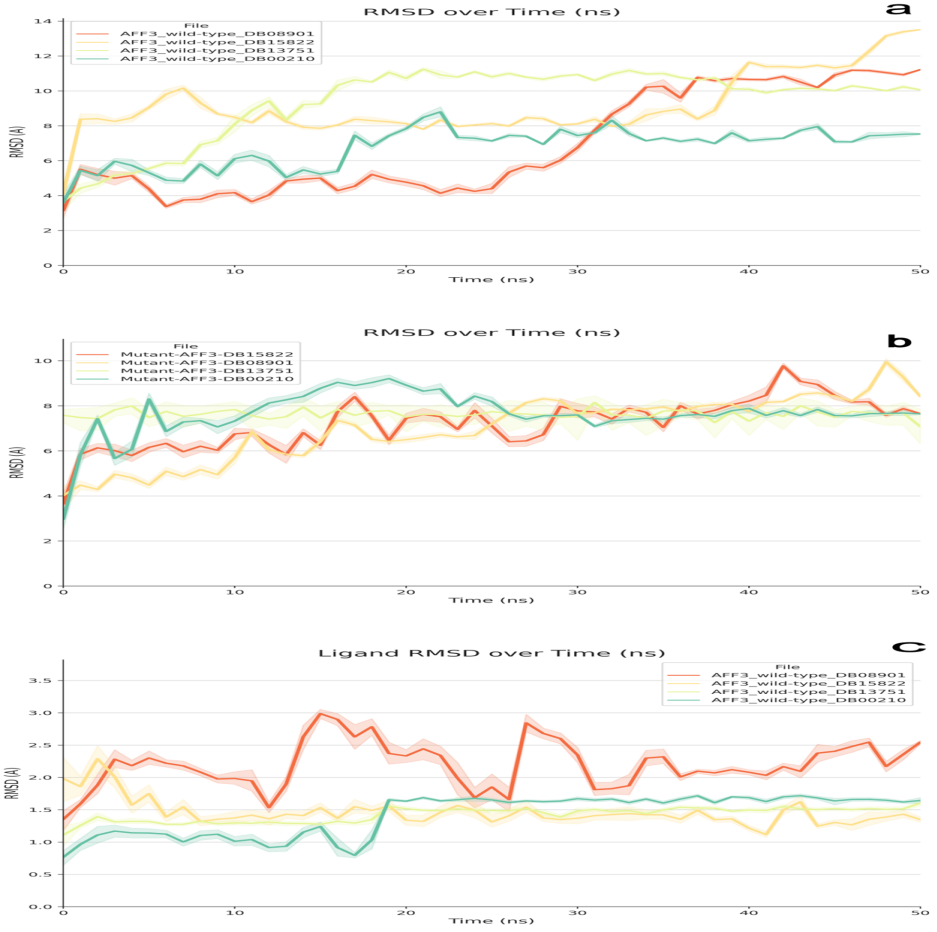

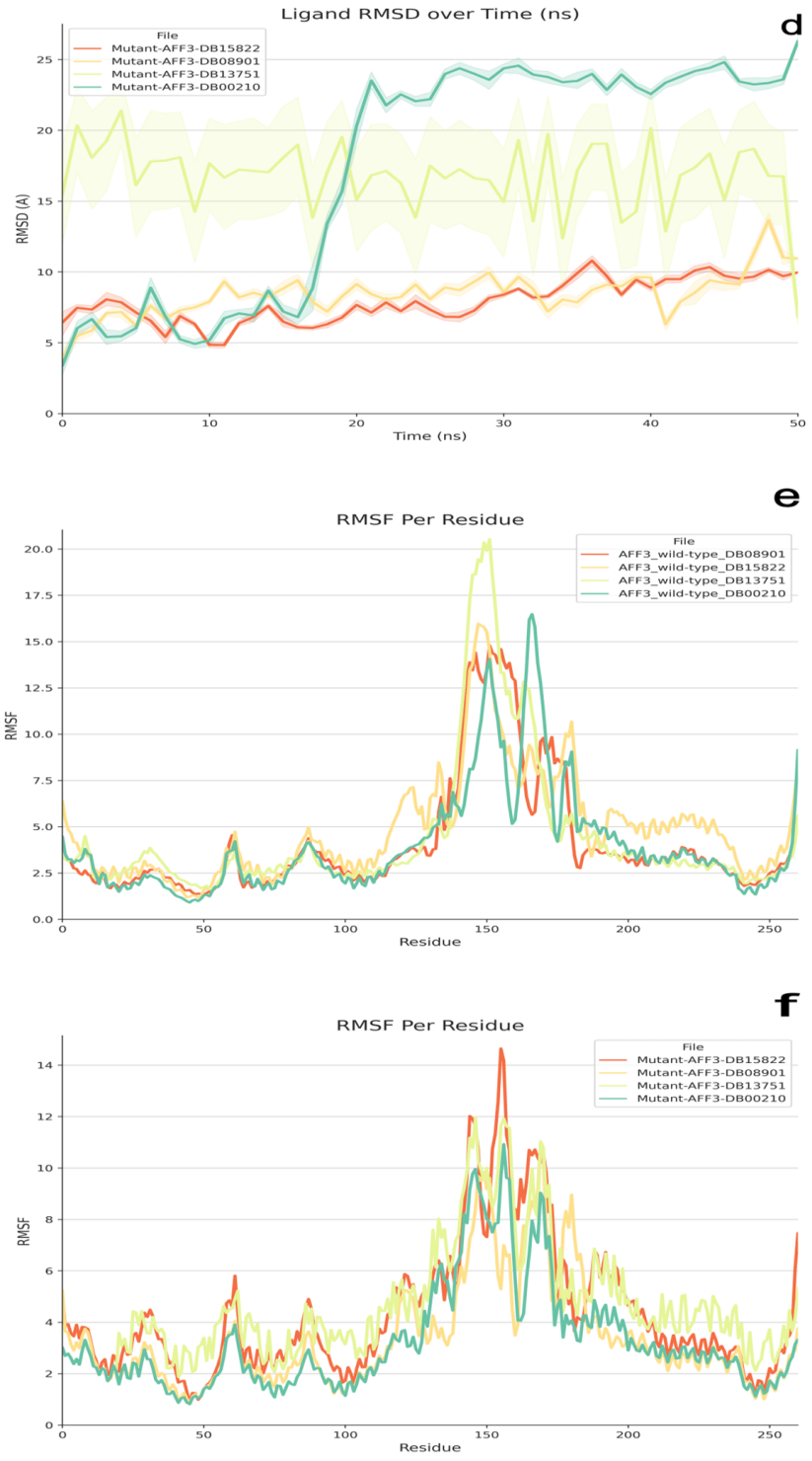

FIGURE 4.51: (a) RMSD graph of wild and (b) mutant ERG representing the conformational differences while docking with selected drug compounds. RMSD graph of ligands (drugs) while docking with wild (c) and mutant ERG (d). The simulations were performed for a period of 50 ns. RMSF graph representing the structural fluctuations observed for amino acid residues between the wild-types (e) and mutant models of ERG (f) protein docked with the selected compounds during a simulation period of 50 ns.

4.17.21 MD Simulation of FAT1 Domains with Selected Drug Compounds

The simulation analysis of the wild-type (D2382A) FAT1-Adapalene complex revealed slight instability in both the protein and the ligand. The RMSD values for complex at the conclusion of the simulation were 3.77 Åand 19.07 Å, respectively (Figure 4.52 a, b). The protein-RMSF figure revealed that only a small number of protein residues exhibited substantial fluctuations. The residue with the greatest fluctuation was PRO (7.27 Å) at position 105 (Figure 4.53). The simulation of the wild-type (D2382A) FAT1-Ponatinib complex revealed that the protein exhibited overall stability with a few minor variations, whereas the ligand displayed modest instability. The RMSD values for complex at the conclusion of the simulation were 3.31 Åand 7.96 Å, respectively, as shown in Figure 4.52 a, b. The protein-RMSF plot indicated that the fluctuation of protein residues was minimal, with the largest fluctuating residue being ASP at position 102, measuring 3.42 Å(Figure 4.53). The simulation outcome of the wild-type (D2382A) FAT1-Glycyrrhizic acid complex indicated that the protein exhibited a little degree of instability, while the ligand displayed a significant level of instability. The RMSD values of the complex at the conclusion of the simulation period were 3.82 Åand 44.37 Å, respectively. These results are depicted in Figure 4.52 a and b. The protein-RMSF figure revealed that only a limited number of protein residues exhibited substantial fluctuations. The residue with the greatest fluctuation was methionine (MET) with a value of 2.89 Åat position 84 (Figure 4.53).

The simulation outcome of the wild-type (DB2382A) FAT1-Pralsetinib complex indicated that the protein exhibited a little degree of instability, whereas the ligand displayed a significant level of instability. At the conclusion of the simulation time, the protein had an RMSD value of 3.29 Åand the ligand had an RMSD value of 12.20 Å(Figure 4.52 a, b). The protein-RMSF plot indicated that only a small number of protein residues exhibited substantial fluctuations. The residue with the greatest variation was serine (SER) with a fluctuation of 3.62 Åat position 29, as seen in Figure 4.53.

The simulation of the wild-type (M7391) FAT1-Adapalene complex revealed that complex exhibit a degree of instability. The RMSD values for the complex at the conclusion of the simulation were 5.28 Åand 3.02 Å, respectively (Figure 4.52 a, b). Analysis of the protein-RMSF revealed that only a small number of protein residues exhibited substantial fluctuations. The residue with the greatest variation was aspartic acid (ASP) with a fluctuation of 5.64 Å, located at position 95 (Figure 4.53).

The modelling of the wild-type (M7391) FAT1-Ponatinib complex revealed that the protein exhibited a minor degree of instability, whereas the ligand shown a high level of instability. As shown in Figure 4.51 a, b, the complex had respective RMSD values of 4.39Åand 24.52 Åat the conclusion of the simulation period. The protein-RMSF analysis revealed that only a small number of protein residues exhibited substantial fluctuations. The residue with the greatest fluctuation was glycine (GLY) with a value of 5.72 Åat position 25 (Figure 4.53). The simulation of the wild-type (M7391) FAT1-Glycyrrhizic acid complex revealed marginal instability. The RMSD values for the complex at the conclusion of the simulation period were 5.28 Åand 9.33 Å, respectively (Figure 4.51 a, b). The protein-RMSF analysis revealed that only a small number of protein residues exhibited substantial fluctuations. The residue with the greatest fluctuation was PRO (10.22 Å) at position 98 (Figure 4.53). The simulation of the wild-type (M7391) FAT1-Pralsetinib complex revealed the instability. As shown in Figure 4.51 a, b, the comlex had respective RMSD values of 4.54 Åand 5.71 Åat the conclusion of the simulation period. The protein-RMSF analysis revealed that only a small number of protein residues exhibited substantial fluctuations. The residue with the greatest fluctuation was aspartic acid (ASP) with a magnitude of 4.2 Å, located at position 95 (Figure 4.53).

The modelling of the wild-type (P4309S) FAT1-Adapalene complex demonstrated the instability of both the protein and the ligand. At the conclusion of the simulation, the ligand and protein had respective RMSD values of 10.01 Åand 8.26nÅ(Figure 4.51 a, b). The protein-RMSF analysis revealed little fluctuations in the protein residues. The residue with the greatest variation was Isoleucine

(10.80 Å) at position 1 (Figure 4.53). The simulation of the wild-type (P4309S) FAT1-Ponatinib complex revealed the instability of both the protein and the ligand. At the conclusion of the simulation period, the ligand's and the protein's RMSD values were 5.07 Åand 7.33 Å, respectively (Figure 4.51 a, b). The protein-RMSF analysis revealed that only a small number of protein residues exhibited substantial fluctuations. The residue with the largest fluctuation was GLN, with a value of 18.61Å, located at position 306 (Figure 4.53). The simulation of the wild-type (P4309S) FAT1-Glycyrrhizic acid complex revealed a modest instability in both the protein and ligand. The RMSD of the protein and the ligand at the conclusion of the simulation period were 6.97 Åand 4.78 Å, respectively (Figure 4.51 a, b). The protein-RMSF analysis revealed that only a small number of protein residues exhibited substantial fluctuations. The residue with the greatest fluctuation was PRO (6.94 Å) at position 40 (Figure 4.53). The simulation of the wild-type (P4309S) FAT1-Pralsetinib complex revealed the instability of both the protein and the ligand. The RMSD of the protein and the ligand at the conclusion of the simulation period were 6.47 Åand 4.05 Å, respectively (Figure 4.51 a, b). The protein-RMSF analysis revealed that only a small number of protein residues exhibited substantial fluctuations. The residue with the greatest fluctuation was GLU (7.46 Å) at position 3 (Figure 4.53).

Similarly, the simulation results of the mutant model (D2382A) FAT1-Adapalene complex indicated that the protein exhibited modest overall instability, whereas the ligand demonstrated significant overall instability. The RMSD values for the protein and the ligand at the conclusion of the simulation period were 5.82 Åand 46.40 Å, respectively (Figure 4.54 a, b). The protein-RMSF plot revealed that the protein residue, PRO (11.13 Å), had the greatest degree of fluctuation at position 105 (Figure 4.55). The simulation results of the mutant model (D2382A) FAT1-Ponatinib complex revealed that the protein exhibited overall instability, whereas the ligand had significant overall instability. As shown in Figure 4.54 a, b, the protein and ligand had respective RMSD values of 4.82 Åand 45.37 Åat the conclusion of the simulation period. The protein-RMSF plot revealed that the protein residue, PRO (12.13 Å) at position 105, had the greatest degree of fluctuation among all protein residues (Figure 4.55). The simulation results of the

mutant model (D2382A) FAT1-Glycyrrhizic acid complex indicated that the protein exhibited a modest overall instability, but the ligand displayed a high overall instability. As shown in Figure 4.54 a, b, the protein and ligand had respective RMSD values of 3.82 Åand 44.40 Åat the conclusion of the simulation. The protein-RMSF plot indicated that the protein residues exhibited little fluctuations, with the exception of residue PRO (12.13 Å) at position 105, which displayed the highest level of fluctuation (Figure 4.55). The simulation results of the mutant model (D2382A) FAT1-Pralsetinib complex revealed that the protein exhibited a minor overall instability, but the ligand displayed a high overall instability. At the conclusion of the simulation, the protein's and the ligand's RMSD values were 5.83 Åand 44.37 Å, respectively (Figure 4.54 a, b). The protein-RMSF plot revealed that the PRO (11.13 Å) residue of the protein exhibited large fluctuations at position 105 (Figure 4.55).

The simulation results of the mutant model (M739I) FAT1-Adapalene complex revealed that the protein exhibited a minor overall instability, but the ligand shown a high overall instability. The RMSD values of the protein and the ligand at the conclusion of the simulation period were 4.82 Åand 45.37 Å, respectively (Figure 4.54 a, b). The protein-RMSF plot indicated that there was no substantial fluctuation in the protein residues. However, the residue with the largest fluctuation was PRO (12.13 Å) at position 105 (Figure 4.55). The simulation results of the mutant model (M739I) FAT1-Ponatinib complex revealed that the protein exhibited overall instability, while the ligand shown significant overall instability. As shown in Figure 4.54 a, b, the protein and ligand had respective RMSD values of 5.82 Åand 43.37 Åat the conclusion of the simulation period. The protein-RMSF plot revealed that the residue PRO (12.13 Å) had the greatest fluctuation at position 105 (Figure 4.55). The simulation results of the mutant model (M739I) FAT1-Glycyrrhizic acid complex revealed that the protein exhibited a modest overall instability, whereas the ligand shown a high overall instability. At the conclusion of the simulation period, the protein's and the ligand's RMSD values were 2.82 Åand 45.37 Å, respectively (Figure 4.54 a, b). The protein-RMSF plot indicated that the protein residue, PRO (12.13 Å), had the greatest degree of fluctuation at position 105 (Figure 4.55). The simulation results of the mutant model (M739I)

FAT1-Pralsetinib complex revealed that the protein exhibited a minor overall instability, but the ligand shown a high overall instability. At the conclusion of the simulation period, the protein's and the ligand's RMSD values were 3.82 Åand 45.37 Å, respectively (Figure 4.54 a, b). The protein-RMSF plot indicated that the protein residue, PRO (11.13 Å) at position 105 exhibited the greatest variability (Figure 4.55).

The simulation results of the mutant model (P4309S) FAT1-Adapalene complex indicated that the protein exhibited a small degree of instability, whereas the ligand shown a high level of instability. As shown in Figure 4.54 a, b, the protein and ligand had respective RMSD values of 4.82 Åand 44.37 Åat the conclusion of the simulation period. The protein-RMSF plot revealed that the protein residues exhibited minimal fluctuations, except for PRO (12.13 Å) at position 105, which displayed the highest degree of variability (Figure 4.55). The simulation results of the mutant model (P4309S) FAT1-Ponatinib complex revealed that the protein exhibited overall instability, whereas the ligand shown overall high instability. As shown in Figure 4.54 a, b, the protein and ligand had respective RMSD values of 5.82 Åand 44.37 Åat the conclusion of the simulation period. The protein-RMSF plot revealed that the protein residues exhibited minimal changes, with the PRO residue (11.13 Å) at position 105 showing the largest variability (Figure 4.55). The simulation results of the mutant model (P4309S) FAT1-Glycyrrhizic acid complex indicated that the protein exhibited overall instability, whereas the ligand shown overall high instability. The RMSD values of the protein and the ligand at the conclusion of the simulation period were 3.82 Åand 43.37 Å, respectively (Figure 4.54 a, b). The RMSF plot revealed that the protein residues exhibited minimal fluctuations, with the most significant fluctuation observed in PRO (11.13 Å) at position 105 (Figure 4.55). The simulation results of the mutant model (P4309S) FAT1-Pralsetinib complex revealed that the protein exhibited a modest overall instability, but the ligand shown a high overall instability. As the simulation came to a finish, the protein's and the ligand's RMSD values were 3.82 Åand 44.37 Å, respectively (Figure 4.54 a, b). The protein-RMSF plot revealed that the protein residues exhibited minor fluctuations, with the most significant fluctuation observed in PRO (11.13 Å) at position 105 (Figure 4.55).

FIGURE 4.52: (a) RMSD graph of wild-type FAT1 domains representing the conformational differences while docking with selected drug compounds. (b) RMSD graph of ligands (drugs) representing the conformational differences while docking with wild-types FAT1 domains. Protein-ligand docked complex simulations were performed for period of 50 ns.

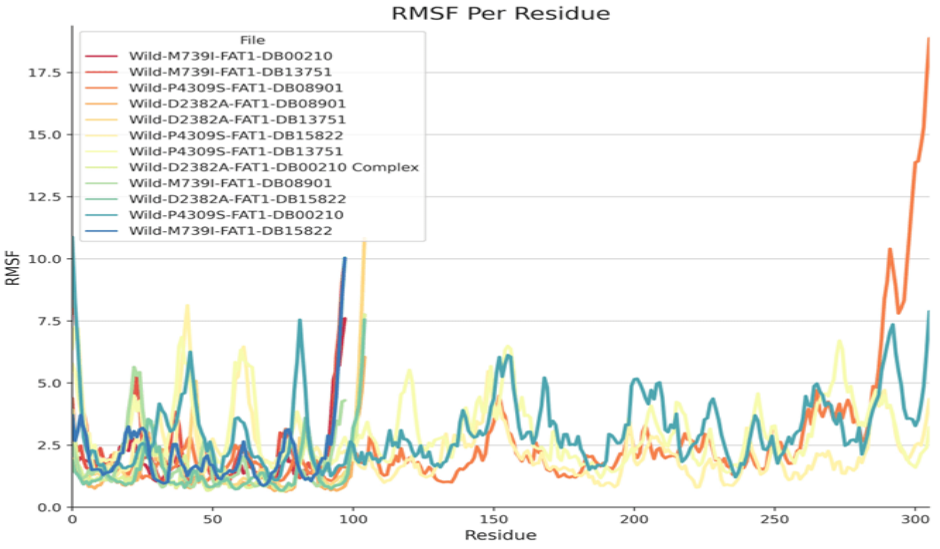

FIGURE 4.53: RMSF graph representing the structural fluctuations observed for amino acid residues between the wild-types FAT1 domains while docked with the selected compounds during a simulation period of 50 ns.

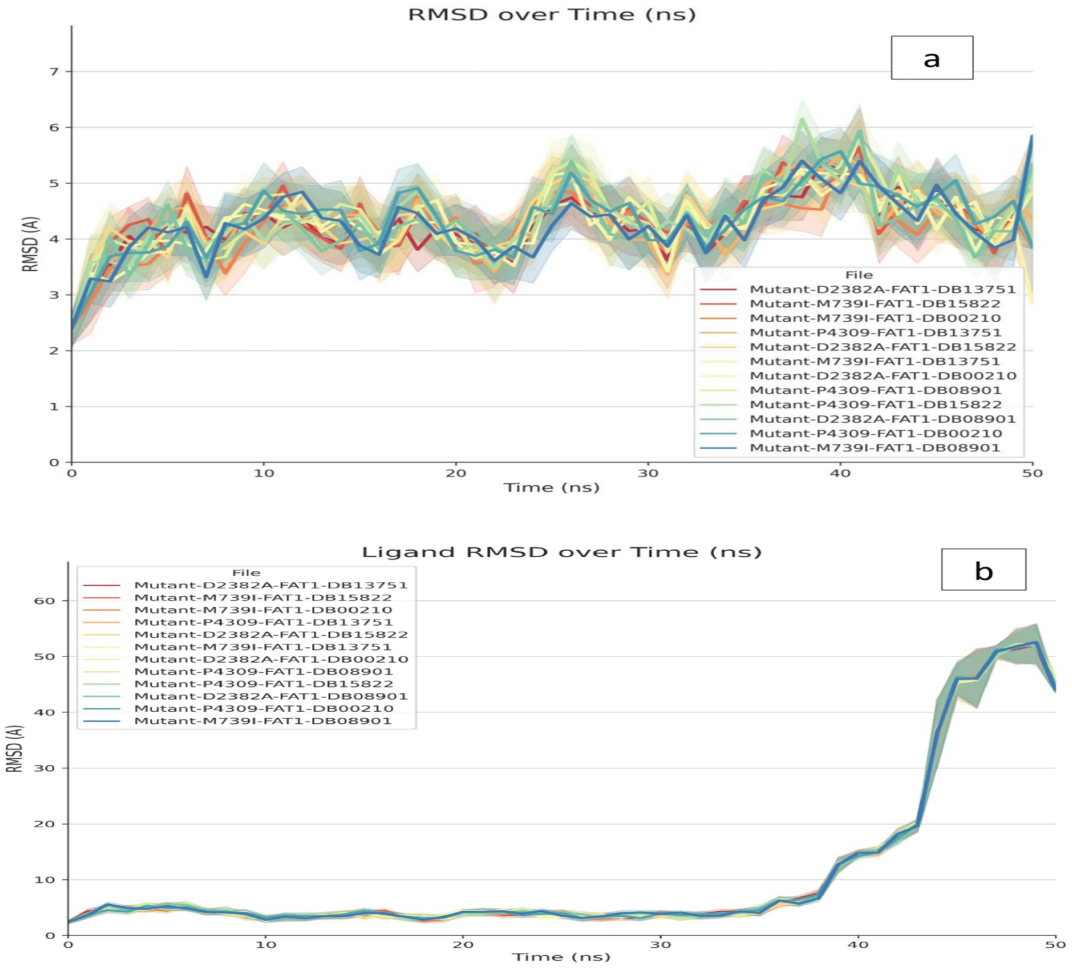

FIGURE 4.54: (a) RMSD graph of mutant FAT1 domains representing the conformational differences while docking with selected drug compounds. (b) RMSD graph of ligands (drugs) representing the conformational differences while docking with mutant FAT1 domains. Protein-ligand docked complex simulations were performed for period of 50 ns.

4.17.22 MD Simulation of KRAS with Selected Drug Compounds

The simulation findings of the wild-type KRAS-Adapalene complex showed that the protein remained stable from 33.90 ns until the completion of the simulation. However, it exhibited fluctuations from the start of the simulation until 18.60 ns, indicating overall slight instability (Figure 4.56 a). Conversely, the ligand exhibited fluctuations between 4.30 ns and 19.70 ns, as well as between 34.20 ns and the conclusion of the simulation. The overall stability of the system was shown to be inadequate, with the smallest difference between the protein and ligand RMSD

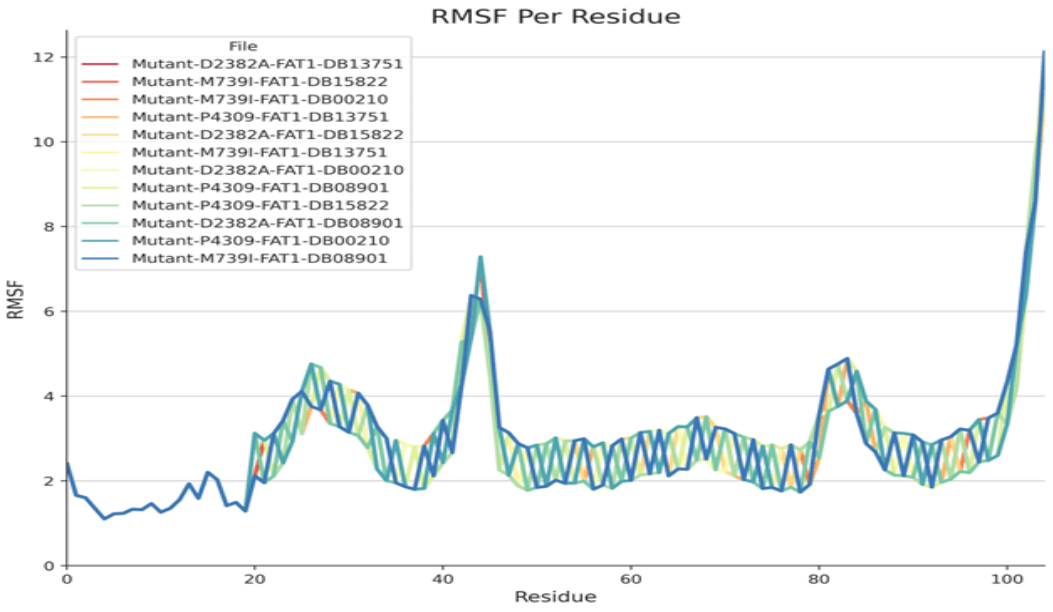

FIGURE 4.55: RMSF graph representing the structural fluctuations observed for amino acid residues between the mutant FAT1 domains while docked with the selected compounds during a simulation period of 50 ns.

values occurring at a time of 0.80 ns. The RMSD values of the protein and the ligand at the conclusion of the simulation were 4.14 Åand 8.02 Å, respectively, as shown in Figure 4.57a. In addition, the protein-RMSF plot revealed that the protein residues exhibited fluctuations at positions 179-183. The greatest variation was seen in the LYS residue (8.47 Å) at position 183, followed by the ILE residue (7.69 Å) at position 182, the LYS residue (7.61 Å) at position 181, the VAL residue (7.03 Å) at position 180, and the CYS residue (5.02 Å) at position 179 (Figure 4.58 a). The simulation findings of the wild-type KRAS-Ponatinib combination demonstrated that the protein remained stable from 11.15 ns to 16.80 ns, with fluctuations occurring only during the first phase of the simulation up to 11.15 ns (Figure 4.56 a). It was shown to exhibit small overall fluctuations. During the simulation, the ligand exhibited fluctuations, reaching a maximum fluctuation of 12.74 Åat 25.50 ns, and these fluctuations continued until 31.95 ns. The RMSD values of the protein and the ligand differed by a minimum of 0.05 ns. At the end of the simulation, the RMSD values for the protein and the ligand were 3.95 Åand 10.54 Å, respectively (Figure 4.57 a). In addition, the protein-RMSF plot revealed that the protein residues exhibited fluctuations at positions 176-180 and 182-183. The greatest variation in distance was observed for GLY (7.29 Å) at position 178,

CYS (6.74 Å) at position 179, PRO (6.32 Å) at position 177, LYS (6.02 Å) at position 183, VAL (5.81 Å) at position 180, and ILE (5.62 Å) at position 182 (Figure 4.58 a).

The simulation findings of the wild-type KRAS-Glycyrrhizic acid complex demonstrated that the protein exhibited stability from 3.15 ns to just before 10.50 ns, followed by fluctuations from 10.50 ns to 27.40 ns. Overall, the protein was seen to be relatively unstable (Figure 4.56 a). Conversely, the ligand exhibited fluctuations ranging from 45.50 ns to the end of the simulation period. The biggest reported fluctuation, measuring 10.47 Å, occurred at 49.95 ns. Overall, the ligand was observed to be unstable. The smallest disparity between the RMSD measurements of the protein and the ligand occurred at the time intervals of 19.70 ns and 20.25 ns. At the conclusion of the simulation, the RMSD values for the protein and the ligand were 4.59 Åand 10.17 Å, respectively (Figure 4.57 a). Nevertheless, the protein-RMSF plot revealed that the protein residues exhibited fluctuations specifically at positions 175-183. The largest variation in distance was observed for the amino acid LYS (14.54 Å) at position 183, followed by ILE (13.98 Å) at position 182, VAL (11.86 Å) at position 180, LYS (11.69 Å) at position 181, CYS (11.37 Å) at position 179, GLY (9.48 Å) at position 178, PRO (8.20 Å) at position 177, THR (7.13 Å) at position 176, and LYS (5.23 Å) at position 175 (Figure 4.58 a). The simulation findings of the wild-type KRAS-Pralsetinib complex demonstrated that the protein maintained stability from 46.60 ns to the end of the simulation. However, between 19.45 ns and 46.60 ns, the protein exhibited fluctuations and overall displayed a relatively low level of stability (Figure 4.56 a). The ligand exhibited a range of fluctuations in time, varying from 25.90 ns to 43.25 ns. The greatest measured fluctuation was 73.45 Åat 28.85 ns. The overall stability of the system was found to be compromised, with the smallest difference between the protein and ligand RMSD values reported at a time of 0.40 ns. The RMSD values of the protein and the ligand at the conclusion of the simulation period were 2.81 Åand 18.98 Å, respectively (Figure 4.57 a). In addition, the protein-RMSF plot revealed notable fluctuations in protein residues at positions 173, as well as 175-183. The residues with the highest fluctuations were LYS and ILE, measuring 13.10 Å, at positions 183 and 182, respectively. This was followed

by LYS at position 181, measuring 12.49 Å, VAL at position 180, measuring 11.87 Å, CYS at position 179, measuring 11.80 Å, GLY at position 178, measuring 9.92 Å, PRO at position 177, measuring 8.83 Å, THR at position 176, measuring 7.23 Å, LYS at position 175, measuring 6.32 Å, and GLU at position 173, measuring 5.22 Å(Figure 4.58 a).

The simulation results of the mutant model (G12V) KRAS-Adapalene complex indicated that the protein exhibited overall instability, while the ligand shown little instability. At the conclusion of the simulation, the RMSD values for the protein and the ligand were 6.09 Åand 3.83 Å, respectively (Figure 4.56 a, Figure 4.57 a). The protein-RMSF plot indicated that the protein residue, LYS, exhibited the greatest fluctuation (14.04 Å) at position 183 (Figure 4.58 a). The simulation results of the KRAS-Ponatinib combination with the mutant model (G12V) demonstrated that the protein exhibited slight overall instability, while the ligand showed considerable instability. The RMSD values of the protein and the ligand at the conclusion of the simulation period were 4.50 Åand 15.83 Å, respectively (Figure 4.56 a, Figure 4.57 a). In the protein-RMSF plot, it was observed that the residue LYS exhibited the largest level of fluctuation (10.18Å) at position 183 (Figure 4.58a). The simulation results of the mutant model (G12V) KRAS-Glycyrrhizic acid complex indicated that both the protein and the ligand exhibited a degree of instability. The RMSD values of the protein and the ligand at the conclusion of the simulation period were 4.40 Åand 7.92 Å, respectively (Figure 4.56 a, Figure 4.57 a). In addition, the protein-RMSF plot revealed that the protein residue LYS had the highest level of fluctuation, measuring 10.09 Å, at position 183 (Figure 4.58 a).

The simulation results of the mutant model (G12V) KRAS-Pralsetinib complex revealed that the protein exhibited fluctuations and overall had a slight degree of instability, whereas the ligand was shown to be unstable. The RMSD values of the protein and the ligand at the conclusion of the simulation period were 4.09 Åand 11.79 Å, respectively (as shown in Figure 4.56 a and Figure 4.57 a). In addition, the plot of protein-RMSF revealed that there were fluctuations in multiple protein residues, with LYS exhibiting the largest degree of fluctuation (11.02 Å) at position 183 (Figure 4.58 a).

The simulation results of the mutant model (G13D) KRAS-Adapalene complex revealed that both the protein and the ligand exhibited overall instability, characterised by fluctuations. The RMSD values of the protein and the ligand at the conclusion of the simulation period were 4.47 Åand 2.73 Å, respectively, as shown in Figure 4.56 a and Figure 4.57 a. In addition, the plot of protein-RMSF revealed that the protein residue LYS had the highest level of fluctuation, measuring 11.27 Å, at position 183 (Figure 4.58 a). The simulation results of the mutant model (G13D) KRAS-Ponatinib complex revealed that both the protein and the ligand exhibited instability due to fluctuations. The RMSD values of the protein and the ligand at the conclusion of the simulation period were 4.92 Åand 12.00 Å, respectively, as shown in Figure 4.56a and Figure 4.57a. In addition, the protein-RMSF plot revealed that the protein residue LYS exhibited the highest degree of variations, measuring 11.39 Å, at position 183 (Figure 4.58 a). The simulation results of the mutant model (G13D) KRAS-Glycyrrhizic acid complex revealed that the protein exhibited slight instability, while the ligand also displayed instability. The RMSD values of the protein and the ligand at the conclusion of the simulation period were 4.40 Åand 9.41 Å, respectively (Figure 4.56 a, Figure 4.57 a). on addition, the protein residue LYS exhibited the highest level of variation, measuring 7.73 Å, at position 183 on the protein-RMSF plot (Figure 4.58 a). The simulation results of the mutant model (G13D) KRAS-Pralsetinib combination revealed that the protein exhibited slight instability, whereas the ligand displayed substantial instability. The RMSD values of the protein and the ligand at the conclusion of the simulation period were 3.51 Åand 20.34 Å, respectively (Figure 4.56 a, Figure 4.57 a). The protein-RMSF plot indicated that the protein residue LYS exhibited the largest level of fluctuation (9.10 Å) at position 183 (Figure 4.58 a).

The simulation results of the mutant model (K117N) KRAS-Adapalene complex revealed that the protein exhibited a minor overall instability, whereas the ligand shown a high level of instability. The RMSD values of the protein and the ligand at the conclusion of the simulation period were 4.70 Åand 10.87 Å, respectively (Figure 4.56 a, Figure 4.57 a). The protein-RMSF figure revealed that only a limited number of protein residues exhibited substantial fluctuations. The largest

variation occurred in the amino acid LYS, with a magnitude of 12.89 Å, at position 183 (Figure 4.58 a). The simulation findings of the mutant model (K117N) KRAS-Ponatinib complex revealed that the protein exhibited a modest overall instability, while the ligand Exhibited significant instability in general. The RMSD values of the protein and the ligand at the conclusion of the simulation period were 3.35 Åand 11.90 Å, respectively (as shown in Figure 4.56 a and Figure 4.57 a). The protein-RMSF plot indicated that the majority of protein residues were rather stable during the simulation, with only a few exhibiting notable fluctuations. The residue with the greatest fluctuation was LYS (13.10 Å) at position 183 (Figure 4.58 a). The simulation findings of the KRAS-Glycyrrhizic acid mutant model (K117N) are presented.

The analysis revealed that the protein exhibited minimal fluctuations and was moderately unstable, but the ligand had significant fluctuations and was generally extremely unstable. The RMSD values of the protein and the ligand at the conclusion of the simulation period were 4.60 Åand 10.50 Å, respectively (Figure 4.56 a, Figure 4.57 a). The protein-RMSF plot revealed large fluctuations in various protein residues, with LYS (14.90 Å) at position 183 exhibiting the highest level of fluctuation.

The residue is variable, as seen in Figure 4.58a. The simulation results of the mutant model (K117N) KRAS-Pralsetinib combination revealed that the protein exhibited a minor overall instability, whereas the ligand displayed a high level of instability. The RMSD values of the protein and the ligand at the conclusion of the simulation period were 3.31Åand 9.81 Å, respectively (Figure 4.56 a, Figure 4.57 a). In addition, the protein-RMSF plot revealed that only a small number of protein residues exhibited substantial fluctuations. The residue with the greatest variation was LYS (13.90 Å) at position 183 (Figure 4.58 a).

The simulation results of the mutant model (Q61E) KRAS-Adapalene complex revealed that the protein exhibited overall instability, whereas the ligand displayed significant instability. The RMSD values of the protein and the ligand at the conclusion of the simulation period were 6.6 Åand 1.3 Å, respectively (Figure 4.56 b, Figure 4.57 b). The RMSF plot of the protein indicated minimal fluctuations in the protein residues. The residue with the greatest fluctuation was LYS (8.73

Å) at position 183 (Figure 4.58 b). The simulation results of the mutant model (Q61E) KRAS-Ponatinib combination revealed that the protein exhibited overall instability, whereas the ligand displayed high instability. The RMSD values for the protein and the ligand at the conclusion of the simulation were 3.6 Åand 6.0 Å, respectively (Figure 4.56 b, Figure 4.57 b). The protein-RMSF figure revealed that only a small number of protein residues exhibited substantial fluctuations. The protein residue with the greatest variation was LYS (9.73 Å) at position 183 (Figure 4.58 b). The simulation results of the mutant model (Q61E) KRAS Glycyrrhizic acid complex indicated that the protein exhibited a small degree of instability, whereas the ligand displayed a significant level of instability. The root mean square deviation (RSMD) values of the protein and the ligand at the conclusion of the simulation period were 6.6 Åand 10.85 Å, respectively, as shown in Figure 4.56 b and Figure 4.57 b. The protein-RMSF figure revealed that only a limited number of protein residues exhibited substantial fluctuations. The greatest variation occurred in the amino acid LYS, with a magnitude of 8.73 Å, at position 183 (Figure 4.58 b). The simulation results of the mutant model (Q61E) KRAS-Pralsetinib combination indicated a marginal degree of protein instability. Although the ligand exhibited significant instability. The RMSD values for the protein and the ligand at the conclusion of the simulation were 4.6 Åand 11.85 Å, respectively (Figure 4.56 b, Figure 4.57 b). The protein-RMSF plot revealed that the residue LYS (9.73 Å) at position 183 exhibited the highest level of fluctuation. However, in general, the protein residues did not demonstrate substantial fluctuations (Figure 4.58 b).

The simulation results of the mutant model (Q61H) KRAS-Adapalene complex indicated that the protein exhibited a minor overall instability, whereas the ligand shown a significant level of instability. The RMSD values for the protein and the ligand at the conclusion of the simulation were 4.6 Åand 10.8 Å, respectively (Figure 4.56 b, Figure 4.57 b). The protein-RMSF plot revealed that the protein residue LYS had the largest level of fluctuation, measuring 8.73 Å, at position 183 (Figure 4.58 b). The simulation results of the mutant model (Q61H) KRAS-Ponatinib complex indicated that the protein exhibited general instability,

whereas the ligand displayed significant instability. The RMSD values of the protein and the ligand at the conclusion of the simulation period were 3.60 Åand 6.0 Å, respectively, as shown in Figure 4.56 b and Figure 4.57 b. The protein-RMSF plot revealed little fluctuations in protein residues. The residue with the greatest fluctuation was LYS (8.73 Å) at position 183 (Figure 4.58 b). The simulation results of the mutant model (Q61H) KRAS-Glycyrrhizic acid complex revealed that the protein exhibited overall instability, while the ligand shown significant overall instability. The RMSD values of the protein and the ligand at the conclusion of the simulation period were 6.6 Åand 10.85 Å, respectively, as shown in Figure 4.56 b and Figure 4.57 b. The protein-RMSF figure indicated that the majority of protein residues exhibited minimal fluctuations, with only a few exceptions. The residue with the greatest fluctuation was LYS (8.73 Å) at position 183 (Figure 4.58 b). The simulation results of the mutant model (Q61H) KRAS-Pralsetinib complex indicated that the protein exhibited overall instability, whereas the ligand shown overall high instability. The RMSD values of the protein and the ligand at the conclusion of the simulation period were 6.6 Åand 9.85 Å, respectively, as shown in Figure 4.56 b and Figure 4.57 b. In the protein-RMSF plot, it was shown that the protein residue LYS had the largest fluctuation, measuring 9.73 Å, at position 183 (Figure 4.58 b).

The simulation results of the mutant model (Q61R) KRAS-Adapalene complex indicated that both the protein and the ligand exhibited significant instability. The RMSD values for the protein and the ligand at the conclusion of the simulation were 4.6 Åand 8.85 Å, respectively (as shown in Figure 4.56 b and Figure 4.57 b). The protein-RMSF figure revealed that only a limited number of protein residues exhibited substantial fluctuations. The residue with the greatest fluctuation was LYS (9.73 Å) at position 183 (Figure 4.58 billion. The simulation results of the mutant model (Q61R) KRAS-Ponatinib complex indicated that the protein exhibited a minor overall instability, but the ligand demonstrated a high overall instability. The RMSD values for the protein and the ligand at the conclusion of the simulation period were 3.6 Åand 6.0 Å, respectively (Figure 4.56 b, Figure 4.57 b). The protein-RMSF plot revealed that the residue LYS (9.73 Å) at position 183 exhibited the greatest fluctuation among all protein residues (Figure 4.58 b). The

simulation results of the mutant model (Q61R) KRAS-Glycyrrhizic acid complex indicated that the protein exhibited overall instability, whereas the ligand shown overall high instability. The RMSD values of the protein and the ligand at the conclusion of the simulation period were 6.6 Åand 8.85 Å, respectively (Figure 4.56 b, Figure 4.57 b). The protein-RMSF plot revealed significant changes in multiple protein residues, with LYS (9.73 Å) exhibiting the largest degree of oscillation at position 183 (Figure 4.58 b). The simulation results of the mutant model (Q61R) KRAS Pralsetinib complex revealed that the protein exhibited overall instability, whereas the ligand displayed overall high instability. The RMSD values for the protein and the ligand at the conclusion of the simulation were 3.6 Åand 6.0 Å, respectively, as shown in Figure 4.56 b and Figure 4.57 b. The protein-RMSF figure indicated that the majority of protein residues exhibited minimal fluctuations, with only a small number showing considerable variation. The residue with the greatest fluctuation was LYS (8.73 Å) at position 183 (Figure 4.58 b).

The simulation results of the mutant model (A59E) KRAS-Adapalene complex indicated that the protein exhibited a generally low level of stability, but the ligand demonstrated overall stability. The RMSD values of the protein and the ligand at the conclusion of the simulation period were 3.53 Åand 1.39 Å, respectively (as shown in Figure 4.56 c and Figure 4.57 c). Nevertheless, the protein-RMSF plot revealed significant fluctuations in multiple protein residues, with LYS (10.11 Å) exhibiting the highest degree of fluctuation.

The residue at position 183 is showing fluctuation, as depicted in Figure 4.58 c. The simulation results of the mutant model (A59E) KRAS-Ponatinib complex indicated that the protein exhibited a general state of little instability, whereas the ligand demonstrated an overall state of instability. The RMSD values of the protein and the ligand at the conclusion of the simulation were 4.10 Åand 6.75 Å, respectively, as shown in Figure 4.56 c and Figure 4.57 c. The protein-RMSF plot revealed significant fluctuations in only eight protein residues. The protein residue with the greatest fluctuation was LYS (11.23 Å) at position 183 (Figure 4.58 c).

The simulation results of the mutant model (A59E) KRAS-Glycyrrhizic acid complex indicated that both the protein and the ligand exhibited general instability, as evidenced by oscillations in their behaviour. The RMSD values of the protein

and the ligand at the conclusion of the simulation period were 4.20 Åand 6.91 Å, respectively, as shown in Figure 4.56 c and Figure 4.57 c. In addition, the protein-RMSF plot revealed significant fluctuations in various protein residues, with the largest fluctuation seen at position 183 for LYS, measuring 11.21 Å(Figure 4.58 c). The simulation results of the mutant model (A59E) KRAS-Pralsetinib complex revealed that both the protein and the ligand exhibited overall instability. The RMSD values of the protein and the ligand at the conclusion of the simulation period were 5.74 Åand 10.96 Å, respectively (Figure 4.56 c, Figure 4.57 c). Moreover, the protein-RMSF plot revealed significant fluctuations in multiple protein residues. The residue with the greatest fluctuation was LYS (12.97 Å) at the specified location. The value is 183, as shown in Figure 4.58 c.

The simulation results of the mutant model (G12D) KRAS-Adapalene complex revealed that the protein exhibited slight overall instability, whereas the ligand demonstrated considerable instability. The RMSD values of the protein and the ligand at the conclusion of the simulation period were 5.42 Åand 14.82 Å, respectively (Figure 4.56 c, Figure 4.57 c). The protein-RMSF plot revealed that the amino acid LYS had the greatest variation of 9.34 Åat position 183 (Figure 4.58 c). The simulation results of the mutant model (G12D) KRAS-Ponatinib complex revealed that the protein exhibited fluctuations and demonstrated a slight overall instability. Similarly, the ligand was observed to be generally unstable. The RMSD values of the protein and the ligand at the conclusion of the simulation period were 4.46 Åand 5.85 Å, respectively (as shown in Figure 4.56 c and Figure 4.57 c). The protein-RMSF plot revealed that the amino acid LYS had the largest level of fluctuation, measuring 11.75 Å, at position 183 (Figure 4.58 c). The simulation findings of the mutant model of the (G12D) KRAS-Glycyrrhizic acid complex revealed that both the protein and the ligand exhibited a degree of instability. The RMSD values of the protein and the ligand at the conclusion of the simulation period were 4.85 Åand 8.82 Å, respectively (Figure 4.56 c, Figure 4.57 c). The protein-RMSF plot revealed that the protein residue ILE had the largest level of fluctuation (7.55 Å) at position 182 (Figure 4.58 c). The simulation results of the mutant model (G12D) KRAS-Pralsetinib complex indicated that the protein exhibited slight overall fluctuations, and the ligand was also observed to

be unstable.

The RMSD values for the protein and the ligand at the conclusion of the simulation were 4.95 Åand 11.39 Å, respectively (Figure 4.56 c, Figure 4.57 c). In addition, the plot of protein-RMSF revealed that the protein residue ILE had the largest level of fluctuation, measuring 11.02 Å, at position 182 (Figure 4.58 c).

The simulation results of the mutant model (G12R) KRAS-Adapalene complex revealed that the protein exhibited slight fluctuations but remained stable overall, but the ligand displayed instability. The RMSD values of the protein and the ligand at the conclusion of the simulation period were 4.37 Åand 4.63 Å, respectively (Figure 4.56 c, Figure 4.57 c). In the protein-RMSF plot, it was seen that the residue LYS exhibited the largest level of fluctuation, measuring 9.05 Å, at position 183 (Figure 4.58 c). The simulation results of the mutant model (G12R) KRAS-Ponatinib complex revealed that both the protein and the ligand were unstable. The RMSD values for the protein and the ligand at the conclusion of the simulation were 4.92 Åand 5.57 Å, respectively (Figure 4.56 c, Figure 4.57 c). In addition, the plot of protein-RMSF revealed that the protein residue LYS had the largest level of fluctuation (8.53 Å) at position 183 (Figure 4.58 c). The simulation results of the mutant model (G12R) KRAS-Glycyrrhizic acid complex demonstrated that the protein exhibited an overall behaviour.

The system exhibited some instability, and the ligand itself was similarly unstable. The RMSD values for the protein and the ligand at the conclusion of the simulation were 3.77 Åand 9.21 Å, respectively (Figure 4.56 c, Figure 4.57 c). In addition, the protein-RMSF plot revealed that the protein residue GLY exhibited the largest level of fluctuation (7.46 Å) at position 178 (Figure 4.58 c). The simulation results of the mutant model (G12R) KRAS-Pralsetinib complex revealed that both the protein and the ligand exhibited a slight overall instability. The RMSD values of the protein and the ligand at the conclusion of the simulation period were 4.69 Åand 11.63 Å, respectively (Figure 4.56 c, Figure 4.57 c). The protein-RMSF plot revealed that the protein residue LYS had the largest level of fluctuation, measuring 11.65 Å, at position 183 (Figure 4.58 c).

The simulation results of the mutant model (G12V) KRAS-Adapalene complex

indicated that the protein exhibited overall instability, while the ligand demonstrated little instability. The RMSD values for the protein and the ligand at the conclusion of the simulation were 6.09 Åand 3.83 Å, respectively (Figure 4.56 c, Figure 4.57 c). The protein-RMSF plot revealed that the protein residue LYS had the greatest fluctuation (14.04 Å) at position 183 (Figure 4.58 c). The simulation results of the mutant model (G12V) KRAS-Ponatinib combination revealed that the protein exhibited slight overall instability, whereas the ligand demonstrated considerable instability. The RMSD values of the protein and the ligand at the conclusion of the simulation period were 4.50 Åand 15.83 Å, respectively (Figure 4.56 c, Figure 4.57 c). The protein-RMSF plot revealed that the protein residue, LYS, exhibited the greatest fluctuation (10.18Å) at position 183 (Figure 4.58 c). The simulation results of the mutant model (G12V) KRAS-Glycyrrhizic acid complex indicated that both the protein and the ligand exhibited a degree of instability. The RMSD values of the protein and the ligand at the conclusion of the simulation period were 4.40 Åand 7.92 Å, respectively (as shown in Figure 4.56 c and Figure 4.57 c). In addition, the protein-RMSF plot revealed that the protein residue LYS had the highest level of fluctuation, measuring 10.09 Å, at position 183 (Figure 4.58 c). The simulation results of the mutant model (G12V) KRAS-Pralsetinib complex revealed that the protein exhibited fluctuations and displayed a slight overall instability. Conversely, the ligand was determined to be unstable. The RMSD values for the protein and the ligand at the conclusion of the simulation were 4.09 Åand 11.79 Å, respectively (as depicted in Figure 4.56 c and Figure 4.57 c). In addition, the protein-RMSF plot revealed that there were fluctuations in multiple protein residues, with LYS exhibiting the greatest change (11.02 Å) at position 183 (Figure 4.58 c).

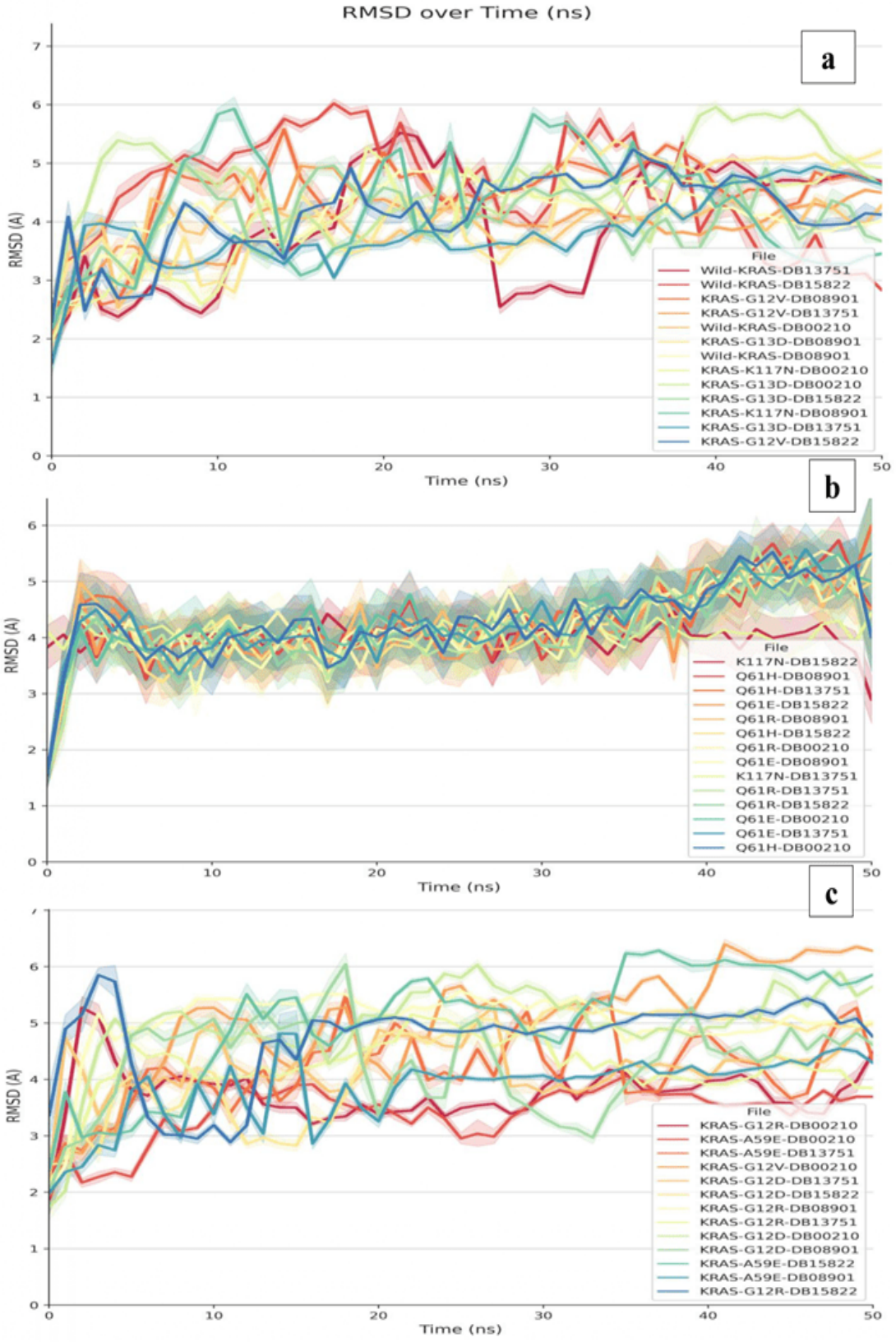

FIGURE 4.56: (a) RMSD graph of wild and KRAS mutant (G12V, G13D, K117N) (b) (Q61H, Q61R, Q61E) (c) (A59E, G12D, G12V, and G12R) representing the conformational differences while docking with selected drug compounds. The simulations were performed for a period of 50 ns

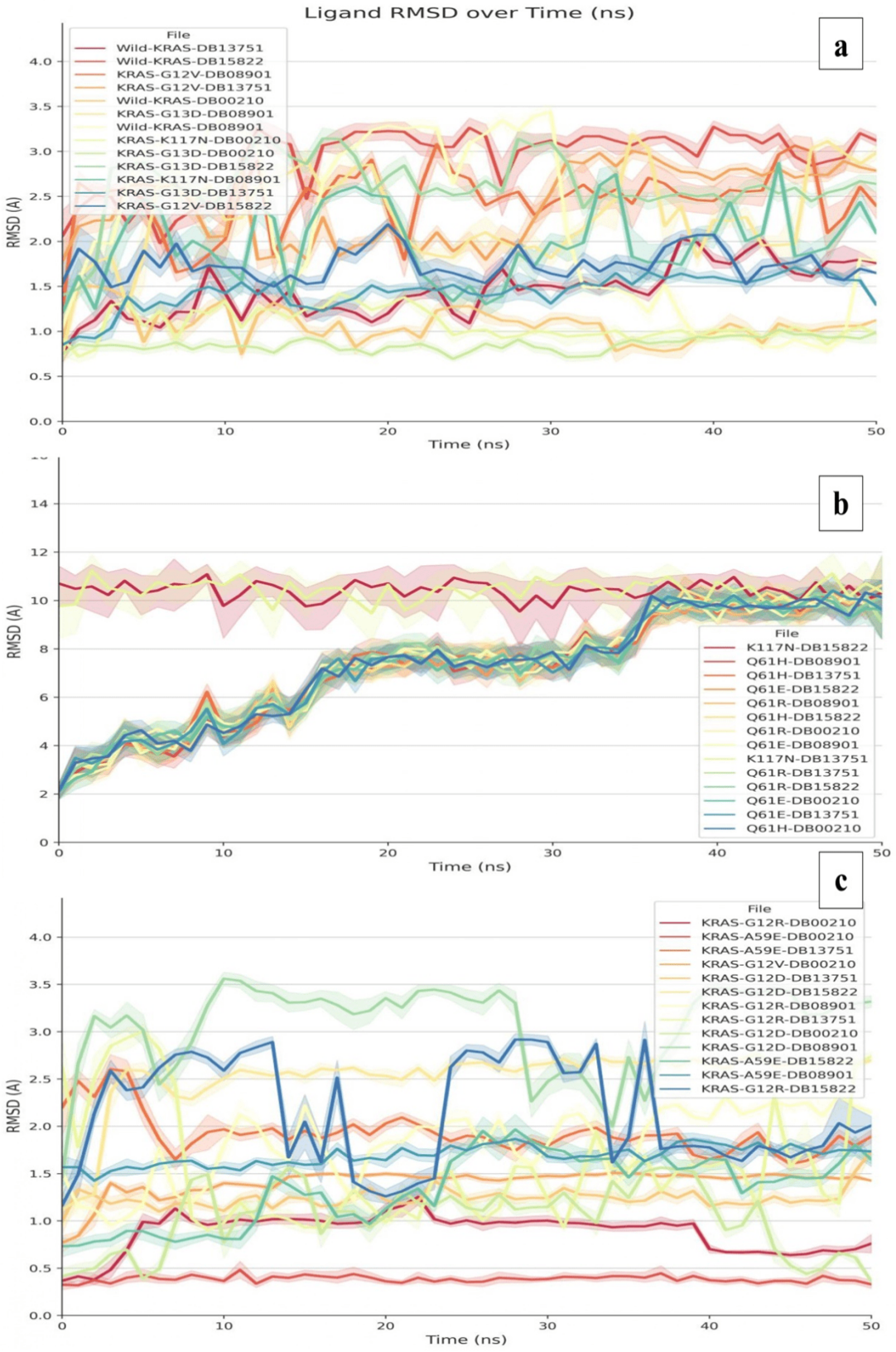

FIGURE 4.57: RMSD graph of ligands (drugs) while docking with (a) wild and KRAS mutant (G12V, G13D, K117N) (b) (Q61H, Q61R, Q61E) (c) (A59E, G12D, G12V, and G12R). The simulations were performed for a period of 50 ns.

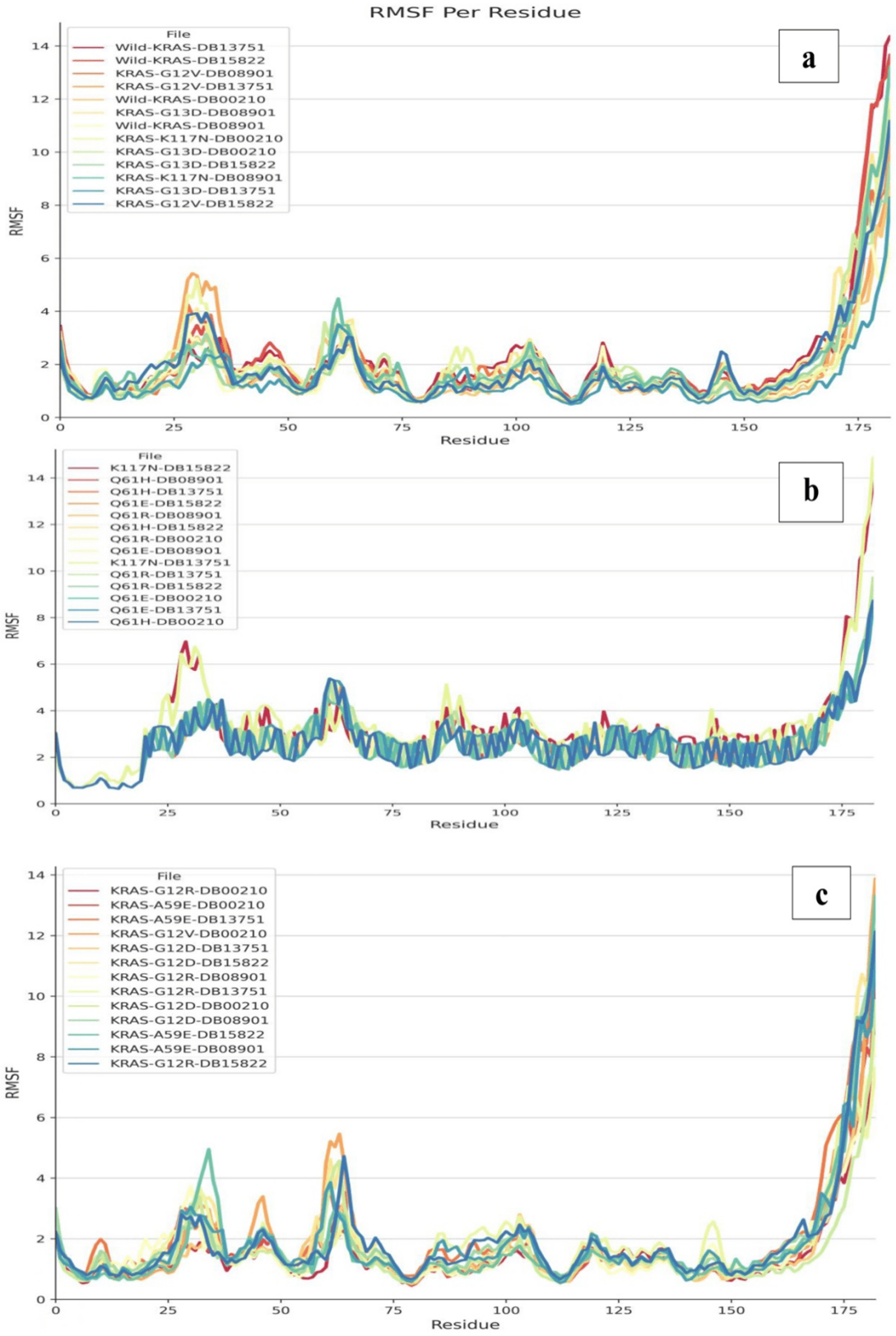

FIGURE 4.58: RMSF graph representing the structural fluctuations observed for amino acid residues between the (a) wild-types and KRAS mutant models (G12V, G13D, K117N) (b) (Q61H, Q61R, Q61E) (c) (A59E, G12D, G12V, and G12R docked with the selected drug compounds during a simulation period of 50 ns.

4.17.23 MD Simulation of KRAS with Selected Drug Compounds

In addition, the simulation results of the wild-type NRAS-Adapalene complex indicated that the protein exhibited overall instability, whereas the ligand shown overall high instability. The RMSD values of the protein and the ligand at the conclusion of the simulation period were 6.15 Åand 7.44 Å, respectively, as depicted in Figure 4.59 a and Figure 4.60 a. The protein-RMSF plot revealed that the residue ASN (8.95 Å) at position 172 exhibited the highest level of fluctuation among all protein residues (Figure 4.61 a). The simulation findings of the wild-type NRAS-Ponatinib complex suggested that the protein was generally slightly unstable, and the ligand also displayed instability. The RMSD values for the protein and the ligand at the conclusion of the simulation period were 3.15 Åand 5.45 Å, respectively (as shown in Figure 4.59 a and Figure 4.60 a). The protein-RMSF plot revealed that the residue ASN (7.95 Å) at position 172 exhibited the largest level of fluctuation (Figure 4.61 a). The simulation results of the wild-type NRAS-Glycyrrhizic acid complex suggested that both the protein and the ligand were generally unstable. The RMSD values of the protein and the ligand at the conclusion of the simulation period were 6.15 Åand 6.45 Å, respectively (Figure 4.59 a, Figure 4.60 a). The protein-RMSF plot indicated that the ASN protein residue saw the largest level of fluctuation at position 172, with a value of 7.95 Å(Figure 4.61 a). The simulation findings of the wild-type NRAS-Pralsetinib complex revealed that both the protein and the ligand exhibited overall instability. The RMSD values of the protein and the ligand at the conclusion of the simulation period were 6.15 Åand 8.45 Å, respectively (as shown in Figure 4.59 a and Figure 4.60 a). The protein-RMSF plot revealed that the protein residue ASN had the largest level of fluctuation, measuring 8.95 Å, at position 172 (Figure 4.61 a).

The simulation results of the mutant model (Y64D) NRAS-Adapalene complex indicated that both the protein and the ligand exhibited overall instability. The RMSD values of the protein and the ligand at the conclusion of the simulation period were 3.15 Åand 6.45 Å, respectively (Figure 4.59 a, Figure 4.60 a). The protein-RMSF plot indicated that the protein residue ASN (7.95 Å) exhibited the

greatest fluctuation among all protein residues at position 172 (Figure 4.61 a). The simulation results of the NRAS-Ponatinib complex with the Y64D mutant model revealed that both the protein and the ligand exhibited overall instability. The RMSD values of the protein and the ligand at the conclusion of the simulation period were 3.15 Åand 7.45 Å, respectively (as shown in Figure 4.59 a and Figure 4.60 a). The protein-RMSF plot revealed that the protein residue ASN, located at position 172, had the largest degree of fluctuation, measuring 7.95 Å(Figure 4.61 a). The simulation results of the NRAS-Glycyrrhizic acid complex with the Y64D mutant model indicated that both the protein and the ligand exhibited overall instability. The RMSD values for the protein and the ligand at the conclusion of the simulation period were 3.15 Åand 8.45 Å, respectively (Figure 4.59 a, Figure 4.60 a). The protein-RMSF plot revealed that the amino acid ASN (8.95 Å) at position 172 exhibited the highest level of fluctuation (Figure 4.61a). The simulation findings of the mutant model (Y64D) NRAS-Pralsetinib complex suggested that both the protein and the ligand were generally unstable. The RMSD values of the protein and the ligand at the conclusion of the simulation period were 3.15 Åand 6.45 Å, respectively (as shown in Figure 4.59 a and Figure 4.60 a). The protein-RMSF plot revealed that the protein residue ASN (8.95 Å) at position 172 exhibited the greatest degree of fluctuation (Figure 4.61 a).

The simulation results of the NRAS-Adapalene complex with the mutant model (Q61R) indicated that both the protein and the ligand exhibited overall instability. The RMSD values of the protein and the ligand at the conclusion of the simulation period were 6.15 Åand 6.45 Å, respectively (Figure 4.59 a, Figure 4.60 a). The protein-RMSF plot revealed that the protein residue ASN (8.95 Å) at position 172 exhibited the highest level of fluctuation (Figure 4.61a). The simulation results of the mutant model (Q61R) NRAS-Ponatinib complex indicated that both the protein and the ligand were generally unstable. The RMSD values of the protein and the ligand at the conclusion of the simulation period were 3.15 Åand 7.45 Å, respectively (Figure 4.59 a, Figure 4.60 a). The protein-RMSF plot indicated that the residue ASN at position 172 exhibited the largest level of fluctuation, measuring 8.95 Å(Figure 4.61 a).

The simulation results of the NRAS-Glycyrrhizic acid complex with the Q61R mutant model indicated that the protein exhibited a modest overall instability, while the ligand also displayed an overall instability. The RMSD values of the protein and the ligand at the conclusion of the simulation period were 5.15 Åand 5.45 Å, respectively (Figure 4.59 a, Figure 4.60 a). The protein-RMSF plot revealed that the protein residues exhibited minimal fluctuations, with the largest fluctuation observed in the residue ASN (7.95 Å) at position 172 (Figure 4.61 a). The simulation results of the NRAS-Pralsetinib complex using the mutant model (Q61R) revealed that both the protein and the ligand exhibited overall instability. The RMSD values of the protein and the ligand at the conclusion of the simulation period were 6.15 Åand 7.45 Å, respectively (Figure 4.59 a, Figure 4.60 a). The protein-RMSF plot revealed that only a few protein residues exhibited significant fluctuations, with the most variable residue being ASN (7.95 Å) at position 172 (Figure 4.61 a).

The simulation results of the NRAS-Adapalene complex with the mutant model (G13R) revealed that both the protein and the ligand exhibited overall instability. The RMSD values for the protein and the ligand at the conclusion of the simulation period were 4.15 Åand 6.45 Å, respectively (as shown in Figure 4.59 b and Figure 4.60 b). In the protein-RMSF plot, it was observed that the residue ASN had the maximum fluctuation at position 172, with a value of 7.95 Å(Figure 4.61 b). The simulation findings of the mutant model (G13R) NRAS-Ponatinib complex revealed that both the protein and the ligand were overall unstable. The RMSD values for the protein and the ligand at the conclusion of the simulation were 3.15 Åand 7.45 Å, respectively (Figure 4.59 b, Figure 4.60 b). The protein-RMSF plot indicated that the residue ASN (8.95 Å) at position 172 exhibited the highest level of fluctuation (Figure 4.61 b). The simulation results of the mutant model (G13R) NRAS-Glycyrrhizic acid complex revealed that both the protein and the ligand were generally unstable. The RMSD values of the protein and the ligand at the conclusion of the simulation period were 5.15 Åand 5.45 Å, respectively (Figure 4.59 b, Figure 4.60 b). The protein-RMSF plot indicated that the protein residue ASN (7.95 Å) exhibited the highest level of fluctuation at position 172 (Figure 4.61 b). The simulation results of the mutant model (G13R) NRAS-Pralsetinib

complex revealed that both the protein and the ligand were generally unstable. The RMSD values of the protein and the ligand at the conclusion of the simulation period were 6.15 Åand 7.45 Å, respectively (Figure 4.59 b, Figure 4.60 b). In the protein-RMSF plot, it was shown that the residue ASN had the largest fluctuation, measuring 8.95 Å, at position 172 (Figure 4.61 b).

The simulation results of the mutant model (Q61H) NRAS-Adapalene complex revealed that the protein exhibited overall instability, while the ligand shown significant instability. The RMSD values of the protein and the ligand at the conclusion of the simulation period were 6.15 Åand 6.45 Å, respectively (as shown in Figure 4.59 b and Figure 4.60 b). The protein-RMSF plot showed minimal fluctuations in the protein residues, with the highest fluctuation observed in the ASN residue (7.95 Å) at position 172 (Figure 4.61 b). The simulation results of the mutant model (Q61H) NRAS-Ponatinib complex revealed overall instability in both the protein and the ligand. The RMSD values for the protein and the ligand at the conclusion of the simulation were 6.15 Åand 7.45 Å, respectively (as shown in Figure 4.59 b and Figure 4.60 b). The protein-RMSF plot revealed that the residue ASN at position 172 had the largest fluctuation, measuring 8.95 Å(Figure 4.61 b). The simulation findings of the mutant model (Q61H) NRAS-Glycyrrhizic acid complex suggested that both the protein and the ligand were generally unstable. The RMSD values of the protein and the ligand at the conclusion of the simulation period were 4.15 Åand 5.45 Å, respectively (Figure 4.59 b, Figure 4.60 b). The protein-RMSF plot indicated that the amino acid ASN exhibited the highest level of fluctuation at position 172, with a value of 7.95 Å(Figure 4.61 b). The simulation findings of the mutant model (Q61H) NRAS-Pralsetinib complex revealed that the protein displayed general instability, whereas the ligand was mostly unstable. The RMSD values for the protein and the ligand at the conclusion of the simulation were 3.15 Åand 6.45 Å, respectively (Figure 4.59 b, Figure 4.60 b). The protein-RMSF plot revealed that the residue ASN had the largest fluctuation at position 172, with a value of 8.95 Å(Figure 4.61 b).

The simulation results of the NRAS-Adapalene complex with the mutant model (Q61K) demonstrated that both the protein and the ligand were determined to

be unstable. The RMSD values of the protein and the ligand at the conclusion of the simulation period were 6.15 Åand 6.45 Å, respectively (as shown in Figure 4.59 b and Figure 4.60 b). The protein-RMSF plot revealed that the protein residue ASN had the largest fluctuation at position 172, with a distance of 7.95 Å(Figure 4.61 b). The simulation findings of the mutant model (Q61K) NRAS-Ponatinib complex suggested that both the protein and the ligand were unstable. The RMSD values of the protein and the ligand at the conclusion of the simulation period were 3.15 Åand 7.45 Å, respectively (as shown in Figure 4.59 b and Figure 4.60 b). The protein-RMSF plot revealed that there was no substantial fluctuation in the protein residues. The protein residue with the highest fluctuation was ASN (8.95 Å) at position 172 (Figure 4.61 b). The simulation findings of the mutant model (Q61K) NRAS-Glycyrrhizic acid complex showed that both the protein and the ligand were generally unstable. The RMSD values of the protein and the ligand at the conclusion of the simulation period were 3.15 Åand 6.45 Å, respectively (as shown in Figure 4.59 b and Figure 4.60 b). The RMSF-plot revealed that there was not significant fluctuation in the protein residues, except for ASN (8.95 Å) at position 172, which exhibited the highest level of fluctuation (Figure 4.61 b). The simulation results of the mutant model (Q61K) NRAS-Pralsetinib complex indicated that both the protein and the ligand were unstable overall. The RMSD values of the protein and the ligand at the conclusion of the simulation period were 4.15 Åand 5.45 Å, respectively (as shown in Figure 4.59 b and Figure 4.60 b). The protein-RMSF plot revealed that the residue ASN had the largest fluctuation at position 172, with a value of 7.95 Å(Figure 4.61 b).

The simulation results of the NRAS-Adapalene complex using the mutant model (E153Q) suggested that the protein exhibited a little overall instability, whereas the ligand was shown to be unstable. The RMSD values of the protein and the ligand at the conclusion of the simulation period were 6.15 Åand 6.45 Å, respectively (as shown in Figure 4.59 c and Figure 4.60 c). The protein-RMSF plot revealed that the protein residue ASN (8.95 Å) exhibited the highest level of fluctuation at position 172 (Figure 4.61 c). The simulation results of the mutant model (E153Q) NRAS-Ponatinib complex demonstrated that the protein was generally unstable, whereas the ligand was also found to be unstable. The RMSD values of the protein

and the ligand at the conclusion of the simulation period were 5.15 Åand 8.45 Å, respectively (as shown in Figure 4.59 c and Figure 4.60 c). The protein-RMSF plot revealed that the protein residues exhibited minimal fluctuations. Nevertheless, the residue with the greatest variation was ASN (7.95 Å) at position 172 (Figure 4.61 c). The simulation findings of the mutant model (E153Q) NRAS-Glycyrrhizic acid complex indicated that both the protein and the ligand were unstable overall. The RMSD values of the protein and the ligand at the conclusion of the simulation period were 6.15 Åand 6.45 Å, respectively (as shown in Figure 4.59 c and Figure 4.60 c). The protein-RMSF figure indicated that the protein residues exhibited little fluctuations. The ASN residue had the greatest variation in position 172, with a fluctuation of 8.95 Å, as depicted in Figure 4.61c. The simulation findings of the NRAS Pralsetinib complex with the mutant model (E153Q) indicated that the protein was generally unstable.

Furthermore, the ligand exhibited instability as well. The RMSD values of the protein and the ligand at the conclusion of the simulation period were 4.15 Åand 8.45 Å, respectively (as shown in Figure 4.59 c and Figure 4.60 c). The protein-RMSF plot indicated that the protein residue ASN had the largest level of fluctuation at position 172, with a distance of 7.95 Å(Figure 4.61 c).

The simulation results of the mutant model (G12D) NRAS-Adapalene complex revealed that both the protein and the ligand were unstable. The root-mean-square deviation (RMSD) values for the protein and the ligand at the conclusion of the simulation were 3.15 Åand 7.45 Å, respectively (as shown in Figure 4.59 c and Figure 4.60 c). The protein-RMSF plot revealed that the residue ASN at position 172 had the largest level of fluctuation, measuring 7.95 Å(Figure 4.61 c). The simulation findings of the NRAS Ponatinib complex with the mutant model (G12D) suggested that the protein was generally slightly unstable, and the ligand was also shown to be generally unstable. The RMSD values of the protein and the ligand at the conclusion of the simulation period were 4.15 Åand 8.45 Å, respectively (as shown in Figure 4.59 c and Figure 4.60 c). The protein-RMSF plot revealed that the residue ASN (7.95 Å) at position 172 exhibited the largest degree of fluctuation, as shown in Figure 4.61 c. The simulation findings of the NRAS-Glycyrrhizic

acid complex mutant model (G12D) demonstrated that both the protein and the ligand were unstable. The RMSD values of the protein and the ligand at the conclusion of the simulation period were 5.15 Åand 8.45 Å, respectively (Figure 4.59 c, Figure 4.60 c). The protein-RMSF plot indicated that residue ASN at position 172 had the highest level of fluctuation, measuring 7.95 Å(Figure 4.61 c). The simulation results of the mutant model (G12D) NRAS-Pralsetinib complex revealed that both the protein and the ligand were characterised by general instability. The RMSD values of the protein and the ligand at the conclusion of the simulation were 3.15Åand 5.45Å, respectively (Figure 4.59 c, Figure 4.60 c). The protein-RMSF figure indicated that there was no substantial fluctuation in the protein residues. The residue with the greatest fluctuation was ASN, measuring 8.95 Å, located at position 172 (Figure 4.61 c).

The simulation results of the mutant model (G13D) NRAS-Adapalene complex indicated that both the protein and the ligand exhibited overall instability.

The RMSD values of the protein and the ligand at the conclusion of the simulation period were 6.15 Åand 6.45 Å, respectively (Figure 4.59 c, Figure 4.60 c). The protein-RMSF plot revealed that the protein residue ASN (7.95 Å) exhibited the highest level of fluctuation at position 172 (Figure 4.61 c). The simulation results of the mutant model (G13D) NRAS-Ponatinib complex indicated that the protein was generally slightly unstable, and the ligand was also found to be generally unstable. The RMSD values of the protein and the ligand at the conclusion of the simulation period were 3.15 Åand 8.45 Å, respectively (Figure 4.59 c, Figure 4.60 c). The protein-RMSF plot indicated minimal fluctuations in the protein residues, with the highest fluctuation observed in ASN (7.95 Å) at position 172 (Figure 4.61 c). The simulation results of the mutant model (G13D) NRAS-Glycyrrhizic acid complex revealed overall instability in both the protein and the ligand. The root-mean-square deviation (RMSD) values of the protein and the ligand at the conclusion of the simulation were 3.15 Åand 7.45 Å, respectively (as shown in Figure 4.59 c and Figure 4.60 c). The protein-RMSF figure indicated that there was minimal fluctuation in the protein residues. The residue with the largest fluctuation was ASN (7.95 Å) at position 172 (Figure 4.61 c). The simulation

results of the mutant model (G13D) NRAS-Pralsetinib complex indicated that both the protein and the ligand were generally unstable. The RMSD values for the protein and the ligand at the conclusion of the simulation were 5.15 Åand 5.45 Å, respectively (Figure 4.59 c, Figure 4.60 c). In the protein-RMSF plot, it was observed that the protein residue ASN had the largest fluctuation at position 172, with a value of 8.95 Å(Figure 4.61 c).

To assess if the drugs may have any inhibitory effect on the proteins by destabilizing the proteins 3D conformation which may assist in inhibition of pathogenic function of the protein, MD simulation was conducted. Finally, the MD simulation results of the docked complexes of the specified proteins with the selected four compounds (Adapalene, Ponatinib, Glycyrrhizic acid, and Pralsetinib) indicated that the Glycyrrhizic acid fluctuated the wild-type TCL1A protein the most, while the TCL1A-T38I was fluctuated the most by Ponatinib. Furthermore, it was observed that both the wild-type and the mutant model (T38I) of the TCL1A protein were slightly iterated and did not show a significant fluctuation as compared to the other proteins. Moreover, the simulation results of the MNX1 protein complexes indicated that all the compounds variate MNX1 wild-type and MNX1-P392L significantly, however Adapalene showed the best results with the MNX1-wild protein and Glycyrrhizic acid showed the best results with the MNX1-P392L. Additionally, the ERG protein complexes showed that the ERG-wild protein was the most iterated with Ponatinib, while the ERG-E353Q was the most variate with Adapalene but the mutation had positive effects over stability of protein. Furthermore, the AFF3-wild and AFF3-P1129L model indicated that both were fluctuated when docked with the selected drug compounds, however, the fluctuations were more pronounced in AFF3-wild as compared to its mutant counterpart. However, The AFF3-wild and the AFF3-P1129L fluctuated most with the same compound, Pralsetinib. Furthermore, the all the wild-type FAT1 models (D2382A, M739I, and P4309S) were less stable than the mutant models of the FAT1 protein. However, the wild and mutant (P4309S) model of FAT1 were most fluctuated with Adapalene. However, the NRAS-wild and the mutant models (Q61R, Q61K, Y64D, Q61H, G13R, G13D, E153Q, G12D) showed somewhat same results as all

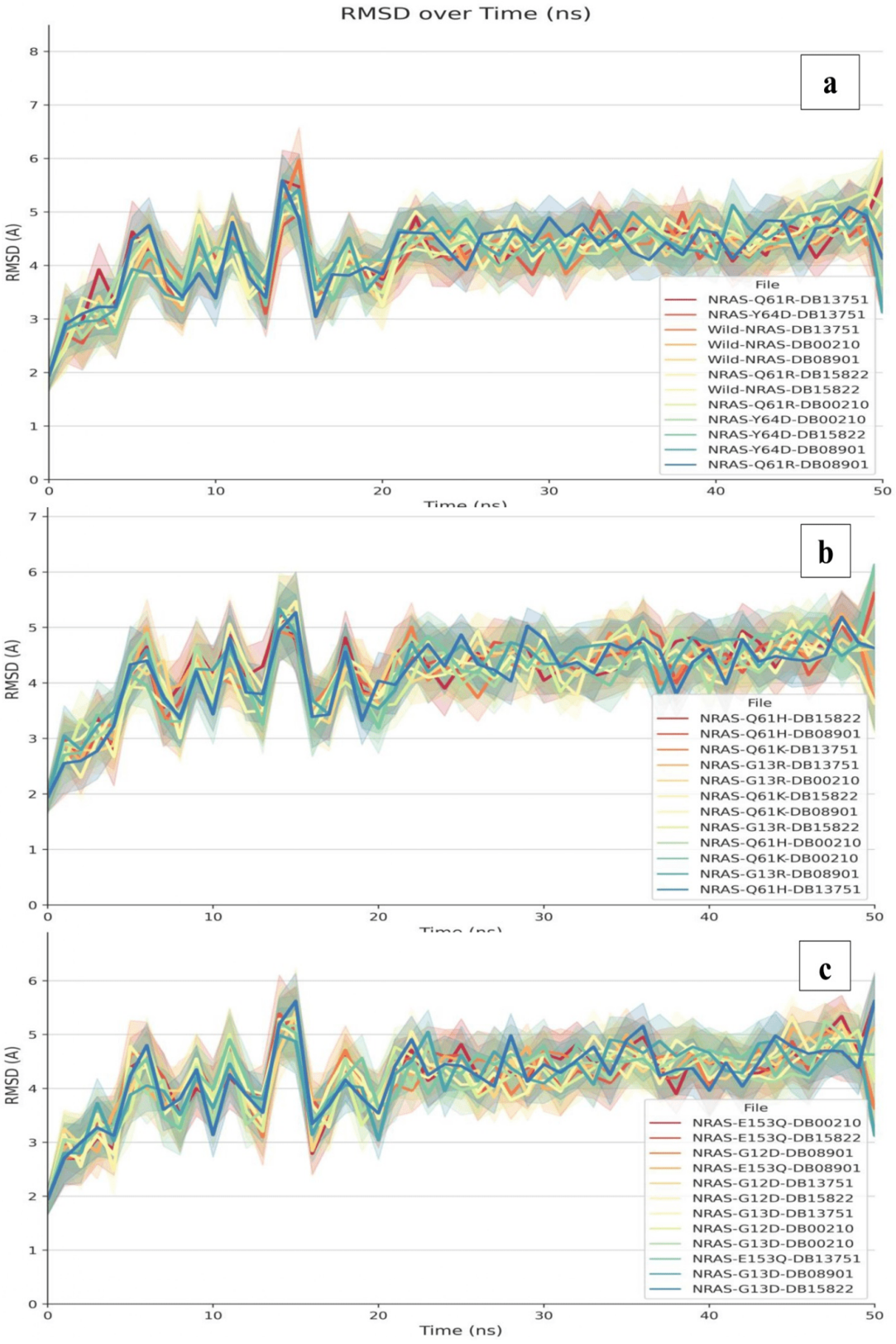

FIGURE 4.59: (a) RMSD graph of wild and NRAS mutant (Q61R, Y64D) (b) (Q61H, Q61K, G13R) (c) (E153Q, G12D, and G13D) representing the conformational differences while docking with selected drug compounds. The simulations were performed for a period of 50 ns.

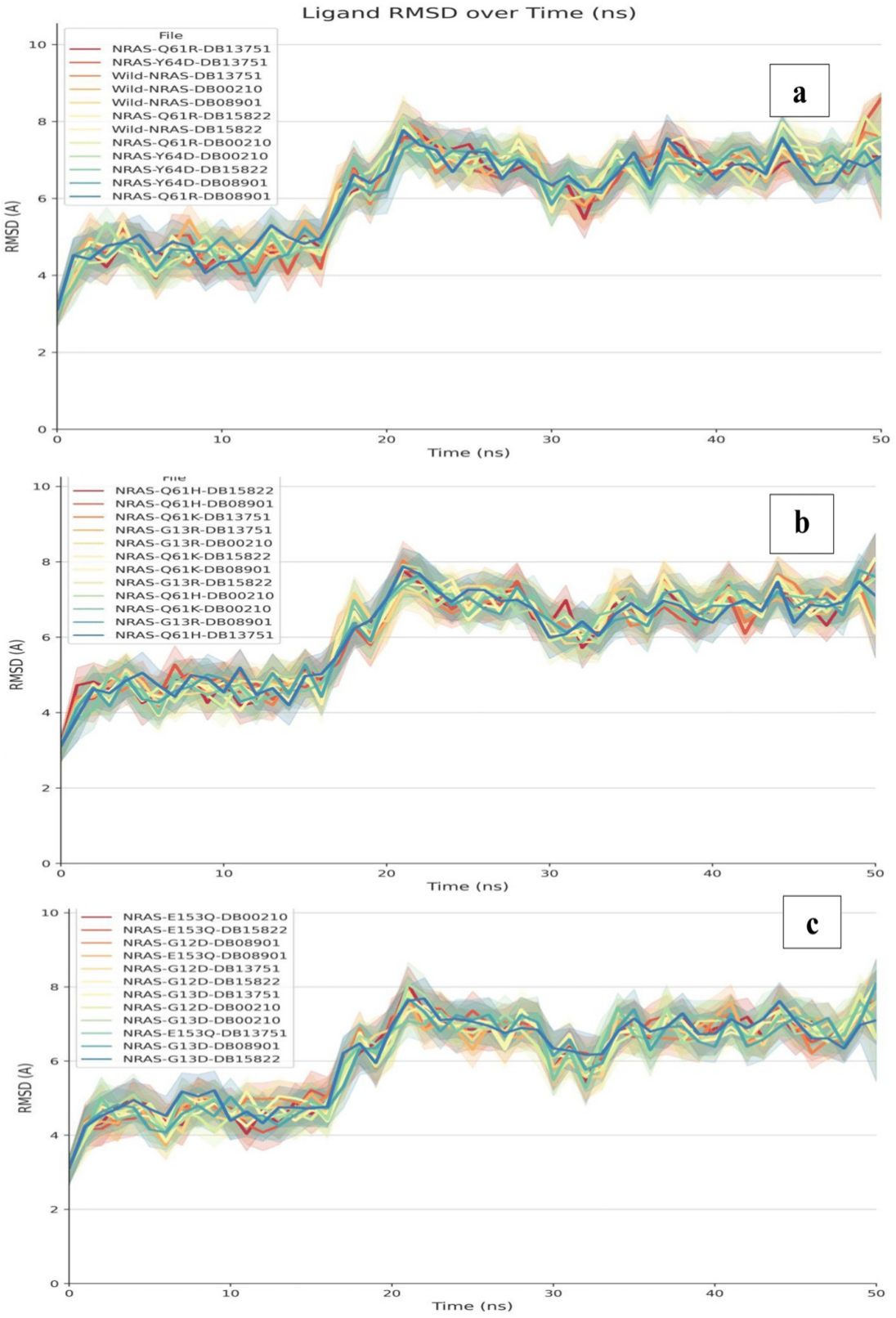

FIGURE 4.60: RMSD graph of ligands (drugs) while docking with (a) wild and NRAS mutant (Q61R, Y64D) (b) (Q61H, Q61K, G13R) (c) (E153Q, G12D, and G13D). The simulations were performed for a period of 50 ns.

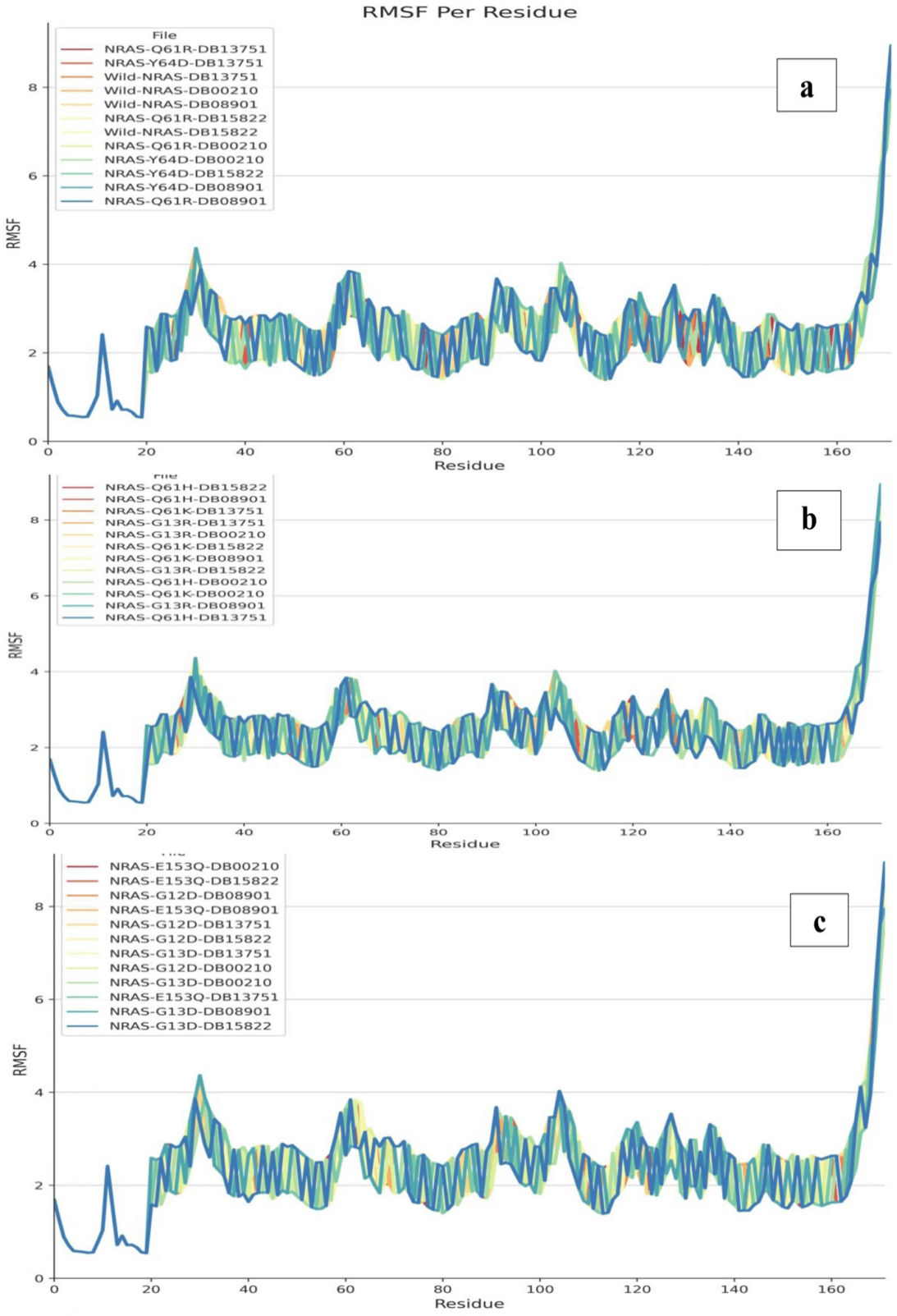

FIGURE 4.61: RMSF graph representing the structural fluctuations observed for amino acid residues between the (a) wild-types and KRAS mutant models (Q61R, Y64D) (b) (Q61H, Q61K, G13R) (c) (E153Q, G12D, and G13D) protein while docking with the selected drug compounds during a simulation period of 50 ns.

the complexes of the wild-type and the mutant models showed instability gradually through the simulation period. Nevertheless, the wild-type NRAS protein showed the most instability with Glycyrrhizic acid, while the mutant model G13D of the NRAS protein showed the most instability with Pralsetinib as compared to the other mutant models. Similarly, the KRAS-wild and the mutant models (Q61H, Q61R, G13D, G12V, G12R, Q61E, K117N, A59E, G12D) indicated more or less same results as all the complexes gradually became less stable through the simulation period. However, the wild-type KRAS protein fluctuated most with Glycyrrhizic acid, while the mutant model G12V of the KRAS variate most with Adapalene. Lastly, the wild and mutant TCL1A proteins were the only protein that showed stability with all selected drug compounds as compared to the other proteins. Conversely, the wild and mutant MNX1 were highly fluctuated with all the selected drug compounds. Conclusively, the selected drug compounds were found to be the best inhibitors for both wild and mutant models of the MNX1 and AFF3 proteins as these proteins were extremely fluctuating when docked with the drug compounds. Among the wild-type and mutant model complexes of MNX1 and AFF3 proteins, the drug compound, Ponatinib (DB08901), was the best inhibitor for mutant model (P392L) MNX1 protein, while Pralsetinib (DB15822) was the best inhibitor found to fluctuate the wild-type AFF3 protein, respectively. Furthermore, these drug compounds (Ponatinib and Pralsetinib) may have the active potential to inhibit these proteins adeptly, hence, the inhibition of these proteins can be affirmed by experimentally corroborating the potential ability of these drug compounds.

A total of 141 drug compounds were retrieved from DrugBank based on sequence searches of candidate relapse biomarkers. Molecular docking results for 18 specified proteins (including MNX1, ERG, TCL1A, and others) with these compounds showed high binding affinities, ranging from -3.1 kcal/mol to -10.9 kcal/mol. Four compounds—adapalene, ponatinib, glycyrrhizic acid, and pralsetinib—exhibited the best binding affinities with most proteins, except for a few complexes. Adapalene had the highest binding affinity with 17 protein models, ponatinib with 15, glycyrrhizic acid with 9, and pralsetinib with 3.

Molecular dynamics simulations revealed varying degrees of instability among the protein-compound complexes. Notably, glycyrrhizic acid caused significant fluctuations in the TCL1A wild-type protein, and ponatinib induced instability in the ERG protein wild-type variant. AFF3, whether wild-type or mutant, was unstable with the selected compounds. The study also found that all drug compounds were effective inhibitors for both wild-type and mutant models of MNX1 and AFF3 proteins, with ponatinib being the most potent for the MNX1 mutant model (P392L) and pralsetinib for the wild-type AFF3 protein.

These results suggest that adapalene and ponatinib are promising candidates for targeting key proteins, with experimental validation needed to confirm their efficacy.

Chapter 5

Conclusion and Future Work

The relapsed, refractory MM (RRMM) is an incurable form of MM that is resistant to most of the available therapies and its genetic heterogeneity is not clearly understood yet. RRMM has been reported to be promoted by chromosomal translocations, gains and deletions, point mutations, genomic instability and epigenetic abnormalities. It has been studied that genetic heterogeneity is associated with therapy resistance caused majorly by genetic alterations and is implicated in cancer relapse It has been reported that mutations in individual genes in MM contribute to its genomic complexity and are thus suggested to have therapeutic implications.

The first objective of the study was to identify biomarkers responsible for relapse of MM. Gene Expression Profiles (GEPs) provides wealth of data at specific condition during course of disease. Hence the differential expression of GEP of MM patients at relapse and at relapse could identify the key mechanisms, pathways and biomarkers that are playing significant role in facilitating relapse of MM. Eighteen biomarkers were selected after comprehensive analysis of literature mining, protein-protein interaction of genetic and gene expression profiles. Among them seven (MNX1, FAT1, ERG, TCL1A, AFF3, KRAS and NRAS) were having SNVs and also upregulates in RRMM. Whereas, CSF1R, VCAN, NRP1, COL22A1, BPI and BIRC5, found as relapse biomarkers in various cancers through literature mining were also upregulated in RRMM. Lastly five hub (IL1B, CD4, ITGAM,

PTPRC and TYROBP) genes with high number of degree were also included in the list of shortlisted candidate relapse biomarkers. The potential of these candidate relapse biomarkers as diagnostic and prognostic biomarkers has been extensively reported in literature but their roles in RRMM is still needed to be explored. The functional annotation analysis of all shortlisted candidate relapse biomarkers revealed significant enrichment in G protein activity, GDP binding, positive regulation of cell population proliferation, serene/threonine kinase activity, endothelial cell proliferation. However, pathway enrichment retrieved PI3K-Akt signaling and prostate cancer, acute myeloid leukemia and CRC pathways were significant along with many cancer pathways. The immune cells infiltration analysis revealed the higher count of neutrophils and lesser level of T cells (CD8+) in TME of RRMM in comparison to NDMM.

The second objective of the study was to evaluate the structural and functional properties of candidate relapse biomarkers. The structural evaluation of predicted proteins corroborated the accuracy of 3D structure prediction utilizing ERRAT, ProSa and QMEAN tools where optimal ERRAT scores were obtained for ERG-wild (94.68), KRAS-Q61R (93.14) and KRAS-A59E (90.29) while the TCL1A and NRAS models obtained the best average QMEAN scores 0.91 and 0.82, respectively. Furthermore, the superimposition of wild-mutant structures to calculate the structural changes in the form of RMSD differences revealed that the TCL1A-T38I, AFF3-P1129L and MNX1-P392L mutants were significantly deviant structurally because the large RMSD values 1.04 Å, 0.52 Å and 0.53 Å were obtained on superimposition, respectively. Meanwhile, the superimposition analysis for mutants of KRAS and NRAS revealed that major structural differences occurred for KRAS-A59E (0.23 Å), KRAS-Q61H (0.17 Å), NRAS-G13R (0.14 Å) and NRAS-G12D (0.13 Å). Moreover, structural visualization through PyMOL to analyze the structure changes and interactions further verified the structural deviations for the mutants AFF3-P1129L, ERG-E353Q, TCL1A-T38I, KRAS-A59E, KRAS-K117N, KRAS-Q61H, KRAS-Q61R, KRAS-Q61E, NRAS-Y64D, NRAS-Q61K, NRAS-Q61R, NRAS-Q61H, NRAS-G13D and NRAS-E153Q suggesting that these mutations may have induced significant alterations in functional properties. Concluding the results of MD simulation results of candidate

relapse biomarkers with SNVs this study proposes TCL1A-T38I, KRAS-K117N and KRAS-Q61E as significantly stable indicating their crucial functional role in RRMM as compared to wild-type models. Meanwhile ERG-E353Q, AFF3-P1129L, KRAS-Q61R, KRAS-G12R, KRAS-A59E, NRAS-Q61H, NRAS-Q61K, NRAS-Q61R, NRAS-G13R, NRAS-E153Q and MNX1-P392L have been identified as more unstable conformtionally, with respect to their wild structures indicating that these structural alterations may have disrupt the native function of these proteins in RRMM.

The third objective of the study was to perform drug repurposing to identify already existing drugs that have potential to treat RRMM. The 141 drug compounds were retrieved from DrugBank using sequence based searched of candidate relapse biomarkers. The molecular docking results of all the specified proteins (MNX1, ERG, TCL1A, AFF3, FAT1, KRAS, NRAS, CD4, ITGAM, PTPRC, TYROBP, IL1B, CSF1R, VCAN, NRP1, COL22A1, BPI, and BIRC5) with the retrieved compounds indicated that the docking scores high binding affinities ranged from as -3.1 kcal/mol with D-norleucine and Dimethyl fumarate to -10.9 kcal/-mol with glycyrrizic acid. However, a four compounds, namely adapalene, ponatinib, glycyrrhizic acid, and pralsetinib, showed the best binding affinities with all the proteins except for two complexes [TYROBP-Glycyrrhizic acid complex, and wild-type (D2382A) FAT1-Adapalene complex], otherwise all the complexes were observed to have the binding affinities of more than -7.0 kcal/mol. Among the 44 protein models analyzed, adapalene exhibited the highest binding affinity with 17 of them, encompassing both wild-type and mutant variants. Meanwhile, ponatinib, glycyrrhizic acid, and pralsetinib demonstrated superior binding affinities with 15, 9, and 3 protein models, respectively. These results suggested that adapalene and ponatinib are promising candidates for targeting key proteins, with only two protein models displaying binding affinities below -7.0 kcal/mol. In the molecular dynamics simulations, different protein-compound complexes displayed varying degrees of instability. Glycyrrhizic acid caused significant fluctuations in the wild-type TCL1A protein, while the mutant model (T38I) of TCL1A exhibited pronounced instability with ponatinib. ERG protein showed increased

instability with wild-type variants when interacting with ponatinib and with mutant models (E353Q) when exposed to adapalene. AFF3, whether wild-type or mutant, exhibited instability when interacting with the selected compounds, with wild-type AFF3 being notably more unstable, especially when binding with pralsetinib. For NRAS, the wild-type protein became unstable with glycyrrhizic acid, while the mutant model G13D showed the most instability with pralsetinib. In the case of KRAS, glycyrrhizic acid destabilized the wild-type protein, while the mutant model G12V was most affected by adapalene. Overall, wild-type FAT1 proteins (D2382A, M739I, and P4309S) were more unstable than their mutant counterparts, with adapalene inducing the most instability in the wild-type FAT1 protein, while the mutant model (P4309S) was most affected by adapalene. However, the study found that all drug compounds were highly effective inhibitors for both wild and mutant models of MNX1 and AFF3 proteins due to their significant binding affinity. Among these compounds, Ponatinib (DB08901) was the most potent inhibitor for the mutant model of MNX1 protein (P392L), while Pralsetinib (DB15822) showed strong inhibition for the wild-type AFF3 protein. These drug compounds, Ponatinib and Pralsetinib, have the potential to effectively inhibit these proteins, which should be confirmed through experimental validation.

Comprehensive molecular investigations are essential to elucidate the precise roles of these biomarkers in relapse. Furthermore, evaluating these identified biomarkers as potential diagnostic and prognostic indicators in extensive clinical cohorts will provide a clearer understanding of their significance in the context of RRMM. Given that the majority of patients in this study belong to the American (white) and African-American (black) populations, with limited representation from Asian populations, it is important to recognize potential limitations in the generalizability of these findings to other ethnic groups. Immunological biomarkers, in addition to the current biomarkers, should be investigated to study the microenvironment of multiple myeloma (MM) and to observe changes in immune cell populations and cytokines. This investigation will help identify the relationship between immune cells, cytokines, and the predicted biomarkers in relapsed and refractory multiple myeloma (RRMM). Robust and reproducible assays can be develop for detecting these biomarkers for diagnostics. Moreover, the resulting variant data can be used

to stratify patients into different risk categories, thereby enabling more personalized treatment approaches. Additionally, considering that these drug molecules have received approvals for other cancer types, further exploration of their efficacy and suitability for RRMM treatment is strongly recommended.

Bibliography

[1] A. Palumbo and K. Anderson, "Multiple myeloma," *N Engl J Med*, vol. 364, pp. 1046–1060, Mar 2011.

[2] R. Eslick and D. Talaulikar, "Multiple myeloma: from diagnosis to treatment," *Australian family physician*, vol. 42, no. 10, pp. 684–688, 2013.

[3] N. C. Institute, "Plasma cell neoplasms (including multiple myeloma) treatment - nci." https://www.cancer.gov/types/myeloma/patient/myeloma-treatment-pdq, 9 2023. (Accessed on 09/27/2023).

[4] K. Kim, J. H. Lee, J. S. Kim, C. K. Min, S. S. Yoon, K. Shimizu, T. Chou, H. Kosugi, K. Suzuki, W. Chen, *et al.*, "Clinical profiles of multiple myeloma in asia?an asian myeloma network study," *American journal of hematology*, vol. 89, no. 7, pp. 751–756, 2014.

[5] F. Bray, J. Ferlay, I. Soerjomataram, R. L. Siegel, L. A. Torre, and A. Jemal, "Global cancer statistics 2018: Globocan estimates of incidence and mortality worldwide for 36 cancers in 185 countries," *CA: a cancer journal for clinicians*, vol. 68, no. 6, pp. 394–424, 2018.

[6] O. Landgren and B. Weiss, "Patterns of monoclonal gammopathy of undetermined significance and multiple myeloma in various ethnic/racial groups: support for genetic factors in pathogenesis," *Leukemia*, vol. 23, no. 10, pp. 1691–1697, 2009.

[7] A. Badros, B. Barlogie, E. Siegel, C. Morris, R. Desikan, M. Zangari, A. Fassas, E. Anaissie, N. Munshi, and G. Tricot, "Autologous stem cell transplantation in elderly multiple myeloma patients over the age of 70 years," *British journal of haematology*, vol. 114, no. 3, pp. 600–607, 2001.

[8] R. Bataille, "Localized plasmacytomas," *Clinics in haematology*, vol. 11, no. 1, pp. 113–122, 1982.

[9] H. B. Jones, "On a new substance occurring in the urine of a patient with mollities ossium," in *Abstracts of the Papers Communicated to the Royal Society of London*, no. 5, pp. 673–673, The Royal Society London, 1851.

[10] J. R. Berenson, A. Lichtenstein, L. Porter, M. A. Dimopoulos, R. Bordoni, S. George, A. Lipton, A. Keller, O. Ballester, M. J. Kovacs, *et al.*, "Efficacy of pamidronate in reducing skeletal events in patients with advanced multiple myeloma," *New England Journal of Medicine*, vol. 334, no. 8, pp. 488–493, 1996.

[11] P. L. Bergsagel and W. M. Kuehl, "Chromosome translocations in multiple myeloma," *Oncogene*, vol. 20, no. 40, pp. 5611–5622, 2001.

[12] B. Bjorkstrand, P. Ljungman, H. Svensson, J. Hermans, A. Alegre, J. Apperley, J. Bladé, K. Carlson, M. Cavo, A. Ferrant, *et al.*, "Allogeneic bone marrow transplantation versus autologous stem cell transplantation in multiple myeloma: a retrospective case-matched study from the european group for blood and marrow transplantation," 1996.

[13] H. Shaheen, I. Ghanghroo, and I. Malik, "Clinicopathological features and management of pakistani patients with multiple myeloma.," *JPMA. The Journal of the Pakistan Medical Association*, vol. 49, no. 10, pp. 233–237, 1999.

[14] R. Hargreaves, J. Lea, H. Griffiths, J. Faux, J. Holt, C. Reid, C. Bunch, M. Lee, and H. Chapel, "Immunological factors and risk of infection in plateau phase myeloma.," *Journal of clinical pathology*, vol. 48, no. 3, pp. 260–266, 1995.

[15] O. Landgren, R. A. Kyle, R. M. Pfeiffer, J. A. Katzmann, N. E. Caporaso, R. B. Hayes, A. Dispenzieri, S. Kumar, R. J. Clark, D. Baris, *et al.*, "Monoclonal gammopathy of undetermined significance (mgus) consistently precedes multiple myeloma: a prospective study," *Blood, The Journal of the American Society of Hematology*, vol. 113, no. 22, pp. 5412–5417, 2009.

[16] A. K. Dutta, D. R. Hewett, J. L. Fink, J. P. Grady, and A. C. Zannettino, "Cutting edge genomics reveal new insights into tumour development, disease progression and therapeutic impacts in multiple myeloma," *British Journal of Haematology*, vol. 178, no. 2, pp. 196–208, 2017.

[17] M. A. Willrich, D. L. Murray, and R. A. Kyle, "Laboratory testing for monoclonal gammopathies: focus on monoclonal gammopathy of undetermined significance and smoldering multiple myeloma," *Clinical Biochemistry*, vol. 51, pp. 38–47, 2018.

[18] D. L. Roberts, C. Dive, and A. G. Renehan, "Biological mechanisms linking obesity and cancer risk: new perspectives," *Annual review of medicine*, vol. 61, pp. 301–316, 2010.

[19] M. Eriksson and M. Karlsson, "Occupational and other environmental factors and multiple myeloma: a population based case-control study.," *Occupational and Environmental Medicine*, vol. 49, no. 2, pp. 95–103, 1992.

[20] S. A. Rezk, X. Zhao, and L. M. Weiss, "Epstein-barr virus (ebv)–associated lymphoid proliferations, a 2018 update," *Human pathology*, vol. 79, pp. 18–41, 2018.

[21] J. Yan, J. Wang, W. Zhang, M. Chen, J. Chen, and W. Liu, "Solitary plasmacytoma associated with epstein-barr virus: a clinicopathologic, cytogenetic study and literature review," *Annals of Diagnostic Pathology*, vol. 27, pp. 1–6, 2017.

[22] R. A. Kyle, M. A. Gertz, T. E. Witzig, J. A. Lust, M. Q. Lacy, A. Dispenzieri, R. Fonseca, S. V. Rajkumar, J. R. Offord, D. R. Larson, *et al.*, "Review of 1027 patients with newly diagnosed multiple myeloma," in *Mayo Clinic Proceedings*, vol. 78, pp. 21–33, Elsevier, 2003.

[23] S. Janz, F. Zhan, F. Sun, Y. Cheng, M. Pisano, Y. Yang, H. Goldschmidt, and P. Hari, "Germline risk contribution to genomic instability in multiple myeloma," *Frontiers in genetics*, vol. 10, p. 424, 2019.

[24] W. M. Kuehl and P. L. Bergsagel, "Early genetic events provide the basis for a clinical classification of multiple myeloma," *ASH Education Program Book*, vol. 2005, no. 1, pp. 346–352, 2005.

[25] P. L. Bergsagel and W. M. Kuehl, "Molecular pathogenesis and a consequent classification of multiple myeloma," *Journal of clinical oncology*, vol. 23, no. 26, pp. 6333–6338, 2005.

[26] P. L. Bergsagel, W. M. Kuehl, F. Zhan, J. Sawyer, B. Barlogie, and J. Shaughnessy Jr, "Cyclin d dysregulation: an early and unifying pathogenic event in multiple myeloma," *Blood*, vol. 106, no. 1, pp. 296–303, 2005.

[27] I. S. Nijhof, N. W. van de Donk, S. Zweegman, and H. M. Lokhorst, "Current and new therapeutic strategies for relapsed and refractory multiple myeloma: an update," *Drugs*, vol. 78, pp. 19–37, 2018.

[28] C. Chen, Y. Li, P. Miao, Y. Xu, Y. Xie, Z. Chen, and S. Qian, "Tumor immune cell infiltration score based model predicts prognosis in multiple myeloma," *Scientific Reports*, vol. 12, no. 1, p. 17082, 2022.

[29] M. S. Raab, K. Podar, I. Breitkreutz, P. G. Richardson, and K. C. Anderson, "Multiple myeloma," *Lancet*, vol. 374, pp. 324–339, Jul 2009.

[30] N. H. Diepenbrock, *Quick reference to critical care*. Lippincott Williams & Wilkins, 2011.

[31] I. M. W. Group *et al.*, "International myeloma working group (imwg) criteria for the diagnosis of multiple myeloma," *International Myeloma Foundation*, 2017.

[32] N. Korde, S. Y. Kristinsson, and O. Landgren, "Monoclonal gammopathy of undetermined significance (mgus) and smoldering multiple myeloma (smm):

novel biological insights and development of early treatment strategies," *Blood, The Journal of the American Society of Hematology*, vol. 117, no. 21, pp. 5573–5581, 2011.

[33] P. R. Greipp, J. S. Miguel, B. G. Durie, J. J. Crowley, B. Barlogie, J. Bladé, M. Boccadoro, J. A. Child, H. Avet-Loiseau, R. A. Kyle, *et al.*, "International staging system for multiple myeloma," *Journal of clinical oncology*, vol. 23, no. 15, pp. 3412–3420, 2005.

[34] H. Quach, H. Prince, *et al.*, "Clinical practice guideline: multiple myeloma," *Australia: Myeloma Australia*, 2019.

[35] M. J. Cejalvo and J. de la Rubia, "Which therapies will move to the front line for multiple myeloma?," *Expert Review of Hematology*, vol. 10, no. 5, pp. 383–392, 2017.

[36] V. Pinto, R. Bergantim, H. R. Caires, H. Seca, J. E. Guimarães, and M. H. Vasconcelos, "Multiple myeloma: Available therapies and causes of drug resistance," *Cancers*, vol. 12, no. 2, p. 407, 2020.

[37] J. Yang, W. Zhou, D. Li, T. Niu, and W. Wang, "Bcma-targeting chimeric antigen receptor t-cell therapy for multiple myeloma," *Cancer Letters*, p. 215949, 2022.

[38] M. F. Berger and E. R. Mardis, "The emerging clinical relevance of genomics in cancer medicine," *Nature reviews Clinical oncology*, vol. 15, no. 6, pp. 353–365, 2018.

[39] D. T. Debela, S. G. Muzazu, K. D. Heraro, M. T. Ndalama, B. W. Mesele, D. C. Haile, S. K. Kitui, and T. Manyazewal, "New approaches and procedures for cancer treatment: Current perspectives," *SAGE open medicine*, vol. 9, p. 20503121211034366, 2021.

[40] Z. D. Kifle, M. Tadele, E. Alemu, T. Gedamu, and A. G. Ayele, "A recent development of new therapeutic agents and novel drug targets for cancer treatment," *SAGE Open Medicine*, vol. 9, p. 20503121211067083, 2021.

[41] P. Antoniou, D. E. Ziogas, M. Mitsis, and D. H. Roukos, "Precision oncology in patients with nonmetastatic disease: emerging reality or illusion," 2019.

[42] N. Coccaro, L. Anelli, A. Zagaria, G. Specchia, and F. Albano, "Next-generation sequencing in acute lymphoblastic leukemia," *International journal of molecular sciences*, vol. 20, no. 12, p. 2929, 2019.

[43] M. Rusch, J. Nakitandwe, S. Shurtleff, S. Newman, Z. Zhang, M. N. Edmonson, M. Parker, Y. Jiao, X. Ma, Y. Liu, *et al.*, "Clinical cancer genomic profiling by three-platform sequencing of whole genome, whole exome and transcriptome," *Nature communications*, vol. 9, no. 1, p. 3962, 2018.

[44] M. D. Ritchie, E. R. Holzinger, R. Li, S. A. Pendergrass, and D. Kim, "Methods of integrating data to uncover genotype–phenotype interactions," *Nature Reviews Genetics*, vol. 16, no. 2, pp. 85–97, 2015.

[45] S. Choi, *Introduction to systems biology*. Springer, 2007.

[46] M.-n. Chen, D. Zeng, Z.-q. Zheng, Z. Li, J.-y. Jin, H.-j. Wang, C.-z. Huang, H.-y. Lin, *et al.*, "Performing data mining and integrative analysis of biomarker in breast cancer using multiple publicly accessible databases," *JoVE (Journal of Visualized Experiments)*, no. 147, p. e59238, 2019.

[47] X. Zhang, C. Kang, N. Li, X. Liu, J. Zhang, F. Gao, and L. Dai, "Identification of special key genes for alcohol-related hepatocellular carcinoma through bioinformatic analysis," *PeerJ*, vol. 7, p. e6375, 2019.

[48] J. Y. Lee, K. Park, E. Lee, T. Ahn, H. H. Jung, S. H. Lim, M. Hong, I.-G. Do, E. Y. Cho, D.-H. Kim, *et al.*, "Gene expression profiling of breast cancer brain metastasis," *Scientific reports*, vol. 6, no. 1, p. 28623, 2016.

[49] X. Cheng, M. Hu, C. Chen, and D. Hou, "Computational analysis of mrna expression profiles identifies a novel triple-biomarker model as prognostic predictor of stage ii and iii colorectal adenocarcinoma patients," *Cancer Management and Research*, pp. 2945–2952, 2018.

[50] S. M. Henshall, D. E. Afar, J. Hiller, L. G. Horvath, D. I. Quinn, K. K. Rasiah, K. Gish, D. Willhite, J. G. Kench, M. Gardiner-Garden, *et al.*,

"Survival analysis of genome-wide gene expression profiles of prostate cancers identifies new prognostic targets of disease relapse," *Cancer research*, vol. 63, no. 14, pp. 4196–4203, 2003.

[51] S. Stratmann, M. Vesterlund, H. M. Umer, S. Eshtad, A. Skaftason, M. K. Herlin, C. Sundström, A. Eriksson, M. Höglund, J. Palle, *et al.*, "Proteogenomic analysis of acute myeloid leukemia associates relapsed disease with reprogrammed energy metabolism both in adults and children," *Leukemia*, vol. 37, no. 3, pp. 550–559, 2023.

[52] S. Stratmann, S. A. Yones, M. Garbulowski, J. Sun, A. Skaftason, M. Mayrhofer, N. Norgren, M. K. Herlin, C. Sundström, A. Eriksson, *et al.*, "Transcriptomic analysis reveals proinflammatory signatures associated with acute myeloid leukemia progression," *Blood advances*, vol. 6, no. 1, pp. 152–164, 2022.

[53] N. J. Dickens, B. A. Walker, P. E. Leone, D. C. Johnson, J. L. Brito, A. Zeisig, M. W. Jenner, K. D. Boyd, D. Gonzalez, W. M. Gregory, *et al.*, "Homozygous deletion mapping in myeloma samples identifies genes and an expression signature relevant to pathogenesis and outcome," *Clinical Cancer Research*, vol. 16, no. 6, pp. 1856–1864, 2010.

[54] R. Kuiper, A. Broyl, Y. a. de Knegt, M. Van Vliet, E. Van Beers, B. van der Holt, L. el Jarari, G. Mulligan, W. Gregory, G. Morgan, *et al.*, "A gene expression signature for high-risk multiple myeloma," *Leukemia*, vol. 26, no. 11, pp. 2406–2413, 2012.

[55] J. D. Shaughnessy Jr, F. Zhan, B. E. Burington, Y. Huang, S. Colla, I. Hanamura, J. P. Stewart, B. Kordsmeier, C. Randolph, D. R. Williams, *et al.*, "A validated gene expression model of high-risk multiple myeloma is defined by deregulated expression of genes mapping to chromosome 1," *Blood*, vol. 109, no. 6, pp. 2276–2284, 2007.

[56] M. Zamani-Ahmadmahmudi, S. M. Nassiri, and F. Soltaninezhad, "Development of an rna sequencing-based prognostic gene signature in multiple

myeloma," *British Journal of Haematology*, vol. 192, no. 2, pp. 310–321, 2021.

[57] S. Manier, K. Z. Salem, J. Park, D. A. Landau, G. Getz, and I. M. Ghobrial, "Genomic complexity of multiple myeloma and its clinical implications," *Nature reviews Clinical oncology*, vol. 14, no. 2, pp. 100–113, 2017.

[58] S. V. Rajkumar, M. A. Dimopoulos, A. Palumbo, J. Blade, G. Merlini, M.-V. Mateos, S. Kumar, J. Hillengass, E. Kastritis, P. Richardson, *et al.*, "International myeloma working group updated criteria for the diagnosis of multiple myeloma," *The lancet oncology*, vol. 15, no. 12, pp. e538–e548, 2014.

[59] S. V. Rajkumar and S. Kumar, "Multiple myeloma current treatment algorithms," *Blood cancer journal*, vol. 10, no. 9, p. 94, 2020.

[60] O. Landgren and B. Weiss, "Patterns of monoclonal gammopathy of undetermined significance and multiple myeloma in various ethnic/racial groups: support for genetic factors in pathogenesis," *Leukemia*, vol. 23, no. 10, pp. 1691–1697, 2009.

[61] R. A. Kyle, M. A. Gertz, T. E. Witzig, J. A. Lust, M. Q. Lacy, A. Dispenzieri, R. Fonseca, S. V. Rajkumar, J. R. Offord, D. R. Larson, *et al.*, "Review of 1027 patients with newly diagnosed multiple myeloma," in *Mayo Clinic Proceedings*, vol. 78, pp. 21–33, Elsevier, 2003.

[62] G. D. Roodman, "Pathogenesis of myeloma bone disease," *Leukemia*, vol. 23, no. 3, pp. 435–441, 2009.

[63] J. Hillengass, S. Usmani, S. V. Rajkumar, B. G. Durie, M.-V. Mateos, S. Lonial, C. Joao, K. C. Anderson, R. García-Sanz, E. Riva, *et al.*, "International myeloma working group consensus recommendations on imaging in monoclonal plasma cell disorders," *The lancet oncology*, vol. 20, no. 6, pp. e302–e312, 2019.

[64] K. D. Short, S. Rajkumar, D. Larson, F. Buadi, S. Hayman, A. Dispenzieri, M. Gertz, S. Kumar, J. Mikhael, V. Roy, *et al.*, "Incidence of extramedullary disease in patients with multiple myeloma in the era of novel therapy, and the

activity of pomalidomide on extramedullary myeloma," *Leukemia*, vol. 25, no. 6, pp. 906–908, 2011.

[65] P. L. Bergsagel, W. M. Kuehl, F. Zhan, J. Sawyer, B. Barlogie, and J. Shaughnessy Jr, "Cyclin d dysregulation: an early and unifying pathogenic event in multiple myeloma," *Blood*, vol. 106, no. 1, pp. 296–303, 2005.

[66] A. I. Clay-Gilmour, M. A. Hildebrandt, E. E. Brown, J. N. Hofmann, J. J. Spinelli, G. G. Giles, W. Cozen, P. Bhatti, X. Wu, R. G. Waller, *et al.*, "Coinherited genetics of multiple myeloma and its precursor, monoclonal gammopathy of undetermined significance," *Blood advances*, vol. 4, no. 12, pp. 2789–2797, 2020.

[67] S. Y. Kristinsson, M. Björkholm, L. R. Goldin, C. Blimark, U.-H. Mellqvist, A. Wahlin, I. Turesson, and O. Landgren, "Patterns of hematologic malignancies and solid tumors among 37,838 first-degree relatives of 13,896 patients with multiple myeloma in sweden," *International journal of cancer*, vol. 125, no. 9, pp. 2147–2150, 2009.

[68] C. M. Vachon, R. A. Kyle, T. M. Therneau, B. J. Foreman, D. R. Larson, C. L. Colby, T. K. Phelps, A. Dispenzieri, S. K. Kumar, J. A. Katzmann, *et al.*, "Increased risk of monoclonal gammopathy in first-degree relatives of patients with multiple myeloma or monoclonal gammopathy of undetermined significance," *Blood, The Journal of the American Society of Hematology*, vol. 114, no. 4, pp. 785–790, 2009.

[69] G. Morgan, D. Johnson, N. Weinhold, H. Goldschmidt, O. Landgren, H. T. Lynch, K. Hemminki, and R. Houlston, "Inherited genetic susceptibility to multiple myeloma," *Leukemia*, vol. 28, no. 3, pp. 518–524, 2014.

[70] N. Goossens, S. Nakagawa, X. Sun, and Y. Hoshida, "Cancer biomarker discovery and validation," *Translational cancer research*, vol. 4, no. 3, p. 256, 2015.

[71] D. T. Koura and A. A. Langston, "Inherited predisposition to multiple myeloma," *Therapeutic advances in hematology*, vol. 4, no. 4, pp. 291–297, 2013.

[72] D. Chubb, N. Weinhold, P. Broderick, B. Chen, D. C. Johnson, A. Försti, J. Vijayakrishnan, G. Migliorini, S. E. Dobbins, A. Holroyd, *et al.*, "Common variation at 3q26. 2, 6p21. 33, 17p11. 2 and 22q13. 1 influences multiple myeloma risk," *Nature genetics*, vol. 45, no. 10, pp. 1221–1225, 2013.

[73] O. Landgren and B. Weiss, "Patterns of monoclonal gammopathy of undetermined significance and multiple myeloma in various ethnic/racial groups: support for genetic factors in pathogenesis," *Leukemia*, vol. 23, no. 10, pp. 1691–1697, 2009.

[74] A. Greenberg, C. Vachon, and S. Rajkumar, "Disparities in the prevalence, pathogenesis and progression of monoclonal gammopathy of undetermined significance and multiple myeloma between blacks and whites," *Leukemia*, vol. 26, no. 4, pp. 609–614, 2012.

[75] L. J. Costa, I. K. Brill, J. Omel, K. Godby, S. K. Kumar, and E. E. Brown, "Recent trends in multiple myeloma incidence and survival by age, race, and ethnicity in the united states," *Blood advances*, vol. 1, no. 4, pp. 282–287, 2017.

[76] A. J. Waxman, P. J. Mink, S. S. Devesa, W. F. Anderson, B. M. Weiss, S. Y. Kristinsson, K. A. McGlynn, and O. Landgren, "Racial disparities in incidence and outcome in multiple myeloma: a population-based study," *Blood, The Journal of the American Society of Hematology*, vol. 116, no. 25, pp. 5501–5506, 2010.

[77] Z. Du, N. Weinhold, G. C. Song, K. A. Rand, D. J. Van Den Berg, A. E. Hwang, X. Sheng, V. Hom, S. Ailawadhi, A. K. Nooka, *et al.*, "A meta-analysis of genome-wide association studies of multiple myeloma among men and women of african ancestry," *Blood advances*, vol. 4, no. 1, pp. 181–190, 2020.

[78] W. Cozen, M. Gebregziabher, D. V. Conti, D. J. Van Den Berg, G. A. Coetzee, S. S. Wang, N. Rothman, L. Bernstein, P. Hartge, A. Morhbacher, *et al.*, "Interleukin-6-related genotypes, body mass index, and risk of multiple myeloma and plasmacytoma," *Cancer Epidemiology Biomarkers & Prevention*, vol. 15, no. 11, pp. 2285–2291, 2006.

[79] N. Weinhold, T. Meissner, D. C. Johnson, A. Seckinger, J. Moreaux, A. Försti, B. Chen, J. Nickel, D. Chubb, A. C. Rawstron, *et al.*, "The 7p15. 3 (rs4487645) association for multiple myeloma shows strong allele-specific regulation of the myc-interacting gene cdca7l in malignant plasma cells," *Haematologica*, vol. 100, no. 3, p. e110, 2015.

[80] N. Li, D. C. Johnson, N. Weinhold, J. B. Studd, G. Orlando, F. Mirabella, J. S. Mitchell, T. Meissner, M. Kaiser, H. Goldschmidt, *et al.*, "Multiple myeloma risk variant at 7p15. 3 creates an irf4-binding site and interferes with cdca7l expression," *Nature communications*, vol. 7, no. 1, p. 13656, 2016.

[81] S. Janz, F. Zhan, F. Sun, Y. Cheng, M. Pisano, Y. Yang, H. Goldschmidt, and P. Hari, "Germline risk contribution to genomic instability in multiple myeloma," *Frontiers in genetics*, vol. 10, p. 424, 2019.

[82] L. B. Baughn, K. Pearce, D. Larson, M.-Y. Polley, E. Elhaik, M. Baird, C. Colby, J. Benson, Z. Li, Y. Asmann, *et al.*, "Differences in genomic abnormalities among african individuals with monoclonal gammopathies using calculated ancestry," *Blood cancer journal*, vol. 8, no. 10, p. 96, 2018.

[83] N. Onodera, N. R. McCabe, and C. M. Rubin, "Formation of a hyperdiploid karyotype in childhood acute lymphoblastic leukemia [see comments]," 1992.

[84] W. M. Kuehl and P. L. Bergsagel, "Early genetic events provide the basis for a clinical classification of multiple myeloma," *ASH Education Program Book*, vol. 2005, no. 1, pp. 346–352, 2005.

[85] P. L. Bergsagel and W. M. Kuehl, "Molecular pathogenesis and a consequent classification of multiple myeloma," *Journal of clinical oncology*, vol. 23, no. 26, pp. 6333–6338, 2005.

[86] G. J. Morgan, B. A. Walker, and F. E. Davies, "The genetic architecture of multiple myeloma," *Nature Reviews Cancer*, vol. 12, no. 5, pp. 335–348, 2012.

[87] F. Zhan, Y. Huang, S. Colla, J. P. Stewart, I. Hanamura, S. Gupta, J. Epstein, S. Yaccoby, J. Sawyer, B. Burington, *et al.*, "The molecular classification of multiple myeloma," *Blood*, vol. 108, no. 6, pp. 2020–2028, 2006.

[88] X. Mao, B. Cao, T. E. Wood, R. Hurren, J. Tong, X. Wang, W. Wang, J. Li, Y. Jin, W. Sun, *et al.*, "A small-molecule inhibitor of d-cyclin transactivation displays preclinical efficacy in myeloma and leukemia via phosphoinositide 3-kinase pathway," *Blood, The Journal of the American Society of Hematology*, vol. 117, no. 6, pp. 1986–1997, 2011.

[89] J. J. Keats, T. Reiman, C. A. Maxwell, B. J. Taylor, L. M. Larratt, M. J. Mant, A. R. Belch, and L. M. Pilarski, "In multiple myeloma, t (4; 14)(p16; q32) is an adverse prognostic factor irrespective of fgfr3 expression," *Blood, The Journal of the American Society of Hematology*, vol. 101, no. 4, pp. 1520–1529, 2003.

[90] H. Chang, S. Sloan, D. Li, L. Zhuang, Q.-L. Yi, C. I. Chen, D. Reece, K. Chun, and A. Keith Stewart, "The t (4; 14) is associated with poor prognosis in myeloma patients undergoing autologous stem cell transplant," *British journal of haematology*, vol. 125, no. 1, pp. 64–68, 2004.

[91] M. Santra, F. Zhan, E. Tian, B. Barlogie, and J. Shaughnessy Jr, "A subset of multiple myeloma harboring the t (4; 14)(p16; q32) translocation lacks fgfr3 expression but maintains an igh/mmset fusion transcript," *Blood, The Journal of the American Society of Hematology*, vol. 101, no. 6, pp. 2374–2376, 2003.

[92] J. J. Keats, C. A. Maxwell, B. J. Taylor, M. J. Hendzel, M. Chesi, P. L. Bergsagel, L. M. Larratt, M. J. Mant, T. Reiman, A. R. Belch, *et al.*, "Overexpression of transcripts originating from the mmset locus characterizes all t (4; 14)(p16; q32)-positive multiple myeloma patients," *Blood*, vol. 105, no. 10, pp. 4060–4069, 2005.

[93] D. Cappellen, C. De Oliveira, D. Ricol, S. de Medina, J. Bourdin, X. Sastre-Garau, D. Chopin, J. P. Thiery, and F. Radvanyi, "Frequent activating mutations of fgfr3 in human bladder and cervix carcinomas," *Nature genetics*, vol. 23, no. 1, pp. 18–20, 1999.

[94] H. Pei, L. Zhang, K. Luo, Y. Qin, M. Chesi, F. Fei, P. L. Bergsagel, L. Wang, Z. You, and Z. Lou, "Mmset regulates histone h4k20 methylation and 53bp1 accumulation at dna damage sites," *Nature*, vol. 470, no. 7332, pp. 124–128, 2011.

[95] H. Avet-Loiseau, X. Leleu, M. Roussel, P. Moreau, C. Guerin-Charbonnel, D. Caillot, G. Marit, L. Benboubker, L. Voillat, C. Mathiot, *et al.*, "Bortezomib plus dexamethasone induction improves outcome of patients with t (4; 14) myeloma but not outcome of patients with del (17p)," *Journal of Clinical Oncology*, vol. 28, no. 30, pp. 4630–4634, 2010.

[96] H. Avet-Loiseau, F. Malard, L. Campion, F. Magrangeas, C. Sebban, B. Lioure, O. Decaux, T. Lamy, L. Legros, J.-G. Fuzibet, *et al.*, "Translocation t (14; 16) and multiple myeloma: is it really an independent prognostic factor?," *Blood, The Journal of the American Society of Hematology*, vol. 117, no. 6, pp. 2009–2011, 2011.

[97] E. M. Hurt, A. Wiestner, A. Rosenwald, A. Shaffer, E. Campo, T. Grogan, P. L. Bergsagel, W. M. Kuehl, and L. M. Staudt, "Overexpression of c-maf is a frequent oncogenic event in multiple myeloma that promotes proliferation and pathological interactions with bone marrow stroma," *Cancer cell*, vol. 5, no. 2, pp. 191–199, 2004.

[98] B. A. Walker, C. P. Wardell, A. Murison, E. M. Boyle, D. B. Begum, N. M. Dahir, P. Z. Proszek, L. Melchor, C. Pawlyn, M. F. Kaiser, *et al.*, "Apobec family mutational signatures are associated with poor prognosis translocations in multiple myeloma," *Nature communications*, vol. 6, no. 1, p. 6997, 2015.

[99] J. Shaughnessy Jr, A. Gabrea, Y. Qi, L. Brents, F. Zhan, E. Tian, J. Sawyer, B. Barlogie, P. L. Bergsagel, and M. Kuehl, "Cyclin d3 at 6p21 is dysregulated by recurrent chromosomal translocations to immunoglobulin loci in multiple myeloma," *Blood, The Journal of the American Society of Hematology*, vol. 98, no. 1, pp. 217–223, 2001.

[100] B. A. Walker, C. P. Wardell, A. Murison, E. M. Boyle, D. B. Begum, N. M. Dahir, P. Z. Proszek, L. Melchor, C. Pawlyn, M. F. Kaiser, *et al.*, "Apobec family mutational signatures are associated with poor prognosis translocations in multiple myeloma," *Nature communications*, vol. 6, no. 1, p. 6997, 2015.

[101] N. Solvason, W. W. Wu, N. Kabra, X. Wu, E. Lees, and M. C. Howard, "Induction of cell cycle regulatory proteins in anti-immunoglobulin-stimulated mature b lymphocytes.," *The Journal of experimental medicine*, vol. 184, no. 2, pp. 407–417, 1996.

[102] B. A. Walker, E. M. Boyle, C. P. Wardell, A. Murison, N. B. Dahir, P. Z. Proszek, D. C. Johnson, M. F. Kaiser, L. Melchor, L. I. Aronson, *et al.*, "Mutational spectrum, copy number changes, and outcome: results of a sequencing study of patients with newly diagnosed myeloma," *Journal of clinical oncology: official journal of the American Society of Clinical Oncology*, vol. 33, no. 33, p. 3911, 2015.

[103] H. Avet-Loiseau, F. Gerson, F. Magrangeas, S. Minvielle, J.-L. Harousseau, and R. Bataille, "Rearrangements of the c-myc oncogene are present in 15% of primary human multiple myeloma tumors," *Blood, The Journal of the American Society of Hematology*, vol. 98, no. 10, pp. 3082–3086, 2001.

[104] J. R. Sawyer, E. Tian, C. J. Heuck, J. Epstein, D. J. Johann, C. M. Swanson, J. L. Lukacs, M. Johnson, R. Binz, A. Boast, *et al.*, "Jumping translocations of 1q12 in multiple myeloma: a novel mechanism for deletion of 17p in cytogenetically defined high-risk disease," *Blood, The Journal of the American Society of Hematology*, vol. 123, no. 16, pp. 2504–2512, 2014.

[105] C. Li, E. B. Wendlandt, B. Darbro, H. Xu, G. S. Thomas, G. Tricot, F. Chen, J. D. Shaughnessy Jr, and F. Zhan, "Genetic analysis of multiple myeloma identifies cytogenetic alterations implicated in disease complexity and progression," *Cancers*, vol. 13, no. 3, p. 517, 2021.

[106] L. Da Silva and S. R. Lakhani, "Pathology of hereditary breast cancer," *Modern Pathology*, vol. 23, pp. S46–S51, 2010.

[107] M. A. Chapman, M. S. Lawrence, J. J. Keats, K. Cibulskis, C. Sougnez, A. C. Schinzel, C. L. Harview, J.-P. Brunet, G. J. Ahmann, M. Adli, *et al.*, "Initial genome sequencing and analysis of multiple myeloma," *Nature*, vol. 471, no. 7339, pp. 467–472, 2011.

[108] K. D. Boyd, F. M. Ross, B. A. Walker, C. P. Wardell, W. J. Tapper, L. Chiecchio, G. Dagrada, Z. J. Konn, W. M. Gregory, G. H. Jackson, *et al.*, "Mapping of chromosome 1p deletions in myeloma identifies fam46c at 1p12 and cdkn2c at 1p32. 3 as being genes in regions associated with adverse survival," *Clinical cancer research*, vol. 17, no. 24, pp. 7776–7784, 2011.

[109] B. A. Walker, P. E. Leone, L. Chiecchio, N. J. Dickens, M. W. Jenner, K. D. Boyd, D. C. Johnson, D. Gonzalez, G. P. Dagrada, R. K. Protheroe, *et al.*, "A compendium of myeloma-associated chromosomal copy number abnormalities and their prognostic value," *Blood, The Journal of the American Society of Hematology*, vol. 116, no. 15, pp. e56–e65, 2010.

[110] R. Fonseca, P. L. Bergsagel, J. Drach, J. Shaughnessy, N. Gutierrez, A. K. Stewart, G. Morgan, B. Van Ness, M. Chesi, S. Minvielle, *et al.*, "International myeloma working group molecular classification of multiple myeloma: spotlight review," *Leukemia*, vol. 23, no. 12, pp. 2210–2221, 2009.

[111] L. Lodé, M. Eveillard, V. Trichet, T. Soussi, S. Wuillème, S. Richebourg, F. Magrangeas, N. Ifrah, L. Campion, C. Traullé, *et al.*, "Mutations in tp53 are exclusively associated with del (17p) in multiple myeloma," *haematologica*, vol. 95, no. 11, p. 1973, 2010.

[112] J. Drach, J. Ackermann, E. Fritz, E. Kromer, R. Schuster, H. Gisslinger, M. DeSantis, N. Zojer, M. Fiegl, S. Roka, *et al.*, "Presence of a p53 gene

deletion in patients with multiple myeloma predicts for short survival after conventional-dose chemotherapy," *Blood, The Journal of the American Society of Hematology*, vol. 92, no. 3, pp. 802–809, 1998.

[113] H. Avet-Loiseau, M. Attal, P. Moreau, C. Charbonnel, F. Garban, C. Hulin, S. Leyvraz, M. Michallet, I. Yakoub-Agha, L. Garderet, *et al.*, "Genetic abnormalities and survival in multiple myeloma: the experience of the intergroupe francophone du myelome," *Blood*, vol. 109, no. 8, pp. 3489–3495, 2007.

[114] A. Gmidene, A. Saad, and H. Avet-Loiseau, "8p21. 3 deletion suggesting a probable role of trail-r1 and trail-r2 as candidate tumor suppressor genes in the pathogenesis of multiple myeloma," *Medical oncology*, vol. 30, pp. 1–4, 2013.

[115] M. Liyanage, A. Coleman, S. d. Manoir, T. Veldman, S. McCormack, R. B. Dickson, C. Barlow, A. Wynshaw-Boris, S. Janz, J. Wienberg, *et al.*, "Multicolour spectral karyotyping of mouse chromosomes," *Nature genetics*, vol. 14, no. 3, pp. 312–315, 1996.

[116] M. Grade, M. J. Difilippantonio, and J. Camps, "Patterns of chromosomal aberrations in solid tumors," *Chromosomal instability in Cancer cells*, pp. 115–142, 2015.

[117] G. Bahr, "The fibrous structure of human chromosomes in relation to rearrangements and aberrations; a theoretical consideration.," in *Federation Proceedings*, vol. 34, pp. 2209–2217, 1975.

[118] Y. Qin, S. Zhang, S. Deng, G. An, X. Qin, F. Li, Y. Xu, M. Hao, Y. Yang, W. Zhou, *et al.*, "Epigenetic silencing of mir-137 induces drug resistance and chromosomal instability by targeting aurka in multiple myeloma," *Leukemia*, vol. 31, no. 5, pp. 1123–1135, 2017.

[119] D. Caracciolo, M. T. Di Martino, N. Amodio, E. Morelli, M. Montesano, C. Botta, F. Scionti, D. Talarico, E. Altomare, M. E. Gallo Cantafio, *et al.*, "mir-22 suppresses dna ligase iii addiction in multiple myeloma," *Leukemia*, vol. 33, no. 2, pp. 487–498, 2019.

[120] B. A. Walker, C. P. Wardell, L. Chiecchio, E. M. Smith, K. D. Boyd, A. Neri, F. E. Davies, F. M. Ross, and G. J. Morgan, "Aberrant global methylation patterns affect the molecular pathogenesis and prognosis of multiple myeloma," *Blood, The Journal of the American Society of Hematology*, vol. 117, no. 2, pp. 553–562, 2011.

[121] G. Tricot, "New insights into role of microenvironment in multiple myeloma," *The Lancet*, vol. 355, no. 9200, pp. 248–250, 2000.

[122] G. Pratt, "Molecular aspects of multiple myeloma," *Molecular Pathology*, vol. 55, no. 5, p. 273, 2002.

[123] B. Nguyen, P. G. Cusumano, K. Deck, D. Kerlin, A. A. Garcia, J. L. Barone, E. Rivera, K. Yao, F. A. De Snoo, J. Van Den Akker, *et al.*, "Comparison of molecular subtyping with blueprint, mammaprint, and targetprint to local clinical subtyping in breast cancer patients," *Annals of surgical oncology*, vol. 19, pp. 3257–3263, 2012.

[124] C. M. Annunziata, R. E. Davis, Y. Demchenko, W. Bellamy, A. Gabrea, F. Zhan, G. Lenz, I. Hanamura, G. Wright, W. Xiao, *et al.*, "Frequent engagement of the classical and alternative nf-κb pathways by diverse genetic abnormalities in multiple myeloma," *Cancer cell*, vol. 12, no. 2, pp. 115–130, 2007.

[125] J. J. Keats, R. Fonseca, M. Chesi, R. Schop, A. Baker, W.-J. Chng, S. Van Wier, R. Tiedemann, C.-X. Shi, M. Sebag, *et al.*, "Promiscuous mutations activate the noncanonical nf-κb pathway in multiple myeloma," *Cancer cell*, vol. 12, no. 2, pp. 131–144, 2007.

[126] W. Zhang and H. T. Liu, "Mapk signal pathways in the regulation of cell proliferation in mammalian cells," *Cell research*, vol. 12, no. 1, pp. 9–18, 2002.

[127] S. Patrawala and I. Puzanov, "Vemurafenib (rg67204, plx4032): a potent, selective braf kinase inhibitor," *Future Oncology*, vol. 8, no. 5, pp. 509–523, 2012.

[128] A. C. Bharti, S. Shishodia, J. M. Reuben, D. Weber, R. Alexanian, S. Raj-Vadhan, Z. Estrov, M. Talpaz, and B. B. Aggarwal, "Nuclear factor–κb and stat3 are constitutively active in cd138+ cells derived from multiple myeloma patients, and suppression of these transcription factors leads to apoptosis," *Blood*, vol. 103, no. 8, pp. 3175–3184, 2004.

[129] Y. S. Chang, E. di Tomaso, D. M. McDonald, R. Jones, R. K. Jain, and L. L. Munn, "Mosaic blood vessels in tumors: frequency of cancer cells in contact with flowing blood," *Proceedings of the National Academy of Sciences*, vol. 97, no. 26, pp. 14608–14613, 2000.

[130] P. Magnowski, H. Bochyński, E. Nowak-Markwitz, M. Zabel, and M. Spaczyński, "Circulating tumor cells (ctcs)–clinical significance in patients with ovarian cancer," *Ginekologia Polska*, vol. 83, no. 4, 2012.

[131] S. Alas and B. Bonavida, "Inhibition of constitutive stat3 activity sensitizes resistant non-hodgkin's lymphoma and multiple myeloma to chemotherapeutic drug-mediated apoptosis," *Clinical cancer research*, vol. 9, no. 1, pp. 316–326, 2003.

[132] M. Osaki, M. Oshimura, , and H. Ito, "Pi3k-akt pathway: its functions and alterations in human cancer," *Apoptosis*, vol. 9, pp. 667–676, 2004.

[133] L. I. Aronson, E. L. Davenport, S. G. Giuntoli, M. Srikanth, E. Smith, G. J. Morgan, and F. Davies, "Autophagy is a key myeloma survival pathway that can be manipulated therapeutically to enhance apoptosis," *Blood*, vol. 116, no. 21, p. 4083, 2010.

[134] T. Uchida, T. Kinoshita, T. Ohno, H. Ohashi, H. Nagai, and H. Saito, "Hypermethylation of p16ink4a gene promoter during the progression of plasma cell dyscrasia," *Leukemia*, vol. 15, no. 1, pp. 157–165, 2001.

[135] A. Kassambara, C. Gourzones-Dmitriev, S. Sahota, T. Rème, J. Moreaux, H. Goldschmidt, A. Constantinou, P. Pasero, D. Hose, and B. Klein, "A dna repair pathway score predicts survival in human multiple myeloma: the potential for therapeutic strategy," *Oncotarget*, vol. 5, no. 9, p. 2487, 2014.

[136] P. Neri, L. Ren, K. Gratton, E. Stebner, J. Johnson, A. Klimowicz, P. Duggan, P. Tassone, A. Mansoor, D. A. Stewart, *et al.*, "Bortezomib-induced "brcaness" sensitizes multiple myeloma cells to parp inhibitors," *Blood, The Journal of the American Society of Hematology*, vol. 118, no. 24, pp. 6368–6379, 2011.

[137] Y. Hu, J. Lin, H. Fang, J. Fang, C. Li, W. Chen, S. Liu, S. Ondrejka, Z. Gong, F. Reu, *et al.*, "Targeting the malat1/parp1/lig3 complex induces dna damage and apoptosis in multiple myeloma," *Leukemia*, vol. 32, no. 10, pp. 2250–2262, 2018.

[138] A. Perrot, V. Lauwers-Cances, J. Corre, N. Robillard, C. Hulin, M.-L. Chretien, T. Dejoie, S. Maheo, A.-M. Stoppa, B. Pegourie, *et al.*, "Minimal residual disease negativity using deep sequencing is a major prognostic factor in multiple myeloma," *Blood, The Journal of the American Society of Hematology*, vol. 132, no. 23, pp. 2456–2464, 2018.

[139] M. Marchesini, E. Fiorini, and S. Colla, "Rna processing: a new player of genomic instability in multiple myeloma," *Oncoscience*, vol. 4, no. 7-8, p. 73, 2017.

[140] B. Pereira, M. Billaud, and R. Almeida, "Rna-binding proteins in cancer: old players and new actors," *Trends in cancer*, vol. 3, no. 7, pp. 506–528, 2017.

[141] M. Marchesini, Y. Ogoti, E. Fiorini, A. A. Samur, L. Nezi, M. D'Anca, P. Storti, M. K. Samur, I. Ganan-Gomez, M. T. Fulciniti, *et al.*, "Ilf2 is a regulator of rna splicing and dna damage response in 1q21-amplified multiple myeloma," *Cancer cell*, vol. 32, no. 1, pp. 88–100, 2017.

[142] J. A. Katzmann, A. Dispenzieri, R. A. Kyle, M. R. Snyder, M. F. Plevak, D. R. Larson, R. S. Abraham, J. A. Lust, L. J. Melton III, and S. V. Rajkumar, "Elimination of the need for urine studies in the screening algorithm for monoclonal gammopathies by using serum immunofixation and free light chain assays," in *Mayo Clinic Proceedings*, vol. 81, pp. 1575–1578, Elsevier, 2006.

[143] S. S. Chawla, S. K. Kumar, A. Dispenzieri, A. J. Greenberg, D. R. Larson, R. A. Kyle, M. Q. Lacy, M. A. Gertz, and S. V. Rajkumar, "Clinical course and prognosis of non-secretory multiple myeloma," *European journal of haematology*, 2015.

[144] A. Dispenzieri, R. Kyle, G. Merlini, J. Miguel, H. Ludwig, R. Hájek, A. Palumbo, S. Jagannath, J. Bladé, S. Lonial, *et al.*, "International myeloma working group guidelines for serum-free light chain analysis in multiple myeloma and related disorders," *Leukemia*, vol. 23, no. 2, pp. 215–224, 2009.

[145] J. R. Mikhael, D. Dingli, V. Roy, C. B. Reeder, F. K. Buadi, S. R. Hayman, A. Dispenzieri, R. Fonseca, T. Sher, R. A. Kyle, *et al.*, "Management of newly diagnosed symptomatic multiple myeloma: updated mayo stratification of myeloma and risk-adapted therapy (msmart) consensus guidelines 2013," in *Mayo Clinic Proceedings*, vol. 88, pp. 360–376, Elsevier, 2013.

[146] O. Dizdar, I. Barista, U. Kalyoncu, O. Karadag, G. Hascelik, A. Cila, A. Pinar, I. Celik, A. Kars, and G. Tekuzman, "Biochemical markers of bone turnover in diagnosis of myeloma bone disease," *American journal of hematology*, vol. 82, no. 3, pp. 185–191, 2007.

[147] F. Silvestris, L. Lombardi, M. De Matteo, A. Bruno, and F. Dammacco, "Myeloma bone disease: pathogenetic mechanisms and clinical assessment," *Leukemia research*, vol. 31, no. 2, pp. 129–138, 2007.

[148] J. Hillengass, L. Moulopoulos, S. Delorme, V. Koutoulidis, J. Mosebach, T. Hielscher, M. Drake, S. Rajkumar, B. Oestergaard, N. Abildgaard, *et al.*, "Whole-body computed tomography versus conventional skeletal survey in patients with multiple myeloma: a study of the international myeloma working group," *Blood cancer journal*, vol. 7, no. 8, pp. e599–e599, 2017.

[149] B. Durie, A. Hoering, S. V. Rajkumar, M. H. Abidi, J. Epstein, S. P. Kahanic, M. C. Thakuri, F. J. Reu, C. M. Reynolds, R. Sexton, *et al.*, "Bortezomib, lenalidomide and dexamethasone vs. lenalidomide and dexamethasone in patients (pts) with previously untreated multiple myeloma without

an intent for immediate autologous stem cell transplant (asct): results of the randomized phase iii trial swog s0777," *Blood*, vol. 126, no. 23, p. 25, 2015.

[150] M. Attal, V. Lauwers-Cances, C. Hulin, X. Leleu, D. Caillot, M. Escoffre, B. Arnulf, M. Macro, K. Belhadj, L. Garderet, *et al.*, "Lenalidomide, bortezomib, and dexamethasone with transplantation for myeloma," *New England Journal of Medicine*, vol. 376, no. 14, pp. 1311–1320, 2017.

[151] H. Goldschmidt, H. Lokhorst, E. Mai, B. van der Holt, I. Blau, S. Zweegman, K. Weisel, E. Vellenga, M. Pfreundschuh, M. J. Kersten, *et al.*, "Bortezomib before and after high-dose therapy in myeloma: long-term results from the phase iii hovon-65/gmmg-hd4 trial," *Leukemia*, vol. 32, no. 2, pp. 383–390, 2018.

[152] A. Perrot, V. Lauwers-Cances, T. Cazaubiel, T. Facon, D. Caillot, L. Clement-Filliatre, M. Macro, O. Decaux, K. Belhadj, M. Mohty, *et al.*, "Early versus late autologous stem cell transplant in newly diagnosed multiple myeloma: long-term follow-up analysis of the ifm 2009 trial," *Blood*, vol. 136, p. 39, 2020.

[153] B. G. Durie and S. E. Salmon, "A clinical staging system for multiple myeloma correlation of measured myeloma cell mass with presenting clinical features, response to treatment, and survival," *Cancer*, vol. 36, no. 3, pp. 842–854, 1975.

[154] P. R. Greipp, J. S. Miguel, B. G. Durie, J. J. Crowley, B. Barlogie, J. Bladé, M. Boccadoro, J. A. Child, H. Avet-Loiseau, R. A. Kyle, *et al.*, "International staging system for multiple myeloma," *Journal of clinical oncology*, vol. 23, no. 15, pp. 3412–3420, 2005.

[155] P. N. Hari, M.-J. Zhang, V. Roy, W. S. Pérez, A. Bashey, L. B. To, G. Elfenbein, C. O. Freytes, R. P. Gale, J. Gibson, *et al.*, "Is the international staging system superior to the durie–salmon staging system? a comparison in multiple myeloma patients undergoing autologous transplant," *Leukemia*, vol. 23, no. 8, pp. 1528–1534, 2009.

[156] S. K. Kumar, A. Dispenzieri, M. Q. Lacy, M. A. Gertz, F. K. Buadi, S. Pandey, P. Kapoor, D. Dingli, S. R. Hayman, N. Leung, *et al.*, "Continued improvement in survival in multiple myeloma: changes in early mortality and outcomes in older patients," *Leukemia*, vol. 28, no. 5, pp. 1122–1128, 2014.

[157] S. Singhal, J. Mehta, R. Desikan, D. Ayers, P. Roberson, P. Eddlemon, N. Munshi, E. Anaissie, C. Wilson, M. Dhodapkar, *et al.*, "Antitumor activity of thalidomide in refractory multiple myeloma," *New England Journal of Medicine*, vol. 341, no. 21, pp. 1565–1571, 1999.

[158] P. G. Richardson, P. Sonneveld, M. W. Schuster, D. Irwin, E. A. Stadtmauer, T. Facon, J.-L. Harousseau, D. Ben-Yehuda, S. Lonial, H. Goldschmidt, *et al.*, "Bortezomib or high-dose dexamethasone for relapsed multiple myeloma," *New England journal of medicine*, vol. 352, no. 24, pp. 2487–2498, 2005.

[159] S. V. Rajkumar, S. R. Hayman, M. Q. Lacy, A. Dispenzieri, S. M. Geyer, B. Kabat, S. R. Zeldenrust, S. Kumar, P. R. Greipp, R. Fonseca, *et al.*, "Combination therapy with lenalidomide plus dexamethasone (rev/dex) for newly diagnosed myeloma," *Blood*, vol. 106, no. 13, pp. 4050–4053, 2005.

[160] P. G. Richardson, E. Blood, C. S. Mitsiades, S. Jagannath, S. R. Zeldenrust, M. Alsina, R. L. Schlossman, S. V. Rajkumar, K. R. Desikan, T. Hideshima, *et al.*, "A randomized phase 2 study of lenalidomide therapy for patients with relapsed or relapsed and refractory multiple myeloma," *Blood*, vol. 108, no. 10, pp. 3458–3464, 2006.

[161] M. Attal, J.-L. Harousseau, A.-M. Stoppa, J.-J. Sotto, J.-G. Fuzibet, J.-F. Rossi, P. Casassus, H. Maisonneuve, T. Facon, N. Ifrah, *et al.*, "A prospective, randomized trial of autologous bone marrow transplantation and chemotherapy in multiple myeloma," *New England Journal of Medicine*, vol. 335, no. 2, pp. 91–97, 1996.

[162] J. A. Child, G. J. Morgan, F. E. Davies, R. G. Owen, S. E. Bell, K. Hawkins, J. Brown, M. T. Drayson, and P. J. Selby, "High-dose chemotherapy with

hematopoietic stem-cell rescue for multiple myeloma," *New England Journal of Medicine*, vol. 348, no. 19, pp. 1875–1883, 2003.

[163] A. Kumar, T. Loughran, M. Alsina, B. G. Durie, and B. Djulbegovic, "Management of multiple myeloma: a systematic review and critical appraisal of published studies," *The lancet oncology*, vol. 4, no. 5, pp. 293–304, 2003.

[164] M. Cavo, P. Tosi, E. Zamagni, C. Cellini, P. Tacchetti, F. Patriarca, F. Di Raimondo, E. Volpe, S. Ronconi, D. Cangini, *et al.*, "Prospective, randomized study of single compared with double autologous stem-cell transplantation for multiple myeloma: Bologna 96 clinical study," *Journal of clinical oncology*, vol. 25, no. 17, pp. 2434–2441, 2007.

[165] J. Fermand, C. Alberti, and J. Marolleau, "Single versus tandem high dose therapy (hdt) supported with autologous stem cell transplantation using unselected or cd-34-enriched absc: results of a two by two designed randomized trial in 230 young patients with multiple myeloma," *The Hematol J*, vol. 4, no. suppl 1, pp. 559–60, 2003.

[166] H. Goldschmidt, "Single vs. tandem autolgous transplantation in multiple myeloma: the gmmg experience," *Hematol J*, vol. 4, no. Suppl 1, p. S61, 2003.

[167] M. Cavo, F. M. Gay, F. Patriarca, E. Zamagni, V. Montefusco, L. Dozza, M. Galli, S. Bringhen, N. Testoni, M. Grasso, *et al.*, "Double autologous stem cell transplantation significantly prolongs progression-free survival and overall survival in comparison with single autotransplantation in newly diagnosed multiple myeloma: an analysis of phase 3 emn02/ho95 study," *Blood*, vol. 130, p. 401, 2017.

[168] E. A. Stadtmauer, M. C. Pasquini, B. Blackwell, P. Hari, A. Bashey, S. Devine, Y. Efebera, S. Ganguly, C. Gasparetto, N. Geller, *et al.*, "Autologous transplantation, consolidation, and maintenance therapy in multiple myeloma: results of the bmt ctn 0702 trial," *Journal of clinical oncology*, vol. 37, no. 7, p. 589, 2019.

[169] T. Facon, S. Kumar, T. Plesner, R. Z. Orlowski, P. Moreau, N. Bahlis, S. Basu, H. Nahi, C. Hulin, H. Quach, *et al.*, "Daratumumab plus lenalidomide and dexamethasone for untreated myeloma," *New England Journal of Medicine*, vol. 380, no. 22, pp. 2104–2115, 2019.

[170] P. Moreau, C. Hulin, M. Macro, D. Caillot, C. Chaleteix, M. Roussel, L. Garderet, B. Royer, S. Brechignac, M. Tiab, *et al.*, "Vtd is superior to vcd prior to intensive therapy in multiple myeloma: results of the prospective ifm2013-04 trial," *Blood, The Journal of the American Society of Hematology*, vol. 127, no. 21, pp. 2569–2574, 2016.

[171] M.-V. Mateos, A. Oriol, J. Martinez, M. T. Cibeira, N. C. Gutierrez, M. J. Terol, R. de Paz, J. Garcia-Larana, E. Bengoechea, A. M. Garcia-Sancho, *et al.*, "A prospective, multicenter, randomized, trial of bortezomib/melphalan/prednisone (vmp) versus bortezomib/thalidomide/prednisone (vtp) as induction therapy followed by maintenance treatment with bortezomib/thalidomide (vt) versus bortezomib/prednisone (vp) in elderly untreated patients with multiple myeloma older than 65 years.," *Blood*, vol. 114, no. 22, p. 3, 2009.

[172] A. Palumbo, S. Bringhen, D. Rossi, M. Cavalli, A. Larocca, R. Ria, M. Offidani, F. Patriarca, C. Nozzoli, T. Guglielmelli, *et al.*, "Bortezomib-melphalan-prednisone-thalidomide followed by maintenance with bortezomib-thalidomide compared with bortezomib-melphalan-prednisone for initial treatment of multiple myeloma: a randomized controlled trial," *J Clin Oncol*, vol. 28, no. 34, pp. 5101–5109, 2010.

[173] Y.-W. Qiang, Y. Chen, O. Stephens, N. Brown, B. Chen, J. Epstein, B. Barlogie, and J. D. Shaughnessy Jr, "Myeloma-derived dickkopf-1 disrupts wnt-regulated osteoprotegerin and rankl production by osteoblasts: a potential mechanism underlying osteolytic bone lesions in multiple myeloma," *Blood, The Journal of the American Society of Hematology*, vol. 112, no. 1, pp. 196–207, 2008.

[174] M. Fulciniti, P. Tassone, T. Hideshima, S. Vallet, P. Nanjappa, S. A. Ettenberg, Z. Shen, N. Patel, Y.-t. Tai, D. Chauhan, *et al.*, "Anti-dkk1 mab (bhq880) as a potential therapeutic agent for multiple myeloma," *Blood, The Journal of the American Society of Hematology*, vol. 114, no. 2, pp. 371–379, 2009.

[175] P. Moreau, M. Attal, C. Hulin, B. Arnulf, K. Belhadj, L. Benboubker, M. C. Béné, A. Broijl, H. Caillon, D. Caillot, *et al.*, "Bortezomib, thalidomide, and dexamethasone with or without daratumumab before and after autologous stem-cell transplantation for newly diagnosed multiple myeloma (cassiopeia): a randomised, open-label, phase 3 study," *The Lancet*, vol. 394, no. 10192, pp. 29–38, 2019.

[176] P. M. Voorhees, J. L. Kaufman, J. P. Laubach, D. W. Sborov, B. Reeves, C. Rodriguez, A. Chari, R. W. Silbermann, L. J. Costa, L. D. Anderson, *et al.*, "Depth of response to daratumumab (dara), lenalidomide, bortezomib, and dexamethasone (rvd) improves over time in patients (pts) with transplant-eligible newly diagnosed multiple myeloma (ndmm): Griffin study update," *Blood*, vol. 134, p. 691, 2019.

[177] B. Barlogie, E. Anaissie, F. Van Rhee, J. Haessler, K. Hollmig, M. Pineda-Roman, M. Cottler-Fox, A. Mohiuddin, Y. Alsayed, G. Tricot, *et al.*, "Incorporating bortezomib into upfront treatment for multiple myeloma: early results of total therapy 3," *British journal of haematology*, vol. 138, no. 2, pp. 176–185, 2007.

[178] F. van Rhee, J. Szymonifka, E. Anaissie, B. Nair, S. Waheed, Y. Alsayed, N. Petty, J. D. Shaughnessy Jr, A. Hoering, J. Crowley, *et al.*, "Total therapy 3 for multiple myeloma: prognostic implications of cumulative dosing and premature discontinuation of vtd maintenance components, bortezomib, thalidomide, and dexamethasone, relevant to all phases of therapy," *Blood, The Journal of the American Society of Hematology*, vol. 116, no. 8, pp. 1220–1227, 2010.

[179] A. Palumbo, V. Magarotto, S. Bringhen, M. Offidani, G. Pietrantuono, A. M. Liberati, G. Benevolo, A. Ledda, M. Gilestro, M. Galli, *et al.*, "A randomized phase 3 trial of melphalan-lenalidomide-prednisone (mpr) or cyclophosphamide-prednisone-lenalidomide (cpr) vs lenalidomide plus dexamethsone (rd) in elderly newly diagnosed multiple myeloma patients," *Blood*, vol. 122, no. 21, p. 536, 2013.

[180] S. K. Kumar, T. M. Therneau, M. A. Gertz, M. Q. Lacy, A. Dispenzieri, S. V. Rajkumar, R. Fonseca, T. E. Witzig, J. A. Lust, D. R. Larson, *et al.*, "Clinical course of patients with relapsed multiple myeloma," in *Mayo Clinic Proceedings*, vol. 79, pp. 867–874, Elsevier, 2004.

[181] P. Moreau, S. K. Kumar, J. San Miguel, F. Davies, E. Zamagni, N. Bahlis, H. Ludwig, J. Mikhael, E. Terpos, F. Schjesvold, *et al.*, "Treatment of relapsed and refractory multiple myeloma: recommendations from the international myeloma working group," *The Lancet Oncology*, vol. 22, no. 3, pp. e105–e118, 2021.

[182] S. Kumar, J. H. Lee, J. J. Lahuerta, G. Morgan, P. G. Richardson, J. Crowley, J. Haessler, J. Feather, A. Hoering, P. Moreau, *et al.*, "Risk of progression and survival in multiple myeloma relapsing after therapy with imids and bortezomib: a multicenter international myeloma working group study," *Leukemia*, vol. 26, no. 1, pp. 149–157, 2012.

[183] M. Pineda-Roman, M. Zangari, F. Van Rhee, E. Anaissie, J. Szymonifka, A. Hoering, N. Petty, J. Crowley, J. Shaughnessy, J. Epstein, *et al.*, "Vtd combination therapy with bortezomib–thalidomide–dexamethasone is highly effective in advanced and refractory multiple myeloma," *Leukemia*, vol. 22, no. 7, pp. 1419–1427, 2008.

[184] P. G. Richardson, E. Weller, S. Jagannath, D. E. Avigan, M. Alsina, R. L. Schlossman, A. Mazumder, N. C. Munshi, I. M. Ghobrial, D. Doss, *et al.*, "Multicenter, phase i, dose-escalation trial of lenalidomide plus bortezomib for relapsed and relapsed/refractory multiple myeloma," *Journal of Clinical Oncology*, vol. 27, no. 34, p. 5713, 2009.

[185] H. M. Lokhorst, T. Plesner, J. P. Laubach, H. Nahi, P. Gimsing, M. Hansson, M. C. Minnema, U. Lassen, J. Krejcik, A. Palumbo, *et al.*, "Targeting cd38 with daratumumab monotherapy in multiple myeloma," *New England Journal of Medicine*, vol. 373, no. 13, pp. 1207–1219, 2015.

[186] M. S. L. Brendan, B. M. Weiss, S. Z. Usmani, *et al.*, "Single-agent daratumumab in heavily pre-treated patients with multiple myeloma: an open-label, international, multicentre phase 2 trial (sirius)," *The Lancet*, vol. 387, no. 10027, pp. 1551–1560, 2016.

[187] S. V. Rajkumar and R. A. Kyle, "Progress in myeloma—a monoclonal breakthrough," 2016.

[188] A. K. Stewart, S. V. Rajkumar, M. A. Dimopoulos, T. Masszi, I. Špička, A. Oriol, R. Hájek, L. Rosiñol, D. S. Siegel, G. G. Mihaylov, *et al.*, "Carfilzomib, lenalidomide, and dexamethasone for relapsed multiple myeloma," *New England Journal of Medicine*, vol. 372, no. 2, pp. 142–152, 2015.

[189] M. A. Dimopoulos, P. Moreau, A. Palumbo, D. Joshua, L. Pour, R. Hájek, T. Facon, H. Ludwig, A. Oriol, H. Goldschmidt, *et al.*, "Carfilzomib and dexamethasone versus bortezomib and dexamethasone for patients with relapsed or refractory multiple myeloma (endeavor): a randomised, phase 3, open-label, multicentre study," *The Lancet Oncology*, vol. 17, no. 1, pp. 27–38, 2016.

[190] M. A. Dimopoulos, H. Goldschmidt, R. Niesvizky, D. Joshua, W.-J. Chng, A. Oriol, R. Z. Orlowski, H. Ludwig, T. Facon, R. Hajek, *et al.*, "Carfilzomib or bortezomib in relapsed or refractory multiple myeloma (endeavor): an interim overall survival analysis of an open-label, randomised, phase 3 trial," *The Lancet Oncology*, vol. 18, no. 10, pp. 1327–1337, 2017.

[191] M. Q. Lacy, S. R. Hayman, M. A. Gertz, A. Dispenzieri, F. Buadi, S. Kumar, P. R. Greipp, J. A. Lust, S. J. Russell, D. Dingli, *et al.*, "Pomalidomide (cc4047) plus low-dose dexamethasone as therapy for relapsed multiple myeloma," *J Clin Oncol*, vol. 27, no. 30, pp. 5008–5014, 2009.

[192] M. Lacy, S. Hayman, M. Gertz, K. Short, A. Dispenzieri, S. Kumar, P. Greipp, J. Lust, S. Russell, D. Dingli, *et al.*, "Pomalidomide (cc4047) plus low dose dexamethasone (pom/dex) is active and well tolerated in lenalidomide refractory multiple myeloma (mm)," *Leukemia*, vol. 24, no. 11, pp. 1934–1939, 2010.

[193] S. Lonial, M. Dimopoulos, A. Palumbo, D. White, S. Grosicki, I. Spicka, A. Walter-Croneck, P. Moreau, M.-V. Mateos, H. Magen, *et al.*, "Elotuzumab therapy for relapsed or refractory multiple myeloma," *New England Journal of Medicine*, vol. 373, no. 7, pp. 621–631, 2015.

[194] P. Moreau, T. Masszi, N. Grzasko, N. J. Bahlis, M. Hansson, L. Pour, I. Sandhu, P. Ganly, B. W. Baker, S. R. Jackson, *et al.*, "Oral ixazomib, lenalidomide, and dexamethasone for multiple myeloma," *New England Journal of Medicine*, vol. 374, no. 17, pp. 1621–1634, 2016.

[195] S. K. Kumar, J. G. Berdeja, R. Niesvizky, S. Lonial, J. P. Laubach, M. Hamadani, A. K. Stewart, P. Hari, V. Roy, R. Vescio, *et al.*, "Safety and tolerability of ixazomib, an oral proteasome inhibitor, in combination with lenalidomide and dexamethasone in patients with previously untreated multiple myeloma: an open-label phase 1/2 study," *The Lancet Oncology*, vol. 15, no. 13, pp. 1503–1512, 2014.

[196] S. Grosicki, M. Simonova, I. Spicka, L. Pour, I. Kriachok, M. Gavriatopoulou, H. Pylypenko, H. W. Auner, X. Leleu, V. Doronin, *et al.*, "Once-per-week selinexor, bortezomib, and dexamethasone versus twice-per-week bortezomib and dexamethasone in patients with multiple myeloma (boston): a randomised, open-label, phase 3 trial," *The Lancet*, vol. 396, no. 10262, pp. 1563–1573, 2020.

[197] A. Chari, D. T. Vogl, M. Gavriatopoulou, A. K. Nooka, A. J. Yee, C. A. Huff, P. Moreau, D. Dingli, C. Cole, S. Lonial, *et al.*, "Oral selinexor–dexamethasone for triple-class refractory multiple myeloma," *New England Journal of Medicine*, vol. 381, no. 8, pp. 727–738, 2019.

[198] L. J. Van't Veer, H. Dai, M. J. Van De Vijver, Y. D. He, A. A. Hart, M. Mao, H. L. Peterse, K. Van Der Kooy, M. J. Marton, A. T. Witteveen, *et al.*, "Gene expression profiling predicts clinical outcome of breast cancer," *nature*, vol. 415, no. 6871, pp. 530–536, 2002.

[199] S. Kumar, J. L. Kaufman, C. Gasparetto, J. Mikhael, R. Vij, B. Pegourie, L. Benboubker, T. Facon, M. Amiot, P. Moreau, *et al.*, "Efficacy of venetoclax as targeted therapy for relapsed/refractory t (11; 14) multiple myeloma," *Blood, The Journal of the American Society of Hematology*, vol. 130, no. 22, pp. 2401–2409, 2017.

[200] S. Kumar and S. V. Rajkumar, "Surrogate endpoints in randomised controlled trials: a reality check," *The Lancet*, vol. 394, no. 10195, pp. 281–283, 2019.

[201] N. Raje, J. Berdeja, Y. Lin, D. Siegel, S. Jagannath, D. Madduri, M. Liedtke, J. Rosenblatt, M. V. Maus, A. Turka, *et al.*, "Anti-bcma car t-cell therapy bb2121 in relapsed or refractory multiple myeloma," *New England Journal of Medicine*, vol. 380, no. 18, pp. 1726–1737, 2019.

[202] S. Lonial, H. C. Lee, A. Badros, S. Trudel, A. K. Nooka, A. Chari, A.-O. Abdallah, N. Callander, N. Lendvai, D. Sborov, *et al.*, "Belantamab mafodotin for relapsed or refractory multiple myeloma (dreamm-2): a two-arm, randomised, open-label, phase 2 study," *The lancet oncology*, vol. 21, no. 2, pp. 207–221, 2020.

[203] K. O. Alfarouk, C.-M. Stock, S. Taylor, M. Walsh, A. K. Muddathir, D. Verduzco, A. H. Bashir, O. Y. Mohammed, G. O. Elhassan, S. Harguindey, *et al.*, "Resistance to cancer chemotherapy: failure in drug response from adme to p-gp," *Cancer cell international*, vol. 15, no. 1, pp. 1–13, 2015.

[204] D. R. Camidge, W. Pao, and L. V. Sequist, "Acquired resistance to tkis in solid tumours: learning from lung cancer," *Nature reviews Clinical oncology*, vol. 11, no. 8, pp. 473–481, 2014.

[205] M. R. Stratton, P. J. Campbell, and P. A. Futreal, "The cancer genome," *Nature*, vol. 458, no. 7239, pp. 719–724, 2009.

[206] N. Wald, "Guidance on terminology," *Journal of medical screening*, vol. 1, no. 2, pp. 139–139, 1994.

[207] B. Budowle and A. Van Daal, "Extracting evidence from forensic dna analyses: future molecular biology directions," *Biotechniques*, vol. 46, no. 5, pp. 339–350, 2009.

[208] A. Ziegler, A. Koch, K. Krockenberger, and A. Großhennig, "Personalized medicine using dna biomarkers: a review," *Human genetics*, vol. 131, pp. 1627–1638, 2012.

[209] C. Greenman, P. Stephens, R. Smith, G. L. Dalgliesh, C. Hunter, G. Bignell, H. Davies, J. Teague, A. Butler, C. Stevens, *et al.*, "Patterns of somatic mutation in human cancer genomes," *Nature*, vol. 446, no. 7132, pp. 153–158, 2007.

[210] M. Goozner, "Duke scandal highlights need for genomics research criteria," 2011.

[211] H. Erichsen and S. Chanock, "Snps in cancer research and treatment," *British journal of cancer*, vol. 90, no. 4, pp. 747–751, 2004.

[212] B. M. Heckman-Stoddard, "Oncology biomarkers: discovery, validation, and clinical use," in *Seminars in oncology nursing*, vol. 28, pp. 93–98, Elsevier, 2012.

[213] J. T. Leek, R. D. Peng, and R. R. Anderson, "Keep a way open for tailored treatments," *Nature*, vol. 484, no. 7394, pp. 318–318, 2012.

[214] R. Rouzier, L. Pusztai, S. Delaloge, A. M. Gonzalez-Angulo, F. Andre, K. R. Hess, A. U. Buzdar, J.-R. Garbay, M. Spielmann, M.-C. Mathieu, *et al.*, "Nomograms to predict pathologic complete response and metastasis-free survival after preoperative chemotherapy for breast cancer," *Journal of Clinical Oncology*, vol. 23, no. 33, pp. 8331–8339, 2005.

[215] M. Kalia, "Biomarkers for personalized oncology: recent advances and future challenges," *Metabolism*, vol. 64, no. 3, pp. S16–S21, 2015.

[216] D. G. Altman, L. M. McShane, W. Sauerbrei, and S. E. Taube, "Reporting recommendations for tumor marker prognostic studies (remark): explanation and elaboration," *BMC medicine*, vol. 10, no. 1, pp. 1–39, 2012.

[217] R. Simon, "Clinical trial designs for evaluating the medical utility of prognostic and predictive biomarkers in oncology," *Personalized medicine*, vol. 7, no. 1, pp. 33–47, 2010.

[218] R. Simon and S. Roychowdhury, "Implementing personalized cancer genomics in clinical trials," *Nature reviews Drug discovery*, vol. 12, no. 5, pp. 358–369, 2013.

[219] D. R. Parkinson, R. T. McCormack, S. M. Keating, S. I. Gutman, S. R. Hamilton, E. A. Mansfield, M. A. Piper, P. DeVerka, F. W. Frueh, J. M. Jessup, *et al.*, "Evidence of clinical utility: an unmet need in molecular diagnostics for patients with cancer," *Clinical Cancer Research*, vol. 20, no. 6, pp. 1428–1444, 2014.

[220] Y. Hoshida, A. Villanueva, A. Sangiovanni, M. Sole, C. Hur, K. L. Andersson, R. T. Chung, J. Gould, K. Kojima, S. Gupta, *et al.*, "Prognostic gene expression signature for patients with hepatitis c–related early-stage cirrhosis," *Gastroenterology*, vol. 144, no. 5, pp. 1024–1030, 2013.

[221] M. Nair, S. Singh Sandhu, and A. K Sharma, "Prognostic and predictive biomarkers in cancer," *Current cancer drug targets*, vol. 14, no. 5, pp. 477–504, 2014.

[222] E. Nalejska, E. Maczyńska, and M. A. Lewandowska, "Prognostic and predictive biomarkers: tools in personalized oncology," *Molecular diagnosis & therapy*, vol. 18, pp. 273–284, 2014.

[223] J. Cui, A. C. Antoniou, G. S. Dite, M. C. Southey, D. J. Venter, D. F. Easton, G. G. Giles, M. R. McCredie, and J. L. Hopper, "After brca1 and brca2—what next? multifactorial segregation analyses of three-generation, population-based australian families affected by female breast cancer," *The American Journal of Human Genetics*, vol. 68, no. 2, pp. 420–431, 2001.

[224] M. Gong, W. Dong, Z. Shi, Y. Xu, W. Ni, and R. An, "Genetic polymorphisms of gstm1, gstt1, and gstp1 with prostate cancer risk: a meta-analysis of 57 studies," *PLoS One*, vol. 7, no. 11, p. e50587, 2012.

[225] A. Plawski and R. Slomski, "Apc gene mutations causing familial adenomatous polyposis in polish patients," *Journal of applied genetics*, vol. 49, pp. 407–414, 2008.

[226] J. Bueno-de Mesquita, S. Linn, R. Keijzer, J. Wesseling, D. Nuyten, C. Van Krimpen, C. Meijers, P. De Graaf, M. Bos, A. Hart, *et al.*, "Validation of 70-gene prognosis signature in node-negative breast cancer," *Breast cancer research and treatment*, vol. 117, pp. 483–495, 2009.

[227] M. Kittaneh, A. J. Montero, and S. Glück, "Molecular profiling for breast cancer: a comprehensive review," *Biomarkers in cancer*, vol. 5, pp. BIC–S9455, 2013.

[228] M. Mego, S. A. Mani, and M. Cristofanilli, "Molecular mechanisms of metastasis in breast cancer—clinical applications," *Nature reviews Clinical oncology*, vol. 7, no. 12, pp. 693–701, 2010.

[229] J. A. DiMasi, R. W. Hansen, and H. G. Grabowski, "The price of innovation: new estimates of drug development costs," *Journal of health economics*, vol. 22, no. 2, pp. 151–185, 2003.

[230] M. Rudrapal, S. J. Khairnar, and A. G. Jadhav, "Drug repurposing (dr): an emerging approach in drug discovery," *Drug repurposing-hypothesis, molecular aspects and therapeutic applications*, vol. 10, 2020.

[231] H. A. Ghofrani, I. H. Osterloh, and F. Grimminger, "Sildenafil: from angina to erectile dysfunction to pulmonary hypertension and beyond," *Nature reviews Drug discovery*, vol. 5, no. 8, pp. 689–702, 2006.

[232] M. Rahmat, R. Sklavenitis Pistofidis, and I. M. Ghobrial, "Repositioning the repurposed drug, a structural study of thalidomide analogs," *The Hematologist*, vol. 16, no. 3, 2019.

[233] T. I. Oprea, J. E. Bauman, C. G. Bologa, T. Buranda, A. Chigaev, B. S. Edwards, J. W. Jarvik, H. D. Gresham, M. K. Haynes, B. Hjelle, *et al.*, "Drug repurposing from an academic perspective," *Drug Discovery Today: Therapeutic Strategies*, vol. 8, no. 3-4, pp. 61–69, 2011.

[234] C. J. Hoban, P. Kidd, S. Jewell, T. Monroe, S. Khoo, D. Rohrer, J. Levy, B. Harrison, S. Lonial, J. Keats, *et al.*, "The mmrf commpasssm study: A prospective, longitudinal, multicenter observational study in newly diagnosed multiple myeloma patients to assess the relationship between patient outcomes, treatment regimens and molecular profiles," *Cancer Research*, vol. 72, no. 8_Supplement, pp. 4561–4561, 2012.

[235] H. M. Berman, J. Westbrook, Z. Feng, G. Gilliland, T. N. Bhat, H. Weissig, I. N. Shindyalov, and P. E. Bourne, "The protein data bank," *Nucleic acids research*, vol. 28, no. 1, pp. 235–242, 2000.

[236] D. S. Wishart, Y. D. Feunang, A. C. Guo, E. J. Lo, A. Marcu, J. R. Grant, T. Sajed, D. Johnson, C. Li, Z. Sayeeda, *et al.*, "Drugbank 5.0: a major update to the drugbank database for 2018," *Nucleic acids research*, vol. 46, no. D1, pp. D1074–D1082, 2018.

[237] R. R Core Team *et al.*, "R: A language and environment for statistical computing," 2013.

[238] G. Sturm, F. Finotello, F. Petitprez, J. D. Zhang, J. Baumbach, W. H. Fridman, M. List, and T. Aneichyk, "Comprehensive evaluation of transcriptome-based cell-type quantification methods for immuno-oncology," *Bioinformatics*, vol. 35, no. 14, pp. i436–i445, 2019.

[239] F. Finotello, C. Mayer, C. Plattner, G. Laschober, D. Rieder, H. Hackl, A. Krogsdam, Z. Loncova, W. Posch, D. Wilflingseder, *et al.*, "Molecular and pharmacological modulators of the tumor immune contexture revealed by deconvolution of rna-seq data," *Genome medicine*, vol. 11, no. 1, pp. 1–20, 2019.

[240] B. Etienne and A. De Reynies, "R package mcpcounter v1.1," 09 2016.

[241] M. I. Love, W. Huber, and S. Anders, "Moderated estimation of fold change and dispersion for rna-seq data with deseq2," *Genome biology*, vol. 15, no. 12, pp. 1–21, 2014.

[242] K. Blighe, S. Rana, and M. Lewis, "Enhancedvolcano: Publication-ready volcano plots with enhanced colouring and labeling," *R package version*, vol. 1, no. 0, 2019.

[243] A. Garcia-Moreno, R. López-Domínguez, J. A. Villatoro-García, A. Ramirez-Mena, E. Aparicio-Puerta, M. Hackenberg, A. Pascual-Montano, and P. Carmona-Saez, "Functional enrichment analysis of regulatory elements," *Biomedicines*, vol. 10, no. 3, p. 590, 2022.

[244] P. Shannon, A. Markiel, O. Ozier, N. S. Baliga, J. T. Wang, D. Ramage, N. Amin, B. Schwikowski, and T. Ideker, "Cytoscape: a software environment for integrated models of biomolecular interaction networks," *Genome research*, vol. 13, no. 11, pp. 2498–2504, 2003.

[245] C.-H. Chin, S.-H. Chen, H.-H. Wu, C.-W. Ho, M.-T. Ko, and C.-Y. Lin, "cytohubba: identifying hub objects and sub-networks from complex interactome," *BMC systems biology*, vol. 8, no. 4, pp. 1–7, 2014.

[246] D. J. Rigden and X. M. ndez, "The 2022 Nucleic Acids Research database issue and the online molecular biology database collection," *Nucleic Acids Res*, vol. 50, pp. D1–D10, Jan 2022.

[247] B. Webb and A. Sali, "Comparative protein structure modeling using modeller," *Current protocols in bioinformatics*, vol. 54, no. 1, pp. 5–6, 2016.

[248] M. A. Martí-Renom, A. C. Stuart, A. Fiser, R. Sánchez, F. Melo, and A. Šali, "Comparative protein structure modeling of genes and genomes," *Annual review of biophysics and biomolecular structure*, vol. 29, no. 1, pp. 291–325, 2000.

[249] A. Šali and T. L. Blundell, "Comparative protein modelling by satisfaction of spatial restraints," *Journal of molecular biology*, vol. 234, no. 3, pp. 779–815, 1993.

[250] A. Fiser, R. K. G. Do, and A. Šali, "Modeling of loops in protein structures," *Protein science*, vol. 9, no. 9, pp. 1753–1773, 2000.

[251] J. Jumper, R. Evans, A. Pritzel, T. Green, M. Figurnov, O. Ronneberger, K. Tunyasuvunakool, R. Bates, A. Žídek, A. Potapenko, *et al.*, "Highly accurate protein structure prediction with alphafold," *Nature*, vol. 596, no. 7873, pp. 583–589, 2021.

[252] R. Wu, F. Ding, R. Wang, R. Shen, X. Zhang, S. Luo, C. Su, Z. Wu, Q. Xie, B. Berger, *et al.*, "High-resolution de novo structure prediction from primary sequence," *BioRxiv*, pp. 2022–07, 2022.

[253] T. E. Lewis, I. Sillitoe, A. Andreeva, T. L. Blundell, D. W. Buchan, C. Chothia, D. Cozzetto, J. M. Dana, I. Filippis, J. Gough, *et al.*, "Genome3d: exploiting structure to help users understand their sequences," *Nucleic Acids Research*, vol. 43, no. D1, pp. D382–D386, 2015.

[254] E. F. Pettersen, T. D. Goddard, C. C. Huang, G. S. Couch, D. M. Greenblatt, E. C. Meng, and T. E. Ferrin, "Ucsf chimera?a visualization system for exploratory research and analysis," *Journal of computational chemistry*, vol. 25, no. 13, pp. 1605–1612, 2004.

[255] C. Colovos and T. O. Yeates, "Verification of protein structures: patterns of nonbonded atomic interactions," *Protein science*, vol. 2, no. 9, pp. 1511–1519, 1993.

[256] M. J. Sippl, "Recognition of errors in three-dimensional structures of proteins," *Proteins: Structure, Function, and Bioinformatics*, vol. 17, no. 4, pp. 355–362, 1993.

[257] M. Wiederstein and M. J. Sippl, "Prosa-web: interactive web service for the recognition of errors in three-dimensional structures of proteins," *Nucleic acids research*, vol. 35, no. suppl_2, pp. W407–W410, 2007.

[258] P. Benkert, M. Biasini, and T. Schwede, "Toward the estimation of the absolute quality of individual protein structure models," *Bioinformatics*, vol. 27, no. 3, pp. 343–350, 2011.

[259] R. Fraczkiewicz and W. Braun, "Exact and efficient analytical calculation of the accessible surface areas and their gradients for macromolecules," *Journal of computational chemistry*, vol. 19, no. 3, pp. 319–333, 1998.

[260] L. Schrödinger and W. DeLano, "Pymol."

[261] J. Eberhardt, D. Santos-Martins, A. F. Tillack, and S. Forli, "Autodock vina 1.2.0: New docking methods, expanded force field, and python bindings," *Journal of chemical information and modeling*, vol. 61, no. 8, pp. 3891–3898, 2021.

[262] O. Trott and A. J. Olson, "Autodock vina: improving the speed and accuracy of docking with a new scoring function, efficient optimization, and multithreading," *Journal of computational chemistry*, vol. 31, no. 2, pp. 455–461, 2010.

[263] X. Ren and P. F. Kuan, "Rnaagecalc: A multi-tissue transcriptional age calculator," *PLoS One*, vol. 15, no. 8, p. e0237006, 2020.

[264] J. Wang, Y. Hu, H. Hamidi, C. Dos Santos, J. Zhang, E. Punnoose, and W. Li, "Immune microenvironment characteristics in multiple myeloma progression from transcriptome profiling," *Frontiers in Oncology*, vol. 12, p. 948548, 2022.

[265] C. Rosales, "Neutrophil: a cell with many roles in inflammation or several cell types?," *Frontiers in physiology*, vol. 9, p. 113, 2018.

[266] N. Parrinello, A. Romano, C. Conticello, M. Cavalli, A. La Fauci, G. Rizzo, P. La Cava, A. Chiarenza, D. Tibullo, C. Giallongo, *et al.*, "Neutrophils of multiple myeloma are dysfunctional and immunosuppressive," *Blood*, vol. 122, no. 21, p. 3138, 2013.

[267] A. Romano, N. Parrinello, V. Simeon, F. Puglisi, P. La Cava, C. Bellofiore, C. Giallongo, G. Camiolo, F. D'Auria, V. Grieco, *et al.*, "High-density neutrophils in mgus and multiple myeloma are dysfunctional and immune-suppressive due to increased stat3 downstream signaling," *Scientific reports*, vol. 10, no. 1, p. 1983, 2020.

[268] N. R. Maimela, S. Liu, and Y. Zhang, "Fates of cd8+ t cells in tumor microenvironment," *Computational and structural biotechnology journal*, vol. 17, pp. 1–13, 2019.

[269] L. Xu, W. Yu, H. Xiao, and K. Lin, "Birc5 is a prognostic biomarker associated with tumor immune cell infiltration," *Scientific Reports*, vol. 11, no. 1, p. 390, 2021.

[270] M. Deng, M. R. Aberle, A. A. van Bijnen, G. van der Kroft, K. Lenaerts, U. P. Neumann, G. Wiltberger, F. G. Schaap, S. W. Olde Damink, and S. S. Rensen, "Lipocalin-2 and neutrophil activation in pancreatic cancer cachexia," *Frontiers in Immunology*, vol. 14, p. 1159411, 2023.

[271] D. Ragusa, S. Tosi, and C. Sisu, "Pan-cancer analysis identifies mnx1 and associated antisense transcripts as biomarkers for cancer," *Cells*, vol. 11, no. 22, p. 3577, 2022.

[272] T. Nilsson, A. Waraky, A. Östlund, S. Li, A. Staffas, J. Asp, L. Fogelstrand, J. Abrahamsson, and L. Palmqvist, "An induced pluripotent stem cell t (7; 12)(q36; p13) acute myeloid leukemia model shows high expression of mnx1 and a block in differentiation of the erythroid and megakaryocytic lineages," *International Journal of Cancer*, vol. 151, no. 5, pp. 770–782, 2022.

[273] X. Yang, Q. Pan, Y. Lu, X. Jiang, S. Zhang, and J. Wu, "Mnx1 promotes cell proliferation and activates wnt/β-catenin signaling in colorectal cancer," *Cell biology international*, vol. 43, no. 4, pp. 402–408, 2019.

[274] C. De Bock, A. Ardjmand, T. Molloy, S. Bone, D. Johnstone, D. Campbell, K. Shipman, T. Yeadon, J. Holst, M. Spanevello, *et al.*, "The fat1 cadherin is overexpressed and an independent prognostic factor for survival in paired diagnosis–relapse samples of precursor b-cell acute lymphoblastic leukemia," *Leukemia*, vol. 26, no. 5, pp. 918–926, 2012.

[275] Z. G. Chen, N. F. Saba, and Y. Teng, "The diverse functions of fat1 in cancer progression: good, bad, or ugly?," *Journal of Experimental & Clinical Cancer Research*, vol. 41, no. 1, p. 248, 2022.

[276] S. Liebig, M. Neumann, P. Silva, J. Ortiz-Tanchez, V. Schulze, K. Isaakidis, C. Schlee, M. P. Schroeder, T. Beder, L. G. Morris, *et al.*, "Fat1 expression in t-cell acute lymphoblastic leukemia (t-all) modulates proliferation and wnt signaling," *Scientific Reports*, vol. 13, no. 1, p. 972, 2023.

[277] P. Adamo and M. Ladomery, "The oncogene erg: a key factor in prostate cancer," *Oncogene*, vol. 35, no. 4, pp. 403–414, 2016.

[278] E. Khosh Kish, M. Choudhry, Y. Gamallat, S. M. Buharideen, and T. A. Bismar, "The expression of proto-oncogene ets-related gene (erg) plays a central role in the oncogenic mechanism involved in the development and progression of prostate cancer," *International Journal of Molecular Sciences*, vol. 23, no. 9, p. 4772, 2022.

[279] W. Zhou, Y. Su, Y. Zhang, B. Han, H. Liu, and X. Wang, "Endothelial cells promote docetaxel resistance of prostate cancer cells by inducing erg expression and activating akt/mtor signaling pathway," *Frontiers in Oncology*, vol. 10, p. 584505, 2020.

[280] F. Paduano, E. Gaudio, A. A. Mensah, S. Pinton, F. Bertoni, and F. Trapasso, "T-cell leukemia/lymphoma 1 (tcl1): an oncogene regulating multiple signaling pathways," *Frontiers in oncology*, vol. 8, p. 317, 2018.

[281] J. Stachelscheid, Q. Jiang, C. Aszyk, K. Warner, N. Bley, T. Müller, O. Vydzhak, K. Symeonidis, G. Crispatzu, P. Mayer, *et al.*, "The proto-oncogene tcl1a deregulates cell cycle and genomic stability in cll," *Blood, The Journal of the American Society of Hematology*, vol. 141, no. 12, pp. 1425–1441, 2023.

[282] H. Li, X. Yan, L. Liu, L. Huang, M. Yin, C. Pan, P. Zhang, and H. Qin, "T-cell leukemia/lymphoma-1a predicts the clinical outcome for patients with stage ii/iii colorectal cancer," *Biomedicine & Pharmacotherapy*, vol. 88, pp. 924–930, 2017.

[283] Y. Shi, Y. Zhao, Y. Zhang, N. AiErken, N. Shao, R. Ye, Y. Lin, and S. Wang, "Aff3 upregulation mediates tamoxifen resistance in breast cancers," *Journal of Experimental & Clinical Cancer Research*, vol. 37, pp. 1–10, 2018.

[284] Q. Yan, X. Qin, J. Liu, Y. Zeng, S. Long, W. Liu, *et al.*, "High expression of affs is related to prognosis of acute myeloid leukemia," 2021.

[285] Y. Zeng, X. Zhang, F. Li, Y. Wang, and M. Wei, "Aff3 is a novel prognostic biomarker and a potential target for immunotherapy in gastric cancer," *Journal of Clinical Laboratory Analysis*, vol. 36, no. 6, p. e24437, 2022.

[286] A. D. Cox and C. J. Der, "Ras history: The saga continues," *Small GTPases*, vol. 1, no. 1, pp. 2–27, 2010.

[287] J. Corre, A. Cleynen, S. Robiou du Pont, L. Buisson, N. Bolli, M. Attal, N. Munshi, and H. Avet-Loiseau, "Multiple myeloma clonal evolution in homogeneously treated patients," *Leukemia*, vol. 32, no. 12, pp. 2636–2647, 2018.

[288] A. Sacco, C. Federico, K. Todoerti, B. Ziccheddu, V. Palermo, A. Giacomini, C. Ravelli, F. Maccarinelli, G. Bianchi, A. Belotti, *et al.*, "Specific targeting of the kras mutational landscape in myeloma as a tool to unveil the elicited antitumor activity," *Blood, The Journal of the American Society of Hematology*, vol. 138, no. 18, pp. 1705–1720, 2021.

[289] Y. Hu, W. Chen, and J. Wang, "Progress in the identification of gene mutations involved in multiple myeloma," *OncoTargets and therapy*, vol. 12, p. 4075, 2019.

[290] A. D. Cox, S. W. Fesik, A. C. Kimmelman, J. Luo, and C. J. Der, "Drugging the undruggable ras: Mission possible?," *Nature reviews Drug discovery*, vol. 13, no. 11, pp. 828–851, 2014.

[291] G. A. Hobbs, N. M. Baker, A. M. Miermont, R. D. Thurman, M. Pierobon, T. H. Tran, A. O. Anderson, A. M. Waters, J. N. Diehl, B. Papke, *et al.*, "Atypical krasg12r mutant is impaired in pi3k signaling and macropinocytosis in pancreatic cancer," *Cancer discovery*, vol. 10, no. 1, pp. 104–123, 2020.

[292] C. J. Weaver and J. D. Tariman, "Multiple myeloma genomics: a systematic review," in *Seminars in oncology nursing*, vol. 33, pp. 237–253, Elsevier, 2017.

[293] C. Li, A. Vides, D. Kim, J. Y. Xue, Y. Zhao, and P. Lito, "The g protein signaling regulator rgs3 enhances the gtpase activity of kras," *Science*, vol. 374, no. 6564, pp. 197–201, 2021.

[294] Y.-Y. Shi, X.-T. Meng, Y.-N. Xu, and X.-J. Tian, "Role of foxo protein's abnormal activation through pi3k/akt pathway in platinum resistance of ovarian cancer," *Journal of Obstetrics and Gynaecology Research*, vol. 47, no. 6, pp. 1946–1957, 2021.

[295] L. Wang, N. Lin, and Y. Li, "The pi3k/akt signaling pathway regulates abcg2 expression and confers resistance to chemotherapy in human multiple myeloma," *Oncology reports*, vol. 41, no. 3, pp. 1678–1690, 2019.

[296] V. Ramakrishnan and S. Kumar, "Pi3k/akt/mtor pathway in multiple myeloma: from basic biology to clinical promise," *Leukemia & lymphoma*, vol. 59, no. 11, pp. 2524–2534, 2018.

[297] T.-M. Hong, Y.-L. Chen, Y.-Y. Wu, A. Yuan, Y.-C. Chao, Y.-C. Chung, M.-H. Wu, S.-C. Yang, S.-H. Pan, J.-Y. Shih, *et al.*, "Targeting neuropilin 1 as an antitumor strategy in lung cancer," *Clinical Cancer Research*, vol. 13, no. 16, pp. 4759–4768, 2007.

[298] S. Chida, H. Okayama, M. Noda, K. Saito, T. Nakajima, K. Aoto, S. Hayase, T. Momma, S. Ohki, K. Kono, *et al.*, "Stromal vcan expression as a potential prognostic biomarker for disease recurrence in stage ii–iii colon cancer," *Carcinogenesis*, vol. 37, no. 9, pp. 878–887, 2016.

[299] Y. Wang, W. Li, X. Jin, X. Jiang, S. Guo, F. Xu, X. Su, G. Wang, Z. Zhao, and X. Gu, "Identification of prognostic immune-related gene signature associated with tumor microenvironment of colorectal cancer," *BMC cancer*, vol. 21, pp. 1–15, 2021.

[300] K. Misawa, T. Kanazawa, A. Imai, S. Endo, D. Mochizuki, H. Fukushima, Y. Misawa, and H. Mineta, "Prognostic value of type xxii and xxiv collagen mrna expression in head and neck cancer patients," *Molecular and clinical oncology*, vol. 2, no. 2, pp. 285–291, 2014.

[301] D. K. Lung, R. M. Reese, and E. T. Alarid, "Intrinsic and extrinsic factors governing the transcriptional regulation of esr1," *Hormones and Cancer*, vol. 11, no. 3-4, pp. 129–147, 2020.

[302] Y. Shi, Y. Zhao, Y. Zhang, N. AiErken, N. Shao, R. Ye, Y. Lin, and S. Wang, "Aff3 upregulation mediates tamoxifen resistance in breast cancers," *Journal of Experimental & Clinical Cancer Research*, vol. 37, pp. 1–10, 2018.

[303] Y. K. Babal, B. Kandemir, and I. A. Kurnaz, "Gene regulatory network of ets domain transcription factors in different stages of glioma," *Journal of Personalized Medicine*, vol. 11, no. 2, p. 138, 2021.

[304] Z. Peng, Y. Gong, and X. Liang, "Role of fat1 in health and disease," *Oncology letters*, vol. 21, no. 5, pp. 1–13, 2021.

[305] S. Li, A. Balmain, and C. M. Counter, "A model for ras mutation patterns in cancers: finding the sweet spot," *Nature Reviews Cancer*, vol. 18, no. 12, pp. 767–777, 2018.

[306] A. Rusu, C. Tanase, G.-A. Pascu, and N. Todoran, "Recent advances regarding the therapeutic potential of adapalene," *Pharmaceuticals*, vol. 13, no. 9, p. 217, 2020.

[307] L. E. Millikan, "Adapalene: an update on newer comparative studies between the various retinoids," *International journal of dermatology*, vol. 39, no. 10, pp. 784–788, 2000.

[308] X.-N. Shi, H. Li, H. Yao, X. Liu, L. Li, K.-S. Leung, H.-F. Kung, and M. C.-M. Lin, "Adapalene inhibits the activity of cyclin-dependent kinase 2 in colorectal carcinoma," *Molecular medicine reports*, vol. 12, no. 5, pp. 6501–6508, 2015.

[309] D. Simoni and M. Tolomeo, "Retinoids, apoptosis and cancer," *Current pharmaceutical design*, vol. 7, no. 17, pp. 1823–1837, 2001.

[310] M. Ocker, C. Herold, M. Ganslmayer, S. Zopf, E. G. Hahn, and D. Schuppan, "Potentiated anticancer effects on hepatoma cells by the retinoid adapalene," *Cancer letters*, vol. 208, no. 1, pp. 51–58, 2004.

[311] J. Y. Wang, "Focus: death: cell death response to dna damage," *The Yale journal of biology and medicine*, vol. 92, no. 4, p. 771, 2019.

[312] M. Ocker, C. Herold, M. Ganslmayer, E. G. Hahn, and D. Schuppan, "The synthetic retinoid adapalene inhibits proliferation and induces apoptosis in colorectal cancer cells in vitro," *International journal of cancer*, vol. 107, no. 3, pp. 453–459, 2003.

[313] H. Li, C. Wang, L. Li, W. Bu, M. Zhang, J. Wei, L. Tao, K. Qian, and P. Ma, "Adapalene suppressed the proliferation of melanoma cells by s-phase arrest and subsequent apoptosis via induction of dna damage," *European Journal of Pharmacology*, vol. 851, pp. 174–185, 2019.

[314] H.-b. Nong, Y.-n. Zhang, Y.-g. Bai, Q. Zhang, M.-f. Liu, Q. Zhou, Z.-h. Shi, G.-f. Zeng, and S.-H. Zong, "Adapalene inhibits prostate cancer cell proliferation in vitro and in vivo by inducing dna damage, s-phase cell cycle arrest, and apoptosis," *Frontiers in Pharmacology*, vol. 13, p. 801624, 2022.

[315] J.-M. Ribera, O. García-Calduch, J. Ribera, P. Montesinos, I. Cano-Ferri, P. Martínez, J. Esteve, D. Esteban, M. García-Fortes, N. Alonso, *et al.*, "Ponatinib, chemotherapy, and transplant in adults with philadelphia chromosome–positive acute lymphoblastic leukemia," *Blood advances*, vol. 6, no. 18, pp. 5395–5402, 2022.

[316] Z. Iqbal, A. Aleem, M. Iqbal, M. I. Naqvi, A. Gill, A. S. Taj, A. Qayyum, N. ur Rehman, A. M. Khalid, I. H. Shah, *et al.*, "Sensitive detection of pre-existing bcr-abl kinase domain mutations in cd34+ cells of newly diagnosed chronic-phase chronic myeloid leukemia patients is associated with imatinib resistance: implications in the post-imatinib era," *PLoS One*, vol. 8, no. 2, p. e55717, 2013.

[317] J.-y. Li, H.-y. Cao, P. Liu, G.-h. Cheng, M.-y. Sun, *et al.*, "Glycyrrhizic acid in the treatment of liver diseases: literature review," *BioMed research international*, vol. 2014, 2014.

[318] L. J. Ming and A. C. Y. Yin, "Therapeutic effects of glycyrrhizic acid," *Natural product communications*, vol. 8, no. 3, p. 1934578X1300800335, 2013.

[319] S. L. Dwivedi, H. D. Upadhyaya, I.-M. Chung, P. De Vita, S. Garcia-Lara, D. Guajardo-Flores, J. A. Gutierrez-Uribe, S. O. Serna-Saldivar, G. Rajakumar, K. L. Sahrawat, *et al.*, "Exploiting phenylpropanoid derivatives to enhance the nutraceutical values of cereals and legumes," *Frontiers in plant science*, vol. 7, p. 763, 2016.

[320] Z. Zuo, L. He, X. Duan, Z. Peng, and J. Han, "Glycyrrhizic acid exhibits strong anticancer activity in colorectal cancer cells via sirt3 inhibition," *Bioengineered*, vol. 13, no. 2, pp. 2720–2731, 2022.

[321] A. Russo, A. R. Lopes, M. G. McCusker, S. G. Garrigues, G. R. Ricciardi, K. E. Arensmeyer, K. A. Scilla, R. Mehra, and C. Rolfo, "New targets in lung cancer (excluding egfr, alk, ros1)," *Current Oncology Reports*, vol. 22, pp. 1–14, 2020.

[322] T. E. Stinchcombe, "Current management of ret rearranged non-small cell lung cancer," *Therapeutic Advances in Medical Oncology*, vol. 12, p. 1758835920928634, 2020.

[323] V. Subbiah, D. Yang, V. Velcheti, A. Drilon, and F. Meric-Bernstam, "State-of-the-art strategies for targeting ret-dependent cancers," *Journal of Clinical Oncology*, vol. 38, no. 11, p. 1209, 2020.

[324] V. Subbiah, J. F. Gainor, R. Rahal, J. D. Brubaker, J. L. Kim, M. Maynard, W. Hu, Q. Cao, M. P. Sheets, D. Wilson, *et al.*, "Precision targeted therapy with blu-667 for ret-driven cancers," *Cancer discovery*, vol. 8, no. 7, pp. 836–849, 2018.

Appendix A

Table 1: Variant Data Retrieved from GDC

Sr.#	ID	DNA Change	Type	Consequences	# of Affected Cases in Cohort	# of Affected Cases Across GDC	Impact
1	chr1:g.114713908T>C	Substitution	Missense		63/833,7.56%	180/13,582	VEP: MODERATE, SIFT: tolerated - score 0.06, PolyPhen: benign - score 0.251
2	chr12:g.25227341T>G	Substitution	Missense	NRAS Q61R	56/833,6.72%	80/13,582	VEP: MODERATE, SIFT: deleterious - score 0, PolyPhen: benign - score 0.121
3	chr1:g.114713909G>T	Substitution	Missense		45/833,5.40%	124/13,582	VEP: MODERATE, SIFT: deleterious - score 0.01, PolyPhen: possibly_damaging - score 0.709
4	chr7:g.140753336A¿T	Substitution	Missense	KRAS Q61H	29/833,3.48%	610/13,582	VEP: MODERATE, SIFT: deleterious - score 0, PolyPhen: probably_damaging - score 0.955
5	chr12:g.25245350C¿T	Substitution	Missense		28/833,3.36%	333/13,582	VEP: MODERATE, SIFT: deleterious - score 0, PolyPhen: benign - score 0.303
6	chr12:g.25245347C¿T	Substitution	Missense	NRAS Q61K	27/833,3.24%	114/13,582	VEP: MODERATE, SIFT: deleterious - score 0.04, PolyPhen: benign - score 0.44
7	chr1:g.114716124C¿G	Substitution	Missense		24/833,2.88%	35/13,582	VEP: MODERATE, SIFT: deleterious - score 0, PolyPhen: probably_damaging - score 0.977
8	chr12:g.25245350C¿A	Substitution	Missense	BRAF V640E	15/833,1.80%	262/13,582	VEP: MODERATE, SIFT: deleterious - score 0, PolyPhen: probably_damaging - score 0.972
9	chr12:g.25245351C¿G	Substitution	Missense		11/833,1.32%	72/13,582	VEP: MODERATE, SIFT: deleterious - score 0.03, PolyPhen: possibly_damaging - score 0.497
10	chr6:g.394972A¿G	Substitution	Missense	KRAS G12D	11/833,1.32%	11/13,582	VEP: MODERATE, SIFT: tolerated - score 0.05, PolyPhen: probably_damaging - score 0.978
11	chr12:g.25227342T¿C	Substitution	Missense		11/833,1.32%	20/13,582	VEP: MODERATE, SIFT: tolerated - score 0.06, PolyPhen: benign - score 0.122
12	chr12:g.25227342T¿A	Substitution	Missense	KRAS G13D	9/833,1.08%	21/13,582	VEP: MODERATE, SIFT: deleterious - score 0, PolyPhen: possibly_damaging - score 0.631

13	chr12:g.25245351C¿T	Substitution Missense		9/833,1.08%	39/13,582	VEP: MODERATE, SIFT: deleterious - score 0.03, PolyPhen: possibly_damaging - score 0.582
14	chr1:g.114716126C¿T	Substitution Missense	NRAS G13R	9/833,1.08%	34/13,582	VEP: MODERATE, SIFT: deleterious - score 0, PolyPhen: benign - score 0.339
15	chr12:g.25245350C¿G	Substitution Missense		9/833,1.08%	54/13,582	VEP: MODERATE, SIFT: deleterious - score 0.02, PolyPhen: possibly_damaging - score 0.723
16	chr7:g.140753355C¿T	Substitution Missense	KRAS G12V	8/833,0.96%	17/13,582	VEP: MODERATE, SIFT: deleterious - score 0, PolyPhen: benign - score 0.267
17	chr1:g.114713907T¿A	Substitution Missense		8/833,0.96%	14/13,582	VEP: MODERATE, SIFT: deleterious - score 0, PolyPhen: benign - score 0.316
18	chr1:g.114713900A¿C	Substitution Missense	KRAS G12R	7/833,0.84%	7/13,582	VEP: MODERATE, SIFT: deleterious - score 0, PolyPhen: probably_damaging - score 0.987
19	chr1:g.114713907T¿G	Substitution Missense		7/833,0.84%	12/13,582	VEP: MODERATE, SIFT: deleterious - score 0, PolyPhen: benign - score 0.316
20	chr1:g.114713908T¿A	Substitution Missense	IRF4 K123R	7/833,0.84%	34/13,582	VEP: MODERATE, SIFT: deleterious - score 0, PolyPhen: possibly_damaging - score 0.861
21	chr12:g.25227341T¿A	Substitution Missense		7/833,0.84%	16/13,582	VEP: MODERATE, SIFT: deleterious - score 0, PolyPhen: benign - score 0.121
22	chr1:g.114716123C¿T	Substitution Missense	KRAS Q61R	6/833,0.72%	15/13,582	VEP: MODERATE, SIFT: deleterious - score 0.05, PolyPhen: benign - score 0.323
23	chr6:g.37170647G¿C	Substitution Missense		6/833,0.72%	7/13,582	VEP: MODERATE, SIFT: tolerated - score 0.48, PolyPhen: benign - score 0.062
24	chr12:g.25227334A¿C	Substitution Missense	KRAS Q61L	6/833,0.72%	6/13,582	VEP: MODERATE, SIFT: deleterious - score 0, PolyPhen: probably_damaging - score 0.991
25	chr7:g.140753354T¿C	Substitution Missense		5/833,0.60%	8/13,582	VEP: MODERATE, SIFT: deleterious - score 0, PolyPhen: benign - score 0.369
26	chr12:g.25225627G¿A	Substitution Missense	KRAS G12S	5/833,0.60%	11/13,582	VEP: MODERATE, SIFT: deleterious - score 0.02, PolyPhen: possibly_damaging - score 0.884

27	chr12:g.112450407A¿G	Substitution Missense		4/833,0.48%	4/13,582	VEP: MODERATE, SIFT: deleterious - score 0, PolyPhen: possibly_damaging - score 0.813
28	chr2:g.208248389G¿A	Substitution Missense	NRAS G12D	4/833,0.48%	71/13,582	VEP: MODERATE, SIFT: deleterious_low_confidence - score 0.03, PolyPhen: benign - score 0.1
29	chr14:g.65093775C¿A	Substitution Missense		4/833,0.48%	5/13,582	VEP: MODERATE, SIFT: deleterious - score 0, PolyPhen: probably_damaging - score 0.976
30	chr8:g.42306376A¿G	Substitution Missense	KRAS G12A	4/833,0.48%	4/13,582	VEP: MODERATE, SIFT: deleterious - score 0, PolyPhen: probably_damaging - score 0.976
31	chr14:g.65093773T¿A	Substitution Missense		3/833,0.36%	3/13,582	VEP: MODERATE, SIFT: deleterious - score 0, PolyPhen: probably_damaging - score 1
32	chr12:g.112450361G¿T	Substitution Missense	BRAF D634N	3/833,0.36%	5/13,582	VEP: MODERATE, SIFT: deleterious - score 0, PolyPhen: probably_damaging - score 0.997
33	chr1:g.114716127C¿T	Substitution Missense		3/833,0.36%	9/13,582	VEP: MODERATE, SIFT: deleterious - score 0.03, PolyPhen: benign - score 0.369
34	chr2:g.197402636T¿G	Substitution Missense	NRAS Q61H	3/833,0.36%	6/13,582	VEP: MODERATE, SIFT: deleterious - score 0, PolyPhen: probably_damaging - score 0.992
35	chr1:g.114716126C¿G	Substitution Missense		3/833,0.36%	7/13,582	VEP: MODERATE, SIFT: deleterious - score 0.02, PolyPhen: possibly_damaging - score 0.525
36	chr12:g.25245321G¿T	Substitution Missense	NRAS Y64D	3/833,0.36%	7/13,582	VEP: MODERATE, SIFT: deleterious - score 0.01, PolyPhen: probably_damaging - score 0.982
37	chr4:g.1801837C¿T	Substitution Missense		3/833,0.36%	7/13,582	VEP: MODERATE, SIFT: deleterious - score 0, PolyPhen: probably_damaging - score 0.982
38	chr7:g.140781611C¿T	Substitution Missense	NRAS Q61H	3/833,0.36%	10/13,582	VEP: MODERATE, SIFT: deleterious - score 0, PolyPhen: probably_damaging - score 0.955
39	chr17:g.7674220C¿T	Substitution Missense		3/833,0.36%	141/13,582	VEP: MODERATE, SIFT: deleterious - score 0, PolyPhen: probably_damaging - score 0.994
40	chr4:g.1804392G¿A	Substitution Missense	NRAS Q61L	3/833,0.36%	7/13,582	VEP: MODERATE, SIFT: tolerated - score 0.14, PolyPhen: possibly_damaging - score 0.637

41	chr14:g.65078030G¿A	Substitution Missense		3/833,0.36%	3/13,582	VEP: MODERATE, SIFT: deleterious - score 0, PolyPhen: probably_damaging - score 1
42	chr12:g.25245351C¿A	Substitution Missense	KRAS Q61H	3/833,0.36%	136/13,582	VEP: MODERATE, SIFT: deleterious - score 0.04, PolyPhen: probably_damaging - score 0.991
43	chr12:g.25225713T¿A	Substitution Missense		3/833,0.36%	7/13,582	VEP: MODERATE, SIFT: deleterious - score 0.01, PolyPhen: probably_damaging - score 0.994
44	chr12:g.25225628C¿T	Substitution Missense	NRAS G13D	3/833,0.36%	32/13,582	VEP: MODERATE, SIFT: deleterious - score 0.03, PolyPhen: possibly_damaging - score 0.844
45	chr14:g.95713954G¿A	Substitution Missense		3/833,0.36%	4/13,582	VEP: MODERATE, SIFT: tolerated - score 1, PolyPhen: benign - score 0.001
46	chr8:g.42306377A¿T	Substitution Missense	PIM1 K24N	3/833,0.36%	3/13,582	VEP: MODERATE, SIFT: deleterious - score 0, PolyPhen: probably_damaging - score 0.994
47	chr11:g.108335039G¿A	Substitution Missense		2/833,0.24%	2/13,582	VEP: MODERATE, SIFT: deleterious - score 0, PolyPhen: probably_damaging - score 0.999
48	chr10:g.102400673T¿C	Substitution Missense	KRAS Y64D	2/833,0.24%	2/13,582	VEP: MODERATE, SIFT: deleterious - score 0, PolyPhen: probably_damaging - score 0.989
49	chr15:g.90088702C¿T	Substitution Missense		2/833,0.24%	14/13,582	VEP: MODERATE, SIFT: deleterious_low_confidence - score 0, PolyPhen: probably_damaging - score 0.987
50	chr16:g.79599772C¿G	Substitution Missense	BRAF D634G	2/833,0.24%	2/13,582	VEP: MODERATE, SIFT: tolerated - score 0.21, PolyPhen: possibly_damaging - score 0.829
51	chr7:g.138879642G¿A	Substitution Missense		2/833,0.24%	2/13,582	VEP: MODERATE, SIFT: deleterious - score 0, PolyPhen: probably_damaging - score 0.999
52	chr1:g.114713900A¿T	Substitution Missense	KRAS A146V	2/833,0.24%	2/13,582	VEP: MODERATE, SIFT: deleterious - score 0, PolyPhen: probably_damaging - score 0.987
53	chr4:g.1806162A¿G	Substitution Missense		2/833,0.24%	5/13,582	VEP: MODERATE, SIFT: deleterious - score 0, PolyPhen: probably_damaging - score 0.999
54	chr3:g.177038423C¿T	Substitution Missense	PTPN11 E76G	2/833,0.24%	2/13,582	VEP: MODERATE, SIFT: deleterious - score 0, PolyPhen: probably_damaging - score 0.972

55	chr7:g.140753334T¿C	Substitution Missense		2/833,0.24%	14/13,582	VEP: MODERATE, SIFT: deleterious - score 0, PolyPhen: benign - score 0.345
56	chr11:g.69641404A¿C	Substitution Missense	IDH1 R132C	2/833,0.24%	2/13,582	VEP: MODERATE, SIFT: tolerated - score 1, PolyPhen: benign - score 0.003
57	chr14:g.65093775C¿T	Substitution Missense		2/833,0.24%	3/13,582	VEP: MODERATE, SIFT: deleterious - score 0, PolyPhen: probably_damaging - score 0.992
58	chr6:g.394920G¿T	Substitution Missense	MAX R35L	2/833,0.24%	3/13,582	VEP: MODERATE, SIFT: deleterious - score 0, PolyPhen: probably_damaging - score 1
59	chr10:g.121503868G¿A	Substitution Missense		2/833,0.24%	4/13,582	VEP: MODERATE, SIFT: deleterious - score 0, PolyPhen: possibly_damaging - score 0.595
60	chr4:g.1805644C¿A	Substitution Missense	IKBKB K171E	2/833,0.24%	2/13,582	VEP: MODERATE, SIFT: deleterious - score 0, PolyPhen: probably_damaging - score 1
61	chr17:g.7674935C¿A	Substitution Missense		2/833,0.24%	10/13,582	VEP: MODERATE, SIFT: deleterious - score 0, PolyPhen: probably_damaging - score 0.999
62	chr12:g.112450395C¿A	Substitution Missense	MAX R36W	2/833,0.24%	5/13,582	VEP: MODERATE, SIFT: deleterious - score 0.05, PolyPhen: probably_damaging - score 0.96
63	chr17:g.7675131C¿T	Substitution Missense		2/833,0.24%	11/13,582	VEP: MODERATE, SIFT: deleterious - score 0, PolyPhen: probably_damaging - score 0.998
64	chr12:g.92145429T¿A	Substitution Missense	PTPN11 D61Y	2/833,0.24%	2/13,582	VEP: MODERATE, SIFT: tolerated - score 0.08, PolyPhen: benign - score 0.03
65	chr12:g.112450406G¿A	Substitution Missense		2/833,0.24%	9/13,582	VEP: MODERATE, SIFT: deleterious - score 0.01, PolyPhen: probably_damaging - score 0.947
66	chr12:g.112450385G¿A	Substitution Missense	NRAS G12S	2/833,0.24%	5/13,582	VEP: MODERATE, SIFT: deleterious - score 0, PolyPhen: probably_damaging - score 0.914
67	chr12:g.25245348C¿A	Substitution Missense		2/833,0.24%	19/13,582	VEP: MODERATE, SIFT: deleterious - score 0.02, PolyPhen: probably_damaging - score 0.997
68	chr6:g.106107035T¿G	Substitution Missense	SF3B1 K666T	2/833,0.24%	2/13,582	VEP: MODERATE, SIFT: deleterious - score 0, PolyPhen: probably_damaging - score 0.999

69	chr7:g.98897855G¿A	Substitution Missense		2/833,0.24%	2/13,582	VEP: MODERATE, SIFT: tolerated - score 0.63, PolyPhen: possibly_damaging - score 0.899
70	chr12:g.25227334A¿T	Substitution Missense	NRAS G12A	2/833,0.24%	2/13,582	VEP: MODERATE, SIFT: deleterious - score 0, PolyPhen: probably_damaging - score 0.991
71	chr7:g.124853021C¿T	Substitution Missense		2/833,0.24%	2/13,582	VEP: MODERATE, SIFT: deleterious - score 0, PolyPhen: probably_damaging - score 1
72	chr8:g.42308940G¿A	Substitution Missense	KRAS Q22K	2/833,0.24%	3/13,582	VEP: MODERATE, SIFT: deleterious - score 0, PolyPhen: probably_damaging - score 0.915
73	chr12:g.122022182T¿A	Substitution Missense		2/833,0.24%	2/13,582	VEP: MODERATE, SIFT: tolerated - score 0.09, PolyPhen: benign - score 0.021
74	chr18:g.25227485G¿T	Substitution Missense	FGFR3 R248C	1/833,0.12%	1/13,582	VEP: MODERATE, SIFT: deleterious - score 0, PolyPhen: probably_damaging - score 0.999
75	chr11:g.108347304T¿G	Substitution Missense		1/833,0.12%	1/13,582	VEP: MODERATE, SIFT: deleterious - score 0, PolyPhen: probably_damaging - score 1
76	chr9:g.99863704G¿A	Substitution Missense	BRAF G506E	1/833,0.12%	1/13,582	VEP: MODERATE, SIFT: deleterious - score 0, PolyPhen: possibly_damaging - score 0.901
77	chr19:g.54152997G¿A	Substitution Missense		1/833,0.12%	1/13,582	VEP: MODERATE, SIFT: tolerated - score 0.06, PolyPhen: probably_damaging - score 0.989
78	chr1:g.92836331G¿A	Substitution Missense	TP53 R248Q	1/833,0.12%	1/13,582	VEP: MODERATE, SIFT: deleterious - score 0.02, PolyPhen: possibly_damaging - score 0.83
79	chr12:g.92144442A¿G	Substitution Missense		1/833,0.12%	1/13,582	VEP: MODERATE, SIFT: deleterious - score 0, PolyPhen: probably_damaging - score 0.999
80	chr2:g.222927061G¿T	Substitution Missense	FGFR3 G382R	1/833,0.12%	1/13,582	VEP: MODERATE, SIFT: deleterious - score 0, PolyPhen: probably_damaging - score 0.997
81	chr4:g.125414970C¿A	Substitution Missense		1/833,0.12%	1/13,582	VEP: MODERATE, SIFT: tolerated - score 0.35, PolyPhen: benign - score 0.408
82	chr19:g.32887813C¿A	Substitution Missense	MAX R60W	1/833,0.12%	1/13,582	VEP: MODERATE, SIFT: deleterious - score 0, PolyPhen: probably_damaging - score 0.997

83	chr4:g.125479802G¿T	Substitution Missense		1/833,0.12%	1/13,582	VEP: MODERATE, SIFT: deleterious - score 0, PolyPhen: probably_damaging - score 0.998
84	chr4:g.105236509G¿A	Substitution Missense	KRAS G12C	1/833,0.12%	1/13,582	VEP: MODERATE, SIFT: tolerated - score 0.17, PolyPhen: benign - score 0.006
85	chr7:g.92001584G¿A	Substitution Missense		1/833,0.12%	1/13,582	VEP: MODERATE, SIFT: tolerated - score 0.21, PolyPhen: benign - score 0.003
86	chr19:g.10812270C¿T	Substitution Missense	KRAS K117N	1/833,0.12%	1/13,582	VEP: MODERATE, SIFT: deleterious - score 0.04, PolyPhen: probably_damaging - score 0.954
87	chr17:g.81996458C¿T	Substitution Missense		1/833,0.12%	1/13,582	VEP: MODERATE, SIFT: deleterious - score 0.01, PolyPhen: probably_damaging - score 0.919
88	chr3:g.37001012G¿C	Substitution Missense	KRAS A146T	1/833,0.12%	1/13,582	VEP: MODERATE, SIFT: deleterious - score 0, PolyPhen: possibly_damaging - score 0.868
89	chr12:g.27650013C¿A	Substitution Missense		1/833,0.12%	1/13,582	VEP: MODERATE, SIFT: tolerated - score 0.05, PolyPhen: possibly_damaging - score 0.816
90	chr10:g.70598877T¿C	Substitution Missense	TCL1A T38I	1/833,0.12%	1/13,582	VEP: MODERATE, SIFT: tolerated - score 0.48, PolyPhen: benign - score 0.17
91	chr12:g.53945173G¿A	Substitution Missense		1/833,0.12%	1/13,582	VEP: MODERATE, SIFT: tolerated - score 0.37, PolyPhen: possibly_damaging - score 0.735
92	chr4:g.186603838A¿C	Substitution Missense	IKBKB K171M	1/833,0.12%	1/13,582	VEP: MODERATE, SIFT: deleterious - score 0, PolyPhen: probably_damaging - score 0.94
93	chr6:g.37171125C¿T	Substitution Missense		1/833,0.12%	2/13,582	VEP: MODERATE, SIFT: tolerated - score 0.25, PolyPhen: benign - score 0.012
94	chr17:g.7675232G¿A	Substitution Missense	ATM G2694E	1/833,0.12%	15/13,582	VEP: MODERATE, SIFT: deleterious - score 0, PolyPhen: probably_damaging - score 1
95	chr18:g.25227436C¿A	Substitution Missense		1/833,0.12%	1/13,582	VEP: MODERATE, SIFT: deleterious - score 0, PolyPhen: probably_damaging - score 1
96	chr2:g.211431082C¿T	Substitution Missense	NFKB2 L606P	1/833,0.12%	2/13,582	VEP: MODERATE, SIFT: deleterious - score 0.04, PolyPhen: benign - score 0.026

97	chr14:g.99174399C¿T	Substitution Missense		1/833,0.12%	1/13,582	VEP: MODERATE, SIFT: deleterious - score 0, PolyPhen: probably_damaging - score 0.998
98	chr2:g.136115796G¿C	Substitution Missense	IDH2 R140Q	1/833,0.12%	1/13,582	VEP: MODERATE, SIFT: deleterious - score 0, PolyPhen: possibly_damaging - score 0.661
99	chr22:g.19233268C¿G	Substitution Missense		1/833,0.12%	1/13,582	VEP: MODERATE, SIFT: deleterious - score 0.03, PolyPhen: benign - score 0.003
100	chr1:g.3432007C¿T	Substitution Missense	MAF S44T	1/833,0.12%	1/13,582	VEP: MODERATE, SIFT: tolerated - score 0.07, PolyPhen: benign - score 0.115
101	chr15:g.55418333G¿C	Substitution Missense		1/833,0.12%	1/13,582	VEP: MODERATE, SIFT: deleterious - score 0.02, PolyPhen: possibly_damaging - score 0.678
102	chr11:g.69641447T¿C	Substitution Missense	KIAA1549 S1414L	1/833,0.12%	1/13,582	VEP: MODERATE, SIFT: deleterious - score 0, PolyPhen: probably_damaging - score 0.976
103	chr1:g.3426128G¿A	Substitution Missense		1/833,0.12%	1/13,582	VEP: MODERATE, SIFT: deleterious - score 0, PolyPhen: probably_damaging - score 0.996
104	chr8:g.102293809C¿T	Substitution Missense	NRAS Y64N	1/833,0.12%	1/13,582	VEP: MODERATE, SIFT: deleterious - score 0.04, PolyPhen: probably_damaging - score 0.976
105	chr7:g.26193340C¿T	Substitution Missense		1/833,0.12%	2/13,582	VEP: MODERATE, SIFT: deleterious - score 0.03, PolyPhen: probably_damaging - score 0.998
106	chr8:g.102296975C¿G	Substitution Missense	FGFR3 K652E	1/833,0.12%	1/13,582	VEP: MODERATE, SIFT: deleterious - score 0, PolyPhen: probably_damaging - score 0.982
107	chr10:g.102400398C¿T	Substitution Missense		1/833,0.12%	1/13,582	VEP: MODERATE, SIFT: deleterious - score 0.01, PolyPhen: probably_damaging - score 0.928
108	chr4:g.125320818T¿G	Substitution Missense	TBL1XR1 D313N	1/833,0.12%	1/13,582	VEP: MODERATE, SIFT: deleterious - score 0.01, PolyPhen: probably_damaging - score 0.971
109	chr2:g.36867851G¿C	Substitution Missense		1/833,0.12%	1/13,582	VEP: MODERATE, SIFT: deleterious - score 0.01, PolyPhen: probably_damaging - score 0.928
110	chr1:g.150826563G¿C	Substitution Missense	BRAF K641E	1/833,0.12%	1/13,582	VEP: MODERATE, SIFT: deleterious - score 0.05, PolyPhen: probably_damaging - score 0.998

111	chr14:g.65078030G¿C	Substitution Missense		1/833,0.12%	1/13,582	VEP: MODERATE, SIFT: deleterious - score 0, PolyPhen: probably_damaging - score 0.996
112	chr17:g.58360162C¿G	Substitution Missense	CCND1 M31L	1/833,0.12%	1/13,582	VEP: MODERATE, SIFT: deleterious - score 0.01, PolyPhen: benign - score 0.39
113	chr17:g.9959212T¿A	Substitution Missense		1/833,0.12%	1/13,582	VEP: MODERATE, SIFT: tolerated - score 0.42, PolyPhen: benign - score 0.007
114	chr11:g.69641446T¿C	Substitution Missense	MAX R35H	1/833,0.12%	1/13,582	VEP: MODERATE, SIFT: deleterious - score 0.02, PolyPhen: benign - score 0.087
115	chr3:g.187725002A¿G	Substitution Missense		1/833,0.12%	1/13,582	VEP: MODERATE, SIFT: deleterious - score 0.05, PolyPhen: probably_damaging - score 0.995
116	chr17:g.31206298G¿C	Substitution Missense	IRF4 D106Y	1/833,0.12%	2/13,582	VEP: MODERATE, SIFT: deleterious - score 0, PolyPhen: probably_damaging - score 1
117	chr16:g.27449105C¿T	Substitution Missense		1/833,0.12%	1/13,582	VEP: MODERATE, SIFT: tolerated - score 0.15, PolyPhen: possibly_damaging - score 0.736
118	chr17:g.8143457G¿T	Substitution Missense	FGFR2 T455M	1/833,0.12%	1/13,582	VEP: MODERATE, SIFT: tolerated - score 0.4, PolyPhen: benign - score 0.001
119	chr20:g.32434645G¿A	Substitution Missense		1/833,0.12%	1/13,582	VEP: MODERATE, SIFT: deleterious - score 0.01, PolyPhen: probably_damaging - score 1
120	chr1:g.47280575G¿A	Substitution Missense	FGFR3 N542K	1/833,0.12%	3/13,582	VEP: MODERATE, SIFT: tolerated - score 0.38, PolyPhen: possibly_damaging - score 0.79
121	chr16:g.13947620A¿G	Substitution Missense		1/833,0.12%	1/13,582	VEP: MODERATE, SIFT: tolerated - score 0.08, PolyPhen: benign - score 0.077
122	chr3:g.37050505T¿C	Substitution Missense	TP53 G199V	1/833,0.12%	1/13,582	VEP: MODERATE, SIFT: tolerated - score 0.59, PolyPhen: benign - score 0
123	chr1:g.47251249T¿C	Substitution Missense		1/833,0.12%	1/13,582	VEP: MODERATE, SIFT: tolerated - score 1, PolyPhen: benign - score 0
124	chr16:g.2173378A¿G	Substitution Missense	PTPN11 A72D	1/833,0.12%	1/13,582	VEP: MODERATE, SIFT: deleterious - score 0.04, PolyPhen: probably_damaging - score 0.96

125	chr5:g.35860918G¿A	Substitution Missense		1/833,0.12%	1/13,582	VEP: MODERATE, SIFT: tolerated - score 0.16, PolyPhen: probably_damaging - score 0.955
126	chr16:g.2076102G¿A	Substitution Missense	TP53 A161T	1/833,0.12%	2/13,582	VEP: MODERATE, SIFT: deleterious - score 0, PolyPhen: probably_damaging - score 0.972
127	chr19:g.4361787T¿C	Substitution Missense		1/833,0.12%	1/13,582	VEP: MODERATE, SIFT: tolerated - score 0.05, PolyPhen: benign - score 0
128	chr7:g.140781612C¿T	Substitution Missense	BTG1 Q36L	1/833,0.12%	1/13,582	VEP: MODERATE, SIFT: deleterious - score 0, PolyPhen: probably_damaging - score 0.966
129	chr4:g.55102005G¿A	Substitution Missense		1/833,0.12%	2/13,582	VEP: MODERATE, SIFT: deleterious - score 0, PolyPhen: probably_damaging - score 0.93
130	chr2:g.176107968G¿A	Substitution Missense	PTPN11 E76K	1/833,0.12%	1/13,582	VEP: MODERATE, SIFT: tolerated - score 0.3, PolyPhen: benign - score 0.053
131	chr14:g.95104102C¿G	Substitution Missense		1/833,0.12%	1/13,582	VEP: MODERATE, SIFT: deleterious - score 0, PolyPhen: probably_damaging - score 0.924
132	chr22:g.31345271G¿A	Substitution Missense	PTPN11 E69K	1/833,0.12%	1/13,582	VEP: MODERATE, SIFT: deleterious_low_confidence - score 0, PolyPhen: possibly_damaging - score 0.897
133	chr11:g.69641418G¿T	Substitution Missense		1/833,0.12%	1/13,582	VEP: MODERATE, SIFT: deleterious - score 0, PolyPhen: probably_damaging - score 0.967
134	chr16:g.79598995T¿C	Substitution Missense	KRAS G13C	1/833,0.12%	1/13,582	VEP: MODERATE, SIFT: deleterious - score 0.03, PolyPhen: probably_damaging - score 0.996
135	chr8:g.118110323G¿A	Substitution Missense		1/833,0.12%	1/13,582	VEP: MODERATE, SIFT: deleterious - score 0, PolyPhen: probably_damaging - score 0.946
136	chr1:g.77967099C¿G	Substitution Missense	PRDM1 L676R	1/833,0.12%	1/13,582	VEP: MODERATE, SIFT: tolerated - score 0.07, PolyPhen: benign - score 0.053
137	chr18:g.26052796C¿T	Substitution Missense		1/833,0.12%	1/13,582	VEP: MODERATE, SIFT: tolerated_low_confidence - score 0.31, PolyPhen: benign - score 0.012
138	chr8:g.108235084C¿T	Substitution Missense	TRRAP E208K	1/833,0.12%	1/13,582	VEP: MODERATE, SIFT: tolerated - score 0.16, PolyPhen: benign - score 0.16

139	chr7:g.124892286G¿A	Substitution Missense		1/833,0.12%	1/13,582	VEP: MODERATE, SIFT: deleterious - score 0, PolyPhen: probably_damaging - score 1
140	chr7:g.98897846G¿C	Substitution Missense	KRAS Y64N	1/833,0.12%	2/13,582	VEP: MODERATE, SIFT: tolerated - score 0.51, PolyPhen: benign - score 0.039
141	chr6:g.117326317G¿T	Substitution Missense		1/833,0.12%	1/13,582	VEP: MODERATE, SIFT: tolerated - score 0.23, PolyPhen: probably_damaging - score 0.963
142	chr3:g.47124188G¿A	Substitution Missense	POT1 G274R	1/833,0.12%	1/13,582	VEP: MODERATE, SIFT: deleterious_low_confidence - score 0.05, PolyPhen: possibly_damaging - score 0.469
143	chrX:g.47180011T¿G	Substitution Missense		1/833,0.12%	1/13,582	VEP: MODERATE, SIFT: deleterious - score 0.04, PolyPhen: possibly_damaging - score 0.571
144	chr7:g.98976583C¿G	Substitution Missense	IKBKB V203I	1/833,0.12%	1/13,582	VEP: MODERATE, SIFT: tolerated - score 0.41, PolyPhen: benign - score 0.012
145	chr22:g.41117784G¿A	Substitution Missense		1/833,0.12%	1/13,582	VEP: MODERATE, SIFT: deleterious - score 0.03, PolyPhen: probably_damaging - score 0.968
146	chr12:g.25227343G¿T	Substitution Missense	BCL7A W31R	1/833,0.12%	9/13,582	VEP: MODERATE, SIFT: deleterious - score 0.01, PolyPhen: benign - score 0.083
147	chr19:g.52216536T¿G	Substitution Missense		1/833,0.12%	1/13,582	VEP: MODERATE, SIFT: tolerated - score 0.06, PolyPhen: benign - score 0.052
148	chr16:g.79599088C¿A	Substitution Missense	ZNF521 P145T	1/833,0.12%	1/13,582	VEP: MODERATE, SIFT: deleterious - score 0, PolyPhen: probably_damaging - score 0.997
149	chr1:g.193236278G¿A	Substitution Missense		1/833,0.12%	2/13,582	VEP: MODERATE, SIFT: deleterious - score 0, PolyPhen: probably_damaging - score 0.968
150	chr16:g.27446041G¿A	Substitution Missense	ATM D2870E	1/833,0.12%	1/13,582	VEP: MODERATE, SIFT: tolerated - score 0.23, PolyPhen: benign - score 0.018
151	chr17:g.58354953T¿G	Substitution Missense		1/833,0.12%	1/13,582	VEP: MODERATE, SIFT: deleterious_low_confidence - score 0.02, PolyPhen: possibly_damaging - score 0.806
152	chr3:g.47057188G¿A	Substitution Missense	NR4A3 G584E	1/833,0.12%	1/13,582	VEP: MODERATE, SIFT: deleterious - score 0, PolyPhen: probably_damaging - score 0.928

153	chr19:g.34221697G¿A	Substitution Missense		1/833,0.12%	1/13,582	VEP: MODERATE, SIFT: tolerated_low_confidence - score 0.17, PolyPhen: probably_damaging - score 1
154	chr16:g.50779951G¿T	Substitution Missense	CNOT3 E679K	1/833,0.12%	1/13,582	VEP: MODERATE, SIFT: deleterious - score 0.01, PolyPhen: possibly_damaging - score 0.883
155	chr10:g.43114674G¿C	Substitution Missense		1/833,0.12%	1/13,582	VEP: MODERATE, SIFT: tolerated - score 0.2, PolyPhen: possibly_damaging - score 0.451
156	chr4:g.186709523C¿G	Substitution Missense	RPL5 G156S	1/833,0.12%	1/13,582	VEP: MODERATE, SIFT: deleterious - score 0.02, PolyPhen: possibly_damaging - score 0.793
157	chr11:g.118755411C¿T	Substitution Missense		1/833,0.12%	1/13,582	VEP: MODERATE, SIFT: deleterious - score 0, PolyPhen: probably_damaging - score 1
158	chr17:g.57529695T¿A	Substitution Missense	BTG1 Y52H	1/833,0.12%	1/13,582	VEP: MODERATE, SIFT: deleterious - score 0.01, PolyPhen: possibly_damaging - score 0.716
159	chr16:g.79599088C¿T	Substitution Missense		1/833,0.12%	1/13,582	VEP: MODERATE, SIFT: deleterious - score 0, PolyPhen: probably_damaging - score 0.999
160	chrX:g.67545925G¿T	Substitution Missense	ACSL3 R446L	1/833,0.12%	1/13,582	VEP: MODERATE, SIFT: deleterious_low_confidence - score 0.03, PolyPhen: probably_damaging - score 0.945
161	chr7:g.75558191C¿A	Substitution Missense		1/833,0.12%	1/13,582	VEP: MODERATE, SIFT: tolerated - score 0.14, PolyPhen: benign - score 0.052
162	chr2:g.29207235G¿A	Substitution Missense	FAT4 L2003I	1/833,0.12%	1/13,582	VEP: MODERATE, SIFT: deleterious - score 0, PolyPhen: probably_damaging - score 1
163	chr7:g.138581732T¿A	Substitution Missense		1/833,0.12%	1/13,582	VEP: MODERATE, SIFT: deleterious - score 0.01, PolyPhen: probably_damaging - score 0.998
164	chr1:g.43339299G¿T	Substitution Missense	CEP89 G635V	1/833,0.12%	1/13,582	VEP: MODERATE, SIFT: tolerated - score 0.09, PolyPhen: benign - score 0.076
165	chr4:g.186628160C¿G	Substitution Missense		1/833,0.12%	1/13,582	VEP: MODERATE, SIFT: tolerated - score 0.13, PolyPhen: probably_damaging - score 0.995
166	chr11:g.128758158C¿T	Substitution Missense	FAT4 D4181Y	1/833,0.12%	1/13,582	VEP: MODERATE, SIFT: tolerated - score 0.05, PolyPhen: benign - score 0.159

167	chr6:g.138889001G¿A	Substitution Missense		1/833,0.12%	1/13,582	VEP: MODERATE, SIFT: tolerated - score 0.09, PolyPhen: benign - score 0.003
168	chrX:g.71118833C¿G	Substitution Missense	TET2 G856E	1/833,0.12%	2/13,582	VEP: MODERATE, SIFT: deleterious - score 0, PolyPhen: possibly_damaging - score 0.904
169	chr17:g.16194503G¿A	Substitution Missense		1/833,0.12%	1/13,582	VEP: MODERATE, SIFT: deleterious - score 0, PolyPhen: benign - score 0.192
170	chr12:g.70556007C¿T	Substitution Missense	AKAP9 S556N	1/833,0.12%	1/13,582	VEP: MODERATE, SIFT: tolerated - score 0.38, PolyPhen: benign - score 0.003
171	chr12:g.124344629G¿A	Substitution Missense		1/833,0.12%	1/13,582	VEP: MODERATE, SIFT: tolerated - score 0.09, PolyPhen: probably_damaging - score 0.929
172	chr7:g.148815001C¿T	Substitution Missense	DNM2 R522C	1/833,0.12%	1/13,582	VEP: MODERATE, SIFT: tolerated - score 0.09, PolyPhen: probably_damaging - score 0.995
173	chr2:g.215326846G¿A	Substitution Missense		1/833,0.12%	1/13,582	VEP: MODERATE, SIFT: deleterious - score 0, PolyPhen: probably_damaging - score 0.927
174	chr16:g.10898683G¿C	Substitution Missense	ASPSCR1 P182L	1/833,0.12%	1/13,582	VEP: MODERATE, SIFT: deleterious - score 0.03, PolyPhen: benign - score 0.132
175	chr12:g.114674533C¿G	Substitution Missense		1/833,0.12%	1/13,582	VEP: MODERATE, SIFT: tolerated - score 0.18, PolyPhen: benign - score 0.058
176	chr11:g.119299756C¿T	Substitution Missense	MLH1 E89Q	1/833,0.12%	1/13,582	VEP: MODERATE, SIFT: deleterious_low_confidence - score 0, PolyPhen: possibly_damaging - score 0.556
177	chr21:g.33027824A¿G	Substitution Missense		1/833,0.12%	1/13,582	VEP: MODERATE, SIFT: deleterious - score 0.04, PolyPhen: possibly_damaging - score 0.584
178	chr15:g.34355672C¿T	Substitution Missense	PPFIBP1 L159I	1/833,0.12%	1/13,582	VEP: MODERATE, SIFT: deleterious - score 0, PolyPhen: benign - score 0.178
179	chr19:g.14097583C¿T	Substitution Missense		1/833,0.12%	1/13,582	VEP: MODERATE, SIFT: tolerated - score 0.11, PolyPhen: benign - score 0.006
180	chr2:g.74369439T¿C	Substitution Missense	PRF1 K282E	1/833,0.12%	1/13,582	VEP: MODERATE, SIFT: deleterious - score 0.03, PolyPhen: probably_damaging - score 0.968

181	chr3:g.52609350T¿C	Substitution Missense		1/833,0.12%	1/13,582	VEP: MODERATE, SIFT: tolerated - score 0.43, PolyPhen: possibly_damaging - score 0.506
182	chr4:g.186620614T¿A	Substitution Missense	HOXC13 V304I	1/833,0.12%	1/13,582	VEP: MODERATE, SIFT: deleterious - score 0, PolyPhen: probably_damaging - score 1
183	chr22:g.19180791C¿T	Substitution Missense		1/833,0.12%	1/13,582	VEP: MODERATE, SIFT: tolerated - score 0.31, PolyPhen: benign - score 0.003
184	chr12:g.124419976C¿T	Substitution Missense	FAT1 V3563G	1/833,0.12%	3/13,582	VEP: MODERATE, SIFT: deleterious - score 0.02, PolyPhen: probably_damaging - score 0.975
185	chr5:g.171205525G¿A	Substitution Missense		1/833,0.12%	1/13,582	VEP: MODERATE, SIFT: tolerated - score 0.08, PolyPhen: possibly_damaging - score 0.902
186	chr7:g.2928632C¿T	Substitution Missense	PIM1 P81S	1/833,0.12%	2/13,582	VEP: MODERATE, SIFT: tolerated - score 0.1, PolyPhen: benign - score 0.013
187	chr2:g.42315965G¿T	Substitution Missense		1/833,0.12%	1/13,582	VEP: MODERATE, SIFT: deleterious - score 0, PolyPhen: probably_damaging - score 0.999
188	chr7:g.157005551G¿A	Substitution Missense	TP53 S127F	1/833,0.12%	1/13,582	VEP: MODERATE, SIFT: deleterious_low_confidence - score 0.05, PolyPhen: benign - score 0
189	chr4:g.186620330A¿C	Substitution Missense		1/833,0.12%	1/13,582	VEP: MODERATE, SIFT: deleterious - score 0, PolyPhen: probably_damaging - score 0.999
190	chr8:g.102259124C¿T	Substitution Missense	ZNF521 R161L	1/833,0.12%	1/13,582	VEP: MODERATE, SIFT: tolerated - score 0.64, PolyPhen: benign - score 0.038
191	chr16:g.11255406G¿A	Substitution Missense		1/833,0.12%	1/13,582	VEP: MODERATE, SIFT: tolerated - score 0.17, PolyPhen: benign - score 0
192	chr12:g.56096537A¿G	Substitution Missense	ERBB4 E836K	1/833,0.12%	1/13,582	VEP: MODERATE, SIFT: tolerated - score 0.11, PolyPhen: benign - score 0.039
193	chr7:g.13986670A¿C	Substitution Missense		1/833,0.12%	1/13,582	VEP: MODERATE, SIFT: deleterious - score 0, PolyPhen: probably_damaging - score 1
194	chr10:g.68690999G¿A	Substitution Missense	BCL11B V813M	1/833,0.12%	1/13,582	VEP: MODERATE, SIFT: tolerated - score 0.61, PolyPhen: benign - score 0.007

195	chr13:g.20031382T¿C	Substitution Missense		1/833,0.12%	1/13,582	VEP: MODERATE, SIFT: deleterious - score 0.02, PolyPhen: probably_damaging - score 0.988
196	chr6:g.106106456A¿G	Substitution Missense	CXCR4 I48M	1/833,0.12%	1/13,582	VEP: MODERATE, SIFT: deleterious - score 0.01, PolyPhen: probably_damaging - score 0.999
197	chr16:g.64947613T¿A	Substitution Missense		1/833,0.12%	1/13,582	VEP: MODERATE, SIFT: deleterious - score 0.03, PolyPhen: possibly_damaging - score 0.462
198	chr1:g.11248001G¿C	Substitution Missense	CLTCL1 M473I	1/833,0.12%	1/13,582	VEP: MODERATE, SIFT: tolerated - score 0.2, PolyPhen: possibly_damaging - score 0.84
199	chr4:g.25662737G¿A	Substitution Missense		1/833,0.12%	1/13,582	VEP: MODERATE, SIFT: tolerated - score 0.1, PolyPhen: benign - score 0.009
200	chr5:g.177294255T¿C	Substitution Missense	PRDM16 P1188L	1/833,0.12%	1/13,582	VEP: MODERATE, SIFT: tolerated_low_confidence - score 0.17, PolyPhen: benign - score 0.003
201	chr9:g.90874233G¿C	Substitution Missense		1/833,0.12%	1/13,582	VEP: MODERATE, SIFT: tolerated - score 0.62, PolyPhen: benign - score 0
202	chr20:g.63534157G¿A	Substitution Missense	C15orf65 K43N	1/833,0.12%	1/13,582	VEP: MODERATE, SIFT: tolerated - score 0.2, PolyPhen: benign - score 0
203	chr7:g.138916753G¿C	Substitution Missense		1/833,0.12%	1/13,582	VEP: MODERATE, SIFT: tolerated - score 0.16, PolyPhen: possibly_damaging - score 0.853
204	chr11:g.32396281G¿T	Substitution Missense	CCND1 F45S	1/833,0.12%	1/13,582	VEP: MODERATE, SIFT: tolerated_low_confidence - score 0.16, PolyPhen: benign - score 0.2
205	chr6:g.106107047T¿G	Substitution Missense		1/833,0.12%	1/13,582	VEP: MODERATE, SIFT: deleterious - score 0, PolyPhen: probably_damaging - score 0.993
206	chr12:g.132680680A¿G	Substitution Missense	PRDM16 A1063T	1/833,0.12%	1/13,582	VEP: MODERATE, SIFT: deleterious - score 0, PolyPhen: benign - score 0.01
207	chr2:g.61492337C¿T	Substitution Missense		1/833,0.12%	11/13,582	VEP: MODERATE, SIFT: deleterious - score 0, PolyPhen: probably_damaging - score 0.999
208	chr17:g.50190872C¿T	Substitution Missense	UBR5 R1462H	1/833,0.12%	1/13,582	VEP: MODERATE, SIFT: deleterious - score 0, PolyPhen: probably_damaging - score 1

209	chr20:g.63532679G¿T	Substitution Missense		1/833,0.12%	1/13,582	VEP: MODERATE, SIFT: tolerated - score 0.11, PolyPhen: benign - score 0.015
210	chr15:g.57063777C¿T	Substitution Missense	HNRNPA2B1 G304E	1/833,0.12%	1/13,582	VEP: MODERATE, SIFT: deleterious - score 0, PolyPhen: benign - score 0
211	chr20:g.58853455G¿C	Substitution Missense		1/833,0.12%	1/13,582	VEP: MODERATE, SIFT: deleterious_low_confidence - score 0.03, PolyPhen: benign - score 0.135
212	chr11:g.108330228T¿A	Substitution Missense	UBR5 E1195Q	1/833,0.12%	1/13,582	VEP: MODERATE, SIFT: deleterious - score 0, PolyPhen: possibly_damaging - score 0.477
213	chr3:g.47122390G¿A	Substitution Missense		1/833,0.12%	1/13,582	VEP: MODERATE, SIFT: tolerated_low_confidence - score 0.11, PolyPhen: benign - score 0
214	chr1:g.198742341C¿A	Substitution Missense	NFKB2 R569W	1/833,0.12%	1/13,582	VEP: MODERATE, SIFT: deleterious - score 0, PolyPhen: probably_damaging - score 0.99
215	chr12:g.45852408A¿G	Substitution Missense		1/833,0.12%	1/13,582	VEP: MODERATE, SIFT: tolerated_low_confidence - score 0.08, PolyPhen: benign - score 0
216	chr5:g.38530614A¿T	Substitution Missense	FAT4 F1469L	1/833,0.12%	1/13,582	VEP: MODERATE, SIFT: tolerated_low_confidence - score 0.75, PolyPhen: benign - score 0
217	chr10:g.112951512A¿C	Substitution Missense		1/833,0.12%	1/13,582	VEP: MODERATE, SIFT: tolerated - score 0.12, PolyPhen: possibly_damaging - score 0.799
218	chr4:g.55114880C¿T	Substitution Missense	STRN L504V	1/833,0.12%	2/13,582	VEP: MODERATE, SIFT: tolerated - score 0.57, PolyPhen: benign - score 0.087
219	chr1:g.3412266G¿A	Substitution Missense		1/833,0.12%	1/13,582	VEP: MODERATE, SIFT: deleterious - score 0.05, PolyPhen: benign - score 0.084
220	chr4:g.54725922A¿T	Substitution Missense	ARNT L408V	1/833,0.12%	1/13,582	VEP: MODERATE, SIFT: deleterious - score 0.01, PolyPhen: probably_damaging - score 0.954
221	chr7:g.138918766G¿C	Substitution Missense		1/833,0.12%	1/13,582	VEP: MODERATE, SIFT: deleterious - score 0.01, PolyPhen: possibly_damaging - score 0.635
222	chr10:g.121498512C¿T	Substitution Missense	MAX R60G	1/833,0.12%	2/13,582	VEP: MODERATE, SIFT: deleterious - score 0, PolyPhen: probably_damaging - score 1

223	chr4:g.1804377G¿T	Substitution Missense		1/833,0.12%	1/13,582	VEP: MODERATE, SIFT: deleterious - score 0.02, PolyPhen: benign - score 0.031
224	chrX:g.65739139A¿T	Substitution Missense	RNF43 M313I	1/833,0.12%	1/13,582	VEP: MODERATE, SIFT: deleterious - score 0.04, PolyPhen: possibly_damaging - score 0.58
225	chr11:g.33869497C¿T	Substitution Missense		1/833,0.12%	1/13,582	VEP: MODERATE, SIFT: tolerated_low_confidence - score 0.57, PolyPhen: benign - score 0
226	chrX:g.77620527C¿T	Substitution Missense	GAS7 N172I	1/833,0.12%	1/13,582	VEP: MODERATE, SIFT: deleterious - score 0, PolyPhen: probably_damaging - score 1
227	chr10:g.59794516G¿A	Substitution Missense		1/833,0.12%	1/13,582	VEP: MODERATE, SIFT: deleterious_low_confidence - score 0.01, PolyPhen: benign - score 0.186
228	chr6:g.128083717C¿T	Substitution Missense	CCND1 F45L	1/833,0.12%	2/13,582	VEP: MODERATE, SIFT: tolerated - score 0.06, PolyPhen: probably_damaging - score 1
229	chr4:g.152326089A¿G	Substitution Missense		1/833,0.12%	1/13,582	VEP: MODERATE, SIFT: tolerated - score 0.24, PolyPhen: possibly_damaging - score 0.456
230	chr16:g.11255207T¿G	Substitution Missense	BCL6 F639S	1/833,0.12%	1/13,582	VEP: MODERATE, SIFT: tolerated - score 0.49, PolyPhen: benign - score 0.012
231	chr12:g.11885947G¿A	Substitution Missense		1/833,0.12%	2/13,582	VEP: MODERATE, SIFT: deleterious - score 0.01, PolyPhen: probably_damaging - score 1
232	chr11:g.102337007C¿T	Substitution Missense	NF1 R440P	1/833,0.12%	1/13,582	VEP: MODERATE, SIFT: deleterious - score 0, PolyPhen: probably_damaging - score 1
233	chr4:g.125319574A¿C	Substitution Missense		1/833,0.12%	1/13,582	VEP: MODERATE, SIFT: tolerated - score 0.11, PolyPhen: probably_damaging - score 0.995
234	chrX:g.71122852G¿C	Substitution Missense	IL21R S480L	1/833,0.12%	1/13,582	VEP: MODERATE, SIFT: tolerated - score 0.19, PolyPhen: benign - score 0.062
235	chr9:g.132901654C¿G	Substitution Missense		1/833,0.12%	1/13,582	VEP: MODERATE, SIFT: tolerated - score 0.07, PolyPhen: probably_damaging - score 0.997
236	chr2:g.127286890G¿C	Substitution Missense	PER1 L961I	1/833,0.12%	1/13,582	VEP: MODERATE, SIFT: tolerated - score 0.21, PolyPhen: benign - score 0.161

237	chr1:g.161328441C¿G	Substitution Missense		1/833,0.12%	1/13,582	VEP: MODERATE, SIFT: deleterious - score 0, PolyPhen: possibly_damaging - score 0.792
238	chr11:g.108250982G¿A	Substitution Missense	ASXL1 G645S	1/833,0.12%	1/13,582	VEP: MODERATE, SIFT: tolerated - score 0.43, PolyPhen: benign - score 0.027
239	chr11:g.118472349G¿A	Substitution Missense		1/833,0.12%	1/13,582	VEP: MODERATE, SIFT: tolerated_low_confidence - score 0.1, PolyPhen: benign - score 0
240	chr4:g.1804389T¿A	Substitution Missense	STIL S628F	1/833,0.12%	1/13,582	VEP: MODERATE, SIFT: deleterious - score 0, PolyPhen: probably_damaging - score 0.986
241	chr3:g.53810246T¿A	Substitution Missense		1/833,0.12%	1/13,582	VEP: MODERATE, SIFT: tolerated_low_confidence - score 1, PolyPhen: benign - score 0.003
242	chr16:g.15748086C¿T	Substitution Missense	ERCC4 Q675R	1/833,0.12%	1/13,582	VEP: MODERATE, SIFT: deleterious - score 0, PolyPhen: probably_damaging - score 0.996
243	chr7:g.101916176G¿T	Substitution Missense		1/833,0.12%	1/13,582	VEP: MODERATE, SIFT: deleterious - score 0, PolyPhen: probably_damaging - score 0.997
244	chr16:g.72795109G¿A	Substitution Missense	MLH1 I708T	1/833,0.12%	1/13,582	VEP: MODERATE, SIFT: deleterious - score 0.03, PolyPhen: probably_damaging - score 0.968
245	chr12:g.124362282G¿A	Substitution Missense		1/833,0.12%	1/13,582	VEP: MODERATE, SIFT: deleterious - score 0.01, PolyPhen: possibly_damaging - score 0.805
246	chr4:g.186707975T¿G	Substitution Missense	STIL I1252V	1/833,0.12%	1/13,582	VEP: MODERATE, SIFT: deleterious - score 0, PolyPhen: benign - score 0.255
247	chr2:g.99560381G¿T	Substitution Missense		1/833,0.12%	1/13,582	VEP: MODERATE, SIFT: tolerated - score 0.72, PolyPhen: benign - score 0.384
248	chr2:g.211623993G¿A	Substitution Missense	TRAF7 K331E	1/833,0.12%	9/13,582	VEP: MODERATE, SIFT: deleterious - score 0.02, PolyPhen: possibly_damaging - score 0.893
249	chr19:g.29817411C¿A	Substitution Missense		1/833,0.12%	2/13,582	VEP: MODERATE, SIFT: deleterious - score 0, PolyPhen: probably_damaging - score 0.963
250	chr1:g.47280654C¿T	Substitution Missense	IL7R G50E	1/833,0.12%	1/13,582	VEP: MODERATE, SIFT: tolerated - score 0.32, PolyPhen: benign - score 0.011

251	chr3:g.142549480T¿C	Substitution Missense		1/833,0.12%	1/13,582	VEP: MODERATE, SIFT: tolerated - score 0.13, PolyPhen: benign - score 0.053
252	chr5:g.177294883G¿C	Substitution Missense	TSC2 V892I	1/833,0.12%	1/13,582	VEP: MODERATE, SIFT: tolerated_low_confidence - score 0.06, PolyPhen: benign - score 0.005
253	chr19:g.44757186C¿T	Substitution Missense		1/833,0.12%	1/13,582	VEP: MODERATE, SIFT: deleterious - score 0.03, PolyPhen: benign - score 0.077
254	chr12:g.25225628C¿G	Substitution Missense	SH3GL1 D307G	1/833,0.12%	2/13,582	VEP: MODERATE, SIFT: deleterious - score 0, PolyPhen: probably_damaging - score 1
255	chr3:g.155914437C¿G	Substitution Missense		1/833,0.12%	2/13,582	VEP: MODERATE, SIFT: tolerated - score 0.08, PolyPhen: benign - score 0.005
256	chr12:g.56720677C¿G	Substitution Missense	BRAF G506R	1/833,0.12%	1/13,582	VEP: MODERATE, SIFT: deleterious_low_confidence - score 0.04, PolyPhen: benign - score 0
257	chr14:g.95712379C¿A	Substitution Missense		1/833,0.12%	1/13,582	VEP: MODERATE, SIFT: deleterious - score 0.01, PolyPhen: benign - score 0.003
258	chr2:g.60460409C¿T	Substitution Missense	KDR R720W	1/833,0.12%	1/13,582	VEP: MODERATE, SIFT: deleterious - score 0, PolyPhen: probably_damaging - score 0.953
259	chr22:g.23181703A¿G	Substitution Missense		1/833,0.12%	1/13,582	VEP: MODERATE, SIFT: deleterious_low_confidence - score 0, PolyPhen: possibly_damaging - score 0.475
260	chr4:g.186619441T¿G	Substitution Missense	HOXD11 E205K	1/833,0.12%	1/13,582	VEP: MODERATE, SIFT: deleterious - score 0, PolyPhen: probably_damaging - score 0.998
261	chr1:g.15928361A¿C	Substitution Missense		1/833,0.12%	1/13,582	VEP: MODERATE, SIFT: deleterious - score 0.02, PolyPhen: probably_damaging - score 0.991
262	chr5:g.38530508T¿C	Substitution Missense	DICER1 W1098C	1/833,0.12%	1/13,582	VEP: MODERATE, SIFT: tolerated - score 0.54, PolyPhen: benign - score 0
263	chr12:g.122022182T¿G	Substitution Missense		1/833,0.12%	1/13,582	VEP: MODERATE, SIFT: deleterious - score 0.03, PolyPhen: possibly_damaging - score 0.461
264	chr16:g.9764425T¿A	Substitution Missense	PATZ1 S111F	1/833,0.12%	1/13,582	VEP: MODERATE, SIFT: tolerated - score 0.16, PolyPhen: benign - score 0.096

265	chr1:g.149009570T¿A	Substitution Missense		1/833,0.12%	1/13,582	VEP: MODERATE, SIFT: deleterious - score 0, PolyPhen: probably_damaging - score 0.999
266	chr7:g.124892271C¿A	Substitution Missense	CCND1 E35D	1/833,0.12%	1/13,582	VEP: MODERATE, SIFT: deleterious - score 0, PolyPhen: probably_damaging - score 1
267	chr8:g.108240013G¿A	Substitution Missense		1/833,0.12%	1/13,582	VEP: MODERATE, SIFT: tolerated - score 0.1, PolyPhen: possibly_damaging - score 0.461
268	chr3:g.10035176G¿C	Substitution Missense	MAF Q303R	1/833,0.12%	1/13,582	VEP: MODERATE, SIFT: tolerated - score 0.41, PolyPhen: benign - score 0.003
269	chr12:g.114683037G¿A	Substitution Missense		1/833,0.12%	1/13,582	VEP: MODERATE, SIFT: tolerated - score 0.28, PolyPhen: benign - score 0.273
270	chr5:g.1294318C¿T	Substitution Missense	EXT1 P242S	1/833,0.12%	1/13,582	VEP: MODERATE, SIFT: tolerated - score 0.62, PolyPhen: benign - score 0.003
271	chr7:g.92042122A¿T	Substitution Missense		1/833,0.12%	1/13,582	VEP: MODERATE, SIFT: deleterious - score 0, PolyPhen: possibly_damaging - score 0.523
272	chr6:g.37170784G¿C	Substitution Missense	FUBP1 R98T	1/833,0.12%	1/13,582	VEP: MODERATE, SIFT: tolerated - score 0.1, PolyPhen: benign - score 0.334
273	chr9:g.5534886C¿G	Substitution Missense		1/833,0.12%	1/13,582	VEP: MODERATE, SIFT: tolerated - score 0.08, PolyPhen: probably_damaging - score 0.931
274	chr11:g.108326176T¿C	Substitution Missense	SS18 M145I	1/833,0.12%	1/13,582	VEP: MODERATE, SIFT: deleterious - score 0, PolyPhen: possibly_damaging - score 0.667
275	chr1:g.164799750C¿T	Substitution Missense		1/833,0.12%	2/13,582	VEP: MODERATE, SIFT: deleterious - score 0, PolyPhen: probably_damaging - score 0.999
276	chr12:g.49041192G¿A	Substitution Missense	EIF3E D129N	1/833,0.12%	1/13,582	VEP: MODERATE, SIFT: tolerated_low_confidence - score 0.09, PolyPhen: benign - score 0.02
277	chr5:g.180630713A¿G	Substitution Missense		1/833,0.12%	1/13,582	VEP: MODERATE, SIFT: deleterious - score 0.05, PolyPhen: benign - score 0.011
278	chr16:g.10909162C¿G	Substitution Missense	POT1 P35L	1/833,0.12%	1/13,582	VEP: MODERATE, SIFT: deleterious - score 0, PolyPhen: probably_damaging - score 1

279	chr6:g.35460613C¿T	Substitution Missense		1/833,0.12%	1/13,582	VEP: MODERATE, SIFT: deleterious - score 0, PolyPhen: possibly_damaging - score 0.875
280	chr11:g.108329198G¿A	Substitution Missense	TRRAP E205Q	1/833,0.12%	1/13,582	VEP: MODERATE, SIFT: deleterious - score 0, PolyPhen: benign - score 0.373
281	chr12:g.114683059G¿A	Substitution Missense		1/833,0.12%	1/13,582	VEP: MODERATE, SIFT: deleterious - score 0.02, PolyPhen: possibly_damaging - score 0.617
282	chr12:g.12718311G¿A	Substitution Missense	ROS1 L1822M	1/833,0.12%	1/13,582	VEP: MODERATE, SIFT: tolerated - score 0.4, PolyPhen: benign - score 0.073
283	chr17:g.61808499C¿T	Substitution Missense		1/833,0.12%	1/13,582	VEP: MODERATE, SIFT: deleterious - score 0, PolyPhen: probably_damaging - score 0.997
284	chr4:g.125320411G¿C	Substitution Missense	SETD2 H150Y	1/833,0.12%	1/13,582	VEP: MODERATE, SIFT: tolerated - score 0.66, PolyPhen: probably_damaging - score 0.981
285	chr18:g.25225284G¿T	Substitution Missense		1/833,0.12%	1/13,582	VEP: MODERATE, SIFT: tolerated - score 0.86, PolyPhen: benign - score 0.02
286	chr5:g.177246776A¿G	Substitution Missense	RBM10 F410V	1/833,0.12%	1/13,582	VEP: MODERATE, SIFT: tolerated - score 0.51, PolyPhen: benign - score 0.015
287	chr10:g.21617164C¿G	Substitution Missense		1/833,0.12%	1/13,582	VEP: MODERATE, SIFT: deleterious - score 0, PolyPhen: probably_damaging - score 0.979
288	chr4:g.125317559C¿T	Substitution Missense	TRRAP S2680C	1/833,0.12%	1/13,582	VEP: MODERATE, SIFT: tolerated - score 0.09, PolyPhen: probably_damaging - score 0.999
289	chr3:g.181712372G¿C	Substitution Missense		1/833,0.12%	1/13,582	VEP: MODERATE, SIFT: tolerated - score 0.08, PolyPhen: benign - score 0.095
290	chr17:g.42323325G¿C	Substitution Missense	EP300 G231E	1/833,0.12%	1/13,582	VEP: MODERATE, SIFT: tolerated - score 0.05, PolyPhen: benign - score 0.071
291	chr14:g.65093766T¿G	Substitution Missense		1/833,0.12%	1/13,582	VEP: MODERATE, SIFT: deleterious - score 0.03, PolyPhen: probably_damaging - score 0.996
292	chr4:g.125490463G¿C	Substitution Missense	KRAS Q61K	1/833,0.12%	1/13,582	VEP: MODERATE, SIFT: deleterious_low_confidence - score 0.02, PolyPhen: probably_damaging - score 0.99

293	chr12:g.1115875G¿T	Substitution Missense		1/833,0.12%	1/13,582	VEP: MODERATE, SIFT: tolerated - score 1, PolyPhen: benign - score 0.013
294	chr2:g.99554347A¿C	Substitution Missense	PPP2R1A V334G	1/833,0.12%	1/13,582	VEP: MODERATE, SIFT: deleterious - score 0, PolyPhen: probably_damaging - score 0.969
295	chr2:g.47799794A¿G	Substitution Missense		1/833,0.12%	1/13,582	VEP: MODERATE, SIFT: deleterious - score 0.02, PolyPhen: benign - score 0.005
296	chr16:g.31190977G¿C	Substitution Missense	MAF R272L	1/833,0.12%	1/13,582	VEP: MODERATE, SIFT: tolerated_low_confidence - score 0.12, PolyPhen: benign - score 0.156
297	chr1:g.110339964G¿A	Substitution Missense		1/833,0.12%	1/13,582	VEP: MODERATE, SIFT: tolerated - score 0.27, PolyPhen: probably_damaging - score 0.968
298	chr18:g.47868449G¿A	Substitution Missense	CDC73 V447M	1/833,0.12%	2/13,582	VEP: MODERATE, SIFT: deleterious - score 0.01, PolyPhen: benign - score 0.142
299	chr5:g.38482026C¿G	Substitution Missense		1/833,0.12%	1/13,582	VEP: MODERATE, SIFT: deleterious - score 0.01, PolyPhen: probably_damaging - score 0.946
300	chr4:g.125317302A¿T	Substitution Missense	IL21R E274K	1/833,0.12%	1/13,582	VEP: MODERATE, SIFT: tolerated - score 0.19, PolyPhen: benign - score 0.005
301	chr7:g.98994638G¿C	Substitution Missense		1/833,0.12%	3/13,582	VEP: MODERATE, SIFT: deleterious - score 0.01, PolyPhen: probably_damaging - score 0.943
302	chr17:g.57258336T¿A	Substitution Missense	RNF43 Q781P	1/833,0.12%	1/13,582	VEP: MODERATE, SIFT: deleterious - score 0.02, PolyPhen: possibly_damaging - score 0.718
303	chr1:g.15932439C¿A	Substitution Missense		1/833,0.12%	2/13,582	VEP: MODERATE, SIFT: tolerated - score 0.65, PolyPhen: benign - score 0
304	chrX:g.47185125A¿G	Substitution Missense	SETD2 S2199F	1/833,0.12%	1/13,582	VEP: MODERATE, SIFT: tolerated - score 0.05, PolyPhen: benign - score 0.088
305	chr2:g.25275078C¿G	Substitution Missense		1/833,0.12%	1/13,582	VEP: MODERATE, SIFT: tolerated - score 0.08, PolyPhen: probably_damaging - score 0.996
306	chr1:g.114713908T¿G	Substitution Missense	LSM14A G443R	1/833,0.12%	2/13,582	VEP: MODERATE, SIFT: deleterious - score 0, PolyPhen: benign - score 0.425
307	chrX:g.133536221A¿G	Substitution Missense		1/833,0.12%	1/13,582	VEP: MODERATE, SIFT: tolerated - score 0.81, PolyPhen: benign - score 0.012

308	chr16:g.3738671G¿A	Substitution	Missense	CYLD L475F	1/833,0.12%	2/13,582	VEP: MODERATE, SIFT: deleterious - score 0, PolyPhen: probably_damaging - score 0.999
309	chr16:g.9764168G¿T	Substitution	Missense		1/833,0.12%	1/13,582	VEP: MODERATE, SIFT: tolerated - score 0.14, PolyPhen: possibly_damaging - score 0.58
310	chr6:g.44251055C¿T	Substitution	Missense	RET A692P	1/833,0.12%	1/13,582	VEP: MODERATE, SIFT: deleterious - score 0.01, PolyPhen: possibly_damaging - score 0.871
311	chr5:g.56884814G¿A	Substitution	Missense		1/833,0.12%	1/13,582	VEP: MODERATE, SIFT: deleterious - score 0, PolyPhen: probably_damaging - score 0.989
312	chr1:g.147619382G¿A	Substitution	Missense	FAT1 G102A	1/833,0.12%	1/13,582	VEP: MODERATE, SIFT: tolerated - score 0.07, PolyPhen: benign - score 0.168
313	chr4:g.186597166T¿C	Substitution	Missense		1/833,0.12%	1/13,582	VEP: MODERATE, SIFT: tolerated - score 0.51, PolyPhen: benign - score 0.134
314	chr1:g.193152393C¿A	Substitution	Missense	DDX6 G423R	1/833,0.12%	1/13,582	VEP: MODERATE, SIFT: deleterious - score 0, PolyPhen: probably_damaging - score 1
315	chr8:g.38413698G¿A	Substitution	Missense		1/833,0.12%	1/13,582	VEP: MODERATE, SIFT: tolerated - score 0.26, PolyPhen: possibly_damaging - score 0.652
316	chr16:g.67610962C¿A	Substitution	Missense	MSI2 M142K	1/833,0.12%	1/13,582	VEP: MODERATE, SIFT: tolerated_low_confidence - score 0.1, PolyPhen: benign - score 0.011
317	chr19:g.1619392G¿A	Substitution	Missense		1/833,0.12%	1/13,582	VEP: MODERATE, SIFT: deleterious - score 0.01, PolyPhen: benign - score 0.266
318	chr1:g.156787094A¿G	Substitution	Missense	MAF R272H	1/833,0.12%	1/13,582	VEP: MODERATE, SIFT: tolerated - score 0.37, PolyPhen: benign - score 0
319	chr6:g.33319077T¿C	Substitution	Missense		1/833,0.12%	1/13,582	VEP: MODERATE, SIFT: deleterious - score 0.01, PolyPhen: probably_damaging - score 0.994
320	chr19:g.42290513C¿T	Substitution	Missense	AR G260V	1/833,0.12%	1/13,582	VEP: MODERATE, SIFT: tolerated_low_confidence - score 0.17, PolyPhen: benign - score 0
321	chr7:g.98965741G¿T	Substitution	Missense		1/833,0.12%	1/13,582	VEP: MODERATE, SIFT: deleterious - score 0, PolyPhen: probably_damaging - score 0.91

322	chr17:g.7675235T¿C	Substitution	Missense	HIP1 Q480H	1/833,0.12%	4/13,582	VEP: MODERATE, SIFT: deleterious - score 0, PolyPhen: probably_damaging - score 1
323	chr3:g.52641972C¿G	Substitution	Missense		1/833,0.12%	1/13,582	VEP: MODERATE, SIFT: tolerated - score 0.08, PolyPhen: probably_damaging - score 0.962
324	chr1:g.77964895A¿T	Substitution	Missense	ALK P1292S	1/833,0.12%	1/13,582	VEP: MODERATE, SIFT: deleterious - score 0, PolyPhen: probably_damaging - score 0.999
325	chr8:g.41934319C¿T	Substitution	Missense		1/833,0.12%	1/13,582	VEP: MODERATE, SIFT: tolerated_low_confidence - score 0.11, PolyPhen: benign - score 0.003
326	chr17:g.7670699C¿A	Substitution	Missense	TRIM24 H918Q	1/833,0.12%	14/13,582	VEP: MODERATE, SIFT: deleterious - score 0.01, PolyPhen: probably_damaging - score 0.946
327	chr7:g.2939769C¿G	Substitution	Missense		1/833,0.12%	1/13,582	VEP: MODERATE, SIFT: deleterious - score 0.04, PolyPhen: possibly_damaging - score 0.856
328	chr7:g.140924615C¿T	Substitution	Missense	MPL K140N	1/833,0.12%	1/13,582	VEP: MODERATE, SIFT: tolerated_low_confidence - score 0.17, PolyPhen: benign - score 0.433
329	chr3:g.53722319G¿A	Substitution	Missense		1/833,0.12%	2/13,582	VEP: MODERATE, SIFT: tolerated - score 0.52, PolyPhen: benign - score 0.075
330	chr1:g.119922339G¿A	Substitution	Missense	FAT1 E1602Q	1/833,0.12%	1/13,582	VEP: MODERATE, SIFT: deleterious - score 0, PolyPhen: probably_damaging - score 0.959
331	chr19:g.32931439G¿T	Substitution	Missense		1/833,0.12%	1/13,582	VEP: MODERATE, SIFT: deleterious - score 0, PolyPhen: probably_damaging - score 0.979
332	chr5:g.35876110C¿T	Substitution	Missense	FLI1 S21L	1/833,0.12%	2/13,582	VEP: MODERATE, SIFT: deleterious - score 0.03, PolyPhen: possibly_damaging - score 0.817
333	chr18:g.63318264C¿G	Substitution	Missense		1/833,0.12%	1/13,582	VEP: MODERATE, SIFT: deleterious - score 0.05, PolyPhen: probably_damaging - score 0.961
334	chr2:g.222232152T¿C	Substitution	Missense	ECT2L C795Y	1/833,0.12%	1/13,582	VEP: MODERATE, SIFT: deleterious - score 0, PolyPhen: probably_damaging - score 0.996
335	chr4:g.53390604G¿A	Substitution	Missense		1/833,0.12%	1/13,582	VEP: MODERATE, SIFT: deleterious - score 0.02, PolyPhen: probably_damaging - score 0.999

336	chr5:g.38484787C¿T	Substitution Missense	MED12 Q27E	1/833,0.12%	1/13,582	VEP: MODERATE, SIFT: tolerated - score 0.14, PolyPhen: benign - score 0.166
337	chr19:g.11033339T¿C	Substitution Missense		1/833,0.12%	1/13,582	VEP: MODERATE, SIFT: deleterious - score 0, PolyPhen: possibly_damaging - score 0.69
338	chr11:g.118436828C¿A	Substitution Missense	NCOR1 H23Y	1/833,0.12%	1/13,582	VEP: MODERATE, SIFT: tolerated_low_confidence - score 0.06, PolyPhen: benign - score 0.111
339	chr19:g.33301707G¿T	Substitution Missense		1/833,0.12%	1/13,582	VEP: MODERATE, SIFT: tolerated - score 0.21, PolyPhen: benign - score 0.052
340	chr16:g.346689C¿T	Substitution Missense	PTPRB R1619K	1/833,0.12%	2/13,582	VEP: MODERATE, SIFT: deleterious - score 0, PolyPhen: probably_damaging - score 0.999
341	chr1:g.3186196G¿A	Substitution Missense	NCOR2 T1561I	1/833,0.12%	2/13,582	VEP: MODERATE, SIFT: deleterious_low_confidence - score 0.01, PolyPhen: benign - score 0.265
342	chr4:g.186628670T¿G	Substitution Missense		1/833,0.12%	1/13,582	VEP: MODERATE, SIFT: deleterious - score 0, PolyPhen: probably_damaging - score 0.946
343	chr12:g.56101952G¿A	Substitution Missense	EZH2 D529N	1/833,0.12%	1/13,582	VEP: MODERATE, SIFT: tolerated - score 0.61, PolyPhen: benign - score 0
344	chr12:g.49050301G¿A	Substitution Missense		1/833,0.12%	1/13,582	VEP: MODERATE, SIFT: deleterious_low_confidence - score 0, PolyPhen: possibly_damaging - score 0.641
345	chr4:g.186636652A¿C	Substitution Missense	ATIC D186N	1/833,0.12%	1/13,582	VEP: MODERATE, SIFT: deleterious - score 0, PolyPhen: probably_damaging - score 0.999
346	chr4:g.125317584C¿A	Substitution Missense		1/833,0.12%	1/13,582	VEP: MODERATE, SIFT: deleterious - score 0, PolyPhen: probably_damaging - score 0.996
347	chr10:g.87961113T¿G	Substitution Missense	CIITA Q103H	1/833,0.12%	9/13,582	VEP: MODERATE, SIFT: deleterious - score 0, PolyPhen: probably_damaging - score 0.998
348	chr1:g.7664237G¿A	Substitution Missense		1/833,0.12%	2/13,582	VEP: MODERATE, SIFT: tolerated_low_confidence - score 0.88, PolyPhen: benign - score 0
349	chr2:g.197400339C¿G	Substitution Missense	TBX3 E468Q	1/833,0.12%	1/13,582	VEP: MODERATE, SIFT: deleterious - score 0, PolyPhen: probably_damaging - score 0.993

350	chr8:g.102272624C¿T	Substitution Missense		1/833,0.12%	2/13,582	VEP: MODERATE, SIFT: deleterious - score 0, PolyPhen: probably_damaging - score 0.996
351	chr17:g.64503994T¿C	Substitution Missense	CBL S899F	1/833,0.12%	2/13,582	VEP: MODERATE, SIFT: deleterious - score 0, PolyPhen: probably_damaging - score 1
352	chr12:g.70539976G¿C	Substitution Missense		1/833,0.12%	1/13,582	VEP: MODERATE, SIFT: deleterious - score 0.01, PolyPhen: possibly_damaging - score 0.74
353	chr21:g.43095524C¿T	Substitution Missense	OLIG2 D321G	1/833,0.12%	1/13,582	VEP: MODERATE, SIFT: deleterious - score 0.01, PolyPhen: probably_damaging - score 0.992
354	chr8:g.31143607A¿G	Substitution Missense		1/833,0.12%	1/13,582	VEP: MODERATE, SIFT: tolerated - score 0.18, PolyPhen: benign - score 0.001
355	chr3:g.142449595G¿T	Substitution Missense	NUTM1 S555F	1/833,0.12%	1/13,582	VEP: MODERATE, SIFT: tolerated - score 0.11, PolyPhen: possibly_damaging - score 0.715
356	chr17:g.40630774C¿G	Substitution Missense		1/833,0.12%	1/13,582	VEP: MODERATE, SIFT: tolerated - score 0.23, PolyPhen: benign - score 0.001
357	chr7:g.92079646G¿A	Substitution Missense	PRKACA S213N	1/833,0.12%	1/13,582	VEP: MODERATE, SIFT: deleterious - score 0.04, PolyPhen: possibly_damaging - score 0.487
358	chr12:g.6600593G¿T	Substitution Missense		1/833,0.12%	1/13,582	VEP: MODERATE, SIFT: deleterious - score 0.05, PolyPhen: possibly_damaging - score 0.748
359	chr11:g.108343253T¿C	Substitution Missense	DCTN1 E482G	1/833,0.12%	1/13,582	VEP: MODERATE, SIFT: deleterious - score 0, PolyPhen: probably_damaging - score 0.997
360	chr13:g.48459811T¿G	Substitution Missense		1/833,0.12%	1/13,582	VEP: MODERATE, SIFT: deleterious - score 0, PolyPhen: probably_damaging - score 0.989
361	chr17:g.9926641C¿A	Substitution Missense	PBRM1 M844V	1/833,0.12%	1/13,582	VEP: MODERATE, SIFT: deleterious - score 0, PolyPhen: possibly_damaging - score 0.738
362	chr2:g.222202132G¿A	Substitution Missense		1/833,0.12%	1/13,582	VEP: MODERATE, SIFT: deleterious_low_confidence - score 0, PolyPhen: possibly_damaging - score 0.807
363	chr3:g.48680220T¿C	Substitution Missense	FAT1 N1991I	1/833,0.12%	1/13,582	VEP: MODERATE, SIFT: tolerated - score 0.52, PolyPhen: benign - score 0

364	chr11:g.128772892G¿A	Substitution Missense		1/833,0.12%	1/13,582	VEP: MODERATE, SIFT: tolerated - score 0.05, PolyPhen: benign - score 0.282
365	chr2:g.74367743C¿T	Substitution Missense	CLTCL1 A1615T	1/833,0.12%	1/13,582	VEP: MODERATE, SIFT: deleterious - score 0, PolyPhen: probably_damaging - score 0.989
366	chr7:g.92108698G¿C	Substitution Intron		/833,0.12%1	/13,582VEP:	MODIFIER
367	chr1:g.114402788G¿A	Substitution Missense	NCOR2 R488Q	1/833,0.12%	3/13,582	VEP: MODERATE, SIFT: tolerated - score 0.48, PolyPhen: benign - score 0
368	chr17:g.16165131G¿C	Substitution Missense		1/833,0.12%	1/13,582	VEP: MODERATE, SIFT: deleterious - score 0.01, PolyPhen: benign - score 0.235
369	chr2:g.36857931A¿C	Substitution Missense	RANBP17 R715H	1/833,0.12%	1/13,582	VEP: MODERATE, SIFT: deleterious - score 0, PolyPhen: benign - score 0.434
370	chr1:g.241519691G¿C	Substitution Missense		1/833,0.12%	1/13,582	VEP: MODERATE, SIFT: tolerated_low_confidence - score 0.19, PolyPhen: benign - score 0
371	chr22:g.41164092G¿C	Substitution Missense	CARD11 V574I	1/833,0.12%	1/13,582	VEP: MODERATE, SIFT: deleterious - score 0, PolyPhen: probably_damaging - score 0.993
372	chr2:g.29920136C¿T	Substitution Missense		1/833,0.12%	1/13,582	VEP: MODERATE, SIFT: deleterious_low_confidence - score 0.02, PolyPhen: benign - score 0
373	chr8:g.56212870A¿G	Substitution Missense	EML4 W657C	1/833,0.12%	1/13,582	VEP: MODERATE, SIFT: tolerated_low_confidence - score 0.86, PolyPhen: benign - score 0.001
374	chr14:g.92014526T¿C	Substitution Missense		1/833,0.12%	1/13,582	VEP: MODERATE, SIFT: tolerated - score 0.07, PolyPhen: benign - score 0.046
375	chr1:g.116393597G¿A	Substitution Missense	MNX1 P392L	1/833,0.12%	2/13,582	VEP: MODERATE, SIFT: deleterious - score 0.01, PolyPhen: probably_damaging - score 1
376	chr14:g.65093775C¿G	Substitution Missense		1/833,0.12%	1/13,582	VEP: MODERATE, SIFT: deleterious - score 0, PolyPhen: probably_damaging - score 0.995
377	chr7:g.2913310A¿G	Substitution Missense	FAT1 Y2086D	1/833,0.12%	2/13,582	VEP: MODERATE, SIFT: deleterious - score 0.02, PolyPhen: benign - score 0.101

378	chr5:g.180620648G¿T	Substitution Missense		1/833,0.12%	1/13,582	VEP: MODERATE, SIFT: deleterious - score 0.03, PolyPhen: possibly_damaging - score 0.463
379	chrX:g.71290743C¿A	Substitution Missense	UBR5 M2654I	1/833,0.12%	1/13,582	VEP: MODERATE, SIFT: deleterious - score 0.01, PolyPhen: benign - score 0.001
380	chr12:g.27656715G¿A	Substitution Missense		1/833,0.12%	1/13,582	VEP: MODERATE, SIFT: tolerated - score 0.06, PolyPhen: benign - score 0.15
381	chr12:g.122377527C¿A	Substitution Missense	SOCS1 P25S	1/833,0.12%	1/13,582	VEP: MODERATE, SIFT: tolerated - score 0.14, PolyPhen: benign - score 0
382	chr11:g.108329108T¿C	Substitution Missense		1/833,0.12%	1/13,582	VEP: MODERATE, SIFT: deleterious - score 0, PolyPhen: possibly_damaging - score 0.49
383	chrX:g.77508484G¿C	Substitution Missense	ERBB3 N697S	1/833,0.12%	1/13,582	VEP: MODERATE, SIFT: deleterious_low_confidence - score 0.02, PolyPhen: probably_damaging - score 0.979
384	chr11:g.32428038G¿A	Substitution Missense		1/833,0.12%	1/13,582	VEP: MODERATE, SIFT: deleterious_low_confidence - score 0, PolyPhen: probably_damaging - score 0.947
385	chr4:g.125490502C¿A	Substitution Missense	ETV1 L50R	1/833,0.12%	2/13,582	VEP: MODERATE, SIFT: deleterious_low_confidence - score 0.01, PolyPhen: probably_damaging - score 0.987
386	chr16:g.56940062A¿G	Substitution Missense		1/833,0.12%	1/13,582	VEP: MODERATE, SIFT: deleterious - score 0, PolyPhen: possibly_damaging - score 0.876
387	chr5:g.171309465G¿A	Substitution Missense	TET1 A1866T	1/833,0.12%	1/13,582	VEP: MODERATE, SIFT: tolerated - score 0.34, PolyPhen: benign - score 0.037
388	chr19:g.44749016C¿G	Substitution Missense		1/833,0.12%	1/13,582	VEP: MODERATE, SIFT: tolerated_low_confidence - score 0.21, PolyPhen: benign - score 0.003
389	chr3:g.53735456G¿C	Substitution Missense	ZMYM2 C639R	1/833,0.12%	1/13,582	VEP: MODERATE, SIFT: deleterious - score 0.01, PolyPhen: possibly_damaging - score 0.521
390	chr22:g.27799913C¿T	Substitution Missense		1/833,0.12%	1/13,582	VEP: MODERATE, SIFT: tolerated_low_confidence - score 0.75, PolyPhen: benign - score 0
391	chr16:g.68808710C¿A	Substitution Missense	PRDM1 K620R	1/833,0.12%	1/13,582	VEP: MODERATE, SIFT: tolerated - score 0.07, PolyPhen: benign - score 0.062

392	chr9:g.107487046G¿A	Substitution Missense		1/833,0.12%	2/13,582	VEP: MODERATE, SIFT: deleterious - score 0, PolyPhen: probably_damaging - score 0.972
393	chr2:g.136115401T¿C	Substitution Missense	CDH11 D794V	1/833,0.12%	1/13,582	VEP: MODERATE, SIFT: tolerated - score 1, PolyPhen: benign - score 0
394	chr2:g.29920308C¿T	Substitution Missense		1/833,0.12%	1/13,582	VEP: MODERATE, SIFT: deleterious_low_confidence - score 0.03, PolyPhen: benign - score 0
395	chr17:g.39716337G¿A	Substitution Missense	MTOR H312D	1/833,0.12%	1/13,582	VEP: MODERATE, SIFT: tolerated - score 0.48, PolyPhen: benign - score 0
396	chr12:g.132667610T¿C	Substitution Missense		1/833,0.12%	1/13,582	VEP: MODERATE, SIFT: deleterious - score 0.01, PolyPhen: benign - score 0.038
397	chr16:g.10904751G¿C	Substitution Missense	SLC34A2 E49K	1/833,0.12%	1/13,582	VEP: MODERATE, SIFT: tolerated - score 0.21, PolyPhen: benign - score 0.098
398	chr15:g.50482007A¿G	Substitution Missense		1/833,0.12%	1/13,582	VEP: MODERATE, SIFT: tolerated - score 0.75, PolyPhen: benign - score 0
399	chr11:g.118491755G¿A	Substitution Missense	NSD1 V2296A	1/833,0.12%	2/13,582	VEP: MODERATE, SIFT: deleterious - score 0.01, PolyPhen: probably_damaging - score 0.951
400	chr15:g.90804278G¿A	Substitution Missense		1/833,0.12%	1/13,582	VEP: MODERATE, SIFT: deleterious - score 0.01, PolyPhen: benign - score 0.281
401	chr17:g.42210216C¿G	Substitution Missense	SYK E315D	1/833,0.12%	1/13,582	VEP: MODERATE, SIFT: deleterious - score 0, PolyPhen: probably_damaging - score 0.999
402	chr7:g.138916877G¿A	Substitution Missense		1/833,0.12%	1/13,582	VEP: MODERATE, SIFT: tolerated - score 0.16, PolyPhen: benign - score 0.374
403	chr11:g.108365354C¿T	Substitution Missense	PTK6 R171W	1/833,0.12%	1/13,582	VEP: MODERATE, SIFT: deleterious - score 0, PolyPhen: probably_damaging - score 0.991
404	chr4:g.55087625T¿C	Substitution Missense		1/833,0.12%	1/13,582	VEP: MODERATE, SIFT: tolerated - score 0.23, PolyPhen: probably_damaging - score 0.999
405	chr16:g.50793557T¿G	Substitution Missense	KIAA1549 T958R	1/833,0.12%	1/13,582	VEP: MODERATE, SIFT: deleterious - score 0, PolyPhen: probably_damaging - score 0.996

406	chr19:g.11027822T¿C	Substitution Missense		1/833,0.12%	1/13,582	VEP: MODERATE, SIFT: deleterious - score 0, PolyPhen: probably_damaging - score 0.998
407	chr3:g.70970794A¿G	Substitution Missense	WT1 Q397K	1/833,0.12%	1/13,582	VEP: MODERATE, SIFT: deleterious - score 0, PolyPhen: probably_damaging - score 1
408	chr6:g.128009182T¿A	Substitution Missense		1/833,0.12%	1/13,582	VEP: MODERATE, SIFT: deleterious - score 0.05, PolyPhen: benign - score 0.189
409	chrX:g.40074834G¿T	Substitution Missense	PRDM1 L680R	1/833,0.12%	1/13,582	VEP: MODERATE, SIFT: deleterious - score 0.02, PolyPhen: benign - score 0.285
410	chr1:g.198749481G¿A	Substitution Missense		1/833,0.12%	1/13,582	VEP: MODERATE, SIFT: deleterious - score 0.02, PolyPhen: possibly_damaging - score 0.824
411	chr17:g.16108854G¿A	Substitution Missense	POLE I71T	1/833,0.12%	1/13,582	VEP: MODERATE, SIFT: deleterious - score 0.05, PolyPhen: probably_damaging - score 0.93
412	chr22:g.29678204C¿A	Substitution Missense		1/833,0.12%	1/13,582	VEP: MODERATE, SIFT: tolerated - score 0.55, PolyPhen: benign - score 0.009
413	chr22:g.19196527G¿T	Substitution Missense	XPO1 E571K	1/833,0.12%	1/13,582	VEP: MODERATE, SIFT: deleterious - score 0.01, PolyPhen: probably_damaging - score 0.998
414	chr4:g.1799305G¿C	Substitution Missense		1/833,0.12%	1/13,582	VEP: MODERATE, SIFT: deleterious - score 0, PolyPhen: probably_damaging - score 0.994
415	chr8:g.91970726C¿T	Substitution Missense	COL1A1 R763H	1/833,0.12%	4/13,582	VEP: MODERATE, SIFT: tolerated - score 0.1, PolyPhen: probably_damaging - score 0.997
416	chr6:g.29942885A¿G	Substitution Missense		1/833,0.12%	1/13,582	VEP: MODERATE, SIFT: deleterious_low_confidence - score 0, PolyPhen: benign - score 0.325
417	chr4:g.55094891C¿A	Substitution Missense	PTK6 L227M	1/833,0.12%	1/13,582	VEP: MODERATE, SIFT: tolerated - score 0.09, PolyPhen: benign - score 0.138
418	chr6:g.41940434G¿A	Substitution Missense		1/833,0.12%	1/13,582	VEP: MODERATE, SIFT: tolerated - score 0.27, PolyPhen: benign - score 0.022
419	chr11:g.118436669G¿T	Substitution Missense	TCF12 S59F	1/833,0.12%	1/13,582	VEP: MODERATE, SIFT: tolerated_low_confidence - score 0.05, PolyPhen: benign - score 0.011

420	chr2:g.25240417C¿T	Substitution Missense		1/833,0.12%	4/13,582	VEP: MODERATE, SIFT: tolerated - score 0.39, PolyPhen: possibly_damaging - score 0.874
421	chr13:g.48380190C¿T	Substitution Missense	GNAS D64H	1/833,0.12%	1/13,582	VEP: MODERATE, SIFT: deleterious - score 0, PolyPhen: probably_damaging - score 1
422	chrX:g.77683775T¿G	Substitution Missense		1/833,0.12%	1/13,582	VEP: MODERATE, SIFT: deleterious_low_confidence - score 0.03, PolyPhen: possibly_damaging - score 0.494
423	chr7:g.148809078C¿T	Substitution Missense	ATM V2441D	1/833,0.12%	1/13,582	VEP: MODERATE, SIFT: deleterious - score 0, PolyPhen: probably_damaging - score 0.997
424	chr21:g.34859564G¿C	Substitution Missense		1/833,0.12%	1/13,582	VEP: MODERATE, SIFT: deleterious - score 0.01, PolyPhen: possibly_damaging - score 0.56
425	chr16:g.67029733T¿C	Substitution Missense	SETD2 T749I	1/833,0.12%	1/13,582	VEP: MODERATE, SIFT: deleterious - score 0, PolyPhen: probably_damaging - score 0.968
426	chr11:g.61430175C¿T	Substitution Missense		1/833,0.12%	2/13,582	VEP: MODERATE, SIFT: tolerated_low_confidence - score 0.83, PolyPhen: benign - score 0
427	chr7:g.152435666G¿A	Substitution Missense	PTPRC Q891K	1/833,0.12%	1/13,582	VEP: MODERATE, SIFT: deleterious - score 0, PolyPhen: possibly_damaging - score 0.876
428	chr14:g.92006127C¿G	Substitution Missense		1/833,0.12%	1/13,582	VEP: MODERATE, SIFT: deleterious - score 0.01, PolyPhen: probably_damaging - score 0.983
429	chrX:g.77664734G¿T	Substitution Missense	ARID2 S1429G	1/833,0.12%	1/13,582	VEP: MODERATE, SIFT: deleterious - score 0, PolyPhen: possibly_damaging - score 0.768
430	chr2:g.189867894T¿G	Substitution Missense		1/833,0.12%	1/13,582	VEP: MODERATE, SIFT: deleterious - score 0, PolyPhen: probably_damaging - score 0.996
431	chr3:g.69964886A¿T	Substitution Missense	LIFR S12T	1/833,0.12%	1/13,582	VEP: MODERATE, SIFT: tolerated - score 0.13, PolyPhen: benign - score 0.148
432	chr10:g.32055889A¿T	Substitution Missense		1/833,0.12%	1/13,582	VEP: MODERATE, SIFT: tolerated - score 0.07, PolyPhen: benign - score 0.011
433	chr12:g.122377514C¿T	Substitution Missense	TCF7L2 K96Q	1/833,0.12%	2/13,582	VEP: MODERATE, SIFT: tolerated - score 0.13, PolyPhen: benign - score 0.097

434	chr15:g.88135113C¿G	Substitution Missense		1/833,0.12%	2/13,582	VEP: MODERATE, SIFT: tolerated - score 0.37, PolyPhen: benign - score 0.028
435	chr14:g.65093794T¿A	Substitution Missense	KDR V218I	1/833,0.12%	1/13,582	VEP: MODERATE, SIFT: deleterious - score 0, PolyPhen: probably_damaging - score 0.999
436	chr12:g.58880730T¿G	Substitution Missense		1/833,0.12%	1/13,582	VEP: MODERATE, SIFT: deleterious - score 0.01, PolyPhen: probably_damaging - score 0.983
437	chr10:g.68645162G¿T	Substitution Missense	PRDM16 G690E	1/833,0.12%	1/13,582	VEP: MODERATE, SIFT: tolerated - score 0.27, PolyPhen: benign - score 0
438	chr11:g.118436618C¿G	Substitution Missense		1/833,0.12%	1/13,582	VEP: MODERATE, SIFT: tolerated_low_confidence - score 0.09, PolyPhen: benign - score 0.007
439	chr5:g.180616465G¿A	Substitution Missense	KIT K471M	1/833,0.12%	2/13,582	VEP: MODERATE, SIFT: deleterious - score 0, PolyPhen: probably_damaging - score 1
440	chr3:g.186065985T¿A	Substitution Missense		1/833,0.12%	1/13,582	VEP: MODERATE, SIFT: tolerated - score 0.14, PolyPhen: probably_damaging - score 0.934
441	chr6:g.41941631C¿T	Substitution Missense	KIAA1549 S287C	1/833,0.12%	1/13,582	VEP: MODERATE, SIFT: deleterious - score 0, PolyPhen: probably_damaging - score 0.998
442	chr6:g.156778765G¿A	Substitution Missense		1/833,0.12%	1/13,582	VEP: MODERATE, SIFT: tolerated_low_confidence - score 0.2, PolyPhen: benign - score 0
443	chr21:g.38445489C¿T	Substitution Missense	FGFR2 G553E	1/833,0.12%	2/13,582	VEP: MODERATE, SIFT: tolerated - score 0.24, PolyPhen: benign - score 0.003
444	chr12:g.132675398C¿T	Substitution Missense		1/833,0.12%	1/13,582	VEP: MODERATE, SIFT: tolerated - score 0.94, PolyPhen: benign - score 0.036
445	chr16:g.2064404A¿C	Substitution Missense	FGFR3 G377C	1/833,0.12%	1/13,582	VEP: MODERATE, SIFT: deleterious - score 0.01, PolyPhen: probably_damaging - score 0.981
446	chr8:g.32763801C¿G	Substitution Missense		1/833,0.12%	1/13,582	VEP: MODERATE, SIFT: tolerated - score 0.06, PolyPhen: probably_damaging - score 0.945
447	chr4:g.125450948C¿A	Substitution Missense	MSN E505V	1/833,0.12%	1/13,582	VEP: MODERATE, SIFT: deleterious - score 0, PolyPhen: probably_damaging - score 0.999

448	chr15:g.87929334C¿T	Substitution Missense		1/833,0.12%	2/13,582	VEP: MODERATE, SIFT: deleterious - score 0, PolyPhen: probably_damaging - score 0.997
449	chr12:g.92145523A¿G	Substitution Missense	LMO2 G33S	1/833,0.12%	1/13,582	VEP: MODERATE, SIFT: tolerated_low_confidence - score 0.51, PolyPhen: benign - score 0.259
450	chrX:g.45020674C¿T	Substitution Missense		1/833,0.12%	1/13,582	VEP: MODERATE, SIFT: deleterious - score 0, PolyPhen: possibly_damaging - score 0.809
451	chr1:g.3432013C¿T	Substitution Missense	ATRX D1714N	1/833,0.12%	1/13,582	VEP: MODERATE, SIFT: tolerated - score 0.09, PolyPhen: benign - score 0.003
452	chr2:g.47480768C¿T	Substitution Missense		1/833,0.12%	1/13,582	VEP: MODERATE, SIFT: deleterious - score 0, PolyPhen: probably_damaging - score 1
453	chr20:g.32429972G¿A	Substitution Missense	CCDC6 P396L	1/833,0.12%	1/13,582	VEP: MODERATE, SIFT: tolerated - score 0.49, PolyPhen: benign - score 0.329
454	chr7:g.92038617G¿C	Substitution Missense		1/833,0.12%	1/13,582	VEP: MODERATE, SIFT: tolerated - score 0.12, PolyPhen: probably_damaging - score 0.957
455	chr7:g.92774800C¿A	Substitution Missense	PTPRK E525K	1/833,0.12%	1/13,582	VEP: MODERATE, SIFT: deleterious - score 0.02, PolyPhen: possibly_damaging - score 0.901
456	chr19:g.1223169C¿T	Substitution Missense		1/833,0.12%	2/13,582	VEP: MODERATE, SIFT: tolerated - score 0.08, PolyPhen: benign - score 0.297
457	chr3:g.47083877G¿A	Substitution Missense	FBXW7 F521L	1/833,0.12%	1/13,582	VEP: MODERATE, SIFT: tolerated - score 0.11, PolyPhen: benign - score 0.034
458	chr22:g.41177079T¿G	Substitution Missense		1/833,0.12%	1/13,582	VEP: MODERATE, SIFT: deleterious - score 0, PolyPhen: probably_damaging - score 0.998
459	chr4:g.125318125C¿G	Substitution Missense	SOCS1 E91A	1/833,0.12%	1/13,582	VEP: MODERATE, SIFT: tolerated - score 0.51, PolyPhen: benign - score 0.003
460	chr4:g.125450425T¿C	Substitution Missense		1/833,0.12%	1/13,582	VEP: MODERATE, SIFT: deleterious - score 0, PolyPhen: probably_damaging - score 0.986
461	chr10:g.121565468C¿T	Substitution Missense	ETV6 E392K	1/833,0.12%	1/13,582	VEP: MODERATE, SIFT: tolerated - score 0.92, PolyPhen: benign - score 0.003

462	chr17:g.7670700G¿A	Substitution Missense		1/833,0.12%	18/13,582	VEP: MODERATE, SIFT: tolerated - score 0.09, PolyPhen: benign - score 0.344
463	chr16:g.79599085T¿A	Substitution Missense	BIRC3 H574Y	1/833,0.12%	1/13,582	VEP: MODERATE, SIFT: deleterious - score 0, PolyPhen: probably_damaging - score 0.999
464	chr16:g.9763379G¿A	Substitution Missense		1/833,0.12%	1/13,582	VEP: MODERATE, SIFT: tolerated - score 0.72, PolyPhen: benign - score 0.005
465	chr17:g.42224835G¿A	Substitution Missense	FAT4 K1055Q	1/833,0.12%	1/13,582	VEP: MODERATE, SIFT: deleterious - score 0, PolyPhen: probably_damaging - score 0.998
466	chr2:g.29233648C¿G	Substitution Missense		1/833,0.12%	1/13,582	VEP: MODERATE, SIFT: deleterious - score 0.01, PolyPhen: probably_damaging - score 0.995
467	chr15:g.74023097G¿A	Substitution Missense	MED12 G488A	1/833,0.12%	1/13,582	VEP: MODERATE, SIFT: tolerated - score 0.62, PolyPhen: benign - score 0.001
468	chr12:g.122022095T¿A	Substitution Missense		1/833,0.12%	1/13,582	VEP: MODERATE, SIFT: deleterious - score 0.01, PolyPhen: benign - score 0.047
469	chr5:g.177209948C¿G	Substitution Missense	TSC1 E813Q	1/833,0.12%	1/13,582	VEP: MODERATE, SIFT: tolerated_low_confidence - score 0.06, PolyPhen: benign - score 0.019
470	chr2:g.29532042C¿T	Substitution Missense		1/833,0.12%	2/13,582	VEP: MODERATE, SIFT: tolerated - score 0.36, PolyPhen: benign - score 0.285
471	chr2:g.174877854C¿T	Substitution Missense	ERCC3 D385E	1/833,0.12%	1/13,582	VEP: MODERATE, SIFT: tolerated - score 0.15, PolyPhen: benign - score 0.005
472	chr4:g.125491044G¿C	Substitution Missense		1/833,0.12%	1/13,582	VEP: MODERATE, SIFT: tolerated - score 0.52, PolyPhen: benign - score 0.125
473	chr12:g.350624T¿G	Substitution Missense	SDHC F41L	1/833,0.12%	1/13,582	VEP: MODERATE, SIFT: tolerated - score 0.67, PolyPhen: benign - score 0.05
474	chr1:g.186318774C¿A	Substitution Missense		1/833,0.12%	1/13,582	VEP: MODERATE, SIFT: deleterious - score 0, PolyPhen: probably_damaging - score 0.996
475	chr6:g.137876104T¿C	Substitution Missense	ATM G506D	1/833,0.12%	1/13,582	VEP: MODERATE, SIFT: deleterious - score 0, PolyPhen: probably_damaging - score 0.937

476	chr10:g.102399338T¿C	Substitution Missense		1/833,0.12%	1/13,582	VEP: MODERATE, SIFT: tolerated - score 0.41, PolyPhen: benign - score 0
477	chr19:g.1622056T¿C	Substitution Missense	KMT2A R397K	1/833,0.12%	1/13,582	VEP: MODERATE, SIFT: tolerated - score 0.09, PolyPhen: benign - score 0.024
478	chr11:g.32435095G¿A	Substitution Missense		1/833,0.12%	1/13,582	VEP: MODERATE, SIFT: deleterious_low_confidence - score 0, PolyPhen: possibly_damaging - score 0.844
479	chr2:g.100007151C¿A	Substitution Missense	FGFR3 Y381N	1/833,0.12%	1/13,582	VEP: MODERATE, SIFT: tolerated - score 0.77, PolyPhen: benign - score 0.003
480	chr7:g.2929995C¿G	Substitution Missense		1/833,0.12%	1/13,582	VEP: MODERATE, SIFT: tolerated - score 0.17, PolyPhen: benign - score 0.214
481	chr2:g.211947591A¿C	Substitution Missense	CACNA1D F2067Y	1/833,0.12%	1/13,582	VEP: MODERATE, SIFT: deleterious - score 0, PolyPhen: probably_damaging - score 1
482	chr12:g.25227348G¿A	Substitution Missense		1/833,0.12%	1/13,582	VEP: MODERATE, SIFT: deleterious - score 0.03, PolyPhen: probably_damaging - score 0.972
483	chr3:g.196065583C¿G	Substitution Missense	MYH11 G721D	1/833,0.12%	1/13,582	VEP: MODERATE, SIFT: tolerated - score 0.11, PolyPhen: probably_damaging - score 0.997
484	chr4:g.55081962G¿C	Substitution Missense		1/833,0.12%	1/13,582	VEP: MODERATE, SIFT: tolerated - score 0.05, PolyPhen: benign - score 0.401
485	chr14:g.36519152T¿G	Substitution Missense	CUX1 R42I	1/833,0.12%	1/13,582	VEP: MODERATE, SIFT: deleterious - score 0, PolyPhen: probably_damaging - score 0.994
486	chr12:g.6668109A¿T	Substitution Missense		1/833,0.12%	1/13,582	VEP: MODERATE, SIFT: deleterious - score 0, PolyPhen: probably_damaging - score 0.999
487	chr2:g.177234118C¿T	Substitution Missense	ZFHX3 P2525S	1/833,0.12%	2/13,582	VEP: MODERATE, SIFT: deleterious - score 0, PolyPhen: probably_damaging - score 0.996
488	chr17:g.43071191G¿T	Substitution Missense		1/833,0.12%	1/13,582	VEP: MODERATE, SIFT: tolerated - score 0.1, PolyPhen: probably_damaging - score 1
489	chr7:g.124892271C¿T	Substitution Missense	NCOR2 H982Y	1/833,0.12%	1/13,582	VEP: MODERATE, SIFT: deleterious - score 0, PolyPhen: probably_damaging - score 1

490	chr11:g.72007247C¿T	Substitution Missense		1/833,0.12%	1/13,582	VEP: MODERATE, SIFT: tolerated - score 0.11, PolyPhen: possibly_damaging - score 0.78
491	chr3:g.41236657C¿T	Substitution Missense	FAT1 N618T	1/833,0.12%	1/13,582	VEP: MODERATE, SIFT: deleterious - score 0, PolyPhen: probably_damaging - score 0.981
492	chr12:g.49022123A¿G	Substitution Missense		1/833,0.12%	1/13,582	VEP: MODERATE, SIFT: deleterious - score 0, PolyPhen: probably_damaging - score 0.999
493	chr7:g.5987365A¿G	Substitution Missense	AFF3 Q1084K	1/833,0.12%	1/13,582	VEP: MODERATE, SIFT: tolerated - score 0.72, PolyPhen: benign - score 0.003
494	chr9:g.121175145C¿G	Substitution Missense		1/833,0.12%	1/13,582	VEP: MODERATE, SIFT: deleterious - score 0, PolyPhen: possibly_damaging - score 0.707
495	chr4:g.87046741G¿A	Substitution Missense	ERBB4 R711C	1/833,0.12%	1/13,582	VEP: MODERATE, SIFT: deleterious - score 0, PolyPhen: probably_damaging - score 1
496	chr19:g.54145676C¿T	Substitution Missense		1/833,0.12%	3/13,582	VEP: MODERATE, SIFT: deleterious - score 0.01, PolyPhen: probably_damaging - score 0.998
497	chrX:g.77589909C¿A	Substitution Missense	CCNE1 A111E	1/833,0.12%	1/13,582	VEP: MODERATE, SIFT: deleterious - score 0, PolyPhen: probably_damaging - score 0.94
498	chr9:g.131151808G¿A	Substitution Missense		1/833,0.12%	1/13,582	VEP: MODERATE, SIFT: tolerated - score 0.12, PolyPhen: benign - score 0.121
499	chr5:g.68293725A¿G	Substitution Missense	STIL V602I	1/833,0.12%	1/13,582	VEP: MODERATE, SIFT: tolerated - score 0.06, PolyPhen: possibly_damaging - score 0.448
500	chr9:g.5534942G¿A	Substitution Missense		1/833,0.12%	1/13,582	VEP: MODERATE, SIFT: deleterious - score 0, PolyPhen: probably_damaging - score 0.998
501	chr16:g.72959206G¿A	Substitution Missense	ATR K1057R	1/833,0.12%	1/13,582	VEP: MODERATE, SIFT: deleterious - score 0, PolyPhen: probably_damaging - score 0.976
502	chr4:g.186617137C¿G	Substitution Missense		1/833,0.12%	1/13,582	VEP: MODERATE, SIFT: deleterious - score 0, PolyPhen: benign - score 0.383
503	chr20:g.32434799T¿C	Substitution Missense	NSD1 E2505D	1/833,0.12%	1/13,582	VEP: MODERATE, SIFT: deleterious - score 0.01, PolyPhen: probably_damaging - score 1

504	chr15:g.40199722G¿A	Substitution Missense		1/833,0.12%	1/13,582	VEP: MODERATE, SIFT: tolerated - score 0.11, PolyPhen: benign - score 0.331
505	chr6:g.37171287G¿C	Substitution Missense	BCL3 P230L	1/833,0.12%	1/13,582	VEP: MODERATE, SIFT: deleterious - score 0.02, PolyPhen: benign - score 0.267
506	chr19:g.11021837C¿A	Substitution Missense		1/833,0.12%	1/13,582	VEP: MODERATE, SIFT: deleterious - score 0.02, PolyPhen: probably_damaging - score 0.939
507	chr14:g.65093742A¿C	Substitution Missense	KRAS A146P	1/833,0.12%	1/13,582	VEP: MODERATE, SIFT: deleterious - score 0, PolyPhen: probably_damaging - score 1
508	chr4:g.54658027C¿T	Substitution Missense		1/833,0.12%	2/13,582	VEP: MODERATE, SIFT: tolerated_low_confidence - score 0.06, PolyPhen: benign - score 0.01
509	chr3:g.177047335T¿C	Substitution Missense	GMPS S302C	1/833,0.12%	1/13,582	VEP: MODERATE, SIFT: deleterious - score 0.03, PolyPhen: benign - score 0.033
510	chr7:g.92045121G¿T	Substitution Missense		1/833,0.12%	1/13,582	VEP: MODERATE, SIFT: deleterious - score 0, PolyPhen: probably_damaging - score 0.967
511	chr3:g.142524032G¿C	Substitution Missense	NACA V285L	1/833,0.12%	1/13,582	VEP: MODERATE, SIFT: tolerated - score 1, PolyPhen: benign - score 0.003
512	chr19:g.10786666C¿T	Substitution Missense		1/833,0.12%	2/13,582	VEP: MODERATE, SIFT: deleterious - score 0, PolyPhen: probably_damaging - score 0.986
513	chr11:g.69643142G¿A	Substitution Missense	TCL1A Q46H	1/833,0.12%	1/13,582	VEP: MODERATE, SIFT: tolerated - score 0.11, PolyPhen: benign - score 0.408
514	chr3:g.10149838C¿A	Substitution Missense		1/833,0.12%	1/13,582	VEP: MODERATE, SIFT: deleterious - score 0, PolyPhen: probably_damaging - score 0.999
515	chr1:g.147621048G¿A	Substitution Missense	BCL11A E801K	1/833,0.12%	1/13,582	VEP: MODERATE, SIFT: tolerated - score 0.46, PolyPhen: benign - score 0.097
516	chr4:g.125316827C¿T	Substitution Missense		1/833,0.12%	1/13,582	VEP: MODERATE, SIFT: deleterious - score 0.02, PolyPhen: probably_damaging - score 0.996
517	chr14:g.65093772C¿T	Substitution Missense	BCR D248G	1/833,0.12%	1/13,582	VEP: MODERATE, SIFT: deleterious - score 0.03, PolyPhen: probably_damaging - score 1

518	chr1:g.50974103G¿C	Substitution Missense		1/833,0.12%	1/13,582	VEP: MODERATE, SIFT: deleterious - score 0, PolyPhen: probably_damaging - score 1
519	chr1:g.36466761C¿T	Substitution Missense	FAT1 D2382A	1/833,0.12%	1/13,582	VEP: MODERATE, SIFT: tolerated - score 0.15, PolyPhen: benign - score 0.058
520	chr2:g.211383970G¿A	Substitution Missense		1/833,0.12%	1/13,582	VEP: MODERATE, SIFT: tolerated - score 0.17, PolyPhen: benign - score 0.039
521	chr9:g.14307310G¿A	Substitution Missense	SPEN E707D	1/833,0.12%	2/13,582	VEP: MODERATE, SIFT: deleterious - score 0, PolyPhen: probably_damaging - score 0.995
522	chr19:g.10783057C¿A	Substitution Missense		1/833,0.12%	1/13,582	VEP: MODERATE, SIFT: deleterious - score 0.03, PolyPhen: probably_damaging - score 0.998
523	chr14:g.99231500G¿T	Substitution Missense	LIFR K47R	1/833,0.12%	1/13,582	VEP: MODERATE, SIFT: deleterious - score 0.01, PolyPhen: probably_damaging - score 0.955
524	chr12:g.49031564C¿G	Substitution Missense		1/833,0.12%	1/13,582	VEP: MODERATE, SIFT: deleterious_low_confidence - score 0.05, PolyPhen: possibly_damaging - score 0.751
525	chr17:g.39463011G¿A	Substitution Missense	BCL7A W31G	1/833,0.12%	1/13,582	VEP: MODERATE, SIFT: tolerated_low_confidence - score 0.11, PolyPhen: possibly_damaging - score 0.833
526	chr16:g.72796780G¿T	Substitution Missense		1/833,0.12%	1/13,582	VEP: MODERATE, SIFT: deleterious - score 0.01, PolyPhen: probably_damaging - score 0.952
527	chrX:g.67546611G¿T	Substitution Missense	GRIN2A E1040V	1/833,0.12%	1/13,582	VEP: MODERATE, SIFT: deleterious_low_confidence - score 0, PolyPhen: probably_damaging - score 0.996
528	chr17:g.61859856C¿T	Substitution Missense		1/833,0.12%	1/13,582	VEP: MODERATE, SIFT: deleterious - score 0, PolyPhen: probably_damaging - score 1
529	chr4:g.125490394C¿G	Substitution Missense	PDE4DIP L1569H	1/833,0.12%	1/13,582	VEP: MODERATE, SIFT: deleterious_low_confidence - score 0, PolyPhen: probably_damaging - score 0.984
530	chr11:g.108330215T¿A	Substitution Missense		1/833,0.12%	1/13,582	VEP: MODERATE, SIFT: deleterious - score 0, PolyPhen: benign - score 0.356
531	chr9:g.130854222C¿G	Substitution Missense	POT1 G40V	1/833,0.12%	1/13,582	VEP: MODERATE, SIFT: deleterious - score 0, PolyPhen: possibly_damaging - score 0.862

532	chr4:g.53453040G¿A	Substitution Missense		1/833,0.12%	1/13,582	VEP: MODERATE, SIFT: deleterious - score 0.05, PolyPhen: possibly_damaging - score 0.745
533	chr4:g.186708043A¿C	Substitution Missense	EIF3E P90S	1/833,0.12%	1/13,582	VEP: MODERATE, SIFT: deleterious - score 0, PolyPhen: probably_damaging - score 0.996
534	chr12:g.124340150G¿A	Substitution Missense		1/833,0.12%	1/13,582	VEP: MODERATE, SIFT: deleterious - score 0.01, PolyPhen: benign - score 0.099
535	chrX:g.67722862G¿A	Substitution Missense	FANCD2 M127I	1/833,0.12%	1/13,582	VEP: MODERATE, SIFT: deleterious - score 0.01, PolyPhen: probably_damaging - score 0.97
536	chr12:g.49054644G¿A	Substitution Missense		1/833,0.12%	1/13,582	VEP: MODERATE, SIFT: tolerated - score 0.14, PolyPhen: benign - score 0.112
537	chr10:g.86919235A¿G	Substitution Missense	TBX3 S55L	1/833,0.12%	1/13,582	VEP: MODERATE, SIFT: deleterious - score 0, PolyPhen: possibly_damaging - score 0.627
538	chr16:g.10907417T¿C	Substitution Missense		1/833,0.12%	1/13,582	VEP: MODERATE, SIFT: deleterious - score 0.01, PolyPhen: possibly_damaging - score 0.834
539	chr4:g.125490024C¿T	Substitution Missense	TERT A190T	1/833,0.12%	1/13,582	VEP: MODERATE, SIFT: deleterious - score 0, PolyPhen: probably_damaging - score 0.996
540	chr14:g.65093771C¿G	Substitution Missense		1/833,0.12%	1/13,582	VEP: MODERATE, SIFT: deleterious - score 0, PolyPhen: probably_damaging - score 1
541	chr15:g.88126363G¿T	Substitution Missense	AKAP9 Q1665L	1/833,0.12%	2/13,582	VEP: MODERATE, SIFT: deleterious - score 0.01, PolyPhen: probably_damaging - score 0.973
542	chr14:g.65077997T¿A	Substitution Missense		1/833,0.12%	1/13,582	VEP: MODERATE, SIFT: deleterious - score 0, PolyPhen: probably_damaging - score 0.999
543	chr12:g.112489084G¿T	Substitution Missense	PIM1 E32Q	1/833,0.12%	10/13,582	VEP: MODERATE, SIFT: deleterious - score 0, PolyPhen: probably_damaging - score 0.999
544	chr18:g.26032466C¿A	Substitution Missense		1/833,0.12%	1/13,582	VEP: MODERATE, SIFT: deleterious_low_confidence - score 0.03, PolyPhen: benign - score 0
545	chr4:g.125451809G¿A	Substitution Missense	PDCD1LG2 T66R	1/833,0.12%	1/13,582	VEP: MODERATE, SIFT: deleterious - score 0.02, PolyPhen: probably_damaging - score 1

546	chr2:g.189864113G¿A	Substitution Missense		1/833,0.12%	1/13,582	VEP: MODERATE, SIFT: tolerated - score 0.85, PolyPhen: benign - score 0.007
547	chr7:g.124863540G¿A	Substitution Missense	ATM L2309P	1/833,0.12%	3/13,582	VEP: MODERATE, SIFT: deleterious - score 0.03, PolyPhen: benign - score 0.009
548	chr14:g.37591925C¿T	Substitution Missense		1/833,0.12%	1/13,582	VEP: MODERATE, SIFT: tolerated - score 0.35, PolyPhen: benign - score 0.011
549	chr19:g.42290510C¿T	Substitution Missense	PBX1 R188W	1/833,0.12%	1/13,582	VEP: MODERATE, SIFT: deleterious_low_confidence - score 0, PolyPhen: probably_damaging - score 0.981
550	chr17:g.65536417C¿T	Substitution Missense		1/833,0.12%	1/13,582	VEP: MODERATE, SIFT: deleterious - score 0.01, PolyPhen: probably_damaging - score 0.976
551	chr17:g.7674953T¿C	Substitution Missense	KMT2D P2193L	1/833,0.12%	38/13,582	VEP: MODERATE, SIFT: deleterious - score 0, PolyPhen: probably_damaging - score 1
552	chr9:g.132897550G¿A	Substitution Missense		1/833,0.12%	1/13,582	VEP: MODERATE, SIFT: deleterious - score 0.03, PolyPhen: benign - score 0.307
553	chr16:g.72960013C¿T	Substitution Missense	FLT4 V81A	1/833,0.12%	2/13,582	VEP: MODERATE, SIFT: deleterious_low_confidence - score 0.01, PolyPhen: benign - score 0.318
554	chr7:g.148809093C¿T	Substitution Missense		1/833,0.12%	2/13,582	VEP: MODERATE, SIFT: deleterious - score 0, PolyPhen: probably_damaging - score 0.995
555	chr2:g.136115854T¿C	Substitution Missense	CIITA L932V	1/833,0.12%	1/13,582	VEP: MODERATE, SIFT: tolerated - score 0.43, PolyPhen: benign - score 0.108
556	chr4:g.125320972G¿C	Substitution Missense		1/833,0.12%	1/13,582	VEP: MODERATE, SIFT: deleterious - score 0.01, PolyPhen: probably_damaging - score 0.999
557	chr8:g.41947813G¿A	Substitution Missense	FANCE R460W	1/833,0.12%	1/13,582	VEP: MODERATE, SIFT: deleterious - score 0, PolyPhen: probably_damaging - score 0.999
558	chr4:g.105242908G¿T	Substitution Missense		1/833,0.12%	1/13,582	VEP: MODERATE, SIFT: deleterious - score 0, PolyPhen: probably_damaging - score 1
559	chr7:g.102248677G¿A	Substitution Missense	ATM E2423K	1/833,0.12%	1/13,582	VEP: MODERATE, SIFT: tolerated - score 0.29, PolyPhen: benign - score 0

560	chr16:g.27449200G¿A	Substitution Missense		1/833,0.12%	1/13,582	VEP: MODERATE, SIFT: tolerated - score 0.15, PolyPhen: possibly_damaging - score 0.844
561	chrX:g.71124329G¿A	Substitution Missense	TBX3 P48S	1/833,0.12%	1/13,582	VEP: MODERATE, SIFT: tolerated - score 0.15, PolyPhen: benign - score 0.06
562	chr19:g.12943743G¿A	Substitution Missense		1/833,0.12%	1/13,582	VEP: MODERATE, SIFT: deleterious - score 0.02, PolyPhen: benign - score 0.003
563	chr6:g.41941535C¿T	Substitution Missense	CDKN1B D158N	1/833,0.12%	2/13,582	VEP: MODERATE, SIFT: tolerated - score 0.23, PolyPhen: benign - score 0.006
564	chr2:g.108765169G¿A	Substitution Missense		1/833,0.12%	1/13,582	VEP: MODERATE, SIFT: deleterious - score 0.04, PolyPhen: possibly_damaging - score 0.739
565	chr9:g.20620685G¿C	Substitution Missense	BRIP1 E296K	1/833,0.12%	1/13,582	VEP: MODERATE, SIFT: tolerated - score 0.16, PolyPhen: benign - score 0.006
566	chr12:g.114674298A¿T	Substitution Missense		1/833,0.12%	1/13,582	VEP: MODERATE, SIFT: deleterious - score 0, PolyPhen: probably_damaging - score 0.991
567	chr13:g.32398479G¿A	Substitution Missense	FAT4 V1334L	1/833,0.12%	1/13,582	VEP: MODERATE, SIFT: tolerated - score 0.45, PolyPhen: benign - score 0.018
568	chr6:g.35458432C¿T	Substitution Missense		1/833,0.12%	1/13,582	VEP: MODERATE, SIFT: deleterious - score 0.02, PolyPhen: probably_damaging - score 0.999
569	chr11:g.32400009G¿A	Substitution Missense	ZNF521 D878E	1/833,0.12%	2/13,582	VEP: MODERATE, SIFT: deleterious_low_confidence - score 0.01, PolyPhen: benign - score 0.445
570	chr3:g.142559413A¿G	Substitution Missense		1/833,0.12%	1/13,582	VEP: MODERATE, SIFT: tolerated_low_confidence - score 0.24, PolyPhen: benign - score 0.024
571	chr19:g.6222395G¿A	Substitution Missense	NSD1 K1493E	1/833,0.12%	1/13,582	VEP: MODERATE, SIFT: tolerated - score 0.2, PolyPhen: possibly_damaging - score 0.713
572	chr1:g.161671490G¿A	Substitution Missense		1/833,0.12%	1/13,582	VEP: MODERATE, SIFT: tolerated - score 0.06, PolyPhen: benign - score 0.007
573	chr17:g.42210454T¿C	Substitution Missense	MLLT10 S219C	1/833,0.12%	1/13,582	VEP: MODERATE, SIFT: tolerated - score 0.61, PolyPhen: probably_damaging - score 0.972

574	chr11:g.64808066G¿A	Substitution Missense		1/833,0.12%	1/13,582	VEP: MODERATE, SIFT: deleterious - score 0, PolyPhen: possibly_damaging - score 0.73
575	chr4:g.125446537C¿G	Substitution Missense	FAT4 T383M	1/833,0.12%	2/13,582	VEP: MODERATE, SIFT: tolerated - score 0.29, PolyPhen: benign - score 0.186
576	chr1:g.193122269C¿G	Substitution Missense		1/833,0.12%	1/13,582	VEP: MODERATE, SIFT: tolerated - score 0.22, PolyPhen: benign - score 0.005
577	chr6:g.106088403C¿T	Substitution Missense	SOX2 M4I	1/833,0.12%	1/13,582	VEP: MODERATE, SIFT: deleterious - score 0, PolyPhen: probably_damaging - score 1
578	chr17:g.7674899G¿A	Substitution Missense		1/833,0.12%	5/13,582	VEP: MODERATE, SIFT: deleterious - score 0.02, PolyPhen: probably_damaging - score 0.989
579	chr4:g.125490910C¿A	Substitution Missense	STAT3 F561L	1/833,0.12%	2/13,582	VEP: MODERATE, SIFT: deleterious - score 0.01, PolyPhen: benign - score 0.068
580	chr19:g.17831321T¿C	Substitution Missense		1/833,0.12%	1/13,582	VEP: MODERATE, SIFT: tolerated - score 1, PolyPhen: benign - score 0.095
581	chr14:g.102101963A¿G	Substitution Missense	MAX H38P	1/833,0.12%	1/13,582	VEP: MODERATE, SIFT: deleterious_low_confidence - score 0.01, PolyPhen: benign - score 0.01
582	chr1:g.110339804T¿A	Substitution Missense		1/833,0.12%	1/13,582	VEP: MODERATE, SIFT: tolerated_low_confidence - score 0.4, PolyPhen: benign - score 0.054
583	chr5:g.143054454C¿G	Substitution Missense	FAT4 K4549N	1/833,0.12%	1/13,582	VEP: MODERATE, SIFT: tolerated - score 0.09, PolyPhen: benign - score 0.048
584	chr3:g.30644846A¿T	Substitution Missense		1/833,0.12%	1/13,582	VEP: MODERATE, SIFT: tolerated - score 0.18, PolyPhen: benign - score 0.159
585	chr2:g.189877371A¿T	Substitution Missense	ERC1 V471L	1/833,0.12%	1/13,582	VEP: MODERATE, SIFT: tolerated - score 0.41, PolyPhen: possibly_damaging - score 0.675
586	chrX:g.49043219T¿C	Substitution Missense		1/833,0.12%	1/13,582	VEP: MODERATE, SIFT: deleterious_low_confidence - score 0.01, PolyPhen: benign - score 0.227
587	chr10:g.68645141G¿A	Substitution Missense	AFF3 W1200G	1/833,0.12%	1/13,582	VEP: MODERATE, SIFT: tolerated - score 0.08, PolyPhen: benign - score 0.027

588	chr11:g.95979017C¿G	Substitution Missense		1/833,0.12%	1/13,582	VEP: MODERATE, SIFT: deleterious - score 0, PolyPhen: probably_damaging - score 0.941
589	chr12:g.92145428C¿A	Substitution Missense	MSH6 E604G	1/833,0.12%	1/13,582	VEP: MODERATE, SIFT: deleterious - score 0, PolyPhen: probably_damaging - score 0.951
590	chr2:g.61502254C¿G	Substitution Missense		1/833,0.12%	1/13,582	VEP: MODERATE, SIFT: tolerated - score 1, PolyPhen: benign - score 0
591	chr14:g.37592111T¿G	Substitution Missense	FUS D470H	1/833,0.12%	1/13,582	VEP: MODERATE, SIFT: deleterious - score 0, PolyPhen: probably_damaging - score 1
592	chr11:g.64810033T¿C	Substitution Missense		1/833,0.12%	1/13,582	VEP: MODERATE, SIFT: deleterious - score 0.02, PolyPhen: possibly_damaging - score 0.498
593	chr11:g.72008740T¿A	Substitution Missense	RBM15 E187K	1/833,0.12%	1/13,582	VEP: MODERATE, SIFT: deleterious - score 0.02, PolyPhen: possibly_damaging - score 0.77
594	chr1:g.155192133G¿C	Substitution Missense		1/833,0.12%	1/13,582	VEP: MODERATE, SIFT: deleterious - score 0.04, PolyPhen: probably_damaging - score 0.997
595	chr16:g.50781247A¿C	Substitution Missense	SMAD2 P177S	1/833,0.12%	1/13,582	VEP: MODERATE, SIFT: deleterious - score 0.01, PolyPhen: probably_damaging - score 0.995
596	chr2:g.47783252C¿G	Substitution Missense		1/833,0.12%	1/13,582	VEP: MODERATE, SIFT: deleterious - score 0.01, PolyPhen: benign - score 0.123
597	chr17:g.43092595C¿T	Substitution Missense	LIFR E955Q	1/833,0.12%	2/13,582	VEP: MODERATE, SIFT: tolerated - score 1, PolyPhen: benign - score 0
598	chr6:g.137879016G¿A	Substitution Missense		1/833,0.12%	1/13,582	VEP: MODERATE, SIFT: deleterious - score 0, PolyPhen: probably_damaging - score 0.997
599	chr3:g.9124767C¿T	Substitution Missense	FAT4 Q297H	1/833,0.12%	1/13,582	VEP: MODERATE, SIFT: deleterious - score 0, PolyPhen: probably_damaging - score 0.991
600	chr8:g.102345491A¿G	Substitution Missense		1/833,0.12%	1/13,582	VEP: MODERATE, SIFT: deleterious - score 0, PolyPhen: possibly_damaging - score 0.888
601	chr2:g.136115731T¿C	Substitution Missense	TRRAP E3353Q	1/833,0.12%	1/13,582	VEP: MODERATE, SIFT: tolerated - score 0.06, PolyPhen: probably_damaging - score 0.986

602	chr19:g.14093726G¿C	Substitution Missense		1/833,0.12%	1/13,582	VEP: MODERATE, SIFT: deleterious - score 0.02, PolyPhen: benign - score 0.406
603	chr7:g.98993678T¿A	Substitution Missense	MSI2 H84Q	1/833,0.12%	1/13,582	VEP: MODERATE, SIFT: tolerated - score 0.17, PolyPhen: benign - score 0.42
604	chr22:g.36289112C¿T	Substitution Missense		1/833,0.12%	1/13,582	VEP: MODERATE, SIFT: tolerated - score 0.49, PolyPhen: benign - score 0.005
605	chr5:g.177093415G¿A	Substitution Missense	SPEN P2067T	1/833,0.12%	1/13,582	VEP: MODERATE, SIFT: tolerated - score 0.07, PolyPhen: possibly_damaging - score 0.551
606	chr4:g.1794037G¿A	Substitution Missense		1/833,0.12%	1/13,582	VEP: MODERATE, SIFT: tolerated_low_confidence - score 0.28, PolyPhen: benign - score 0.053
607	chr5:g.1264536A¿T	Substitution Missense	RBM10 Q739R	1/833,0.12%	1/13,582	VEP: MODERATE, SIFT: deleterious - score 0, PolyPhen: possibly_damaging - score 0.867
608	chr20:g.58853956G¿A	Substitution Missense		1/833,0.12%	1/13,582	VEP: MODERATE, SIFT: deleterious_low_confidence - score 0.05, PolyPhen: benign - score 0.109
609	chr15:g.74023354G¿A	Substitution Missense	DNMT3A G168R	1/833,0.12%	1/13,582	VEP: MODERATE, SIFT: tolerated - score 0.14, PolyPhen: benign - score 0.024
610	chr12:g.122022108T¿A	Substitution Missense		1/833,0.12%	1/13,582	VEP: MODERATE, SIFT: deleterious - score 0, PolyPhen: possibly_damaging - score 0.862
611	chr2:g.15945895G¿A	Substitution Missense	NRAS Q61P	1/833,0.12%	1/13,582	VEP: MODERATE, SIFT: deleterious - score 0, PolyPhen: probably_damaging - score 0.98
612	chr5:g.132934779C¿T	Substitution Missense		1/833,0.12%	1/13,582	VEP: MODERATE, SIFT: tolerated - score 0.5, PolyPhen: benign - score 0.062
613	chrX:g.153559871G¿A	Substitution Missense	GPC3 I572T	1/833,0.12%	3/13,582	VEP: MODERATE, SIFT: deleterious - score 0.01, PolyPhen: possibly_damaging - score 0.549
614	chrX:g.71136314C¿A	Substitution Missense		1/833,0.12%	1/13,582	VEP: MODERATE, SIFT: deleterious - score 0.03, PolyPhen: possibly_damaging - score 0.833
615	chr17:g.58358673C¿T	Substitution Missense	CREBBP R1428C	1/833,0.12%	1/13,582	VEP: MODERATE, SIFT: tolerated - score 0.57, PolyPhen: benign - score 0

616	chr11:g.118503505C¿T	Substitution Missense		1/833,0.12%	1/13,582	VEP: MODERATE, SIFT: deleterious_low_confidence - score 0, PolyPhen: possibly_damaging - score 0.483
617	chr1:g.155188221G¿A	Substitution Missense	GRIN2A P1126T	1/833,0.12%	1/13,582	VEP: MODERATE, SIFT: deleterious - score 0, PolyPhen: probably_damaging - score 0.997
618	chr10:g.113159986C¿G	Substitution Missense		1/833,0.12%	1/13,582	VEP: MODERATE, SIFT: deleterious - score 0, PolyPhen: possibly_damaging - score 0.764
619	chr9:g.21971097C¿T	Substitution Missense	HSP90AB1 S322F	1/833,0.12%	5/13,582	VEP: MODERATE, SIFT: deleterious - score 0.04, PolyPhen: possibly_damaging - score 0.485
620	chr14:g.95713997A¿C	Substitution Missense		1/833,0.12%	1/13,582	VEP: MODERATE, SIFT: tolerated - score 0.51, PolyPhen: benign - score 0.011
621	chr19:g.11061784G¿A	Substitution Missense	MAP3K1 E1324K	1/833,0.12%	1/13,582	VEP: MODERATE, SIFT: tolerated_low_confidence - score 0.68, PolyPhen: benign - score 0
622	chr15:g.50499012C¿A	Substitution Missense		1/833,0.12%	1/13,582	VEP: MODERATE, SIFT: deleterious - score 0, PolyPhen: possibly_damaging - score 0.639
623	chr11:g.118495875C¿T	Substitution Missense	BCL9 M409I	1/833,0.12%	1/13,582	VEP: MODERATE, SIFT: tolerated - score 0.22, PolyPhen: benign - score 0.133
624	chr11:g.128694269C¿T	Substitution Missense		1/833,0.12%	1/13,582	VEP: MODERATE, SIFT: deleterious - score 0.03, PolyPhen: benign - score 0.015
625	chr6:g.106095676G¿C	Substitution Missense	FAT1 Q4125R	1/833,0.12%	1/13,582	VEP: MODERATE, SIFT: deleterious - score 0, PolyPhen: probably_damaging - score 1
626	chr3:g.41235800G¿A	Substitution Missense		1/833,0.12%	8/13,582	VEP: MODERATE, SIFT: deleterious - score 0, PolyPhen: probably_damaging - score 0.987
627	chr1:g.186332197C¿T	Substitution Missense	CDC73 F307L	1/833,0.12%	1/13,582	VEP: MODERATE, SIFT: tolerated - score 0.05, PolyPhen: probably_damaging - score 0.978
628	chr8:g.102281485T¿G	Substitution Missense		1/833,0.12%	1/13,582	VEP: MODERATE, SIFT: tolerated - score 0.68, PolyPhen: benign - score 0
629	chr9:g.5465536C¿A	Substitution Missense	FGFR1 P831L	1/833,0.12%	1/13,582	VEP: MODERATE, SIFT: deleterious - score 0.02, PolyPhen: possibly_damaging - score 0.482

630	chr3:g.38139017G¿A	Substitution Missense		1/833,0.12%	1/13,582	VEP: MODERATE, SIFT: tolerated - score 0.99, PolyPhen: benign - score 0.117
631	chr8:g.116847667C¿T	Substitution Missense	CTCF Q44K	1/833,0.12%	1/13,582	VEP: MODERATE, SIFT: tolerated - score 0.53, PolyPhen: benign - score 0.142
632	chr17:g.80328430T¿C	Substitution Missense		1/833,0.12%	1/13,582	VEP: MODERATE, SIFT: deleterious - score 0.04, PolyPhen: possibly_damaging - score 0.887
633	chrX:g.47179128G¿A	Substitution Missense	TCF3 T417M	1/833,0.12%	1/13,582	VEP: MODERATE, SIFT: deleterious - score 0.01, PolyPhen: possibly_damaging - score 0.704
634	chr16:g.89765012C¿T	Substitution Missense		1/833,0.12%	1/13,582	VEP: MODERATE, SIFT: deleterious - score 0.04, PolyPhen: benign - score 0.388
635	chr8:g.42306397C¿G	Substitution Missense	PRCC M335V	1/833,0.12%	1/13,582	VEP: MODERATE, SIFT: tolerated - score 0.17, PolyPhen: benign - score 0.392
636	chr14:g.50758127C¿T	Substitution Missense		1/833,0.12%	1/13,582	VEP: MODERATE, SIFT: tolerated - score 0.48, PolyPhen: benign - score 0.007
637	chr6:g.28923249G¿T	Substitution Missense	DAXX T695A	1/833,0.12%	1/13,582	VEP: MODERATE, SIFT: tolerated - score 0.1, PolyPhen: benign - score 0.001
638	chr17:g.20096662C¿T	Substitution Missense		1/833,0.12%	1/13,582	VEP: MODERATE, SIFT: tolerated_low_confidence - score 0.1, PolyPhen: benign - score 0.007
639	chrX:g.48683985G¿C	Substitution Missense	CIC A582V	1/833,0.12%	1/13,582	VEP: MODERATE, SIFT: tolerated - score 0.46, PolyPhen: benign - score 0.326
640	chr4:g.186611475G¿A	Substitution Missense		1/833,0.12%	1/13,582	VEP: MODERATE, SIFT: tolerated - score 0.31, PolyPhen: benign - score 0.059
641	chr16:g.79599533G¿C	Substitution Missense	TRRAP R2334L	1/833,0.12%	1/13,582	VEP: MODERATE, SIFT: tolerated - score 0.58, PolyPhen: benign - score 0.005
642	chr1:g.18635132G¿A	Substitution Missense		1/833,0.12%	1/13,582	VEP: MODERATE, SIFT: tolerated - score 0.11, PolyPhen: probably_damaging - score 0.972
643	chr6:g.393328A¿G	Substitution Missense	TP53 Y126C	1/833,0.12%	1/13,582	VEP: MODERATE, SIFT: deleterious - score 0.04, PolyPhen: probably_damaging - score 0.952

644	chr4:g.105276421C¿G	Substitution Missense		1/833,0.12%	1/13,582	VEP: MODERATE, SIFT: deleterious - score 0.04, PolyPhen: probably_damaging - score 0.994
645	chr3:g.47124028G¿A	Substitution Missense	PBRM1 E357Q	1/833,0.12%	1/13,582	VEP: MODERATE, SIFT: tolerated_low_confidence - score 0.27, PolyPhen: benign - score 0
646	chr4:g.87114704C¿T	Substitution Missense		1/833,0.12%	1/13,582	VEP: MODERATE, SIFT: tolerated - score 0.19, PolyPhen: benign - score 0
647	chr6:g.108664226T¿C	Substitution Missense	FUBP1 I237N	1/833,0.12%	1/13,582	VEP: MODERATE, SIFT: deleterious - score 0, PolyPhen: possibly_damaging - score 0.797
648	chrX:g.153560786G¿C	Substitution Missense		1/833,0.12%	1/13,582	VEP: MODERATE, SIFT: deleterious - score 0.02, PolyPhen: probably_damaging - score 0.915
649	chr7:g.129206247C¿A	Substitution Missense	KAT6A E1301K	1/833,0.12%	1/13,582	VEP: MODERATE, SIFT: tolerated - score 0.08, PolyPhen: benign - score 0.012
650	chr2:g.15942438A¿T	Substitution Missense		1/833,0.12%	1/13,582	VEP: MODERATE, SIFT: deleterious - score 0, PolyPhen: probably_damaging - score 0.996
651	chrX:g.71096659C¿A	Substitution Missense	TP53 R337L	1/833,0.12%	1/13,582	VEP: MODERATE, SIFT: tolerated - score 0.14, PolyPhen: benign - score 0.333
652	chr17:g.39708354G¿A	Substitution Missense		1/833,0.12%	2/13,582	VEP: MODERATE, SIFT: deleterious - score 0, PolyPhen: probably_damaging - score 0.998
653	chr10:g.121500905T¿A	Substitution Missense	CARD11 E282Q	1/833,0.12%	1/13,582	VEP: MODERATE, SIFT: deleterious - score 0.01, PolyPhen: probably_damaging - score 0.996
654	chr20:g.58855210C¿T	Substitution Missense		1/833,0.12%	1/13,582	VEP: MODERATE, SIFT: tolerated - score 0.1, PolyPhen: benign - score 0.048
655	chr19:g.42287009C¿A	Substitution Missense	BRAF G30D	1/833,0.12%	1/13,582	VEP: MODERATE, SIFT: deleterious_low_confidence - score 0.01, PolyPhen: probably_damaging - score 0.996
656	chr16:g.10918484C¿T	Substitution Missense		1/833,0.12%	1/13,582	VEP: MODERATE, SIFT: deleterious - score 0, PolyPhen: possibly_damaging - score 0.821
657	chr17:g.58358619C¿T	Substitution Missense	CACNA1D R524H	1/833,0.12%	1/13,582	VEP: MODERATE, SIFT: tolerated - score 0.35, PolyPhen: benign - score 0.267

658	chr3:g.69879379T¿C	Substitution Missense		1/833,0.12%	1/13,582	VEP: MODERATE, SIFT: deleterious - score 0, PolyPhen: benign - score 0.38
659	chrX:g.67723709C¿A	Substitution Missense	NOTCH2 R1704C	1/833,0.12%	1/13,582	VEP: MODERATE, SIFT: deleterious - score 0, PolyPhen: probably_damaging - score 0.989
660	chrX:g.71119697C¿A	Substitution Missense		1/833,0.12%	1/13,582	VEP: MODERATE, SIFT: tolerated - score 0.17, PolyPhen: benign - score 0.379
661	chr2:g.197402029C¿A	Substitution Missense	CEP89 S340Y	1/833,0.12%	2/13,582	VEP: MODERATE, SIFT: deleterious - score 0, PolyPhen: possibly_damaging - score 0.801
662	chr11:g.118763256C¿T	Substitution Missense		1/833,0.12%	1/13,582	VEP: MODERATE, SIFT: tolerated - score 0.13, PolyPhen: benign - score 0.038
663	chr1:g.92841857G¿A	Substitution Missense	IL7R S335F	1/833,0.12%	2/13,582	VEP: MODERATE, SIFT: tolerated - score 0.11, PolyPhen: benign - score 0.003
664	chr17:g.82009043G¿A	Substitution Missense		1/833,0.12%	1/13,582	VEP: MODERATE, SIFT: tolerated - score 0.36, PolyPhen: possibly_damaging - score 0.728
665	chr19:g.17830218C¿G	Substitution Missense	BCL2 E135Q	1/833,0.12%	1/13,582	VEP: MODERATE, SIFT: tolerated - score 0.06, PolyPhen: possibly_damaging - score 0.458
666	chr2:g.74367363C¿T	Substitution Missense		1/833,0.12%	1/13,582	VEP: MODERATE, SIFT: tolerated - score 0.26, PolyPhen: probably_damaging - score 0.994
667	chr2:g.222220196G¿C	Substitution Missense	PAX3 R240G	1/833,0.12%	1/13,582	VEP: MODERATE, SIFT: tolerated_low_confidence - score 0.18, PolyPhen: benign - score 0.009
668	chr9:g.99863623G¿C	Substitution Missense		1/833,0.12%	1/13,582	VEP: MODERATE, SIFT: deleterious - score 0, PolyPhen: probably_damaging - score 0.971
669	chr16:g.65004787C¿T	Substitution Missense	FIP1L1 E161K	1/833,0.12%	2/13,582	VEP: MODERATE, SIFT: tolerated - score 0.65, PolyPhen: benign - score 0.063
670	chr1:g.205620581C¿G	Substitution Missense		1/833,0.12%	1/13,582	VEP: MODERATE, SIFT: deleterious - score 0, PolyPhen: probably_damaging - score 0.997
671	chr4:g.86769933G¿A	Substitution Missense	LIFR R860Q	1/833,0.12%	1/13,582	VEP: MODERATE, SIFT: deleterious - score 0, PolyPhen: probably_damaging - score 1

672	chr9:g.95508193C¿T	Substitution Missense		1/833,0.12%	3/13,582	VEP: MODERATE, SIFT: tolerated - score 0.34, PolyPhen: possibly_damaging - score 0.511
673	chr9:g.131144462G¿C	Substitution Missense	SMARCA4 V1199A	1/833,0.12%	1/13,582	VEP: MODERATE, SIFT: tolerated - score 0.11, PolyPhen: benign - score 0.007
674	chr1:g.114713914G¿C	Substitution Missense		1/833,0.12%	1/13,582	VEP: MODERATE, SIFT: deleterious - score 0.01, PolyPhen: benign - score 0.418
675	chr8:g.18025604T¿A	Substitution Missense	KMT2A L106I	1/833,0.12%	1/13,582	VEP: MODERATE, SIFT: deleterious - score 0, PolyPhen: benign - score 0.225
676	chr18:g.25322158C¿T	Substitution Missense		1/833,0.12%	1/13,582	VEP: MODERATE, SIFT: tolerated_low_confidence - score 0.44, PolyPhen: possibly_damaging - score 0.899
677	chr12:g.124344662A¿T	Substitution Missense	CEBPA H236Q	1/833,0.12%	1/13,582	VEP: MODERATE, SIFT: tolerated - score 1, PolyPhen: possibly_damaging - score 0.754
678	chr4:g.54695665C¿T	Substitution Missense		1/833,0.12%	1/13,582	VEP: MODERATE, SIFT: tolerated - score 0.23, PolyPhen: benign - score 0
679	chr9:g.133102570A¿C	Substitution Missense	AXIN1 D113N	1/833,0.12%	1/13,582	VEP: MODERATE, SIFT: deleterious - score 0, PolyPhen: probably_damaging - score 0.987
680	chr5:g.143121113T¿C	Substitution Missense		1/833,0.12%	1/13,582	VEP: MODERATE, SIFT: deleterious - score 0, PolyPhen: probably_damaging - score 0.971
681	chr22:g.19216127C¿T	Substitution Missense	PRDM16 E37K	1/833,0.12%	1/13,582	VEP: MODERATE, SIFT: tolerated - score 0.19, PolyPhen: benign - score 0.047
682	chr4:g.186604457C¿T	Substitution Missense		1/833,0.12%	1/13,582	VEP: MODERATE, SIFT: tolerated - score 0.77, PolyPhen: benign - score 0.111
683	chr4:g.1801519C¿T	Substitution Missense	FAT1 T1473P	1/833,0.12%	2/13,582	VEP: MODERATE, SIFT: deleterious - score 0, PolyPhen: probably_damaging - score 0.999
684	chr17:g.7673776G¿A	Substitution Missense		1/833,0.12%	98/13,582	VEP: MODERATE, SIFT: deleterious - score 0, PolyPhen: probably_damaging - score 1
685	chr4:g.186609965A¿G	Substitution Missense	ERBB3 R1309H	1/833,0.12%	1/13,582	VEP: MODERATE, SIFT: deleterious - score 0, PolyPhen: probably_damaging - score 0.999

686	chr6:g.37170987A¿G	Substitution Missense		1/833,0.12%	1/13,582	VEP: MODERATE, SIFT: tolerated - score 0.49, PolyPhen: benign - score 0.05
687	chr7:g.75556034T¿A	Substitution Missense	KMT2D S1096F	1/833,0.12%	1/13,582	VEP: MODERATE, SIFT: deleterious - score 0, PolyPhen: benign - score 0.013
688	chr17:g.31330430T¿A	Substitution Missense		1/833,0.12%	1/13,582	VEP: MODERATE, SIFT: deleterious - score 0, PolyPhen: probably_damaging - score 0.999
689	chr2:g.36869725G¿C	Substitution Missense	FAT1 I1302S	1/833,0.12%	1/13,582	VEP: MODERATE, SIFT: tolerated - score 0.28, PolyPhen: benign - score 0.003
690	chr2:g.108782305A¿G	Substitution Missense		1/833,0.12%	1/13,582	VEP: MODERATE, SIFT: deleterious - score 0, PolyPhen: probably_damaging - score 0.932
691	chr11:g.3683437G¿A	Substitution Missense	FAT4 N391K	1/833,0.12%	2/13,582	VEP: MODERATE, SIFT: deleterious - score 0, PolyPhen: probably_damaging - score 0.997
692	chr1:g.116390407G¿C	Substitution Missense		1/833,0.12%	1/13,582	VEP: MODERATE, SIFT: tolerated - score 0.11, PolyPhen: benign - score 0.103
693	chr15:g.90607390T¿G	Substitution Missense	PTEN F341V	1/833,0.12%	1/13,582	VEP: MODERATE, SIFT: deleterious - score 0, PolyPhen: probably_damaging - score 0.999
694	chr11:g.108335854G¿A	Substitution Missense		1/833,0.12%	2/13,582	VEP: MODERATE, SIFT: deleterious - score 0.01, PolyPhen: probably_damaging - score 0.999
695	chr11:g.95979722C¿A	Substitution Missense	CAMTA1 A564T	1/833,0.12%	1/13,582	VEP: MODERATE, SIFT: deleterious - score 0.02, PolyPhen: possibly_damaging - score 0.86
696	chr9:g.133108283G¿A	Substitution Missense		1/833,0.12%	1/13,582	VEP: MODERATE, SIFT: tolerated - score 0.52, PolyPhen: benign - score 0.007
697	chr13:g.40665815T¿C	Substitution Missense	SF3B1 W938C	1/833,0.12%	1/13,582	VEP: MODERATE, SIFT: tolerated - score 0.38, PolyPhen: benign - score 0.025
698	chr17:g.39517529G¿A	Substitution Missense		1/833,0.12%	1/13,582	VEP: MODERATE, SIFT: deleterious - score 0.01, PolyPhen: probably_damaging - score 0.998
699	chr12:g.56094497C¿G	Substitution Missense	UBR5 R2293Q	1/833,0.12%	1/13,582	VEP: MODERATE, SIFT: deleterious - score 0, PolyPhen: probably_damaging - score 0.998

700	chr2:g.42286366A¿G	Substitution Missense		1/833,0.12%	1/13,582	VEP: MODERATE, SIFT: tolerated - score 0.21, PolyPhen: benign - score 0.075
701	chr11:g.102324904G¿C	Substitution Missense	DDX5 K144E	1/833,0.12%	1/13,582	VEP: MODERATE, SIFT: deleterious - score 0.04, PolyPhen: possibly_damaging - score 0.506
702	chr11:g.118504561G¿A	Substitution Missense		1/833,0.12%	1/13,582	VEP: MODERATE, SIFT: deleterious_low_confidence - score 0, PolyPhen: probably_damaging - score 0.959
703	chr5:g.180620906C¿T	Substitution Missense	PTPRB R1881G	1/833,0.12%	1/13,582	VEP: MODERATE, SIFT: tolerated - score 0.16, PolyPhen: possibly_damaging - score 0.581
704	chr4:g.186603557C¿A	Substitution Missense		1/833,0.12%	1/13,582	VEP: MODERATE, SIFT: deleterious - score 0, PolyPhen: probably_damaging - score 0.998
705	chr15:g.87929304G¿A	Substitution Missense	U2AF1 E88K	1/833,0.12%	1/13,582	VEP: MODERATE, SIFT: deleterious - score 0, PolyPhen: probably_damaging - score 0.991
706	chr1:g.35190834T¿A	Substitution Missense		1/833,0.12%	1/13,582	VEP: MODERATE, SIFT: tolerated - score 0.21, PolyPhen: benign - score 0.018
707	chr22:g.36302626C¿T	Substitution Missense	WRN N1123D	1/833,0.12%	2/13,582	VEP: MODERATE, SIFT: deleterious - score 0, PolyPhen: possibly_damaging - score 0.614
708	chr3:g.12609306T¿G	Substitution Missense		1/833,0.12%	1/13,582	VEP: MODERATE, SIFT: tolerated - score 0.09, PolyPhen: benign - score 0.361
709	chr4:g.125490230G¿C	Substitution Missense	ATR T2590N	1/833,0.12%	1/13,582	VEP: MODERATE, SIFT: deleterious_low_confidence - score 0, PolyPhen: probably_damaging - score 0.999
710	chr16:g.79599694G¿A	Substitution Missense		1/833,0.12%	1/13,582	VEP: MODERATE, SIFT: deleterious - score 0, PolyPhen: probably_damaging - score 0.997
711	chr15:g.52384291T¿G	Substitution Missense	SMARCE1 E323Q	1/833,0.12%	1/13,582	VEP: MODERATE, SIFT: deleterious - score 0.04, PolyPhen: benign - score 0.005
712	chr11:g.108345851G¿A	Substitution Missense		1/833,0.12%	1/13,582	VEP: MODERATE, SIFT: deleterious - score 0, PolyPhen: benign - score 0.295
713	chr7:g.102227565G¿A	Substitution Missense	AKAP9 E2505K	1/833,0.12%	1/13,582	VEP: MODERATE, SIFT: deleterious - score 0.02, PolyPhen: probably_damaging - score 1

714	chr10:g.74843138G¿A	Substitution Missense		1/833,0.12%	1/13,582	VEP: MODERATE, SIFT: tolerated - score 0.67, PolyPhen: benign - score 0.007
715	chr17:g.7674887C¿G	Substitution Missense	CHD4 S335Y	1/833,0.12%	1/13,582	VEP: MODERATE, SIFT: deleterious - score 0, PolyPhen: probably_damaging - score 1
716	chr5:g.143134021C¿T	Substitution Missense		1/833,0.12%	1/13,582	VEP: MODERATE, SIFT: deleterious - score 0.03, PolyPhen: possibly_damaging - score 0.897
717	chr13:g.40665754G¿C	Substitution Missense	ATM L2767P	1/833,0.12%	1/13,582	VEP: MODERATE, SIFT: deleterious - score 0, PolyPhen: probably_damaging - score 0.988
718	chr9:g.95476803G¿A	Substitution Missense		1/833,0.12%	1/13,582	VEP: MODERATE, SIFT: deleterious - score 0, PolyPhen: probably_damaging - score 0.986
719	chr19:g.18465878C¿G	Substitution Missense	RB1 M695R	1/833,0.12%	1/13,582	VEP: MODERATE, SIFT: deleterious - score 0.01, PolyPhen: probably_damaging - score 0.918
720	chr19:g.53577562G¿T	Substitution Missense		1/833,0.12%	1/13,582	VEP: MODERATE, SIFT: deleterious - score 0, PolyPhen: probably_damaging - score 0.983
721	chr1:g.3412658G¿A	Substitution Missense	GAS7 K338N	1/833,0.12%	1/13,582	VEP: MODERATE, SIFT: deleterious - score 0, PolyPhen: possibly_damaging - score 0.452
722	chr12:g.25227340C¿T	Substitution Missense		1/833,0.12%	3/13,582	VEP: MODERATE, SIFT: deleterious - score 0.01, PolyPhen: possibly_damaging - score 0.669
723	chr15:g.88126319A¿T	Substitution Missense	PAX3 A411V	1/833,0.12%	1/13,582	VEP: MODERATE, SIFT: tolerated - score 0.06, PolyPhen: benign - score 0.074
724	chr12:g.122474060C¿T	Substitution Missense		1/833,0.12%	1/13,582	VEP: MODERATE, SIFT: deleterious - score 0, PolyPhen: probably_damaging - score 0.996
725	chr4:g.186620809T¿C	Substitution Missense	NCKIPSD M368V	1/833,0.12%	1/13,582	VEP: MODERATE, SIFT: tolerated - score 0.37, PolyPhen: probably_damaging - score 0.998
726	chr12:g.70576498G¿A	Substitution Missense		1/833,0.12%	1/13,582	VEP: MODERATE, SIFT: deleterious - score 0.01, PolyPhen: possibly_damaging - score 0.637
727	chr11:g.3773735G¿A	Substitution Missense	FLI1 E166K	1/833,0.12%	1/13,582	VEP: MODERATE, SIFT: tolerated - score 0.23, PolyPhen: benign - score 0.056

728	chr12:g.6669179C¿T	Substitution	Missense		1/833,0.12%	1/13,582	VEP: MODERATE, SIFT: deleterious - score 0, PolyPhen: probably_damaging - score 0.99
729	chr12:g.124341892C¿T	Substitution	Missense	DCTN1 E713K	1/833,0.12%	1/13,582	VEP: MODERATE, SIFT: deleterious - score 0.03, PolyPhen: probably_damaging - score 0.995
730	chr3:g.12379743C¿A	Substitution	Missense		1/833,0.12%	1/13,582	VEP: MODERATE, SIFT: tolerated_low_confidence - score 0.1, PolyPhen: benign - score 0.14
731	chr17:g.80388655A¿T	Substitution	Missense	AKAP9 1	1/833,0.12%	1/13,582	VEP: MODERATE, SIFT: tolerated - score 0.2, PolyPhen: benign - score 0.005
732	chr5:g.171309684G¿A	Substitution	Missense		1/833,0.12%	1/13,582	VEP: MODERATE, SIFT: deleterious - score 0.01, PolyPhen: benign - score 0.042
733	chr9:g.121138577G¿T	Substitution	Missense	TRIM33 A955V	1/833,0.12%	1/13,582	VEP: MODERATE, SIFT: deleterious - score 0.02, PolyPhen: probably_damaging - score 0.978
734	chr3:g.37047625A¿G	Substitution	Missense		1/833,0.12%	1/13,582	VEP: MODERATE, SIFT: deleterious - score 0.02, PolyPhen: benign - score 0.249
735	chr4:g.125320418C¿A	Substitution	Missense	NCOR1 P156A	1/833,0.12%	1/13,582	VEP: MODERATE, SIFT: tolerated - score 0.16, PolyPhen: probably_damaging - score 0.995
736	chr11:g.3693344T¿C	Substitution	Missense		1/833,0.12%	1/13,582	VEP: MODERATE, SIFT: deleterious - score 0, PolyPhen: probably_damaging - score 0.997
737	chr10:g.8058488C¿T	Substitution	Missense	STRN S588A	1/833,0.12%	2/13,582	VEP: MODERATE, SIFT: tolerated - score 0.15, PolyPhen: benign - score 0.001
738	chr3:g.142562889C¿A	Substitution	Missense		1/833,0.12%	1/13,582	VEP: MODERATE, SIFT: tolerated_low_confidence - score 0.06, PolyPhen: probably_damaging - score 0.997
739	chr11:g.108353777G¿A	Substitution	Missense	FH S11W	1/833,0.12%	1/13,582	VEP: MODERATE, SIFT: deleterious - score 0, PolyPhen: probably_damaging - score 0.999
740	chr7:g.152136891C¿A	Substitution	Missense		1/833,0.12%	1/13,582	VEP: MODERATE, SIFT: deleterious - score 0, PolyPhen: probably_damaging - score 0.998
741	chr3:g.37050544A¿C	Substitution	Missense	EP300 Q1256H	1/833,0.12%	1/13,582	VEP: MODERATE, SIFT: deleterious - score 0.02, PolyPhen: possibly_damaging - score 0.763

742	chr19:g.18683732C¿A	Substitution Missense		1/833,0.12%	1/13,582	VEP: MODERATE, SIFT: deleterious - score 0, PolyPhen: probably_damaging - score 0.999
743	chr15:g.90769545G¿C	Substitution Missense	ALK S175N	1/833,0.12%	1/13,582	VEP: MODERATE, SIFT: deleterious - score 0, PolyPhen: probably_damaging - score 0.981
744	chr12:g.25245328C¿G	Substitution Missense		1/833,0.12%	7/13,582	VEP: MODERATE, SIFT: deleterious - score 0.01, PolyPhen: probably_damaging - score 0.999
745	chr19:g.16093566G¿C	Substitution Missense	CHCHD7 H7R	1/833,0.12%	1/13,582	VEP: MODERATE, SIFT: tolerated - score 0.11, PolyPhen: probably_damaging - score 0.98
746	chr4:g.186618821C¿T	Substitution Missense		1/833,0.12%	1/13,582	VEP: MODERATE, SIFT: deleterious - score 0.03, PolyPhen: benign - score 0.157
747	chr10:g.68572387G¿A	Substitution Missense	TRIP11 K292R	1/833,0.12%	1/13,582	VEP: MODERATE, SIFT: deleterious - score 0.03, PolyPhen: benign - score 0.014
748	chr15:g.40185344G¿A	Substitution Missense		1/833,0.12%	1/13,582	VEP: MODERATE, SIFT: deleterious - score 0.01, PolyPhen: probably_damaging - score 0.983
749	chr16:g.64947920G¿T	Substitution Missense	ATP1A1 E512K	1/833,0.12%	1/13,582	VEP: MODERATE, SIFT: tolerated - score 0.48, PolyPhen: benign - score 0.444
750	chr19:g.10829253G¿C	Substitution Missense		1/833,0.12%	1/13,582	VEP: MODERATE, SIFT: tolerated - score 0.63, PolyPhen: benign - score 0
751	chr5:g.56882741A¿G	Substitution Missense	MAX R35P	1/833,0.12%	1/13,582	VEP: MODERATE, SIFT: tolerated - score 0.4, PolyPhen: possibly_damaging - score 0.824
752	chr17:g.7674918A¿G	Substitution Missense		1/833,0.12%	5/13,582	VEP: MODERATE, SIFT: deleterious - score 0.01, PolyPhen: possibly_damaging - score 0.634
753	chr9:g.97684994T¿G	Substitution Missense	CARD11 M999T	1/833,0.12%	1/13,582	VEP: MODERATE, SIFT: tolerated - score 0.13, PolyPhen: possibly_damaging - score 0.529
754	chr1:g.47251588C¿T	Substitution Missense		1/833,0.12%	1/13,582	VEP: MODERATE, SIFT: deleterious - score 0, PolyPhen: probably_damaging - score 0.96
755	chr1:g.114716127C¿A	Substitution Missense	FLT4 F789L	1/833,0.12%	8/13,582	VEP: MODERATE, SIFT: deleterious - score 0.04, PolyPhen: possibly_damaging - score 0.541

756	chr22:g.19239354C¿T	Substitution Missense		1/833,0.12%	1/13,582	VEP: MODERATE, SIFT: deleterious - score 0.04, PolyPhen: probably_damaging - score 1
757	chr2:g.108764045G¿A	Substitution Missense	NONO P36T	1/833,0.12%	1/13,582	VEP: MODERATE, SIFT: tolerated - score 0.36, PolyPhen: probably_damaging - score 0.999
758	chr16:g.10898970C¿A	Substitution Missense		1/833,0.12%	1/13,582	VEP: MODERATE, SIFT: tolerated - score 0.3, PolyPhen: benign - score 0.078
759	chr5:g.180624059C¿T	Substitution Missense	PPFIBP1 E297K	1/833,0.12%	1/13,582	VEP: MODERATE, SIFT: tolerated - score 0.6, PolyPhen: benign - score 0.022
760	chr7:g.140753345A¿T	Substitution Missense		1/833,0.12%	2/13,582	VEP: MODERATE, SIFT: deleterious - score 0, PolyPhen: possibly_damaging - score 0.852
761	chr14:g.95126725A¿G	Substitution Missense	CLIP1 Q173H	1/833,0.12%	1/13,582	VEP: MODERATE, SIFT: tolerated - score 0.28, PolyPhen: benign - score 0.023
762	chr14:g.36520080C¿T	Substitution Missense		1/833,0.12%	1/13,582	VEP: MODERATE, SIFT: deleterious_low_confidence - score 0.01, PolyPhen: benign - score 0
763	chr6:g.394900G¿C	Substitution Missense	ATM F2393L	1/833,0.12%	1/13,582	VEP: MODERATE, SIFT: deleterious - score 0, PolyPhen: probably_damaging - score 0.998
764	chr14:g.92000027C¿T	Substitution Missense		1/833,0.12%	1/13,582	VEP: MODERATE, SIFT: tolerated - score 0.06, PolyPhen: probably_damaging - score 0.999
765	chr15:g.90642082C¿T	Substitution Missense	ATRX S2449C	1/833,0.12%	1/13,582	VEP: MODERATE, SIFT: deleterious - score 0, PolyPhen: probably_damaging - score 0.913
766	chr12:g.331890G¿C	Substitution Missense		1/833,0.12%	1/13,582	VEP: MODERATE, SIFT: deleterious - score 0, PolyPhen: benign - score 0.325
767	chr11:g.32396310T¿G	Substitution Missense	WT1 P269S	1/833,0.12%	1/13,582	VEP: MODERATE, SIFT: deleterious_low_confidence - score 0.01, PolyPhen: possibly_damaging - score 0.482
768	chr3:g.49368506C¿T	Substitution Missense		1/833,0.12%	1/13,582	VEP: MODERATE, SIFT: deleterious - score 0.02, PolyPhen: benign - score 0.236
769	chr10:g.121485407C¿A	Substitution Missense	FAT4 D4562E	1/833,0.12%	1/13,582	VEP: MODERATE, SIFT: deleterious - score 0, PolyPhen: probably_damaging - score 1

770	chr16:g.65004712C¿T	Substitution Missense		1/833,0.12%	1/13,582	VEP: MODERATE, SIFT: deleterious - score 0, PolyPhen: probably_damaging - score 0.999
771	chr4:g.186603583G¿T	Substitution Missense	HERPUD1 N241S	1/833,0.12%	1/13,582	VEP: MODERATE, SIFT: tolerated - score 0.59, PolyPhen: probably_damaging - score 0.915
772	chr17:g.5378203T¿A	Substitution Missense		1/833,0.12%	1/13,582	VEP: MODERATE, SIFT: deleterious - score 0.03, PolyPhen: probably_damaging - score 0.953
773	chr4:g.125320543C¿G	Substitution Missense	TLX3 A34T	1/833,0.12%	1/13,582	VEP: MODERATE, SIFT: tolerated - score 0.07, PolyPhen: probably_damaging - score 0.986
774	chr11:g.95991702G¿C	Substitution Missense		1/833,0.12%	1/13,582	VEP: MODERATE, SIFT: tolerated - score 0.32, PolyPhen: benign - score 0.428
775	chr13:g.40560196C¿T	Substitution Missense	BCL3 L76V	1/833,0.12%	1/13,582	VEP: MODERATE, SIFT: tolerated - score 1, PolyPhen: benign - score 0
776	chr5:g.38511897G¿T	Substitution Missense		1/833,0.12%	1/13,582	VEP: MODERATE, SIFT: deleterious - score 0, PolyPhen: probably_damaging - score 0.999
777	chr19:g.1611759G¿A	Substitution Missense	CACNA1D A922P	1/833,0.12%	1/13,582	VEP: MODERATE, SIFT: tolerated - score 0.15, PolyPhen: benign - score 0.261
778	chr2:g.47801128T¿C	Substitution Missense		1/833,0.12%	1/13,582	VEP: MODERATE, SIFT: tolerated - score 0.06, PolyPhen: benign - score 0.167
779	chr8:g.42316721C¿G	Substitution Missense	MN1 G211S	1/833,0.12%	1/13,582	VEP: MODERATE, SIFT: deleterious - score 0, PolyPhen: benign - score 0.263
780	chr17:g.16032450A¿T	Substitution Missense		1/833,0.12%	1/13,582	VEP: MODERATE, SIFT: deleterious - score 0, PolyPhen: benign - score 0.057
781	chr2:g.197408033C¿T	Substitution Missense	CDH1 D183E	1/833,0.12%	1/13,582	VEP: MODERATE, SIFT: deleterious - score 0.02, PolyPhen: possibly_damaging - score 0.864
782	chr5:g.158840060G¿A	Substitution Missense		1/833,0.12%	1/13,582	VEP: MODERATE, SIFT: deleterious - score 0, PolyPhen: possibly_damaging - score 0.785
783	chr2:g.25234289G¿A	Substitution Missense	KLF4 H416Y	1/833,0.12%	2/13,582	VEP: MODERATE, SIFT: deleterious - score 0, PolyPhen: benign - score 0.428

784	chr19:g.52206007C¿G	Substitution Missense		1/833,0.12%	1/13,582	VEP: MODERATE, SIFT: tolerated - score 1, PolyPhen: benign - score 0.003
785	chr7:g.98881160G¿A	Substitution Missense	CXCR4 N180S	1/833,0.12%	1/13,582	VEP: MODERATE, SIFT: tolerated_low_confidence - score 0.06, PolyPhen: benign - score 0.011
786	chr4:g.186596932C¿T	Substitution Missense		1/833,0.12%	2/13,582	VEP: MODERATE, SIFT: deleterious - score 0.01, PolyPhen: probably_damaging - score 0.98
787	chr4:g.186707033T¿G	Substitution Missense	ALK A118T	1/833,0.12%	1/13,582	VEP: MODERATE, SIFT: tolerated - score 0.08, PolyPhen: possibly_damaging - score 0.896
788	chr4:g.125319824C¿A	Substitution Missense		1/833,0.12%	1/13,582	VEP: MODERATE, SIFT: tolerated - score 0.17, PolyPhen: possibly_damaging - score 0.506
789	chr2:g.236581283T¿C	Substitution Missense	ERBB2 R517Q	1/833,0.12%	1/13,582	VEP: MODERATE, SIFT: deleterious - score 0, PolyPhen: probably_damaging - score 0.964
790	chr8:g.38428352G¿A	Substitution Missense		1/833,0.12%	1/13,582	VEP: MODERATE, SIFT: tolerated - score 0.25, PolyPhen: benign - score 0.355
791	chr1:g.186345596C¿T	Substitution Missense	POLE K738E	1/833,0.12%	1/13,582	VEP: MODERATE, SIFT: deleterious - score 0.03, PolyPhen: possibly_damaging - score 0.885
792	chr9:g.125158252T¿C	Substitution Missense		1/833,0.12%	1/13,582	VEP: MODERATE, SIFT: deleterious - score 0, PolyPhen: probably_damaging - score 0.978
793	chr1:g.179131356A¿T	Substitution Missense	CIITA K316N	1/833,0.12%	1/13,582	VEP: MODERATE, SIFT: deleterious - score 0, PolyPhen: probably_damaging - score 0.999
794	chr11:g.108333912C¿T	Substitution Missense		1/833,0.12%	1/13,582	VEP: MODERATE, SIFT: tolerated - score 0.08, PolyPhen: benign - score 0.041
795	chr2:g.174824505C¿G	Substitution Missense	USP8 K582R	1/833,0.12%	1/13,582	VEP: MODERATE, SIFT: tolerated - score 0.06, PolyPhen: probably_damaging - score 0.926
796	chr9:g.77797643A¿C	Substitution Missense		1/833,0.12%	1/13,582	VEP: MODERATE, SIFT: deleterious - score 0, PolyPhen: probably_damaging - score 0.999
797	chr14:g.95712390C¿G	Substitution Missense	KMT2A E1611K	1/833,0.12%	1/13,582	VEP: MODERATE, SIFT: tolerated - score 0.07, PolyPhen: benign - score 0.363

798	chr9:g.121138578A¿G	Substitution Missense		1/833,0.12%	1/13,582	VEP: MODERATE, SIFT: deleterious - score 0, PolyPhen: benign - score 0.239
799	chr16:g.13922185A¿G	Substitution Missense	BLM E1224K	1/833,0.12%	2/13,582	VEP: MODERATE, SIFT: deleterious - score 0.04, PolyPhen: benign - score 0.003
800	chr17:g.7674256T¿G	Substitution Missense		1/833,0.12%	2/13,582	VEP: MODERATE, SIFT: deleterious - score 0, PolyPhen: probably_damaging - score 0.996
801	chr2:g.25244558C¿A	Substitution Missense	STAT5B D621H	1/833,0.12%	1/13,582	VEP: MODERATE, SIFT: deleterious - score 0, PolyPhen: possibly_damaging - score 0.625
802	chr4:g.186663339A¿T	Substitution Missense		1/833,0.12%	1/13,582	VEP: MODERATE, SIFT: deleterious - score 0, PolyPhen: probably_damaging - score 0.954
803	chr4:g.125491470A¿T	Substitution Missense	KIAA1549 P917S	1/833,0.12%	1/13,582	VEP: MODERATE, SIFT: deleterious - score 0, PolyPhen: benign - score 0.109
804	chr12:g.12718077G¿C	Substitution Missense		1/833,0.12%	1/13,582	VEP: MODERATE, SIFT: deleterious - score 0.03, PolyPhen: benign - score 0.286
805	chr7:g.152144744G¿A	Substitution Missense	ATM A3006V	1/833,0.12%	1/13,582	VEP: MODERATE, SIFT: deleterious - score 0, PolyPhen: probably_damaging - score 0.991
806	chr17:g.61801374A¿C	Substitution Missense		1/833,0.12%	1/13,582	VEP: MODERATE, SIFT: deleterious - score 0, PolyPhen: probably_damaging - score 0.987
807	chr7:g.92082542T¿G	Substitution Missense	KDR D1215G	1/833,0.12%	1/13,582	VEP: MODERATE, SIFT: tolerated - score 0.22, PolyPhen: benign - score 0.001
808	chr16:g.72794800C¿T	Substitution Missense		1/833,0.12%	3/13,582	VEP: MODERATE, SIFT: deleterious - score 0, PolyPhen: possibly_damaging - score 0.695
809	chr6:g.157207803G¿A	Substitution Missense	CYLD C788G	1/833,0.12%	2/13,582	VEP: MODERATE, SIFT: deleterious - score 0, PolyPhen: probably_damaging - score 0.996
810	chr17:g.7675124T¿C	Substitution Missense		1/833,0.12%	31/13,582	VEP: MODERATE, SIFT: deleterious - score 0, PolyPhen: probably_damaging - score 0.999
811	chr1:g.7249612G¿T	Substitution Missense	SMARCA4 L1085P	1/833,0.12%	1/13,582	VEP: MODERATE, SIFT: deleterious - score 0, PolyPhen: probably_damaging - score 0.999

812	chr17:g.7675208C¿T	Substitution Missense		1/833,0.12%	12/13,582	VEP: MODERATE, SIFT: deleterious - score 0, PolyPhen: probably_damaging - score 1
813	chr12:g.25227343G¿C	Substitution Missense	FOXP1 L571P	1/833,0.12%	2/13,582	VEP: MODERATE, SIFT: deleterious - score 0, PolyPhen: possibly_damaging - score 0.509
814	chr3:g.186048818C¿T	Substitution Missense		1/833,0.12%	1/13,582	VEP: MODERATE, SIFT: deleterious - score 0, PolyPhen: possibly_damaging - score 0.787
815	chr1:g.198699704G¿T	Substitution Missense	PTPRK I761F	1/833,0.12%	1/13,582	VEP: MODERATE, SIFT: deleterious - score 0.01, PolyPhen: possibly_damaging - score 0.556
816	chr3:g.53751880G¿C	Substitution Missense		1/833,0.12%	1/13,582	VEP: MODERATE, SIFT: tolerated - score 0.26, PolyPhen: benign - score 0.006
817	chr1:g.3432006C¿A	Substitution Missense	BCOR P171H	1/833,0.12%	1/13,582	VEP: MODERATE, SIFT: tolerated - score 0.14, PolyPhen: benign - score 0.058
818	chr7:g.143356648C¿T	Substitution Missense		1/833,0.12%	1/13,582	VEP: MODERATE, SIFT: tolerated - score 0.05, PolyPhen: possibly_damaging - score 0.447
819	chr6:g.128322253T¿G	Substitution Missense	PTPRC D1002N	1/833,0.12%	1/13,582	VEP: MODERATE, SIFT: deleterious - score 0.01, PolyPhen: benign - score 0.071
820	chr9:g.133112116C¿T	Substitution Missense		1/833,0.12%	1/13,582	VEP: MODERATE, SIFT: deleterious - score 0, PolyPhen: probably_damaging - score 0.948
821	chr22:g.23180968A¿C	Substitution Missense	NCOR1 T705I	1/833,0.12%	1/13,582	VEP: MODERATE, SIFT: deleterious_low_confidence - score 0.01, PolyPhen: benign - score 0.255
822	chr17:g.31360538T¿G	Substitution Missense		1/833,0.12%	1/13,582	VEP: MODERATE, SIFT: deleterious - score 0.01, PolyPhen: benign - score 0.387
823	chr8:g.91986211C¿T	Substitution Missense	NF2 N485K	1/833,0.12%	2/13,582	VEP: MODERATE, SIFT: tolerated - score 0.06, PolyPhen: probably_damaging - score 0.997
824	chr1:g.15872997C¿T	Substitution Missense		1/833,0.12%	1/13,582	VEP: MODERATE, SIFT: deleterious - score 0, PolyPhen: probably_damaging - score 0.999
825	chr8:g.102271221C¿T	Substitution Missense	CLTCL1 H1335N	1/833,0.12%	2/13,582	VEP: MODERATE, SIFT: tolerated - score 0.16, PolyPhen: possibly_damaging - score 0.614

826	chr15:g.87929204G¿A	Substitution	Missense		1/833,0.12%	1/13,582	VEP: MODERATE, SIFT: tolerated - score 0.05, PolyPhen: possibly_damaging - score 0.858
827	chr1:g.155192219C¿A	Substitution	Missense	FGFR3 G54A	1/833,0.12%	1/13,582	VEP: MODERATE, SIFT: tolerated - score 0.22, PolyPhen: benign - score 0.006
828	chrX:g.40062805C¿G	Substitution	Missense		1/833,0.12%	1/13,582	VEP: MODERATE, SIFT: deleterious - score 0.01, PolyPhen: possibly_damaging - score 0.464
829	chr19:g.14097668C¿T	Substitution	Missense	RUNX1T1 A550T	1/833,0.12%	1/13,582	VEP: MODERATE, SIFT: deleterious - score 0, PolyPhen: probably_damaging - score 1
830	chr10:g.102397583C¿A	Substitution	Missense		1/833,0.12%	1/13,582	VEP: MODERATE, SIFT: deleterious - score 0, PolyPhen: probably_damaging - score 1
831	chr14:g.65093794T¿C	Substitution	Missense	HLA-A R68G	1/833,0.12%	1/13,582	VEP: MODERATE, SIFT: deleterious - score 0, PolyPhen: probably_damaging - score 0.992
832	chr3:g.47123269C¿A	Substitution	Missense		1/833,0.12%	1/13,582	VEP: MODERATE, SIFT: deleterious_low_confidence - score 0, PolyPhen: probably_damaging - score 0.997
833	chr17:g.7675214A¿G	Substitution	Missense	KDR R961L	1/833,0.12%	1/13,582	VEP: MODERATE, SIFT: deleterious - score 0, PolyPhen: benign - score 0.089
834	chr13:g.32370403T¿C	Substitution	Missense		1/833,0.12%	1/13,582	VEP: MODERATE, SIFT: deleterious - score 0, PolyPhen: possibly_damaging - score 0.769
835	chrX:g.47179973G¿A	Substitution	Missense	CCND3 T117M	1/833,0.12%	1/13,582	VEP: MODERATE, SIFT: deleterious - score 0, PolyPhen: probably_damaging - score 0.992
836	chr10:g.43114619G¿C	Substitution	Missense		1/833,0.12%	1/13,582	VEP: MODERATE, SIFT: tolerated - score 0.06, PolyPhen: probably_damaging - score 0.942
837	chr4:g.105241411G¿C	Substitution	Missense	KMT2A A53S	1/833,0.12%	1/13,582	VEP: MODERATE, SIFT: deleterious - score 0, PolyPhen: probably_damaging - score 0.999
838	chr1:g.147620299G¿A	Substitution	Missense		1/833,0.12%	1/13,582	VEP: MODERATE, SIFT: tolerated - score 0.27, PolyPhen: benign - score 0
839	chr16:g.2076147G¿T	Substitution	Missense	DNMT3A R736H	1/833,0.12%	1/13,582	VEP: MODERATE, SIFT: deleterious - score 0, PolyPhen: probably_damaging - score 0.996

840	chr15:g.90087189A¿C	Substitution Missense		1/833,0.12%	1/13,582	VEP: MODERATE, SIFT: deleterious_low_confidence - score 0.02, PolyPhen: benign - score 0.393
841	chr7:g.152158994T¿C	Substitution Missense	RB1 H483Y	1/833,0.12%	1/13,582	VEP: MODERATE, SIFT: deleterious - score 0, PolyPhen: probably_damaging - score 0.985
842	chr17:g.43094471T¿A	Substitution Missense		1/833,0.12%	1/13,582	VEP: MODERATE, SIFT: deleterious - score 0.01, PolyPhen: possibly_damaging - score 0.888
843	chr8:g.41987505C¿T	Substitution Missense	ATRX K494T	1/833,0.12%	1/13,582	VEP: MODERATE, SIFT: deleterious - score 0.02, PolyPhen: probably_damaging - score 0.998
844	chr17:g.80344789C¿G	Substitution Missense		1/833,0.12%	1/13,582	VEP: MODERATE, SIFT: deleterious - score 0, PolyPhen: probably_damaging - score 0.997
845	chr17:g.59681832T¿A	Substitution Missense	EZH2 D730N	1/833,0.12%	1/13,582	VEP: MODERATE, SIFT: tolerated - score 0.33, PolyPhen: benign - score 0.038
846	chr20:g.58853342C¿A	Substitution Missense		1/833,0.12%	1/13,582	VEP: MODERATE, SIFT: deleterious_low_confidence - score 0, PolyPhen: probably_damaging - score 0.996
847	chr3:g.12406066G¿C	Substitution Missense	RUNX1 L175V	1/833,0.12%	1/13,582	VEP: MODERATE, SIFT: tolerated - score 0.06, PolyPhen: possibly_damaging - score 0.863
848	chrX:g.77508433C¿A	Substitution Missense		1/833,0.12%	1/13,582	VEP: MODERATE, SIFT: deleterious_low_confidence - score 0, PolyPhen: probably_damaging - score 0.998
849	chr16:g.72958476G¿A	Substitution Missense	CBFB Y29H	1/833,0.12%	1/13,582	VEP: MODERATE, SIFT: deleterious_low_confidence - score 0.01, PolyPhen: possibly_damaging - score 0.624
850	chr1:g.26696833C¿T	Substitution Missense		1/833,0.12%	1/13,582	VEP: MODERATE, SIFT: tolerated_low_confidence - score 0.19, PolyPhen: benign - score 0.062
851	chr16:g.9840980G¿A	Substitution Missense	SDHAF2 S10L	1/833,0.12%	1/13,582	VEP: MODERATE, SIFT: deleterious - score 0, PolyPhen: probably_damaging - score 0.996
852	chr11:g.108326160G¿C	Substitution Missense		1/833,0.12%	1/13,582	VEP: MODERATE, SIFT: deleterious - score 0, PolyPhen: probably_damaging - score 0.936
853	chr12:g.132687293C¿T	Substitution Missense	KMT2C R41C	1/833,0.12%	1/13,582	VEP: MODERATE, SIFT: tolerated - score 0.18, PolyPhen: possibly_damaging - score 0.885

854	chr4:g.53399830C¿G	Substitution Missense		1/833,0.12%	1/13,582	VEP: MODERATE, SIFT: deleterious - score 0.01, PolyPhen: probably_damaging - score 0.93
855	chr1:g.64879127T¿C	Substitution Missense	TRIP11 E617Q	1/833,0.12%	1/13,582	VEP: MODERATE, SIFT: tolerated - score 0.3, PolyPhen: probably_damaging - score 0.985
856	chr14:g.81087959T¿G	Substitution Missense		1/833,0.12%	1/13,582	VEP: MODERATE, SIFT: deleterious - score 0, PolyPhen: probably_damaging - score 1
857	chr1:g.156879288G¿C	Substitution Missense	ATRX S1285Y	1/833,0.12%	1/13,582	VEP: MODERATE, SIFT: deleterious - score 0, PolyPhen: benign - score 0.051
858	chr6:g.398931C¿A	Substitution Missense		1/833,0.12%	1/13,582	VEP: MODERATE, SIFT: tolerated - score 0.76, PolyPhen: benign - score 0
859	chr4:g.125452519G¿C	Substitution Missense	PMS1 L813R	1/833,0.12%	1/13,582	VEP: MODERATE, SIFT: tolerated - score 0.47, PolyPhen: benign - score 0.053
860	chr5:g.159099436T¿G	Substitution Missense		1/833,0.12%	1/13,582	VEP: MODERATE, SIFT: tolerated_low_confidence - score 1, PolyPhen: benign - score 0
861	chr8:g.144511729C¿T	Substitution Missense	MITF I407F	1/833,0.12%	1/13,582	VEP: MODERATE, SIFT: deleterious - score 0, PolyPhen: benign - score 0.137
862	chr7:g.66991258T¿A	Substitution Missense		1/833,0.12%	1/13,582	VEP: MODERATE, SIFT: deleterious - score 0.04, PolyPhen: possibly_damaging - score 0.72
863	chr2:g.157738511C¿T	Substitution Missense	KIF5B Y29N	1/833,0.12%	1/13,582	VEP: MODERATE, SIFT: deleterious - score 0, PolyPhen: probably_damaging - score 0.97
864	chr16:g.64973017T¿G	Substitution Missense		1/833,0.12%	1/13,582	VEP: MODERATE, SIFT: deleterious - score 0, PolyPhen: probably_damaging - score 0.996
865	chr7:g.148817311C¿T	Substitution Missense	CLIP1 E178K	1/833,0.12%	1/13,582	VEP: MODERATE, SIFT: deleterious - score 0.04, PolyPhen: probably_damaging - score 0.994
866	chr1:g.164807667C¿G	Substitution Missense		1/833,0.12%	1/13,582	VEP: MODERATE, SIFT: deleterious - score 0, PolyPhen: probably_damaging - score 0.996
867	chr7:g.102196673G¿A	Substitution Missense	NTRK3 E398Q	1/833,0.12%	1/13,582	VEP: MODERATE, SIFT: tolerated - score 0.79, PolyPhen: benign - score 0.007

868	chr6:g.44265397G¿C	Substitution Missense		1/833,0.12%	1/13,582	VEP: MODERATE, SIFT: tolerated_low_confidence - score 0.84, PolyPhen: benign - score 0
869	chrX:g.47180240A¿C	Substitution Missense	MAX N29Y	1/833,0.12%	1/13,582	VEP: MODERATE, SIFT: deleterious - score 0.03, PolyPhen: probably_damaging - score 0.974
870	chr1:g.114716124C¿A	Substitution Missense		1/833,0.12%	2/13,582	VEP: MODERATE, SIFT: deleterious - score 0.02, PolyPhen: probably_damaging - score 0.992
871	chr9:g.15466809G¿C	Substitution Missense	LRIG3 H551P	1/833,0.12%	1/13,582	VEP: MODERATE, SIFT: tolerated_low_confidence - score 0.06, PolyPhen: possibly_damaging - score 0.9
872	chr16:g.23635375C¿T	Substitution Missense		1/833,0.12%	1/13,582	VEP: MODERATE, SIFT: tolerated - score 1, PolyPhen: benign - score 0.005
873	chr11:g.3699244G¿C	Substitution Missense	TET1 M811I	1/833,0.12%	1/13,582	VEP: MODERATE, SIFT: tolerated - score 0.05, PolyPhen: benign - score 0.396
874	chr2:g.108766083A¿C	Substitution Missense		1/833,0.12%	1/13,582	VEP: MODERATE, SIFT: tolerated_low_confidence - score 0.2, PolyPhen: benign - score 0.044
875	chr17:g.39494564G¿C	Substitution Missense	KMT2A P36A	1/833,0.12%	1/13,582	VEP: MODERATE, SIFT: deleterious - score 0.01, PolyPhen: probably_damaging - score 0.994
876	chr1:g.110340999C¿T	Substitution Missense		1/833,0.12%	1/13,582	VEP: MODERATE, SIFT: tolerated - score 0.13, PolyPhen: benign - score 0.04
877	chr3:g.186789186G¿A	Substitution Missense	FLT4 R1041W	1/833,0.12%	1/13,582	VEP: MODERATE, SIFT: deleterious - score 0.01, PolyPhen: possibly_damaging - score 0.878
878	chrX:g.77664747T¿G	Substitution Missense		1/833,0.12%	1/13,582	VEP: MODERATE, SIFT: tolerated - score 0.06, PolyPhen: benign - score 0.03
879	chr11:g.69641372C¿A	Substitution Missense	ETV5 Q246H	1/833,0.12%	1/13,582	VEP: MODERATE, SIFT: deleterious - score 0.02, PolyPhen: benign - score 0.003
880	chr1:g.204542789G¿C	Substitution Missense		1/833,0.12%	1/13,582	VEP: MODERATE, SIFT: tolerated - score 0.08, PolyPhen: benign - score 0.029
881	chr12:g.120997635G¿C	Substitution Missense	CCND3 E7K	1/833,0.12%	1/13,582	VEP: MODERATE, SIFT: deleterious - score 0, PolyPhen: probably_damaging - score 0.929

882	chr10:g.87933161G¿A	Substitution Missense		1/833,0.12%	1/13,582	VEP: MODERATE, SIFT: deleterious - score 0, PolyPhen: probably_damaging - score 0.977
883	chr14:g.92015764C¿T	Substitution Missense	ARID1B S362N	1/833,0.12%	2/13,582	VEP: MODERATE, SIFT: deleterious - score 0.04, PolyPhen: benign - score 0.118
884	chr12:g.12718022T¿A	Substitution Missense		1/833,0.12%	1/13,582	VEP: MODERATE, SIFT: deleterious - score 0.03, PolyPhen: probably_damaging - score 0.955
885	chr3:g.169116667C¿A	Substitution Missense	ERG V58I	1/833,0.12%	2/13,582	VEP: MODERATE, SIFT: deleterious - score 0, PolyPhen: probably_damaging - score 0.996
886	chr6:g.117326295C¿G	Substitution Missense		1/833,0.12%	1/13,582	VEP: MODERATE, SIFT: deleterious - score 0, PolyPhen: probably_damaging - score 0.991
887	chr12:g.58885889T¿A	Substitution Missense	POLE R409K	1/833,0.12%	1/13,582	VEP: MODERATE, SIFT: deleterious - score 0, PolyPhen: probably_damaging - score 0.999
888	chr9:g.37033986C¿T	Substitution Missense		1/833,0.12%	1/13,582	VEP: MODERATE, SIFT: deleterious - score 0.04, PolyPhen: probably_damaging - score 0.999
889	chr20:g.51432610G¿C	Substitution Missense	TSC2 S526R	1/833,0.12%	1/13,582	VEP: MODERATE, SIFT: tolerated - score 0.15, PolyPhen: benign - score 0.197
890	chr7:g.2937127C¿A	Substitution Missense		1/833,0.12%	1/13,582	VEP: MODERATE, SIFT: tolerated - score 0.05, PolyPhen: benign - score 0.003
891	chr16:g.72795229G¿T	Substitution Missense	NRG1 T441R	1/833,0.12%	1/13,582	VEP: MODERATE, SIFT: tolerated - score 0.2, PolyPhen: benign - score 0.011
892	chr7:g.98921928C¿G	Substitution Missense		1/833,0.12%	1/13,582	VEP: MODERATE, SIFT: tolerated - score 0.3, PolyPhen: benign - score 0.005
893	chr7:g.140787550C¿T	Substitution Missense	FAT4 A3313D	1/833,0.12%	1/13,582	VEP: MODERATE, SIFT: tolerated - score 0.08, PolyPhen: possibly_damaging - score 0.76
894	chr12:g.25245285G¿T	Substitution Missense		1/833,0.12%	1/13,582	VEP: MODERATE, SIFT: deleterious - score 0, PolyPhen: probably_damaging - score 1
895	chr12:g.363037C¿A	Substitution Missense	NTRK3 A664T	1/833,0.12%	1/13,582	VEP: MODERATE, SIFT: deleterious - score 0.03, PolyPhen: benign - score 0.013

896	chr1:g.26697103C¿T	Substitution Missense		1/833,0.12%	1/13,582	VEP: MODERATE, SIFT: tolerated_low_confidence - score 0.15, PolyPhen: possibly_damaging - score 0.878
897	chr4:g.125318744T¿C	Substitution Missense	BTG1 Y5H	1/833,0.12%	1/13,582	VEP: MODERATE, SIFT: tolerated - score 0.55, PolyPhen: benign - score 0.172
898	chr11:g.69641449A¿G	Substitution Missense		1/833,0.12%	1/13,582	VEP: MODERATE, SIFT: tolerated - score 0.13, PolyPhen: benign - score 0.075
899	chr4:g.86784493C¿T	Substitution Missense	KDM6A H170Y	1/833,0.12%	2/13,582	VEP: MODERATE, SIFT: tolerated - score 0.39, PolyPhen: benign - score 0
900	chr17:g.61684135G¿C	Substitution Missense		1/833,0.12%	1/13,582	VEP: MODERATE, SIFT: tolerated_low_confidence - score 0.1, PolyPhen: benign - score 0.254
901	chr7:g.26197710T¿C	Substitution Missense	PRDM16 P1190L	1/833,0.12%	1/13,582	VEP: MODERATE, SIFT: deleterious - score 0.01, PolyPhen: probably_damaging - score 0.985
902	chr16:g.314577C¿T	Substitution Missense		1/833,0.12%	1/13,582	VEP: MODERATE, SIFT: tolerated - score 0.09, PolyPhen: possibly_damaging - score 0.804
903	chr17:g.7675089G¿C	Substitution Missense	MSH2 A844V	1/833,0.12%	10/13,582	VEP: MODERATE, SIFT: deleterious - score 0, PolyPhen: probably_damaging - score 0.99
904	chr20:g.40687919G¿A	Substitution Missense		1/833,0.12%	1/13,582	VEP: MODERATE, SIFT: deleterious - score 0, PolyPhen: probably_damaging - score 0.971
905	chr1:g.119955193T¿C	Substitution Missense	ASXL1 G213S	1/833,0.12%	1/13,582	VEP: MODERATE, SIFT: tolerated - score 0.34, PolyPhen: benign - score 0.007
906	chr18:g.25227436C¿T	Substitution Missense		1/833,0.12%	1/13,582	VEP: MODERATE, SIFT: deleterious - score 0, PolyPhen: probably_damaging - score 0.999
907	chr10:g.68572886G¿C	Substitution Missense	AKAP9 E1513Q	1/833,0.12%	1/13,582	VEP: MODERATE, SIFT: deleterious - score 0.02, PolyPhen: benign - score 0.04
908	chr3:g.12417038G¿A	Substitution Missense		1/833,0.12%	3/13,582	VEP: MODERATE, SIFT: deleterious - score 0.02, PolyPhen: probably_damaging - score 0.999
909	chr3:g.52576554C¿T	Substitution Missense	CDK6 D89Y	1/833,0.12%	1/13,582	VEP: MODERATE, SIFT: tolerated - score 0.33, PolyPhen: possibly_damaging - score 0.758

910	chr16:g.15759659C¿T	Substitution Missense		1/833,0.12%	3/13,582	VEP: MODERATE, SIFT: deleterious - score 0, PolyPhen: probably_damaging - score 0.946
911	chr5:g.150412676G¿C	Substitution Missense	STK11 P369S	1/833,0.12%	1/13,582	VEP: MODERATE, SIFT: deleterious - score 0, PolyPhen: probably_damaging - score 0.998
912	chr9:g.129902886C¿T	Substitution Missense		1/833,0.12%	2/13,582	VEP: MODERATE, SIFT: deleterious - score 0, PolyPhen: possibly_damaging - score 0.857
913	chr17:g.7673776G¿C	Substitution Missense	SETD2 T1968I	1/833,0.12%	4/13,582	VEP: MODERATE, SIFT: deleterious - score 0.03, PolyPhen: possibly_damaging - score 0.801
914	chr13:g.32339867G¿A	Substitution Missense		1/833,0.12%	1/13,582	VEP: MODERATE, SIFT: tolerated - score 0.48, PolyPhen: probably_damaging - score 0.978
915	chr12:g.6672404C¿T	Substitution Missense	EP300 C1790G	1/833,0.12%	1/13,582	VEP: MODERATE, SIFT: deleterious - score 0, PolyPhen: probably_damaging - score 0.949
916	chr15:g.52340309C¿T	Substitution Missense		1/833,0.12%	1/13,582	VEP: MODERATE, SIFT: tolerated - score 0.08, PolyPhen: benign - score 0.04
917	chr12:g.70622464G¿T	Substitution Missense	FAT4 L572V	1/833,0.12%	1/13,582	VEP: MODERATE, SIFT: tolerated_low_confidence - score 0.23, PolyPhen: benign - score 0.014
918	chr18:g.47845395T¿A	Substitution Missense		1/833,0.12%	1/13,582	VEP: MODERATE, SIFT: deleterious - score 0.02, PolyPhen: probably_damaging - score 0.979
919	chr3:g.187725015A¿C	Substitution Missense	FAT4 F3139L	1/833,0.12%	1/13,582	VEP: MODERATE, SIFT: deleterious - score 0.01, PolyPhen: probably_damaging - score 0.995
920	chr6:g.157201000A¿G	Substitution Missense		1/833,0.12%	1/13,582	VEP: MODERATE, SIFT: tolerated_low_confidence - score 0.06, PolyPhen: probably_damaging - score 0.979
921	chr12:g.47987109G¿A	Substitution Missense	FGFR2 E116K	1/833,0.12%	1/13,582	VEP: MODERATE, SIFT: tolerated - score 0.08, PolyPhen: probably_damaging - score 0.926
922	chr11:g.72013080T¿G	Substitution Missense		1/833,0.12%	1/13,582	VEP: MODERATE, SIFT: tolerated - score 0.24, PolyPhen: benign - score 0.28
923	chr2:g.99593269C¿T	Substitution Missense	TP53 R337C	1/833,0.12%	1/13,582	VEP: MODERATE, SIFT: tolerated - score 0.78, PolyPhen: benign - score 0.005

924	chr15:g.66435076G¿A	Substitution Missense		1/833,0.12%	1/13,582	VEP: MODERATE, SIFT: tolerated - score 0.07, PolyPhen: benign - score 0.427
925	chr19:g.34196690C¿G	Substitution Missense	MAF E273V	1/833,0.12%	1/13,582	VEP: MODERATE, SIFT: deleterious - score 0.01, PolyPhen: possibly_damaging - score 0.548
926	chr16:g.79599836T¿C	Substitution Missense		1/833,0.12%	1/13,582	VEP: MODERATE, SIFT: deleterious - score 0.04, PolyPhen: probably_damaging - score 0.99
927	chr2:g.24707229G¿A	Substitution Missense	GRIN2A H1389Y	1/833,0.12%	1/13,582	VEP: MODERATE, SIFT: deleterious - score 0.03, PolyPhen: possibly_damaging - score 0.874
928	chr4:g.86722400C¿T	Substitution Missense		1/833,0.12%	1/13,582	VEP: MODERATE, SIFT: tolerated - score 0.05, PolyPhen: benign - score 0.382
929	chr10:g.43100528C¿T	Substitution Missense	STAT5B R107C	1/833,0.12%	2/13,582	VEP: MODERATE, SIFT: tolerated_low_confidence - score 0.13, PolyPhen: benign - score 0.143
930	chr4:g.86735717G¿C	Substitution Missense		1/833,0.12%	1/13,582	VEP: MODERATE, SIFT: deleterious - score 0.02, PolyPhen: probably_damaging - score 0.966
931	chr4:g.54267320T¿A	Substitution Missense	ALK E802Q	1/833,0.12%	1/13,582	VEP: MODERATE, SIFT: tolerated - score 0.54, PolyPhen: benign - score 0
932	chr3:g.169128033C¿G	Substitution Missense		1/833,0.12%	1/13,582	VEP: MODERATE, SIFT: deleterious - score 0.04, PolyPhen: probably_damaging - score 0.996
933	chr1:g.35192344G¿C	Substitution Missense	PML R291Q	1/833,0.12%	2/13,582	VEP: MODERATE, SIFT: deleterious_low_confidence - score 0, PolyPhen: benign - score 0.038
934	chr6:g.128322175G¿C	Substitution Missense		1/833,0.12%	1/13,582	VEP: MODERATE, SIFT: deleterious - score 0, PolyPhen: probably_damaging - score 0.964
935	chr3:g.14146048G¿C	Substitution Missense	BCL7A S2T	1/833,0.12%	1/13,582	VEP: MODERATE, SIFT: deleterious - score 0.03, PolyPhen: benign - score 0.406
936	chr7:g.152167363T¿C	Substitution Missense		1/833,0.12%	1/13,582	VEP: MODERATE, SIFT: tolerated - score 0.36, PolyPhen: benign - score 0.151
937	chr20:g.41159648C¿T	Substitution Missense	NSD1 Q517E	1/833,0.12%	1/13,582	VEP: MODERATE, SIFT: deleterious - score 0, PolyPhen: probably_damaging - score 0.98

938	chr7:g.128092029G¿A	Substitution Missense		1/833,0.12%	1/13,582	VEP: MODERATE, SIFT: tolerated - score 0.05, PolyPhen: benign - score 0.124
939	chr11:g.119278181T¿G	Substitution Missense	ALK E343K	1/833,0.12%	1/13,582	VEP: MODERATE, SIFT: deleterious - score 0, PolyPhen: probably_damaging - score 0.998
940	chr14:g.92006087G¿T	Substitution Missense		1/833,0.12%	1/13,582	VEP: MODERATE, SIFT: deleterious - score 0.02, PolyPhen: possibly_damaging - score 0.652
941	chr17:g.59648294C¿G	Substitution Missense	CHN1 V179M	1/833,0.12%	1/13,582	VEP: MODERATE, SIFT: deleterious - score 0, PolyPhen: probably_damaging - score 0.992
942	chr11:g.102336974A¿G	Substitution Missense		1/833,0.12%	1/13,582	VEP: MODERATE, SIFT: deleterious - score 0, PolyPhen: possibly_damaging - score 0.525
943	chr9:g.90895589G¿A	Substitution Missense	FAT4 G4743A	1/833,0.12%	2/13,582	VEP: MODERATE, SIFT: deleterious - score 0.01, PolyPhen: possibly_damaging - score 0.725
944	chr7:g.2906692G¿C	Substitution Missense		1/833,0.12%	1/13,582	VEP: MODERATE, SIFT: tolerated - score 0.52, PolyPhen: benign - score 0
945	chr11:g.69641384A¿C	Substitution Missense	KDM5A E435D	1/833,0.12%	1/13,582	VEP: MODERATE, SIFT: tolerated - score 0.24, PolyPhen: benign - score 0
946	chr10:g.102400712T¿A	Substitution Missense		1/833,0.12%	1/13,582	VEP: MODERATE, SIFT: deleterious - score 0, PolyPhen: probably_damaging - score 0.964
947	chr11:g.69641366C¿T	Substitution Missense	TPR G2208V	1/833,0.12%	1/13,582	VEP: MODERATE, SIFT: tolerated - score 0.45, PolyPhen: benign - score 0
948	chr12:g.122022125A¿G	Substitution Missense		1/833,0.12%	1/13,582	VEP: MODERATE, SIFT: deleterious - score 0, PolyPhen: possibly_damaging - score 0.904
949	chr20:g.51523921G¿A	Substitution Missense	TNFAIP3 I248T	1/833,0.12%	1/13,582	VEP: MODERATE, SIFT: deleterious - score 0.01, PolyPhen: benign - score 0.021
950	chr14:g.61745815C¿G	Substitution Missense		1/833,0.12%	1/13,582	VEP: MODERATE, SIFT: deleterious - score 0, PolyPhen: possibly_damaging - score 0.906
951	chr3:g.169116353G¿T	Substitution Missense	NFKB2 S390P	1/833,0.12%	1/13,582	VEP: MODERATE, SIFT: deleterious - score 0.01, PolyPhen: probably_damaging - score 0.999

952	chr7:g.13935712G¿A	Substitution Missense		1/833,0.12%	1/13,582	VEP: MODERATE, SIFT: deleterious - score 0.01, PolyPhen: probably_damaging - score 0.943
953	chr7:g.152203002C¿T	Substitution Missense	TCF3 M274V	1/833,0.12%	1/13,582	VEP: MODERATE, SIFT: deleterious - score 0.01, PolyPhen: benign - score 0.197
954	chr19:g.53577348G¿A	Substitution Missense		1/833,0.12%	1/13,582	VEP: MODERATE, SIFT: tolerated - score 0.27, PolyPhen: probably_damaging - score 0.995
955	chr11:g.95979480G¿A	Substitution Missense	WT1 P89L	1/833,0.12%	1/13,582	VEP: MODERATE, SIFT: tolerated - score 0.06, PolyPhen: benign - score 0.082
956	chr2:g.177231151C¿T	Substitution Missense		1/833,0.12%	1/13,582	VEP: MODERATE, SIFT: deleterious - score 0.03, PolyPhen: possibly_damaging - score 0.541
957	chr14:g.95117663G¿A	Substitution Missense	AFF3 A187S	1/833,0.12%	1/13,582	VEP: MODERATE, SIFT: tolerated - score 0.12, PolyPhen: probably_damaging - score 0.91
958	chr10:g.102400772A¿G	Substitution Missense		1/833,0.12%	1/13,582	VEP: MODERATE, SIFT: deleterious - score 0, PolyPhen: possibly_damaging - score 0.572
959	chr3:g.47083767T¿A	Substitution Missense	CARD11 K550N	1/833,0.12%	1/13,582	VEP: MODERATE, SIFT: tolerated - score 0.21, PolyPhen: benign - score 0.025
960	chr1:g.205620097A¿T	Substitution Missense		1/833,0.12%	1/13,582	VEP: MODERATE, SIFT: tolerated - score 0.11, PolyPhen: possibly_damaging - score 0.628
961	chr8:g.38417389T¿C	Substitution Missense	ERBB4 V87G	1/833,0.12%	1/13,582	VEP: MODERATE, SIFT: deleterious - score 0, PolyPhen: probably_damaging - score 0.995
962	chr18:g.25226849T¿C	Substitution Missense		1/833,0.12%	1/13,582	VEP: MODERATE, SIFT: tolerated_low_confidence - score 1, PolyPhen: benign - score 0.015
963	chr2:g.197400833A¿C	Substitution Missense	KRAS A59V	1/833,0.12%	1/13,582	VEP: MODERATE, SIFT: deleterious - score 0, PolyPhen: probably_damaging - score 0.993
964	chr3:g.186048656C¿T	Substitution Missense		1/833,0.12%	1/13,582	VEP: MODERATE, SIFT: tolerated - score 0.72, PolyPhen: possibly_damaging - score 0.469
965	chr5:g.132934887C¿T	Substitution Missense	TFRC C353S	1/833,0.12%	1/13,582	VEP: MODERATE, SIFT: deleterious - score 0, PolyPhen: probably_damaging - score 0.996

966	chr3:g.149527842A¿C	Substitution Missense		1/833,0.12%	1/13,582	VEP: MODERATE, SIFT: deleterious - score 0, PolyPhen: possibly_damaging - score 0.69
967	chr17:g.31336785C¿A	Substitution Missense	KDR S1281C	1/833,0.12%	1/13,582	VEP: MODERATE, SIFT: deleterious - score 0, PolyPhen: possibly_damaging - score 0.893
968	chr12:g.6577820C¿T	Substitution Missense		1/833,0.12%	1/13,582	VEP: MODERATE, SIFT: deleterious - score 0, PolyPhen: probably_damaging - score 0.992
969	chr22:g.19233209G¿T	Substitution Missense	NKX2-1 H99P	1/833,0.12%	1/13,582	VEP: MODERATE, SIFT: deleterious - score 0.01, PolyPhen: possibly_damaging - score 0.833
970	chr11:g.118473735C¿T	Substitution Missense		1/833,0.12%	1/13,582	VEP: MODERATE, SIFT: deleterious_low_confidence - score 0, PolyPhen: possibly_damaging - score 0.641
971	chr17:g.43092326G¿C	Substitution Missense	ZNF384 Y447N	1/833,0.12%	1/13,582	VEP: MODERATE, SIFT: deleterious - score 0.01, PolyPhen: benign - score 0.26
972	chrX:g.48688304A¿G	Substitution Missense		1/833,0.12%	1/13,582	VEP: MODERATE, SIFT: deleterious - score 0.01, PolyPhen: possibly_damaging - score 0.475
973	chr3:g.52609374G¿A	Substitution Missense	NFE2L2 E67K	1/833,0.12%	2/13,582	VEP: MODERATE, SIFT: deleterious - score 0, PolyPhen: probably_damaging - score 0.992
974	chr15:g.87880367T¿A	Substitution Missense		1/833,0.12%	1/13,582	VEP: MODERATE, SIFT: deleterious - score 0, PolyPhen: probably_damaging - score 0.999
975	chr11:g.69641341G¿A	Substitution Missense	BRCA1 P1596T	1/833,0.12%	1/13,582	VEP: MODERATE, SIFT: tolerated - score 0.17, PolyPhen: benign - score 0.001
976	chr22:g.29661241G¿A	Substitution Missense		1/833,0.12%	1/13,582	VEP: MODERATE, SIFT: deleterious - score 0, PolyPhen: probably_damaging - score 0.977
977	chr14:g.61720512A¿C	Substitution Missense	POT1 G40E	1/833,0.12%	1/13,582	VEP: MODERATE, SIFT: deleterious - score 0, PolyPhen: probably_damaging - score 0.998
978	chr6:g.117578999T¿G	Substitution Missense		1/833,0.12%	1/13,582	VEP: MODERATE, SIFT: tolerated - score 0.11, PolyPhen: benign - score 0.066
979	chr4:g.186618224C¿T	Substitution Missense	NUMA1 R1802H	1/833,0.12%	1/13,582	VEP: MODERATE, SIFT: tolerated - score 0.06, PolyPhen: benign - score 0.031

980	chr7:g.13931648T¿C	Substitution Missense		1/833,0.12%	1/13,582	VEP: MODERATE, SIFT: tolerated - score 0.23, PolyPhen: benign - score 0.003
981	chr21:g.38383633G¿T	Substitution Missense	CTNNB1 S675L	1/833,0.12%	1/13,582	VEP: MODERATE, SIFT: tolerated - score 1, PolyPhen: benign - score 0.007
982	chr4:g.54278430G¿A	Substitution Missense		1/833,0.12%	2/13,582	VEP: MODERATE, SIFT: tolerated - score 0.05, PolyPhen: possibly_damaging - score 0.759
983	chr4:g.186618224C¿G	Substitution Missense	KMT2D C5481R	1/833,0.12%	1/13,582	VEP: MODERATE, SIFT: deleterious - score 0.03, PolyPhen: possibly_damaging - score 0.608
984	chr16:g.11255013C¿T	Substitution Missense		1/833,0.12%	1/13,582	VEP: MODERATE, SIFT: tolerated - score 0.69, PolyPhen: benign - score 0.017
985	chr9:g.107489016C¿T	Substitution Missense	PMS2 V467A	1/833,0.12%	1/13,582	VEP: MODERATE, SIFT: deleterious - score 0.04, PolyPhen: benign - score 0.079
986	chr7:g.26197630C¿G	Substitution Missense		1/833,0.12%	2/13,582	VEP: MODERATE, SIFT: deleterious - score 0.01, PolyPhen: probably_damaging - score 0.994
987	chr2:g.136114872G¿T	Substitution Missense	CNTRL S2292C	1/833,0.12%	1/13,582	VEP: MODERATE, SIFT: deleterious_low_confidence - score 0.01, PolyPhen: probably_damaging - score 0.996
988	chr14:g.95713948T¿C	Substitution Missense		1/833,0.12%	1/13,582	VEP: MODERATE, SIFT: deleterious - score 0.01, PolyPhen: benign - score 0.394
989	chr7:g.152273849G¿T	Substitution Missense	AFF1 G69E	1/833,0.12%	1/13,582	VEP: MODERATE, SIFT: deleterious - score 0.03, PolyPhen: probably_damaging - score 0.994
990	chr12:g.12718102A¿G	Substitution Missense		1/833,0.12%	1/13,582	VEP: MODERATE, SIFT: deleterious - score 0, PolyPhen: probably_damaging - score 0.999
991	chr9:g.97675528C¿T	Substitution Missense	CNOT3 R188C	1/833,0.12%	1/13,582	VEP: MODERATE, SIFT: tolerated - score 0.07, PolyPhen: benign - score 0.003
992	chr19:g.32939868G¿T	Substitution Missense		1/833,0.12%	1/13,582	VEP: MODERATE, SIFT: tolerated - score 0.06, PolyPhen: possibly_damaging - score 0.549
993	chr16:g.50791608A¿G	Substitution Missense	ATRX D2048Y	1/833,0.12%	1/13,582	VEP: MODERATE, SIFT: deleterious - score 0.03, PolyPhen: benign - score 0.089

994	chr16:g.72798535C¿T	Substitution Missense		1/833,0.12%	2/13,582	VEP: MODERATE, SIFT: deleterious - score 0.01, PolyPhen: possibly_damaging - score 0.877
995	chr7:g.140753349C¿T	Substitution Missense	NUP214 E784K	1/833,0.12%	2/13,582	VEP: MODERATE, SIFT: deleterious - score 0, PolyPhen: possibly_damaging - score 0.766
996	chr15:g.88137443A¿G	Substitution Missense		1/833,0.12%	1/13,582	VEP: MODERATE, SIFT: tolerated - score 0.21, PolyPhen: benign - score 0.078
997	chr10:g.75020776C¿A	Substitution Missense	PIK3R1 E439G	1/833,0.12%	1/13,582	VEP: MODERATE, SIFT: deleterious - score 0.04, PolyPhen: probably_damaging - score 0.978
998	chr19:g.52216661G¿A	Substitution Missense		1/833,0.12%	1/13,582	VEP: MODERATE, SIFT: deleterious - score 0.01, PolyPhen: benign - score 0.255
999	chr2:g.29193396G¿A	Substitution Missense	PDCD1LG2 A85T	1/833,0.12%	2/13,582	VEP: MODERATE, SIFT: deleterious - score 0.02, PolyPhen: benign - score 0.313
1000	chr17:g.16118018T¿A	Substitution Missense		1/833,0.12%	1/13,582	VEP: MODERATE, SIFT: deleterious - score 0, PolyPhen: possibly_damaging - score 0.707
1001	chr5:g.158731079C¿T	Substitution Missense	ZFHX3 R314W	1/833,0.12%	2/13,582	VEP: MODERATE, SIFT: deleterious - score 0, PolyPhen: possibly_damaging - score 0.884
1002	chr17:g.42329753A¿C	Substitution Missense		1/833,0.12%	1/13,582	VEP: MODERATE, SIFT: tolerated - score 0.17, PolyPhen: possibly_damaging - score 0.787
1003	chr9:g.130884094G¿A	Substitution Missense	FAT1 K2981N	1/833,0.12%	1/13,582	VEP: MODERATE, SIFT: tolerated_low_confidence - score 0.12, PolyPhen: benign - score 0.014
1004	chr3:g.69941287G¿A	Substitution Missense		1/833,0.12%	1/13,582	VEP: MODERATE, SIFT: deleterious - score 0, PolyPhen: benign - score 0.354
1005	chr1:g.116397973G¿A	Substitution Missense	ASXL1 L696P	1/833,0.12%	1/13,582	VEP: MODERATE, SIFT: deleterious - score 0, PolyPhen: probably_damaging - score 0.998
1006	chr2:g.197393033C¿G	Substitution Missense		1/833,0.12%	1/13,582	VEP: MODERATE, SIFT: tolerated - score 0.07, PolyPhen: benign - score 0.001
1007	chr9:g.5073699C¿T	Substitution Missense	BUB1B D466N	1/833,0.12%	1/13,582	VEP: MODERATE, SIFT: deleterious - score 0, PolyPhen: probably_damaging - score 0.964

1008	chr5:g.177091022C¿T	Substitution Missense		1/833,0.12%	1/13,582	VEP: MODERATE, SIFT: tolerated - score 0.09, PolyPhen: probably_damaging - score 0.938
1009	chr8:g.42306377A¿G	Substitution Missense	PIM1 E135Q	1/833,0.12%	2/13,582	VEP: MODERATE, SIFT: deleterious - score 0.02, PolyPhen: possibly_damaging - score 0.707
1010	chr11:g.118436774T¿C	Substitution Missense		1/833,0.12%	1/13,582	VEP: MODERATE, SIFT: deleterious_low_confidence - score 0.04, PolyPhen: benign - score 0
1011	chr2:g.108764158G¿A	Substitution Missense	SMARCA4 T910K	1/833,0.12%	1/13,582	VEP: MODERATE, SIFT: deleterious - score 0.02, PolyPhen: benign - score 0.444
1012	chr2:g.25247628C¿T	Substitution Missense		1/833,0.12%	1/13,582	VEP: MODERATE, SIFT: deleterious - score 0, PolyPhen: probably_damaging - score 0.969
1013	chr17:g.50194798G¿A	Substitution Missense	MAX L46W	1/833,0.12%	1/13,582	VEP: MODERATE, SIFT: tolerated - score 0.06, PolyPhen: possibly_damaging - score 0.509
1014	chr11:g.85983969G¿T	Substitution Missense		1/833,0.12%	1/13,582	VEP: MODERATE, SIFT: tolerated - score 0.33, PolyPhen: benign - score 0.079
1015	chr1:g.205662036C¿T	Substitution Missense	KIT R5C	1/833,0.12%	1/13,582	VEP: MODERATE, SIFT: deleterious - score 0.01, PolyPhen: probably_damaging - score 0.944
1016	chr11:g.119285427C¿G	Substitution Missense		1/833,0.12%	1/13,582	VEP: MODERATE, SIFT: deleterious_low_confidence - score 0.03, PolyPhen: benign - score 0.219
1017	chr2:g.189854636A¿G	Substitution Missense	TBL1XR1 K277E	1/833,0.12%	1/13,582	VEP: MODERATE, SIFT: tolerated - score 0.4, PolyPhen: benign - score 0.035
1018	chr3:g.169131447T¿C	Substitution Missense		1/833,0.12%	1/13,582	VEP: MODERATE, SIFT: tolerated - score 0.59, PolyPhen: probably_damaging - score 0.961
1019	chr3:g.177026437C¿T	Substitution Missense	AKAP9 R1759I	1/833,0.12%	2/13,582	VEP: MODERATE, SIFT: deleterious - score 0.02, PolyPhen: benign - score 0.275
1020	chr12:g.53945165A¿G	Substitution Missense		1/833,0.12%	1/13,582	VEP: MODERATE, SIFT: deleterious - score 0, PolyPhen: probably_damaging - score 1
1021	chr11:g.118472453G¿A	Substitution Missense	ATR F1371L	1/833,0.12%	2/13,582	VEP: MODERATE, SIFT: deleterious_low_confidence - score 0.04, PolyPhen: probably_damaging - score 0.985

1022	chr6:g.117389427G¿A	Substitution Missense		1/833,0.12%	2/13,582	VEP: MODERATE, SIFT: deleterious - score 0, PolyPhen: probably_damaging - score 0.997
1023	chr12:g.124402459C¿T	Substitution Missense	DNM2 R318W	1/833,0.12%	1/13,582	VEP: MODERATE, SIFT: tolerated - score 0.46, PolyPhen: benign - score 0.001
1024	chr17:g.7675236A¿G	Substitution Missense		1/833,0.12%	2/13,582	VEP: MODERATE, SIFT: deleterious - score 0, PolyPhen: probably_damaging - score 0.999
1025	chr10:g.8058443C¿T	Substitution Missense	CCND1 A104T	1/833,0.12%	1/13,582	VEP: MODERATE, SIFT: tolerated - score 0.1, PolyPhen: benign - score 0.289
1026	chr15:g.87929339T¿C	Substitution Missense		1/833,0.12%	1/13,582	VEP: MODERATE, SIFT: deleterious - score 0.04, PolyPhen: probably_damaging - score 0.967
1027	chr7:g.152224465G¿A	Substitution Missense	VHL P172H	1/833,0.12%	1/13,582	VEP: MODERATE, SIFT: deleterious - score 0, PolyPhen: probably_damaging - score 0.985
1028	chr7:g.98915737G¿T	Substitution Missense		1/833,0.12%	1/13,582	VEP: MODERATE, SIFT: tolerated - score 0.29, PolyPhen: benign - score 0.014
1029	chr11:g.108354845T¿A	Substitution Missense	BCL9 V965I	1/833,0.12%	1/13,582	VEP: MODERATE, SIFT: deleterious - score 0, PolyPhen: possibly_damaging - score 0.492
1030	chr4:g.186619877T¿C	Substitution Missense		1/833,0.12%	1/13,582	VEP: MODERATE, SIFT: tolerated - score 0.12, PolyPhen: benign - score 0.174
1031	chr8:g.102281486C¿A	Substitution Missense	FAT4 S139F	1/833,0.12%	1/13,582	VEP: MODERATE, SIFT: tolerated - score 0.4, PolyPhen: benign - score 0.005
1032	chr20:g.63530089A¿C	Substitution Missense		1/833,0.12%	1/13,582	VEP: MODERATE, SIFT: tolerated - score 0.06, PolyPhen: benign - score 0.197
1033	chr7:g.2928608G¿A	Substitution Missense	MAX R36K	1/833,0.12%	1/13,582	VEP: MODERATE, SIFT: tolerated - score 0.07, PolyPhen: benign - score 0.035
1034	chr11:g.64804714G¿A	Substitution Missense		1/833,0.12%	1/13,582	VEP: MODERATE, SIFT: deleterious - score 0.01, PolyPhen: probably_damaging - score 0.996
1035	chr19:g.16101343A¿G	Substitution Missense	CDKN2C G114R	1/833,0.12%	1/13,582	VEP: MODERATE, SIFT: tolerated_low_confidence - score 0.5, PolyPhen: benign - score 0.006

1036	chr12:g.47993492C¿T	Substitution Missense		1/833,0.12%	1/13,582	VEP: MODERATE, SIFT: deleterious - score 0, PolyPhen: probably_damaging - score 0.998
1037	chr8:g.91960481A¿T	Substitution Missense	CSF3R E730K	1/833,0.12%	2/13,582	VEP: MODERATE, SIFT: deleterious - score 0, PolyPhen: probably_damaging - score 0.991
1038	chr8:g.70162765G¿C	Substitution Missense		1/833,0.12%	1/13,582	VEP: MODERATE, SIFT: tolerated - score 0.09, PolyPhen: possibly_damaging - score 0.634
1039	chr1:g.77967096G¿C	Substitution Missense	ERBB4 A1191V	1/833,0.12%	1/13,582	VEP: MODERATE, SIFT: deleterious - score 0.01, PolyPhen: probably_damaging - score 0.912
1040	chr12:g.57091421T¿A	Substitution Missense		1/833,0.12%	1/13,582	VEP: MODERATE, SIFT: deleterious - score 0, PolyPhen: benign - score 0.205
1041	chr14:g.95094151A¿G	Substitution Missense	NFIB R81C	1/833,0.12%	1/13,582	VEP: MODERATE, SIFT: deleterious - score 0, PolyPhen: probably_damaging - score 0.998
1042	chr3:g.186048752G¿A	Substitution Missense		1/833,0.12%	1/13,582	VEP: MODERATE, SIFT: tolerated - score 1, PolyPhen: benign - score 0.023
1043	chrX:g.47145480G¿A	Substitution Missense	DNM2 H262Q	1/833,0.12%	1/13,582	VEP: MODERATE, SIFT: tolerated_low_confidence - score 0.07, PolyPhen: benign - score 0.059
1044	chr7:g.2919372C¿T	Substitution Missense		1/833,0.12%	1/13,582	VEP: MODERATE, SIFT: deleterious - score 0, PolyPhen: probably_damaging - score 0.929
1045	chr12:g.50090275G¿T	Substitution Missense	BCL11B P162H	1/833,0.12%	1/13,582	VEP: MODERATE, SIFT: deleterious - score 0.01, PolyPhen: possibly_damaging - score 0.609
1046	chr10:g.87960925T¿C	Substitution Missense		1/833,0.12%	1/13,582	VEP: MODERATE, SIFT: deleterious - score 0.02, PolyPhen: probably_damaging - score 0.977
1047	chr11:g.108353877G¿A	Substitution Missense	KMT2D D4381H	1/833,0.12%	1/13,582	VEP: MODERATE, SIFT: deleterious - score 0, PolyPhen: probably_damaging - score 0.943
1048	chr17:g.31252971G¿A	Substitution Missense		1/833,0.12%	1/13,582	VEP: MODERATE, SIFT: deleterious_low_confidence - score 0.04, PolyPhen: probably_damaging - score 0.956
1049	chr17:g.31993887G¿T	Substitution Missense	CDK12 E314K	1/833,0.12%	2/13,582	VEP: MODERATE, SIFT: deleterious - score 0, PolyPhen: possibly_damaging - score 0.533

1050	chr16:g.10907524G¿C	Substitution Missense		1/833,0.12%	1/13,582	VEP: MODERATE, SIFT: deleterious - score 0.01, PolyPhen: possibly_damaging - score 0.466
1051	chr7:g.138894356G¿C	Substitution Missense	ZFHX3 Q1968K	1/833,0.12%	1/13,582	VEP: MODERATE, SIFT: deleterious - score 0, PolyPhen: probably_damaging - score 0.996
1052	chr12:g.70538207G¿T	Substitution Missense		1/833,0.12%	1/13,582	VEP: MODERATE, SIFT: deleterious - score 0, PolyPhen: probably_damaging - score 0.971
1053	chr17:g.55268027C¿T	Substitution Missense	AR G489W	1/833,0.12%	1/13,582	VEP: MODERATE, SIFT: deleterious - score 0.02, PolyPhen: benign - score 0.259
1054	chr1:g.164821553A¿C	Substitution Missense		1/833,0.12%	1/13,582	VEP: MODERATE, SIFT: deleterious_low_confidence - score 0, PolyPhen: benign - score 0.007
1055	chr4:g.125452222A¿G	Substitution Missense	BRIP1 G49R	1/833,0.12%	1/13,582	VEP: MODERATE, SIFT: tolerated - score 0.33, PolyPhen: benign - score 0.037
1056	chr15:g.57282451A¿T	Substitution Missense		1/833,0.12%	1/13,582	VEP: MODERATE, SIFT: deleterious - score 0, PolyPhen: probably_damaging - score 0.996
1057	chr3:g.53730489G¿A	Substitution Missense	FAT4 I4526M	1/833,0.12%	1/13,582	VEP: MODERATE, SIFT: deleterious - score 0, PolyPhen: possibly_damaging - score 0.882
1058	chrX:g.130069603T¿G	Substitution Missense		1/833,0.12%	1/13,582	VEP: MODERATE, SIFT: tolerated - score 0.33, PolyPhen: benign - score 0.097
1059	chr1:g.186335487A¿C	Substitution Missense	ATM Y2437N	1/833,0.12%	1/13,582	VEP: MODERATE, SIFT: tolerated - score 0.19, PolyPhen: probably_damaging - score 0.991
1060	chr6:g.127990842C¿G	Substitution Missense		1/833,0.12%	1/13,582	VEP: MODERATE, SIFT: deleterious - score 0.01, PolyPhen: probably_damaging - score 0.954
1061	chr16:g.2077664G¿C	Substitution Missense	ABL1 L99V	1/833,0.12%	1/13,582	VEP: MODERATE, SIFT: tolerated - score 0.52, PolyPhen: benign - score 0.001
1062	chr4:g.152337818G¿A	Substitution Missense		1/833,0.12%	1/13,582	VEP: MODERATE, SIFT: deleterious - score 0, PolyPhen: probably_damaging - score 0.997
1063	chr9:g.129979358A¿T	Substitution Missense	FIP1L1 R469K	1/833,0.12%	1/13,582	VEP: MODERATE, SIFT: deleterious - score 0, PolyPhen: probably_damaging - score 1

1064	chr11:g.3676260G¿A	Substitution Missense		1/833,0.12%	1/13,582	VEP: MODERATE, SIFT: tolerated - score 0.06, PolyPhen: benign - score 0.187
1065	chr17:g.31327775G¿C	Substitution Missense	FAT1 D595E	1/833,0.12%	1/13,582	VEP: MODERATE, SIFT: deleterious - score 0, PolyPhen: probably_damaging - score 0.992
1066	chr5:g.157228361A¿C	Substitution Missense		1/833,0.12%	1/13,582	VEP: MODERATE, SIFT: tolerated - score 0.11, PolyPhen: benign - score 0.13
1067	chrX:g.53201606C¿T	Substitution Missense	NCOR2 P1848L	1/833,0.12%	1/13,582	VEP: MODERATE, SIFT: deleterious - score 0, PolyPhen: possibly_damaging - score 0.566
1068	chr11:g.108345900C¿T	Substitution Missense		1/833,0.12%	1/13,582	VEP: MODERATE, SIFT: deleterious - score 0, PolyPhen: probably_damaging - score 0.991
1069	chrX:g.15809276G¿A	Substitution Missense	AR D829N	1/833,0.12%	1/13,582	VEP: MODERATE, SIFT: tolerated - score 0.06, PolyPhen: probably_damaging - score 1
1070	chr17:g.31993868C¿G	Substitution Missense		1/833,0.12%	1/13,582	VEP: MODERATE, SIFT: tolerated - score 0.23, PolyPhen: probably_damaging - score 0.967
1071	chr8:g.38414249C¿T	Substitution Missense	KMT2D P95L	1/833,0.12%	1/13,582	VEP: MODERATE, SIFT: deleterious - score 0.01, PolyPhen: probably_damaging - score 1
1072	chr19:g.4090697G¿T	Substitution Missense		1/833,0.12%	1/13,582	VEP: MODERATE, SIFT: deleterious - score 0.01, PolyPhen: possibly_damaging - score 0.844
1073	chr1:g.110345576G¿C	Substitution Missense	BMPR1A Y311C	1/833,0.12%	1/13,582	VEP: MODERATE, SIFT: deleterious_low_confidence - score 0, PolyPhen: benign - score 0.003
1074	chr12:g.70560709C¿G	Substitution Missense		1/833,0.12%	1/13,582	VEP: MODERATE, SIFT: deleterious - score 0.03, PolyPhen: probably_damaging - score 0.987
1075	chr1:g.58782599C¿T	Substitution Missense	CIITA V643A	1/833,0.12%	1/13,582	VEP: MODERATE, SIFT: tolerated - score 0.97, PolyPhen: benign - score 0.018
1076	chr2:g.99565551C¿T	Substitution Missense		1/833,0.12%	1/13,582	VEP: MODERATE, SIFT: deleterious - score 0, PolyPhen: probably_damaging - score 0.98
1077	chr11:g.108307902G¿C	Substitution Missense	FAT4 P4403L	1/833,0.12%	1/13,582	VEP: MODERATE, SIFT: tolerated - score 0.17, PolyPhen: benign - score 0.033

1078	chr2:g.99601520T¿A	Substitution Missense		1/833,0.12%	1/13,582	VEP: MODERATE, SIFT: deleterious - score 0, PolyPhen: probably_damaging - score 0.96
1079	chr4:g.86734386A¿T	Substitution Missense	MAX R36S	1/833,0.12%	1/13,582	VEP: MODERATE, SIFT: tolerated_low_confidence - score 1, PolyPhen: benign - score 0.001
1080	chr17:g.9946944C¿G	Substitution Missense		1/833,0.12%	1/13,582	VEP: MODERATE, SIFT: deleterious - score 0.01, PolyPhen: possibly_damaging - score 0.676
1081	chr3:g.155910776A¿G	Substitution Missense	NTRK3 A435E	1/833,0.12%	1/13,582	VEP: MODERATE, SIFT: tolerated - score 0.24, PolyPhen: benign - score 0.005
1082	chr12:g.120999349C¿A	Substitution Missense		1/833,0.12%	1/13,582	VEP: MODERATE, SIFT: tolerated - score 0.22, PolyPhen: benign - score 0.009
1083	chr12:g.27691780A¿T	Substitution Missense	MAX I71F	1/833,0.12%	1/13,582	VEP: MODERATE, SIFT: deleterious - score 0, PolyPhen: benign - score 0.196
1084	chr5:g.160119307C¿T	Substitution Missense		1/833,0.12%	1/13,582	VEP: MODERATE, SIFT: deleterious_low_confidence - score 0, PolyPhen: benign - score 0.187
1085	chr3:g.169116233T¿C	Substitution Missense	PTPN11 G503V	1/833,0.12%	1/13,582	VEP: MODERATE, SIFT: tolerated - score 0.4, PolyPhen: probably_damaging - score 0.915
1086	chr10:g.102401297G¿T	Substitution Missense		1/833,0.12%	1/13,582	VEP: MODERATE, SIFT: deleterious - score 0.01, PolyPhen: possibly_damaging - score 0.904
1087	chr11:g.114063339C¿A	Substitution Missense	SS18 G388V	1/833,0.12%	1/13,582	VEP: MODERATE, SIFT: deleterious - score 0, PolyPhen: probably_damaging - score 0.991
1088	chr4:g.125415135T¿C	Substitution Missense		1/833,0.12%	1/13,582	VEP: MODERATE, SIFT: tolerated - score 0.24, PolyPhen: probably_damaging - score 0.997
1089	chr3:g.53810036C¿T	Substitution Missense	FAT4 G3600E	1/833,0.12%	3/13,582	VEP: MODERATE, SIFT: tolerated_low_confidence - score 0.48, PolyPhen: probably_damaging - score 0.998
1090	chr14:g.95126707G¿A	Substitution Missense		1/833,0.12%	1/13,582	VEP: MODERATE, SIFT: tolerated - score 0.09, PolyPhen: benign - score 0.019
1091	chr9:g.20414050C¿T	Substitution Missense	PMS1 E743K	1/833,0.12%	1/13,582	VEP: MODERATE, SIFT: tolerated - score 0.09, PolyPhen: benign - score 0.056

1092	chr1:g.35189303C¿G	Substitution Missense		1/833,0.12%	1/13,582	VEP: MODERATE, SIFT: deleterious - score 0.03, PolyPhen: possibly_damaging - score 0.867
1093	chr22:g.23181032G¿C	Substitution Missense	POT1 S119L	1/833,0.12%	1/13,582	VEP: MODERATE, SIFT: tolerated_low_confidence - score 0.22, PolyPhen: benign - score 0.019
1094	chr13:g.40666110A¿G	Substitution Missense		1/833,0.12%	1/13,582	VEP: MODERATE, SIFT: tolerated - score 0.25, PolyPhen: benign - score 0
1095	chr11:g.69641365C¿T	Substitution Missense	FOXA1 A287T	1/833,0.12%	1/13,582	VEP: MODERATE, SIFT: tolerated - score 0.66, PolyPhen: benign - score 0
1096	chr1:g.26780169T¿G	Substitution Missense		1/833,0.12%	1/13,582	VEP: MODERATE, SIFT: deleterious - score 0.01, PolyPhen: probably_damaging - score 0.998
1097	chr2:g.99593748C¿T	Substitution Missense	CIC P581L	1/833,0.12%	1/13,582	VEP: MODERATE, SIFT: deleterious - score 0, PolyPhen: probably_damaging - score 0.954
1098	chr7:g.124863558G¿C	Substitution Missense		1/833,0.12%	1/13,582	VEP: MODERATE, SIFT: deleterious - score 0, PolyPhen: probably_damaging - score 0.956
1099	chr12:g.111792105G¿C	Substitution Missense	AXIN2 D682N	1/833,0.12%	1/13,582	VEP: MODERATE, SIFT: deleterious - score 0, PolyPhen: probably_damaging - score 1
1100	chr17:g.50188540C¿T	Substitution Missense		1/833,0.12%	2/13,582	VEP: MODERATE, SIFT: deleterious - score 0, PolyPhen: probably_damaging - score 0.994
1101	chrX:g.53196839C¿T	Substitution Missense	TP53 H193R	1/833,0.12%	1/13,582	VEP: MODERATE, SIFT: tolerated - score 1, PolyPhen: benign - score 0.003
1102	chr7:g.148826522G¿C	Substitution Missense		1/833,0.12%	1/13,582	VEP: MODERATE, SIFT: deleterious - score 0, PolyPhen: probably_damaging - score 0.995
1103	chr16:g.89749892G¿C	Substitution Missense	TSC1 L896F	1/833,0.12%	1/13,582	VEP: MODERATE, SIFT: tolerated - score 0.19, PolyPhen: benign - score 0.003
1104	chr12:g.92144376G¿A	Substitution Missense		1/833,0.12%	1/13,582	VEP: MODERATE, SIFT: deleterious - score 0, PolyPhen: probably_damaging - score 0.987
1105	chr13:g.19993589G¿A	Substitution Missense	ZFHX3 E45K	1/833,0.12%	1/13,582	VEP: MODERATE, SIFT: tolerated_low_confidence - score 0.12, PolyPhen: possibly_damaging - score 0.747

1106	chr18:g.25227107C¿T	Substitution Missense		1/833,0.12%	1/13,582	VEP: MODERATE, SIFT: tolerated - score 0.46, PolyPhen: benign - score 0.402
1107	chr10:g.21673603T¿A	Substitution Missense	EZH2 E725K	1/833,0.12%	1/13,582	VEP: MODERATE, SIFT: tolerated - score 0.34, PolyPhen: benign - score 0.04
1108	chr10:g.113152422G¿T	Substitution Missense		1/833,0.12%	1/13,582	VEP: MODERATE, SIFT: deleterious - score 0, PolyPhen: probably_damaging - score 1
1109	chr5:g.55964244G¿A	Substitution Missense	CXCR4 K29R	1/833,0.12%	1/13,582	VEP: MODERATE, SIFT: tolerated - score 0.1, PolyPhen: benign - score 0.007
1110	chr17:g.7674885C¿T	Substitution Missense		1/833,0.12%	17/13,582	VEP: MODERATE, SIFT: deleterious - score 0, PolyPhen: probably_damaging - score 1
1111	chr10:g.74975766C¿T	Substitution Missense	FAT4 D1521H	1/833,0.12%	1/13,582	VEP: MODERATE, SIFT: tolerated_low_confidence - score 0.45, PolyPhen: benign - score 0.015
1112	chr7:g.92086262C¿T	Substitution Missense		1/833,0.12%	1/13,582	VEP: MODERATE, SIFT: tolerated - score 0.09, PolyPhen: benign - score 0.003
1113	chr5:g.160093423T¿G	Substitution Missense	KAT6A L614F	1/833,0.12%	1/13,582	VEP: MODERATE, SIFT: tolerated - score 0.13, PolyPhen: benign - score 0.3
1114	chr2:g.136115377T¿C	Substitution Missense		1/833,0.12%	1/13,582	VEP: MODERATE, SIFT: tolerated - score 0.08, PolyPhen: possibly_damaging - score 0.751
1115	chr1:g.186345671G¿C	Substitution Missense	TET2 G1192V	1/833,0.12%	1/13,582	VEP: MODERATE, SIFT: deleterious - score 0, PolyPhen: possibly_damaging - score 0.65
1116	chr7:g.50400158C¿T	Substitution Missense		1/833,0.12%	1/13,582	VEP: MODERATE, SIFT: tolerated - score 0.21, PolyPhen: benign - score 0.001
1117	chr3:g.41234275G¿A	Substitution Missense	CUX1 D1396N	1/833,0.12%	1/13,582	VEP: MODERATE, SIFT: deleterious - score 0.02, PolyPhen: benign - score 0.014
1118	chr9:g.133108392G¿A	Substitution Missense		1/833,0.12%	1/13,582	VEP: MODERATE, SIFT: tolerated - score 0.4, PolyPhen: benign - score 0
1119	chr4:g.186596803G¿T	Substitution Missense	IL21R D512N	1/833,0.12%	1/13,582	VEP: MODERATE, SIFT: deleterious - score 0, PolyPhen: probably_damaging - score 0.999

1120	chr17:g.7675088C¿T	Substitution Missense		1/833,0.12%	183/13,582	VEP: MODERATE, SIFT: tolerated - score 0.11, PolyPhen: benign - score 0.319
1121	chr2:g.211387147G¿T	Substitution Missense	MED12 D639N	1/833,0.12%	2/13,582	VEP: MODERATE, SIFT: tolerated - score 0.52, PolyPhen: probably_damaging - score 0.93
1122	chr20:g.32436767C¿T	Substitution Missense		1/833,0.12%	1/13,582	VEP: MODERATE, SIFT: deleterious - score 0.01, PolyPhen: benign - score 0.014
1123	chr5:g.143054488G¿C	Substitution Missense	CALR D362N	1/833,0.12%	1/13,582	VEP: MODERATE, SIFT: tolerated - score 0.91, PolyPhen: benign - score 0.091
1124	chr11:g.95979669C¿T	Substitution Missense		1/833,0.12%	1/13,582	VEP: MODERATE, SIFT: tolerated - score 0.14, PolyPhen: benign - score 0
1125	chr12:g.122022174T¿A	Substitution Missense	CCND3 V39I	1/833,0.12%	1/13,582	VEP: MODERATE, SIFT: deleterious - score 0.01, PolyPhen: benign - score 0.206
1126	chr12:g.122377460T¿A	Substitution Missense		1/833,0.12%	1/13,582	VEP: MODERATE, SIFT: deleterious - score 0, PolyPhen: benign - score 0.236
1127	chr3:g.47106043C¿T	Substitution Missense	RANBP2 E1544K	1/833,0.12%	2/13,582	VEP: MODERATE, SIFT: deleterious - score 0.02, PolyPhen: probably_damaging - score 0.998
1128	chrX:g.1466357T¿C	Substitution Missense		1/833,0.12%	1/13,582	VEP: MODERATE, SIFT: tolerated - score 0.07, PolyPhen: possibly_damaging - score 0.493
1129	chr16:g.72960093A¿G	Substitution Missense	MLLT3 H54Q	1/833,0.12%	1/13,582	VEP: MODERATE, SIFT: tolerated_low_confidence - score 1, PolyPhen: benign - score 0.044
1130	chr14:g.37592176A¿C	Substitution Missense		1/833,0.12%	1/13,582	VEP: MODERATE, SIFT: deleterious - score 0, PolyPhen: probably_damaging - score 1
1131	chr4:g.25664205G¿C	Substitution Missense	TBX3 V546D	1/833,0.12%	1/13,582	VEP: MODERATE, SIFT: tolerated - score 0.14, PolyPhen: benign - score 0.03
1132	chr17:g.16146522A¿C	Substitution Missense		1/833,0.12%	1/13,582	VEP: MODERATE, SIFT: deleterious - score 0, PolyPhen: benign - score 0.437
1133	chr16:g.3740531A¿G	Substitution Missense	BRCA2 M3322I	1/833,0.12%	1/13,582	VEP: MODERATE, SIFT: deleterious - score 0, PolyPhen: probably_damaging - score 0.997

1134	chr20:g.32369101G¿A	Substitution Missense		1/833,0.12%	1/13,582	VEP: MODERATE, SIFT: deleterious - score 0, PolyPhen: probably_damaging - score 0.94
1135	chr14:g.102086255C¿G	Substitution Missense	FANCE L369F	1/833,0.12%	1/13,582	VEP: MODERATE, SIFT: deleterious_low_confidence - score 0, PolyPhen: probably_damaging - score 0.977
1136	chr12:g.112450407A¿C	Substitution Missense		1/833,0.12%	3/13,582	VEP: MODERATE, SIFT: deleterious - score 0, PolyPhen: possibly_damaging - score 0.813
1137	chr10:g.43128160G¿C	Substitution Missense	WT1 T334M	1/833,0.12%	1/13,582	VEP: MODERATE, SIFT: deleterious_low_confidence - score 0, PolyPhen: probably_damaging - score 0.995
1138	chr22:g.36304122G¿A	Substitution Missense		1/833,0.12%	1/13,582	VEP: MODERATE, SIFT: deleterious - score 0.02, PolyPhen: probably_damaging - score 1
1139	chr4:g.125450603C¿A	Substitution Missense	ATR S524P	1/833,0.12%	1/13,582	VEP: MODERATE, SIFT: deleterious - score 0.03, PolyPhen: possibly_damaging - score 0.52
1140	chr17:g.43528707C¿T	Substitution Missense		1/833,0.12%	1/13,582	VEP: MODERATE, SIFT: deleterious - score 0, PolyPhen: possibly_damaging - score 0.519
1141	chrX:g.40054322C¿A	Substitution Missense	MLLT1 P279L	1/833,0.12%	1/13,582	VEP: MODERATE, SIFT: deleterious - score 0, PolyPhen: probably_damaging - score 0.999
1142	chr14:g.99175678G¿T	Substitution Missense		1/833,0.12%	1/13,582	VEP: MODERATE, SIFT: tolerated - score 0.19, PolyPhen: possibly_damaging - score 0.694
1143	chr16:g.10916395G¿A	Substitution Missense	FCGR2B E78K	1/833,0.12%	1/13,582	VEP: MODERATE, SIFT: deleterious - score 0, PolyPhen: probably_damaging - score 0.999
1144	chr1:g.11144979G¿C	Substitution Missense		1/833,0.12%	1/13,582	VEP: MODERATE, SIFT: deleterious - score 0, PolyPhen: probably_damaging - score 0.998
1145	chr9:g.131164105G¿C	Substitution Missense	STAT5B D575G	1/833,0.12%	1/13,582	VEP: MODERATE, SIFT: deleterious - score 0, PolyPhen: possibly_damaging - score 0.714
1146	chr16:g.13926718G¿A	Substitution Missense		1/833,0.12%	1/13,582	VEP: MODERATE, SIFT: deleterious - score 0, PolyPhen: possibly_damaging - score 0.506
1147	chr3:g.179203764A¿G	Substitution Missense	MEN1 A165V	1/833,0.12%	1/13,582	VEP: MODERATE, SIFT: deleterious - score 0.02, PolyPhen: probably_damaging - score 0.996

1148	chr14:g.50757315C¿G	Substitution Missense		1/833,0.12%	2/13,582	VEP: MODERATE, SIFT: deleterious - score 0, PolyPhen: probably_damaging - score 0.997
1149	chr2:g.60553224T¿G	Substitution Missense	FAT4 L2482V	1/833,0.12%	1/13,582	VEP: MODERATE, SIFT: tolerated_low_confidence - score 0.14, PolyPhen: benign - score 0.012
1150	chr6:g.135194430G¿T	Substitution Missense		1/833,0.12%	1/13,582	VEP: MODERATE, SIFT: deleterious - score 0, PolyPhen: probably_damaging - score 0.994
1151	chrX:g.40063868A¿G	Substitution Missense	CDC73 D23E	1/833,0.12%	1/13,582	VEP: MODERATE, SIFT: deleterious - score 0.03, PolyPhen: probably_damaging - score 0.97
1152	chr3:g.14170477C¿T	Substitution Missense		1/833,0.12%	1/13,582	VEP: MODERATE, SIFT: tolerated - score 0.38, PolyPhen: benign - score 0.054
1153	chr7:g.140781611C¿A	Substitution Missense	PRDM1 S82F	1/833,0.12%	8/13,582	VEP: MODERATE, SIFT: deleterious - score 0, PolyPhen: probably_damaging - score 0.987
1154	chr4:g.41747479C¿A	Substitution Missense		1/833,0.12%	1/13,582	VEP: MODERATE, SIFT: deleterious - score 0, PolyPhen: probably_damaging - score 0.996
1155	chr18:g.25225171C¿T	Substitution Missense	TP53 T211I	1/833,0.12%	1/13,582	VEP: MODERATE, SIFT: tolerated - score 0.56, PolyPhen: benign - score 0.313
1156	chr1:g.15873034G¿C	Substitution Missense		1/833,0.12%	1/13,582	VEP: MODERATE, SIFT: tolerated - score 0.14, PolyPhen: possibly_damaging - score 0.867
1157	chr11:g.85976667C¿T	Substitution Missense	FAT4 N4698K	1/833,0.12%	1/13,582	VEP: MODERATE, SIFT: tolerated - score 0.15, PolyPhen: benign - score 0.342
1158	chr3:g.186786643G¿A	Substitution Missense		1/833,0.12%	1/13,582	VEP: MODERATE, SIFT: deleterious - score 0, PolyPhen: benign - score 0.264
1159	chr16:g.9938303C¿G	Substitution Missense	JAK3 H962R	1/833,0.12%	1/13,582	VEP: MODERATE, SIFT: tolerated - score 0.06, PolyPhen: probably_damaging - score 0.938
1160	chr7:g.152145249C¿T	Substitution Missense		1/833,0.12%	6/13,582	VEP: MODERATE, SIFT: deleterious - score 0, PolyPhen: probably_damaging - score 0.998
1161	chr6:g.157084696G¿T	Substitution Missense	HSP90AA1 V93A	1/833,0.12%	1/13,582	VEP: MODERATE, SIFT: deleterious_low_confidence - score 0, PolyPhen: probably_damaging - score 1

1162	chr1:g.170736049G¿A	Substitution Missense		1/833,0.12%	2/13,582	VEP: MODERATE, SIFT: tolerated - score 0.75, PolyPhen: benign - score 0.003
1163	chr12:g.57751648G¿A	Substitution Missense	RBM15 N133K	1/833,0.12%	2/13,582	VEP: MODERATE, SIFT: deleterious - score 0.02, PolyPhen: benign - score 0.129
1164	chr19:g.10786582C¿T	Substitution Missense		1/833,0.12%	2/13,582	VEP: MODERATE, SIFT: deleterious - score 0.01, PolyPhen: probably_damaging - score 0.941
1165	chr11:g.108316030G¿A	Substitution Missense	ARHGAP26 S434C	1/833,0.12%	4/13,582	VEP: MODERATE, SIFT: deleterious - score 0, PolyPhen: possibly_damaging - score 0.585
1166	chr9:g.130714414C¿T	Substitution Missense		1/833,0.12%	2/13,582	VEP: MODERATE, SIFT: deleterious_low_confidence - score 0.01, PolyPhen: benign - score 0.11
1167	chr12:g.65121113C¿T	Substitution Missense	TGFBR2 K90I	1/833,0.12%	1/13,582	VEP: MODERATE, SIFT: tolerated - score 0.64, PolyPhen: benign - score 0.005
1168	chr8:g.102254496T¿C	Substitution Missense		1/833,0.12%	1/13,582	VEP: MODERATE, SIFT: deleterious - score 0, PolyPhen: probably_damaging - score 0.976
1169	chr4:g.186606135C¿T	Substitution Missense	PMS1 I912F	1/833,0.12%	1/13,582	VEP: MODERATE, SIFT: deleterious - score 0.04, PolyPhen: probably_damaging - score 0.994
1170	chr2:g.197393123A¿C	Substitution Missense		1/833,0.12%	1/13,582	VEP: MODERATE, SIFT: deleterious - score 0.02, PolyPhen: possibly_damaging - score 0.832
1171	chr7:g.124852991C¿T	Substitution Missense	TFE3 H3R	1/833,0.12%	2/13,582	VEP: MODERATE, SIFT: deleterious - score 0.01, PolyPhen: possibly_damaging - score 0.9
1172	chr4:g.55090006C¿A	Substitution Missense		1/833,0.12%	1/13,582	VEP: MODERATE, SIFT: deleterious - score 0, PolyPhen: probably_damaging - score 1
1173	chr5:g.157211338C¿T	Substitution Missense	TET1 M804I	1/833,0.12%	3/13,582	VEP: MODERATE, SIFT: deleterious - score 0, PolyPhen: probably_damaging - score 0.984
1174	chr7:g.98992143C¿T	Substitution Missense		1/833,0.12%	1/13,582	VEP: MODERATE, SIFT: deleterious - score 0, PolyPhen: probably_damaging - score 0.987
1175	chr6:g.117418463G¿A	Substitution Missense	MAML2 K1134N	1/833,0.12%	1/13,582	VEP: MODERATE, SIFT: tolerated - score 0.09, PolyPhen: benign - score 0

1176	chr5:g.112767374G¿A	Substitution Missense		1/833,0.12%	3/13,582	VEP: MODERATE, SIFT: deleterious - score 0, PolyPhen: probably_damaging - score 0.972
1177	chr17:g.57675055G¿T	Substitution Missense	BTG1 Q36H	1/833,0.12%	1/13,582	VEP: MODERATE, SIFT: deleterious - score 0, PolyPhen: probably_damaging - score 0.969
1178	chr13:g.40665598G¿C	Substitution Missense		1/833,0.12%	1/13,582	VEP: MODERATE, SIFT: deleterious - score 0, PolyPhen: probably_damaging - score 0.982
1179	chr3:g.128620503T¿G	Substitution Missense	XPO1 V120L	1/833,0.12%	1/13,582	VEP: MODERATE, SIFT: tolerated - score 0.35, PolyPhen: benign - score 0.066
1180	chr17:g.59682791G¿C	Substitution Missense		1/833,0.12%	1/13,582	VEP: MODERATE, SIFT: tolerated - score 0.59, PolyPhen: probably_damaging - score 0.999
1181	chr12:g.58887891C¿T	Substitution Missense	FOXA1 N225H	1/833,0.12%	1/13,582	VEP: MODERATE, SIFT: deleterious - score 0.01, PolyPhen: probably_damaging - score 0.912
1182	chr9:g.129957431C¿G	Substitution Missense		1/833,0.12%	1/13,582	VEP: MODERATE, SIFT: deleterious - score 0, PolyPhen: probably_damaging - score 0.975
1183	chr16:g.65004686C¿T	Substitution Missense	MEN1 E26G	1/833,0.12%	3/13,582	VEP: MODERATE, SIFT: deleterious - score 0, PolyPhen: probably_damaging - score 1
1184	chr6:g.36596919T¿G	Substitution Missense		1/833,0.12%	1/13,582	VEP: MODERATE, SIFT: deleterious - score 0, PolyPhen: probably_damaging - score 0.995
1185	chr7:g.127652417C¿T	Substitution Missense	NUMA1 I1722F	1/833,0.12%	1/13,582	VEP: MODERATE, SIFT: tolerated - score 0.1, PolyPhen: benign - score 0
1186	chr1:g.204537468A¿G	Substitution Missense		1/833,0.12%	1/13,582	VEP: MODERATE, SIFT: tolerated - score 0.74, PolyPhen: benign - score 0
1187	chr16:g.11255295C¿G	Substitution Missense	MUC1 S79C	1/833,0.12%	1/13,582	VEP: MODERATE, SIFT: tolerated - score 0.22, PolyPhen: possibly_damaging - score 0.681
1188	chr17:g.31983093C¿T	Substitution Missense		1/833,0.12%	1/13,582	VEP: MODERATE, SIFT: tolerated - score 0.38, PolyPhen: possibly_damaging - score 0.888
1189	chr3:g.47113994A¿T	Substitution Missense	CYLD E507A	1/833,0.12%	1/13,582	VEP: MODERATE, SIFT: deleterious - score 0, PolyPhen: benign - score 0.141

1190	chr3:g.47121284C¿T	Substitution Missense		1/833,0.12%	1/13,582	VEP: MODERATE, SIFT: deleterious_low_confidence - score 0.05, PolyPhen: benign - score 0.031
1191	chr3:g.142507990A¿G	Substitution Missense	MSH6 L7V	1/833,0.12%	1/13,582	VEP: MODERATE, SIFT: tolerated - score 0.23, PolyPhen: benign - score 0.202
1192	chr2:g.211947484A¿T	Substitution Missense		1/833,0.12%	1/13,582	VEP: MODERATE, SIFT: deleterious - score 0.03, PolyPhen: probably_damaging - score 0.998
1193	chr12:g.70635842T¿C	Substitution Missense	BRCA1 R979H	1/833,0.12%	1/13,582	VEP: MODERATE, SIFT: deleterious_low_confidence - score 0.02, PolyPhen: possibly_damaging - score 0.721
1194	chr8:g.17947354G¿A	Substitution Missense		1/833,0.12%	1/13,582	VEP: MODERATE, SIFT: deleterious - score 0, PolyPhen: probably_damaging - score 0.999
1195	chr11:g.72014541G¿C	Substitution Missense	TNFAIP3 C524Y	1/833,0.12%	1/13,582	VEP: MODERATE, SIFT: deleterious - score 0, PolyPhen: probably_damaging - score 0.99
1196	chr8:g.38421938C¿T	Substitution Missense		1/833,0.12%	1/13,582	VEP: MODERATE, SIFT: tolerated - score 0.1, PolyPhen: benign - score 0.388
1197	chr3:g.53723470G¿A	Substitution Missense	SRGAP3 R73H	1/833,0.12%	1/13,582	VEP: MODERATE, SIFT: deleterious - score 0.02, PolyPhen: possibly_damaging - score 0.6
1198	chr8:g.38414808G¿A	Substitution Missense		1/833,0.12%	1/13,582	VEP: MODERATE, SIFT: deleterious - score 0.02, PolyPhen: probably_damaging - score 0.995
1199	chr3:g.37048550G¿C	Substitution Missense	UBR5 I264T	1/833,0.12%	1/13,582	VEP: MODERATE, SIFT: deleterious - score 0, PolyPhen: probably_damaging - score 0.917
1200	chr4:g.125319733T¿G	Substitution Missense		1/833,0.12%	1/13,582	VEP: MODERATE, SIFT: tolerated - score 0.53, PolyPhen: probably_damaging - score 0.911
1201	chr19:g.29822497C¿T	Substitution Missense	CXCR4 Q70R	1/833,0.12%	1/13,582	VEP: MODERATE, SIFT: tolerated - score 0.23, PolyPhen: possibly_damaging - score 0.476
1202	chr5:g.177211533G¿A	Substitution Missense		1/833,0.12%	1/13,582	VEP: MODERATE, SIFT: tolerated_low_confidence - score 0.11, PolyPhen: benign - score 0
1203	chr12:g.58872718G¿A	Substitution Missense	PRKACA L278V	1/833,0.12%	1/13,582	VEP: MODERATE, SIFT: tolerated_low_confidence - score 0.64, PolyPhen: benign - score 0

1204	chr11:g.108329112C¿T	Substitution Missense		1/833,0.12%	2/13,582	VEP: MODERATE, SIFT: deleterious - score 0, PolyPhen: possibly_damaging - score 0.535
1205	chr17:g.1365024C¿G	Substitution Missense	TRRAP S3316T	1/833,0.12%	1/13,582	VEP: MODERATE, SIFT: tolerated_low_confidence - score 0.1, PolyPhen: benign - score 0.038
1206	chr17:g.31223475T¿G	Substitution Missense		1/833,0.12%	1/13,582	VEP: MODERATE, SIFT: tolerated - score 0.07, PolyPhen: probably_damaging - score 0.916
1207	chr8:g.31076229G¿A	Substitution Missense	MYH9 M1510I	1/833,0.12%	1/13,582	VEP: MODERATE, SIFT: tolerated - score 1, PolyPhen: benign - score 0.005
1208	chr3:g.9064531G¿T	Substitution Missense		1/833,0.12%	1/13,582	VEP: MODERATE, SIFT: deleterious - score 0.01, PolyPhen: benign - score 0.08
1209	chr3:g.10060355T¿G	Substitution Missense	FGFR4 E421K	1/833,0.12%	1/13,582	VEP: MODERATE, SIFT: deleterious - score 0, PolyPhen: probably_damaging - score 0.973
1210	chr7:g.138917504T¿C	Substitution Missense		1/833,0.12%	1/13,582	VEP: MODERATE, SIFT: tolerated - score 0.14, PolyPhen: benign - score 0
1211	chr5:g.142770811A¿C	Substitution Missense	FGFR3 A35T	1/833,0.12%	1/13,582	VEP: MODERATE, SIFT: tolerated - score 0.2, PolyPhen: benign - score 0.124
1212	chr11:g.44171721A¿C	Substitution Missense		1/833,0.12%	1/13,582	VEP: MODERATE, SIFT: tolerated - score 0.97, PolyPhen: benign - score 0.007
1213	chr7:g.152149050G¿A	Substitution Missense	TERT V904E	1/833,0.12%	1/13,582	VEP: MODERATE, SIFT: deleterious - score 0.04, PolyPhen: possibly_damaging - score 0.88
1214	chr12:g.49044448C¿G	Substitution Missense		1/833,0.12%	1/13,582	VEP: MODERATE, SIFT: tolerated - score 0.06, PolyPhen: possibly_damaging - score 0.879
1215	chr4:g.186707245A¿C	Substitution Missense	GNAS E231K	1/833,0.12%	1/13,582	VEP: MODERATE, SIFT: tolerated - score 0.3, PolyPhen: possibly_damaging - score 0.526
1216	chr2:g.177231107C¿T	Substitution Missense		1/833,0.12%	1/13,582	VEP: MODERATE, SIFT: tolerated - score 0.06, PolyPhen: possibly_damaging - score 0.841
1217	chr7:g.98992140G¿A	Substitution Missense	PML D377N	1/833,0.12%	1/13,582	VEP: MODERATE, SIFT: deleterious - score 0.04, PolyPhen: probably_damaging - score 0.992

1218	chrX:g.71294407G¿C	Substitution Missense		1/833,0.12%	1/13,582	VEP: MODERATE, SIFT: deleterious - score 0, PolyPhen: probably_damaging - score 0.984
1219	chr9:g.37034012T¿C	Substitution Missense	BCL7A V6D	1/833,0.12%	1/13,582	VEP: MODERATE, SIFT: tolerated - score 0.12, PolyPhen: benign - score 0.395
1220	chr17:g.61781000G¿A	Substitution Missense		1/833,0.12%	1/13,582	VEP: MODERATE, SIFT: tolerated - score 0.08, PolyPhen: probably_damaging - score 0.999
1221	chr4:g.1806163A¿C	Substitution Missense	MYCN R398Q	1/833,0.12%	1/13,582	VEP: MODERATE, SIFT: deleterious - score 0, PolyPhen: probably_damaging - score 1
1222	chr7:g.13935763C¿A	Substitution Missense		1/833,0.12%	1/13,582	VEP: MODERATE, SIFT: tolerated - score 0.81, PolyPhen: benign - score 0.026
1223	chr9:g.130878451G¿A	Substitution Missense	AFF4 E96K	1/833,0.12%	1/13,582	VEP: MODERATE, SIFT: deleterious - score 0, PolyPhen: probably_damaging - score 1
1224	chr20:g.51523702G¿A	Substitution Missense		1/833,0.12%	1/13,582	VEP: MODERATE, SIFT: deleterious - score 0, PolyPhen: probably_damaging - score 0.994
1225	chr1:g.156134489G¿A	Substitution Missense	ATP2B3 R923H	1/833,0.12%	1/13,582	VEP: MODERATE, SIFT: deleterious - score 0.03, PolyPhen: benign - score 0.003
1226	chr19:g.1223132C¿G	Substitution Missense		1/833,0.12%	1/13,582	VEP: MODERATE, SIFT: tolerated - score 0.12, PolyPhen: benign - score 0.057
1227	chr7:g.92083613T¿G	Substitution Missense	MED12 P1687T	1/833,0.12%	1/13,582	VEP: MODERATE, SIFT: deleterious - score 0, PolyPhen: probably_damaging - score 1
1228	chr17:g.7674262T¿C	Substitution Missense		1/833,0.12%	22/13,582	VEP: MODERATE, SIFT: deleterious - score 0, PolyPhen: probably_damaging - score 0.98
1229	chr4:g.125318152G¿A	Substitution Missense	RNF43 R368Q	1/833,0.12%	1/13,582	VEP: MODERATE, SIFT: tolerated - score 0.2, PolyPhen: possibly_damaging - score 0.679
1230	chr16:g.2053375G¿T	Substitution Missense		1/833,0.12%	2/13,582	VEP: MODERATE, SIFT: deleterious - score 0, PolyPhen: probably_damaging - score 0.999
1231	chr4:g.54274890A¿G	Substitution Missense	KMT2A S2538F	1/833,0.12%	1/13,582	VEP: MODERATE, SIFT: deleterious - score 0, PolyPhen: benign - score 0.355

1232	chr3:g.129171634C¿T	Substitution Missense		1/833,0.12%	1/13,582	VEP: MODERATE, SIFT: tolerated - score 0.19, PolyPhen: possibly_damaging - score 0.533
1233	chr12:g.53973855A¿G	Substitution Missense	MUC1 S286F	1/833,0.12%	1/13,582	VEP: MODERATE, SIFT: tolerated - score 1, PolyPhen: benign - score 0
1234	chr14:g.37592548G¿A	Substitution Missense		1/833,0.12%	1/13,582	VEP: MODERATE, SIFT: deleterious - score 0.02, PolyPhen: benign - score 0.103
1235	chr10:g.68645916C¿G	Substitution Missense	TCF7L2 P456R	1/833,0.12%	1/13,582	VEP: MODERATE, SIFT: tolerated - score 0.5, PolyPhen: benign - score 0.049
1236	chr16:g.56935283C¿T	Substitution Missense		1/833,0.12%	1/13,582	VEP: MODERATE, SIFT: deleterious - score 0, PolyPhen: probably_damaging - score 0.948
1237	chr4:g.186709020C¿T	Substitution Missense	CDKN2A E88K	1/833,0.12%	1/13,582	VEP: MODERATE, SIFT: tolerated - score 0.18, PolyPhen: probably_damaging - score 0.982
1238	chr7:g.98955255C¿T	Substitution Missense		1/833,0.12%	1/13,582	VEP: MODERATE, SIFT: tolerated - score 0.07, PolyPhen: benign - score 0.067
1239	chr10:g.102401874G¿A	Substitution Missense	TCL1A F24V	1/833,0.12%	2/13,582	VEP: MODERATE, SIFT: tolerated - score 0.16, PolyPhen: benign - score 0.041
1240	chr9:g.121150265G¿A	Substitution Missense		1/833,0.12%	1/13,582	VEP: MODERATE, SIFT: deleterious - score 0, PolyPhen: probably_damaging - score 0.956
1241	chr16:g.64992975C¿T	Substitution Missense	SMARCA4 D1638N	1/833,0.12%	2/13,582	VEP: MODERATE, SIFT: deleterious - score 0, PolyPhen: possibly_damaging - score 0.7
1242	chr12:g.70556076G¿A	Substitution Missense		1/833,0.12%	1/13,582	VEP: MODERATE, SIFT: deleterious - score 0, PolyPhen: probably_damaging - score 0.997
1243	chr19:g.3119338G¿C	Substitution Missense	USP8 S1094Y	1/833,0.12%	1/13,582	VEP: MODERATE, SIFT: tolerated - score 0.08, PolyPhen: probably_damaging - score 0.92
1244	chr1:g.36467883C¿G	Substitution Missense		1/833,0.12%	1/13,582	VEP: MODERATE, SIFT: deleterious - score 0, PolyPhen: possibly_damaging - score 0.623
1245	chr4:g.186707397C¿T	Substitution Missense	KMT2A P1847S	1/833,0.12%	3/13,582	VEP: MODERATE, SIFT: tolerated - score 0.21, PolyPhen: benign - score 0.214

1246	chr22:g.23803344G¿A	Substitution Missense		1/833,0.12%	1/13,582	VEP: MODERATE, SIFT: deleterious - score 0, PolyPhen: possibly_damaging - score 0.804
1247	chr15:g.67184768G¿A	Substitution Missense	FLI1 T4I	1/833,0.12%	1/13,582	VEP: MODERATE, SIFT: deleterious - score 0.03, PolyPhen: probably_damaging - score 0.978
1248	chr5:g.171241083G¿C	Substitution Missense		1/833,0.12%	1/13,582	VEP: MODERATE, SIFT: deleterious - score 0.03, PolyPhen: benign - score 0.248
1249	chr16:g.72795831C¿G	Substitution Missense	PRDM1 G118A	1/833,0.12%	1/13,582	VEP: MODERATE, SIFT: deleterious - score 0, PolyPhen: probably_damaging - score 0.999
1250	chr12:g.318160A¿C	Substitution Missense		1/833,0.12%	1/13,582	VEP: MODERATE, SIFT: deleterious - score 0, PolyPhen: possibly_damaging - score 0.857
1251	chr17:g.42333924C¿A	Substitution Missense	CTNNB1 R587Q	1/833,0.12%	1/13,582	VEP: MODERATE, SIFT: deleterious - score 0, PolyPhen: benign - score 0.285
1252	chr17:g.80337918T¿G	Substitution Missense		1/833,0.12%	1/13,582	VEP: MODERATE, SIFT: deleterious - score 0, PolyPhen: benign - score 0.101
1253	chr3:g.12608780G¿C	Substitution Missense	TPR E1868K	1/833,0.12%	1/13,582	VEP: MODERATE, SIFT: tolerated - score 0.33, PolyPhen: benign - score 0.001
1254	chr9:g.121162195G¿A	Substitution Missense		1/833,0.12%	1/13,582	VEP: MODERATE, SIFT: tolerated - score 0.06, PolyPhen: possibly_damaging - score 0.696
1255	chr9:g.5089839T¿G	Substitution Missense	UBR5 M1911L	1/833,0.12%	1/13,582	VEP: MODERATE, SIFT: deleterious - score 0, PolyPhen: probably_damaging - score 0.995
1256	chr17:g.50199909G¿A	Substitution Missense		1/833,0.12%	1/13,582	VEP: MODERATE, SIFT: tolerated - score 0.34, PolyPhen: benign - score 0
1257	chr16:g.9764807A¿G	Substitution Missense	CD274 H240Q	1/833,0.12%	1/13,582	VEP: MODERATE, SIFT: deleterious - score 0.04, PolyPhen: probably_damaging - score 0.995
1258	chrX:g.47179972C¿T	Substitution Missense		1/833,0.12%	1/13,582	VEP: MODERATE, SIFT: deleterious - score 0, PolyPhen: probably_damaging - score 0.992
1259	chr11:g.46317469G¿A	Substitution Missense	MYD88 G106E	1/833,0.12%	2/13,582	VEP: MODERATE, SIFT: tolerated - score 1, PolyPhen: benign - score 0

1260	chr1:g.11133148C¿G	Substitution Missense		1/833,0.12%	1/13,582	VEP: MODERATE, SIFT: tolerated - score 0.11, PolyPhen: benign - score 0.14
1261	chr9:g.99828178G¿A	Substitution Missense	RAD21 E577K	1/833,0.12%	1/13,582	VEP: MODERATE, SIFT: deleterious - score 0.04, PolyPhen: benign - score 0.224
1262	chr11:g.120460702G¿A	Substitution Missense		1/833,0.12%	2/13,582	VEP: MODERATE, SIFT: deleterious - score 0.01, PolyPhen: probably_damaging - score 0.953
1263	chr16:g.15771658A¿G	Substitution Missense	RNF213 V1157A	1/833,0.12%	1/13,582	VEP: MODERATE, SIFT: tolerated - score 0.05, PolyPhen: possibly_damaging - score 0.573
1264	chr14:g.95091292T¿C	Substitution Missense		1/833,0.12%	4/13,582	VEP: MODERATE, SIFT: deleterious - score 0, PolyPhen: probably_damaging - score 0.998
1265	chr4:g.186596615G¿A	Substitution Missense	RBM10 R295Q	1/833,0.12%	1/13,582	VEP: MODERATE, SIFT: deleterious - score 0, PolyPhen: probably_damaging - score 0.998
1266	chr2:g.197402637T¿G	Substitution Missense		1/833,0.12%	1/13,582	VEP: MODERATE, SIFT: deleterious - score 0, PolyPhen: probably_damaging - score 0.988
1267	chr19:g.1220596G¿A	Substitution Missense	FANCA E886K	1/833,0.12%	1/13,582	VEP: MODERATE, SIFT: tolerated - score 0.1, PolyPhen: benign - score 0.084
1268	chr13:g.20019616G¿A	Substitution Missense		1/833,0.12%	1/13,582	VEP: MODERATE, SIFT: tolerated - score 0.2, PolyPhen: benign - score 0
1269	chr4:g.186707523T¿C	Substitution Missense	IKBKB L178V	1/833,0.12%	1/13,582	VEP: MODERATE, SIFT: tolerated - score 0.07, PolyPhen: benign - score 0.078
1270	chr12:g.4276209C¿G	Substitution Missense		1/833,0.12%	1/13,582	VEP: MODERATE, SIFT: tolerated - score 1, PolyPhen: benign - score 0.01
1271	chr1:g.147612890A¿G	Substitution Missense	NIN R968Q	1/833,0.12%	1/13,582	VEP: MODERATE, SIFT: deleterious_low_confidence - score 0, PolyPhen: probably_damaging - score 0.978
1272	chr4:g.25676358C¿A	Substitution Missense		1/833,0.12%	1/13,582	VEP: MODERATE, SIFT: deleterious - score 0, PolyPhen: probably_damaging - score 0.994
1273	chr17:g.50186675C¿T	Substitution Missense	TRIM27 S128R	1/833,0.12%	1/13,582	VEP: MODERATE, SIFT: deleterious - score 0.01, PolyPhen: probably_damaging - score 0.991
1274	chr4:g.1801956G¿T	Substitution Missense		1/833,0.12%	1/13,582	VEP: MODERATE, SIFT: deleterious - score 0, PolyPhen: probably_damaging - score 0.987

1275	chr14:g.55627978G¿T	Substitution	Missense	SPECC1 A4V	1/833,0.12%	1/13,582	VEP: MODERATE, SIFT: tolerated - score 0.67, PolyPhen: benign - score 0.001
1276	chr9:g.5029800C¿A	Substitution	Missense		1/833,0.12%	1/13,582	VEP: MODERATE, SIFT: deleterious - score 0.04, PolyPhen: benign - score 0.184
1277	chr3:g.169115986A¿G	Substitution	Missense	WAS L44F	1/833,0.12%	1/13,582	VEP: MODERATE, SIFT: tolerated - score 0.33, PolyPhen: probably_damaging - score 0.956
1278	chr16:g.50794215C¿T	Substitution	Missense		1/833,0.12%	1/13,582	VEP: MODERATE, SIFT: deleterious - score 0, PolyPhen: probably_damaging - score 0.992
1279	chr4:g.1801472C¿T	Substitution	Missense	FAT1 A3255V	1/833,0.12%	1/13,582	VEP: MODERATE, SIFT: deleterious - score 0, PolyPhen: probably_damaging - score 0.978
1280	chr4:g.186628615T¿A	Substitution	Missense		1/833,0.12%	1/13,582	VEP: MODERATE, SIFT: tolerated - score 0.17, PolyPhen: benign - score 0.083
1281	chr6:g.106107299G¿A	Substitution	Missense	MAF L124V	1/833,0.12%	1/13,582	VEP: MODERATE, SIFT: tolerated - score 1, PolyPhen: benign - score 0.05
1282	chr22:g.27798274G¿A	Substitution	Missense		1/833,0.12%	1/13,582	VEP: MODERATE, SIFT: deleterious_low_confidence - score 0, PolyPhen: benign - score 0.116
1283	chr16:g.2070499A¿G	Substitution	Missense	PAX7 E115K	1/833,0.12%	2/13,582	VEP: MODERATE, SIFT: deleterious - score 0, PolyPhen: probably_damaging - score 0.999
1284	chr11:g.108365085C¿G	Substitution	Missense		1/833,0.12%	1/13,582	VEP: MODERATE, SIFT: deleterious - score 0.01, PolyPhen: possibly_damaging - score 0.62
1285	chr5:g.170892471T¿G	Substitution	Missense	IRF4 K59R	1/833,0.12%	1/13,582	VEP: MODERATE, SIFT: deleterious - score 0, PolyPhen: benign - score 0.421
1286	chr5:g.170896097G¿T	Substitution	Missense		1/833,0.12%	1/13,582	VEP: MODERATE, SIFT: deleterious - score 0, PolyPhen: probably_damaging - score 0.996
1287	chr21:g.38383435G¿A	Substitution	Missense	TET2 L1971V	1/833,0.12%	1/13,582	VEP: MODERATE, SIFT: deleterious - score 0, PolyPhen: probably_damaging - score 0.969
1288	chr10:g.102401001G¿C	Substitution	Missense		1/833,0.12%	1/13,582	VEP: MODERATE, SIFT: deleterious - score 0, PolyPhen: possibly_damaging - score 0.864

1289	chr3:g.179218303G¿A	Substitution	Missense	SETD2 S203L	1/833,0.12%	302/13,582	VEP: MODERATE, SIFT: deleterious - score 0.02, PolyPhen: probably_damaging - score 0.909
1290	chr17:g.50190846G¿A	Substitution	Missense		1/833,0.12%	1/13,582	VEP: MODERATE, SIFT: deleterious - score 0.03, PolyPhen: probably_damaging - score 0.998
1291	chr7:g.140778006T¿G	Substitution	Missense	AFF1 S624L	1/833,0.12%	1/13,582	VEP: MODERATE, SIFT: deleterious - score 0, PolyPhen: probably_damaging - score 0.973
1292	chr7:g.152203056C¿T	Substitution	Missense		1/833,0.12%	1/13,582	VEP: MODERATE, SIFT: deleterious - score 0.01, PolyPhen: probably_damaging - score 0.98
1293	chr3:g.30644816A¿T	Substitution	Missense	FOXO3 Y465H	1/833,0.12%	1/13,582	VEP: MODERATE, SIFT: deleterious - score 0.02, PolyPhen: probably_damaging - score 0.995
1294	chr2:g.211673210G¿T	Substitution	Missense		1/833,0.12%	1/13,582	VEP: MODERATE, SIFT: deleterious - score 0, PolyPhen: benign - score 0.112
1295	chr14:g.102084961T¿G	Substitution	Missense	ATP2B3 E984Q	1/833,0.12%	1/13,582	VEP: MODERATE, SIFT: deleterious_low_confidence - score 0.02, PolyPhen: benign - score 0.359
1296	chr4:g.86775228G¿T	Substitution	Missense		1/833,0.12%	1/13,582	VEP: MODERATE, SIFT: tolerated - score 0.21, PolyPhen: possibly_damaging - score 0.693
1297	chr3:g.188609782C¿T	Substitution	Missense	SMO H340N	1/833,0.12%	2/13,582	VEP: MODERATE, SIFT: tolerated - score 0.16, PolyPhen: benign - score 0.169
1298	chr5:g.132898292C¿T	Substitution	Missense		1/833,0.12%	1/13,582	VEP: MODERATE, SIFT: deleterious - score 0.01, PolyPhen: probably_damaging - score 0.992
1299	chr12:g.114671938G¿A	Substitution	Missense	MYCN K125M	1/833,0.12%	1/13,582	VEP: MODERATE, SIFT: tolerated - score 0.05, PolyPhen: benign - score 0.01
1300	chr15:g.52379693T¿A	Substitution	Missense		1/833,0.12%	1/13,582	VEP: MODERATE, SIFT: tolerated - score 0.09, PolyPhen: benign - score 0.01
1301	chr1:g.147624160G¿T	Substitution	Missense	FOXO4 P44Q	1/833,0.12%	1/13,582	VEP: MODERATE, SIFT: tolerated - score 0.51, PolyPhen: benign - score 0.203
1302	chr17:g.59685092G¿A	Substitution	Missense		1/833,0.12%	1/13,582	VEP: MODERATE, SIFT: tolerated - score 0.1, PolyPhen: probably_damaging - score 0.999

1303	chr16:g.50779983G¿A	Substitution	Missense	ERBB2 A87T	1/833,0.12%	1/13,582	VEP: MODERATE, SIFT: deleterious - score 0, PolyPhen: probably_damaging - score 1
1304	chr9:g.20414246C¿T	Substitution	Missense		1/833,0.12%	1/13,582	VEP: MODERATE, SIFT: tolerated - score 0.08, PolyPhen: benign - score 0.003
1305	chr2:g.189795917G¿A	Substitution	Missense	FGFR2 Q495H	1/833,0.12%	1/13,582	VEP: MODERATE, SIFT: deleterious - score 0, PolyPhen: probably_damaging - score 1
1306	chr2:g.189805671C¿T	Substitution	Missense		1/833,0.12%	1/13,582	VEP: MODERATE, SIFT: deleterious - score 0, PolyPhen: probably_damaging - score 0.997
1307	chr7:g.124863600G¿C	Substitution	Missense	GNAS R649C	1/833,0.12%	1/13,582	VEP: MODERATE, SIFT: tolerated - score 0.18, PolyPhen: possibly_damaging - score 0.712
1308	chr2:g.174811574C¿T	Substitution	Missense		1/833,0.12%	1/13,582	VEP: MODERATE, SIFT: deleterious - score 0, PolyPhen: probably_damaging - score 1
1309	chr4:g.1801841C¿G	Substitution	Missense	CIC P74H	1/833,0.12%	37/13,582	VEP: MODERATE, SIFT: deleterious - score 0.01, PolyPhen: probably_damaging - score 0.978
1310	chr2:g.174824491A¿G	Substitution	Missense		1/833,0.12%	1/13,582	VEP: MODERATE, SIFT: deleterious - score 0, PolyPhen: probably_damaging - score 1
1311	chr4:g.87131204C¿G	Substitution	Missense	CIITA A1037V	1/833,0.12%	1/13,582	VEP: MODERATE, SIFT: deleterious - score 0.02, PolyPhen: possibly_damaging - score 0.815
1312	chr20:g.58895629A¿G	Substitution	Missense		1/833,0.12%	1/13,582	VEP: MODERATE, SIFT: deleterious - score 0, PolyPhen: probably_damaging - score 1
1313	chr16:g.68833311G¿A	Substitution	Missense	RNF43 R386Q	1/833,0.12%	1/13,582	VEP: MODERATE, SIFT: deleterious - score 0, PolyPhen: probably_damaging - score 1
1314	chr6:g.106106990G¿A	Substitution	Missense		1/833,0.12%	1/13,582	VEP: MODERATE, SIFT: tolerated - score 0.07, PolyPhen: probably_damaging - score 1
1315	chrX:g.124050294G¿T	Substitution	Missense	MITF L117P	1/833,0.12%	1/13,582	VEP: MODERATE, SIFT: deleterious - score 0, PolyPhen: probably_damaging - score 1
1316	chr16:g.9763529T¿C	Substitution	Missense		1/833,0.12%	1/13,582	VEP: MODERATE, SIFT: tolerated - score 0.31, PolyPhen: benign - score 0.013

1317	chr9:g.77721426G¿C	Substitution	Missense	AR F877L	1/833,0.12%	1/13,582	VEP: MODERATE, SIFT: tolerated - score 0.13, PolyPhen: benign - score 0.14
1318	chr10:g.21670642G¿A	Substitution	Missense		1/833,0.12%	1/13,582	VEP: MODERATE, SIFT: tolerated - score 0.66, PolyPhen: probably_damaging - score 0.931
1319	chr18:g.47848519T¿C	Substitution	Missense	MED12 N72K	1/833,0.12%	1/13,582	VEP: MODERATE, SIFT: deleterious - score 0.02, PolyPhen: probably_damaging - score 0.993
1320	chr18:g.25224411G¿T	Substitution	Missense		1/833,0.12%	1/13,582	VEP: MODERATE, SIFT: tolerated_low_confidence - score 0.08, PolyPhen: benign - score 0.034
1321	chr20:g.32429967C¿T	Substitution	Missense	SF3B1 V727L	1/833,0.12%	1/13,582	VEP: MODERATE, SIFT: deleterious - score 0.02, PolyPhen: probably_damaging - score 0.91
1322	chr17:g.81996722C¿T	Substitution	Missense		1/833,0.12%	1/13,582	VEP: MODERATE, SIFT: tolerated - score 0.06, PolyPhen: benign - score 0.048
1323	chr1:g.26697062G¿C	Substitution	Missense	DDX6 G233R	1/833,0.12%	1/13,582	VEP: MODERATE, SIFT: tolerated_low_confidence - score 1, PolyPhen: benign - score 0.084
1324	chr12:g.50085425C¿T	Substitution	Missense		1/833,0.12%	1/13,582	VEP: MODERATE, SIFT: tolerated_low_confidence - score 0.15, PolyPhen: benign - score 0
1325	chr7:g.92097253G¿A	Substitution	Missense	RPL5 E296K	1/833,0.12%	1/13,582	VEP: MODERATE, SIFT: deleterious - score 0, PolyPhen: probably_damaging - score 0.964
1326	chr5:g.1278711T¿A	Substitution	Missense		1/833,0.12%	1/13,582	VEP: MODERATE, SIFT: tolerated - score 0.07, PolyPhen: probably_damaging - score 0.999
1327	chrX:g.53211571C¿G	Substitution	Missense	ASPSCR1 D314N	1/833,0.12%	1/13,582	VEP: MODERATE, SIFT: deleterious - score 0, PolyPhen: probably_damaging - score 0.999
1328	chr22:g.27799676C¿T	Substitution	Missense		1/833,0.12%	1/13,582	VEP: MODERATE, SIFT: tolerated_low_confidence - score 0.14, PolyPhen: benign - score 0.006
1329	chr4:g.55104937C¿G	Substitution	Missense	JAK3 E1033Q	1/833,0.12%	1/13,582	VEP: MODERATE, SIFT: tolerated - score 1, PolyPhen: benign - score 0.11
1330	chr4:g.1799305G¿A	Substitution	Missense		1/833,0.12%	1/13,582	VEP: MODERATE, SIFT: deleterious - score 0, PolyPhen: probably_damaging - score 0.995

1331	chr22:g.23181172A¿G	Substitution	Missense	DCTN1 D748N	1/833,0.12%	1/13,582	VEP: MODERATE, SIFT: deleterious_low_confidence - score 0.01, PolyPhen: probably_damaging - score 0.994
1332	chr1:g.32279883C¿G	Substitution	Missense		1/833,0.12%	1/13,582	VEP: MODERATE, SIFT: deleterious - score 0.01, PolyPhen: possibly_damaging - score 0.611
1333	chr3:g.38138729C¿T	Substitution	Missense	PAX3 P373A	1/833,0.12%	1/13,582	VEP: MODERATE, SIFT: tolerated - score 0.12, PolyPhen: possibly_damaging - score 0.61
1334	chr1:g.164812069C¿T	Substitution	Missense		1/833,0.12%	1/13,582	VEP: MODERATE, SIFT: tolerated - score 0.05, PolyPhen: possibly_damaging - score 0.836
1335	chr8:g.38429868G¿A	Substitution	Missense	NR4A3 R557T	1/833,0.12%	1/13,582	VEP: MODERATE, SIFT: deleterious - score 0.01, PolyPhen: possibly_damaging - score 0.893
1336	chrX:g.130071144C¿G	Substitution	Missense		1/833,0.12%	1/13,582	VEP: MODERATE, SIFT: deleterious - score 0, PolyPhen: possibly_damaging - score 0.739
1337	chr19:g.42287215G¿A	Substitution	Missense	CDH11 R28Q	1/833,0.12%	1/13,582	VEP: MODERATE, SIFT: deleterious_low_confidence - score 0, PolyPhen: probably_damaging - score 0.968
1338	chr7:g.6009012C¿T	Substitution	Missense		1/833,0.12%	2/13,582	VEP: MODERATE, SIFT: tolerated_low_confidence - score 0.32, PolyPhen: benign - score 0.001
1339	chr17:g.50199255C¿T	Substitution	Missense	ELK4 L155F	1/833,0.12%	2/13,582	VEP: MODERATE, SIFT: deleterious - score 0, PolyPhen: probably_damaging - score 0.939
1340	chr7:g.116775096G¿A	Substitution	Missense		1/833,0.12%	1/13,582	VEP: MODERATE, SIFT: deleterious - score 0.03, PolyPhen: benign - score 0.031
1341	chr10:g.59792939G¿A	Substitution	Missense	PTPN13 D1557N	1/833,0.12%	1/13,582	VEP: MODERATE, SIFT: tolerated_low_confidence - score 1, PolyPhen: benign - score 0
1342	chr3:g.47120567G¿A	Substitution	Missense		1/833,0.12%	1/13,582	VEP: MODERATE, SIFT: tolerated_low_confidence - score 0.71, PolyPhen: benign - score 0
1343	chr1:g.77949219T¿C	Substitution	Missense	PTCH1 D57N	1/833,0.12%	1/13,582	VEP: MODERATE, SIFT: deleterious - score 0.03, PolyPhen: probably_damaging - score 0.932
1344	chr4:g.1804963G¿A	Substitution	Missense		1/833,0.12%	2/13,582	VEP: MODERATE, SIFT: deleterious - score 0, PolyPhen: probably_damaging - score 0.96

1345	chr8:g.92095063G¿C	Substitution	Missense	NUP214 A493P	1/833,0.12%	1/13,582	VEP: MODERATE, SIFT: deleterious_low_confidence - score 0.01, PolyPhen: unknown - score 0
1346	chr12:g.49024815C¿T	Substitution	Missense		1/833,0.12%	1/13,582	VEP: MODERATE, SIFT: deleterious - score 0, PolyPhen: probably_damaging - score 0.998
1347	chr6:g.106105923C¿G	Substitution	Missense	NRAS A59G	1/833,0.12%	1/13,582	VEP: MODERATE, SIFT: deleterious - score 0, PolyPhen: probably_damaging - score 0.998
1348	chr21:g.41476586G¿A	Substitution	Missense		1/833,0.12%	1/13,582	VEP: MODERATE, SIFT: deleterious - score 0, PolyPhen: probably_damaging - score 0.967
1349	chr1:g.39897827A¿G	Substitution	Missense	PCM1 C1999S	1/833,0.12%	1/13,582	VEP: MODERATE, SIFT: deleterious - score 0, PolyPhen: probably_damaging - score 0.989
1350	chr9:g.20354821C¿A	Substitution	Missense		1/833,0.12%	1/13,582	VEP: MODERATE, SIFT: tolerated - score 0.57, PolyPhen: benign - score 0.081
1351	chr5:g.157252619C¿T	Substitution	Missense	ZNF521 E24K	1/833,0.12%	3/13,582	VEP: MODERATE, SIFT: deleterious - score 0, PolyPhen: probably_damaging - score 1
1352	chr10:g.102594025G¿A	Substitution	Missense		1/833,0.12%	1/13,582	VEP: MODERATE, SIFT: tolerated - score 0.06, PolyPhen: benign - score 0.428
1353	chr7:g.140753349C¿G	Substitution	Missense	NCOR2 F1550Y	1/833,0.12%	4/13,582	VEP: MODERATE, SIFT: deleterious - score 0.01, PolyPhen: benign - score 0.316
1354	chr2:g.24707319G¿C	Substitution	Missense		1/833,0.12%	1/13,582	VEP: MODERATE, SIFT: deleterious - score 0, PolyPhen: benign - score 0.044
1355	chr13:g.48379606G¿A	Substitution	Missense	KIT T74M	1/833,0.12%	1/13,582	VEP: MODERATE, SIFT: deleterious - score 0, PolyPhen: probably_damaging - score 0.999
1356	chr6:g.128184714G¿T	Substitution	Missense		1/833,0.12%	1/13,582	VEP: MODERATE, SIFT: deleterious - score 0, PolyPhen: probably_damaging - score 1
1357	chr11:g.118504852C¿G	Substitution	Missense	RALGDS Y639D	1/833,0.12%	1/13,582	VEP: MODERATE, SIFT: tolerated_low_confidence - score 1, PolyPhen: benign - score 0
1358	chr16:g.15759664G¿A	Substitution	Missense		1/833,0.12%	1/13,582	VEP: MODERATE, SIFT: tolerated - score 0.4, PolyPhen: benign - score 0.015

1359	chr7:g.55174818G¿A	Substitution	Missense	ARHGAP26 I555T	1/833,0.12%	1/13,582	VEP: MODERATE, SIFT: deleterious - score 0, PolyPhen: probably_damaging - score 0.923
1360	chrX:g.134377753A¿C	Substitution	Missense		1/833,0.12%	1/13,582	VEP: MODERATE, SIFT: tolerated - score 0.14, PolyPhen: possibly_damaging - score 0.887
1361	chr19:g.10823816G¿A	Substitution	Missense	CLTCL1 V1017I	1/833,0.12%	1/13,582	VEP: MODERATE, SIFT: deleterious - score 0.01, PolyPhen: possibly_damaging - score 0.837
1362	chr12:g.25245314A¿T	Substitution	Missense		1/833,0.12%	1/13,582	VEP: MODERATE, SIFT: deleterious - score 0, PolyPhen: probably_damaging - score 0.992
1363	chr9:g.78031133C¿T	Substitution	Missense	FAT1 E3490K	1/833,0.12%	1/13,582	VEP: MODERATE, SIFT: tolerated - score 0.4, PolyPhen: benign - score 0.02
1364	chr17:g.50189714C¿T	Substitution	Missense		1/833,0.12%	1/13,582	VEP: MODERATE, SIFT: deleterious - score 0, PolyPhen: probably_damaging - score 0.999
1365	chr6:g.108561621C¿T	Substitution	Missense	FGFR3 R200C	1/833,0.12%	1/13,582	VEP: MODERATE, SIFT: deleterious - score 0.03, PolyPhen: benign - score 0.001
1366	chr7:g.116699333G¿T	Substitution	Missense		1/833,0.12%	1/13,582	VEP: MODERATE, SIFT: deleterious - score 0.03, PolyPhen: probably_damaging - score 0.938
1367	chr17:g.50194026C¿A	Substitution	Missense	TP53 R282W	1/833,0.12%	1/13,582	VEP: MODERATE, SIFT: deleterious - score 0, PolyPhen: probably_damaging - score 0.998
1368	chr9:g.121168267C¿G	Substitution	Missense		1/833,0.12%	1/13,582	VEP: MODERATE, SIFT: deleterious - score 0, PolyPhen: probably_damaging - score 0.991
1369	chr9:g.95111618C¿T	Substitution	Missense	FAT1 Y3302H	1/833,0.12%	1/13,582	VEP: MODERATE, SIFT: deleterious - score 0, PolyPhen: possibly_damaging - score 0.763
1370	chr1:g.157589348T¿G	Substitution	Missense		1/833,0.12%	1/13,582	VEP: MODERATE, SIFT: tolerated - score 0.07, PolyPhen: probably_damaging - score 0.934
1371	chr12:g.70596268G¿T	Substitution	Missense	PIM1 I66V	1/833,0.12%	1/13,582	VEP: MODERATE, SIFT: tolerated - score 0.1, PolyPhen: benign - score 0.039
1372	chr6:g.135197131G¿C	Substitution	Missense		1/833,0.12%	1/13,582	VEP: MODERATE, SIFT: tolerated - score 0.49, PolyPhen: benign - score 0.003

1373	chrX:g.133953208G¿A	Substitution Missense	HIP1 S607C	1/833,0.12%	1/13,582	VEP: MODERATE, SIFT: tolerated - score 0.18, PolyPhen: benign - score 0.035
1374	chr11:g.108335053C¿T	Substitution Missense		1/833,0.12%	1/13,582	VEP: MODERATE, SIFT: deleterious - score 0, PolyPhen: possibly_damaging - score 0.867
1375	chrX:g.40076471G¿A	Substitution Missense	NF1 L1915Q	1/833,0.12%	1/13,582	VEP: MODERATE, SIFT: tolerated_low_confidence - score 0.35, PolyPhen: benign - score 0.445
1376	chr2:g.61533807C¿T	Substitution Missense		1/833,0.12%	1/13,582	VEP: MODERATE, SIFT: deleterious - score 0, PolyPhen: probably_damaging - score 0.947
1377	chr2:g.201266629T¿G	Substitution Missense	STRN A443G	1/833,0.12%	1/13,582	VEP: MODERATE, SIFT: deleterious - score 0, PolyPhen: probably_damaging - score 1
1378	chr4:g.125491010A¿G	Substitution Missense		1/833,0.12%	1/13,582	VEP: MODERATE, SIFT: tolerated - score 0.33, PolyPhen: benign - score 0
1379	chr20:g.58854800G¿A	Substitution Missense	RANBP2 K2980E	1/833,0.12%	1/13,582	VEP: MODERATE, SIFT: deleterious_low_confidence - score 0.01, PolyPhen: benign - score 0.012
1380	chr18:g.25091997C¿T	Substitution Missense		1/833,0.12%	1/13,582	VEP: MODERATE, SIFT: deleterious - score 0.01, PolyPhen: possibly_damaging - score 0.88
1381	chr7:g.148829842C¿T	Substitution Missense	NUP98 R1561C	1/833,0.12%	1/13,582	VEP: MODERATE, SIFT: deleterious - score 0, PolyPhen: benign - score 0.246
1382	chr1:g.186325839C¿T	Substitution Missense		1/833,0.12%	1/13,582	VEP: MODERATE, SIFT: tolerated - score 0.1, PolyPhen: probably_damaging - score 0.984
1383	chr5:g.177257007C¿G	Substitution Missense	ATP1A1 Q406H	1/833,0.12%	1/13,582	VEP: MODERATE, SIFT: tolerated - score 0.46, PolyPhen: benign - score 0.082
1384	chr7:g.152156028G¿C	Substitution Missense		1/833,0.12%	1/13,582	VEP: MODERATE, SIFT: tolerated - score 0.16, PolyPhen: benign - score 0.039
1385	chr12:g.124472953T¿A	Substitution Missense	CRTC3 D163E	1/833,0.12%	1/13,582	VEP: MODERATE, SIFT: deleterious - score 0, PolyPhen: probably_damaging - score 0.996
1386	chr16:g.79598837A¿G	Substitution Missense		1/833,0.12%	2/13,582	VEP: MODERATE, SIFT: deleterious - score 0.02, PolyPhen: benign - score 0.402

1387	chr22:g.41177756G¿A	Substitution	Missense	ATM D2721N	1/833,0.12%	1/13,582	VEP: MODERATE, SIFT: tolerated - score 0.1, PolyPhen: benign - score 0
1388	chr7:g.152177802G¿A	Substitution	Missense		1/833,0.12%	1/13,582	VEP: MODERATE, SIFT: deleterious - score 0, PolyPhen: probably_damaging - score 0.994
1389	chr11:g.72018453T¿C	Substitution	Missense	MAML2 L899F	1/833,0.12%	1/13,582	VEP: MODERATE, SIFT: deleterious - score 0, PolyPhen: probably_damaging - score 0.979
1390	chr4:g.1801918T¿G	Substitution	Missense		1/833,0.12%	1/13,582	VEP: MODERATE, SIFT: deleterious - score 0, PolyPhen: possibly_damaging - score 0.864
1391	chr12:g.45851950C¿T	Substitution	Missense	RALGDS P301L	1/833,0.12%	1/13,582	VEP: MODERATE, SIFT: deleterious_low_confidence - score 0.03, PolyPhen: benign - score 0.006
1392	chrX:g.49030473C¿A	Substitution	Missense		1/833,0.12%	1/13,582	VEP: MODERATE, SIFT: tolerated - score 0.54, PolyPhen: benign - score 0.042
1393	chr3:g.47103357C¿T	Substitution	Missense	FOXO1 Q133R	1/833,0.12%	1/13,582	VEP: MODERATE, SIFT: deleterious - score 0, PolyPhen: probably_damaging - score 0.998
1394	chr2:g.211383770A¿T	Substitution	Missense		1/833,0.12%	1/13,582	VEP: MODERATE, SIFT: deleterious - score 0.05, PolyPhen: benign - score 0.109
1395	chrX:g.153553072G¿C	Substitution	Missense	CDK12 R979Q	1/833,0.12%	1/13,582	VEP: MODERATE, SIFT: tolerated - score 0.44, PolyPhen: benign - score 0.001
1396	chr11:g.118505191G¿C	Substitution	Missense		1/833,0.12%	1/13,582	VEP: MODERATE, SIFT: deleterious_low_confidence - score 0, PolyPhen: possibly_damaging - score 0.725
1397	chr3:g.188609570G¿T	Substitution	Missense	ERBB3 I600M	1/833,0.12%	1/13,582	VEP: MODERATE, SIFT: tolerated - score 0.09, PolyPhen: benign - score 0.001
1398	chr5:g.55951466A¿C	Substitution	Missense		1/833,0.12%	1/13,582	VEP: MODERATE, SIFT: deleterious - score 0, PolyPhen: probably_damaging - score 0.974
1399	chr20:g.45330540C¿G	Substitution	Missense	EML4 D370G	1/833,0.12%	1/13,582	VEP: MODERATE, SIFT: deleterious - score 0.01, PolyPhen: possibly_damaging - score 0.476
1400	chr6:g.44252088G¿C	Substitution	Missense		1/833,0.12%	1/13,582	VEP: MODERATE, SIFT: deleterious - score 0, PolyPhen: probably_damaging - score 1

1401	chr9:g.21971112G¿A	Substitution	Missense	BIRC3 G132A	1/833,0.12%	18/13,582	VEP: MODERATE, SIFT: deleterious - score 0, PolyPhen: probably_damaging - score 1
1402	chr17:g.42333700G¿C	Substitution	Missense		1/833,0.12%	1/13,582	VEP: MODERATE, SIFT: deleterious - score 0, PolyPhen: probably_damaging - score 0.945
1403	chr7:g.152273716G¿A	Substitution	Missense	KMT2A R2890H	1/833,0.12%	1/13,582	VEP: MODERATE, SIFT: deleterious - score 0, PolyPhen: probably_damaging - score 0.996
1404	chrX:g.71122231T¿G	Substitution	Missense		1/833,0.12%	1/13,582	VEP: MODERATE, SIFT: deleterious - score 0, PolyPhen: probably_damaging - score 1
1405	chr5:g.157222866C¿T	Substitution	Missense	FLT4 V757I	1/833,0.12%	1/13,582	VEP: MODERATE, SIFT: tolerated - score 0.55, PolyPhen: benign - score 0
1406	chr17:g.7674227T¿G	Substitution	Missense		1/833,0.12%	1/13,582	VEP: MODERATE, SIFT: deleterious - score 0, PolyPhen: probably_damaging - score 0.968
1407	chr6:g.37171170G¿A	Substitution	Missense	FAT1 G3657C	1/833,0.12%	3/13,582	VEP: MODERATE, SIFT: deleterious - score 0, PolyPhen: benign - score 0.438
1408	chr4:g.125449126G¿C	Substitution	Missense		1/833,0.12%	1/13,582	VEP: MODERATE, SIFT: tolerated - score 0.32, PolyPhen: possibly_damaging - score 0.575
1409	chr4:g.152322901A¿C	Substitution	Missense	NTRK3 H674Y	1/833,0.12%	1/13,582	VEP: MODERATE, SIFT: deleterious - score 0, PolyPhen: probably_damaging - score 0.999
1410	chr11:g.108272536C¿G	Substitution	Missense		1/833,0.12%	2/13,582	VEP: MODERATE, SIFT: deleterious - score 0.01, PolyPhen: possibly_damaging - score 0.615
1411	chr2:g.99593817C¿T	Substitution	Missense	SFPQ Q393H	1/833,0.12%	2/13,582	VEP: MODERATE, SIFT: tolerated - score 0.87, PolyPhen: benign - score 0.02
1412	chr1:g.147624049C¿A	Substitution	Missense		1/833,0.12%	1/13,582	VEP: MODERATE, SIFT: deleterious - score 0.03, PolyPhen: possibly_damaging - score 0.543
1413	chr14:g.65093773T¿C	Substitution	Missense	MYH9 R814Q	1/833,0.12%	1/13,582	VEP: MODERATE, SIFT: deleterious - score 0, PolyPhen: probably_damaging - score 1
1414	chr17:g.7673779C¿T	Substitution	Missense		1/833,0.12%	4/13,582	VEP: MODERATE, SIFT: deleterious - score 0.01, PolyPhen: probably_damaging - score 0.985

1415	chr12:g.68836738A¿T	Substitution	Missense	RAF1 D117A	1/833,0.12%	1/13,582	VEP: MODERATE, SIFT: deleterious - score 0, PolyPhen: possibly_damaging - score 0.554
1416	chr13:g.28037253C¿A	Substitution	Missense		1/833,0.12%	1/13,582	VEP: MODERATE, SIFT: deleterious - score 0, PolyPhen: probably_damaging - score 0.922
1417	chr12:g.70635692C¿T	Substitution	Missense	FAT4 G4472R	1/833,0.12%	1/13,582	VEP: MODERATE, SIFT: tolerated_low_confidence - score 0.39, PolyPhen: benign - score 0.053
1418	chr19:g.29823679A¿G	Substitution	Missense		1/833,0.12%	2/13,582	VEP: MODERATE, SIFT: tolerated - score 0.58, PolyPhen: benign - score 0
1419	chr16:g.79599628T¿G	Substitution	Missense	MAF S70F	1/833,0.12%	1/13,582	VEP: MODERATE, SIFT: deleterious - score 0.02, PolyPhen: probably_damaging - score 0.919
1420	chr1:g.186326175C¿T	Substitution	Missense		1/833,0.12%	2/13,582	VEP: MODERATE, SIFT: deleterious_low_confidence - score 0.05, PolyPhen: benign - score 0.026
1421	chr5:g.68273990A¿C	Substitution	Missense	MYO5A D595A	1/833,0.12%	1/13,582	VEP: MODERATE, SIFT: tolerated - score 0.1, PolyPhen: benign - score 0.013
1422	chr16:g.72793575C¿T	Substitution	Missense		1/833,0.12%	2/13,582	VEP: MODERATE, SIFT: tolerated - score 0.07, PolyPhen: probably_damaging - score 0.992
1423	chr5:g.68297578G¿T	Substitution	Missense	ATM A2843T	1/833,0.12%	1/13,582	VEP: MODERATE, SIFT: deleterious - score 0, PolyPhen: possibly_damaging - score 0.653
1424	chr17:g.65537550C¿T	Substitution	Missense		1/833,0.12%	1/13,582	VEP: MODERATE, SIFT: tolerated - score 0.46, PolyPhen: benign - score 0.001
1425	chr5:g.38482591C¿G	Substitution	Missense	CUX1 G1121E	1/833,0.12%	1/13,582	VEP: MODERATE, SIFT: tolerated - score 0.11, PolyPhen: benign - score 0.041
1426	chr21:g.38383807C¿G	Substitution	Missense		1/833,0.12%	1/13,582	VEP: MODERATE, SIFT: deleterious - score 0, PolyPhen: probably_damaging - score 0.995
1427	chr6:g.128218996T¿G	Substitution	Missense	KAT6B G94E	1/833,0.12%	1/13,582	VEP: MODERATE, SIFT: tolerated - score 0.15, PolyPhen: probably_damaging - score 0.969
1428	chr1:g.77964284C¿A	Substitution	Missense		1/833,0.12%	1/13,582	VEP: MODERATE, SIFT: deleterious - score 0, PolyPhen: probably_damaging - score 0.979

1429	chr8:g.92017261C¿A	Substitution	Missense	TP53 S215T	1/833,0.12%	1/13,582	VEP: MODERATE, SIFT: deleterious - score 0, PolyPhen: probably_damaging - score 1
1430	chr1:g.155187780G¿T	Substitution	Missense		1/833,0.12%	1/13,582	VEP: MODERATE, SIFT: tolerated - score 0.52, PolyPhen: benign - score 0.086
1431	chr15:g.34356428G¿A	Substitution	Missense	ARHGAP26 R585W	1/833,0.12%	1/13,582	VEP: MODERATE, SIFT: tolerated - score 0.29, PolyPhen: benign - score 0.062
1432	chr9:g.131175597C¿T	Substitution	Missense		1/833,0.12%	1/13,582	VEP: MODERATE, SIFT: deleterious - score 0, PolyPhen: probably_damaging - score 0.999
1433	chr4:g.186708726C¿G	Substitution	Missense	FOXO1 S153R	1/833,0.12%	2/13,582	VEP: MODERATE, SIFT: deleterious - score 0.04, PolyPhen: probably_damaging - score 0.926
1434	chr1:g.18700678G¿A	Substitution	Missense		1/833,0.12%	1/13,582	VEP: MODERATE, SIFT: deleterious - score 0, PolyPhen: probably_damaging - score 0.973
1435	chr9:g.95459639G¿A	Substitution	Missense	PTCH1 H520Y	1/833,0.12%	1/13,582	VEP: MODERATE, SIFT: deleterious - score 0.05, PolyPhen: benign - score 0.348
1436	chr11:g.120446407G¿C	Substitution	Missense		1/833,0.12%	1/13,582	VEP: MODERATE, SIFT: tolerated - score 0.08, PolyPhen: probably_damaging - score 0.984
1437	chr16:g.15748155T¿C	Substitution	Missense	ELL R75P	1/833,0.12%	1/13,582	VEP: MODERATE, SIFT: deleterious - score 0.01, PolyPhen: possibly_damaging - score 0.662
1438	chr7:g.116699546A¿G	Substitution	Missense		1/833,0.12%	1/13,582	VEP: MODERATE, SIFT: deleterious - score 0.02, PolyPhen: possibly_damaging - score 0.859
1439	chr8:g.31143608A¿C	Substitution	Missense	ZNF331 K334N	1/833,0.12%	1/13,582	VEP: MODERATE, SIFT: tolerated - score 0.14, PolyPhen: benign - score 0.012
1440	chr4:g.125450839G¿A	Substitution	Missense		1/833,0.12%	2/13,582	VEP: MODERATE, SIFT: deleterious - score 0.02, PolyPhen: probably_damaging - score 0.926
1441	chr11:g.69641466G¿C	Substitution	Missense	PRDM16 E821K	1/833,0.12%	1/13,582	VEP: MODERATE, SIFT: tolerated - score 1, PolyPhen: benign - score 0.003
1442	chr17:g.59661570C¿T	Substitution	Missense		1/833,0.12%	1/13,582	VEP: MODERATE, SIFT: deleterious - score 0.01, PolyPhen: probably_damaging - score 0.999

1443	chr17:g.43082556T¿A	Substitution	Missense	KRAS E62K	1/833,0.12%	1/13,582	VEP: MODERATE, SIFT: deleterious - score 0, PolyPhen: benign - score 0.015
1444	chr7:g.138869688C¿T	Substitution	Missense		1/833,0.12%	3/13,582	VEP: MODERATE, SIFT: deleterious - score 0, PolyPhen: probably_damaging - score 0.989
1445	chr12:g.58872813G¿A	Substitution	Missense	NTRK3 F450I	1/833,0.12%	1/13,582	VEP: MODERATE, SIFT: deleterious_low_confidence - score 0, PolyPhen: probably_damaging - score 0.996
1446	chr10:g.102401841G¿C	Substitution	Missense		1/833,0.12%	1/13,582	VEP: MODERATE, SIFT: deleterious - score 0.02, PolyPhen: probably_damaging - score 0.966
1447	chr2:g.99727108C¿G	Substitution	Missense	ZCCHC8 E283K	1/833,0.12%	1/13,582	VEP: MODERATE, SIFT: tolerated - score 0.07, PolyPhen: benign - score 0.014
1448	chr6:g.157207761G¿C	Substitution	Missense		1/833,0.12%	1/13,582	VEP: MODERATE, SIFT: deleterious - score 0.01, PolyPhen: benign - score 0.382
1449	chr12:g.114672238G¿A	Substitution	Missense	FAT1 K1926R	1/833,0.12%	1/13,582	VEP: MODERATE, SIFT: deleterious - score 0, PolyPhen: probably_damaging - score 0.98
1450	chr3:g.48682407C¿T	Substitution	Missense		1/833,0.12%	1/13,582	VEP: MODERATE, SIFT: tolerated - score 0.14, PolyPhen: benign - score 0.395
1451	chr17:g.55267792G¿A	Substitution	Missense	PTPRB A909V	1/833,0.12%	1/13,582	VEP: MODERATE, SIFT: tolerated - score 0.06, PolyPhen: benign - score 0.057
1452	chr7:g.140781602C¿T	Substitution	Missense		1/833,0.12%	2/13,582	VEP: MODERATE, SIFT: deleterious - score 0, PolyPhen: probably_damaging - score 0.998
1453	chr1:g.3411386G¿A	Substitution	Missense	NUP98 P167L	1/833,0.12%	1/13,582	VEP: MODERATE, SIFT: deleterious - score 0.03, PolyPhen: probably_damaging - score 0.978
1454	chr19:g.32931533G¿C	Substitution	Missense		1/833,0.12%	1/13,582	VEP: MODERATE, SIFT: deleterious - score 0.02, PolyPhen: probably_damaging - score 0.997
1455	chr19:g.18768533T¿C	Substitution	Missense	ZNF384 R395Q	1/833,0.12%	1/13,582	VEP: MODERATE, SIFT: tolerated - score 0.22, PolyPhen: benign - score 0.011
1456	chr8:g.56167261G¿A	Substitution	Missense		1/833,0.12%	2/13,582	VEP: MODERATE, SIFT: deleterious - score 0, PolyPhen: probably_damaging - score 0.998

1457	chr14:g.65093776G¿A	Substitution	Missense	NCOR2 A1707T	1/833,0.12%	2/13,582	VEP: MODERATE, SIFT: deleterious - score 0, PolyPhen: possibly_damaging - score 0.741
1458	chr16:g.15724372C¿T	Substitution	Missense		1/833,0.12%	1/13,582	VEP: MODERATE, SIFT: tolerated - score 0.26, PolyPhen: benign - score 0.009
1459	chr17:g.63930129C¿G	Substitution	Missense	PPARG T41N	1/833,0.12%	1/13,582	VEP: MODERATE, SIFT: tolerated - score 0.07, PolyPhen: benign - score 0
1460	chr3:g.12618592C¿T	Substitution	Missense		1/833,0.12%	1/13,582	VEP: MODERATE, SIFT: tolerated - score 0.09, PolyPhen: benign - score 0.014
1461	chr10:g.102401798G¿C	Substitution	Missense	RNF213 H4989L	1/833,0.12%	1/13,582	VEP: MODERATE, SIFT: deleterious - score 0.03, PolyPhen: probably_damaging - score 0.919
1462	chr20:g.58903754T¿C	Substitution	Missense		1/833,0.12%	1/13,582	VEP: MODERATE, SIFT: deleterious - score 0, PolyPhen: probably_damaging - score 0.964
1463	chr4:g.86762838G¿A	Substitution	Missense	TLX3 A107T	1/833,0.12%	2/13,582	VEP: MODERATE, SIFT: tolerated - score 0.22, PolyPhen: benign - score 0.006
1464	chr9:g.77721390C¿T	Substitution	Missense		1/833,0.12%	1/13,582	VEP: MODERATE, SIFT: tolerated - score 0.05, PolyPhen: benign - score 0.104
1465	chrX:g.77682203T¿C	Substitution	Missense	CNTRL E745D	1/833,0.12%	1/13,582	VEP: MODERATE, SIFT: tolerated_low_confidence - score 0.05, PolyPhen: benign - score 0.007
1466	chr17:g.39462804G¿T	Substitution	Missense		1/833,0.12%	2/13,582	VEP: MODERATE, SIFT: deleterious_low_confidence - score 0.01, PolyPhen: probably_damaging - score 0.986
1467	chr3:g.47103417C¿A	Substitution	Missense	MLH1 E613G	1/833,0.12%	1/13,582	VEP: MODERATE, SIFT: deleterious - score 0, PolyPhen: probably_damaging - score 1
1468	chrX:g.49039363G¿C	Substitution	Missense		1/833,0.12%	1/13,582	VEP: MODERATE, SIFT: deleterious - score 0, PolyPhen: benign - score 0.258
1469	chr6:g.127996921C¿T	Substitution	Missense	FAT4 S1336Y	1/833,0.12%	2/13,582	VEP: MODERATE, SIFT: deleterious - score 0.01, PolyPhen: probably_damaging - score 1
1470	chr4:g.86722291C¿A	Substitution	Missense		1/833,0.12%	1/13,582	VEP: MODERATE, SIFT: deleterious - score 0.03, PolyPhen: benign - score 0.441

1471	chr1:g.193212395C¿G	Substitution	Missense	NUP98 N1400S	1/833,0.12%	1/13,582	VEP: MODERATE, SIFT: deleterious - score 0, PolyPhen: probably_damaging - score 0.97
1472	chr10:g.87965396A¿T	Substitution	Missense		1/833,0.12%	1/13,582	VEP: MODERATE, SIFT: tolerated_low_confidence - score 0.22, PolyPhen: probably_damaging - score 0.956
1473	chr6:g.37171028G¿C	Substitution	Missense	GATA3 S142L	1/833,0.12%	2/13,582	VEP: MODERATE, SIFT: tolerated - score 0.19, PolyPhen: benign - score 0.031
1474	chr3:g.149527969C¿T	Substitution	Missense		1/833,0.12%	1/13,582	VEP: MODERATE, SIFT: deleterious - score 0, PolyPhen: probably_damaging - score 0.956
1475	chr17:g.42227562C¿G	Substitution	Missense	ATR W171C	1/833,0.12%	1/13,582	VEP: MODERATE, SIFT: deleterious - score 0.03, PolyPhen: benign - score 0.271
1476	chr16:g.10906795C¿T	Substitution	Missense		1/833,0.12%	1/13,582	VEP: MODERATE, SIFT: tolerated - score 0.08, PolyPhen: benign - score 0.033
1477	chr10:g.121500872T¿G	Substitution	Missense	ATM E2895K	1/833,0.12%	1/13,582	VEP: MODERATE, SIFT: deleterious - score 0.01, PolyPhen: probably_damaging - score 0.999
1478	chrX:g.71096877G¿A	Substitution	Missense		1/833,0.12%	1/13,582	VEP: MODERATE, SIFT: deleterious - score 0.04, PolyPhen: benign - score 0.364
1479	chr16:g.64947764C¿T	Substitution	Missense	KMT2C D4893Y	1/833,0.12%	2/13,582	VEP: MODERATE, SIFT: deleterious - score 0.01, PolyPhen: probably_damaging - score 0.972
1480	chr22:g.41127545G¿T	Substitution	Missense		1/833,0.12%	1/13,582	VEP: MODERATE, SIFT: tolerated - score 0.06, PolyPhen: probably_damaging - score 0.968
1481	chr1:g.116388221T¿C	Substitution	Missense	MLH1 Y721S	1/833,0.12%	1/13,582	VEP: MODERATE, SIFT: deleterious - score 0, PolyPhen: probably_damaging - score 0.998
1482	chr3:g.37012023G¿A	Substitution	Missense		1/833,0.12%	1/13,582	VEP: MODERATE, SIFT: tolerated - score 0.11, PolyPhen: benign - score 0.028
1483	chr3:g.52563404C¿A	Substitution	Missense	CRTC1 F10L	1/833,0.12%	1/13,582	VEP: MODERATE, SIFT: tolerated - score 0.14, PolyPhen: possibly_damaging - score 0.58
1484	chr7:g.143356648C¿A	Substitution	Missense		1/833,0.12%	1/13,582	VEP: MODERATE, SIFT: deleterious - score 0.01, PolyPhen: probably_damaging - score 0.914

1485	chr8:g.17966022C¿T	Substitution Missense	BLM Q838H	1/833,0.12%	2/13,582	VEP: MODERATE, SIFT: tolerated - score 0.1, PolyPhen: benign - score 0.395
1486	chr14:g.65076604C¿G	Substitution Missense		1/833,0.12%	1/13,582	VEP: MODERATE, SIFT: deleterious - score 0.02, PolyPhen: possibly_damaging - score 0.805
1487	chr4:g.125320808G¿T	Substitution Missense	KRAS L19F	1/833,0.12%	1/13,582	VEP: MODERATE, SIFT: tolerated - score 0.08, PolyPhen: probably_damaging - score 0.999
1488	chr3:g.47083947C¿T	Substitution Missense		1/833,0.12%	1/13,582	VEP: MODERATE, SIFT: deleterious - score 0.01, PolyPhen: benign - score 0.115
1489	chrX:g.47179889T¿C	Substitution Missense	TPM4 E98Q	1/833,0.12%	1/13,582	VEP: MODERATE, SIFT: deleterious - score 0, PolyPhen: probably_damaging - score 0.988
1490	chr4:g.186708478C¿A	Substitution Missense		1/833,0.12%	1/13,582	VEP: MODERATE, SIFT: tolerated - score 0.47, PolyPhen: benign - score 0.282
1491	chr20:g.45330540C¿T	Substitution Missense	FAT1 D2589N	1/833,0.12%	2/13,582	VEP: MODERATE, SIFT: deleterious - score 0.01, PolyPhen: benign - score 0.226
1492	chr12:g.132632767C¿T	Substitution Missense		1/833,0.12%	1/13,582	VEP: MODERATE, SIFT: tolerated - score 0.37, PolyPhen: benign - score 0.003
1493	chr4:g.98421332G¿A	Substitution Missense	TET1 D17N	1/833,0.12%	1/13,582	VEP: MODERATE, SIFT: tolerated - score 0.23, PolyPhen: possibly_damaging - score 0.885
1494	chr16:g.56939334T¿C	Substitution Missense		1/833,0.12%	1/13,582	VEP: MODERATE, SIFT: deleterious - score 0, PolyPhen: probably_damaging - score 0.982
1495	chr19:g.11059756T¿A	Substitution Missense	BUB1B G311S	1/833,0.12%	1/13,582	VEP: MODERATE, SIFT: deleterious - score 0, PolyPhen: probably_damaging - score 0.99
1496	chr1:g.64879119C¿A	Substitution Missense		1/833,0.12%	1/13,582	VEP: MODERATE, SIFT: deleterious - score 0.02, PolyPhen: benign - score 0.248
1497	chr17:g.7670703C¿T	Substitution Missense	CDH11 P692T	1/833,0.12%	1/13,582	VEP: MODERATE, SIFT: tolerated - score 0.31, PolyPhen: benign - score 0.031
1498	chr12:g.56098852G¿T	Substitution Missense		1/833,0.12%	1/13,582	VEP: MODERATE, SIFT: deleterious - score 0, PolyPhen: probably_damaging - score 1

1499	chr12:g.49046643G¿A	Substitution	Missense	DNM2 S759T	1/833,0.12%	1/13,582	VEP: MODERATE, SIFT: deleterious - score 0.04, PolyPhen: probably_damaging - score 0.915
1500	chr3:g.186048795G¿C	Substitution	Missense		1/833,0.12%	1/13,582	VEP: MODERATE, SIFT: deleterious - score 0.02, PolyPhen: benign - score 0.257
1501	chr16:g.79598860T¿C	Substitution	Missense	MAP3K1 M1181V	1/833,0.12%	1/13,582	VEP: MODERATE, SIFT: tolerated - score 0.09, PolyPhen: benign - score 0.365
1502	chr7:g.26196995T¿G	Substitution	Missense		1/833,0.12%	1/13,582	VEP: MODERATE, SIFT: deleterious - score 0.02, PolyPhen: benign - score 0.215
1503	chr6:g.37170643C¿T	Substitution	Missense	TP53 Y205H	1/833,0.12%	1/13,582	VEP: MODERATE, SIFT: tolerated - score 0.2, PolyPhen: benign - score 0.006
1504	chr14:g.99175727A¿G	Substitution	Missense		1/833,0.12%	1/13,582	VEP: MODERATE, SIFT: deleterious - score 0, PolyPhen: probably_damaging - score 0.995
1505	chr4:g.87114800G¿A	Substitution	Missense	XPA E201A	1/833,0.12%	1/13,582	VEP: MODERATE, SIFT: tolerated - score 0.12, PolyPhen: benign - score 0.046
1506	chr4:g.25667931C¿G	Substitution	Missense		1/833,0.12%	1/13,582	VEP: MODERATE, SIFT: deleterious - score 0.01, PolyPhen: probably_damaging - score 0.993
1507	chr16:g.15738631C¿T	Substitution	Missense	STIL E1139K	1/833,0.12%	1/13,582	VEP: MODERATE, SIFT: deleterious - score 0.01, PolyPhen: probably_damaging - score 0.967
1508	chr6:g.127976940C¿T	Substitution	Missense		1/833,0.12%	3/13,582	VEP: MODERATE, SIFT: tolerated - score 0.06, PolyPhen: benign - score 0.151
1509	chr7:g.116700037A¿T	Substitution	Missense	NRAS G12C	1/833,0.12%	1/13,582	VEP: MODERATE, SIFT: deleterious - score 0, PolyPhen: probably_damaging - score 0.999
1510	chrX:g.77558691T¿G	Substitution	Missense		1/833,0.12%	1/13,582	VEP: MODERATE, SIFT: deleterious - score 0.04, PolyPhen: possibly_damaging - score 0.899
1511	chr6:g.401730A¿G	Substitution	Missense	CLTCL1 G239E	1/833,0.12%	1/13,582	VEP: MODERATE, SIFT: deleterious - score 0, PolyPhen: probably_damaging - score 0.998
1512	chr19:g.10825174A¿G	Substitution	Missense		1/833,0.12%	1/13,582	VEP: MODERATE, SIFT: tolerated - score 0.3, PolyPhen: benign - score 0.181

1513	chr1:g.193122231T¿C	Substitution	Missense	RANBP2 G1169D	1/833,0.12%	1/13,582	VEP: MODERATE, SIFT: deleterious - score 0.04, PolyPhen: probably_damaging - score 0.929
1514	chr2:g.36869686T¿G	Substitution	Missense		1/833,0.12%	2/13,582	VEP: MODERATE, SIFT: deleterious - score 0, PolyPhen: probably_damaging - score 0.986
1515	chr10:g.87957924G¿A	Substitution	Missense	CIITA P136Q	1/833,0.12%	1/13,582	VEP: MODERATE, SIFT: tolerated - score 0.28, PolyPhen: benign - score 0.174
1516	chr11:g.108249025G¿T	Substitution	Missense		1/833,0.12%	1/13,582	VEP: MODERATE, SIFT: deleterious - score 0, PolyPhen: possibly_damaging - score 0.691
1517	chr1:g.198732555A¿C	Substitution	Missense	FLT4 R475Q	1/833,0.12%	1/13,582	VEP: MODERATE, SIFT: deleterious - score 0, PolyPhen: probably_damaging - score 0.995
1518	chr4:g.125320024G¿T	Substitution	Missense		1/833,0.12%	1/13,582	VEP: MODERATE, SIFT: deleterious - score 0, PolyPhen: probably_damaging - score 0.999
1519	chr16:g.72959380C¿T	Substitution	Missense	BRAF L637Q	1/833,0.12%	2/13,582	VEP: MODERATE, SIFT: deleterious - score 0.01, PolyPhen: probably_damaging - score 0.987
1520	chr16:g.15727039C¿G	Substitution	Missense		1/833,0.12%	1/13,582	VEP: MODERATE, SIFT: deleterious - score 0, PolyPhen: possibly_damaging - score 0.866
1521	chr16:g.11255430C¿G	Substitution	Missense	DICER1 I253T	1/833,0.12%	1/13,582	VEP: MODERATE, SIFT: tolerated - score 0.08, PolyPhen: benign - score 0
1522	chr6:g.106099438T¿G	Substitution	Missense		1/833,0.12%	1/13,582	VEP: MODERATE, SIFT: deleterious - score 0, PolyPhen: probably_damaging - score 0.999
z	chr12:g.58877594C¿T	Substitution	Missense	NKX2-1 G17E	1/833,0.12%	1/13,582	VEP: MODERATE, SIFT: tolerated - score 0.48, PolyPhen: benign - score 0.057
1524	chr12:g.49040641G¿A	Substitution	Missense		1/833,0.12%	1/13,582	VEP: MODERATE, SIFT: deleterious - score 0.01, PolyPhen: benign - score 0.036
1525	chr7:g.116775033G¿A	Substitution	Missense	IRF4 C99S	1/833,0.12%	1/13,582	VEP: MODERATE, SIFT: deleterious - score 0.01, PolyPhen: benign - score 0.347
1526	chr16:g.2056759C¿A	Substitution	Missense		1/833,0.12%	1/13,582	VEP: MODERATE, SIFT: deleterious - score 0.02, PolyPhen: probably_damaging - score 0.999

1527	chr4:g.186709388G¿A	Substitution	Missense	TRIP11 D1547N	1/833,0.12%	2/13,582	VEP: MODERATE, SIFT: deleterious - score 0, PolyPhen: probably_damaging - score 0.999
1528	chr2:g.201258310C¿T	Substitution	Missense		1/833,0.12%	1/13,582	VEP: MODERATE, SIFT: deleterious_low_confidence - score 0, PolyPhen: benign - score 0.011
1529	chr7:g.140753353A¿T	Substitution	Missense	CRTC3 S601F	1/833,0.12%	1/13,582	VEP: MODERATE, SIFT: deleterious - score 0, PolyPhen: benign - score 0.003
1530	chr1:g.47220028G¿A	Substitution	Missense		1/833,0.12%	1/13,582	VEP: MODERATE, SIFT: deleterious - score 0, PolyPhen: probably_damaging - score 1
1531	chr11:g.108310230G¿T	Substitution	Missense	KDM5A R568G	1/833,0.12%	1/13,582	VEP: MODERATE, SIFT: deleterious - score 0, PolyPhen: probably_damaging - score 0.974
1532	chr7:g.75562973C¿G	Substitution	Missense		1/833,0.12%	1/13,582	VEP: MODERATE, SIFT: tolerated - score 0.07, PolyPhen: benign - score 0.372
1533	chr17:g.80347130T¿C	Substitution	Missense	WT1 N387T	1/833,0.12%	1/13,582	VEP: MODERATE, SIFT: deleterious - score 0, PolyPhen: probably_damaging - score 0.972
1534	chr17:g.7670714A¿G	Substitution	Missense		1/833,0.12%	1/13,582	VEP: MODERATE, SIFT: deleterious - score 0, PolyPhen: probably_damaging - score 0.956
1535	chr1:g.204549426C¿T	Substitution	Missense	RHOA D67N	1/833,0.12%	1/13,582	VEP: MODERATE, SIFT: tolerated - score 0.21, PolyPhen: benign - score 0.003
1536	chr6:g.28923298A¿T	Substitution	Missense		1/833,0.12%	1/13,582	VEP: MODERATE, SIFT: tolerated - score 0.58, PolyPhen: benign - score 0
1537	chr2:g.15946015A¿T	Substitution	Missense	FGFR2 C729F	1/833,0.12%	1/13,582	VEP: MODERATE, SIFT: tolerated - score 0.45, PolyPhen: benign - score 0
1538	chr1:g.58782086G¿C	Substitution	Missense		1/833,0.12%	1/13,582	VEP: MODERATE, SIFT: tolerated - score 0.19, PolyPhen: benign - score 0.074
1539	chr10:g.43128251G¿A	Substitution	Missense	CDH11 R53H	1/833,0.12%	1/13,582	VEP: MODERATE, SIFT: tolerated_low_confidence - score 0.07, PolyPhen: benign - score 0.014
1540	chr12:g.124343094C¿T	Substitution	Missense		1/833,0.12%	1/13,582	VEP: MODERATE, SIFT: tolerated - score 0.17, PolyPhen: probably_damaging - score 0.99

1541	chr1:g.15934432C¿T	Substitution Missense	FAT1 A3648D	1/833,0.12%	1/13,582	VEP: MODERATE, SIFT: tolerated_low_confidence - score 0.26, PolyPhen: benign - score 0.017
1542	chr1:g.11212906T¿A	Substitution Missense		1/833,0.12%	1/13,582	VEP: MODERATE, SIFT: deleterious - score 0.01, PolyPhen: benign - score 0.338
1543	chr20:g.45330545A¿T	Substitution Missense	RABEP1 L748I	1/833,0.12%	1/13,582	VEP: MODERATE, SIFT: deleterious - score 0, PolyPhen: probably_damaging - score 0.985
1544	chr17:g.61683656G¿C	Substitution Missense		1/833,0.12%	1/13,582	VEP: MODERATE, SIFT: deleterious_low_confidence - score 0.02, PolyPhen: possibly_damaging - score 0.745
1545	chr19:g.40236318C¿T	Substitution Missense	FAT4 L1378V	1/833,0.12%	1/13,582	VEP: MODERATE, SIFT: tolerated - score 0.57, PolyPhen: benign - score 0.013
1546	chr22:g.31327225G¿A	Substitution Missense		1/833,0.12%	1/13,582	VEP: MODERATE, SIFT: tolerated - score 0.5, PolyPhen: benign - score 0.175
1547	chr10:g.68572939A¿C	Substitution Missense	MAML2 Q721E	1/833,0.12%	1/13,582	VEP: MODERATE, SIFT: tolerated - score 0.12, PolyPhen: benign - score 0
1548	chr7:g.99011396G¿C	Substitution Missense		1/833,0.12%	1/13,582	VEP: MODERATE, SIFT: tolerated - score 0.27, PolyPhen: possibly_damaging - score 0.714
1549	chr12:g.70534518G¿A	Substitution Missense	FOXO1 S432N	1/833,0.12%	1/13,582	VEP: MODERATE, SIFT: deleterious - score 0.01, PolyPhen: probably_damaging - score 0.99
1550	chr8:g.42997590G¿A	Substitution Missense		1/833,0.12%	1/13,582	VEP: MODERATE, SIFT: deleterious - score 0.01, PolyPhen: probably_damaging - score 0.993
1551	chr17:g.20205752C¿T	Substitution Missense	LIFR P210H	1/833,0.12%	1/13,582	VEP: MODERATE, SIFT: tolerated - score 0.05, PolyPhen: benign - score 0.011
1552	chr16:g.72788285A¿G	Substitution Missense		1/833,0.12%	1/13,582	VEP: MODERATE, SIFT: deleterious - score 0, PolyPhen: probably_damaging - score 0.99
1553	chr2:g.197401760C¿T	Substitution Missense	TCF3 S638L	1/833,0.12%	1/13,582	VEP: MODERATE, SIFT: deleterious - score 0.01, PolyPhen: probably_damaging - score 0.999
1554	chr15:g.34348461T¿C	Substitution Missense		1/833,0.12%	1/13,582	VEP: MODERATE, SIFT: tolerated - score 1, PolyPhen: benign - score 0

1555	chr8:g.32605579T¿G	Substitution Missense	MSH6 S1049P	1/833,0.12%	1/13,582	VEP: MODERATE, SIFT: deleterious - score 0, PolyPhen: probably_damaging - score 0.999
1556	chr17:g.7675216C¿G	Substitution Missense		1/833,0.12%	13/13,582	VEP: MODERATE, SIFT: deleterious - score 0, PolyPhen: probably_damaging - score 0.999
1557	chr4:g.41746103C¿A	Substitution Missense	IKBKB I314M	1/833,0.12%	1/13,582	VEP: MODERATE, SIFT: deleterious_low_confidence - score 0.01, PolyPhen: possibly_damaging - score 0.496
1558	chr6:g.394965C¿A	Substitution Missense		1/833,0.12%	1/13,582	VEP: MODERATE, SIFT: deleterious - score 0, PolyPhen: probably_damaging - score 1
1559	chr3:g.158592547G¿A	Substitution Missense	NCOR1 M2390K	1/833,0.12%	2/13,582	VEP: MODERATE, SIFT: tolerated - score 0.49, PolyPhen: benign - score 0.003
1560	chr20:g.41123293T¿C	Substitution Missense		1/833,0.12%	1/13,582	VEP: MODERATE, SIFT: deleterious - score 0, PolyPhen: probably_damaging - score 1
1561	chr13:g.40666005A¿G	Substitution Missense	SF3B1 E402K	1/833,0.12%	1/13,582	VEP: MODERATE, SIFT: tolerated - score 0.23, PolyPhen: benign - score 0.33
1562	chr12:g.6577819T¿G	Substitution Missense		1/833,0.12%	1/13,582	VEP: MODERATE, SIFT: deleterious - score 0, PolyPhen: probably_damaging - score 0.992
1563	chr14:g.102082239T¿A	Substitution Missense	EBF1 A202V	1/833,0.12%	1/13,582	VEP: MODERATE, SIFT: deleterious_low_confidence - score 0, PolyPhen: probably_damaging - score 0.987
1564	chr12:g.49031782G¿A	Substitution Missense		1/833,0.12%	1/13,582	VEP: MODERATE, SIFT: tolerated_low_confidence - score 0.19, PolyPhen: benign - score 0.24
1565	chr3:g.48681649G¿T	Substitution Missense	DNMT3A A910V	1/833,0.12%	1/13,582	VEP: MODERATE, SIFT: deleterious - score 0.05, PolyPhen: probably_damaging - score 0.997
1566	chr1:g.148961897C¿G	Substitution Missense		1/833,0.12%	2/13,582	VEP: MODERATE, SIFT: deleterious - score 0, PolyPhen: possibly_damaging - score 0.758
1567	chr6:g.127973679G¿A	Substitution Missense	PPP2R1A Q72E	1/833,0.12%	3/13,582	VEP: MODERATE, SIFT: deleterious - score 0, PolyPhen: probably_damaging - score 0.997
1568	chr5:g.170924484G¿A	Substitution Missense		1/833,0.12%	1/13,582	VEP: MODERATE, SIFT: tolerated - score 0.06, PolyPhen: benign - score 0.049

1569	chr1:g.92834888G¿T	Substitution	Missense	TRRAP V4I	1/833,0.12%	2/13,582	VEP: MODERATE, SIFT: deleterious - score 0, PolyPhen: benign - score 0.213
1570	chr14:g.95103378C¿T	Substitution	Missense		1/833,0.12%	1/13,582	VEP: MODERATE, SIFT: deleterious - score 0, PolyPhen: probably_damaging - score 0.997
1571	chr15:g.90629241G¿C	Substitution	Missense	FAT1 R4203H	1/833,0.12%	1/13,582	VEP: MODERATE, SIFT: tolerated - score 0.52, PolyPhen: probably_damaging - score 0.956
1572	chr1:g.26696747A¿G	Substitution	Missense		1/833,0.12%	1/13,582	VEP: MODERATE, SIFT: tolerated_low_confidence - score 0.1, PolyPhen: benign - score 0.024
1573	chr16:g.79599653G¿C	Substitution	Missense	FAT1 Y932S	1/833,0.12%	1/13,582	VEP: MODERATE, SIFT: tolerated - score 0.1, PolyPhen: possibly_damaging - score 0.532
1574	chr16:g.72794598C¿T	Substitution	Missense		1/833,0.12%	1/13,582	VEP: MODERATE, SIFT: deleterious - score 0, PolyPhen: probably_damaging - score 0.997
1575	chr10:g.112950870G¿C	Substitution	Missense	FAT4 S1138Y	1/833,0.12%	1/13,582	VEP: MODERATE, SIFT: deleterious - score 0.01, PolyPhen: benign - score 0.173
1576	chr1:g.205620360A¿G	Substitution	Missense		1/833,0.12%	1/13,582	VEP: MODERATE, SIFT: tolerated - score 0.43, PolyPhen: benign - score 0
1577	chr2:g.207575341C¿T	Substitution	Missense	ACKR3 L273P	1/833,0.12%	1/13,582	VEP: MODERATE, SIFT: deleterious - score 0.02, PolyPhen: possibly_damaging - score 0.69
1578	chr3:g.155893521G¿C	Substitution	Missense		1/833,0.12%	1/13,582	VEP: MODERATE, SIFT: tolerated_low_confidence - score 0.15, PolyPhen: benign - score 0.094
1579	chr11:g.33869475G¿A	Substitution	Missense	FGFR1 P181S	1/833,0.12%	1/13,582	VEP: MODERATE, SIFT: tolerated_low_confidence - score 0.09, PolyPhen: benign - score 0.005
1580	chr12:g.70532115A¿T	Substitution	Missense		1/833,0.12%	1/13,582	VEP: MODERATE, SIFT: deleterious - score 0, PolyPhen: possibly_damaging - score 0.864
1581	chr19:g.11033470C¿T	Substitution	Missense	TPR R1066H	1/833,0.12%	4/13,582	VEP: MODERATE, SIFT: deleterious - score 0, PolyPhen: probably_damaging - score 0.988
1582	chr16:g.64950929C¿T	Substitution	Missense		1/833,0.12%	1/13,582	VEP: MODERATE, SIFT: deleterious - score 0.05, PolyPhen: probably_damaging - score 0.997

1583	chr12:g.49043676T¿C	Substitution	Missense	PPP6C Y160C	1/833,0.12%	1/13,582	VEP: MODERATE, SIFT: deleterious - score 0.03, PolyPhen: possibly_damaging - score 0.607
1584	chr3:g.47106086G¿A	Substitution	Missense		1/833,0.12%	1/13,582	VEP: MODERATE, SIFT: deleterious - score 0.01, PolyPhen: probably_damaging - score 0.999
1585	chr16:g.3850542G¿A	Substitution	Missense	ABL2 Y116N	1/833,0.12%	1/13,582	VEP: MODERATE, SIFT: tolerated_low_confidence - score 0.1, PolyPhen: benign - score 0.44
1586	chr14:g.99175686G¿A	Substitution	Missense		1/833,0.12%	1/13,582	VEP: MODERATE, SIFT: deleterious - score 0, PolyPhen: probably_damaging - score 0.998
1587	chr16:g.9829566G¿C	Substitution	Missense	ATM P2652S	1/833,0.12%	1/13,582	VEP: MODERATE, SIFT: deleterious - score 0.01, PolyPhen: probably_damaging - score 0.998
1588	chr11:g.114064286A¿G	Substitution	Missense		1/833,0.12%	1/13,582	VEP: MODERATE, SIFT: tolerated - score 0.41, PolyPhen: benign - score 0.003
1589	chr6:g.128089845T¿C	Substitution	Missense	CHN1 R214T	1/833,0.12%	1/13,582	VEP: MODERATE, SIFT: tolerated - score 0.32, PolyPhen: benign - score 0.039
1590	chr5:g.180625876G¿A	Substitution	Missense		1/833,0.12%	1/13,582	VEP: MODERATE, SIFT: deleterious - score 0.01, PolyPhen: possibly_damaging - score 0.846
1591	chr7:g.27165051G¿A	Substitution	Missense	GNAQ L161R	1/833,0.12%	1/13,582	VEP: MODERATE, SIFT: deleterious - score 0.04, PolyPhen: possibly_damaging - score 0.581
1592	chr1:g.119969744C¿A	Substitution	Missense		1/833,0.12%	1/13,582	VEP: MODERATE, SIFT: deleterious - score 0, PolyPhen: probably_damaging - score 1
1593	chr8:g.108235080G¿A	Substitution	Missense	TCL1A D43H	1/833,0.12%	2/13,582	VEP: MODERATE, SIFT: tolerated - score 0.11, PolyPhen: benign - score 0.287
1594	chr4:g.53458661A¿T	Substitution	Missense		1/833,0.12%	1/13,582	VEP: MODERATE, SIFT: deleterious - score 0, PolyPhen: probably_damaging - score 0.966
1595	chr6:g.37170782A¿T	Substitution	Missense	CNTRL K746E	1/833,0.12%	1/13,582	VEP: MODERATE, SIFT: deleterious - score 0, PolyPhen: possibly_damaging - score 0.894
1596	chr5:g.68294660A¿G	Substitution	Missense		1/833,0.12%	1/13,582	VEP: MODERATE, SIFT: deleterious - score 0.04, PolyPhen: benign - score 0.242

1597	chr12:g.122043912G¿A	Substitution	Missense	ERCC4 D121G	1/833,0.12%	2/13,582	VEP: MODERATE, SIFT: deleterious - score 0.04, PolyPhen: probably_damaging - score 0.998
1598	chr9:g.131197273G¿C	Substitution	Missense		1/833,0.12%	1/13,582	VEP: MODERATE, SIFT: tolerated - score 0.08, PolyPhen: benign - score 0.164
1599	chr9:g.131228240G¿A	Substitution	Missense	TP53 Y236S	1/833,0.12%	1/13,582	VEP: MODERATE, SIFT: deleterious - score 0.02, PolyPhen: probably_damaging - score 1
1600	chr9:g.131222876G¿A	Substitution	Missense		1/833,0.12%	2/13,582	VEP: MODERATE, SIFT: deleterious - score 0, PolyPhen: probably_damaging - score 1
1601	chr20:g.40688222C¿T	Substitution	Missense	DNMT3A G550V	1/833,0.12%	1/13,582	VEP: MODERATE, SIFT: tolerated - score 0.1, PolyPhen: possibly_damaging - score 0.564
1602	chr12:g.132675814G¿T	Substitution	Missense		1/833,0.12%	1/13,582	VEP: MODERATE, SIFT: deleterious - score 0.04, PolyPhen: probably_damaging - score 0.99
1603	chr17:g.39463079C¿A	Substitution	Missense	FAT1 S1180R	1/833,0.12%	1/13,582	VEP: MODERATE, SIFT: tolerated_low_confidence - score 0.07, PolyPhen: benign - score 0.13
1604	chr5:g.38523448G¿A	Substitution	Missense		1/833,0.12%	3/13,582	VEP: MODERATE, SIFT: deleterious - score 0.03, PolyPhen: possibly_damaging - score 0.866
1605	chr4:g.125415081A¿C	Substitution	Missense	FAT4 N4885I	1/833,0.12%	1/13,582	VEP: MODERATE, SIFT: tolerated - score 0.08, PolyPhen: possibly_damaging - score 0.902
1606	chr8:g.144512024C¿T	Substitution	Missense		1/833,0.12%	2/13,582	VEP: MODERATE, SIFT: tolerated - score 0.08, PolyPhen: benign - score 0.031
1607	chr5:g.1294666C¿T	Substitution	Missense	CDKN1B E80Q	1/833,0.12%	1/13,582	VEP: MODERATE, SIFT: deleterious - score 0.01, PolyPhen: possibly_damaging - score 0.655
1608	chr5:g.55968355C¿T	Substitution	Missense		1/833,0.12%	2/13,582	VEP: MODERATE, SIFT: tolerated - score 0.06, PolyPhen: possibly_damaging - score 0.465
1609	chr1:g.7751320A¿G	Substitution	Missense	KMT2C S4771F	1/833,0.12%	1/13,582	VEP: MODERATE, SIFT: deleterious - score 0, PolyPhen: probably_damaging - score 1
1610	chr16:g.3727884G¿A	Substitution	Missense		1/833,0.12%	1/13,582	VEP: MODERATE, SIFT: tolerated_low_confidence - score 0.64, PolyPhen: benign - score 0.117

1611	chrX:g.53193534T¿C	Substitution	Missense	BRIP1 L340R	1/833,0.12%	1/13,582	VEP: MODERATE, SIFT: deleterious - score 0.03, PolyPhen: probably_damaging - score 0.999
1612	chr17:g.16039444G¿A	Substitution	Missense		1/833,0.12%	1/13,582	VEP: MODERATE, SIFT: tolerated - score 0.11, PolyPhen: probably_damaging - score 0.977
1613	chr2:g.197400430G¿A	Substitution	Missense	AKAP9 H2680Q	1/833,0.12%	1/13,582	VEP: MODERATE, SIFT: tolerated - score 0.37, PolyPhen: benign - score 0.003
1614	chr12:g.122030705A¿C	Substitution	Missense		1/833,0.12%	1/13,582	VEP: MODERATE, SIFT: deleterious - score 0, PolyPhen: probably_damaging - score 0.998
1615	chr1:g.77964911C¿G	Substitution	Missense	ZFHX3 E2628K	1/833,0.12%	1/13,582	VEP: MODERATE, SIFT: deleterious - score 0, PolyPhen: probably_damaging - score 0.983
1616	chr8:g.17938833A¿T	Substitution	Missense		1/833,0.12%	1/13,582	VEP: MODERATE, SIFT: tolerated - score 1, PolyPhen: probably_damaging - score 0.985
1617	chr1:g.110341134G¿A	Substitution	Missense	ARID1B R2304Q	1/833,0.12%	1/13,582	VEP: MODERATE, SIFT: deleterious - score 0.01, PolyPhen: benign - score 0.291
1618	chr1:g.114410217G¿A	Substitution	Missense		1/833,0.12%	1/13,582	VEP: MODERATE, SIFT: deleterious - score 0, PolyPhen: probably_damaging - score 0.992
1619	chr5:g.177135687A¿C	Substitution	Missense	TP53 Y163C	1/833,0.12%	1/13,582	VEP: MODERATE, SIFT: tolerated_low_confidence - score 0.26, PolyPhen: benign - score 0.018
1620	chrX:g.77683452C¿A	Substitution	Missense		1/833,0.12%	2/13,582	VEP: MODERATE, SIFT: deleterious_low_confidence - score 0.01, PolyPhen: possibly_damaging - score 0.819
1621	chr17:g.31232881G¿A	Substitution	Missense	CAMTA1 V142F	1/833,0.12%	1/13,582	VEP: MODERATE, SIFT: tolerated - score 0.5, PolyPhen: benign - score 0.05
1622	chr11:g.72004686C¿T	Substitution	Missense		1/833,0.12%	2/13,582	VEP: MODERATE, SIFT: deleterious - score 0.01, PolyPhen: probably_damaging - score 0.99
1623	chr12:g.25227348G¿T	Substitution	Missense	TP53 C135Y	1/833,0.12%	2/13,582	VEP: MODERATE, SIFT: deleterious - score 0.02, PolyPhen: probably_damaging - score 0.999
1624	chr11:g.128809167G¿T	Substitution	Missense		1/833,0.12%	1/13,582	VEP: MODERATE, SIFT: deleterious - score 0.02, PolyPhen: possibly_damaging - score 0.67

1625	chr20:g.32366417C¿T	Substitution	Missense	KRAS Q61E	1/833,0.12%	1/13,582	VEP: MODERATE, SIFT: deleterious - score 0.01, PolyPhen: probably_damaging - score 0.999
1626	chr1:g.3412356C¿G	Substitution	Missense		1/833,0.12%	1/13,582	VEP: MODERATE, SIFT: deleterious - score 0, PolyPhen: possibly_damaging - score 0.462
1627	chrX:g.47185571C¿T	Substitution	Missense	ETV5 D452N	1/833,0.12%	1/13,582	VEP: MODERATE, SIFT: deleterious - score 0, PolyPhen: probably_damaging - score 1
1628	chr9:g.90844043G¿A	Substitution	Missense		1/833,0.12%	1/13,582	VEP: MODERATE, SIFT: deleterious - score 0, PolyPhen: probably_damaging - score 1
1629	chr5:g.150403212C¿G	Substitution	Missense	PTPRC D147Y	1/833,0.12%	1/13,582	VEP: MODERATE, SIFT: deleterious - score 0, PolyPhen: probably_damaging - score 0.999
1630	chr2:g.29296952C¿T	Substitution	Missense		1/833,0.12%	1/13,582	VEP: MODERATE, SIFT: tolerated - score 0.31, PolyPhen: benign - score 0.121
1631	chr12:g.65066721C¿T	Substitution	Missense	CACNA1D M1236I	1/833,0.12%	2/13,582	VEP: MODERATE, SIFT: tolerated - score 0.96, PolyPhen: benign - score 0
1632	chr12:g.47993828G¿A	Substitution	Missense		1/833,0.12%	1/13,582	VEP: MODERATE, SIFT: tolerated - score 0.18, PolyPhen: benign - score 0.104
1633	chr12:g.92145411T¿C	Substitution	Missense	PRDM16 P1188T	1/833,0.12%	1/13,582	VEP: MODERATE, SIFT: tolerated - score 0.55, PolyPhen: benign - score 0.003
1634	chr16:g.9840769C¿T	Substitution	Missense		1/833,0.12%	1/13,582	VEP: MODERATE, SIFT: deleterious - score 0, PolyPhen: probably_damaging - score 1
1635	chr7:g.152148547C¿T	Substitution	Missense	FAM131B D329N	1/833,0.12%	1/13,582	VEP: MODERATE, SIFT: tolerated - score 0.13, PolyPhen: possibly_damaging - score 0.876
1636	chr9:g.121173400G¿C	Substitution	Missense		1/833,0.12%	1/13,582	VEP: MODERATE, SIFT: tolerated - score 0.51, PolyPhen: benign - score 0.095
1637	chr2:g.36894005C¿A	Substitution	Missense	PTPRK Q94P	1/833,0.12%	1/13,582	VEP: MODERATE, SIFT: tolerated - score 0.18, PolyPhen: benign - score 0.027
1638	chr9:g.125189577G¿A	Substitution	Missense		1/833,0.12%	1/13,582	VEP: MODERATE, SIFT: tolerated_low_confidence - score 0.67, PolyPhen: benign - score 0

1639	chr4:g.125319976C¿G	Substitution	Missense	RALGDS G74R	1/833,0.12%	1/13,582	VEP: MODERATE, SIFT: tolerated_low_confidence - score 0.14, PolyPhen: benign - score 0.04
1640	chr10:g.87933231G¿C	Substitution	Missense		1/833,0.12%	1/13,582	VEP: MODERATE, SIFT: tolerated - score 0.28, PolyPhen: possibly_damaging - score 0.626
1641	chr7:g.127702465T¿A	Substitution	Missense	BCR D3A	1/833,0.12%	1/13,582	VEP: MODERATE, SIFT: deleterious - score 0, PolyPhen: benign - score 0.238
1642	chr11:g.118436726G¿C	Substitution	Missense		1/833,0.12%	1/13,582	VEP: MODERATE, SIFT: tolerated_low_confidence - score 0.08, PolyPhen: benign - score 0
1643	chr17:g.68528961A¿C	Substitution	Missense	NF1 L2738V	1/833,0.12%	1/13,582	VEP: MODERATE, SIFT: tolerated - score 0.42, PolyPhen: benign - score 0.003
1644	chr1:g.156138518G¿A	Substitution	Missense		1/833,0.12%	1/13,582	VEP: MODERATE, SIFT: deleterious_low_confidence - score 0.01, PolyPhen: benign - score 0.041
1645	chr4:g.186619199G¿C	Substitution	Missense	RUNX1T1 D457N	1/833,0.12%	1/13,582	VEP: MODERATE, SIFT: deleterious - score 0.01, PolyPhen: benign - score 0.039
1646	chr2:g.108768215A¿C	Substitution	Missense		1/833,0.12%	1/13,582	VEP: MODERATE, SIFT: tolerated - score 0.54, PolyPhen: benign - score 0.021
1647	chr5:g.159097071G¿A	Substitution	Missense	SPEN R89W	1/833,0.12%	1/13,582	VEP: MODERATE, SIFT: deleterious - score 0, PolyPhen: probably_damaging - score 0.964
1648	chr9:g.37034028C¿G	Substitution	Missense		1/833,0.12%	1/13,582	VEP: MODERATE, SIFT: deleterious_low_confidence - score 0.01, PolyPhen: benign - score 0.264
1649	chr4:g.54290542G¿T	Substitution	Missense	UBR5 R2333Q	1/833,0.12%	1/13,582	VEP: MODERATE, SIFT: deleterious - score 0.04, PolyPhen: probably_damaging - score 0.997
1650	chrX:g.71101297G¿C	Substitution	Missense		1/833,0.12%	1/13,582	VEP: MODERATE, SIFT: tolerated - score 0.69, PolyPhen: benign - score 0.219
1651	chr3:g.12379922G¿C	Substitution	Missense	NTRK3 T707M	1/833,0.12%	1/13,582	VEP: MODERATE, SIFT: tolerated_low_confidence - score 0.16, PolyPhen: possibly_damaging - score 0.541
1652	chr17:g.80347789G¿A	Substitution	Missense		1/833,0.12%	1/13,582	VEP: MODERATE, SIFT: deleterious - score 0, PolyPhen: probably_damaging - score 0.994

1653	chr17:g.20204416C¿T	Substitution	Missense	MUC1 Q50H	1/833,0.12%	1/13,582	VEP: MODERATE, SIFT: deleterious - score 0.02, PolyPhen: probably_damaging - score 1
1654	chr19:g.53577122G¿A	Substitution	Missense		1/833,0.12%	2/13,582	VEP: MODERATE, SIFT: tolerated - score 0.28, PolyPhen: benign - score 0.023
1655	chr4:g.186606105C¿T	Substitution	Missense	BCOR E1372Q	1/833,0.12%	2/13,582	VEP: MODERATE, SIFT: tolerated - score 0.1, PolyPhen: benign - score 0.003
1656	chr2:g.197400881G¿C	Substitution	Missense		1/833,0.12%	1/13,582	VEP: MODERATE, SIFT: deleterious - score 0.03, PolyPhen: possibly_damaging - score 0.571
1657	chr16:g.72794289G¿A	Substitution	Missense	PRKACA D185N	1/833,0.12%	1/13,582	VEP: MODERATE, SIFT: deleterious - score 0.04, PolyPhen: benign - score 0.109
1658	chr15:g.88184272G¿C	Substitution	Missense		1/833,0.12%	1/13,582	VEP: MODERATE, SIFT: tolerated - score 0.86, PolyPhen: benign - score 0
1659	chr17:g.39723916T¿A	Substitution	Missense	NFKB2 L187M	1/833,0.12%	1/13,582	VEP: MODERATE, SIFT: deleterious - score 0, PolyPhen: possibly_damaging - score 0.53
1660	chr8:g.32754375C¿T	Substitution	Missense		1/833,0.12%	1/13,582	VEP: MODERATE, SIFT: deleterious - score 0.02, PolyPhen: benign - score 0.206
1661	chr17:g.16108837C¿A	Substitution	Missense	MAX N29D	1/833,0.12%	1/13,582	VEP: MODERATE, SIFT: deleterious - score 0, PolyPhen: probably_damaging - score 0.96
1662	chr4:g.125321060T¿G	Substitution	Missense		1/833,0.12%	1/13,582	VEP: MODERATE, SIFT: deleterious - score 0, PolyPhen: benign - score 0.192
1663	chrX:g.67686030G¿A	Substitution	Missense	SETD2 R456L	1/833,0.12%	3/13,582	VEP: MODERATE, SIFT: deleterious - score 0, PolyPhen: probably_damaging - score 0.998
1664	chr10:g.3784953T¿C	Substitution	Missense		1/833,0.12%	1/13,582	VEP: MODERATE, SIFT: tolerated - score 0.05, PolyPhen: possibly_damaging - score 0.903
1665	chr12:g.292891C¿G	Substitution	Missense	TP53 M133T	1/833,0.12%	1/13,582	VEP: MODERATE, SIFT: tolerated - score 0.38, PolyPhen: benign - score 0.005
1666	chr22:g.23787245T¿A	Substitution	Missense		1/833,0.12%	1/13,582	VEP: MODERATE, SIFT: deleterious_low_confidence - score 0, PolyPhen: possibly_damaging - score 0.495

1667	chr3:g.142550167C¿T	Substitution	Missense	BRCA2 I2778T	1/833,0.12%	1/13,582	VEP: MODERATE, SIFT: tolerated - score 0.15, PolyPhen: benign - score 0.314
1668	chr7:g.26197629T¿G	Substitution	Missense		1/833,0.12%	1/13,582	VEP: MODERATE, SIFT: deleterious - score 0, PolyPhen: possibly_damaging - score 0.843
1669	chr10:g.26860808A¿C	Substitution	Missense	RBM10 R397H	1/833,0.12%	1/13,582	VEP: MODERATE, SIFT: deleterious - score 0, PolyPhen: probably_damaging - score 0.999
1670	chr7:g.124863423G¿A	Substitution	Missense		1/833,0.12%	1/13,582	VEP: MODERATE, SIFT: deleterious - score 0, PolyPhen: benign - score 0.326
1671	chr12:g.58880892G¿A	Substitution	Missense	RET E673D	1/833,0.12%	1/13,582	VEP: MODERATE, SIFT: tolerated - score 0.16, PolyPhen: probably_damaging - score 0.999
1672	chr4:g.125318291C¿G	Substitution	Missense		1/833,0.12%	1/13,582	VEP: MODERATE, SIFT: tolerated - score 1, PolyPhen: benign - score 0.001
1673	chrX:g.49038418T¿C	Substitution	Missense	TET2 R1161T	1/833,0.12%	1/13,582	VEP: MODERATE, SIFT: deleterious - score 0.01, PolyPhen: probably_damaging - score 0.987
1674	chr8:g.32754425G¿A	Substitution	Missense		1/833,0.12%	3/13,582	VEP: MODERATE, SIFT: deleterious - score 0, PolyPhen: possibly_damaging - score 0.835
1675	chr4:g.125448527C¿T	Substitution	Missense	BCL9 G715E	1/833,0.12%	1/13,582	VEP: MODERATE, SIFT: tolerated - score 0.06, PolyPhen: probably_damaging - score 0.997
1676	chr1:g.155188426T¿G	Substitution	Missense		1/833,0.12%	1/13,582	VEP: MODERATE, SIFT: tolerated - score 0.22, PolyPhen: benign - score 0.207
1677	chr17:g.7675136G¿A	Substitution	Missense	TSC2 D907Y	1/833,0.12%	16/13,582	VEP: MODERATE, SIFT: deleterious - score 0, PolyPhen: possibly_damaging - score 0.772
1678	chr12:g.25225714T¿C	Substitution	Missense		1/833,0.12%	1/13,582	VEP: MODERATE, SIFT: deleterious - score 0, PolyPhen: probably_damaging - score 0.975
1679	chr4:g.87047019G¿A	Substitution	Missense	IDH2 V297G	1/833,0.12%	1/13,582	VEP: MODERATE, SIFT: tolerated - score 0.49, PolyPhen: possibly_damaging - score 0.474
1680	chr11:g.119299626C¿G	Substitution	Missense		1/833,0.12%	1/13,582	VEP: MODERATE, SIFT: tolerated_low_confidence - score 0.15, PolyPhen: benign - score 0.026

1681	chr17:g.80288025C¿A	Substitution	Missense	KMT2C K3847E	1/833,0.12%	1/13,582	VEP: MODERATE, SIFT: tolerated - score 0.26, PolyPhen: benign - score 0.09
1682	chrX:g.49030219G¿T	Substitution	Missense		1/833,0.12%	1/13,582	VEP: MODERATE, SIFT: deleterious - score 0, PolyPhen: probably_damaging - score 0.922
1683	chr7:g.138460653T¿G	Substitution	Missense	BRCA1 N354Y	1/833,0.12%	1/13,582	VEP: MODERATE, SIFT: deleterious - score 0, PolyPhen: benign - score 0.298
1684	chr7:g.152162455A¿G	Substitution	Missense		1/833,0.12%	1/13,582	VEP: MODERATE, SIFT: tolerated - score 0.39, PolyPhen: benign - score 0
1685	chr6:g.106107029T¿A	Substitution	Missense	KAT6A R220Q	1/833,0.12%	1/13,582	VEP: MODERATE, SIFT: deleterious - score 0, PolyPhen: probably_damaging - score 0.953
1686	chr12:g.53939010G¿T	Substitution	Missense		1/833,0.12%	1/13,582	VEP: MODERATE, SIFT: tolerated_low_confidence - score 0.39, PolyPhen: probably_damaging - score 0.953
1687	chr14:g.37591762G¿A	Substitution	Missense	RNF213 P2152A	1/833,0.12%	1/13,582	VEP: MODERATE, SIFT: tolerated - score 0.11, PolyPhen: benign - score 0.039
1688	chr2:g.211947609C¿T	Substitution	Missense		1/833,0.12%	1/13,582	VEP: MODERATE, SIFT: tolerated - score 1, PolyPhen: benign - score 0.327
1689	chr2:g.47823184A¿T	Substitution	Missense	CLTC N1149K	1/833,0.12%	1/13,582	VEP: MODERATE, SIFT: tolerated - score 0.1, PolyPhen: possibly_damaging - score 0.495
1690	chr14:g.99175344G¿A	Substitution	Missense		1/833,0.12%	1/13,582	VEP: MODERATE, SIFT: deleterious - score 0.02, PolyPhen: possibly_damaging - score 0.563
1691	chr11:g.111354446G¿C	Substitution	Missense	GNAS P26H	1/833,0.12%	1/13,582	VEP: MODERATE, SIFT: tolerated - score 1, PolyPhen: benign - score 0.01
1692	chr19:g.29817524C¿A	Substitution	Missense		1/833,0.12%	1/13,582	VEP: MODERATE, SIFT: deleterious - score 0, PolyPhen: probably_damaging - score 1
1693	chr19:g.1621134G¿A	Substitution	Missense	PPARG K268N	1/833,0.12%	1/13,582	VEP: MODERATE, SIFT: deleterious - score 0.02, PolyPhen: possibly_damaging - score 0.619
1694	chr6:g.37170801G¿C	Substitution	Missense		1/833,0.12%	1/13,582	VEP: MODERATE, SIFT: tolerated - score 0.31, PolyPhen: benign - score 0.003
1695	chr12:g.53975317C¿G	Substitution	Missense	ATRX G2466V	1/833,0.12%	1/13,582	VEP: MODERATE, SIFT: tolerated - score 0.09, PolyPhen: probably_damaging - score 1

1696	chr4:g.105261817A¿C	Substitution Missense		1/833,0.12%	1/13,582	VEP: MODERATE, SIFT: deleterious - score 0, PolyPhen: probably_damaging - score 0.981
1697	chr5:g.160118995C¿T	Substitution Missense	ZFHX3 S557F	1/833,0.12%	1/13,582	VEP: MODERATE, SIFT: tolerated_low_confidence - score 0.27, PolyPhen: benign - score 0.012
1698	chr13:g.40665985C¿G	Substitution Missense		1/833,0.12%	1/13,582	VEP: MODERATE, SIFT: deleterious - score 0.02, PolyPhen: probably_damaging - score 0.994
1699	chr4:g.125320543C¿A	Substitution Missense	ARID1A P144S	1/833,0.12%	1/13,582	VEP: MODERATE, SIFT: deleterious - score 0, PolyPhen: probably_damaging - score 0.996
1700	chr19:g.54144105G¿A	Substitution Missense		1/833,0.12%	1/13,582	VEP: MODERATE, SIFT: deleterious - score 0, PolyPhen: probably_damaging - score 0.992
1701	chr1:g.119950796G¿A	Substitution Missense	GRIN2A H485Y	1/833,0.12%	1/13,582	VEP: MODERATE, SIFT: deleterious - score 0, PolyPhen: probably_damaging - score 0.999
1702	chr17:g.38918768A¿T	Substitution Missense		1/833,0.12%	1/13,582	VEP: MODERATE, SIFT: deleterious - score 0, PolyPhen: probably_damaging - score 0.994
1703	chr3:g.186784998G¿A	Substitution Missense	ATM E2304Q	1/833,0.12%	1/13,582	VEP: MODERATE, SIFT: deleterious - score 0, PolyPhen: probably_damaging - score 0.974
1704	chr20:g.40688186C¿T	Substitution Missense		1/833,0.12%	1/13,582	VEP: MODERATE, SIFT: deleterious - score 0, PolyPhen: probably_damaging - score 1
1705	chr16:g.3740415G¿C	Substitution Missense	POLE R8Q	1/833,0.12%	1/13,582	VEP: MODERATE, SIFT: deleterious - score 0.02, PolyPhen: probably_damaging - score 0.984
1706	chr15:g.52340387C¿T	Substitution Missense		1/833,0.12%	1/13,582	VEP: MODERATE, SIFT: deleterious - score 0.01, PolyPhen: possibly_damaging - score 0.885
1707	chr17:g.7675211A¿G	Substitution Missense	FIP1L1 P269R	1/833,0.12%	1/13,582	VEP: MODERATE, SIFT: deleterious - score 0, PolyPhen: probably_damaging - score 1
1708	chr9:g.125153692G¿C	Substitution Missense		1/833,0.12%	1/13,582	VEP: MODERATE, SIFT: deleterious - score 0.01, PolyPhen: probably_damaging - score 0.918
1709	chr22:g.31345308C¿T	Substitution Missense	JAK1 N76S	1/833,0.12%	1/13,582	VEP: MODERATE, SIFT: deleterious_low_confidence - score 0.02, PolyPhen: probably_damaging - score 0.934

1710	chr12:g.45852210G¿A	Substitution Missense		1/833,0.12%	1/13,582	VEP: MODERATE, SIFT: deleterious_low_confidence - score 0, PolyPhen: probably_damaging - score 0.996
1711	chrX:g.153553189G¿A	Substitution Missense	TSHR I108S	1/833,0.12%	1/13,582	VEP: MODERATE, SIFT: tolerated - score 0.39, PolyPhen: benign - score 0.026
1712	chr12:g.122377539C¿A	Substitution Missense		1/833,0.12%	2/13,582	VEP: MODERATE, SIFT: tolerated - score 0.7, PolyPhen: benign - score 0
1713	chr17:g.80353541C¿T	Substitution Missense	NTRK1 V658L	1/833,0.12%	1/13,582	VEP: MODERATE, SIFT: tolerated - score 0.1, PolyPhen: benign - score 0.15
1714	chr15:g.90798302G¿A	Substitution Missense		1/833,0.12%	1/13,582	VEP: MODERATE, SIFT: deleterious - score 0.01, PolyPhen: benign - score 0.127
1715	chr8:g.32764103G¿A	Substitution Missense	IRF4 F247L	1/833,0.12%	5/13,582	VEP: MODERATE, SIFT: tolerated - score 0.29, PolyPhen: benign - score 0.003
1716	chr19:g.34172715A¿T	Substitution Missense		1/833,0.12%	1/13,582	VEP: MODERATE, SIFT: deleterious - score 0.01, PolyPhen: possibly_damaging - score 0.551
1717	chr7:g.55154104C¿T	Substitution Missense	FAT4 V3837L	1/833,0.12%	1/13,582	VEP: MODERATE, SIFT: deleterious - score 0.03, PolyPhen: possibly_damaging - score 0.526
1718	chr11:g.69641455G¿A	Substitution Missense		1/833,0.12%	1/13,582	VEP: MODERATE, SIFT: deleterious - score 0, PolyPhen: probably_damaging - score 0.991
1719	chr16:g.64947815C¿T	Substitution Missense	EBF1 M15L	1/833,0.12%	1/13,582	VEP: MODERATE, SIFT: deleterious - score 0, PolyPhen: possibly_damaging - score 0.902
1720	chr7:g.152176923C¿G	Substitution Missense		1/833,0.12%	1/13,582	VEP: MODERATE, SIFT: deleterious - score 0.04, PolyPhen: benign - score 0.046
1721	chr12:g.70622632C¿T	Substitution Missense	RECQL4 E1152K	1/833,0.12%	2/13,582	VEP: MODERATE, SIFT: deleterious_low_confidence - score 0.04, PolyPhen: possibly_damaging - score 0.54
1722	chr8:g.32764329G¿A	Substitution Missense		1/833,0.12%	1/13,582	VEP: MODERATE, SIFT: tolerated - score 0.14, PolyPhen: probably_damaging - score 0.999
1723	chr16:g.79599607T¿G	Substitution Missense	SBDS E168V	1/833,0.12%	1/13,582	VEP: MODERATE, SIFT: deleterious - score 0.01, PolyPhen: possibly_damaging - score 0.682

1724	chr12:g.25245348C¿G	Substitution Missense		1/833,0.12%	1/13,582	VEP: MODERATE, SIFT: deleterious - score 0, PolyPhen: probably_damaging - score 0.986
1725	chr1:g.26780445C¿T	Substitution Missense	ACVR1 E442K	1/833,0.12%	1/13,582	VEP: MODERATE, SIFT: deleterious - score 0, PolyPhen: probably_damaging - score 0.999
1726	chr1:g.15938740T¿C	Substitution Missense		1/833,0.12%	1/13,582	VEP: MODERATE, SIFT: deleterious - score 0, PolyPhen: probably_damaging - score 0.996
1727	chr4:g.125415793G¿A	Substitution Missense	CDH11 D426A	1/833,0.12%	1/13,582	VEP: MODERATE, SIFT: tolerated - score 1, PolyPhen: benign - score 0.001
1728	chrX:g.47171183G¿T	Substitution Missense		1/833,0.12%	1/13,582	VEP: MODERATE, SIFT: tolerated_low_confidence - score 0.47, PolyPhen: benign - score 0
1729	chrX:g.71120038G¿A	Substitution Missense	EZH2 E441K	1/833,0.12%	1/13,582	VEP: MODERATE, SIFT: deleterious - score 0, PolyPhen: benign - score 0.298
1730	chr16:g.50782466G¿A	Substitution Missense		1/833,0.12%	1/13,582	VEP: MODERATE, SIFT: deleterious - score 0.04, PolyPhen: probably_damaging - score 0.998
1731	chr17:g.7675220T¿G	Substitution Missense	PBX1 T276R	1/833,0.12%	1/13,582	VEP: MODERATE, SIFT: deleterious - score 0.02, PolyPhen: probably_damaging - score 0.992
1732	chr20:g.51474074C¿G	Substitution Missense		1/833,0.12%	1/13,582	VEP: MODERATE, SIFT: deleterious - score 0, PolyPhen: probably_damaging - score 1
1733	chr7:g.116758538T¿G	Substitution Missense	CUX1 R432Q	1/833,0.12%	1/13,582	VEP: MODERATE, SIFT: tolerated - score 0.25, PolyPhen: benign - score 0.275
1734	chr4:g.186614238G¿A	Substitution Missense		1/833,0.12%	1/13,582	VEP: MODERATE, SIFT: deleterious - score 0.01, PolyPhen: probably_damaging - score 0.959
1735	chr2:g.127293628G¿A	Substitution Missense	NFKBIE L123V	1/833,0.12%	2/13,582	VEP: MODERATE, SIFT: tolerated - score 0.2, PolyPhen: benign - score 0.03
1736	chr19:g.6270725C¿T	Substitution Missense		1/833,0.12%	1/13,582	VEP: MODERATE, SIFT: deleterious - score 0.04, PolyPhen: possibly_damaging - score 0.883
1737	chr8:g.41933827C¿T	Substitution Missense	RBM10 Q429P	1/833,0.12%	1/13,582	VEP: MODERATE, SIFT: deleterious - score 0.01, PolyPhen: possibly_damaging - score 0.684

1738	chr17:g.76737155G¿C	Substitution Missense		1/833,0.12%	1/13,582	VEP: MODERATE, SIFT: deleterious - score 0, PolyPhen: probably_damaging - score 0.939
1739	chr6:g.117341284A¿C	Substitution Missense	NRAS G13C	1/833,0.12%	1/13,582	VEP: MODERATE, SIFT: deleterious - score 0, PolyPhen: probably_damaging - score 0.991
1740	chr4:g.125450956G¿T	Substitution Missense		1/833,0.12%	1/13,582	VEP: MODERATE, SIFT: deleterious - score 0, PolyPhen: probably_damaging - score 1
1741	chr7:g.55173074C¿G	Substitution Missense	PSIP1 Q491E	1/833,0.12%	1/13,582	VEP: MODERATE, SIFT: deleterious - score 0, PolyPhen: possibly_damaging - score 0.818
1742	chr11:g.32392746G¿T	Substitution Missense		1/833,0.12%	1/13,582	VEP: MODERATE, SIFT: deleterious_low_confidence - score 0, PolyPhen: probably_damaging - score 0.977
1743	chr15:g.52327928G¿A	Substitution Missense	PALB2 A391T	1/833,0.12%	2/13,582	VEP: MODERATE, SIFT: deleterious - score 0, PolyPhen: possibly_damaging - score 0.493
1744	chr4:g.54270659G¿A	Substitution Missense		1/833,0.12%	1/13,582	VEP: MODERATE, SIFT: deleterious - score 0, PolyPhen: probably_damaging - score 0.937
1745	chr10:g.75029559G¿A	Substitution Missense	NUP98 L1283V	1/833,0.12%	1/13,582	VEP: MODERATE, SIFT: tolerated - score 0.19, PolyPhen: benign - score 0.118
1746	chr12:g.47996570A¿C	Substitution Missense		1/833,0.12%	1/13,582	VEP: MODERATE, SIFT: tolerated - score 0.09, PolyPhen: benign - score 0.221
1747	chr12:g.53945062T¿G	Substitution Missense	RANBP2 K1848N	1/833,0.12%	1/13,582	VEP: MODERATE, SIFT: deleterious - score 0, PolyPhen: probably_damaging - score 1
1748	chr12:g.114674728G¿C	Substitution Missense		1/833,0.12%	1/13,582	VEP: MODERATE, SIFT: tolerated - score 0.08, PolyPhen: benign - score 0.142
1749	chr10:g.113040036G¿A	Substitution Missense	CDK12 E763D	1/833,0.12%	1/13,582	VEP: MODERATE, SIFT: tolerated - score 0.08, PolyPhen: possibly_damaging - score 0.688
1750	chr4:g.125318820T¿G	Substitution Missense		1/833,0.12%	1/13,582	VEP: MODERATE, SIFT: tolerated - score 0.63, PolyPhen: probably_damaging - score 0.981
1751	chr7:g.98948667G¿C	Substitution Missense	RBM15 R532C	1/833,0.12%	1/13,582	VEP: MODERATE, SIFT: tolerated - score 0.1, PolyPhen: benign - score 0.055

1752	chr7:g.124823973C¿T	Substitution Missense		1/833,0.12%	1/13,582	VEP: MODERATE, SIFT: deleterious - score 0.02, PolyPhen: benign - score 0.056
1753	chrX:g.1206556G¿A	Substitution Missense	EIF4A2 D381N	1/833,0.12%	1/13,582	VEP: MODERATE, SIFT: deleterious - score 0.04, PolyPhen: possibly_damaging - score 0.61
1754	chr16:g.3769329C¿G	Substitution Missense		1/833,0.12%	1/13,582	VEP: MODERATE, SIFT: deleterious - score 0, PolyPhen: possibly_damaging - score 0.67
1755	chr5:g.180618910G¿A	Substitution Missense	ATRX K1281Q	1/833,0.12%	1/13,582	VEP: MODERATE, SIFT: deleterious - score 0.02, PolyPhen: benign - score 0.007
1756	chr6:g.157206320G¿A	Substitution Missense		1/833,0.12%	1/13,582	VEP: MODERATE, SIFT: tolerated_low_confidence - score 0.12, PolyPhen: benign - score 0.32
1757	chr18:g.25227533G¿A	Substitution Missense	CCND1 A20D	1/833,0.12%	2/13,582	VEP: MODERATE, SIFT: deleterious - score 0, PolyPhen: probably_damaging - score 1
1758	chr16:g.79599068G¿C	Substitution Missense		1/833,0.12%	1/13,582	VEP: MODERATE, SIFT: deleterious - score 0, PolyPhen: probably_damaging - score 0.996
1759	chr4:g.125398824T¿A	Substitution Missense	MDM4 D173H	1/833,0.12%	1/13,582	VEP: MODERATE, SIFT: deleterious - score 0.02, PolyPhen: possibly_damaging - score 0.643
1760	chr16:g.15750242T¿C	Substitution Missense		1/833,0.12%	1/13,582	VEP: MODERATE, SIFT: deleterious - score 0.01, PolyPhen: probably_damaging - score 0.945
1761	chr17:g.81996549G¿C	Substitution Missense	HNF1A A491P	1/833,0.12%	1/13,582	VEP: MODERATE, SIFT: tolerated - score 0.08, PolyPhen: benign - score 0.387
1762	chr1:g.47225615C¿G	Substitution Missense		1/833,0.12%	2/13,582	VEP: MODERATE, SIFT: deleterious - score 0.02, PolyPhen: possibly_damaging - score 0.615
1763	chr5:g.38502658G¿C	Substitution Missense	PTEN M134I	1/833,0.12%	1/13,582	VEP: MODERATE, SIFT: tolerated - score 0.61, PolyPhen: benign - score 0
1764	chr9:g.105662584C¿T	Substitution Missense		1/833,0.12%	1/13,582	VEP: MODERATE, SIFT: deleterious - score 0, PolyPhen: probably_damaging - score 1
1765	chr4:g.1801853C¿A	Substitution Missense	TRIP11 R252Q	1/833,0.12%	1/13,582	VEP: MODERATE, SIFT: deleterious - score 0, PolyPhen: probably_damaging - score 0.981

1766	chr2:g.197402110T¿C	Substitution Missense		1/833,0.12%	21/13,582	VEP: MODERATE, SIFT: deleterious - score 0, PolyPhen: probably_damaging - score 0.999
1767	chr17:g.31182598T¿G	Substitution Missense	CDKN1B N61K	1/833,0.12%	1/13,582	VEP: MODERATE, SIFT: deleterious - score 0, PolyPhen: probably_damaging - score 0.999
1768	chr8:g.92014808G¿C	Substitution Missense		1/833,0.12%	1/13,582	VEP: MODERATE, SIFT: tolerated - score 0.17, PolyPhen: possibly_damaging - score 0.876
1769	chrX:g.71127943C¿T	Substitution Missense	MECOM R279I	1/833,0.12%	1/13,582	VEP: MODERATE, SIFT: deleterious - score 0, PolyPhen: benign - score 0.154
1770	chr12:g.53973315G¿A	Substitution Missense		1/833,0.12%	2/13,582	VEP: MODERATE, SIFT: deleterious - score 0.02, PolyPhen: probably_damaging - score 0.988
1771	chr16:g.11255373G¿A	Substitution Missense	ROS1 R1829T	1/833,0.12%	1/13,582	VEP: MODERATE, SIFT: tolerated - score 0.35, PolyPhen: benign - score 0
1772	chr9:g.134048385C¿T	Substitution Missense		1/833,0.12%	1/13,582	VEP: MODERATE, SIFT: tolerated - score 0.09, PolyPhen: benign - score 0.026
1773	chr4:g.25662785G¿A	Substitution Missense	LRIG3 N396Y	1/833,0.12%	2/13,582	VEP: MODERATE, SIFT: tolerated - score 0.09, PolyPhen: benign - score 0.007
1774	chr16:g.79599080T¿G	Substitution Missense		1/833,0.12%	1/13,582	VEP: MODERATE, SIFT: deleterious - score 0, PolyPhen: probably_damaging - score 0.999
1775	chr11:g.102336951G¿C	Substitution Missense	PAX5 G16R	1/833,0.12%	1/13,582	VEP: MODERATE, SIFT: deleterious - score 0, PolyPhen: probably_damaging - score 0.999
1776	chr12:g.334389T¿C	Substitution Missense		1/833,0.12%	1/13,582	VEP: MODERATE, SIFT: deleterious - score 0, PolyPhen: benign - score 0.04
1777	chr12:g.132636024G¿C	Substitution Missense	NFATC2 P727A	1/833,0.12%	1/13,582	VEP: MODERATE, SIFT: deleterious - score 0.04, PolyPhen: probably_damaging - score 0.972
1778	chr6:g.157084873G¿A	Substitution Missense		1/833,0.12%	1/13,582	VEP: MODERATE, SIFT: deleterious_low_confidence - score 0.03, PolyPhen: probably_damaging - score 0.991
1779	chr1:g.119916286C¿T	Substitution Missense	CARD11 M417I	1/833,0.12%	1/13,582	VEP: MODERATE, SIFT: tolerated - score 0.08, PolyPhen: possibly_damaging - score 0.77

1780	chr7:g.129210369G¿T	Substitution Missense		1/833,0.12%	1/13,582	VEP: MODERATE, SIFT: deleterious - score 0.01, PolyPhen: possibly_damaging - score 0.6
1781	chr4:g.186708447G¿A	Substitution Missense	ZFHX3 P2485T	1/833,0.12%	1/13,582	VEP: MODERATE, SIFT: deleterious - score 0, PolyPhen: probably_damaging - score 0.998
1782	chr4:g.125415704T¿G	Substitution Missense		1/833,0.12%	1/13,582	VEP: MODERATE, SIFT: deleterious - score 0.03, PolyPhen: possibly_damaging - score 0.805
1783	chr12:g.25245345C¿T	Substitution Missense	TRRAP A933G	1/833,0.12%	4/13,582	VEP: MODERATE, SIFT: deleterious - score 0, PolyPhen: probably_damaging - score 0.959
1784	chr7:g.143356621G¿A	Substitution Missense		1/833,0.12%	3/13,582	VEP: MODERATE, SIFT: deleterious - score 0, PolyPhen: probably_damaging - score 1
1785	chr16:g.67029813C¿G	Substitution Missense	BRAF G392E	1/833,0.12%	1/13,582	VEP: MODERATE, SIFT: tolerated - score 0.09, PolyPhen: benign - score 0.038
1786	chr12:g.112450394G¿A	Substitution Missense		1/833,0.12%	4/13,582	VEP: MODERATE, SIFT: deleterious - score 0, PolyPhen: probably_damaging - score 0.972
1787	chr4:g.55115301G¿T	Substitution Missense	KRAS P34T	1/833,0.12%	1/13,582	VEP: MODERATE, SIFT: deleterious - score 0, PolyPhen: probably_damaging - score 0.997
1788	chr6:g.158818090G¿C	Substitution Missense		1/833,0.12%	1/13,582	VEP: MODERATE, SIFT: deleterious - score 0.02, PolyPhen: benign - score 0.125
1789	chr11:g.128810963C¿G	Substitution Missense	KDM5A D200Y	1/833,0.12%	1/13,582	VEP: MODERATE, SIFT: deleterious - score 0, PolyPhen: benign - score 0.14
1790	chr19:g.54152289G¿A	Substitution Missense		1/833,0.12%	1/13,582	VEP: MODERATE, SIFT: deleterious - score 0.01, PolyPhen: benign - score 0.05
1791	chrX:g.77681735G¿C	Substitution Missense	ARID1A P234S	1/833,0.12%	1/13,582	VEP: MODERATE, SIFT: deleterious_low_confidence - score 0.01, PolyPhen: benign - score 0.078
1792	chr9:g.35074991C¿G	Substitution Missense		1/833,0.12%	1/13,582	VEP: MODERATE, SIFT: deleterious - score 0, PolyPhen: possibly_damaging - score 0.841
1793	chr4:g.186708738G¿C	Substitution Missense	FAT4 I778T	1/833,0.12%	1/13,582	VEP: MODERATE, SIFT: tolerated - score 0.26, PolyPhen: benign - score 0.005

1794	chr1:g.43339351G¿A	Substitution Missense		1/833,0.12%	1/13,582	VEP: MODERATE, SIFT: tolerated - score 0.69, PolyPhen: possibly_damaging - score 0.632
1795	chr11:g.118436718G¿A	Substitution Missense	CCND1 K46E	1/833,0.12%	1/13,582	VEP: MODERATE, SIFT: deleterious_low_confidence - score 0.02, PolyPhen: benign - score 0.036
1796	chr7:g.138579384C¿T	Substitution Missense		1/833,0.12%	1/13,582	VEP: MODERATE, SIFT: tolerated - score 0.4, PolyPhen: benign - score 0.04
1797	chr1:g.114713832A¿T	Substitution Missense	PTPN13 S2023L	1/833,0.12%	1/13,582	VEP: MODERATE, SIFT: deleterious - score 0.04, PolyPhen: benign - score 0.069
1798	chr12:g.114672103G¿A	Substitution Missense		1/833,0.12%	1/13,582	VEP: MODERATE, SIFT: deleterious - score 0, PolyPhen: benign - score 0.051
1799	chr14:g.95713980C¿G	Substitution Missense	BRIP1 P971A	1/833,0.12%	1/13,582	VEP: MODERATE, SIFT: deleterious - score 0, PolyPhen: probably_damaging - score 0.978
1800	chr17:g.31975536A¿C	Substitution Missense		1/833,0.12%	2/13,582	VEP: MODERATE, SIFT: deleterious - score 0, PolyPhen: probably_damaging - score 0.991
1801	chr2:g.29320819G¿A	Substitution Missense	HNRNPA2B1 K22R	1/833,0.12%	1/13,582	VEP: MODERATE, SIFT: tolerated - score 0.16, PolyPhen: benign - score 0
1802	chr7:g.152162691A¿G	Substitution Missense		1/833,0.12%	1/13,582	VEP: MODERATE, SIFT: tolerated - score 0.07, PolyPhen: benign - score 0.001
1803	chrX:g.47171104C¿A	Substitution Missense	AXIN1 D329N	1/833,0.12%	1/13,582	VEP: MODERATE, SIFT: tolerated - score 0.06, PolyPhen: possibly_damaging - score 0.634
1804	chr2:g.112482476G¿T	Substitution Missense		1/833,0.12%	1/13,582	VEP: MODERATE, SIFT: deleterious - score 0.01, PolyPhen: possibly_damaging - score 0.879
1805	chr12:g.56094528C¿T	Substitution Missense	TP53 R175G	1/833,0.12%	2/13,582	VEP: MODERATE, SIFT: tolerated - score 0.14, PolyPhen: benign - score 0
1806	chr9:g.130042970G¿C	Substitution Missense		1/833,0.12%	1/13,582	VEP: MODERATE, SIFT: deleterious - score 0, PolyPhen: benign - score 0.355
1807	chr2:g.222295558C¿T	Substitution Missense	MAFB S311F	1/833,0.12%	1/13,582	VEP: MODERATE, SIFT: deleterious - score 0.02, PolyPhen: benign - score 0.057

1808	chr12:g.58887882C¿T	Substitution Missense		1/833,0.12%	1/13,582	VEP: MODERATE, SIFT: tolerated - score 0.2, PolyPhen: probably_damaging - score 0.971
1809	chrX:g.49034141C¿G	Substitution Missense	NOTCH2 N689S	1/833,0.12%	1/13,582	VEP: MODERATE, SIFT: deleterious - score 0.01, PolyPhen: probably_damaging - score 0.967
1810	chr8:g.56167313C¿T	Substitution Missense		1/833,0.12%	1/13,582	VEP: MODERATE, SIFT: deleterious - score 0, PolyPhen: probably_damaging - score 0.992
1811	chr1:g.164792577G¿A	Substitution Missense	ZNF521 R161Q	1/833,0.12%	4/13,582	VEP: MODERATE, SIFT: deleterious - score 0.05, PolyPhen: probably_damaging - score 0.995
1812	chr10:g.113159975C¿A	Substitution Missense		1/833,0.12%	1/13,582	VEP: MODERATE, SIFT: tolerated - score 0.18, PolyPhen: benign - score 0.003
1813	chr10:g.68691473C¿T	Substitution Missense	TET1 G183A	1/833,0.12%	1/13,582	VEP: MODERATE, SIFT: deleterious - score 0, PolyPhen: probably_damaging - score 0.998
1814	chr4:g.125317468G¿T	Substitution Missense		1/833,0.12%	1/13,582	VEP: MODERATE, SIFT: tolerated - score 0.1, PolyPhen: probably_damaging - score 0.976
1815	chr3:g.128650541T¿G	Substitution Missense	PPARG R385Q	1/833,0.12%	1/13,582	VEP: MODERATE, SIFT: tolerated - score 0.22, PolyPhen: possibly_damaging - score 0.46
1816	chr8:g.42906207C¿A	Substitution Missense		1/833,0.12%	1/13,582	VEP: MODERATE, SIFT: tolerated - score 0.13, PolyPhen: benign - score 0.026
1817	chr8:g.70156378C¿G	Substitution Missense	PBRM1 M1201I	1/833,0.12%	1/13,582	VEP: MODERATE, SIFT: deleterious - score 0.02, PolyPhen: possibly_damaging - score 0.784
1818	chr15:g.52405340G¿T	Substitution Missense		1/833,0.12%	1/13,582	VEP: MODERATE, SIFT: deleterious - score 0.01, PolyPhen: probably_damaging - score 0.998
1819	chr16:g.9769039C¿T	Substitution Missense	MYH11 V447M	1/833,0.12%	1/13,582	VEP: MODERATE, SIFT: deleterious - score 0, PolyPhen: probably_damaging - score 0.993
1820	chr12:g.25227349C¿A	Substitution Missense		1/833,0.12%	1/13,582	VEP: MODERATE, SIFT: deleterious - score 0.04, PolyPhen: possibly_damaging - score 0.774
1821	chr2:g.47463133A¿G	Substitution Missense	CD74 S25C	1/833,0.12%	1/13,582	VEP: MODERATE, SIFT: tolerated - score 0.3, PolyPhen: benign - score 0

1822	chr6:g.108663579G¿A	Substitution Missense		1/833,0.12%	1/13,582	VEP: MODERATE, SIFT: deleterious - score 0, PolyPhen: probably_damaging - score 0.999
1823	chr14:g.65093787A¿G	Substitution Missense	FNBP1 E471K	1/833,0.12%	1/13,582	VEP: MODERATE, SIFT: deleterious - score 0, PolyPhen: probably_damaging - score 1
1824	chr7:g.102189852G¿C	Substitution Missense		1/833,0.12%	1/13,582	VEP: MODERATE, SIFT: deleterious - score 0.04, PolyPhen: benign - score 0.384
1825	chr3:g.9124765A¿G	Substitution Missense	TP53 R282G	1/833,0.12%	1/13,582	VEP: MODERATE, SIFT: deleterious - score 0.02, PolyPhen: benign - score 0.132
1826	chr1:g.120069377C¿A	Substitution Missense		1/833,0.12%	1/13,582	VEP: MODERATE, SIFT: tolerated - score 0.16, PolyPhen: benign - score 0
1827	chr17:g.65536884T¿G	Substitution Missense	BRCA2 E1838K	1/833,0.12%	1/13,582	VEP: MODERATE, SIFT: deleterious - score 0, PolyPhen: possibly_damaging - score 0.806
1828	chr2:g.176107385C¿A	Substitution Missense		1/833,0.12%	1/13,582	VEP: MODERATE, SIFT: deleterious - score 0.01, PolyPhen: benign - score 0.424
1829	chr11:g.108303001T¿A	Substitution Missense	ZNF384 C347Y	1/833,0.12%	1/13,582	VEP: MODERATE, SIFT: tolerated - score 0.06, PolyPhen: possibly_damaging - score 0.69
1830	chr5:g.55956079G¿C	Substitution Missense		1/833,0.12%	1/13,582	VEP: MODERATE, SIFT: tolerated - score 0.52, PolyPhen: benign - score 0
1831	chr19:g.18768752G¿C	Substitution Missense	MYO5A E1376K	1/833,0.12%	1/13,582	VEP: MODERATE, SIFT: tolerated_low_confidence - score 0.54, PolyPhen: benign - score 0.073
1832	chr17:g.50186340C¿T	Substitution Missense		1/833,0.12%	1/13,582	VEP: MODERATE, SIFT: deleterious - score 0.01, PolyPhen: probably_damaging - score 0.982
1833	chr17:g.64503231A¿T	Substitution Missense	PTPRB L212M	1/833,0.12%	1/13,582	VEP: MODERATE, SIFT: deleterious - score 0, PolyPhen: probably_damaging - score 0.998
1834	chr4:g.54261253G¿C	Substitution Missense		1/833,0.12%	1/13,582	VEP: MODERATE, SIFT: tolerated - score 0.51, PolyPhen: benign - score 0.057
1835	chr6:g.44260489C¿T	Substitution Missense	SMAD2 T409S	1/833,0.12%	1/13,582	VEP: MODERATE, SIFT: tolerated - score 0.38, PolyPhen: benign - score 0.018
1836	chr12:g.25225713T¿G	Substitution Missense		1/833,0.12%	6/13,582	VEP: MODERATE, SIFT: deleterious - score 0.01, PolyPhen: probably_damaging - score 0.994

1837	chr7:g.6374769G¿C	Substitution	Missense	BCL6 C635G	1/833,0.12%	1/13,582	VEP: MODERATE, SIFT: deleterious - score 0.02, PolyPhen: possibly_damaging - score 0.629
1838	chr5:g.180612595T¿C	Substitution	Missense		1/833,0.12%	1/13,582	VEP: MODERATE, SIFT: tolerated - score 1, PolyPhen: benign - score 0
1839	chr14:g.81143960C¿G	Substitution	Missense	ARID1B N1552S	1/833,0.12%	1/13,582	VEP: MODERATE, SIFT: deleterious - score 0, PolyPhen: probably_damaging - score 0.997
1840	chr6:g.106107136T¿A	Substitution	Missense		1/833,0.12%	1/13,582	VEP: MODERATE, SIFT: deleterious - score 0, PolyPhen: possibly_damaging - score 0.542
1841	chr17:g.5144859C¿T	Substitution	Missense	COL2A1 A445V	1/833,0.12%	1/13,582	VEP: MODERATE, SIFT: tolerated_low_confidence - score 0.27, PolyPhen: possibly_damaging - score 0.681
1842	chr11:g.69641438T¿C	Substitution	Missense		1/833,0.12%	1/13,582	VEP: MODERATE, SIFT: tolerated - score 0.71, PolyPhen: benign - score 0.009
1843	chr17:g.42217203G¿A	Substitution	Missense	NUMA1 K1475Q	1/833,0.12%	1/13,582	VEP: MODERATE, SIFT: deleterious - score 0, PolyPhen: probably_damaging - score 0.992
1844	chr7:g.2937093C¿G	Substitution	Missense		1/833,0.12%	1/13,582	VEP: MODERATE, SIFT: tolerated - score 0.16, PolyPhen: benign - score 0.11
1845	chr2:g.61502299A¿T	Substitution	Missense	AFF3 E823K	1/833,0.12%	1/13,582	VEP: MODERATE, SIFT: deleterious - score 0, PolyPhen: probably_damaging - score 0.99
1846	chr19:g.45361601T¿C	Substitution	Missense		1/833,0.12%	1/13,582	VEP: MODERATE, SIFT: deleterious - score 0.04, PolyPhen: benign - score 0.12
1847	chr11:g.69641453G¿C	Substitution	Missense	MAP2K1 E44K	1/833,0.12%	1/13,582	VEP: MODERATE, SIFT: tolerated - score 0.05, PolyPhen: benign - score 0.043
1848	chr3:g.52628901A¿C	Substitution	Missense		1/833,0.12%	1/13,582	VEP: MODERATE, SIFT: deleterious - score 0, PolyPhen: possibly_damaging - score 0.724
1849	chr15:g.87940694A¿T	Substitution	Missense	LSM14A F114L	1/833,0.12%	1/13,582	VEP: MODERATE, SIFT: deleterious - score 0, PolyPhen: probably_damaging - score 0.994
1850	chr7:g.138525323T¿C	Substitution	Missense		1/833,0.12%	1/13,582	VEP: MODERATE, SIFT: tolerated - score 0.08, PolyPhen: benign - score 0.012

1851	chrX:g.124078025G¿C	Substitution	Missense	MAF N23D	1/833,0.12%	2/13,582	VEP: MODERATE, SIFT: tolerated - score 0.29, PolyPhen: probably_damaging - score 0.926
1852	chr13:g.40665822G¿C	Substitution	Missense		1/833,0.12%	1/13,582	VEP: MODERATE, SIFT: tolerated - score 0.53, PolyPhen: benign - score 0.085
1853	chr5:g.112841717A¿C	Substitution	Missense	NCOA1 E587K	1/833,0.12%	1/13,582	VEP: MODERATE, SIFT: deleterious - score 0, PolyPhen: probably_damaging - score 0.992
1854	chr17:g.1361101C¿T	Substitution	Missense		1/833,0.12%	1/13,582	VEP: MODERATE, SIFT: deleterious_low_confidence - score 0.04, PolyPhen: benign - score 0.071
1855	chr9:g.107487091C¿T	Substitution	Missense	PTPN13 A525V	1/833,0.12%	1/13,582	VEP: MODERATE, SIFT: tolerated - score 0.17, PolyPhen: benign - score 0.031
1856	chr1:g.26731559G¿C	Substitution	Missense		1/833,0.12%	1/13,582	VEP: MODERATE, SIFT: deleterious_low_confidence - score 0.04, PolyPhen: probably_damaging - score 0.986
1857	chr8:g.31132502G¿C	Substitution	Missense	RET T48M	1/833,0.12%	1/13,582	VEP: MODERATE, SIFT: deleterious - score 0.01, PolyPhen: probably_damaging - score 0.982
1858	chr19:g.13099485G¿T	Substitution	Missense		1/833,0.12%	1/13,582	VEP: MODERATE, SIFT: tolerated - score 0.12, PolyPhen: benign - score 0.415
1859	chr1:g.155188303G¿A	Substitution	Missense	PTPN13 E759Q	1/833,0.12%	1/13,582	VEP: MODERATE, SIFT: deleterious - score 0.02, PolyPhen: probably_damaging - score 0.924
1860	chr22:g.23834152G¿A	Substitution	Missense		1/833,0.12%	5/13,582	VEP: MODERATE, SIFT: deleterious - score 0, PolyPhen: probably_damaging - score 0.912
1861	chr2:g.99554707G¿A	Substitution	Missense	PDGFRA I264N	1/833,0.12%	1/13,582	VEP: MODERATE, SIFT: deleterious - score 0, PolyPhen: possibly_damaging - score 0.768
1862	chr3:g.30672294C¿T	Substitution	Missense		1/833,0.12%	1/13,582	VEP: MODERATE, SIFT: tolerated - score 0.06, PolyPhen: benign - score 0.3
1863	chr21:g.34880583A¿G	Substitution	Missense	MECOM C90S	1/833,0.12%	2/13,582	VEP: MODERATE, SIFT: deleterious - score 0, PolyPhen: probably_damaging - score 1
1864	chr4:g.86762792C¿G	Substitution	Missense		1/833,0.12%	1/13,582	VEP: MODERATE, SIFT: tolerated - score 0.24, PolyPhen: benign - score 0.117

1865	chr2:g.47416300C¿T	Substitution	Missense	SFPQ R236G	1/833,0.12%	1/13,582	VEP: MODERATE, SIFT: tolerated - score 0.51, PolyPhen: possibly_damaging - score 0.873
1866	chr11:g.108316024G¿A	Substitution	Missense		1/833,0.12%	1/13,582	VEP: MODERATE, SIFT: deleterious - score 0.01, PolyPhen: benign - score 0.219
1867	chr5:g.112843327C¿T	Substitution	Missense	PTPRK P120R	1/833,0.12%	1/13,582	VEP: MODERATE, SIFT: deleterious - score 0, PolyPhen: probably_damaging - score 0.994
1868	chrX:g.47179982A¿T	Substitution	Missense		1/833,0.12%	1/13,582	VEP: MODERATE, SIFT: deleterious - score 0, PolyPhen: possibly_damaging - score 0.894
1869	chr10:g.103106646G¿T	Substitution	Missense	XPC Q906E	1/833,0.12%	1/13,582	VEP: MODERATE, SIFT: deleterious - score 0.05, PolyPhen: possibly_damaging - score 0.533
1870	chr4:g.54280345G¿C	Substitution	Missense		1/833,0.12%	1/13,582	VEP: MODERATE, SIFT: deleterious - score 0.03, PolyPhen: benign - score 0.443
1871	chr13:g.32337507T¿C	Substitution	Missense	KMT2C K3178R	1/833,0.12%	1/13,582	VEP: MODERATE, SIFT: tolerated - score 0.23, PolyPhen: benign - score 0.388
1872	chr10:g.68573700C¿A	Substitution	Missense		1/833,0.12%	1/13,582	VEP: MODERATE, SIFT: deleterious - score 0.02, PolyPhen: benign - score 0.249
1873	chr9:g.132900816G¿T	Substitution	Missense	PLCG1 S87L	1/833,0.12%	1/13,582	VEP: MODERATE, SIFT: tolerated - score 0.13, PolyPhen: possibly_damaging - score 0.868
1874	chr1:g.114716127C¿G	Substitution	Missense		1/833,0.12%	4/13,582	VEP: MODERATE, SIFT: deleterious - score 0.03, PolyPhen: possibly_damaging - score 0.538
1875	chr18:g.51076747G¿T	Substitution	Missense	SND1 D902N	1/833,0.12%	1/13,582	VEP: MODERATE, SIFT: tolerated - score 0.1, PolyPhen: probably_damaging - score 0.981
1876	chr17:g.7675125A¿C	Substitution	Missense		1/833,0.12%	3/13,582	VEP: MODERATE, SIFT: deleterious - score 0, PolyPhen: probably_damaging - score 1
1877	chr9:g.134041929G¿A	Substitution	Missense	CBL Y371D	1/833,0.12%	1/13,582	VEP: MODERATE, SIFT: deleterious - score 0, PolyPhen: probably_damaging - score 0.946
1878	chr12:g.53945146G¿A	Substitution	Missense		1/833,0.12%	2/13,582	VEP: MODERATE, SIFT: tolerated - score 0.11, PolyPhen: benign - score 0.166

1879	chr19:g.17842555C¿T	Substitution	Missense	TRIP11 S630Y	1/833,0.12%	1/13,582	VEP: MODERATE, SIFT: tolerated - score 0.09, PolyPhen: benign - score 0.013
1880	chr5:g.171400172G¿A	Substitution	Missense		1/833,0.12%	1/13,582	VEP: MODERATE, SIFT: tolerated - score 0.13, PolyPhen: benign - score 0.046
1881	chr4:g.86741758G¿C	Substitution	Missense	CLTC Q196E	1/833,0.12%	2/13,582	VEP: MODERATE, SIFT: deleterious - score 0.03, PolyPhen: probably_damaging - score 1
1882	chr17:g.39726577C¿G	Substitution	Missense		1/833,0.12%	1/13,582	VEP: MODERATE, SIFT: deleterious - score 0.01, PolyPhen: probably_damaging - score 0.919
1883	chr11:g.108272726A¿G	Substitution	Missense	BIRC3 K563E	1/833,0.12%	1/13,582	VEP: MODERATE, SIFT: deleterious - score 0, PolyPhen: probably_damaging - score 0.996
1884	chr14:g.50748015C¿G	Substitution	Missense		1/833,0.12%	1/13,582	VEP: MODERATE, SIFT: deleterious - score 0.01, PolyPhen: probably_damaging - score 0.943
1885	chr16:g.15745189C¿G	Substitution	Missense	SYK V633M	1/833,0.12%	1/13,582	VEP: MODERATE, SIFT: deleterious - score 0, PolyPhen: probably_damaging - score 1
1886	chr7:g.55156647T¿G	Substitution	Missense		1/833,0.12%	1/13,582	VEP: MODERATE, SIFT: deleterious - score 0.04, PolyPhen: benign - score 0.124
1887	chr22:g.41117787G¿A	Substitution	Missense	CARD11 D1137E	1/833,0.12%	1/13,582	VEP: MODERATE, SIFT: deleterious - score 0.01, PolyPhen: probably_damaging - score 0.978
1888	chr10:g.70598388C¿T	Substitution	Missense		1/833,0.12%	1/13,582	VEP: MODERATE, SIFT: tolerated - score 0.2, PolyPhen: possibly_damaging - score 0.457
1889	chr17:g.8146938A¿G	Substitution	Missense	CCND1 N24T	1/833,0.12%	1/13,582	VEP: MODERATE, SIFT: tolerated - score 0.28, PolyPhen: probably_damaging - score 0.921
1890	chr7:g.124863379C¿G	Substitution	Missense		1/833,0.12%	1/13,582	VEP: MODERATE, SIFT: tolerated - score 0.33, PolyPhen: benign - score 0.003
1891	chr1:g.77966907C¿A	Substitution	Missense	NFKB2 L619Q	1/833,0.12%	1/13,582	VEP: MODERATE, SIFT: deleterious - score 0, PolyPhen: probably_damaging - score 0.997
1892	chr3:g.52550496C¿T	Substitution	Missense		1/833,0.12%	1/13,582	VEP: MODERATE, SIFT: deleterious - score 0.01, PolyPhen: probably_damaging - score 0.987

1893	chr4:g.125490755C¿A	Substitution	Missense	CCND1 P18L	1/833,0.12%	1/13,582	VEP: MODERATE, SIFT: tolerated - score 0.29, PolyPhen: probably_damaging - score 0.946
1894	chr4:g.125448569T¿A	Substitution	Missense		1/833,0.12%	1/13,582	VEP: MODERATE, SIFT: tolerated - score 0.61, PolyPhen: possibly_damaging - score 0.841
1895	chr10:g.8058716C¿A	Substitution	Missense	BCL7A S12G	1/833,0.12%	1/13,582	VEP: MODERATE, SIFT: deleterious - score 0.01, PolyPhen: benign - score 0.379
1896	chr5:g.55964157G¿T	Substitution	Missense		1/833,0.12%	2/13,582	VEP: MODERATE, SIFT: deleterious - score 0, PolyPhen: probably_damaging - score 0.999
1897	chr6:g.117389505C¿T	Substitution	Missense	NFATC2 S107L	1/833,0.12%	1/13,582	VEP: MODERATE, SIFT: tolerated - score 0.26, PolyPhen: benign - score 0
1898	chr4:g.86759018T¿A	Substitution	Missense		1/833,0.12%	1/13,582	VEP: MODERATE, SIFT: deleterious - score 0.01, PolyPhen: benign - score 0.156
1899	chr14:g.99175803A¿T	Substitution	Missense	HIF1A S800C	1/833,0.12%	1/13,582	VEP: MODERATE, SIFT: deleterious - score 0.02, PolyPhen: probably_damaging - score 0.998
1900	chr3:g.9013780C¿T	Substitution	Missense		1/833,0.12%	2/13,582	VEP: MODERATE, SIFT: deleterious - score 0, PolyPhen: possibly_damaging - score 0.631
1901	chr12:g.111418392C¿T	Substitution	Missense	MECOM P384T	1/833,0.12%	1/13,582	VEP: MODERATE, SIFT: tolerated - score 0.19, PolyPhen: benign - score 0
1902	chr19:g.53577860A¿G	Substitution	Missense		1/833,0.12%	1/13,582	VEP: MODERATE, SIFT: deleterious - score 0, PolyPhen: benign - score 0.007
1903	chr1:g.11240432G¿A	Substitution	Missense	ETV1 H184Y	1/833,0.12%	1/13,582	VEP: MODERATE, SIFT: tolerated - score 0.06, PolyPhen: possibly_damaging - score 0.586
1904	chr5:g.170919493G¿C	Substitution	Missense		1/833,0.12%	1/13,582	VEP: MODERATE, SIFT: deleterious - score 0, PolyPhen: probably_damaging - score 0.986
1905	chr7:g.98988874C¿T	Substitution	Missense	KMT2C E1342K	1/833,0.12%	3/13,582	VEP: MODERATE, SIFT: deleterious - score 0, PolyPhen: probably_damaging - score 0.987
1906	chr4:g.125317667T¿G	Substitution	Missense		1/833,0.12%	1/13,582	VEP: MODERATE, SIFT: deleterious - score 0.01, PolyPhen: probably_damaging - score 0.998

1907	chr14:g.37592092A¿G	Substitution	Missense	ZNF331 R263K	1/833,0.12%	1/13,582	VEP: MODERATE, SIFT: deleterious - score 0, PolyPhen: probably_damaging - score 0.999
1908	chr19:g.11010397G¿C	Substitution	Missense		1/833,0.12%	1/13,582	VEP: MODERATE, SIFT: deleterious - score 0.04, PolyPhen: possibly_damaging - score 0.688
1909	chr16:g.79599079T¿C	Substitution	Missense	MAML2 T980M	1/833,0.12%	1/13,582	VEP: MODERATE, SIFT: deleterious - score 0, PolyPhen: probably_damaging - score 0.993
1910	chr7:g.92003107G¿C	Substitution	Missense		1/833,0.12%	1/13,582	VEP: MODERATE, SIFT: deleterious - score 0.03, PolyPhen: benign - score 0.007
1911	chr7:g.138918436G¿A	Substitution	Missense	NFE2L2 M484I	1/833,0.12%	1/13,582	VEP: MODERATE, SIFT: tolerated - score 0.07, PolyPhen: benign - score 0.115
1912	chr11:g.69641366C¿G	Substitution	Missense		1/833,0.12%	1/13,582	VEP: MODERATE, SIFT: tolerated - score 0.8, PolyPhen: benign - score 0
1913	chr16:g.2172262G¿C	Substitution	Missense	DICER1 R490C	1/833,0.12%	1/13,582	VEP: MODERATE, SIFT: tolerated - score 0.09, PolyPhen: benign - score 0.231
1914	chr10:g.75030830G¿A	Substitution	Missense		1/833,0.12%	1/13,582	VEP: MODERATE, SIFT: deleterious - score 0, PolyPhen: possibly_damaging - score 0.661
1915	chr7:g.152152897T¿C	Substitution	Missense	NFKB2 H639R	1/833,0.12%	1/13,582	VEP: MODERATE, SIFT: deleterious - score 0.01, PolyPhen: possibly_damaging - score 0.787
1916	chr4:g.186621545T¿G	Substitution	Missense		1/833,0.12%	1/13,582	VEP: MODERATE, SIFT: tolerated - score 0.55, PolyPhen: benign - score 0.003
1917	chr1:g.35192965G¿A	Substitution	Missense	SETD2 I2005L	1/833,0.12%	1/13,582	VEP: MODERATE, SIFT: deleterious_low_confidence - score 0, PolyPhen: possibly_damaging - score 0.775
1918	chr4:g.125452407G¿T	Substitution	Missense		1/833,0.12%	1/13,582	VEP: MODERATE, SIFT: tolerated - score 0.16, PolyPhen: benign - score 0.133
1919	chr11:g.118436675C¿T	Substitution	Missense	ELK4 S317T	1/833,0.12%	1/13,582	VEP: MODERATE, SIFT: tolerated_low_confidence - score 0.16, PolyPhen: benign - score 0
1920	chr7:g.124851950C¿A	Substitution	Missense		1/833,0.12%	1/13,582	VEP: MODERATE, SIFT: tolerated - score 1, PolyPhen: benign - score 0.014
1921	chr17:g.43104193T¿C	Substitution	Missense	FGFR1 D558G	1/833,0.12%	1/13,582	VEP: MODERATE, SIFT: tolerated - score 0.23, PolyPhen: benign - score 0.017

1922	chr3:g.142561385C¿T	Substitution Missense		1/833,0.12%	1/13,582	VEP: MODERATE, SIFT: deleterious_low_confidence - score 0.01, PolyPhen: benign - score 0.162
1923	chr8:g.56216491C¿T	Substitution Missense	ZNF521 T357A	1/833,0.12%	1/13,582	VEP: MODERATE, SIFT: deleterious - score 0.01, PolyPhen: benign - score 0.211
1924	chr11:g.46320371G¿A	Substitution Missense		1/833,0.12%	1/13,582	VEP: MODERATE, SIFT: tolerated_low_confidence - score 0.34, PolyPhen: benign - score 0.014
1925	chr1:g.186331558A¿C	Substitution Missense	SF3B1 M867R	1/833,0.12%	1/13,582	VEP: MODERATE, SIFT: deleterious - score 0, PolyPhen: probably_damaging - score 0.991
1926	chr16:g.11254865C¿G	Substitution Missense		1/833,0.12%	1/13,582	VEP: MODERATE, SIFT: tolerated - score 0.57, PolyPhen: benign - score 0.288
1927	chr3:g.53747400C¿G	Substitution Missense	ETV5 E506K	1/833,0.12%	1/13,582	VEP: MODERATE, SIFT: deleterious - score 0.01, PolyPhen: possibly_damaging - score 0.879
1928	chr13:g.32339147C¿T	Substitution Missense		1/833,0.12%	2/13,582	VEP: MODERATE, SIFT: tolerated - score 0.11, PolyPhen: probably_damaging - score 0.986
1929	chr3:g.185443543C¿T	Substitution Missense	AFF4 D60N	1/833,0.12%	1/13,582	VEP: MODERATE, SIFT: deleterious - score 0, PolyPhen: probably_damaging - score 0.985
1930	chr8:g.41987493G¿A	Substitution Missense		1/833,0.12%	1/13,582	VEP: MODERATE, SIFT: deleterious - score 0, PolyPhen: probably_damaging - score 0.955
1931	chrX:g.67546670G¿T	Substitution Missense	WWTR1 L300R	1/833,0.12%	1/13,582	VEP: MODERATE, SIFT: deleterious_low_confidence - score 0.01, PolyPhen: benign - score 0.015
1932	chrX:g.45090753A¿T	Substitution Missense		1/833,0.12%	2/13,582	VEP: MODERATE, SIFT: tolerated - score 0.08, PolyPhen: probably_damaging - score 0.995
1933	chr11:g.108247048G¿C	Substitution Missense	NF1 L2100I	1/833,0.12%	2/13,582	VEP: MODERATE, SIFT: deleterious - score 0, PolyPhen: probably_damaging - score 0.994
1934	chr6:g.106106474C¿T	Substitution Missense		1/833,0.12%	1/13,582	VEP: MODERATE, SIFT: deleterious - score 0, PolyPhen: probably_damaging - score 1
1935	chr11:g.108299759C¿G	Substitution Missense	CHD4 E1765K	1/833,0.12%	2/13,582	VEP: MODERATE, SIFT: deleterious - score 0, PolyPhen: benign - score 0.227

1936	chr12:g.12718024T¿G	Substitution Missense		1/833,0.12%	1/13,582	VEP: MODERATE, SIFT: deleterious - score 0, PolyPhen: probably_damaging - score 0.998
1937	chr17:g.42333695C¿T	Substitution Missense	CLTCL1 A493E	1/833,0.12%	2/13,582	VEP: MODERATE, SIFT: tolerated - score 0.2, PolyPhen: possibly_damaging - score 0.76
1938	chr1:g.204530696T¿G	Substitution Missense		1/833,0.12%	1/13,582	VEP: MODERATE, SIFT: deleterious - score 0, PolyPhen: probably_damaging - score 0.984
1939	chr19:g.42290753C¿A	Substitution Missense	KMT2A S859F	1/833,0.12%	1/13,582	VEP: MODERATE, SIFT: deleterious_low_confidence - score 0.01, PolyPhen: benign - score 0
1940	chr12:g.112450394G¿C	Substitution Missense		1/833,0.12%	1/13,582	VEP: MODERATE, SIFT: deleterious - score 0, PolyPhen: possibly_damaging - score 0.454
1941	chr3:g.53673741C¿T	Substitution Missense	BRCA1 Q1069E	1/833,0.12%	1/13,582	VEP: MODERATE, SIFT: deleterious - score 0, PolyPhen: probably_damaging - score 0.999
1942	chr17:g.8143534G¿T	Substitution Missense		1/833,0.12%	1/13,582	VEP: MODERATE, SIFT: deleterious - score 0.01, PolyPhen: possibly_damaging - score 0.887
1943	chr1:g.47260441G¿T	Substitution Missense	WAS N261S	1/833,0.12%	1/13,582	VEP: MODERATE, SIFT: tolerated - score 0.1, PolyPhen: benign - score 0.219
1944	chr16:g.3731371C¿T	Substitution Missense		1/833,0.12%	1/13,582	VEP: MODERATE, SIFT: deleterious - score 0, PolyPhen: probably_damaging - score 0.99
1945	chr1:g.150829932A¿G	Substitution Missense	PBRM1 R836W	1/833,0.12%	1/13,582	VEP: MODERATE, SIFT: tolerated - score 0.18, PolyPhen: probably_damaging - score 0.959
1946	chr5:g.180621108G¿A	Substitution Missense		1/833,0.12%	1/13,582	VEP: MODERATE, SIFT: deleterious - score 0, PolyPhen: probably_damaging - score 0.979
1947	chr4:g.152411707T¿C	Substitution Missense	NTRK3 K746M	1/833,0.12%	1/13,582	VEP: MODERATE, SIFT: deleterious_low_confidence - score 0.01, PolyPhen: benign - score 0.001
1948	chr16:g.72957872C¿G	Substitution Missense		1/833,0.12%	1/13,582	VEP: MODERATE, SIFT: deleterious - score 0, PolyPhen: probably_damaging - score 0.997
1949	chr11:g.72018917C¿G	Substitution Missense	CCND1 V10M	1/833,0.12%	1/13,582	VEP: MODERATE, SIFT: tolerated - score 0.07, PolyPhen: benign - score 0.001

1950	chr4:g.125415289C¿A	Substitution Missense		1/833,0.12%	1/13,582	VEP: MODERATE, SIFT: deleterious - score 0.01, PolyPhen: possibly_damaging - score 0.707
1951	chr1:g.119925642G¿T	Substitution Missense	NF2 A238T	1/833,0.12%	1/13,582	VEP: MODERATE, SIFT: tolerated - score 0.87, PolyPhen: benign - score 0
1952	chr3:g.30650416C¿T	Substitution Missense		1/833,0.12%	1/13,582	VEP: MODERATE, SIFT: deleterious - score 0.03, PolyPhen: probably_damaging - score 0.986
1953	chr19:g.11060176G¿C	Substitution Missense	HIF1A K80Q	1/833,0.12%	1/13,582	VEP: MODERATE, SIFT: deleterious_low_confidence - score 0.01, PolyPhen: benign - score 0.076
1954	chr7:g.140834757G¿A	Substitution Missense		1/833,0.12%	1/13,582	VEP: MODERATE, SIFT: tolerated - score 0.09, PolyPhen: benign - score 0.125
1955	chr9:g.107488182G¿T	Substitution Missense	GOPC K117N	1/833,0.12%	1/13,582	VEP: MODERATE, SIFT: tolerated - score 0.68, PolyPhen: benign - score 0.109
1956	chr1:g.7736387G¿A	Substitution Missense		1/833,0.12%	1/13,582	VEP: MODERATE, SIFT: deleterious - score 0, PolyPhen: probably_damaging - score 0.994
1957	chr6:g.37170604C¿T	Substitution Missense	FAT1 E2788K	1/833,0.12%	1/13,582	VEP: MODERATE, SIFT: deleterious_low_confidence - score 0.01, PolyPhen: benign - score 0.189
1958	chr19:g.3110299C¿T	Substitution Missense		1/833,0.12%	1/13,582	VEP: MODERATE, SIFT: tolerated - score 0.15, PolyPhen: benign - score 0.062
1959	chr3:g.100736639C¿T	Substitution Missense	ETV1 N219S	1/833,0.12%	1/13,582	VEP: MODERATE, SIFT: deleterious - score 0, PolyPhen: probably_damaging - score 0.966
1960	chr13:g.28034382G¿T	Substitution Missense		1/833,0.12%	1/13,582	VEP: MODERATE, SIFT: tolerated - score 0.13, PolyPhen: benign - score 0
1961	chr19:g.50876543G¿T	Substitution Missense	ERG P411T	1/833,0.12%	1/13,582	VEP: MODERATE, SIFT: tolerated - score 0.09, PolyPhen: benign - score 0.152
1962	chr4:g.105243756C¿T	Substitution Missense		1/833,0.12%	1/13,582	VEP: MODERATE, SIFT: deleterious - score 0, PolyPhen: probably_damaging - score 1
1963	chr5:g.112840737G¿A	Substitution Missense	PDGFRA D691N	1/833,0.12%	1/13,582	VEP: MODERATE, SIFT: tolerated_low_confidence - score 0.13, PolyPhen: benign - score 0.136

1964	chr1:g.186345633C¿T	Substitution Missense		1/833,0.12%	1/13,582	VEP: MODERATE, SIFT: tolerated - score 0.13, PolyPhen: benign - score 0.29
1965	chr5:g.112754928T¿G	Substitution Missense	FAT1 E2788Q	1/833,0.12%	1/13,582	VEP: MODERATE, SIFT: deleterious - score 0.02, PolyPhen: probably_damaging - score 0.998
1966	chr4:g.125317618G¿A	Substitution Missense		1/833,0.12%	1/13,582	VEP: MODERATE, SIFT: deleterious - score 0.03, PolyPhen: probably_damaging - score 0.99
1967	chr18:g.25225251G¿T	Substitution Missense	SOCS1 A156T	1/833,0.12%	1/13,582	VEP: MODERATE, SIFT: tolerated - score 0.05, PolyPhen: possibly_damaging - score 0.684
1968	chr4:g.125451707G¿A	Substitution Missense		1/833,0.12%	1/13,582	VEP: MODERATE, SIFT: deleterious - score 0, PolyPhen: probably_damaging - score 1
1969	chr15:g.34356692T¿C	Substitution Missense	KLF4 D14N	1/833,0.12%	1/13,582	VEP: MODERATE, SIFT: tolerated - score 0.09, PolyPhen: benign - score 0.063
1970	chr11:g.128810942G¿A	Substitution Missense		1/833,0.12%	2/13,582	VEP: MODERATE, SIFT: tolerated - score 0.06, PolyPhen: benign - score 0.072
1971	chr7:g.92001565A¿T	Substitution Missense	HNRNPA2B1 D49H	1/833,0.12%	1/13,582	VEP: MODERATE, SIFT: tolerated - score 0.28, PolyPhen: benign - score 0.3
1972	chrX:g.53210472A¿G	Substitution Missense		1/833,0.12%	1/13,582	VEP: MODERATE, SIFT: deleterious - score 0, PolyPhen: probably_damaging - score 1
1973	chr6:g.44265139C¿T	Substitution Missense	CXCR4 S356R	1/833,0.12%	1/13,582	VEP: MODERATE, SIFT: deleterious - score 0, PolyPhen: possibly_damaging - score 0.896
1974	chr11:g.118436687G¿A	Substitution Missense		1/833,0.12%	1/13,582	VEP: MODERATE, SIFT: tolerated_low_confidence - score 0.16, PolyPhen: benign - score 0.039
1975	chr2:g.208248388C¿T	Substitution Missense	TCL1A E40G	1/833,0.12%	389/13,582	VEP: MODERATE, SIFT: deleterious_low_confidence - score 0.01, PolyPhen: benign - score 0.047
1976	chr2:g.60553228G¿A	Substitution Missense		1/833,0.12%	1/13,582	VEP: MODERATE, SIFT: deleterious_low_confidence - score 0, PolyPhen: probably_damaging - score 0.988
1977	chr16:g.72788759G¿A	Substitution Missense	KMT2C H290N	1/833,0.12%	1/13,582	VEP: MODERATE, SIFT: tolerated - score 0.17, PolyPhen: benign - score 0.057

1978	chr17:g.40628799C¿G	Substitution Missense		1/833,0.12%	1/13,582	VEP: MODERATE, SIFT: deleterious_low_confidence - score 0.01, PolyPhen: benign - score 0.188
1979	chr15:g.88183483G¿C	Substitution Missense	CDKN1B Y88C	1/833,0.12%	1/13,582	VEP: MODERATE, SIFT: deleterious - score 0, PolyPhen: probably_damaging - score 0.989
1980	chr14:g.37591385G¿A	Substitution Missense		1/833,0.12%	1/13,582	VEP: MODERATE, SIFT: tolerated - score 0.39, PolyPhen: probably_damaging - score 0.994
1981	chr16:g.79599691G¿T	Substitution Missense	XPA E245K	1/833,0.12%	1/13,582	VEP: MODERATE, SIFT: deleterious - score 0, PolyPhen: probably_damaging - score 0.999
1982	chrX:g.47145478C¿T	Substitution Missense		1/833,0.12%	1/13,582	VEP: MODERATE, SIFT: deleterious_low_confidence - score 0.02, PolyPhen: benign - score 0.04
1983	chr11:g.108253854G¿C	Substitution Missense	CEP89 L205M	1/833,0.12%	1/13,582	VEP: MODERATE, SIFT: tolerated - score 0.16, PolyPhen: benign - score 0.031
1984	chr13:g.40666092T¿G	Substitution Missense		1/833,0.12%	1/13,582	VEP: MODERATE, SIFT: deleterious - score 0, PolyPhen: probably_damaging - score 0.987
1985	chr8:g.17966349A¿T	Substitution Missense	CYLD E720G	1/833,0.12%	1/13,582	VEP: MODERATE, SIFT: tolerated - score 0.2, PolyPhen: probably_damaging - score 0.998
1986	chr12:g.27671511G¿T	Substitution Missense		1/833,0.12%	1/13,582	VEP: MODERATE, SIFT: tolerated - score 0.35, PolyPhen: benign - score 0
1987	chr4:g.87114949G¿A	Substitution Missense	ZFHX3 E1383K	1/833,0.12%	1/13,582	VEP: MODERATE, SIFT: deleterious - score 0.03, PolyPhen: benign - score 0.223
1988	chrX:g.77696648T¿C	Substitution Missense		1/833,0.12%	1/13,582	VEP: MODERATE, SIFT: tolerated - score 0.13, PolyPhen: probably_damaging - score 0.992
1989	chr4:g.125321206C¿T	Substitution Missense	BRAF G636S	1/833,0.12%	1/13,582	VEP: MODERATE, SIFT: tolerated - score 0.06, PolyPhen: probably_damaging - score 0.996
1990	chr2:g.212124756A¿T	Substitution Missense		1/833,0.12%	1/13,582	VEP: MODERATE, SIFT: deleterious - score 0, PolyPhen: probably_damaging - score 0.992
1991	chr12:g.49034424G¿A	Substitution Missense	NTRK3 S195P	1/833,0.12%	1/13,582	VEP: MODERATE, SIFT: tolerated - score 0.39, PolyPhen: benign - score 0.026

1992	chr17:g.7673796C¿T	Substitution Missense		1/833,0.12%	23/13,582	VEP: MODERATE, SIFT: deleterious - score 0, PolyPhen: probably_damaging - score 0.997
1993	chr16:g.50750025G¿T	Substitution Missense	KAT6B L942M	1/833,0.12%	1/13,582	VEP: MODERATE, SIFT: deleterious - score 0, PolyPhen: probably_damaging - score 0.977
1994	chr17:g.40354346G¿A	Substitution Missense		1/833,0.12%	1/13,582	VEP: MODERATE, SIFT: tolerated - score 0.06, PolyPhen: possibly_damaging - score 0.543
1995	chr17:g.31225188C¿T	Substitution Missense	PPP2R1A E376K	1/833,0.12%	2/13,582	VEP: MODERATE, SIFT: tolerated - score 0.14, PolyPhen: benign - score 0.031
1996	chr5:g.170924404A¿G	Substitution Missense		1/833,0.12%	1/13,582	VEP: MODERATE, SIFT: deleterious - score 0.01, PolyPhen: probably_damaging - score 0.987
1997	chr10:g.102398787C¿A	Substitution Missense	ALK A1564V	1/833,0.12%	1/13,582	VEP: MODERATE, SIFT: tolerated - score 0.09, PolyPhen: benign - score 0.01
1998	chr4:g.125449583C¿G	Substitution Missense		1/833,0.12%	1/13,582	VEP: MODERATE, SIFT: deleterious - score 0, PolyPhen: probably_damaging - score 0.998
1999	chr16:g.72794892G¿A	Substitution Missense	NCOR1 E642V	1/833,0.12%	1/13,582	VEP: MODERATE, SIFT: deleterious - score 0, PolyPhen: benign - score 0.111
2000	chr19:g.54149600G¿A	Substitution Missense	NTRK3 S195P	1/833,0.12%	1/13,582	VEP: MODERATE, SIFT: tolerated - score 0.06, PolyPhen: possibly_damaging - score 0.838
2001	chr16:g.89770215C¿T	Substitution Missense		1/833,0.12%	1/13,582	VEP: MODERATE, SIFT: tolerated - score 0.97, PolyPhen: benign - score 0
2002	chrX:g.77682135C¿T	Substitution Missense	KAT6B L942M	1/833,0.12%	1/13,582	VEP: MODERATE, SIFT: tolerated_low_confidence - score 0.17, PolyPhen: benign - score 0.031
2003	chr12:g.120979072G¿T	Substitution Missense		1/833,0.12%	1/13,582	VEP: MODERATE, SIFT: tolerated - score 0.06, PolyPhen: benign - score 0.291
2004	chr9:g.107487433G¿C	Substitution Missense	PPP2R1A E376K	1/833,0.12%	1/13,582	VEP: MODERATE, SIFT: deleterious - score 0.03, PolyPhen: benign - score 0
2005	chr7:g.152152915G¿T	Substitution Missense		1/833,0.12%	1/13,582	VEP: MODERATE, SIFT: tolerated - score 0.2, PolyPhen: benign - score 0.236

2006	chr2:g.15945999C¿G	Substitution Missense	ALK A1564V	1/833,0.12%	1/13,582	VEP: MODERATE, SIFT: tolerated - score 0.1, PolyPhen: probably_damaging - score 0.984
2007	chr1:g.15934140T¿G	Substitution Missense	BRAF G636S	1/833,0.12%	1/13,582	VEP: MODERATE, SIFT: tolerated_low_confidence - score 0.29, PolyPhen: possibly_damaging - score 0.746

TABLE 2: Candidate relapse Biomarkers Proteins IDs and Sequences

Sr#	Homo sapien Genes	Sequence	Accession no
1	TCL1A	MAECPTLGEAVTDHPDRLWAWEKFVYLDEKQH AWLPL TIEIKDRLQLRVLLRREDVVLGRPMTPT QIGPSLLPIMW QLYPDGRYRSSDSSFWRLVYH IKIDGVEDMLLELLPDD MEKSKNFRIDALLAVDPPRAASAQSAPLALVT SLAAAA SGTGGGGGGGGASGGTSGSCSPASSE PPAAPADRLRAE SPSPPRLLAAHCALLPKPGF LGAGGGGGGTGGGHGGP HHHAHPGAAAAAAAAA AAAAAAGGLALGLHPGGAQG	P56279
2	MNX1	GAGLPAQAALYG HPVYGYSAAAAAAALAGQHPALSY SYPQVQGA HPAHPADPIKLGAGTFQLDQWLRASTAGMI LP KMPDFNSQAQSNLLGKCRRPRTAFTSQQLLEL EHQF KLNKYLSRPKRFEVATSLMLTETQVKIW FQNRRMKWK RSKKAKEQAAQEAEKQKGGGGGA GKGGAEEPGAEEL LGPPAPGDKGSGRRLRDLRDSDPEEDEDEDDEDHFPYS NGASVHAASSDCS SEDDSPPPRPSHQPAPQ	P50219
3	ERG	MASTIKEALSVVSEDQSLFECAYGTPHLAKTE MTASSSS DYGQTSKMSPRVPQQDWLSQPPARV TIKMECNPSQVNG SRNSPDECSVAKGGKMVGS PDTVGMNYGSYMEEKHMP PPNMTTNERRVIVP ADPTLWSTDHVRQWLEWAVKEYGL PDVNILLF QNIDGKELCKMTKDDFQRLTPSYNADILLSHL HYLRETPLPHLTSDDVDKALQNSPRLMHARNT GGAAFIF PNTSVYPEATQRITTRPDLPYEPPR RSAWTGHGHPTPQSK AAQPSPSTVPKTEDQRP QLDPYQILGPTSSRLANPGSGQI QLWQFLLEL LSDSSNSSCITWEGTNGEFKMTDPDEVARR WG ERKSKPNMNYDKLSRALRYYYDKNIMTKVHGK RY AYKFDFHGIAQALQPHPPESSLYKYPSDLP YMGSYHAHP QKMNFVAPHPPALPVTSSSFFAA PNPYWNSPTGGIYPNT RLPTSHMPSHLGTYY	P11308

Sr#	Homo sapien Genes	Sequence	Accession no
4	AFF3	MDSFDLALLQEWDLESLCVYEPDRNALRRKER ERRN QETQQDDGTFNSSYSLFSEPYKTNKGDE LSNRIQNTL GNYDEMKDFLTDRSNQSHLVGVP KPGVPQTPVNKID EHFVADSRAQNQPSSICST TTSTPAAVPVQQSKRGTMG WQKAGHPPSDGQQ RATQQGSLRTLLGDGVGRQQPRA KQVCNVEVG LQTQERPPAMAAKHSSSGHCVQNFPPSL ASKP SLVQQKPTAYVRPMDGQDQAPDESPKLKSSSETS VHCTSYRGVPASKPEPARAKAKLSKFSIPK QGEESRSG ETNSCVEEIIREMTWLPPLSAIQA PGKVEPTKFPFPNKDS QLVSSGHNNPKKGDAE PESPDNGTSNTSMLEDDLKLSS DEEENEQQAA QRTALRALSDSAVVQQPNCRTSVPSSKG SSSS SSSGSSSSSSDSESSSGSDSETESSSSESEGS KPPHFS SPEAEPASSNKWQLDKWLNKVNPHKP PILIQNESHGSES NQYYNPVKEDVQDCGKVPD VCQPSLREKEIKSTCKEEQ RPRTANKAPGSKG VKQKSPPAAVAVAVSAAAPPPAVPCAP AENAP APARRSAGKKPTRRTERTSAGDGANCHRPEEPAA ADALGTSVVVPPEPTKTRPCGNNRASHRKE LRSSVTCEK RRTRGLSRIVPKSKEFIETESSS SSSSSDSDLESEQEEYPLS KAQTVAASASSGN DQRLKEAAANGGSGPRAPVGSINAR TTSDIAK ELEEQFYTLVPFGRNELLSPLKDSDEIRSLWVK IDLTLLSRIPEHLPQEPGVLSAPATKDSESA PPSHTSDTPAE KALPKSKRKRKCDNEDDYREI KKSQGEKDSSSRLATSTS NTLSANHCNMNINS VAIPINKNEKMLRSPISPLSDASKHK YTSEDL TSSSRPNGNSLFTSASSSKKPKADSQLQPHGGDL TKAAHNNSENIPLHKSRPQTKPWSPGSNGH RDCKRQKLV FDDMPRSADYFMQEAKRMKHKAD AMVEKFGKALNYAE AALSFIECGNAMEQGPME SKSPYTMYSETVELIRYAMRL KTHSGPNATPE DKQLAALCYRCLALLYWRMFRLKRDHA VKYSK ALIDYFKNSSKAAQAPSPWGASGKSTGTPSPMSP NPSPASSVGSQGSLSNASALSPSTIVSIPQ RIHQMAANHVS ITNSILHSYDYWEMADNLAKE NREFFNDLDLLMGPVTLH SSMEHLVQYSQQGLHWLRNSAHLS	P51826
5	KRAS	MTEYKLVVVGAGGVGKSALTIQLIQNHFVDEY DPTIEDSY RKQVVIDGETCLLDILDTAGQEEY SAMRDQYMRTGEGFL CVFAINNTKSFEDIHHY REQIKRVKDSEDVPMVLVGNKCD LPSRTVDTK QAQDLARSYGIPFIETSAKTRQRVEDAFYTLV REIRQYRLKKISKEEKTPGCVKIKKCIIM	P01116
6	NRAS	MTEYKLVVVGAGGVGKSALTIQLIQNHFVDEY DPTIEDSY RKQVVIDGETCLLDILDTAGQEEY SAMRDQYMRTGEGFL CVFAINNSKSFADINLY REQIKRVKDSDDVPMVLVGNKCD LPTRTVDTK QAHELAKSYGIPFIETSAKTRQGVEDAFYTLV REIRQYRMKKLNSSDDGTQGCMGLPCVVM	P01111

Sr#	Homo sapien Genes	Sequence	Accession no
7	FAT1	MGRHLALLLLLLLLFQHFGDSDGSQRLEQTPLQFTHLEYN VTVQENSAAKTYVGHPVKMGVYITHPAWEVRYKIVSGDS ENLFKAEEYILGDFCFLRIRTKGGNTAILNREVKDHYTLIVK ALEKNTNVEARTKVRVQVLDTNDLRPLFSPTSYSVSLPENT AIRTSIARVSATDADIGTNGEFYYSFKDRTDMFAIHPTSGVIV LTGRLDYLETKLYEMEILAADRGMKLYGSSGISSMAKLTVH IEQANECAPVITAVTLSPSELDRDPAYAIVTVDDCDQGANGD IASLSIVAGDLLQQFRTVRSFPGSKEYKVKAIGGIDWDSHPF GYNLTLQAKDKGTPPQFSSVKVIHVTSPQFKAGPVKFEKDV YRAEISEFAPPNTPVVMVKAIPAYSHLRYVFKSTPGKAKFSL NYNTGLISILEPVKRQQAAHFELEVTTSDRKASTKVLVKVL GANSNPPEFTQTAYKAAFDENVPIGTTVMSLSAVDPDEGEN GYVTYSIANLNHVPFAIDHFTGAVSTSENLDYELMPRVYTL RIRASDWGLPYRREVEVLATITLNNLNDNTPLFEKINCEGTI PRDLGVGEQITTVSAIDADELQLVQYQIEAGNELDFFSLNPN SGVLSLKRSLMDGLGAKVSFHSLRITATDGENFATPLYINITV AASHKLVNLQCEETGVAKMLAEKLLQANKLHNQGEVEDIF FDSHSVNAHIPQFRSTLPTGIQVKENQPVGSSVIFMNSTDLD TGFNGKLVYAVSGGNEDSCFMIDMETGMLKILSPLDRETTD KYTLNITVYDLGIPQKAAWRLLHVVVVDANDNPPEFLQESY FVEVSEDKEVHSEIIQVEATDKDLGPNGHVTYSIVTDTDTFS IDSVTGVVNIARPLDRELQHEHSLKIEARDQAREEPQLFSTV VVKVSLEDVNDNPPTFIPPNYRVKVREDLPEGTVIMWLEAH DPDLGQSGQVRYSLLDHGEGNFDVDKLSGAVRIVQQLDFEK KQVYNLTVRAKDKGKPVSLSSTCYVEVEVVDVNENLHPPV FSSFVEKGTVKEDAPVGSLVMTVSAHDEDARRDGEIRYSIRD GSGVGVFKIGEETGVIETSDRLDRESTSHYWLTVFATDQGVV PLSSFIEIYIEVEDVNDNAPQTSEPVYYPEIMENSPKDVSVVQI EAFDPDSSSNDKLMYKITSGNPQGFFSIHPKTGLITTTSRKLD REQQDEHILEVTVTDNGSPPKSTIARVIVKILDENDNKPQFLQ KFYKIRLPEREKPDRERNARREPLYHVIATDKDEGPNAEISYSI EDGNEHGKFFIEPKTGVVSSKRFSAAGEYDILSIKAVDNGRPQ KSSTTRLHIEWISKPKPSLEPISFEESFFTFTVMESDPVAHMIGV ISVEPPGIPLWFDITGGNYDSHFDVDKGTGTIIVAKPLDAEQK	Q14517

Sr#	Homo sapien Genes	Sequence	Accession no
		SNYNLTVEATDGTTTILTQVFIKVIDTNDHRPQFSTSKYEVV	
		IPEDTAPETEILQISAVDQDEKNKLIYTLQSSRDPLSLKKFRL	
		DPATGSLYTSEKLDHEAVHQHTLTVMVRDQDVPVKRNFAR	
		IVVNVSDTNDHAPWFTASSYKGRVYESAAVGSVVLQVTA	
		LDKDKGKNAEVLYSIESGNIGNSFMIDPVLGSIKTAKELDR	
		SNQAEYDLMVKATDKGSPPMSEITSVRIFVTIADNASPKFTS	
		KEYSVELSETVSIGSFVGMVTAHSQSSVVYEIKDGNTGDAFD	
		INPHSGTIITQKALDFETLPIYTLIIQGTNMAGLSTNTTVLVHL	
		QDENDNAPVFMQAEYTGLISESASINSVVLTDRNVPLVIRAA	
		ADKDSNALLVYHIVEPSVHTYFAIDSSTGAIHTVLSLDYEETS	
		FHFTVQVHDMGTPRLFAEYAANVTVHVIDINDCPPVFAKPLY	
		ASLLLPTYKGVKVITVNATDADSSAFSQLIYSITEGNIGEKFSM	
		YKTGALTVQNTTQLRSRYELTVRASDGRFAGLTSVKINVKESK	
		SHLKFTQDVYSAVVKENSTEAETLAVITAIGNPINEPLFYHILNP	
		RRFKISRTSGVLSTTGTPFDREQQEAFDVVVEVTEEHKPSAVAH	
		VVVKVIVEDQNDNAPVFVNLPYYAVVKVDTEVGHVIRYVTAV	
		DRDSGRNGEVHYYLKEHHEHFQIGPLGEISLKKQFELDTLNKE	
		YLVTVVAKDGGNPAFSAEVIVPITVMNKAMPVFEKPFYSAEIAE	
		SIQVHSPVVHVQANSPEGLKVFYSITDGDPFSQFTINFNTGVINV	
		IAPLDFEAHPAYKLSIRATDSLTGAHAEVFVDIIVDDINDNPPVFA	
		QQSYAVTLSEASVIGTSVVQVRATDSDSEPNRGISYQMFGNHSK	
		SHDHFHVDSSTGLISLLRTLDYEQSRQHTIFVRAVDGGMPTLSS	
		VIVTVDVTDLNDNPPLFEQQIYEARISEHAPHGHFVTCVKAYDA	
		SSDIDKLQYSILSGNDHKHFVIDSATGIITLSNLHRHALKPFYSLN	
		SVSDGVFRSSTQVHVTVIGGNLHSPAFLQNEYEVELAENAPLHT	
		VMEVKTTDGDSGIYGHVTYHIVNDFAKDRFYINERGQIFTLEKL	
		RETPAEKVISVRLMAKDAGGKVAFCTVNVILTDDNDNAPQFRAT	
		KYEVNIGSSAAKGTSVVKVLASDADEGSNADITYAIEADSESVKE	
		NLEINKLSGVITTKESLIGLENEFFTFFVRAVDNGSPSKESVVLVY	
		VKILPPEMQLPKFSEPFYTFTVSEDVPIGTEIDLIRAEHSGTVLYSL	
		VKGNTPESNRDESFVIDRQSGRLKLEKSLDHETTKWYQFSILAR	
		CTQDDHEMVASVDVSIQVKDANDNSPVFESSPYEAFIVENLPGG	
		SRVIQIRASDADSGTNGQVMYSLDQSQSVEVIESFAINMETGWIT	
		TLKELDHEKRDNYQIKVVASDHGEKIQLSSTAIVDVTVTDVNDSP	
		PRFTAEIYKGTVSEDDPQGGVIAILSTTDADSEEINRQVTYFITGGD	
		PLGQFAVETIQNEWKVYVKKPLDREKRDNYLLTITATDGTFSSKAI	

Sr#	Homo sapien Genes	Sequence	Accession no
8	BIRC5	VEVKVLDANDNSPVCEKTLYSDTIPEDVLPGKLIMQISATDADIRS NAEITYTLLGSGAEKFKLNPDTGELKTSTPLDREEQAVYHLLVRA TDGGGRFCQASIVLTLEDVNDNAPEFSADPYAITVFENTEPGTLLTR VQATDADAGLNRKILYSLIDSADGQFSINELSGIIQLEKPLDRELQA VYTLSLKAVDQGLPRRLTATGTVIVSVLDINDNPPVFEYREYGATV SEDILVGTEVLQVYAASRDIEANAEITYSIISGNEHGKFSIDSKTGAV FIIENLDYESSHEYYLTVEATDGGTPSLSDVATVNVNVTDINDNTPV FSQDTYTTVISEDAVLEQSVITVMADDADGPSNSHIHYSIIDGNQGS SFTIDPVRGEVKVTKLLDRETISGYTLTVQASDNGSPPRVNTTTVNI DVSDVNDNAPVFSRGNYSVIIQENKPVGFSVLQLVVTDEDSSHNGP PFFFTIVTGNDEKAFEVNPQGVLLTSSAIKRKEKDHYLLQVKVADN GKPQLSSLTYIDIRVIEESIYPPAILPLEIFITSSGEEYSGGVIGKIHATD QDVYDTLTYSLDPQMDNLFSVSSTGGKLIAHKKLDIGQYLLNVSV TDGKFTTVADITVHIRQVTQEMLNHTIAIRFANLTPEEFVGDYWRN FQRALRNILGVRRNDIQIVSLQSSEPHPHLDVLLFVEKPGSAQISTK QLLHKINSSVTDIEEIIGVRILNVFQKLCAGLDCPWKFCDEKVSVDE SVMSTHSTARLSFVTPRHHRAAVCLCKEGRCPPVHHGCEDDPCPE GSECVSDPWEEKHTCVCPSGRFGQCPGSSSMTLTGNSYVKYRLTE NENKLEMKLTMRLRTYSTHAVVMYARGTDYSILEIHHGRLQYKF DCGSGPGIVSVQSIQVNDGQWHAVALEVNGNYARLVLDQVHTAS GTAPGTLKTLNLDNYVFFGGHIRQQGTRHGRSPQVGNGFRGCMD SIYLNGQELPLNSKPRSYAHIEESVDVSPGCFLTATEDCASNPCQNG GVCNPSPAGGYYCKCSALYIGTHCEISVNPCSSKPCLYGGTCVVDN GGFVCQCRGLYTGQRCQLSPYCKDEPCKNGGTCFDSLDGAVCQCD SGFRGERCQSDIDECSGNPCLHGALCENTHGSYHCNCSHEYRGRHC EDAAPNQYVSTPWNIGLAEGIGIVVFVAGIFLLVVVFVLCRKMISRK KKHQAEPKDKHLGPATAFLQRPYFDSKLNKNIYSDIPPQVPVRPISY TPSIPSDSRNNLDRNSFEGSAIPEHPEFSTFNPESVHGHRKAVAVCSV APNLPPPPPSNSPSDSDSIQKPSWDFDYDTKVVDLDPCLSKKPLEEK PSQPYSARESLSEVQSLSSFQSESCDDNGYHWDTSDWMPSVPLPDI QEFPNYEVIDEQTPLYSADPNAIDTDYYPGGYDIESDFPPPPEDFPAA DELPPLPPEFSNQFESIHPPRDMPAAGSLGSSSRNRQRFNLNQYLPNF YPLDMSEPQTKGTGENSTCREPHAPYPPGYQRHFEAPAVESMPMSV YASTASCSDVSACCEVESEVMMSDYESGDDGHFEEVTIPPLDSQQH MGAPTLPPAWQPFLKDHRISTFKNWPFLEGCACTPERMAE CPTENEPDLAQCFFCFKELEGWEPDDDPIEEHKKHSSGC KQFEELTLGEFLKLDRERAKNKIAKETNNKKKEFEETAK EQLAAMD	O15392

Sr#	Homo sapien Genes	Sequence	Accession no
9	CD4	MNRGVPFRHLLLVLQLALLPAATQGKKVVLGKKGDTVE QKKSIQFHWKNSNQIKILGNQGSFLTKGPSKLNDRADSRR QGNFPLIIKNLKIEDSDTYICEVEDQKEEVQLLVFGLTANSL QGQSLTLTLESPPGSSPSVQCRSPRGKNIQGGKTLSVSQLG TWTCTVLQNQKKVEFKIDIVVLAFQKASSIVYKKEGEQPL AFTVEKLTGSGELWWQAERASSSKSWITFDLKNKEVSVQD PKLQMGKKLPLHLTLPQALPQYAGSGNLTLALEAKTGVN LVVMRATQLQKNLTCEVWGPTSPKLMLSLKLENVSKREKA VWVLNPEAGMWQCLLSDSGQVLLESNIKVLPTWMALIL GGVAGLLLFIGLGIFFCVRCRHRRRQAERMSQIKRLLSQCP HRFQKTCSPI	P01730
10	IL1B	MAEVPELASEMMAYYSGNEDDLFFEADGPKQMKCSFQDLDLCP LDGGIQLRISDHHYSKGFRQAASVVVAMDKLRKMLVPCPQTFQE NDLSTFFPFIFEEEPIFFDTWDNEAYVHDAPVRSLNCTLRDSQQK SLVMSGPYELKALHLQGQDMEQQVVFSMSFVQGEESNDKIPVA LGLKEKNLYLSCVLKDDKPTLQLESVDPKNYPKKKMEKRFVFN KIEINNKLEFESAQFPNWYISTSQAENMPVFLGGTKGGQDITDFT MQFVSS	P01584
11	ITGAM	MALRVLLLTALTLCHGFNLDTENAMTFQENARGFGQSVVQLQG SRVVVGAPQEIVAANQRGSLYQCDYSTGSCEPIRLQVPVEAVNM SLGLSLAATTSPPQLLACGPTVHQTCSENTYVKGLCFLFGSNLR QQPQKFPEALRGCPQEDSDIAFLIDGSGSIIPHDFRRMKEFVSTV MEQLKKSKTLFSLMQYSEEFRIHFTFKEFQNNPNPRSLVKPITQL LGRTHTATGIRKVVRELFNITNGARKNAFKILVVITDGEKFGDPL GYEDVIPEADREGVIRYVIGVGDAFRSEKSRQELNTIASKPPRDH VFQVNNFEALKTIQNQLREKIFAIEGTQTGSSSSFEHEMSQEGFS AAITSNGPLLSTVGSYDWAGGVFLYTSKEKSTFINMTRVDSDMN DAYLGYAAAIILRNRVQSLVLGAPRYQHIGLVAMFRQNTGMWES NANVKGTQIGAYFGASLCSVDVDSNGSTDLVLIGAPHYYEQTRG GQVSVCPLPRGRARWQCDAVLYGEQGQPWGRFGAALTVLGDV NGDKLTDVAIGAPGEEDNRGAVYLFHGTSGSGISPSHSQRIAGSKL PRLQYFGQSLSGGQDLTMDGLVDLTVGAQGHVLLLRSQPVLRVK AIMEFNPREVARNVFECNDQVVKGKEAGEVRVCLHVQKSTRDRL REGQIQSVVTYDLALDSGRPHSRAVFNETKNSTRRQTQVLGLTQT CETLKLQLPNCIEDPVSPIVLRLNFSLVGTPLSAFGNLRPVLAEDAQ RLFTALFPFEKNCGNDNICQDDLSITFSFMSLDCLVVGGPREFNVT VTVRNDGEDSYRTQVTFFFPLDLSYRKVSTLQNQRSQRSWRLACES ASSTEVSGALKSTSCSINHPIFPENSEVTFNITFDVDSKASLGNKLLL KANVTSENNMPRTNKTEFQLELPVKYAVYMVVTSHGVSTKYLNFT ASENTSRVMQHQYQVSNLGQRSLPISLVFLVPVRLNQTVIWDRPQV TFSENLSSTCHTKERLPSHSDFLAELRKAPVVNCSIAVCQRIQCDIPFF GIQEEFNATLKGNLSFDWYIKTSHNHLLIVSTAEILFNDSVFTLLPGQ GAFVRSQTETKVEPFEVPNPLPLIVGSSVGGLLLLALITAALYKLGFFK RQYKDMMSEGGPPGAEPQ	P11215

Sr#	Homo sapien Genes	Sequence	Accession no
12	TYROBP	MGGLEPCSRLLLLPLLLAVSGLRPVQAQAQSDCSCSTVSPGVLAGIV MGDLVLTVLIALAVYFLGRLVPRGRGAAEAATRKQRITETESPYQEL QGQRSDVYSDLNTQRPYYK	O43914
13	PTPRC	MTMYLWLKLLAFGFAFLDTEVFVTGQSPTPSPTGLTTAKMPSVPL SSDPLPTHTTAFSPASTFERENDFSETTTSLSPDNTSTQVSPDSLDN ASAFNTTGVSSVQTPHLPTHADSQTPSAGTDTQTFSGSAANAKL NPTPGSNAISDVPGERSTASTFPTDPVSPLTTTLSLAHHSSAALPAR TSNTTITANTSDAYLNASETTTLSPSGSAVISTTTIATTPSKPTCDEK YANITVDYLYNKETKLFTAKLNVNENVECGNNTCTNNEVHNLTE CKNASVSISHNSCTAPDKTLILDVPPGVEKFQLHDCTQVEKADTTI CLKWKNIETFTCDTQNITYRFQCGNMIFDNKEIKLENLEPEHEYK CDSEILYNNHKFTNASKIIKTDFGSPGEPQIIFCRSEAAHQGVITWN PPQRSFHNFTLCYIKETEKDCLNLDKNLIKYDLQNLKPYTKYVLS LHAYIIAKVQRNGSAAMCHFTTKSAPPSQVWNMTVSMTSDNSMH VKCRPPRDRNGPHERYHLEVEAGNTLVRNESHKNCDFRVKDLQY STDYTFKAYFHNGDYPGEPFILHHSTSYNSKALIAFLAFLIIVTSIAL LVVLYKIYDLHKKRSCNLDEQQELVERDDEKQLMNVEPIHADILL ETYKRKIADEGRLFLAEFQSIPRVFSKFPIKEARKPFNQNKNRYVDI LPYDYNRVELSEINGDAGSNYINASYIDGFKEPRKYIAAQGPRDET VDDFWRMIWEQKATVIVMVTRCEEGNRNKCAEYWPSMEEGTRA FGDVVVKINQHKRCPDYIIQKLNIVNKKEKATGREVTHIQFTSWPD HGVPEDPHLLLKLRRRVNAFSNFFSGPIVVHCSAGVGRTGTYIGID AMLEGLEAENKVDVYGYVVKLRRQRCLMVQVEAQYILIHQALVE YNQFGETEVNLSELHPYLHNMKKRDPPSEPSPLEAEFQRLPSYRSW RTQHIGNQEENKSKNRNSNVIPYDYNRVPLKHELEMSKESEHDSDE SSDDDSDSEEPSKYINASFIMSYWKPEVMIAAQGPLKETIGDFWQM IFQRKVKVIVMLTELKHGDQEICAQYWGEGKQTYGDIEVDLKDTD KSSTYTLRVFELRHSKRKDSRTVYQYQYTNWSVEQLPAEPKELISMI QVVKQKLPQKNSSEGNKHHKSTPLLIHCRDGSQQTGIFCALLNLLES AETEEVVDIFQVVKALRKARPGMVSTFEQYQFLYDVIASTYPAQNG QVKKNNHQEDKIEFDNEVDKVKQDANCVNPLGAPEKLPEAKEQA EGSEPTSGTEGPEHSVNGPASPALNQGS	

Sr#	Homo sapien Genes	Sequence	Accession no
14	CSF1R	MGPGVLLLLLVATAWHGQGIPVIEPSVPELVVKPGATVTLRCVGNG SVEWDGPPSPHWTLYSDGSSSILSTNNATFQNTGTYRCTEPGDPLG GSAAIHLYVKDPARPWNVLAQEVVVFEDQDALLPCLLTDPVLEAG VSLVRVRGRPLMRHTNYSFSPWHGFTIHRAKFIQSQDYQCSALMG GRKVMSISIRLKVQKVIPGPPALTLVPAELVRIRGEAAQIVCSASSVD VNFDVFLQHNNTKLAIPQQSDFHNNRYQKVLTLNLDQVDFQHAGN YSCVASNVQGKHSTSMFFRVVESAYLNLSSEQNLIQEVTVGEGLNL KVMVEAYPGLQGFNWTYLGPFSDHQPEPKLANATTKDTYRHTFTLS LPRLKPSEAGRYSFLARNPGGWRALTFELTLRYPPEVSVIWTFINGSG TLLCAASGYPQPNVTWLQCSGHTDRCDEAQVLQVWDDPYPEVLSQ EPFHKVTVQSLLTVETLEHNQTYECRAHNSVGSGSWAFIPISAGAHT HPPDEFLFTPVVVACMSIMALLLLLLLLLLYKYKQKPKYQVRWKIIE SYEGNSYTFIDPTQLPYNEKWEFPRNNLQFGKTLGAGAFGKVVEATA FGLGKEDAVLKVAVKMLKSTAHADEKEALMSELKIMSHLGQHENIV NLLGACTHGGPVLVITEYCCYGDLLNFLRRKAEAMLGPSLSPGQDP EGGVDYKNIHLEKKYVRRDSGFSSQGVDTYVEMRPVSTSSNDSFSE QDLDKEDGRPLELRDLLHFSSQVAQGMAFLASKNCIHRDVAARNVL LTNGHVAKIGDFGLARDIMNDSNYIVKGNARLPVKWMAPESIFDCV YTVQSDVWSYGILLWEIFSLGLNPYPGILVNSKFYKLVKDGYQMAQP AFAPKNIYSIMQACWALEPTHRPTFQQICSFLQEQAQEDRRERDYTNL PSSSRSGGSGSSSSELEEESSSEHLTCCEQGDIAQPLLQPNNYQFC	P07333

Sr#	Homo sapien Genes	Sequence	Accession no
15	VCAN	MFINIKSILWMCSTLIVTHALHKVKVGKSPPVRGSLSGKVSLPCHF STMPTLPPSYNTSEFLRIKWSKIEVDKNGKDLKETTVLVAQNGNIK IGQDYKGRVSVPTHPEAVGDASLTVVKLLASDAGLYRCDVMYGIE DTQDTVSLTVDGVVFHYRAATSRYTLNFEAAQKACLDVGAVIATPE QLFAAYEDGFEQCDAGWLADQTVRYPIRAPRVGCYGDKMGKAGV RTYGFRSPQETYDVYCYVDHLDGDVFHLTVPSKFTFEEAAKECEN QDARLATVGELQAAWRNGFDQCDYGWLSDASVRHPVTVARAQC GGGLLGVRTLYRFENQTGFPPPDSRFDAYCFKPKEATTIDLSILAETA SPSLSKEPQMVSDRTTPIIPLVDELPVIPTEFPPVGNIVSFEQKATVQP QAITDSLATKLPTPTGSTKKPWDMDDYSPSASGPLGKLDISEIKEEV LQSTTGVSHYATDSWDGVVEDKQTQESVTQIEQIEVGPLVTSMEIL KHIPSKEFPVTETPLVTARMILESKTEKKMVSTVSELVTTGHYGFTL GEEDDEDRTLTVGSDESTLIFDQIPEVITVSKTSEDTIHTHLEDLESV SASTTVSPLIMPDNNGSSMDDWEERQTSGRITEEFLGKYLSTTPFP SQHRTEIELFPYSGDKILVEGISTVIYPSLQTEMTHRRERTETLIPEMR TDTYTDEIQEEITKSPFMGKTEEEVFSGMKLSTSLSEPIHVTESSVE MTKSFDFPTLITKLSAEPTEVRDMEEDFTATPGTTKYDENITTVLL AHGTLSVEAATVSKWSWDEDNTTSKPLESTEPSASSKLPPALLTTV GMNGKDKDIPSFTEDGADEFTLIPDSTQKQLEEVTDEDIAAHGKF TIRFQPTTSTGIAEKSTLRDSTTEEKVPPITSTEGQVYATMEGSALG EVEDVDLSKPVSTVPQFAHTSEVEGLAFVSYSSTQEPTTYVDSSHT IPLSVIPKTDWGVLVPSVPSEDEVLGEPSQDILVIDQTRLEATISPET MRTTKITEGTTQEEFPWKEQTAEKPVPALSSTAWTPKEAVTPLDEQ EGDGSAYTVSEDELLTGSERVPVLETTPVGKIDHSVSYPPGAVTEH KVKTDEVVTLTPRIGPKVSLSPGPEQKYETEGSSTTGFTSSLSPFST HITQLMEETTTEKTSLEDIDLGSGLFEKPKATELIEFSTIKVTVPSDI TTAFSSVDRLHTTSAFKPSSAITKKPPLIDREPGEETTSDMVIIGEST SHVPPTTLEDIVAKETETDIDREYFTTSSPPATQPTRPPTVEDKEAFG RWQESRR	P13611

Sr#	Homo sapien Genes	Sequence	Accession no
16	NRP1	MERGLPLLCAVLALVLAPAGAFRNDKCGDTIKIESPGYLTSPGYPH SYHPSEKCEWLIQAPDPYQRIMINFNPHFDLEDRDCKYDYVEVFD GENENGHFRGKFCGKIAPPPVVSSGPFLFIKFVSDYETHGAGFSIR YEIFKRGPECSQNYTTPSGVIKSPGFPEKYPNSLECTYIVFVPKMSE IILEFESFDLEPDSNPPGGMFCRYDRLEIWDGFPDVGPHIGRYCGQ KTPGRIRSSSGILSMVFYTDSAIAKEGFSANYSVLQSSVSEDFKCM EALGMESGEIHSDQITASSQYSTNWSAERSRLNYPENGWTPGEDS YREWIQVDLGLLRFVTAVGTQGAISKETKKKYYVKTYKIDVSSNG EDWITIKEGNKPVLFQGNTNPTDVVVAVFPKPLITRFVRIKPATWET GISMRFEVYGCKITDYPCSGMLGMVSGLISDSQITSSNQGDRNWM PENIRLVTSRSGWALPPAPHSYINEWLQIDLGEEKIVRGIIIQGGKHR ENKVFMRKFKIGYSNNGSDWKMIMDDSKRKAKSFEGNNNYDTPE LRTFPALSTRFIRIYPERATHGGLGLRMELLGCEVEAPTAGPTTPNGN LVDECDDDQANCHSGTGDDFQLTGGTTVLATEKPTVIDSTIQSEFPT YGFNCEFGWGSHKTFCHWEHDNHVQLKWSVLTSKTGPIQDHTGD GNFIYSQADENQKGKVARLVSPVVYSQNSAHCMTFWYHMSGSHV GTLRVKLRYQKPEEYDQLVWMAIGHQGDHWKEGRVLLHKSLKLY QVIFEGEIGKGNLGGIAVDDISINNHISQEDCAKPADLDKKNPEIKID ETGSTPGYEGEGEGDKNISRKPGNVLKTLDPILITIIAMSALGVLLG AVCGVVLYCACWHNGMSERNLSALENYNFELVDGVKLKKDKLNT QSTYSEA	O14786

Sr#	Homo sapien Genes	Sequence	Accession no
17	COL22A1	MAGLRGNAVAGLLWMLLLWSGGGGCQAQRAGCKSVHYDLVFLLD TSSSVGKEDFEKVRQWVANLVDTFEVGPDRTRVGVVRYSDRPTTAF ELGLFGSQEEVKAAARRLAYHGGNTNTGDALRYITARSFSPHAGGR PRDRAYKQVAILLTDGRSQDLVLDAAAAAHRAGIRIFAVGVGEALKE ELEEIASEPKSAHVFHVSDFNAIDKIRGKLRRRLCENVLCPSVRVEGD RFKHTNGGTKEITGFDLMDLFSVKEILGKRENGAQSSYVRMGSFPV VQSTEDVFPQGLPDEYAFVTTFRFRKTSRKEDWYIWQVIDQYSIPQV SIRLDGENKAVEYNAVGAMKDAVRVVFRGSRVNDLFDRDWHKMAL SIQAQNVSLHIDCALVQTLPIEERENIDIQGKTVIGKRLYDSVPIDFDL QRIVIYCDSRHAELETCCDIPSGPCQVTVVTEPPPPPPPQRPPTPGSEQ IGFLKTINCSCPAGEKGEMGVAGPMGLPGPKGDIGAIGPVGAPGPKG EKGDVGIGPFGQGEKGEKGSLGLPGPPGRDGSKGMRGEPGELGEPG LPGEVGMRGPQGPPGLPGPPGRVGAPGLQGERGEKGTRGEKGERGL DGFPGKPGDTGQQGRPGPSGVAGPQGEKGDVGPAGPPGVPGSVVQ QEGLKGEQGAPGPRGHQGAPGPPGARGPIGPEGRDGPPGLQGLRG KKGDMGPPGIPGLLGLQGPPGPPGVPGPPGPGGSPGLPGEIGFPGKP GPPGPTGPPGKDGPNGPPGPPGTKGEPGERGEDGLPGKPGLRGEIG EQGLAGRPGEKGEAGLPGAPGFPGVRGEKGDQGEKGELGLPGLK GDRGEKGEAGPAGPPGLPGTTSLFTPHPRMPGEQGPKGEKGDPGLP GEPGLQGRPGELGPQGPTGPPGAKGQEGAHGAPGAAGNPGAPGHV GAPGPSGPPGSVGAPGLRGTPGKDGERGEKGAAGEEGSPGPVGPRG DPGAPGLPGPPGKGKDGEPGLRGSPGLPGPLGTKAACGKVRGSENC ALGGQCVKGDRGAPGIPGSPGSRGDPGIGVAGPPGPSGPPGDKGSPG SRGLPGFPGPQGPAGRDGAPGNPGERGPPGKPGLSSLLSPGDINLLAK DVCNDCPPGPPGLPGLPGFKGDKGVPGKPGREGTEGKKGEAGPPGLP GPPGIAGPQGSQGERGADGEVGQKGDQGHPGVPGFMGPPGNPGPPGA DGIAGAAGPPGIQGSPGKEGPPGPQGPSGLPGIPGEEGKEGRDGKPGPP GEPGKAGEPGLPGPEGARGPPGFKGHTGDSGAPGPRGESGAMGLPGQ EGLPGKDGDTGPTGPQGPQGPRGPPGKNGSPGSPGEPGPSGTPGQKGS KGENGSPGLPGFLGPRGPPGEPGEKGVPGKEGVPGKPGEPGFKGERGD PGIKGDKGPPGGKGQPGDPGIPGHKGHTGLMGPQGLPGENGPVGPPG PPGQPGFPGLRGESPSMETLRRLIQEELGKQLETRLAYLLAQMPPAYM KSSQGRPGPPGPPGKDGLPGRAGPMGEPGRPGQGGLEGPSGPIGPKGE RGAKGDPGAPGVGLRGEMGPPGIPGQPGEPGYAKDGLPGIPGPQGET GPAGHPGLPGPPGPPGQCDPSQCAYFASLAARPGNVKGP	Q8NFW1

Sr#	Homo sapien Genes	Sequence	Accession no
18	BPI	MRENMARGPCNAPRWASLMVLVAIGTAVTAAVNPGVVVRISQKGLD YASQQGTAALQKELKRIKIPDYSDSFKIKHLGKGHYSFYSMDIREFQL PSSQISMVPNVGLKFSISNANIKISGKWKAQKRFLKMSGNFDLSIEGM SISADLKLGSNPTSGKPTITCSSCSSHINSVHVHISKSKVGWLIQLFHKK IESALRNKMNSQVCEKVTNSVSSELQPYFQTLPVMTKIDSVAGINYGL VAPPATTAETLDVQMKGEFYSENHHNPPPFAPPVMEFPAAHDRMVYL GLSDYFFNTAGLVYQEAGVLKMTLRDDMIPKESKFRLTTKFFGTFLPE VAKKFPNMKIQIHVSASTPPHLSVQPTGLTFYPAVDVQAFAVLPNSSLA SLFLIGMHTTGSMEVSAESNRLVGELKLDRLLLELKHSNIGPFPVELLQ DIMNYIVPILVLPRVNEKLQKGFPLPTPARVQLYNVVLQPHQNFLLFGAD VVYK	P17213

TABLE 3: Candidate Relapse Biomarkers Domain Data

Gene	No. of Domains	Domain Names	Domain Length
ERG	2	ETS Domain Pointed domain	310-395
AFF3	1	AF4/FMR2, C-terminal homology domain	113-199
MNX1	1	Homeobox domain	962-1225
KRAS	1	Small GTP-binding protein domain	239-303
NRAS	1	Small GTP-binding protein domain	1-159
CD4	12	Immunoglobulin subtype 2 Immunoglobulin subtype 2	1-159
		Immunoglobulin subtype	32-116
		Immunoglobulin subtype	134-191
		Immunoglobulin subtype	26-123
		Immunoglobulin-like domain	128-202
		Immunoglobulin C2-set	208-317
		Immunoglobulin C2-set	20-119
		Immunoglobulin V-set domain	126-202
		Immunoglobulin	317-388
		CD4, extracellular	36-111
		T-cell CD4 receptor C-terminal region	25-112
IL1B	1	Interleukin-1 propeptide	206-316
ITGAM	2	von Willebrand factor, type A	426-452
		Integrin alpha-2	1-103
PTPRC	9	Tyrosine-specific protein phosphatase, PTPase domain	148-333
		Tyrosine-specific protein phosphatase, PTPase domain	614-980
		Tyrosine-specific protein phosphatases domain	652-914
		Tyrosine-specific protein phosphatases domain	943-1230
		Protein-tyrosine phosphatase, catalytic	832-903
		Protein-tyrosine phosphatase, catalytic	1135-1219
		Fibronectin type III	810-911
		Fibronectin type III	1116-1227
		Protein-tyrosine phosphatase, receptor type, N-terminal	391-483
CSF1R	14	Protein kinase domain	484-576

Gene	No. of Domains	Domain Names	Domain Length
		Serine-threonine/tyrosine-protein kinase, catalytic domain	7-32
		Immunoglobulin subtype 2	582-910
		Immunoglobulin subtype 2	582-910
		Immunoglobulin subtype	215-285
		Immunoglobulin subtype	410-492
		Immunoglobulin subtype	27-102
		Immunoglobulin subtype	112-196
		Immunoglobulin subtype	209-296
		Immunoglobulin-like domain	308-399
		Immunoglobulin-like domain	404-504
		Immunoglobulin-like domain	21-85
		Immunoglobulin	203-290
		Tyrosine-protein kinase, catalytic domain	402-502
VCAN	12	Sushi/SCR/CCP domain	209-292
		Link domain	582-910
		Link domain	3294-3354
		EGF-like domain	148-248
		EGF-like domain	249-347
		C-type lectin-like	3089-3125
		EGF-like calcium-binding domain	3127-3163
		EGF-like calcium-binding domain	3169-3291
		Immunoglobulin subtype	3093-3125
		Immunoglobulin-like domain	3127-3163
		Immunoglobulin V-set domain	29-148
		Aggrecan/versican, C-type lectin-like domain	34-146
NRP1	6	Coagulation factor 5/8 C-terminal domain	29-147
		Coagulation factor 5/8 C-terminal domain	3169-3292
		CUB domain	274-424
		CUB domain	430-583
		MAM domain	27-141
		Neuropilin, C-terminal	147-265
COL22A1	2	Laminin G domain	645-811
		von Willebrand factor, type A	845-923
BPI	2	Lipid-binding serum glycoprotein, C-terminal	239-427
		Lipid-binding serum glycoprotein, N-terminal	36-218
FAT1	43	EGF-like domain	249-486
		EGF-like domain	39-264
		EGF-like domain	3790-3827
		EGF-like domain	4013-4050
		EGF-like domain	4052-4088
		Laminin G domain	4089-4125
		EGF-like calcium-binding domain	4127-4163
		EGF-like calcium-binding domain	3829-4009
		EGF-like calcium-binding domain	4016-4050
		EGF-like calcium-binding domain	4052-4088
		Cadherin-like	4093-4125
		Cadherin-like	4127-4163

Gene	No. of Domains	Domain Names	Domain Length
		Cadherin-like	35-149
		Cadherin-like	150-257
		Cadherin-like	276-358
		Cadherin-like	368-463
		Cadherin-like	463-569
		Cadherin-like	577-669
		Cadherin-like	718-822
		Cadherin-like	823-1034
		Cadherin-like	1035-1139
		Cadherin-like	1140-1245
		Cadherin-like	1246-1357
		Cadherin-like	1359-1456
		Cadherin-like	1457-1562
		Cadherin-like	1563-1667
		Cadherin-like	1668-1765
		Cadherin-like	1766-1879
		Cadherin-like	1880-1979
		Cadherin-like	1980-2081
		Cadherin-like	2082-2182
		Cadherin-like	2183-2283
		Cadherin-like	2284-2390
		Cadherin-like	2391-2492
		Cadherin-like	2493-2596
		Cadherin-like	2597-2703
		Cadherin-like	2704-2809
		Cadherin-like	2810-2918
		Cadherin-like	2919-3023
		Cadherin-like	3024-3125
		Cadherin-like	3126-3230
		Cadherin-like	3231-3335
		Cadherin-like	3336-3440

TABLE 4: Docking of Relapsed biomarkers with drugs results

	TCL1A		AFF3		ERG		MNX1	
ID	mutant	wild	mutant	wild	mutant	wild	mutant	wild
DB00136	-6.6	-6	-6.4	-6.7	-7.3	-7	-7	-6.7
DB00176	-5.5	-5.7	-5.9	-5	-6	-5.7	-5	-5.3
DB00199	-6.1	-6.2	-6.6	-6	-6.9	-6.6	-6.4	-6.1
DB00204	-5.3	-5.2	-6.1	-6	-5.2	-5.8	-5.9	-6.5
DB00210	-8.3	-8.7	-8.4	-8.2	-9	-9	-8.3	-8.2
DB00228	-4.1	-4.2	-5	-5.1	-4	-4.1	-4	-4
DB00252	-6.8	-6.5	-6.5	-5.8	-6	-6.3	-5.7	-6.1
DB00276	-6.8	-7.3	-6.9	-7.3	-7.4	-7.4	-6.4	-6.7
DB00280	-5.9	-5.2	-4.9	-5.7	-5.5	-5.7	-6.1	-6.1
DB00308	-5.1	-5.4	-4.9	-4.4	-5.2	-5.2	-4.7	-5

ID	mutant	wild	mutant	wild	mutant	wild	mutant	wild
DB00321	-6.6	-7	-6.7	-5.9	-6.5	-6.5	-5.8	-5.5
DB00342	-7.5	-8.6	-7	-6.9	-6.6	-7.2	-7	-6.2
DB00398	-6.5	-6.7	-7	-7.1	-7.4	-6.7	-7.7	-7.3
DB00455	-5.8	-5.5	-7	-6.1	-7.5	-7.3	-5.9	-6
DB00457	-5.9	-5.7	-6.6	-5.5	-5.3	-5.7	-6.5	-5.6
DB00458	-6.4	-5	-6.3	-7.6	-6.4	-6.3	-6.1	-5.6
DB00472	-6.4	-6.9	-6.2	-7	-6.5	-6.6	-6.6	-6.3
DB00477	-5.2	-5.3	-4.7	-7	-6	-6.6	-4.3	-5
DB00480	-5.8	-6.1	-6.4	-6.4	-6.9	-6.6	-5.8	-5.6
DB00482	-6.7	-7.3	-7.6	-7	-7.6	-7.6	-7.2	-7
DB00489	-5.3	-5.5	-5.8	-5.1	-5.8	-5.7	-4.9	-5.2
DB00537	-5.8	-5.9	-6.5	-6.6	-6.5	-6.4	-5.9	-5.6
DB00557	-6	-5.4	-6.5	-6	-6.1	-6.4	-5.6	-5.9
DB00570	-6.5	-6.3	-6.7	-6.9	-7	-7.1	-6.2	-7
DB00590	-6.1	-6.4	-6.6	-7.4	-7	-7.6	-6.5	-6.1
DB00604	-6.2	-5.8	-6	-7.7	-6.8	-5.8	-6.2	-6.6
DB00619	-6.7	-7.3	-7.5	-6.9	-7.4	-8.2	-7	-7.6
DB00637	-7.9	-7.3	-7.8	-7.7	-7.2	-7.2	-7.6	-7.6
DB00661	-5.9	-6.3	-6.7	-6.2	-6.4	-6.1	-5.4	-5.8
DB00675	-6.3	-7.2	-6.9	-8.2	-7.4	-7.4	-6.6	-6.8
DB00679	-6.2	-6.4	-6.3	-6.1	-5.9	-6.3	-6.1	-5.7
DB00795	-7.1	-7.6	-7.4	-7.2	-7.2	-6.3	-6.8	-7
DB00836	-6.6	-6.8	-7.9	-7	-7.2	-8.4	-7.9	-7.4
DB00843	-7	-5.5	-6.6	-6.7	-6	-6.6	-6.7	-7.2
DB00852	-3.7	-4.6	-4.3	-4.4	-4.6	-4.5	-4.3	-4.3
DB00908	-5.8	-6.1	-5.7	-6	-6.7	-6.6	-5.7	-6.2
DB00945	-4.5	-6.1	-5	-5.9	-4.9	-5.1	-4.8	-4.7
DB01025	-6.2	-6.8	-6.4	-6.1	-7.4	-6.8	-6.3	-6.6
DB01026	-7.4	-6.3	-7.4	-7.7	-7.1	-7.5	-7.4	-7.1
DB01029	-6.8	-7.5	-7.1	-6.8	-7.7	-7.5	-6.8	-7.7
DB01035	-4.9	-4.7	-4.7	-4.6	-5.1	-5.5	-4.8	-4.7
DB01074	-7.4	-6.9	-7.3	-7.8	-6.8	-6.9	-6.9	-6.5
DB01097	-6	-6.4	-6.1	-6.3	-6.4	-6.3	-5.7	-5.6
DB01100	-7	-7.6	-7.2	-7.9	-7.7	-7.7	-6.9	-7.5
DB01110	-7	-6.9	-6.7	-6.6	-8	-7.3	-7.4	-7.3
DB01118	-6.5	-5.8	-6.2	-6.3	-7	-6.9	-6.1	-7
DB01136	-9.2	-7	-7.3	-8.2	-7.6	-7.2	-8	-7.6
DB01142	-6.2	-7.4	-6.3	-6	-6.3	-6.5	-6.3	-5.8
DB01149	-6.1	-6.2	-6.3	-6.5	-7	-6.5	-6.5	-6.7
DB01162	-5.3	-5.7	-6.5	-6.2	-6.3	-6.3	-5.8	-5.7
DB01182	-7.1	-7.5	-6.5	-6.7	-7.3	-7.6	-7.1	-7.4
DB01195	-5.9	-5.9	-6.6	-6.2	-6.4	-6.1	-6.4	-6.5
DB01211	-6.2	-5.8	-6.3	-6.2	-5.9	-6.6	-5.8	-5.9
DB01218	-6.1	-6.5	-6.8	-7	-7.9	-5.1	-6.3	-6.5
DB01244	-5.5	-6.8	-6.3	-7.4	-7.1	-7.1	-6	-6.2
DB01268	-5.6	-5.3	-6	-5.9	-6.7	-5.9	-6.4	-5.5
DB01296	-4.7	-4	-5.3	-5.2	-4.5	-4.9	-4.5	-4.3
DB01411	-7.8	-8.2	-7.8	-8.5	-7.8	-7.6	-7.5	-7.4

ID	mutant	wild	mutant	wild	mutant	wild	mutant	wild
DB01645	-6.2	-6.1	-6.9	-6.8	-6.8	-6.7	-6.6	-6.1
DB01750	-5.6	-6.2	-5.6	-5.5	-5.9	-6	-6.6	-5.7
DB01809	-5.6	-6.2	-5.4	-5.8	-6.4	-6.3	-6.5	-5.8
DB01863	-5	-4.9	-6	-5.9	-5.3	-5.2	-4.9	-5.4
DB02709	-6.1	-6.3	-5.7	-6.6	-6.1	-6.3	-6.3	-5.6
DB03017	-6.1	-6.7	-6.6	-5.3	-5.8	-5.9	-5.5	-5.9
DB03309	-4.7	-5	-5.9	-4.9	-5.1	-5.2	-4.7	-4.7
DB03459	-4.6	-4.6	-4.8	-6.1	-5.5	-5.9	-5.3	-5.1
DB03701	-6.6	-7.2	-7.3	-6.7	-8.3	-7.6	-6.7	-6.8
DB03721	-5.7	-5.3	-5.2	-6.7	-5.2	-5	-5.4	-4.9
DB03756	-6.1	-6.4	-6.5	-7.7	-7.4	-6.8	-6.9	-6.7
DB03796	-7.1	-7.5	-7.3	-7.2	-7	-7	-6.5	-6.8
DB04147	-3.9	-4.5	-3.5	-3.8	-4	-4.3	-3.6	-3.7
DB04419	-4.1	-3.9	-4	-4.8	-4.4	-3.8	-3.6	-3.6
DB04855	-5.8	-6.2	-6.3	-6.1	-7.2	-6.5	-6.5	-6.3
DB04891	-6.4	-5.7	-5.9	-6.6	-7.2	-6.9	-6.5	-6
DB04957	-5.8	-6.3	-6.3	-6.2	-6.1	-6.6	-6.8	-6.9
DB05212	-6.4	-7.2	-6.9	-6.7	-6.7	-7.3	-6.8	-6.9
DB05294	-6.8	-6.9	-7.9	-7.3	-7	-7.1	-7.7	-6.9
DB05767	-6.4	-7	-7.2	-7.3	-6.6	-7.7	-6.9	-6.7
DB05785	-6.8	-7.7	-8.3	-7.5	-8.3	-7.3	-6.8	-7.3
DB05786	-5.2	-5.7	-5.4	-5.8	-5.7	-5.9	-5.6	-5.7
DB05943	-5.8	-5.9	-6.1	-6.3	-6.1	-6.1	-5.9	-6.1
DB06080	-6.7	-6.9	-7.8	-7.4	-8.4	-7.3	-7.2	-7.1
DB06144	-6.3	-6.2	-7.1	-6.8	-7.2	-6.9	-6.9	-6.9
DB06207	-6.5	-6.6	-6.8	-6	-7.1	-7	-6.1	-6.2
DB06217	-5.4	-6.7	-5.5	-6	-6.2	-6	-5.4	-6
DB06457	-6.7	-7.1	-6.9	-7.3	-7	-6.5	-6.2	-7.4
DB06486	-7.1	-6.9	-7.5	-7.7	-8	-8	-7.7	-7.5
DB06595	-8.4	-9.1	-7.9	-7.6	-8	-7.7	-8.2	-7.5
DB06641	-5.2	-4.4	-6.1	-5.8	-5.2	-5.1	-5.9	-5.3
DB06732	-7.4	-4.4	-7.8	-7.7	-6.9	-7.9	-6.5	-6.7
DB06884	-6.2	-6.6	-6.8	-6.6	-6.1	-5.8	-6.5	-6.1
DB06980	-4.7	-5.9	-5.9	-6.7	-5.6	-5.4	-5.1	-5.7
DB06981	-5.9	-5.9	-5.8	-6.7	-6	-5.7	-5.5	-5.4
DB06982	-5.8	-4.9	-5.5	-7.3	-5.5	-5.6	-5.2	-5.2
DB07167	-5.4	-6.2	-6.4	-5.3	-6.6	-6.1	-5.6	-5.5
DB07202	-5.7	-6.7	-6.6	-6.4	-6.5	-7.3	-6.5	-6.3
DB07584	-5.4	-5.7	-5.6	-7.6	-6.7	-6.8	-6	-6.3
DB07585	-4.9	-4.7	-4.8	-5.4	-5.1	-5.4	-5.6	-4.8
DB07812	-6.2	-5.6	-6.5	-7	-6.8	-6	-5.9	-6.1
DB07859	-6.8	-7.9	-7.4	-7.2	-8.2	-7.5	-6.9	-6.9
DB07947	-5.2	-5.7	-5.6	-4.4	-6.3	-5.7	-5.4	-4.1
DB07950	-5.3	-5	-5.5	-4.6	-5.4	-5	-4.9	-4.7
DB08073	-7.7	-6.2	-5.2	-7.7	-7.2	-7.1	-6.1	-5.1
DB08231	-5.1	-4.8	4.4	-4.8	-4.8	-4.3	-4.6	-4.7
DB08341	-6.2	-6.3	-6.6	-6.1	-6.8	-6.7	-6.3	-6.4
DB08814	-5.7	-5.2	-5.5	-6.2	-5.6	-4.7	-5.3	-5.3

ID	mutant	wild	mutant	wild	mutant	wild	mutant	wild
DB08865	-6.7	-7.4	-7.9	-7.2	-7.4	-7.5	-6.8	-7.3
DB08875	-6.1	-6.5	-7.9	-7.2	-6.9	-8.2	-7.5	-7.7
DB08896	-7	-7.9	-7.5	-7.6	-7.1	-7.8	-8.1	-7.6
DB08901	-7.7	-8.3	-8.6	-8	-8.2	-8.1	-8.7	-8.3
DB08908	-3.4	-3.6	-3.9	-3.9	-4.1	-3.8	-3.5	-3.6
DB09063	-6.1	-6.7	-6.8	-7.3	-7	-7.1	-6.9	-6.8
DB09078	-5.6	-6.1	-5.9	-6.2	-6.6	-6.7	-6.3	-6.1
DB09079	-7.5	-7.1	-7.8	-8.4	-7.5	-7.9	-7.4	-7.9
DB09221	-4.8	-4.7	-5.6	-5.2	-4.8	-5.8	-4.8	-4.8
DB11186	-4.8	-5.5	-5.4	-5.1	-5.7	-5.6	-5.5	-5.3
DB11363	-7.8	-7.8	-7.6	-7.3	-8.2	-7.4	-7.1	-7.2
DB11386	-3.3	-3.5	-3.7	-3.5	-4	-4.2	-3.5	-3.4
DB11633	-6.8	-6.2	-6.9	-7.4	-6.8	-6.9	-7.5	-6.9
DB11642	-5.6	-5.3	-5	-5.4	-5.1	-5.2	-4.8	-5.3
DB11697	-7.4	-7.7	-7.9	-8.2	-7.2	-7.8	-7	-7.4
DB11718	-5.4	-6.1	-6.4	-6.9	-7.2	-6.4	-6.1	-6.5
DB11752	-7	-6	-7.2	-7.6	-6.9	-6.2	-6.3	-6.4
DB11800	-6.8	-7	-6.4	-7.1	-7.3	-7	-6.1	-6.5
DB12010	-6.4	-6.4	-7.1	-7.2	-6.9	-7.8	-6.7	-6.7
DB12130	-6.5	-7	-7.1	-7.1	-7	-7.3	-6.7	-7.3
DB12141	-6.2	-6.1	-7.1	-7.2	-6.1	-6.6	-6.7	-6.4
DB12267	-7.2	-7.1	-7.2	-6.9	-7	-7.1	-7.3	-7.2
DB12364	-6.8	-6.4	-6.9	-7.4	-6.6	-6.9	-6.6	-7.2
DB12500	-5.6	-6.3	-6.7	-6.9	-6.4	-7.4	-6.6	-6.8
DB12742	-6.1	-6.3	-8.3	-6.8	-7.9	-6.5	-7	-6.9
DB12816	-5.8	-5.4	-5.2	-6.3	-5	-5.1	-4.5	-4.9
DB12978	-7	-7.5	-7	-7.7	-6.6	-6.8	-6.7	-7.2
DB13751	-7.5	-7.2	-8	-8	-8.3	-8.3	-7.2	-7.9
DB14059	-6.4	-7	-7.2	-6.6	-7.7	-7.2	-7.1	-7
DB15035	-7.3	-7.3	-7.3	-7.6	-8.2	-7.4	-7	-7.3
DB15685	-7.3	-6.2	-7.5	-7.2	-7.5	-7.8	-6.6	-6.9
DB15822	-7.8	-8.5	-8.1	-7.9	-8.3	-8.1	-8.2	-8.2
Ellagicacid	-6.2	-6.6	-7.2	-7	-7	-7.3	-6.8	-6.5
Epicatechin	-6.5	-7	-7.2	-6.9	-6.6	-6.8	-6.4	-6.4
EpigallocatechinGallate	-6.9	-6.4	-7.3	-7	-7.2	-7.1	-7	-6.9
Hydnocarpin D	-7.6	-7.7	-7.9	-7.6	-8.4	-7.9	-7.9	-7.8
Isookanin	-6.8	-7.2	-7.3	-7.2	-7	-7	-7	-6.6
Quercetin	-6.5	-7.3	-7.1	-7.1	-6.6	-6.7	-6.8	-6.9
Silandrin	-7.4	-7.3	-7.8	-7.3	-6.9	-7.8	-7.2	-7.6
Theaflavine	-7.5	-7.4	-7.9	-8.2	-9	-8.2	-7.4	-7.2
UrolithinC	-6.4	-7.7	-6.6	-7.8	-6.3	-6.8	-5.7	-6.2
Xanthone	-5.7	-6.8	-6.9	-5.9	-6.4	-6.2	-6.2	-6.2

TABLE 5: Docking of relapsed biomarkers with drugs

	CD4	**IL1B**	**ITGAM**	**TYROBP**	**PTPRC**
ID	**Wild**	**Wild**	**Wild**	**Wild**	**Wild**
DB00136	-5.8	-7	-9.6	-6.5	-7.1
DB00176	-5	-5.4	-6.1	-4.5	-6.5
DB00199	-6	-6.7	-9.2	-5.5	-7.6
DB00204	-4.9	-5.4	-5.9	-4.2	-6.7
DB00210	-7.8	-9	-10.8	-8	-9.3
DB00228	-3.7	-4.2	-5	-3.4	-4.8
DB00252	-6.2	-6.7	-7.1	-5.5	-7.5
DB00276	-6.7	-7.1	-8.5	-6	-7.8
DB00280	-5	-5.9	-7.4	-5.7	-6.5
DB00308	-4.7	-5.7	-6.2	-4.6	-5.5
DB00321	-5.8	-6	-7.1	-5.9	-6.4
DB00342	-5.8	-7.8	-8.7	-5.4	-7.5
DB00398	-6.3	-7.3	-8.6	-5.4	-7.5
DB00455	-5.3	-6.3	-8.2	-5.4	-7.3
DB00457	-5.1	-6.2	-7.8	-5	-6.4
DB00458	-5.7	-6.1	-7.3	-5.7	-6.4
DB00472	-5.4	-6.5	-7.7	-5.2	-6.6
DB00477	-4.5	-5.6	-5.9	-4.6	-5.5
DB00480	-5.5	-6.8	-7.4	-5.6	-7.8
DB00482	-6.2	-7.8	-9	-6.3	-7.4
DB00489	-4.5	-6.1	-6.8	-5	-6.3
DB00537	-5.9	-7	-7.9	-5.8	-6.6
DB00557	-4.7	-6.2	-7.4	-5.9	-6.6
DB00570	-6.3	-7.3	-8.1	-6.8	-8.1
DB00590	-6.1	-6.9	-8.7	-6.4	-7.7
DB00604	-5.8	-6.8	-7.5	-6.2	-7.2
DB00619	-6.4	-7.6	-9.1	-6.2	-8.7
DB00637	-6.2	-8.1	-9.2	-6.9	-8.1
DB00661	-4.2	-6.6	-7.1	-6.4	-6.3
DB00675	-5.8	-7.3	-7.9	-6.6	-7.2
DB00679	-4.9	-6.3	-6.5	-4.8	-6.4
DB00795	-6	-7.6	-8.5	-6.4	-7.7
DB00836	-6.9	-7.8	-8.7	-6.2	-7.9
DB00843	-5.3	-7.5	-7.1	-5.7	-6.7
DB00852	-5	-4.8	-5.2	-3.6	-5.3
DB00908	-5.5	-6.4	-7.4	-5.2	-6.9
DB00945	-4.5	-5.1	-5.4	-3.6	-5.8
DB01025	-6.1	-7.4	-8.5	-6.2	-7.3
DB01026	-5.7	-7.7	-9.3	-7.2	-7.7
DB01029	-6.1	-7.6	-9.3	-7	-7.8
DB01035	-4	-5	-5.5	-4.3	-5.2
DB01074	-6.7	-6.9	-7.2	-6	-7
DB01097	-5.6	-6.2	-7.1	-5.8	-6.6
DB01100	-6.6	-7.9	-9.6	-6.9	-8.2
DB01110	-6	-6.6	-8.7	-6.8	-8

ID	Wild	Wild	Wild	Wild	Wild
DB01118	-5.2	-7.1	-8.6	-6.2	-7.1
DB01136	-6.6	-7.9	-8.7	-7	-8.6
DB01142	-5.6	-6	-7.3	-5.7	-6.5
DB01149	-5.5	-6.6	-7.3	-5.4	-7.3
DB01162	-4.8	-6	-7.5	-4.9	-7.4
DB01182	-5.9	-7.6	-7.6	-5.9	-7.3
DB01195	-5.5	-6.3	-7.5	-5.3	-6.8
DB01211	-5.6	-6	-8.2	-5.2	-7.1
DB01218	-5.5	-7.2	-7.3	-6.7	-7
DB01244	-5.7	-6.2	-8	-6.2	-6.9
DB01268	-5.1	-6.2	-6.6	-5.9	-6.2
DB01296	-4.1	-4.5	-5.3	-4.1	-6.1
DB01411	-6.7	-8.4	-9.3	-6.4	-8.5
DB01645	-5.8	-6.9	-7.5	-5.8	-8.4
DB01750	-5.5	-5.4	-6.5	-5.1	-6
DB01809	-5.8	-6.2	-7.6	-5.4	-6.5
DB01863	-4.7	-5.1	-6.9	-4.9	-6.1
DB02709	-5.2	-6.2	-7.1	-5.8	-6.7
DB03017	-4.8	-5.9	-7	-5.2	-5.9
DB03309	-4.6	-4.8	-5.8	-4.4	-5.9
DB03459	-4.9	-5.2	-6.5	-3.7	-6.1
DB03701	-6.2	-7.4	-8.5	-6.3	-7.9
DB03721	-5	-5.7	-6.1	-4.3	-6.2
DB03756	-5.9	-7.4	-8.7	-6.8	-7.6
DB03796	-6	-7	-7.8	-6.2	-6.8
DB04147	-3.3	-3.7	-4.5	-3.5	-4.5
DB04419	-3.6	-3.8	-4.7	-3.1	-5.2
DB04855	-6.5	-7.2	-7.8	-6.2	-7.3
DB04891	-5.6	-6.5	-8.6	-5	-7
DB04957	-6	-5.9	-7.9	-6.3	-7.7
DB05212	-5.7	-7.2	-8.8	-5.8	-7.5
DB05294	-6.4	-7.8	-10.5	-7.4	-8
DB05767	-5.6	-6.9	-8.7	-5.4	-7.2
DB05785	-5.6	-8.1	-8.3	-6.9	-7.5
DB05786	-5.4	-5.8	-5.8	-4.5	-5.5
DB05943	-5	-6.4	-7.3	-5.3	-6.7
DB06080	-6.2	-7.3	-7.3	-6.6	-7.5
DB06144	-5.3	-7	-7.5	-6.2	-7.2
DB06207	-5.9	-6.9	-7.6	-4.7	-7.2
DB06217	-5	-6.9	-7.8	-5.3	-6.9
DB06457	-6	-6.4	-8	-6.2	-7.2
DB06486	-7.7	-8.6	-9.7	-7.3	-8.7
DB06595	-6.8	-8	-8.3	-6.8	-8.7
DB06641	-4.5	-5.9	-6.2	-5.1	-7.5
DB06732	-6	-7.5	-9.1	-6.8	-7.6
DB06884	-5.8	-6.6	-8.2	-5.9	-7
DB06980	-5.1	-5.9	-6.5	-5.3	-5.9
DB06981	-5	-5.7	-6.5	-4.9	-6

ID	Wild	Wild	Wild	Wild	Wild
DB06982	-4.7	-6	-6.1	-4.9	-5.9
DB07167	-5.7	-6	-7.6	-6	-6.1
DB07202	-5.5	-7.3	-7	-5.7	-8
DB07584	-5	-6.3	-7.6	-4.9	-7.8
DB07585	-4.7	-5.8	-7	-4.2	-6.1
DB07812	-5.5	-6.9	-8.4	-6.1	-7
DB07859	-6.2	-7.6	-8.7	-6.5	-8.2
DB07947	-5.2	-6.1	-7.6	-5.6	-5.8
DB07950	-4.9	-5.1	-6.1	-4.5	-5.3
DB08073	-4	-8	-8.3	-6.1	-7.6
DB08231	-3.9	-4.9	-5	-4.2	-4.8
DB08341	-5.7	-6.7	-8.5	-6.4	-6.8
DB08814	-4.7	-4.9	-7.2	-4.8	-6
DB08865	-6.9	-7.9	-9.5	-6.7	-7.9
DB08875	-7.1	-7.8	-10.5	-5.7	-7.9
DB08896	-5.9	-7.7	-9.4	-6.6	-7.6
DB08901	-6.4	-9.4	-9.3	-8.1	-8.4
DB08908	-3.4	-3.6	-4.2	-3.1	-4.3
DB09063	-6.6	-7.6	-9.7	-7.3	-7.7
DB09078	-5.6	-6	-8.9	-5.5	-7.8
DB09079	-6.3	-8.3	-9.8	-6.9	-8.3
DB09221	-4.9	-5.2	-6.5	-4.1	-6.9
DB11186	-4.7	-5.4	-6.8	-5.1	-5.6
DB11363	-7	-8.2	-8.1	-7.1	-9
DB11386	-3.6	-3.9	-4.3	-3.4	-4.2
DB11633	-6.3	-7.3	-8.4	-5.2	-7.4
DB11642	-3.6	-5.3	-5.7	-4.6	-6.4
DB11697	-7.3	-8	-10	-6.9	-8.7
DB11718	-6.8	-6.8	-8	-5.5	-7.1
DB11752	-6.2	-6.7	-8.7	-5.9	-7.8
DB11800	-5.4	-6.7	-9.2	-5.6	-7.8
DB12010	-6.3	-7.4	-8.3	-6.1	-8.1
DB12130	-6.6	-8.1	-9.3	-6	-8.1
DB12141	-5.8	-8.2	-9	-6.5	-7.5
DB12267	-6.2	-7.6	-9.7	-6.1	-8.4
DB12364	-6.4	-7.8	-9	-5.9	-7.8
DB12500	-5.5	-6.5	-8	-5.6	-7.4
DB12742	-6.3	-7.2	-8.8	-6.8	-7.5
DB12816	-4.4	-4.9	-5.9	-4.4	-5.7
DB12978	-5.9	-7.6	-9.1	-5.6	-7.4
DB13751	-7.7	-9.1	-10.9	-6.7	-8.4
DB14059	-6.8	-8.3	-8.4	-6.4	-7.7
DB15035	-6.5	-8	-8.9	-6.3	-8.9
DB15685	-6.5	-7.6	-8.6	-6.3	-8.2
DB15822	-7.4	-8.3	-9.8	-7.4	-8.1
Ellagic acid	-6.3	-6.6	-8.5	-6.5	-8.3
Epicate chin	-6.2	-7.1	-9	-5.8	-7.8
Epigallo catechin Gallate	-6.6	-7.5	-9.8	-5.5	-8.1

ID	Wild	Wild	Wild	Wild	Wild
Hydnocar pin D	-7.5	-8.3	-10.2	-6.8	-9
Isooka nin	-6.3	-7.3	-9.1	-6.1	-7.5
Querce tin	-6.4	-6.7	-8.6	-5.5	-7.4
Siland rin	-6.5	-8.9	-10.3	-7	-8.4
Theafla vine	-7.3	-8.2	-10.8	-6.9	-8.4
Urolith in C	-5.7	-6.6	-8	-5.4	-7
Xan thone	-5.6	-6.3	-7.5	-5.8	-6.8

TABLE 6: Docking of KRAS and Variants with drugs

	KRAS									
ID	**Wild**	**mutant _Q61H**	**mutant _Q61R**	**mutant _G13D**	**mutant _G12V**	**mutant _G12R**	**mutant _Q61E**	**mutant _K117N**	**mutant _A59E**	**mutant _G12D**
DB00136	-7	-6.3	-7.1	-6.5	-5.7	-6	-6.4	-7.1	-5.9	-5.9
DB00176	-5.8	-6.2	-5.6	-6	-6.8	-5.7	-5.1	-6.4	-5.5	-5.6
DB00199	-6.3	-6.4	-6.5	-6.6	-6.9	-6.8	-6.1	-6.6	-6.3	-6.1
DB00204	-5.3	-5.2	-5.2	-6.2	-5.9	-5.3	-5.2	-5.7	-5.8	-5.4
DB00210	-7.8	-7.9	-8.8	-8.2	-8.2	-8.2	-7.5	-8.5	-8.3	-7.8
DB00228	-4.4	-4.8	-3.9	-4.1	-3.9	-4.3	-5.3	-5.2	-4.2	-4.2
DB00252	-6.6	-6.4	-6.1	-6.3	-6.9	-6.4	-6.5	-7.5	-7.1	-6.4
DB00276	-7.1	-7.3	-7.1	-7.3	-7.2	-6.8	-6.9	-7.9	-6.6	-7.1
DB00280	-5.3	-5.7	-6	-6.8	-5.6	-6.1	-5.8	-5.1	-5.8	-5.5
DB00308	-4	-5.3	-4.2	-5.1	-5.2	-5.2	-5	-5.1	-5	-4.6
DB00321	-6	-5.7	-5.9	-5.6	-5.5	-5.9	-5.8	-6.4	-5.6	-5.9
DB00342	-5.7	-5.6	-5.8	-6.9	-7.9	-6.6	-6.2	-6.3	-7.9	-7.9
DB00398	-7.4	-7.2	-6.6	-6.7	-6.8	-7.3	-7.4	-6.9	-7.1	-7.4
DB00455	-5.9	-5.6	-7.2	-5.9	-6.1	-6	-6.1	-6.2	-5.4	-6.9
DB00457	-6.2	-6.1	-5.8	-5.6	-6.1	-6	-5.7	-6	-5.6	-6.2
DB00458	-5.9	-5.7	-6.1	-5.7	-6.6	-5.7	-5.8	-6.4	-5.9	-5.6
DB00472	-5.8	-6.5	-6.4	-5.8	-6.1	-5.9	-7.2	-7.1	-6.2	-6.2
DB00477	-4.9	-5.9	-4.9	-5.2	-5.1	-5.1	-5.8	-5.7	-4.7	-6.1
DB00480	-6.5	-6.6	-6.5	-6.8	-5.7	-5.9	-5.8	-6.5	-6.2	-5.9
DB00482	-6.7	-6.7	-6.8	-6.7	-7	-6.8	-7.9	-6.7	-7	-6.9
DB00489	-4.9	-4.7	-5.4	-5.1	-4.7	-5	-5	-5	-5.2	-4.9
DB00537	-5.5	-6.5	-5.8	-5.9	-6	-6.1	-6.1	-5.6	-5.9	-6
DB00557	-6	-6.1	-5.6	-6.3	-6.9	-6.4	-6.1	-6.4	-6.7	-6.8
DB00570	-6.3	-6.7	-6.8	-6.8	-7	-7.1	-6.3	-6.3	-7	-5.9
DB00590	-6.7	-7.4	-6.2	-6.7	-6.5	-6.8	-7	-6.6	-6.7	-7
DB00604	-6.3	-6	-6.4	-6.6	-7	-7.2	-5.9	-6.6	-6.3	-6.2
DB00619	-7.2	-7.2	-7.4	-6.7	-6.8	-7.5	-7.4	-7.4	-8.1	-6.6
DB00637	-7.1	-8	-7.2	-7.4	-8.4	-7.6	-7.4	-6.9	-7.9	-6.8
DB00661	-6.3	-6.6	-5.3	-6.2	-5.6	-5.4	-5.9	-6	-6.7	-6.2
DB00675	-6.9	-6.9	-6.4	-7	-6.8	-6.6	-6.4	-7.2	-6.3	-6.2
DB00679	-5.8	-5.9	-5.5	-5.5	-5.6	-5.1	-5.5	-5.7	-5.9	-5.9
DB00795	-6.9	-7.6	-6.9	-6.8	-7.3	-7.9	-7.7	-7.1	-7.6	-7.2
DB00836	-6.9	-7.6	-6.8	-7.2	-7.7	-7.3	-6.8	-7	-7.6	-6.4
DB00843	-6.6	-6.5	-6.4	-6.7	-6.4	-5.7	-6.6	-6.3	-6.7	-6.4

ID	Wild	mutant _Q61H	mutant _Q61R	mutant _G13D	mutant _G12V	mutant _G12R	mutant _Q61E	mutant _K117N	mutant _A59E	mutant _G12D
DB00852	-3.9	-4.6	-3.9	-5.2	-4.4	-4.5	-5.5	-4.9	-5	-4.4
DB00908	-6.2	-6.4	-7.1	-6.4	-5.7	-6.2	-6	-6.5	-5.7	-5.8
DB00945	-4.8	-5	-4.6	-4.6	-4.9	-4.3	-4.3	-5.9	-4.8	-5
DB01025	-6	-6.4	-6.5	-6.6	-7	-6.3	-6.6	-6.6	-6.8	-7
DB01026	-7.5	-6.4	-7.3	-7.2	-6.9	-7.1	-6.8	-7.4	-7.4	-6.4
DB01029	-6.9	-7.3	-7.5	-7	-6.8	-7.1	-7.1	-7.5	-7.3	-6.3
DB01035	-4.7	-4.7	-5.4	-4.8	-4.7	-4.7	-4.5	-5	-4.6	-5
DB01074	-6.5	-7.1	-6.4	-6.3	-6.6	-5.8	-5.8	-6.5	-6.8	-6
DB01097	-6.2	-6.6	-5.8	-5.9	-5.9	-5.5	-6.2	-6.9	-6.1	-6.1
DB01100	-7.3	-7.4	-7.4	-7	-7.7	-7	-7	-7.1	-6.9	-6.7
DB01110	-7.2	-7	-7.1	-7.2	-7.3	-6.8	-6.8	-7	-7.5	-6.9
DB01118	-6.4	-6.2	-5.9	-6	-6.8	-6.4	-6.1	-6.7	-6	-6.4
DB01136	-7.4	-7.2	-7.5	-7.6	-7.7	-7.1	-7.5	-8.3	-7.4	-7.2
DB01142	-6	-6.3	-6.7	-5.9	-6.3	-5.4	-6.9	-7	-5.9	-7.1
DB01149	-6.4	-5.9	-5.7	-6	-6	-6.1	-6.3	-6	-6.9	-6.4
DB01162	-5.2	-5.8	-6.2	-6.1	-5.8	-6.3	-6.5	-6	-6.1	-6
DB01182	-7.2	-7	-7.2	-6.8	-6.6	-7.2	-6.9	-7	-6.7	-7.3
DB01195	-5.5	-6.7	-6.2	-6.1	-6.5	-6.2	-6.4	-6.7	-7	-6.2
DB01211	-6.7	-6.2	-6.5	-6.1	-6.4	-6.6	-5.9	-6.8	-5.9	-6.5
DB01218	-6	-7.7	-6.7	-5.9	-7	-6.3	-6.2	-6.6	-7.3	-6.3
DB01244	-6	-6.9	-6	-6.7	-6.7	-6.4	-6.1	-6.4	-6.6	-5.9
DB01268	-5.7	-6.3	-6.1	-6.5	-5.9	-5.9	-5.5	-5.8	-6.4	-6.2
DB01296	-4.4	-4.3	-4.3	-3.9	-4.5	-4.3	-5.2	-4.8	-4.3	-4.5
DB01411	-8.2	-7.1	-7.3	-7.4	-7.5	-7.5	-7.3	-7.7	-7.2	-7.8
DB01645	-6.2	-6.1	-6.1	-6.2	-6.9	-6.5	-6.4	-6.3	-6.4	-6.9
DB01750	-5.7	-6.2	-5.5	-5.7	-6.2	-5.2	-6.9	-6.9	-5.6	-6.8
DB01809	-6.1	-6	-5.9	-5.9	-5.7	-6	-5.7	-5.8	-5.9	-5.9
DB01863	-5.6	-5.5	-5.3	-5.5	-5.4	-5.5	-5.3	-5.5	-5.8	-5.9
DB02709	-6.5	-6	-7.3	-6.7	-8	-6.6	-6.3	-5.5	-5.7	-6.5
DB03017	-6.3	-5.7	-5.5	-5.7	-6	-5.4	-6.9	-7.1	-5.4	-6.5
DB03309	-5.1	-5.2	-4.7	-4.8	-4.9	-5.1	-5.2	-5.4	-5.6	-4.5
DB03459	-4.6	-5	-5.1	-5.6	-4.5	-5.8	-4.5	-5	-5.3	-5.2
DB03701	-6.8	-6.7	-6.9	-6.6	-7.3	-6.3	-6.9	-7.4	-7.1	-7.5
DB03721	-5.2	-5.4	-5.2	-4.7	-5.7	-5.4	-5.1	-5.8	-5	-5.5
DB03756	-6.6	-7	-6.6	-7.1	-7.4	-7	-6.7	-6.9	-7.4	-7.1
DB03796	-6.4	-6	-6.2	-6.1	-6.2	-5.9	-6.2	-6.3	-5.9	-5.7
DB04147	-3.5	-3.8	-3.4	-3.8	-3.7	-3.9	-4	-4.2	-3.8	-4.3
DB04419	-4.3	-4.4	-3.9	-4.5	-4.1	-4.1	-4.6	-4.6	-3.7	-3.8
DB04855	-5.6	-6.2	-6.4	-6.2	-7.2	-5.9	-6.7	-6.2	-6	-5.9
DB04891	-5.8	-6.2	-5.6	-5.9	-6.4	-6.1	-6.3	-6.2	-6.3	-6.2
DB04957	-6.1	-6.3	-6.8	-6.8	-6.4	-6.2	-6.7	-7	-6.6	-6.5
DB05212	-6	-5.9	-6.9	-6.5	-6.3	-6.7	-6.4	-6.8	-7	-6.2
DB05294	-7.1	-7.2	-7.2	-7.5	-7.2	-7.4	-7.2	-7.1	-7.3	-7.4
DB05767	-6.7	-6.2	-6.3	-6.3	-6.1	-5.9	-6.4	-5.9	-6	-5.6
DB05785	-6.7	-6.9	-7.7	-7.3	-8	-6.9	-7.3	-7	-7.3	-7.1
DB05786	-5.5	-5.1	-6.2	-5.4	-5.4	-5.3	-5.6	-5.9	-5.5	-5.6
DB05943	-5.8	-5.8	-5.8	-5.7	-5.8	-5.3	-5	-6.4	-5.4	-6.2

ID	Wild	mutant _Q61H	mutant _Q61R	mutant _G13D	mutant _G12V	mutant _G12R	mutant _Q61E	mutant _K117N	mutant _A59E	mutant _G12D
DB06080	-7.2	-6.8	-6.9	-7.4	-7.1	-6.7	-7.6	-7.2	-8.2	-6.8
DB06144	-6.7	-7.1	-7.9	-6.4	-5.9	-7.3	-6.9	-7.1	-7	-8.3
DB06207	-6.1	-6.3	-6.3	-6.9	-6.4	-7.3	-5.8	-6.3	-6.5	-6
DB06217	-5.6	-6	-5.7	-6.1	-5.9	-5.7	-6.5	-5.8	-6.2	-5.6
DB06457	-6.4	-6.2	-6.3	-7.1	-6.7	-6.8	-6.7	-7.3	-7.1	-6.5
DB06486	-8.4	-7.4	-7.6	-8.9	-8.8	-7.2	-7.5	-7.6	-7.3	-6.9
DB06595	-8.3	-7.6	-9.1	-8.3	-7.8	-8	-7.4	-8.7	-8.3	-8.3
DB06641	-4.8	-5	-5	-4.9	-4.9	-5.4	-5.4	-6.1	-5.5	-5.6
DB06732	-6.6	-6.8	-6.9	-7	-6.7	-6.5	-6.7	-7.4	-6.6	-6.5
DB06884	-6.2	-6.4	-6.1	-5.9	-6.3	-6.1	-6.4	-6.2	-5.9	-6.8
DB06980	-5.3	-5.5	-5.7	-5.4	-5.1	-5.2	-4.9	-5.9	-5.4	-5.3
DB06981	-5.7	-5.8	-5.4	-5.6	-5.7	-5.2	-5.3	-6.1	-5.4	-6.2
DB06982	-5.4	-4.8	-5.4	-5.5	-5.1	-5.3	-5.4	-6.8	-5.6	-5.6
DB07167	-6.4	-6.2	-5.9	-5.7	-6.4	-6.8	-5.8	-5.3	-6	-6
DB07202	-6.2	-7.1	-6.9	-6.6	-6.6	-6.3	-6.5	-7.1	-6.4	-7
DB07584	-6.5	-6.5	-6.6	-7.1	-6.2	-5.9	-5.5	-7	-6.3	-5.9
DB07585	-4.9	-4.7	-5.1	-4.9	-5.6	-5	-5.4	-5.4	-5.3	-5.5
DB07812	-6.5	-6	-6.7	-6.6	-6.4	-6.9	-6.3	-7	-6	-7
DB07859	-6.7	-6.5	-6.8	-6.5	-7.3	-6.7	-6.4	-7	-6.2	-6.8
DB07947	-5.2	-6.2	-6.5	-5.7	-6.2	-4.1	-6.1	-5.3	-6.1	-5.8
DB07950	-5.3	-4.6	-4.9	-5.2	-5.3	-4.9	-6	-5.8	-4.6	-5.2
DB08073	-5.5	-5	-6.2	-7.1	-5.7	-6.6	-7.3	-5.3	-5.9	-6.6
DB08231	-4.4	-4	-4.7	-4.3	-4.7	-4.3	-4.5	-4.6	-4.8	-4.4
DB08341	-6.5	-7	-6.9	-6.6	-7.1	-6.8	-6.6	-7.2	-6.4	-6.4
DB08814	-5.6	-5.7	-5.5	-5.5	-5.7	-5.5	-4.9	-5.1	-5.1	-5.7
DB08865	-6.6	-6.8	-6.7	-7.6	-7.1	-6.7	-6.8	-6.8	-7.1	-6.7
DB08875	-7.2	-7.9	-7.3	-7.5	-8	-7.6	-7.5	-7.7	-7.6	-7.1
DB08896	-7.3	-7.2	-7.6	-7.8	-7.4	-7.5	-7	-7	-7.7	-7.1
DB08901	-8.1	-7.8	-7.5	-7.9	-7.4	-8.3	-7.8	-8	-8.5	-9.6
DB08908	-4.1	-3.5	-3.9	-4	-3.7	-4.1	-3.7	-3.9	-3.8	-3.5
DB09063	-6.9	-7.5	-6.6	-7.2	-7.4	-7.7	-6.8	-7.4	-7.1	-7.3
DB09078	-5.4	-5.8	-5.4	-6	-5.2	-5.6	-5.8	-6.1	-6.1	-5.5
DB09079	-7.4	-7.5	-7.5	-7.9	-7.6	-8.6	-6.9	-7.8	-7.2	-8.7
DB09221	-5.4	-4.9	-4.9	-4.5	-5.4	-4.8	-5	-5.4	-5.1	-5.4
DB11186	-6	-5.5	-5.2	-5.4	-5.6	-5.2	-4.5	-5.1	-5.3	-5.4
DB11363	-7.3	-8.1	-7.7	-7.7	-8.2	-8.1	-7.1	-7.8	-7.6	-8.1
DB11386	-3.7	-3.8	-3.5	-3.5	-3.4	-4	-3.6	-3.8	-3.8	-3.5
DB11633	-6.2	-6.9	-6.3	-6.6	-6.8	-7	-6.4	-7.2	-6.1	-6.7
DB11642	-5	-5.9	-5.1	-5.7	-5.4	-5	-4.8	-5.6	-5.7	-5.9
DB11697	-7.6	-7.7	-7.5	-7.9	-7.9	-7.6	-7.7	-7.7	-7.5	-8.5
DB11718	-6.4	-6.7	-6.3	-6.3	-7.1	-6.9	-6.3	-6.8	-6.4	-6.9
DB11752	-7.4	-7.5	-7.3	-6.9	-7.1	-7.4	-6.8	-7.6	-6.6	-6.7
DB11800	-6.4	-6.7	-6.1	-7	-6.4	-6.7	-6.2	-6.9	-7.3	-6.3
DB12010	-6.8	-6.6	-6.5	-7.1	-7.1	-6.9	-6.5	-6.7	-6.9	-6.7
DB12130	-7	-7.7	-7.4	-7	-7.1	-7.4	-7.3	-7.3	-7.7	-7.6
DB12141	-6.9	-7.3	-7.2	-6.8	-7.4	-7.6	-7.2	-7.3	-7.4	-7.2
DB12267	-6.8	-7.3	-7.5	-7.9	-7.1	-6.8	-7.1	-7.6	-8.7	-7.5

ID	Wild	mutant _Q61H	mutant _Q61R	mutant _G13D	mutant _G12V	mutant _G12R	mutant _Q61E	mutant _K117N	mutant _A59E	mutant _G12D
DB12364	-7.2	-6.9	-6.7	-7.1	-7.1	-6.6	-7.1	-7.3	-7	-7.1
DB12500	-7.6	-6.5	-6	-6.8	-7.1	-7.7	-6.6	-7	-6	-6.4
DB12742	-6.5	-6.5	-7.1	-6.8	-7	-6.3	-6.2	-6.8	-6.5	-6.9
DB12816	-4.9	-5.3	-5.3	-5.3	-5	-5.3	-6.1	-4.5	-4.8	-4.6
DB12978	-6.4	-7	-7	-7.1	-6.4	-6.7	-6.7	-6.8	-6.9	-7.2
DB13751	-8.1	-8.1	-8.5	-8.1	-7.9	-7.9	-8.5	-7.3	-8.6	-8.3
DB14059	-6.7	-6.9	-6.5	-6.6	-7	-6.6	-7.4	-6.5	-6.5	-6.6
DB15035	-7.1	-7.7	-7.2	-7.3	-6.9	-6.9	-7	-7.1	-7.2	-7.3
DB15685	-6.6	-7.9	-6.7	-7.3	-7.4	-7	-7.3	-7	-7.5	-6.6
DB15822	-7.6	-7.5	-7.4	-7.4	-8.1	-7.5	-7.7	-8.3	-7.8	-8.6
Ellagic acid	-6.9	-6.3	-6.7	-6.3	-7.4	-6.5	-6.3	-6.7	-6.6	-6.4
Epicatechin	-6.8	-6.3	-6.1	-7.1	-6.3	-6.2	-7	-6.2	-7	-6.8
Epigallocatechin Gallate	-6.7	-7.1	-6.8	-6.9	-6.6	-6.6	-6.8	-6.5	-7.6	-6.6
Hydnocarpin D	-8.4	-9	-8.2	-8.2	-7.4	-8.1	-7.7	-7	-8.7	-8.4
Isookanin	-6.6	-7	-6.3	-6.7	-7.1	-6.6	-7.8	-7.3	-6.8	-7.1
Quercetin	-6.9	-7.1	-6.2	-6.5	-6.9	-6.6	-6.5	-6.5	-7.1	-6.5
Silandrin	-8.7	-7.1	-7.7	-8.7	-7.9	-7.5	-7.3	-7.5	-7.7	-7
Theaflavine	-8.1	-8.7	-8.1	-7.7	-8.3	-7.8	-8.1	-8	-7.9	-8.1
Urolithin C	-6.4	-6.1	-6.4	-6.1	-6.1	-6.1	-6	-6.3	-6.3	-6.7
Xanthone	-6.5	-6.1	-5.6	-6.2	-6.1	-5.9	-6.9	-7.2	-5.9	-6.5

TABLE 7: Docking of NRAS and Variants with Drugs

	NRAS								
ID	**Wild**	**mutant _Q61R**	**mutant _Q61K**	**mutant _Y64D**	**mutant _Q61H**	**mutant _G13R**	**mutant _G13D**	**mutant _E153Q**	**mutant _G12D**
DB00136	-6	-6	-6	-5.6	-5.9	-6.3	-6.9	-6.1	-6.6
DB00176	-5.9	-5.5	-5.2	-5.9	-4.7	-4.6	-5.7	-5.4	-5
DB00199	-6.2	-6.2	-6.1	-6.1	-6.1	-6.1	-5.9	-6.5	-5.8
DB00204	-5.6	-5.3	-5.6	-5	-5.4	-4.9	-5.1	-5.3	-4.6
DB00210	-7.3	-7.3	-7.3	-7.9	-7.1	-8	-7.4	-7.7	-7.6
DB00228	-4.6	-4.3	-4	-4.4	-4.5	-4.5	-4.2	-4.3	-4.2
DB00252	-7.6	-5.7	-6.8	-7.2	-5.6	-5.3	-5.3	-6.3	-6
DB00276	-6.7	-6.5	-7.7	-6.6	-6.8	-6.7	-6.5	-6.5	-8.3

ID	Wild	mutant _Q61R	mutant _Q61K	mutant _Y64D	mutant _Q61H	mutant _G13R	mutant _G13D	mutant _E153Q	mutant _G12D
DB00280	-5.5	-5.1	-5.5	-5.3	-5.5	-6.3	-5.1	-5.4	-5.6
DB00308	-5.1	-4.8	-5.1	-4.4	-4.5	-4.2	-4.8	-4.1	-4.4
DB00321	-4.9	-5.9	-6.6	-6.1	-5.4	-5	-5.3	-6.1	-6.3
DB00342	-7	-6.6	-7.2	-7	-6.4	-6.5	-5.4	-6.8	-7.2
DB00398	-6.2	-6.5	-6.9	-7.1	-6.3	-6.7	-6.3	-6.9	-6.2
DB00455	-6.1	-5.8	-6.1	-5.6	-6.4	-5.8	-5.6	-6	-5.5
DB00457	-5	-5.6	-5.7	-5.5	-5.2	-5.8	-5.5	-6.7	-5.1
DB00458	-5.7	-5.8	-7	-5.7	-5.6	-5.8	-5.7	-7	-5.4
DB00472	-7.4	-6.6	-5.6	-5.2	-5.8	-6.5	-5.5	-5.5	-6
DB00477	-5.3	-4.7	-4.9	-4.5	-4.5	-5	-4.8	-5	-6
DB00480	-6.4	-5.8	-5.9	-7	-5.7	-6.2	-5.8	-7	-5.6
DB00482	-8.1	-7.3	-7.5	-7.1	-7.2	-6.3	-7.4	-7.1	-7.5
DB00489	-5.5	-5	-4.9	-5.6	-5.1	-5.5	-5.5	-5.5	-6.3
DB00537	-5.7	-5.5	-5.6	-5.7	-6.1	-6.2	-5.2	-5.8	-6.8
DB00557	-6.1	-5.7	-5.6	-6.1	-6.1	-5.7	-5.7	-5.6	-6.7
DB00570	-6.9	-6.9	-7.2	-6.2	-6.2	-6.3	-6.3	-6.2	-6.9
DB00590	-6.2	-6.2	-7.3	-7.3	-6.1	-6.9	-6.2	-6.5	-7
DB00604	-6.3	-6.7	-6.2	-6.1	-6.2	-7.1	-6.2	-6.2	-6.2
DB00619	-7	-6.5	-7	-7.2	-7.6	-7.4	-6.6	-6.9	-7
DB00637	-7.1	-6.2	-7.6	-6.4	-7.1	-6.7	-6.7	-7	-7.4
DB00661	-6	-5.4	-6.6	-4.9	-5.7	-6	-5.9	-5.3	-6.3
DB00675	-6.4	-6.5	-6.5	-6.9	-6.6	-6.8	-5.8	-6.2	-7.6
DB00679	-5.1	-5.1	-5.5	-5.2	-5.2	-5.5	-5.3	-5.6	-5.2
DB00795	-6.7	-6.4	-6.7	-6.4	-6.2	-6.9	-6.7	-6.3	-6.7
DB00836	-6.4	-6.4	-7.2	-7.1	-6.7	-7	-6.8	-7.1	-6.8
DB00843	-5.9	-6.3	-6.1	-6.2	-7	-6.3	-6.3	-6.3	-5.8
DB00852	-4.1	-3.9	-4.2	-4.2	-3.7	-3.9	-4.8	-4.3	-5.7
DB00908	-5.6	-6.6	-7	-7.5	-5.6	-5.4	-6	-7.5	-7.5
DB00945	-5.2	-4	-4.6	-4.3	-5.3	-4.7	-5.5	-5.1	-6.2
DB01025	-6.2	-6.1	-6.6	-6	-6.5	-6.4	-6	-6.5	-5.9
DB01026	-7.1	-6.9	-6.4	-7.1	-7	-6.9	-6.5	-6.9	-7.8
DB01029	-6.7	-6	-7.1	-7.9	-6.5	-7	-6.6	-6	-8.4
DB01035	-5.9	-4.3	-4	-4.3	-4.5	-4.4	-4.1	-5	-6.2
DB01074	-7.7	-5.9	-6	-6.6	-6.5	-6.3	-5.8	-7.6	-5.9
DB01097	-6.8	-6	-5.9	-6.7	-5.7	-5.8	-5.4	-6.4	-5.3
DB01100	-7.3	-7	-7.2	-7.1	-7.2	-6.8	-6.8	-7.2	-6.6
DB01110	-7	-6.5	-5.8	-7.1	-6.6	-6.7	-6.3	-6.5	-7.7
DB01118	-5.9	-5.7	-5.8	-6.4	-5.5	-5.5	-5.4	-5.7	-5.2
DB01136	-7.2	-7.5	-7.4	-7.8	-7.7	-7.5	-7.3	-6.9	-7.4
DB01142	-6.2	-5.9	-6.3	-6	-5.8	-5.5	-5.5	-6	-6.6
DB01149	-6.7	-6.2	-6.3	-5.8	-6.1	-6.3	-6.6	-7.1	-7.1
DB01162	-5.5	-5.6	-5.6	-5.7	-5.3	-6.2	-5.8	-5.5	-5.9
DB01182	-7.7	-6.5	-7	-6.3	-6.5	-6.7	-6.4	-6.4	-6.1
DB01195	-6.9	-5.9	-5.8	-7.1	-6.2	-5.8	-6.8	-6.7	-7.2
DB01211	-5.9	-5.8	-5.8	-5.7	-5.8	-5.9	-5.8	-5.7	-5.6
DB01218	-5.9	-5.7	-5.7	-6.8	-5.8	-5.9	-6.3	-6.9	-7
DB01244	-7.1	-6.5	-6.9	-6.1	-6.5	-6.2	-5.6	-5.8	-6.9

ID	Wild	mutant _Q61R	mutant _Q61K	mutant _Y64D	mutant _Q61H	mutant _G13R	mutant _G13D	mutant _E153Q	mutant _G12D
DB01268	-6	-5.3	-5.9	-5.3	-5.7	-5.2	-5.4	-5.5	-6.2
DB01296	-5.2	-5.1	-5.1	-5.1	-5.1	-5	-4.9	-5.1	-5.9
DB01411	-7.6	-7.8	-7.4	-7.7	-7.4	-7.5	-7	-7.1	-7.7
DB01645	-7	-6.1	-7	-7.6	-5.9	-5.9	-5.6	-6.9	-7.9
DB01750	-6	-5.7	-6.4	-5.4	-5.2	-5.9	-5.4	-5.5	-6.4
DB01809	-6.4	-5.2	-5.7	-5.9	-5.4	-6	-5.3	-5.2	-7.1
DB01863	-6.5	-5.5	-6.3	-5.1	-5.1	-6.1	-5.1	-6.2	-6.3
DB02709	-8	-5.6	-5.4	-5.4	-5.4	-5.9	-5.4	-7	-8.2
DB03017	-6.3	-5.3	-6.5	-4.8	-5.5	-5.4	-5.8	-6.2	-6.6
DB03309	-4.4	-5.7	-4.4	-5.7	-5.4	-4.7	-4.1	-5.9	-6.2
DB03459	-7.1	-5.7	-4.5	-4.7	-5	-5.9	-4.7	-6.9	-6.5
DB03701	-7.3	-6.4	-6.4	-6.6	-6.4	-6.1	-7	-6.1	-6.5
DB03721	-5.1	-6	-5.7	-6.1	-6	-4.5	-6.1	-5.8	-6.2
DB03756	-6.4	-6.5	-6.5	-6.2	-6.2	-6.8	-6.5	-6.6	-7.9
DB03796	-5.8	-5.9	-5.7	-6.1	-6	-5.9	-6.1	-6.3	-6.8
DB04147	-4.5	-3.5	-3.4	-3.4	-3.2	-3.5	-3.6	-3.8	-3.5
DB04419	-4.6	-4.4	-4.6	-4.3	-4.6	-4.6	-3.6	-4.6	-4.5
DB04855	-5.4	-6.3	-5.2	-6.4	-5.4	-6	-6.2	-7.2	-6.1
DB04891	-7	-5.7	-6.5	-6	-5.4	-5.5	-5.5	-6	-6.7
DB04957	-6.8	-5.9	-6.9	-6.8	-6.3	-6.8	-6.1	-6.1	-5.7
DB05212	-5.6	-6.4	-6.4	-6.8	-6.4	-6.9	-6.1	-6.1	-6.3
DB05294	-7	-6.9	-6.7	-7	-7.3	-7.2	-6.7	-6.7	-7.1
DB05767	-6.2	-5.7	-6.3	-5.7	-6.1	-5.8	-6.2	-6.1	-6.9
DB05785	-7	-6.4	-6.3	-6.3	-7	-6.3	-6.5	-7.2	-6
DB05786	-5.2	-5.2	-5.7	-5.2	-5.4	-4.8	-5.4	-5.2	-4.7
DB05943	-7	-5.5	-6	-5.3	-5.5	-5.3	-5.8	-5.2	-6.8
DB06080	-7.3	-6.4	-7.9	-6.6	-6.6	-6.5	-6.2	-6.3	-8.4
DB06144	-7	-5.7	-6.5	-6.7	-6.6	-5.8	-6.6	-6.1	-6.4
DB06207	-5.9	-6.1	-6.4	-6.9	-5.8	-6.5	-6.5	-5.6	-6.3
DB06217	-5.9	-5.7	-6.7	-6	-5.4	-5.7	-5.7	-6.1	-6.5
DB06457	-6.4	-6.3	-7.4	-6.1	-6.3	-6	-6.2	-7.2	-7.8
DB06486	-6.7	-7.8	-7.7	-7.1	-7.9	-7.2	-7.7	-7	-8.6
DB06595	-8.1	-7	-8.2	-7.1	-7.9	-6.8	-7.3	-6.7	-8
DB06641	-5.1	-4.8	-5.1	-5	-4.9	-5.3	-5.4	-5	-5.2
DB06732	-7.5	-6.2	-7.4	-7	-6.5	-6.9	-7.3	-6.4	-8.2
DB06884	-6.6	-5.6	-6	-5.7	-5.6	-5.9	-5.5	-6.3	-6.2
DB06980	-6.2	-5.6	-5	-4.9	-6	-5.7	-4.8	-6.5	-6.5
DB06981	-5.3	-5.4	-6.2	-5.2	-5.5	-5	-5.4	-5.1	-6.1
DB06982	-5.4	-5	-4.6	-5	-4.8	-4.8	-5	-4.6	-5.4
DB07167	-6.6	-5.6	-6.1	-5.6	-5.3	-5.5	-5.2	-6.2	-5.4
DB07202	-6.1	-6.1	-6.1	-6.5	-6.2	-5.8	-6.2	-6.6	-6
DB07584	-7	-5.8	-6.9	-6.6	-5.4	-5.7	-6.1	-6.3	-5.8
DB07585	-4.7	-4.2	-5.4	-6	-5.4	-4.9	-5	-5.3	-5.2
DB07812	-6.6	-6	-6.8	-5.7	-6.2	-6.4	-5.7	-6.5	-6
DB07859	-7.9	-6.5	-6.9	-7.1	-6.6	-6.2	-6.2	-6.1	-8
DB07947	-4.5	-5.1	-5	-4.6	-5.1	-4	-5.6	-5.3	-4.7
DB07950	-5.8	-4.9	-6.3	-5.9	-5.5	-4.8	-4.7	-4.7	-6

ID	Wild	mutant _Q61R	mutant _Q61K	mutant _Y64D	mutant _Q61H	mutant _G13R	mutant _G13D	mutant _E153Q	mutant _G12D
DB08073	-4.4	-6	-6.1	-5.1	-6	-5.4	-6.1	-6.7	-6.5
DB08231	-4.6	-4	-4.2	-4.1	-4.1	-4.2	-4.1	-4.2	-5.9
DB08341	-7	-5.8	-7.1	-7	-6.5	-6.6	-6.4	-6.2	-6.8
DB08814	-5.1	-5.6	-5.3	-5.7	-5.3	-5.5	-5	-6.5	-6.2
DB08865	-6.7	-7	-6.5	-6.5	-7.6	-6.9	-6.2	-6.4	-6.4
DB08875	-6.6	-7.2	-7.5	-7.5	-7.2	-6.8	-6.7	-6.5	-6.7
DB08896	-6.9	-6.9	-7.4	-7.1	-7.3	-7.3	-7	-7.7	-6.7
DB08901	-7.4	-7.1	-7.9	-8.1	-7.4	-7.5	-7.5	-7.5	-7.4
DB08908	-4.3	-4.4	-4.3	-3.3	-4.1	-4.1	-4.3	-4.3	-4.3
DB09063	-6.5	-6.7	-7	-6.7	-6.6	-5.9	-6.6	-6.9	-7.3
DB09078	-5.3	-6.1	-6.2	-7.1	-6.3	-5.9	-5.9	-5.9	-5.4
DB09079	-6.9	-6.7	-8	-7.5	-7.2	-6.8	-7.1	-7	-8.1
DB09221	-5.1	-5	-5.4	-4.7	-5.7	-6	-5.7	-5.7	-6.2
DB11186	-5	-4.7	-5.9	-5.5	-5.6	-5.3	-4.8	-5.5	-4.6
DB11363	-7	-7.4	-7.4	-7.3	-7.2	-7.3	-6.7	-8.6	-8.6
DB11386	-3.4	-3.3	-3.8	-3.4	-3.8	-4	-3.3	-3.8	-3.9
DB11633	-6.6	-6.6	-6.1	-8.3	-6.5	-6.5	-5.7	-6.4	-7.2
DB11642	-5.2	-4.8	-4.4	-4.4	-5.1	-4.4	-4.7	-5.1	-5.1
DB11697	-7.3	-7.4	-7.4	-7.7	-7.6	-7.5	-7.8	-7.8	-7.5
DB11718	-5.7	-6.2	-6	-6	-6.3	-5.8	-5.9	-6.1	-6.6
DB11752	-6.5	-7.2	-6.6	-6.6	-7.1	-7.1	-7.1	-7	-7.2
DB11800	-6.8	-6.6	-6.2	-6.7	-6.5	-6.6	-6.5	-7.2	-7.5
DB12010	-5.9	-6.2	-7.3	-6.3	-7.2	-5.9	-6.9	-6	-6.9
DB12130	-8	-7.3	-7.4	-7.1	-7.9	-7.1	-6.7	-7.6	-7.8
DB12141	-6.6	-6.5	-6.2	-6.5	-6.9	-6.8	-6.7	-7.5	-6
DB12267	-7	-7.7	-7.1	-6.8	-7.6	-7.5	-6.9	-7	-7.4
DB12364	-7.2	-6.2	-6.6	-6	-6.7	-6.3	-6.3	-6.6	-6.6
DB12500	-7.4	-6.9	-7	-6.4	-6.6	-6.2	-6.9	-6.1	-6.5
DB12742	-6.3	-6.6	-6.2	-6	-6.5	-6.7	-6.1	-7.4	-6.5
DB12816	-4.1	-5.1	-5.3	-5.5	-4.4	-5	-4.5	-5.1	-5.4
DB12978	-6.6	-6.2	-6.7	-6.2	-6.1	-6.6	-6.2	-6.1	-6.8
DB13751	-8	-7.3	-7.6	-7.7	-7.5	-8.9	-7.6	-7.5	-7.2
DB14059	-6.7	-6.2	-6.6	-6.4	-6.7	-6.4	-6.5	-6.8	-7.6
DB15035	-6.8	-6.5	-7.4	-6.8	-6.7	-7.2	-6.7	-7.3	-7.2
DB15685	-7.5	-7.6	-6.8	-6.9	-6.6	-6.5	-6.2	-6.9	-7.1
DB15822	-7.6	-7.3	-7	-8.2	-7.7	-7.8	-7.7	-7.5	-7.1
Ellagicacid	-7	-6.7	-7.3	-7.1	-7	-7.4	-6	-7.1	-7.8
Epicatechin	-8.4	-6	-8.8	-6	-6	-5.9	-7.6	-5.8	-6.3
Epigallo catechin Gallate	-6.3	-7	-6.7	-6.5	-6.1	-6.9	-6.1	-7.1	-8.5
Hydno carpin D	-6.8	-6.9	-7.3	-7.3	-8.2	-7.2	-7.5	-7.1	-6.9
Isookanin	-8.4	-6.3	-8.7	-5.9	-6.6	-6.6	-6.7	-8.4	-8.5
Quercetin	-6.1	-6.1	-6	-6.1	-6.9	-6.8	-7.5	-7.4	-7.9
Silandrin	-7.4	-7.5	-7.1	-7.6	-7.5	-7.1	-7.2	-7.1	-8.4
Theaflavine	-8.6	-7.6	-7.4	-7.8	-7.1	-7.5	-7.2	-7.1	-8.8

ID	Wild	mutant _Q61R	mutant _Q61K	mutant _Y64D	mutant _Q61H	mutant _G13R	mutant _G13D	mutant _E153Q	mutant _G12D
UrolithinC	-7.5	-6.3	-7.4	-7.1	-6.5	-6.1	-6.2	-6.6	-7.5
Xanthone	-6.7	-6	-5.6	-6.7	-6.2	-6.2	-6.5	-5.9	-6.7

TABLE 8: Docking of Relapsed Biomarkers with Drugs

	DB00210	DB08901	DB13751	DB15822
CSF1R	-8.9	-9.5	-8.9	-8.6
BIRC5	-8.6	-9.2	-8.7	-9
NRP1	-10	-10.5	-9.5	-9.9
VCAN	-10.3	-10	-8.6	-8.8
BPI	-10.6	-10.2	-7.8	-10.5
COL22A1	-8.7	-8.1	-8.9	-8.9
FAT1_D2382A_wild	-6.9	-7.4	-7.8	-7.5
FAT1_D2382A	-7.1	-7.2	-7.3	-7.2
FAT1_M739I_Wild	-7.4	-8.5	-8.1	-7.4
FAT1_M739I	-7.6	-8.5	-8.1	-7.4
FAT1_P4309S_wild	-8.6	-9.6	-8.9	-8.9
FAT1_P4309S	-9.4	-8.8	-8.1	-9.1

Appendix B

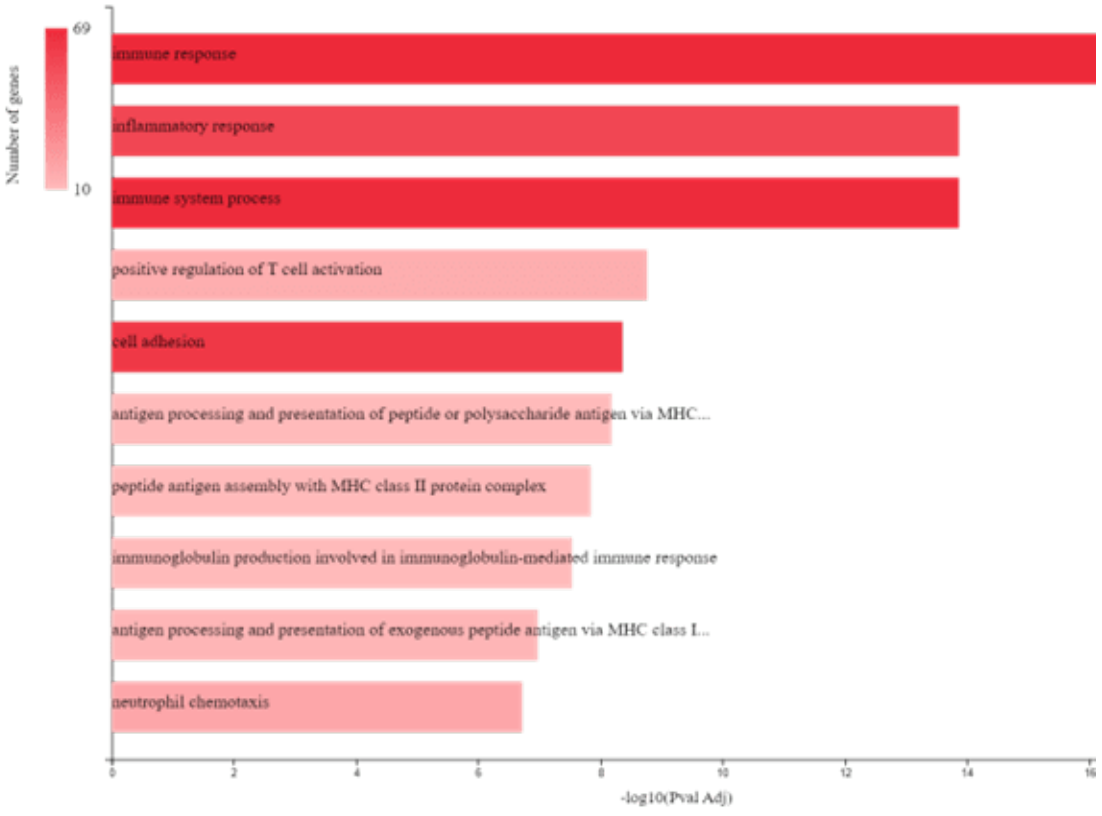

FIGURE 1: The GO Biological Process analysis of upregulated DEGs

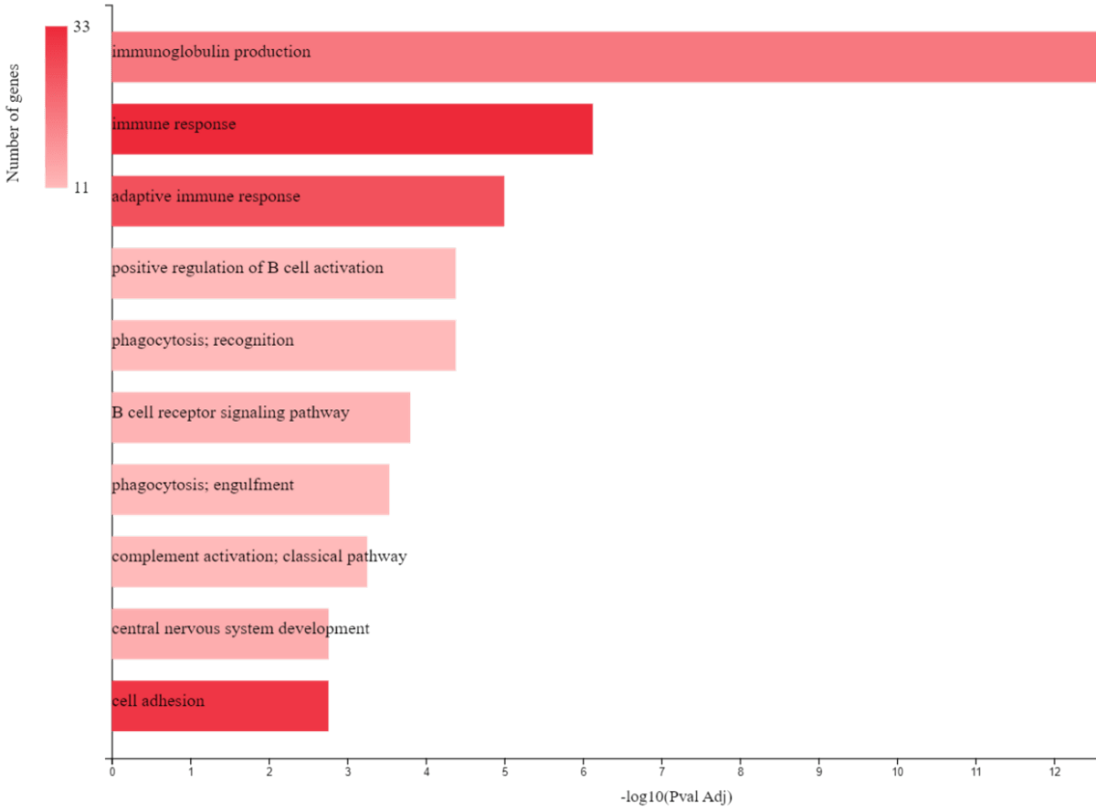

FIGURE 2: The GO Biological Process analysis of downregulated DEGs

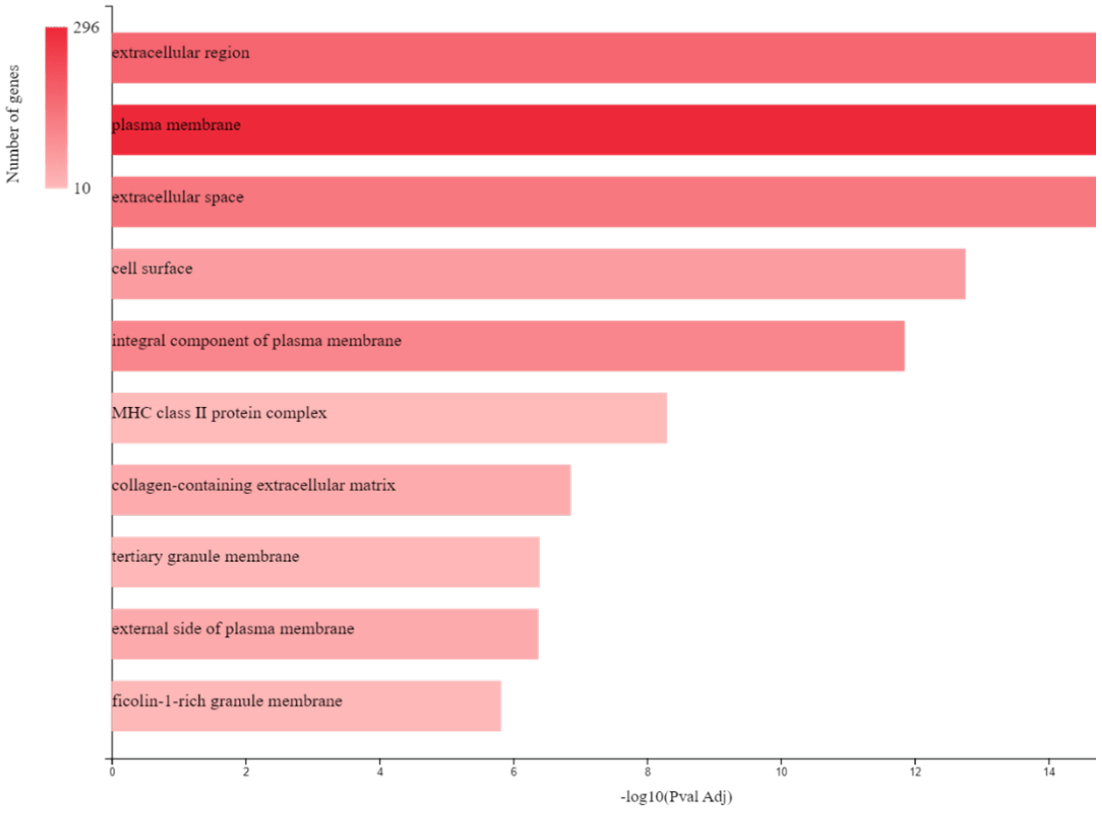

FIGURE 3: The GO Cellular Component analysis of upregulated DEGs

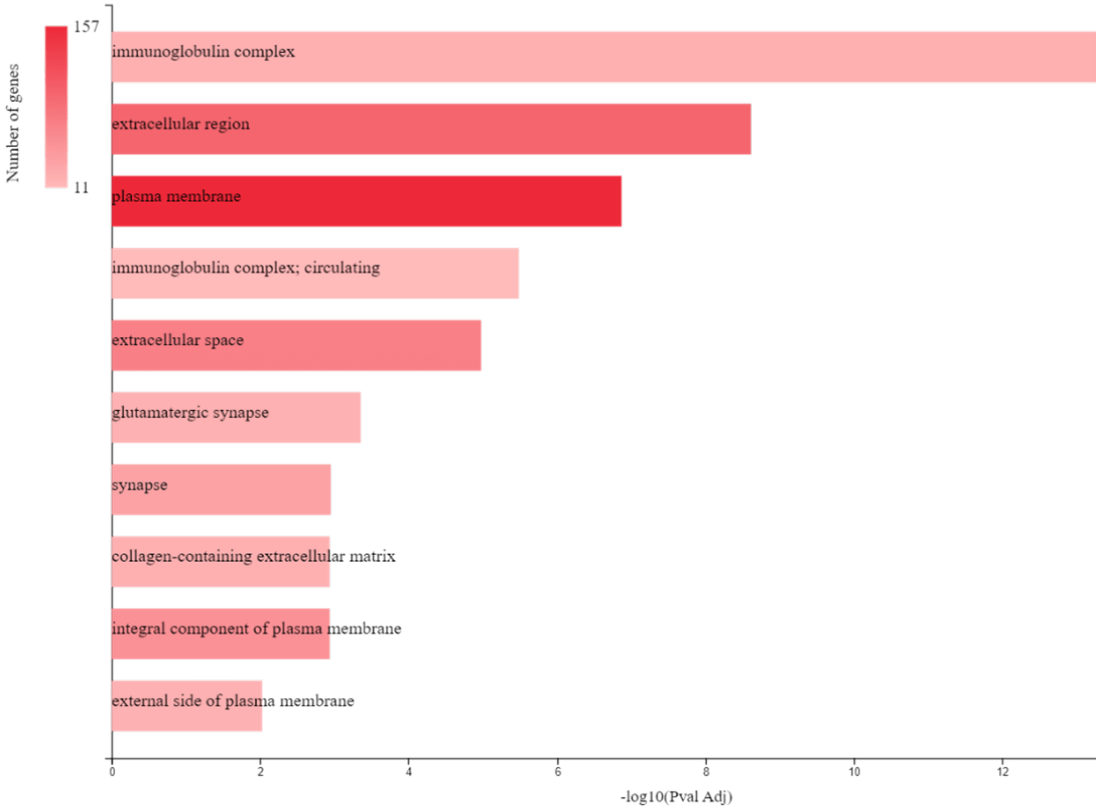

FIGURE 4: The GO Cellular Component analysis of downregulated DEGs

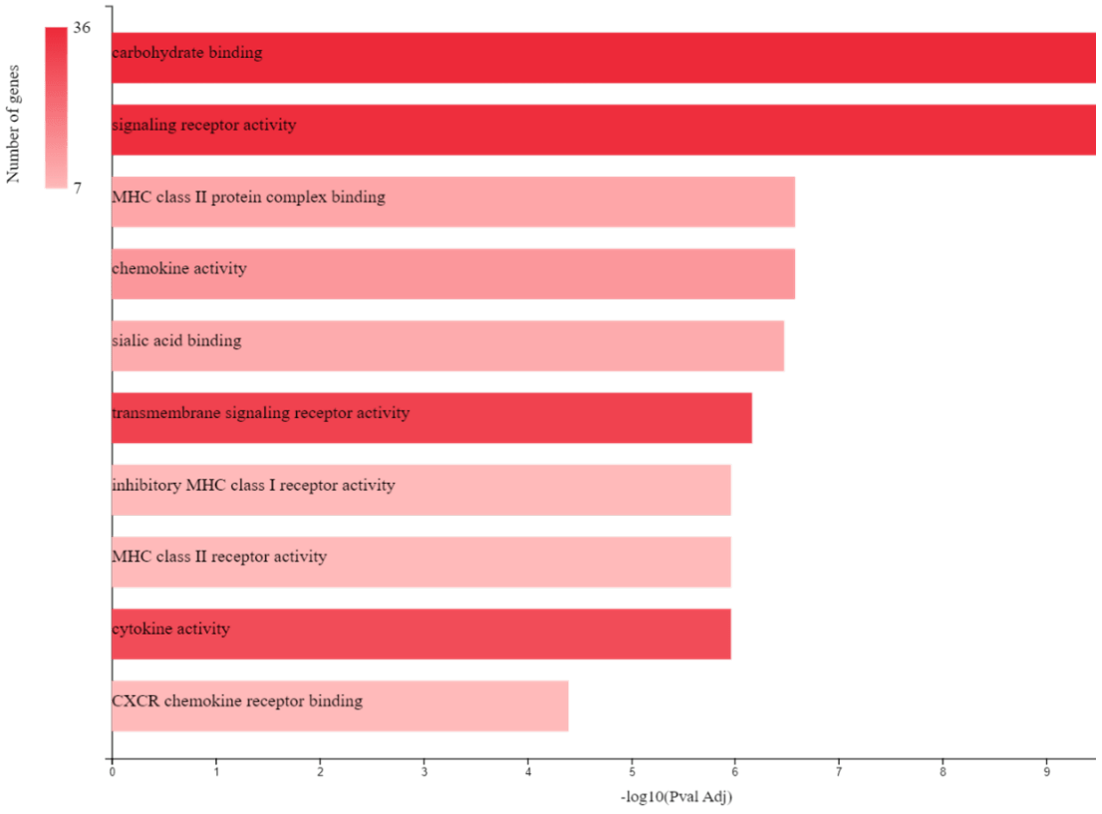

FIGURE 5: The GO Molecular Function analysis of upregulated DEGs

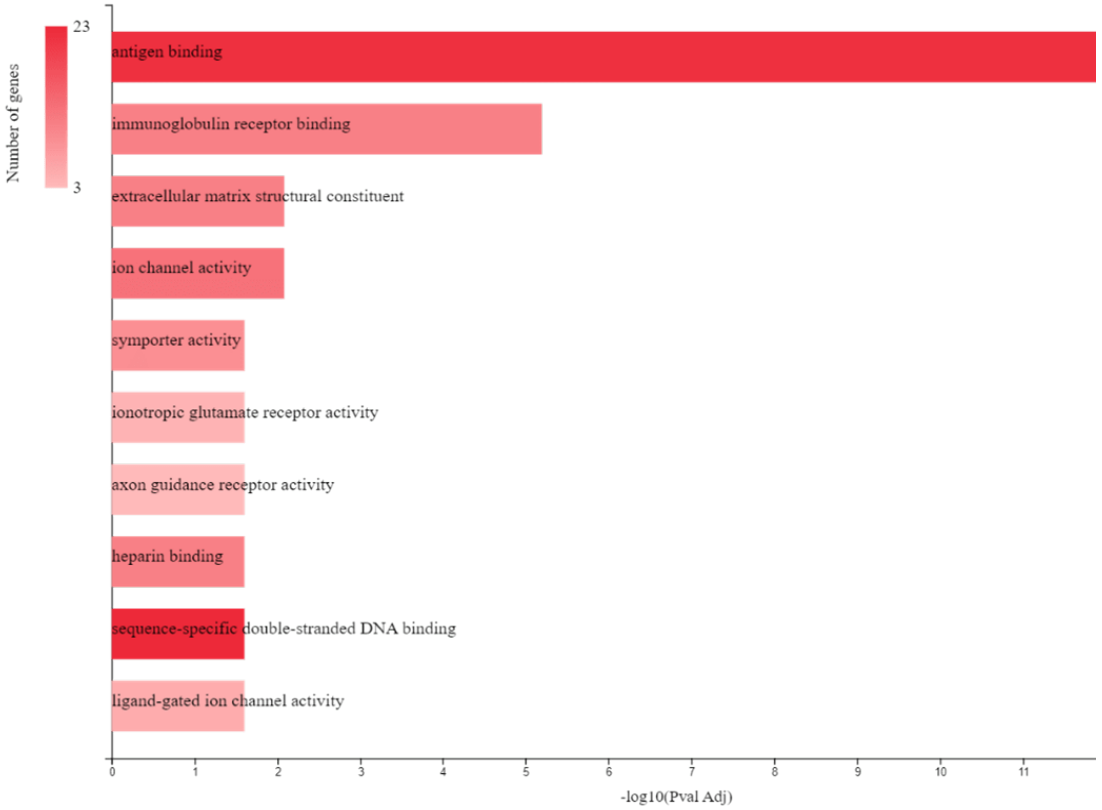

FIGURE 6: The GO Molecular Function analysis of upregulated DEGs

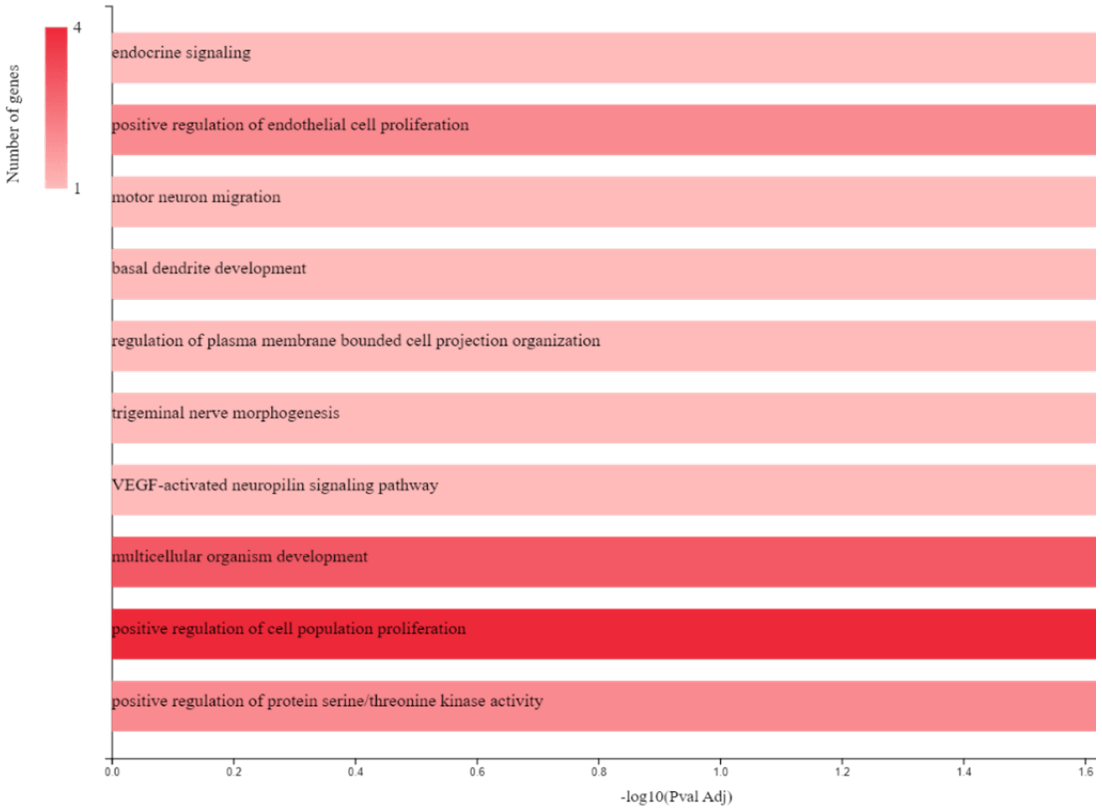

FIGURE 7: The GO Biological Function analysis of shortlisted candidate relapse biomarkers

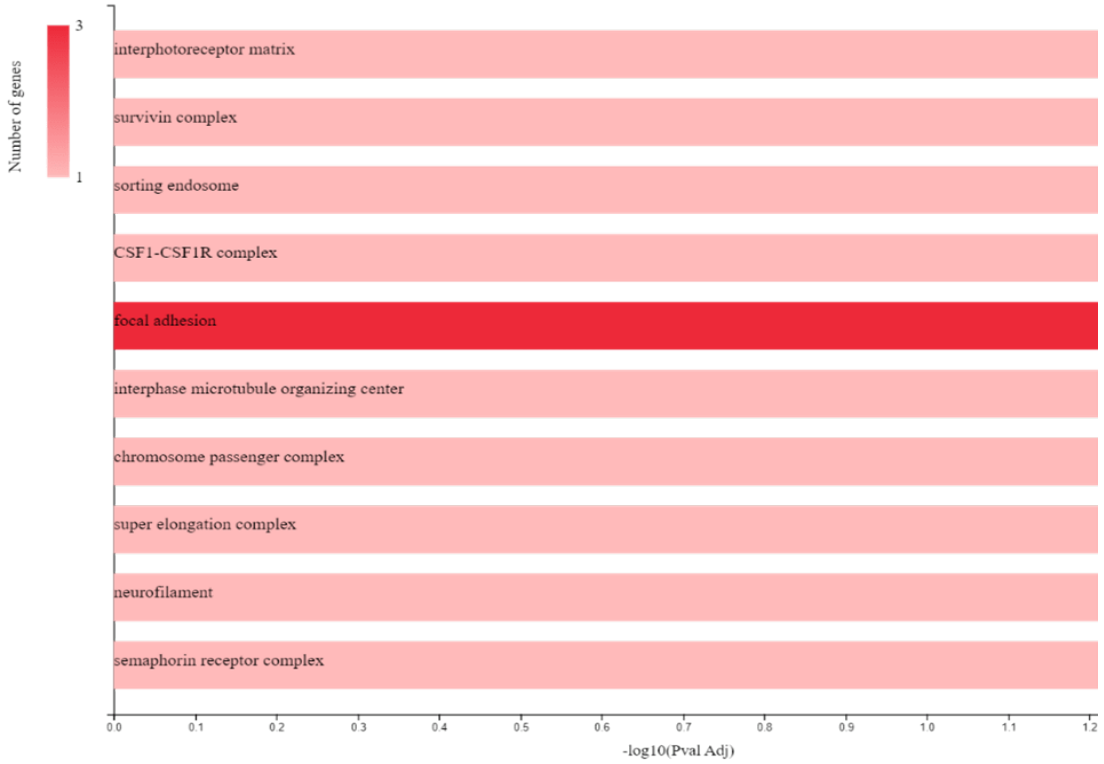

FIGURE 8: The GO Cellular Component analysis of shortlisted candidate relapse biomarkers

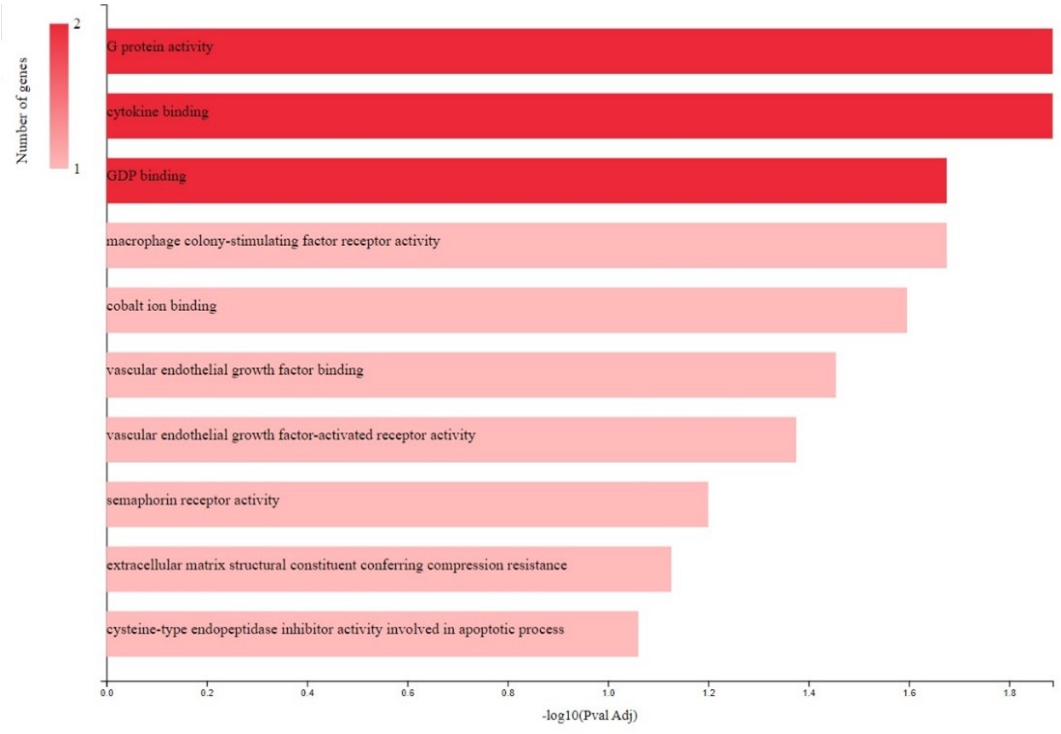

FIGURE 9: The GO Molecular Function analysis of shortlisted candidate relapse biomarkers